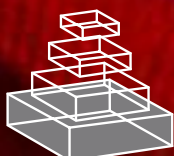


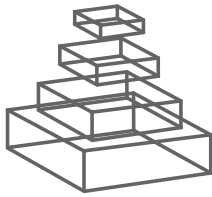
# frontiers RESEARCH TOPICS

MIND THE GAP!  
GAP JUNCTION CHANNELS  
AND THEIR IMPORTANCE IN  
PATHOGENESIS

Topic Editors  
Aida Salameh, Katja Blanke  
and Stefan Dhein



frontiers in  
**PHARMACOLOGY**



## **FRONTIERS COPYRIGHT STATEMENT**

© Copyright 2007-2014  
Frontiers Media SA.  
All rights reserved.

All content included on this site, such as text, graphics, logos, button icons, images, video/audio clips, downloads, data compilations and software, is the property of or is licensed to Frontiers Media SA ("Frontiers") or its licensees and/or subcontractors. The copyright in the text of individual articles is the property of their respective authors, subject to a license granted to Frontiers.

The compilation of articles constituting this e-book, wherever published, as well as the compilation of all other content on this site, is the exclusive property of Frontiers. For the conditions for downloading and copying of e-books from Frontiers' website, please see the Terms for Website Use. If purchasing Frontiers e-books from other websites or sources, the conditions of the website concerned apply.

Images and graphics not forming part of user-contributed materials may not be downloaded or copied without permission.

Individual articles may be downloaded and reproduced in accordance with the principles of the CC-BY licence subject to any copyright or other notices. They may not be re-sold as an e-book.

As author or other contributor you grant a CC-BY licence to others to reproduce your articles, including any graphics and third-party materials supplied by you, in accordance with the Conditions for Website Use and subject to any copyright notices which you include in connection with your articles and materials.

All copyright, and all rights therein, are protected by national and international copyright laws.

The above represents a summary only. For the full conditions see the Conditions for Authors and the Conditions for Website Use.

**ISSN** 1664-8714  
**ISBN** 978-2-88919-238-0  
**DOI** 10.3389/978-2-88919-238-0

## **ABOUT FRONTIERS**

Frontiers is more than just an open-access publisher of scholarly articles: it is a pioneering approach to the world of academia, radically improving the way scholarly research is managed. The grand vision of Frontiers is a world where all people have an equal opportunity to seek, share and generate knowledge. Frontiers provides immediate and permanent online open access to all its publications, but this alone is not enough to realize our grand goals.

## **FRONTIERS JOURNAL SERIES**

The Frontiers Journal Series is a multi-tier and interdisciplinary set of open-access, online journals, promising a paradigm shift from the current review, selection and dissemination processes in academic publishing.

All Frontiers journals are driven by researchers for researchers; therefore, they constitute a service to the scholarly community. At the same time, the Frontiers Journal Series operates on a revolutionary invention, the tiered publishing system, initially addressing specific communities of scholars, and gradually climbing up to broader public understanding, thus serving the interests of the lay society, too.

## **DEDICATION TO QUALITY**

Each Frontiers article is a landmark of the highest quality, thanks to genuinely collaborative interactions between authors and review editors, who include some of the world's best academicians. Research must be certified by peers before entering a stream of knowledge that may eventually reach the public - and shape society; therefore, Frontiers only applies the most rigorous and unbiased reviews.

Frontiers revolutionizes research publishing by freely delivering the most outstanding research, evaluated with no bias from both the academic and social point of view.

By applying the most advanced information technologies, Frontiers is catapulting scholarly publishing into a new generation.

## **WHAT ARE FRONTIERS RESEARCH TOPICS?**

Frontiers Research Topics are very popular trademarks of the Frontiers Journals Series: they are collections of at least ten articles, all centered on a particular subject. With their unique mix of varied contributions from Original Research to Review Articles, Frontiers Research Topics unify the most influential researchers, the latest key findings and historical advances in a hot research area!

Find out more on how to host your own Frontiers Research Topic or contribute to one as an author by contacting the Frontiers Editorial Office: [researchtopics@frontiersin.org](mailto:researchtopics@frontiersin.org)

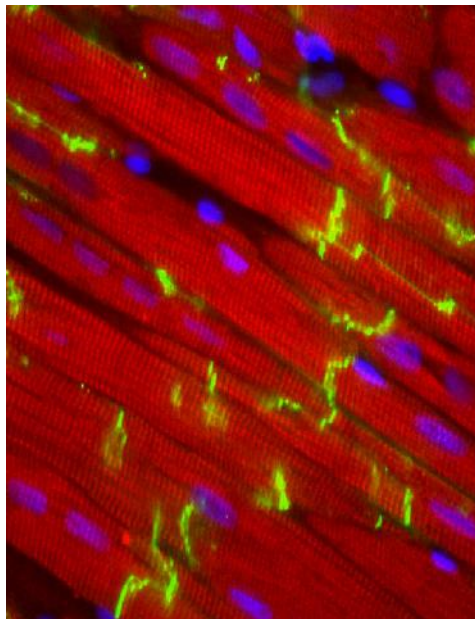
# MIND THE GAP! GAP JUNCTION CHANNELS AND THEIR IMPORTANCE IN PATHOGENESIS

Topic Editors:

**Aida Salameh**, Heart Centre University of Leipzig, Germany

**Katja Blanke**, Heart Center Leipzig, Germany

**Stefan Dhein**, Universitätsklinik Leipzig Herzzentrum Leipzig GmbH, Germany



“Cells live together, but die singly”, this sentence wrote the German physiologist Theodor Engelmann in 1875 and although he had no particular knowledge of gap junction channels (their structure was discovered around 100 years later) he described their functions very well: gap junction channels are essential for intercellular communication and crucial for the development of tissue and organs. But besides providing an opportunity for cells to communicate gap junction channels might also prevent intercellular communication by channel closure thereby preserving the surrounding healthy tissue in case of cellular necrosis.

According to today’s understanding gap junction channels play an important role during embryonic development, during growth, wound healing and cell

differentiation and are also involved in the process of learning. In the past decades most intensive research was done not only to unravel the physiological role of gap junction channels but also to extend our knowledge of the contribution of these channels in pathogenesis. A new frontier emerges in the field “pharmacology of gap junctions” with the aim to control growth, differentiation, or electrical coupling via targeting gap junction channels pharmacologically.

As we know today disturbances in gap junction synthesis, assembly and cellular distribution may account for various organic disorders from most different medical fields, such as the Charcot-Marie-Tooth neuropathy, epilepsy, Chagas-disease, Naxos-syndrome, congenital cardiac malformations, arrhythmias, cancer and as a very common disease in industrial countries atherosclerosis. Point mutations in gap junction channels have been found to cause hereditary diseases like the congenital deafness or the Charcot-Marie-Tooth neuropathy but the exact molecular mechanisms of gap junction malfunction from most of the mentioned illnesses are not fully understood. Moreover, in the last few years research has expanded on the role and function of connexin hemichannels and on a relatively new field the pannexins. The purpose of this volume is to give a comprehensive overview of the involvement of gap junction channels, hemichannels and pannexins on pathogenesis of inborn and acquired diseases and on emerging pharmacological strategies to target these channels.

We welcome our colleagues to contribute their findings on the influence of gap junctions on pathogenesis and to unravel the secrets of intercellular communication. Take the lid off!

# Table of Contents

- 06 Mind the Gap! Connexins and Pannexins in Physiology, Pharmacology and Disease**  
Aida Salameh, Katja Blanke and Stefan Dhein
- 08 Managing the Complexity of Communication: Regulation of Gap Junctions by Post-Translational Modification**  
Lene Nygaard Axelsen, Kirstine Calloe, Niels-Henrik Holstein-Rathlou and Morten Schak Nielsen
- 26 Connixin Diversity in the Heart: Insights From Transgenic Mouse Models**  
Sander Verheule and Sven Kaese
- 40 Cyclic Nucleotide Permeability Through Unopposed Connixin Hemichannels**  
Virginijus Valiunas
- 52 Connixin Expression and Gap-Junctional Intercellular Communication in ES Cells and iPS Cells**  
Masahito Oyamada, Kumiko Takebe, Aya Endo, Sachiko Hara and Yumiko Oyamada
- 60 Connixin 43 Impacts on Mitochondrial Potassium Uptake**  
Kerstin Boengler, Elvira Ungefug, Gerd Heusch, Luc Leybaert and Rainer Schulz
- 65 Interfering Amino Terminal Peptides and Functional Implications for Heteromeric Gap Junction Formation**  
Eric C. Beyer, Xianming Lin and Richard D. Veenstra
- 74 Together and Apart: Inhibition of DNA Synthesis by Connixin-43 and Its Relationship to Transforming Growth Factor  $\beta$**   
Maya Madhumathy Jeyaraman, Robert R. Fandrich and Elissavet Kardami
- 83 Histone Deacetylase Inhibition Reduces Cardiac Connixin43 Expression and Gap Junction Communication**  
Qin Xu, Xianming Lin, Laura Andrews, Dakshesh Patel, Paul D. Lampe and Richard D. Veenstra
- 99 The Effects of the Histone Deacetylase Inhibitor 4-Phenylbutyrate on Gap Junction Conductance and Permeability**  
Joshua Kaufman, Chris Gordon, Roberto Bergamaschi, Hong Zhan Wang, Ira S. Cohen, Virginijus Valiunas and Peter R. Brink
- 106 The Oligodendroglial Precursor Cell Line Oli-Neu Represents a Cell Culture System to Examine Functional Expression of the Mouse Gap Junction Gene Connixin29 (Cx29)**  
Goran Christoph Söhl, Sonja Hombach, Joachim Degen and Benjamin Odermatt

- 122 An Escherichia Coli Strain for Expression of the Connexin45 Carboxyl Terminus Attached to the 4th Transmembrane Domain**  
Jennifer L. Kopanic, Mona Al-Mugotir, Sydney Zach, Srustidhar Das, Rosslyn Grosely and Paul L. Sorgen
- 130 Promises and Pitfalls of a Pannexin1 Transgenic Mouse Line**  
Regina Hanstein, Hiromitsu Negoro, Naman K. Patel, Anne Charollais, Paolo Meda, David C. Spray, Sylvia O. Suadicani and Eliana Scemes
- 140 Connexin and Pannexin Hemichannels in Brain Glial Cells: Properties, Pharmacology, and Roles**  
Christian Giaume, Luc Leybaert, Christian C. Naus and Juan-Carlos Sáez
- 157 A Comparative Antibody Analysis of Pannexin1 Expression in Four Rat Brain Regions Reveals Varying Subcellular Localizations**  
Angela C. Cone, Cinzia Ambrosi, Eliana Scemes, Maryann E. Martone and Gina E. Sosinsky
- 176 Regulation of Gap Junctions by Nitric Oxide Influences the Generation of Arrhythmias Resulting From Acute Ischemia and Reperfusion in Vivo**  
Ágnes Végh, Márton Gönczi, Gottfried Miskolczi and Mária Kovács
- 186 Inverse Relationship Between Tumor Proliferation Markers and Connexin Expression in a Malignant Cardiac Tumor Originating From Mesenchymal Stem Cell Engineered Tissue in a Rat in Vivo Model**  
Cathleen Spath, Franziska Schlegel, Sergey Leontyev, Friedrich-Wilhelm Mohr and Stefan Dhein
- 198 Role of Connexins in Human Congenital Heart Disease: The Chicken and Egg Problem**  
Aida Salameh, Katja Blanke and Ingo Dähnert
- 209 Connexin Mutants and Cataracts**  
Eric C. Beyer, Lisa Ebihara and Viviana M. Berthoud
- 223 Role of Connexins in Infantile Hemangiomas**  
Katja Blanke, Ingo Dähnert and Aida Salameh
- 232 Neurological Manifestations of Oculodentodigital Dysplasia: A Cx43 Channelopathy of the Central Nervous System?**  
Marijke De Bock, Marianne Kerrebrouck, Nan Wang and Luc Leybaert



# Mind the gap! Connexins and pannexins in physiology, pharmacology and disease

**Aida Salameh<sup>1\*</sup>, Katja Blanke<sup>1</sup> and Stefan Dhein<sup>2</sup>**

<sup>1</sup> Department of Paediatric Cardiology, Heart Centre University of Leipzig, Leipzig, Germany

<sup>2</sup> Department of Cardiac Surgery, Heart Centre University of Leipzig, Leipzig, Germany

\*Correspondence: [aida.salameh@med.uni-leipzig.de](mailto:aida.salameh@med.uni-leipzig.de)

**Edited by:**

Philippe Lory, CNRS and University of Montpellier, France

**Keywords:** connexin, pannexin, mutation, stem cells, hemichannels, arrhythmia, inborn heart disease, cancer

Among other aspects it is the communication which makes the difference between a crowd of individuals and a society. Similarly, a key feature of an organism or of organs is the communication between their individual cells realized by mediators, hormones, and by direct intercellular communication via gap junction channels allowing the transmission of electrical signals and the exchange of small molecules to regulate growth and differentiation. This enables the organ or the organism to adapt very efficiently to the actual needs. Due to the important role of gap junction intercellular communication (GJIC) for the correct functioning of organs, and tissues a tight regulation of the expression of gap junction channel proteins, the connexins, their localization, and function is required. Besides connexins, another group of proteins, the pannexins, showing many molecular similarities with connexins have been identified. They seem to form hemichannels which may regulate cytosolic homeostasis or the release of small molecules. The present issue provides a comprehensive picture of recent developments and current research in this fascinating, fast developing area comprising review and original research articles on both connexins and pannexins written by leading experts in their research areas. The articles are organized in three parts:

A: role of gap junctions in cell biology; regulation and targeting of connexins (11 articles)

B: connexins and pannexins (3 articles)

C: gap junctions in various diseases (6 articles)

Regarding part A, regulation of connexin function is not only realized via regulation of expression but also by various post-translational modifications as reviewed by Axelsen et al. (2013). Verheule and Kaese (2013) shed light on the different roles of cardiac connexins for cardiac phenotypes in various knock-out models. Connexins not only form intercellular dodecameric channels but also may form unopposed hemichannels, which may allow cAMP release as a new pathway for intercellular cAMP signaling as shown by Valiunas (2013). With regard to their role in differentiation and growth Oyamada et al. (2013) review the role of GJIC and connexins in development and re-programming of embryonic stem cells and induced pluripotent stem cells in comparison to the undifferentiated state. According to recent findings connexins not only have functions in the membrane, but also may control gene expression, and -as found by Boengler et al. (2013)-are expressed in the mitochondria where they control

mitochondrial K<sup>+</sup>-influx. Another puzzling aspect of gap junction research is the ability or non-ability of certain connexins to form heteromeric channels which are composed of more than only one isoform. Regarding this aspect Beyer et al. (2013a) investigate the heteromeric interactions between Cx40 and Cx43 focusing on the role of the N-terminal. Regarding growth control by GJIC Kardami's group investigated the inhibition of DNA synthesis by Cx43 and S262-Cx43 de-phosphorylation Jeyaraman et al. (2013). In the next two articles histone-deacetylase is examined as a possible pharmacological target for influencing Cx43 expression with reduced expression when using trichostatin A (Xu et al., 2013) or with enhanced expression when using 4-phenylbutyrate (Kaufman et al., 2013). The section is closed with two more methodological articles showing a new cell culture system for the study of Cx29 (Söhl et al., 2013) and a new Escherichia coli expression system for Cx45 carboxyl terminus allowing the yield of large protein amounts as needed for NMR analysis (Kopanic et al., 2013).

Part B starts with an original article about pannexin 1 elucidating the problems with Panx1 knock outs and showing the generation of astrocyte and neuron-specific Panx1 deletions (Hanstein et al., 2013). The role of Panx1 and connexin hemichannels in brain glial cells in health and disease as well their impact for neuroglial interaction and possible pharmacological approaches are reviewed by Giaume et al. (2013). The distribution of Panx1 in four rat brain regions using different antibodies in a comparative study is investigated by Cone et al. (2013).

Part C focuses on the role of gap junctions in various diseases starting with an interesting hypothesis article by Végh et al. (2013) on the regulation of cardiac gap junctions by nitric oxide in ischemia and reperfusion and its relation to arrhythmia. In the next article the inverse relationship between proliferative activity of a tumor induced by cardiac transplantation of bone marrow stem cells and intra-tumor connexin expression. Spath et al. (2013) conclude that the lack of connexin expression in the most proliferative areas of the tumor results in absence of differentiation and growth stop signals so that invasive growth is facilitated. The role of gap junction mutations or alteration in inborn human heart disease is reviewed by Salameh et al. (2013) in comparison to the findings in various mouse models. Beyer et al. (2013b) review the role of connexin mutations in the pathogenesis of lens cataracts and discuss altered hemichannel functions and formation of cytoplasmic accumulations. Interesting new aspects about a possible pathogenetic role of gap junctions are given by Blanke et al. (2013) with regard to the formation of

infantile hemangiomas and possible interference between beta-adrenoceptors and connexins. The section closes with a review on the most recent advances in research on GJIC and oculodentoglia dysplasia focussing on the possible relationship between channel dysfunction and neurological symptoms in these patients De Bock et al. (2013).

This compilation of articles on most recent developments in connexin and pannexin research hopefully encourages more scientists to investigate these highly interesting cell biology mechanisms in their research areas. When cellular interaction or interplay is of relevance this recent research suggests: mid the gap!

## REFERENCES

- Axelsen, L. N., Calloe, K., Holstein-Rathlou, N. H., and Schak Nielsen, M. (2013). Managing the complexity of communication; regulation of gap junctions by post-translational modification. *Front. Pharmacol.* 4:130. doi: 10.3389/fphar.2013.00130
- Beyer, E. C., Lin, X., and Veenstra, R. D. (2013a). Interfering amino terminal peptides and functional implications for heteromeric gap junction formation. *Front. Pharmacol.* 4:67. doi: 10.3389/fphar.2013.00067
- Beyer, E. C., Ebihara, L., and Berthoud, V. M. (2013b). Connexin mutants and cataracts. *Front. Pharmacol.* 4:43. doi: 10.3389/fphar.2013.00043
- Blanke, K., Dähnert, I., and Salameh, A. (2013). Role of connexins in infantile hemangiomas. *Front. Pharmacol.* 4:41. doi: 10.3389/fphar.2013.00041
- Boengler, K., Ungefug, E., Heusch, G., Leybaert, L., and Schulz, R. (2013). Connexin 43 impacts on mitochondrial potassium uptake. *Front. Pharmacol.* 4:73. doi: 10.3389/fphar.2013.00073
- Cone, A. C., Ambrosi, C., Scemes, E., Martone, M. E., and Sosinsky, G. E. (2013). A comparative antibody analysis of pannexin1 expression in four rat brain regions reveals varying subcellular localizations. *Front. Pharmacol.* 4:6. doi: 10.3389/fphar.2013.00006
- De Bock, M., Kerrebrouck, M., Wang, N., and Leybaert, L. (2013). Neurological manifestations of oculodentodigital dysplasia: a Cx43 channelopathy of the central nervous system. *Front. Pharmacol.* 4:120. doi: 10.3389/fphar.2013.00120
- Giaume, C., Leybaert, L., Naus, C. C., Sáez, J. C. (2013). Connexin and pannexin hemichannels in brain glial cells: properties, pharmacology, and roles. *Front. Pharmacol.* 4:88. doi: 10.3389/fphar.2013.00088
- Hanstein, R., Negoro, H., Patel, N. K., Charollais, A., Meda, P., Spray, D. C., et al. (2013). Promises and pitfalls of a Pannexin1 transgenic mouse line. *Front. Pharmacol.* 4:61. doi: 10.3389/fphar.2013.00061
- Jeyaraman, M. M., Fandrich, R. R., and Kardami, E. (2013). Together and apart: inhibition of DNA synthesis by connexin-43 and its relationship to transforming growth factor  $\beta$ . *Front. Pharmacol.* 4:90. doi: 10.3389/fphar.2013.00090
- Kaufman, J., Gordon, C., Bergamaschi, R., Wang, H. Z., Cohen, I. S., Valiunas, V., et al. (2013). The effects of the histone deacetylase inhibitor 4-phenylbutyrate on gap junction conductance and permeability. *Front. Pharmacol.* 4:111. doi: 10.3389/fphar.2013.00111
- Kopanic, J. L., Al-Mugotir, M., Zach, S., Das, S., Grosely, R., and Sorgen, P. L. (2013). An Escherichia coli strain for expression of the connexin45 carboxyl terminus attached to the 4th transmembrane domain. *Front. Pharmacol.* 4:106. doi: 10.3389/fphar.2013.00106
- Oyamada, M., Takebe, K., Endo, A., Hara, S., and Oyamada, Y. (2013). Connexin expression and gap-junctional intercellular communication in ES cells and iPS cells. *Front. Pharmacol.* 4:85. doi: 10.3389/fphar.2013.00085
- Salameh, A., Blanke, K., and Daehnert, I. (2013). Role of connexins in human congenital heart disease: the chicken and egg problem. *Front. Pharmacol.* 4:70. doi: 10.3389/fphar.2013.00070
- Söhl, G., Hombach, S., Degen, J., and Odermatt, B. (2013). The oligodendroglial precursor cell line Oli-neu represents a cell culture system to examine functional expression of the mouse gap junction gene connexin29 (Cx29). *Front. Pharmacol.* 4:83. doi: 10.3389/fphar.2013.00083
- Spath, C., Schlegel, F., Leontyev, S., Mohr, F. W., and Dhein, S. (2013). Inverse relationship between tumor proliferation markers and connexin expression in a malignant cardiac tumor originating from mesenchymal stem cell engineered tissue in a rat *in vivo* model. *Front. Pharmacol.* 4:42. doi: 10.3389/fphar.2013.00042
- Valiunas, V. (2013). Cyclic nucleotide permeability through unopposed connexin hemichannels. *Front. Pharmacol.* 4:75. doi: 10.3389/fphar.2013.00075
- Végh, A., Gönczi, M., Miskolczi, G., and Kovács, M. (2013). Regulation of gap junctions by nitric oxide influences the generation of arrhythmias resulting from acute ischemia and reperfusion *in vivo*. *Front. Pharmacol.* 4:76. doi: 10.3389/fphar.2013.00076
- Verheule, S., and Kaese, S. (2013). Connexin diversity in the heart: insights from transgenic mouse models. *Front. Pharmacol.* 4:81. doi: 10.3389/fphar.2013.00081
- Xu, Q., Lin, X., Andrews, L., Patel, D., Lampe, P. D., and Veenstra, R. D. (2013). Histone deacetylase inhibition reduces cardiac connexin43 expression and gap junction communication. *Front. Pharmacol.* 4:44. doi: 10.3389/fphar.2013.00044

Received: 14 October 2013; accepted: 04 November 2013; published online: 21 November 2013.

Citation: Salameh A, Blanke K and Dhein S (2013) Mind the gap! Connexins and pannexins in physiology, pharmacology and disease. *Front. Pharmacol.* 4:144. doi: 10.3389/fphar.2013.00144

This article was submitted to Pharmacology of Ion Channels and Channelopathies, a section of the journal *Frontiers in Pharmacology*.

Copyright © 2013 Salameh, Blanke and Dhein. This is an open-access article distributed under the terms of the Creative Commons Attribution License (CC BY). The use, distribution or reproduction in other forums is permitted, provided the original author(s) or licensor are credited and that the original publication in this journal is cited, in accordance with accepted academic practice. No use, distribution or reproduction is permitted which does not comply with these terms.



# Managing the complexity of communication: regulation of gap junctions by post-translational modification

Lene N. Axelsen<sup>1</sup>, Kirstine Calloe<sup>2</sup>, Niels-Henrik Holstein-Rathlou<sup>1</sup> and Morten S. Nielsen<sup>1\*</sup>

<sup>1</sup> Department of Biomedical Sciences and The Danish National Research Foundation Centre for Cardiac Arrhythmia, Faculty of Health and Medical Sciences, University of Copenhagen, Copenhagen, Denmark

<sup>2</sup> Department of Veterinary Clinical and Animal Sciences and The Danish National Research Foundation Centre for Cardiac Arrhythmia, Faculty of Health and Medical Sciences, University of Copenhagen, Copenhagen, Denmark

**Edited by:**

Stefan Dhein, Universitätsklinik Leipzig, Herzzentrum Leipzig GmbH, Leipzig, Germany

**Reviewed by:**

Stefan Dhein, Universitätsklinik Leipzig, Herzzentrum Leipzig GmbH, Leipzig, Germany

John Philip Winpenny, University of East Anglia, UK

**\*Correspondence:**

Morten S. Nielsen, Department of Biomedical Sciences and The Danish National Research Foundation Centre for Cardiac Arrhythmia, Faculty of Health and Medical Sciences, University of Copenhagen, Blegdamsvej 3, 10.5, 2200 Copenhagen, Denmark  
e-mail: schak@sund.ku.dk

Gap junctions are comprised of connexins that form cell-to-cell channels which couple neighboring cells to accommodate the exchange of information. The need for communication does, however, change over time and therefore must be tightly controlled. Although the regulation of connexin protein expression by transcription and translation is of great importance, the trafficking, channel activity and degradation are also under tight control. The function of connexins can be regulated by several post translational modifications, which affect numerous parameters; including number of channels, open probability, single channel conductance or selectivity. The most extensively investigated post translational modifications are phosphorylations, which have been documented in all mammalian connexins. Besides phosphorylations, some connexins are known to be ubiquitinated, SUMOylated, nitrosylated, hydroxylated, acetylated, methylated, and  $\gamma$ -carboxyglutamated. The aim of the present review is to summarize our current knowledge of post translational regulation of the connexin family of proteins.

**Keywords:** connexin, post translational modification, phosphorylation, sumoylation, nitrosylation, methylation, acetylation, ubiquitination

## INTRODUCTION

Connexins are a family of membrane proteins forming gap junctional channels. Each connexin is a four membrane spanning protein with two extracellular loops, an intracellular loop and intracellular N- and C-termini (see **Figure 1**). Six connexins oligomerize to form a connexon, which, once inserted in the plasma membrane, may dock with a connexon from a neighboring cell and form an intercellular gap junctional channel. When many intercellular channels aggregate, they form a gap junction plaque, which present a typical penta-laminar structure when viewed in transmission electron microscope images (**Figure 1**, right panel). In some cases, free connexons may open directly to the extracellular medium in which case they are often referred to as hemichannels. This review will primarily deal with intercellular gap junctional channels.

Gap junctions are responsible for direct intercellular communication in vertebrates and the connexin family has 21 members in humans and 20 in mice (Willecke et al., 2002). The connexins are named after their approximate molecular weight (e.g., Cx43 is a protein of app. 43 kDa), whereas the genes encoding them are named GJX followed by a number with X indicating group ( $\alpha$ ,  $\beta$ ,  $\gamma$ ,  $\delta$  or  $\epsilon$ ) based on homology and length of their cytoplasmic loop (for more information about nomenclature, see Nielsen et al., 2012). A list of gene and protein names for human and mouse connexins is given in **Table 1**. In the present review, we use the name of the human ortholog in general but may also state species dependent names where relevant to avoid confusion.

Gap junctions are instrumental in many physiological phenomena, from embryonic development to propagation of cardiac action potentials. Giving the diversity of these tasks, it is not surprising that the connexins, which form the gap junctional channels, come in many isoforms. By the expression of different connexins, cells can regulate coupling in a tissue and time dependent manner.

The connexin isoforms differ in their permeability to larger molecules, termed metabolic coupling; and current in the form of atomic ions, termed electrical coupling. Although it is often stated that gap junctional channels are permeable to substances up to 1 kDa, metabolic coupling is highly variable among isoforms and permeability is often unpredictable with respect to permeant size and charge. Most of our current knowledge on metabolic coupling comes from studies of fluorescent tracer molecules and some caution is needed when comparing studies using different tracers, also it should be kept in mind that permeability to biologically relevant molecules cannot necessarily be inferred from tracer permeability. More information about permeability of connexin channels can be found in (Harris and Locke, 2009; Nielsen et al., 2012). Electrical coupling can be measured by dual patch clamp and investigated as either the total conductance between cells in a pair, termed macroscopic coupling, or single channel conductance, which is usually determined under partial uncoupling by agents like octanol.

The characteristics of the various connexin isoforms enable them to fulfill different physiological roles that may be more or less connexin specific. In the case of the development of cardiac morphology, Cx43 may be exchanged with Cx40 without consequence

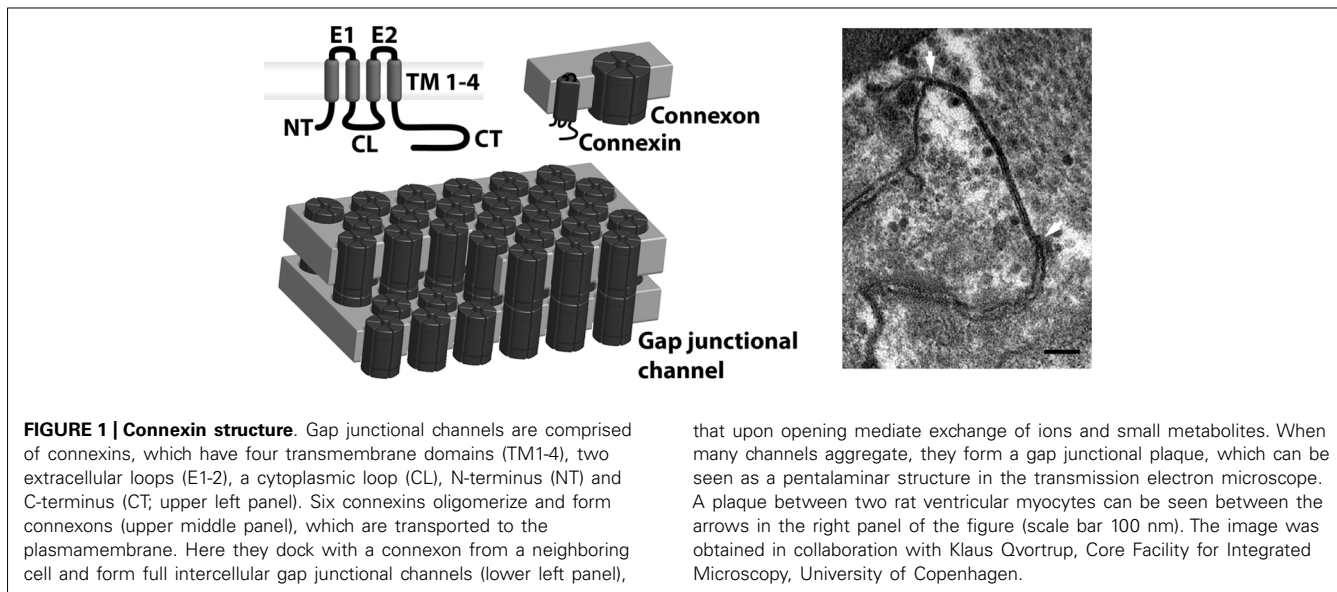


**FIGURE 1 | Connexin structure.** Gap junctional channels are comprised of connexins, which have four transmembrane domains (TM1-4), two extracellular loops (E1-2), a cytoplasmic loop (CL), N-terminus (NT) and C-terminus (CT; upper left panel). Six connexins oligomerize and form connexons (upper middle panel), which are transported to the plasmamembrane. Here they dock with a connexon from a neighboring cell and form full intercellular gap junctional channels (lower left panel).

that upon opening mediate exchange of ions and small metabolites. When many channels aggregate, they form a gap junctional plaque, which can be seen as a pentalaminar structure in the transmission electron microscope. A plaque between two rat ventricular myocytes can be seen between the arrows in the right panel of the figure (scale bar 100 nm). The image was obtained in collaboration with Klaus Qvortrup, Core Facility for Integrated Microscopy, University of Copenhagen.

and is thus relatively unspecific; however, the same exchange renders homozygous females unable to wean their pups and males infertile, which shows that these processes are highly dependent on the specific properties of Cx43 (Plum et al., 2000).

Despite the possibility of altering intercellular coupling by changing the connexin expression profile, cells often need to regulate communication acutely by altering the function and localization of the connexins at hand. This is often mediated by post translational modifications (PTMs). The most widely investigated PTMs in connexins are phosphorylations and ubiquitinizations, but in recent years studies have shown how other PTM such as ubiquitination, SUMOylation, nitrosylation, hydroxylation, acetylation, methylation, and  $\gamma$ -carboxyglutamyl also play important roles in the regulation of intercellular communication.

Intercellular coupling is determined by both the number of channels incorporated in gap junctions, their activity and selectivity. The number of channels is regulated by transcription, translation, oligomerization, trafficking to and from the membrane, and degradation. Pre-translational events (transcription and translation) does of course not involve PTM (for review of these processes in connexins, see Nielsen et al., 2012), but PTMs are involved in the regulation of all other aspects of the connexin lifecycle. The activity of gap junctional channels is determined by their open probability, conductance and selectivity, each of which can be regulated by PTMs. In the following, we will review the state of knowledge of how various PTMs regulate connexin function.

## PHOSPHORYLATION – A KEY PLAYER IN THE REGULATION OF GAP JUNCTIONS

The covalent binding of phosphate groups to either serine, threonine or tyrosine residues of proteins is termed protein phosphorylation. The addition of a phosphate group to a protein is facilitated by various protein kinases, whereas removal of a phosphate group, dephosphorylation, is mediated by protein phosphatases. Protein phosphorylation was first described by Edmond Fischer and Edwin Krebs, who were awarded the Nobel

Prize for “*their discoveries concerning reversible protein phosphorylation as a biological regulatory mechanism*” in 1992. Today, phosphorylation and dephosphorylation is well described and potentially the most common way of controlling the activity and function of proteins in biological systems. Following translation of a protein, the phosphorylation state of the protein usually determine the three-dimensional folding and conformation, the intracellular trafficking and activity of the protein, as well as its interaction with other proteins. Phosphorylation of proteins is therefore a key player in the regulation of all forms of cellular processes.

The first evidence that connexins are phosphoproteins was published in the 1980s (Saez et al., 1986; Takeda et al., 1987). Since then, tremendous amounts of work have contributed to our current knowledge of site-specific phosphorylation and dephosphorylation and its contribution to the post-translational regulation of connexins. All the connexin family members are now known to be phosphoproteins and connexin phosphorylation/dephosphorylation is involved in all stages of the connexin life-cycle, the regulation of electrical and metabolic coupling of gap junction channels, as well as regulation of connexin interaction with other proteins. The phosphorylation state of connexins is dependent on interplay between various kinases and phosphatases, it is often cell- or tissue-type specific and it is further affected by various physiological and pathological conditions. This part of the review aims at summarizing the current knowledge of connexin phosphorylation, while highlighting the contradictions that exist and turning attention to the areas, which need further elucidation.

## PHOSPHORYLATION OF CONNEXIN43

Of the 21 identified members of the connexin family, the 43 kDa subtype, connexin 43 (Cx43) is not only the most widely expressed in mammalian cells, it is also the most intensively studied connexin. Cx43 is translated as a 40 kDa protein, which becomes phosphorylated to a 41 kDa form soon after synthesis (Puranam et al., 1993). The early phosphorylation of Cx43, which results in

**Table 1 | Nomenclature of human and mouse connexin genes and proteins.**

<b>Human Gene name</b>	<b>Human Protein name</b>	<b>Mouse gene name</b>	<b>Mouse protein name</b>
GJE1	hCx23	Gje1	mCx23
GJB7	hCx25	No mouse ortholog	No mouse ortholog
GJB2	hCx26	Gjb2	mCx26
GJC3	hCx30.2	Gjc3	mCx29
GJB6	hCx30	Gjb6	mCx30
GJB4	hCx30.3	Gjb4	mCx30.3
GJB3	hCx31	Gjb3	mCx31
GJB5	hCx31.1	Gjb5	mCx31.1
GJD3	hCx31.9	Gjd3	mCx30.2
GJB1	hCx32	Gjb1	mCx32
No human ortholog	No human ortholog	Gja6	mCx33
GJD2	hCx36	Gjd2	mCx36
GJA4	hCx37	Gja4	mCx37
GJA5	hCx40	Gja5	mCx40
GJD4	hCx40.1	Gjd4	mCx39
GJA1	hCx43	Gja1	mCx43
GJC1	hCx45	Gjc1	mCx45
GJA3	hCx46	Gja3	mCx46
GJC2	hCx47	Gjc2	mCx47
GJA8	hCx50	Gja8	mCx50
GJA9*	hCx59	No mouse ortholog	No mouse ortholog
GJA10	hCx62	Gja10	mCx57

\*Previously named GJA10

the 41 kDa form, occurs in the ER or *cis-medial* Golgi (Puranam et al., 1993). A more extensive phosphorylation, however, takes place later in the secretory pathway or following formation of gap junction channels at the plasma membrane. Today, 21 phosphorylation sites are described for Cx43 and a substantial amount of experimental work have demonstrated that all stages of the Cx43 “life cycle” are modified by post-translational phosphorylation of Cx43. In addition, pathophysiological conditions, such as ischemia (Beardslee et al., 2000; Axelsen et al., 2006), hemodynamic volume overload (Rucker-Martin et al., 2006; Qu et al., 2009) and diabetes (Lin et al., 2006; Howarth et al., 2008), may affect Cx43 phosphorylation and thereby gap junction coupling between Cx43 expressing cells.

#### SITE SPECIFIC CX43 PHOSPHORYLATION AND THE RESPONSIBLE PROTEIN KINASES

**Figure 2** illustrates all the specific phosphorylation sites identified in Cx43, as well as the specific kinases that facilitate their phosphorylation. In addition to the sites and kinases shown in

**Figure 2**, bioinformatics has identified additional phosphorylation consensus sites in Cx43 and heat map analysis reveal that the majority of the phosphorylation sites may be recognized by multiple kinases (reviewed by Chen et al., 2013). In the following, we will focus on the specific phospho-sites and kinases shown in **Figure 2**, since they are all verified by biological experiments.

#### **Ser244 AND Ser314**

Ser244 and Ser314 were recently identified as potential phosphorylation sites in Cx43. Using high-resolution mass spectrometry and a peptide containing the full length of the C-terminal tail of Cx43, Huang et al. (2010) showed that Ser244 and Ser314, along with 13 other serine sites (see **Table 2**), are targets for *in vitro* phosphorylation by  $\text{Ca}^{2+}$ /calmodulin-dependent kinase II (CaMKII). CaMKII is involved in a variety of cellular processes, such as  $\text{Ca}^{2+}$  homeostasis, transcription and apoptosis (reviewed by Braun and Schulman, 1995), however, the specific role of CaMKII in the regulation of Cx43, and whether phosphorylation of Ser244 and Ser314 plays a role *in vivo* remains to be investigated.

#### **Tyr247 AND Tyr265**

Tyr247 and Tyr265 are the only 2 out of the 21 described phosphorylation sites in Cx43, which are tyrosine sites, and both sites are targets of the oncoprotein and tyrosine Src kinase. Activation of c-Src causes direct phosphorylation of Tyr265, which leads to reduced electrical conductance in the absence of changes in the amount of Cx43 gap junction channels (Postma et al., 1998; Geppmans et al., 2001). In addition, v-Src (the constitutively active Src kinase isoform) is reported to co-localize with Cx43 present in the plasma membrane (Loo et al., 1999), an interaction, which depends on the Src-homology-2 (SH2) and SH3 domains in v-Src, as well as the Pro274-Pro284 region and phosphorylation of Tyr265 in the cytoplasmic tail of Cx43 (Kanemitsu et al., 1997). A study on Cx43 mutants has implied that phosphorylation of Tyr265 alone is not sufficient for complete gap junction closure. Instead, phosphorylation of both Tyr265 and Tyr247 are required to disrupt metabolic coupling through Cx43 gap junction channels (Lin et al., 2001). Together, these results support a model for v-Src induced Cx43 tyrosine phosphorylation, where interaction is initiated by binding of the v-Src SH3 domain to the Pro274-Pro284 region of Cx43. This interaction facilitates the phosphorylation of Tyr265, which then acts as a binding site for the SH2 domain. Binding of the v-Src SH2 domain to P-Tyr265 then strengthens the interaction between Cx43 and v-Src and facilitates the subsequent phosphorylation of Tyr247 and closure of the Cx43 gap junction channel (Lin et al., 2001). This mechanism for direct Src induced gap junction closure seems reasonable and experimentally supported. Nevertheless, a study by Zhou et al. (1999) showed that substitution of Tyr265 and/or Tyr247 with phenylalanine (which mimics a constitutive dephosphorylated tyrosine) did not interfere with the ability of v-Src to cause electrical uncoupling of gap junction channels. Instead, their study implied that phosphorylation of the mitogen-activated protein kinase (MAP kinase) sites Ser255, Ser279, and Ser282 (which are further described below) is essential for v-Src induced regulation of electrical coupling. In addition, a recent study found that Akt activation is crucial to disrupt dye transfer in v-Src transformed cells, but

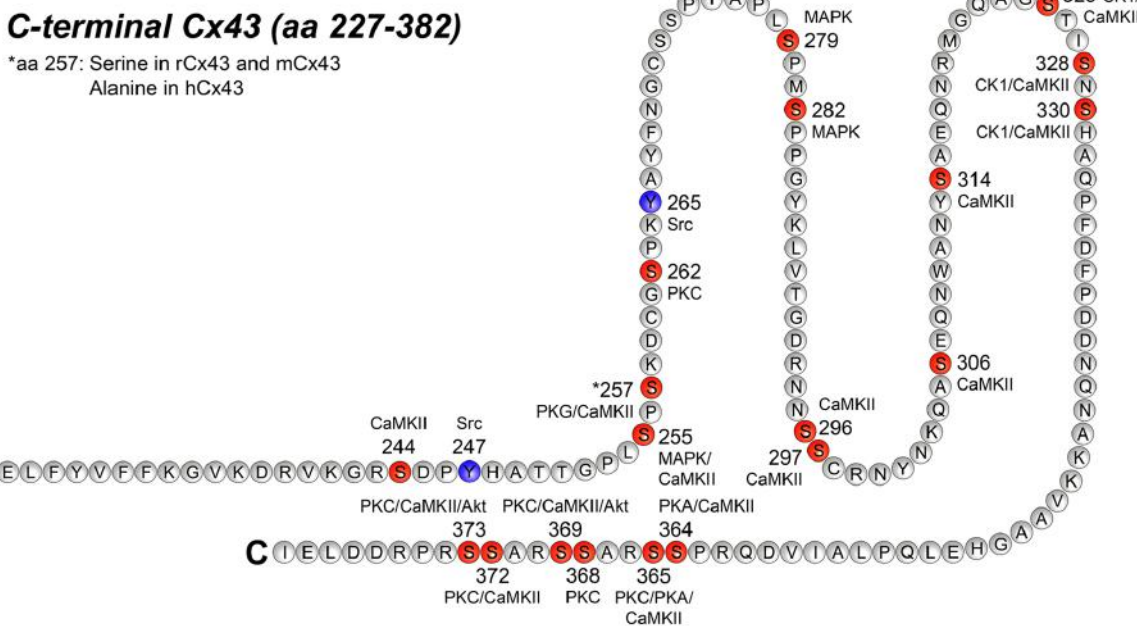


**FIGURE 2 | Phosphorylation sites in the C-terminal tail of Cx43.** This figure represents the C-terminal tail of Connexin43 (Cx43; amino acid, aa 227–382) including its phosphorylation sites and its respective kinases. Serine (S) phosphorylation sites are presented in red and tyrosine (Y)

phosphorylation sites are presented in purple. CaMKII, Ca<sup>2+</sup>/calmodulin-dependent kinase II; PKG, protein kinase G; PKC, protein kinase C, MAPK, mitogen-activated protein kinase; CK1, casein kinase 1; PKA, protein kinase A. For references see text and **Table 2**.

inhibition of Akt only recovered the metabolic coupling to 60% (Ito et al., 2010). Since Akt may cause phosphorylation of Ser369 and Ser373 in Cx43 (Park et al., 2007; for details see section on Ser364, Ser365, Ser368, Ser369, Ser372, and Ser373), this indicates that Src kinases controls several intracellular signaling pathways, and thereby affects the phosphorylation of both serine and tyrosine residues in the C-terminal tail of Cx43 with different effects on electrical and metabolic coupling. Together, these studies outlines that the control of gap junction coupling by Src kinases is extremely complex; It depends of a combination of direct phosphorylation of both Tyr247 and Tyr265, as well as interplay with several intracellular signaling pathways controlling Cx43 serine phosphorylation.

In addition to the control of gap junction channels, Src may also regulate gap junction localization. Binding of Src to Cx43 and phosphorylation of Tyr265 inhibits the endogenous interaction between Cx43 and the cytoskeleton protein zonula occludens 1 (ZO-1) in cardiomyocytes (Toyofuku et al., 2001). ZO-1 is important for the localization of Cx43 channels at the intercalated discs of the heart, and therefore, an interruption of the Cx43-ZO-1 interaction may reduce the amount of Cx43 present at the cell surface. This is further supported by Duffy et al. (2004) who found that intracellular acidification in astrocytes causes Cx43 internalization accompanied by decreased binding of ZO-1 and increased binding of Src to Cx43.

Based on the complex nature of Src kinase regulation of Cx43 gap junction channels, it is not surprising that Src induced alterations in gap junction coupling is found in several pathological conditions. Since gap junction communication is essential for

controlled cell growth and cell differentiation, Src kinase induced Cx43 phosphorylation seems to play an essential role in tumorigenesis (reviewed by Pahuja et al., 2007). Furthermore, tyrosine phosphorylation of Cx43 is suggested to play a role in cardiac arrhythmias caused by either increased activation of the renin-angiotensin-aldosterone system or metabolic inhibition. More specifically, it was shown that treatment with a c-Src inhibitor interrupts Angiotensin II mediated loss of Cx43 gap junction channels and reduces the risk of ventricular tachycardia in mice with over expression of angiotensin-converting-enzyme (ACE; Sovari et al., 2011). Furthermore, metabolic inhibition of cultured neonatal cardiomyocytes also induces tyrosine phosphorylation of Cx43 and increased association between c-Src and Cx43 (Chung et al., 2007, 2009), which indicates a role for tyrosine phosphorylation in gap junction uncoupling and/or remodeling during myocardial ischemia.

Ser255, Ser279, AND Ser282

As indicated above, Ser255, Ser279, and Ser282 are all targets for MAP kinase phosphorylation (Warn-Cramer et al., 1996; Cameron et al., 2003). In HeLa cells, Cx43 phosphorylated at Ser255, Ser279, and Ser282 is transported correctly to gap junctional plaques, but phosphorylation of Ser279 and/or Ser282 impairs channel function and decreases both electrical and metabolic coupling (Warn-Cramer et al., 1998). In addition, a recent study demonstrates that Ser279 and Ser282 are involved in the regulation of gap junction plaque size in human pancreatic cancer cells; Johnson et al. (2013) found that phosphorylation of Ser279 and Ser282 disrupts gap junction plaque growth by

**Table 2 | Connexin 43 post translational modification (PTM) sites including kinases responsible for phosphorylation (P).**

Residue	PTM (Kinase(s))	Reference
K114	SUMOylation	Kjenseth et al. (2012)
K234	SUMOylation	Kjenseth et al. (2012)
S244	P (CaMKII)	Huang et al. (2010)
Y247	P (Src)	Lin et al. (2001), Solan and Lampe (2007)
S255	P (MAPK/CaMKII)	Warn-Cramer et al. (1996), Cameron et al. (2003), Huang et al. (2010)
S257*	P (PKG/CaMKII)	Kwak et al. (1995a), Kwak and Jongsma (1996), Huang et al. (2010)
S262	P (PKC $\epsilon$ )	Doble et al. (2004), Axelsen et al. (2006), Srisakuldee et al. (2009)
Y265	P (Src)	Giepmans et al. (2001), Lin et al. (2001), Toyofuku et al. (2001), Solan and Lampe (2007)
C271	Nitrosylation	Straub et al. (2011)
S279	P (MAPK)	Warn-Cramer et al. (1996)
S282	P (MAPK)	Warn-Cramer et al. (1996)
S296	P (CaMKII)	Axelsen et al. (2006), Huang et al. (2010)
S297	P (CaMKII)	Axelsen et al. (2006), Huang et al. (2010)
S306	P (CaMKII)	Axelsen et al. (2006), Huang et al. (2010)
S314	P (CaMKII)	Huang et al. (2010)
S325	P (CK1/CaMKII)	Cooper and Lampe (2002), Huang et al. (2010)
S328	P (CK1/CaMKII)	Cooper and Lampe (2002), Huang et al. (2010)
S330	P (CK1/CaMKII)	Cooper and Lampe (2002), Huang et al. (2010)
S364	P (PKA/CaMKII)	TenBroek et al. (2001), Shah et al. (2002), Huang et al. (2010)
S365	P (PKC/PKA/CaMKII)	Shah et al. (2002), Huang et al. (2010)
S368	P (PKC)	Saez et al. (1997), Lampe et al. (2000), Shah et al. (2002), Bao et al. (2004), Axelsen et al. (2006), Ek-Vitorin et al. (2006)
S369	P (PKC/Akt/CaMKII)	Shah et al. (2002), Park et al. (2007), Huang et al. (2010)
S372	P (PKC/CaMKII)	Saez et al. (1997), Shah et al. (2002), Huang et al. (2010)
S372	P (PKC/Akt/CaMKII)	Shah et al. (2002), Park et al. (2007), Huang et al. (2010)

\*Amino acid residue 257 of rat Cx43 is a serine. In human Cx43, residue 257 is an alanine.

CaMKII,  $Ca^{2+}$ /calmodulin-dependent kinase II; MAPK, mitogen-activated protein kinase; PKG, protein kinase G; PKC, protein kinase C; CK1, casein kinase 1; PKA, protein kinase A. Akt is also known as protein kinase B.

triggering clathrin-mediated endocytosis of Cx43. Based upon these results, it seems that MAP kinase controlled phosphorylation of Ser255 and especially Ser279 and Ser282 regulate both electric and metabolic coupling of gap junction channels, as well as gap junction plaque size by controlling the rate of Cx43 endocytosis. However, the effects of MAP kinase induced Cx43 phosphorylation maybe cell type specific and further studies are needed to determine the specific effects *in vivo*.

### Ser257

Amino acid residue 257 of Cx43 is a serine in rats, whereas it is an alanine in the human genome. Since alanine mimics a constitutive dephosphorylated form of a serine, it could be assumed that Ser257 is not a target for phosphorylation in the rat. Nevertheless, Kwak et al. (1995a) found that activation of PKG by 8-bromoguanosine 3':5'-cyclicmonophosphate (8Br-cGMP) increase the incorporation of P<sup>32</sup> into rat Cx43 but not human Cx43 expressed in SKHep1 cells. Furthermore, phosphorylation of Cx43 by protein

kinase G (PKG) was associated with a decreased macroscopic and single channel conductance in SKHep1 cells (Kwak et al., 1995a). Kwak and Jongsma (1996) also showed that PKG causes decreased macroscopic – and single channel conductance in cardiomyocytes from rats. These data shows that electrical coupling is regulated by PKG induced phosphorylation of Ser257 in the rat, whereas PKG is not involved in the regulation of Cx43 in humans.

### Ser262

Fibroblast growth factor 2 (FGF2) induced stimulation of protein kinase C (PKC; subtype  $\epsilon$ ) in cultured cardiomyocytes induces Ser262 phosphorylation along with increased cardiomyocyte proliferation (Doble et al., 2004). The same study also found that Cx43 overexpression is associated with decreased DNA synthesis and thereby decreased cell proliferation. In addition, the effect of Cx43 overexpression was inhibited when Ser262 was exchanged with aspartate that mimics a constitutive phosphorylation. These

findings support a central role for Ser262 phosphorylation in Cx43 mediated control of cell proliferation.

Ser262 phosphorylation may also play a role in cardio protection against ischemic injuries and arrhythmias. Both FGF2 and ischemic preconditioning causes increased phosphorylation of Ser262, as well as protection against ischemic injury in isolated rat hearts (Srisakuldee et al., 2009). Furthermore, expression of a Cx43 mutant, where Ser262 is exchanged with alanine, exacerbate injury and death of cardiomyocytes following simulated ischemia *in vitro* (Srisakuldee et al., 2009). In addition, it was recently shown that Ser262 phosphorylation is essential for Cx43 interaction with the ATP sensitive K<sup>+</sup> channel Kir6.1 in NIH3T3 cells (Waza et al., 2012). Together these data supports a role for Ser262 phosphorylation in ischemic cardio protection, potentially mediated through the interaction with Kir6.1. Nevertheless, further studies are needed to determine exactly what the physiological consequences of the Cx43-Kir6.1 interaction are.

#### **Ser296, Ser297, AND Ser306**

That Ser296, Ser297 and Ser306 of Cx43 are subjects for phosphorylation was first identified by a mass spectrometry analysis of Cx43 purified from rat hearts (Axelsen et al., 2006). This study further showed that Ser306 is dephosphorylated within 7 min of cardiac ischemia, while Ser297 (together with Ser368, which will be discussed later in this chapter) is dephosphorylated between 15 and 30 min of ischemia, where gap junction electrical uncoupling is also known to occur (Smith et al., 1995; Beardslee et al., 2000). Furthermore, the study showed that the anti-arrhythmic peptide analog rotigaptide (which is known to prevent and convert conduction slowing during metabolic stress, Haugan et al., 2005a,b) preserves Ser297 and Ser368 phosphorylation during ischemia. The preserved phosphorylation of Ser297 and Ser368 was further correlated to a delayed onset of ischemia induced arrhythmias (Axelsen et al., 2006). In other words, these findings indicate that dephosphorylation of Ser297 and/or Ser368 is responsible for gap junction uncoupling during cardiac ischemia. Another study evaluated the effect of serine to alanine substitutions of Ser306, Ser296, and Ser297 in Cx43 transfected into HeLa cells (Procida et al., 2009). Here it was found that an alanine substitution of Ser296 and Ser297 has no significant effects on either macroscopic electrical coupling or single channel conductance. In contrast, substitution of Ser306 to alanine resulted in a 57% reduction in electrical coupling, possibly mediated by a reduction of single channel conductance. Based on these findings, it seems reasonable to conclude that several phospho-sites, including Ser297 and Ser306 are involved in the regulation of electrical coupling through Cx43 channels during ischemia or metabolic stress.

The kinase(s) responsible for phosphorylation of Ser296, Ser297, and Ser306 is still a matter of debate; While Axelsen et al. (2006) were not able to detect CaMKII induced P<sup>32</sup> incorporation into a synthetic peptide containing Ser296, Ser297, and Ser306, the previously discussed mass spectrometry based study by Huang et al. (2010) did detect CaMKII induced phosphorylation on all of these specific sites. Further studies are needed to clarify these contradictory findings.

#### **Ser325, Ser328, AND Ser330**

That Cx43 phosphorylation is involved in the regulation of trafficking, assembly and dis-assembly, as well as the localization of Cx43 gap junction channels was first suggested by Musil and Goodenough (Musil et al., 1990; Musil and Goodenough, 1991). Since then, Cooper and Lampe (2002) have shown that casein kinase 1 (CK1) induced phosphorylation of Ser325, Ser328, and Ser330 in Cx43 is a key regulatory mechanism for the formation of gap junctions channels. Furthermore, it is indicated that these specific serine phosphorylation sites are only phosphorylated when Cx43 is located in gap junction plaques (Solan and Lampe, 2007). In further support of the importance of phosphorylation of these specific sites, substitution of Ser325, Ser328, and Ser330 to alanine (which mimics a constitutively dephosphorylated serine residue) causes decreased dye coupling, as well as delayed development of electrical coupling in mouse fibroblasts (Lampe et al., 2006).

In isolated Langendorff perfused rat hearts, Ser330 becomes phosphorylated within 7 min of global no-flow ischemia, whereas it returns to the dephosphorylated state between 30 and 45 min of ischemia (Axelsen et al., 2006). In addition, ischemia induced dislocation of Cx43 from the intercalated disks to the lateral edges of cardiomyocytes (a process known as lateralization) correlates with dephosphorylation of Ser325, Ser328, and/or Ser330 (Lampe et al., 2006).

Chronic hemodynamic overload also causes dephosphorylation and delocalization of atrial Cx43 in both rats and humans, which may be related to the development of atrial fibrillation (Rucker-Martin et al., 2006). Furthermore, in mice, such hemodynamic overload induced by aortic constriction causes a time-dependent reduction in Ser325, Ser328, Ser330 phosphorylation along with progressive loss of junctional Cx43, conduction velocity slowing and increased arrhythmogenicity (Qu et al., 2009). To further explore the physiological significance of Ser325, Ser328, and Ser330 phosphorylation, Remo et al. (2011) conducted an elegant study in mutant knock-in mice where Ser325, Ser328, and Ser330 were replaced by either phosphomimetic glutamic acids or non-phosphomimetic alanines. The introduction of glutamic acid as a pseudophosphorylation resulted in gap junctions that were resistant to gap junction remodeling associated with both acute ischemia and chronic hemodynamic overload. In contrast, the phosphorylation deficient mice where Ser325, Ser328, and Ser330 were replaced by alanines, displayed aberrant gap junction expression even at baseline and increased arrhythmic susceptibility (Remo et al., 2011). Collectively, these studies verify that the phosphorylation state of Ser325, Ser328, and/or Ser330 plays an important role in both physiological and pathological regulation of Cx43 gap junction localization and function.

#### **Ser364, Ser365, Ser368, Ser369, Ser372, AND Ser373**

Ser364 is phosphorylated by protein kinase A (PKA; TenBroek et al., 2001; Shah et al., 2002), while Ser365 may be phosphorylated by both PKA and PKC (Shah et al., 2002). PKC is also known to phosphorylate Ser368, Ser369, Ser372, and Ser373 (Saez et al., 1997; Lampe and Lau, 2000; Shah et al., 2002; Bao et al., 2004). Even though Cx43 is a relatively poor substrate for PKA compared

to PKC, it was shown that initial PKA activation accelerates subsequent PKC phosphorylation (Shah et al., 2002). The link between PKA and PKC phosphorylation is further supported by the finding that FSH-induced Cx43 phosphorylation, which is mediated by PKC, is depressed by the use of the selective PKA inhibitor H89 (Yogo et al., 2006).

Besides being a potential target for both PKA and PKC, Ser365 is proposed to be a “gatekeeper,” which controls the ability of other serine residues in Cx43 to become phosphorylated. More specifically, it was reported that phosphorylation of Ser365 causes a conformational change in the c-terminal region of Cx43, which prevents PKC induced phosphorylation of Ser368 (Solan et al., 2007). These data underline the complexity of Cx43 phosphorylation and demonstrate that the phosphorylation state of one site may influence the ability of other sites to become phosphorylated.

Along with the ability of PKC to phosphorylate Cx43 at several serine residues, activation of PKC by 12-O-tetradecanoyl-phorbol 13-acetate (TPA), is also known to increase cardiac macroscopic conductance along with reduced single-channel conductance (Kwak et al., 1995b; Lampe et al., 2000). This PKC effect on gap junction conductance is, however, prevented when Ser368 is exchanged with an alanine (Lampe et al., 2000). These findings suggest that PKC induced Cx43 phosphorylation, and especially phosphorylation of Ser368, affects electrical coupling and the open probability of gap junction channels.

The role of Ser368 phosphorylation during myocardial ischemia and its connection to electrical conductance is, however, subject of contradicting findings. As earlier mentioned, Axelsen et al. (2006) found that Ser368 becomes dephosphorylated during no-flow ischemia in isolated rat hearts, at a time course similar to that of electric uncoupling (Smith et al., 1995; Beardslee et al., 2000). In addition, rotigaptide, which prevents and reverse conduction slowing during metabolic stress (Haugan et al., 2005a,b) and suppresses the development of cardiac arrhythmias (Xing et al., 2005; Axelsen et al., 2006), preserved phosphorylation of Ser368 during ischemia (Axelsen et al., 2006). Based on this study, it is tempting to conclude that preservation of Ser368 phosphorylation contributes to an improved electrical coupling during cardiac ischemia. The findings by Axelsen et al. (2006) are, however, in contrast to findings by Ek-Vitorin et al. (2006). They reported that phosphorylation of Ser368 causes a reduction in gap junction conductance and that 30 min of no-flow ischemia in excised mice hearts results in increased levels of Ser368 phosphorylation, despite an overall Cx43 dephosphorylation when examined by western blotting. Currently, there are no clear explanations for these contradicting findings and further research is needed to clarify the role of Ser368 phosphorylation during pathological conditions.

In addition to the regulatory role of Ser368 with respect to electrical coupling, the Cx43 PKC phosphorylation sites are also involved in the regulation of metabolic coupling. In HeLa cells, it was found that alanine substitutions of Ser365, Ser368, Ser369, and Ser373 all at once, cause a marked drop in gap junction dye transfer (Yogo et al., 2002). This effect on metabolic coupling was, however, blunted if the alanine substitution was restricted to Ser368. These findings suggest that while dephosphorylation of Ser368 alone seems sufficient to alter the electrical coupling, the

metabolic coupling appears to depend on several of the specific PKC sites. In contrast to the findings in HeLa cells, where reduced metabolic coupling is related to Cx43 dephosphorylation, PKC mediated increases in Cx43 phosphorylation reduces metabolic coupling in both fibroblasts (Lampe et al., 2000) and neonatal cardiomyocytes (Kwak et al., 1995b). The reason for these contradicting findings on the connection between metabolic coupling and the phosphorylation state of Cx43 is currently unknown. It could, however, simply be a matter of the different cell-systems used and further studies are needed in order to determine the effect *in vivo*.

As described above, phosphorylation of Ser369 and Ser373 can be mediated by PKC. Both these sites are, however, also subject to phosphorylation by Akt kinase (also known as protein kinase B) (Park et al., 2007). Akt induced phosphorylation of Ser369 and Ser373 facilitates an interaction between Cx43 and 14-3-3, which plays a role in trafficking of Cx43 multimers and/or their incorporation into gap junction plaques (Park et al., 2007).

Finally, the previously discussed mass spectrometry study by Huang et al. (2010) also identified Ser364, Ser365, Ser369, Ser372, and Ser373 as CaMKII targets *in vitro*. However, it is still unknown whether CaMKII phosphorylates Cx43 *in vivo* and the potential physiological role of CaMKII induced Cx43 phosphorylation remains to be established.

## THE ROLE OF PROTEIN PHOSPHATASES

Most experimental studies have focused on the protein kinases, which are responsible for Cx43 phosphorylation. Nevertheless, regulation of Cx43 phosphorylation is not only dependent on the kinases, but also on the equilibrium between protein phosphatase and kinase activity. Even so, experimental data regarding the phosphatases that dephosphorylate Cx43 remain limited.

Under normal physiological conditions, both protein phosphatase 1 (PP1) and protein phosphatase 2A (PP2A) co-localize with Cx43 in rabbit hearts (Ai and Pogwizd, 2005), indicating a physiological role for these enzymes in the regulation of Cx43. The role of these endogenous protein phosphatases on Cx43 gap junction uncoupling during ischemia or ATP-depletion have further been evaluated in neonatal rat cardiomyocytes, adult rat cardiomyocytes, as well as isolated rat hearts; in neonatal cardiomyocytes, selective PP1 inhibitors postpone electrical uncoupling of gap junctions during ATP-depletion (Duthe et al., 2001). At the same time, addition of a specific PP1 stimulator facilitated a gradual decrease in electrical coupling, even in the presence of ATP (Duthe et al., 2001). Likewise, PP1 inhibitors decreased Cx43 dephosphorylation during ischemia in both isolated perfused rat hearts and adult cardiomyocytes (Jeyaraman et al., 2003). This study also found that treatment with the selective PP2A inhibitor fostriecin did not prevent Cx43 dephosphorylation during ischemic conditions. This indicates that PP1 is the key player in Cx43 dephosphorylation during ischemia in the rat.

Both PP1 and PP2A are also expressed in mini pig hearts, but in contrast to what was found in rabbit hearts, only PP2A co-localizes with Cx43 in the mini pig (Totzeck et al., 2008). Furthermore, when isolated mini pig hearts were exposed to 90 min of low flow ischemia, it resulted in Cx43 dephosphorylation along with an increase in total PP2A levels. The amount of Cx43-PP2A

co-precipitation was, however, not affected during ischemia and ischemic pre-conditioning preserved Cx43 phosphorylation, without any effect on either PP2A levels or activity (Totzeck et al., 2008). In contrast to the findings during cardiac ischemia, another study have reported a >2.5-fold increase in the amount of PP2A, which co-localizes with Cx43 in a rabbit model of non-ischemic heart failure (Ai and Pogwizd, 2005). The increase in PP2A-Cx43 co-localization was further associated with increased levels of dephosphorylated Cx43 and decreased metabolic coupling, which was prevented in the presence of okadaic acid in a concentration, which should only inhibit PP2A. The same study also examined the amount of co-localized Cx43 and PP1, before and after long-term aortic constriction, but here they found no changes (Ai and Pogwizd, 2005). Together, these studies show that both PP1 and PP2A may affect Cx43 phosphorylation *in vivo*. Based on the available data, it seems that PP1 is the main player during acute dephosphorylation of Cx43, as seen during cardiac ischemia, whereas PP2A may become the dominant player during long-term pathological alterations such as non-ischemic heart failure. The different results may, however, also be species dependent and further studies are needed before the final conclusion can be drawn.

#### A PERSPECTIVE ON CONNEXIN43 PHOSPHORYLATION

As outlined above, phosphorylation of Cx43 has been a subject for intense investigation for more than three decades. These investigations have clarified that the regulation of Cx43 gap junction channels by phosphorylation is an extremely complex matter, which includes at least 21 different phosphorylation sites and a growing list of more than 10 different kinases and phosphatases. In addition, it is now clear that the different phosphorylation sites may interact and depend upon each other and site specific changes in phosphorylation may exert different effects on electric and metabolic coupling. Furthermore, it seems that the effects of altered Cx43 phosphorylation may be both species and cell type dependent. All of these considerations should be taken into account when planning future studies on Cx43 phosphorylation, as well as during the interpretation of such studies.

#### PHOSPHORYLATION OF CONNEXIN26

For many years, it was generally thought that Cx26 was not a phospho-protein, because of its fairly short C-terminal tail, consisting of only 11 amino acids. A mass spectrometry study, however, showed that Cx26 is phosphorylated in the intracellular N-terminal tail at either position Asp2, Thr5, or Ser8 when expressed in HeLa cells (Locke et al., 2006). Importantly, the same phosphorylation was not detected in Cx26 from liver tissue, where the same amino residues were found to be hydroxylated instead (Locke et al., 2006). In a later study, Harris and Locke (2009) also found indications for potential phosphorylation sites in the cytoplasmic loop (Thr123) and the extracellular loop (E2; Thr177, Ser183 and Thr186) of Cx26 (Locke et al., 2009). Nevertheless, the physiological role of Cx26 phosphorylation remains unknown.

#### PHOSPHORYLATION OF CONNEXIN32

As for Cx26, Cx32 also contains phosphorylation sites in the N-terminal domain, more specifically Thr4, Tyr7, Thr8, or Ser11, which was identified as phosphorylated in Cx32 from both HeLa

cells and mouse liver (Locke et al., 2006). In addition, Cx32 from HeLa cells was phosphorylated in the C-terminal tail at position His237, Ser233, and/or Ser240 (Locke et al., 2006). In support of the findings by mass spectrometry, work on isolated hepatocytes have shown that both PKA and PKC may phosphorylate Ser233, whereas CaMKII may phosphorylate other serine and threonine sites in Cx32, but not Ser233 (Saez et al., 1990). Cx32 is also identified as a target for epidermal growth factor (EGF)-receptor tyrosine kinase (Díez et al., 1998). The specific tyrosine residue(s), which is/are targeted by EGF-receptor tyrosine kinase, was not revealed, but the study showed that binding of calmodulin to Cx32 prevented EGF-receptor tyrosine kinase induced phosphorylation. Based on this finding, it is likely that the target for EGF-receptor tyrosine kinase phosphorylation is located in one of the calmodulin binding sites in Cx32, which is amino acid no. 1–27 in the N-terminal tail and amino acid no. 216–230 located in the C-terminal tail (Török et al., 1997).

Further experimental studies are needed in order to reveal to physiological role of Cx32 phosphorylation in biological systems.

#### PHOSPHORYLATION OF CONNEXIN40

Cx40 is also regulated by post-translational phosphorylation (Traub et al., 1994; van Rijen et al., 2000), but the specific sites are yet to be studied in detail. So far, it is known that both PKA and PKC are able to incorporate P<sup>32</sup> into Cx40 in transfected human cells and that 8-Br-cAMP induced PKA activation causes an electrophoretic mobility shift of Cx40. Furthermore, van Rijen et al. (2000) showed that Cx40 gap junction channels increase both macroscopic conductance and metabolic coupling, when subjected to PKA-induced phosphorylation in SKHep1 cells.

Recently, it was also shown that reduced serine phosphorylation of Cx40 correlates with reduced electrical coupling between microvascular endothelial cells (EC) during sepsis (Bolon et al., 2008). This process was prevented by PKA activation and mimicked in control cells by PKA inhibition, which indicates that the involved phosphorylation site(s) is/are a target for PKA.

Since Cx40 is the predominant connxin found in the atria, it can be hypothesized that dephosphorylation of Cx40 and decreased electrical coupling in the atria may play a role in the patogenesis of atrial fibrillation. This, however, remains an interesting question for future research.

#### PHOSPHORYLATION OF CONNEXIN45

Cx45 is expressed in many different tissues and the only member of the connxin family, whose absence is lethal in the embryonic state (Kruger et al., 2000; Kumai et al., 2000). Even so, the post-translational regulation of Cx45 has been less extensively studied compared to other connexins. Serine phosphorylation of Cx45 is found in both mouse kidney (Butterweck et al., 1994), cultured neonatal rat ventricular myocytes (Darrow et al., 1995), as well as in HeLa transfectants (Hertlein et al., 1998). The latter study found that exchange of the serine residues at position 374, 376, 378, 381, 382, 384, 385, 387, and 393 for other amino acids or deletion of this part of the carboxy-terminal led to an 89% decrease in the phosphorylation signal. This indicates that these nine serine residues are the main sites for Cx45 phosphorylation. They did, however, also find signals for phosphothreonine and phosphotyrosine after

metabolically labeling with  $^{32}\text{P}$ -orthophosphate. Even when all the above mentioned carboxy-terminal serine residues of Cx45 were replaced, it did not interfere with intracellular trafficking or assembly of gap junction channels at the plasma membrane. Furthermore, HeLa cells transfected with the Cx45 mutant showed the same extend of dye transfer as cells transfected with wild type Cx45 (Hertlein et al., 1998). Instead, they found that mutation of the nine serine residues in the cytoplasmic tail caused an increased Cx45 degradation. When all nine serine residues or the double serine residues Ser381 – Ser382 or Ser384 – Ser385 were exchanged, the Cx45 half-life time was reduced with up to 50%.

A recent study based on tandem mass spectrometry showed that CaMKII and CK1 phosphorylates Cx45 *in vitro* (Bao et al., 2011). Specifically, CaMKII was found to phosphorylate serine 326, 381, 382, 384, 385, 387, and 393 along with threonine 337, whereas CK1 phosphorylate serine 326, 382, 384, 387, and 393. Another study, also based on HeLa cells transfected with Cx45, reported that activation of PKA and MAP kinase increases Cx45 phosphorylation when analyzed by western blotting (van Veen et al., 2000). PKA and MAP kinase induced Cx45 phosphorylation was associated with a decreased macroscopic junctional conductance, whereas activation of PKC was found to increase macroscopic conductance of Cx45 channels. However, the effect of PKC occurred in the absence in any apparent changes in Cx45 phosphorylation. Together, all of these studies show that Cx45 contains several phosphorylation sites, which are involved in the regulation of Cx45 degradation and macroscopic conductance, at least in HeLa cells. However, the role of Cx45 phosphorylation *in vivo* during both physiological and pathophysiological conditions remains an open question for future research.

### PHOSPHORYLATION OF Cx46 AND Cx50

Cx46 and Cx50 are known to combine and form heteromeric gap junction channels in ocular lens fibers and both connexins play an important role in lens growth and maintenance of lens transparency. Mass spectrometry analysis of Cx46 and Cx50 isolated from bovine lenses identified a total of 11 and 18 phosphorylation sites, respectively (Wang and Schey, 2009). All of the identified phosphorylation sites in Cx46 are located in the C-terminal tail, whereas three of the identified sites in Cx50 are located in the cytoplasmic loop. The physiological response to altered Cx46 and Cx50 phosphorylation is not yet fully understood. In chicken, however, caspase-3-like protease induced truncation of lens Cx45.6 (the chicken homolog of Cx50) is inhibited by casein kinase II (CKII) induced phosphorylation of Ser363 (Yin et al., 2001). Calpain mediated cleavage of lens Cx46 and Cx50 is proposed to occur naturally during the maturation of lens fibers (Lin et al., 1997; Yin et al., 2001), and the data by Yin et al. (2001) implies that Cx46 and Cx50 cleavage may be regulated by Cx46 and Cx50 phosphorylation.

### UBIQUITINATION

Ubiquitin is a 76 amino acid polypeptide that is found in almost all eukaryotic cells. Structurally, it consists of a globular domain, formed by a  $\beta$ -sheet and an  $\alpha$ -helix, with the N- and C-termini protruding out. It is important for protein trafficking, in particular for labeling proteins for proteasomal

destruction and recycling. Aaron Ciechanover, Avram Hershko, and Irwin Rose were awarded the Nobel Prize in Chemistry in 2004 for the discovery of ubiquitin-mediated protein degradation.

The enzymatic process of ubiquitin binding (ubiquitination or ubiquitylation) to a target protein begins with activation of ubiquitin by an E1 ubiquitin activating enzyme that forms a bond between the carboxyl group of the C-terminal glycine residue (Gly 76) of ubiquitin and an E1 cysteine. This step is followed by transfer of ubiquitin from E1 to a cysteine residue of the ubiquitin-conjugating enzyme E2. Finally, the E2-ubiquitin conjugated enzyme associates with an E3 ubiquitin-protein ligase (as reviewed by Schulman and Harper, 2009; Weissman et al., 2011). The E3 enzymes function as substrate recognition module and facilitates the formation of a bond between a lysine of the target protein and the C-terminal glycine of ubiquitin. In most organisms, there is only one E1, several different E2 and hundreds of E3s. By determining the timing and the substrate of the ubiquitination process, the E3 ubiquitin-protein ligases are the central regulatory determinants of the ubiquitination process. The E3 ubiquitin-protein ligases can be classified into (1) The HECT (homologous to E6-AP carboxy terminal) E3s (Huibregtse et al., 1995), (2) The RING (really interesting new gene) E3s (Lorick et al., 1999) or the closely related U-box E3s.

Homologous to E6-AP carboxy terminal E3 participates directly in ubiquitination by forming a bond with ubiquitin prior to the transfer of ubiquitin to the target protein. HECT E3s contain 3 WW domains, WW1–3. WW domains are short domains containing 38 to 40 amino acid residues, including two conserved tryptophan residues, hence the name WW domain. The domain form a triple-stranded  $\beta$  sheet that binds proteins with particular proline-motifs (PY motifs, XXPPXY, where P is a proline, X is any amino acid and Y is tyrosine) and/or phosphoserine and phosphothreonin containing motifs and thereby mediate target recognition (Nguyen et al., 1998).

An ubiquitin molecule contains a total of seven lysine residues. Following addition of a single ubiquitin to a protein (monoubiquitination), further ubiquitin molecules can be conjugated to lysine residues in the bound ubiquitin, resulting in a polyubiquitin chain. The first identified type of polyubiquitin chains were linked via lysine 48 (Lys48 forming an isopeptide bond to Gly76), however, a wide variety of linkages involving all possible lysine residues (Lys6, 11, 27, 29, 33 and 63) have been demonstrated, reviewed by (Ikeda and Dikic, 2008; Kulathu and Komander, 2012). Further, some substrates contain multiple lysine residues that can be modified by addition of ubiquitin molecules or ubiquitin chains (multiubiquitination).

The various types of ubiquitin modifications have been linked to distinct physiological functions in cells. Multi-monoubiquitination is associated with DNA repair and receptor endocytosis, and lysosomal degradation or recycling to the surface (Dikic et al., 2009) whereas lysine 48-linked polyubiquitin chains label proteins for proteasomal degradation (Hershko and Ciechanover, 1998). Homotypic ubiquitin chains (e.g., chains consisting of only Lys6, 11, 27, or 29 linkages) are also found, and may be involved in different cellular processes such as signaling, trafficking, DNA damage response, cell cycle regulation

or endoplasmic reticulum associated degradation (ERAD) as reviewed by (Komander, 2009).

### UBIQUITINATION OF CONNEXINS

Ubiquitination may be involved in several important steps in the life cycle of connexins (reviewed by Kjenseth et al., 2010 and Su and Lau, 2012). The newly synthesized connexins undergo quality control in the endoplasmic reticulum and polyubiquitination targets misfolded connexin proteins to ERAD and proteasomal degradation (VanSlyke and Musil, 2002). CIP75 (connexin interacting protein 75) facilitates this process (Li et al., 2008). After insertion into gap junction plaques in the membrane, ubiquitination by the E3 ubiquitin ligase Nedd4 is thought to target connexins for endocytosis and lysosomal degradation (Leykauf et al., 2006). The connexins remain ubiquitinated throughout the internalization process that is assisted by EGF receptor pathway substrate 15 (Esp15; Girao et al., 2009). In the early endosomes, the ubiquitin binding proteins Hrs (hepatocyte growth factor-regulated tyrosine kinase substrate) and Tsg101 (tumor susceptibility gene product 101) interacts with ubiquitinated connexins and determines whether the connexins are targeted for recycling or for deubiquitination followed by degradation (Leithe et al., 2009). Connexins targeted for destruction may follow several alternative endocytic pathways, however, there is increasing evidence suggesting that the final destination is lysosomal degradation (Laing et al., 1997; Musil et al., 2000; Girao and Pereira, 2003; Rivedal and Leithe, 2005; Piehl et al., 2007; Falk et al., 2012).

### ERAD AND CIP75

Approximately 40% of newly synthesized Cx43 and Cx32 may undergo ERAD (VanSlyke and Musil, 2002). The level of ERAD is strongly dependent on cellular stress. Oxidative and thermal stress reduce ERAD and more connexins reach the membrane and form functional gap junctions (VanSlyke and Musil, 2002). The mechanism behind cellular stress-induced ERAD is not known (VanSlyke and Musil, 2002). Interestingly, a Cx32 mutation, where Glu 208 is replaced by a lysine from a patient with X-linked peripheral neuropathy Charcot-Marie-Tooth was found to cause nearly a 100% of the newly synthesized Cx32 to undergo ERAD (VanSlyke et al., 2000; Kelly et al., 2007), however, under cellular stress, the polyubiquitination of this Cx32 mutation is reduced. The mutated proteins accumulate in the ER and may contribute to the disease by co-assembling with wild type connexin (VanSlyke et al., 2000; Kelly et al., 2007).

The CIP75 protein is involved in ERAD by translocating the ubiquitinated connexins across the endoplasmatic reticulum membrane as well as bringing the connexins targeted for degradation to the proteasomes during the ERAD process (Li et al., 2008). The Cx43 C-terminal harbors a proline-rich area corresponding to the PY motif (Thomas et al., 2003a), that is important for E3 ubiquitin-ligase target recognition (Nguyen et al., 1998). The interaction between CIP75 and Cx43, takes place between a C-terminal ubiquitin-associated domain of CIP75 and this PY motif, as well as multiple phosphorylation sites located between Lys264 and Asn302 of Cx43 (Li et al., 2008). CIP75 contains domains that interact with the proteasomal complex and

overexpression experiments suggested that CIP75 stimulates proteasomal degradation of Cx43 (Li et al., 2008). CIP75 can bind free mono-ubiquitin and Lys48-linked ubiquitin chains *in vitro* as well as ubiquitinated proteins in cellular lysates (Su et al., 2010). However, it was demonstrated that Cx43 associated with CIP75 is not ubiquitinated, and a mutant form of Cx43 lacking lysine residues and thus incapable of ubiquitination retained the capacity to interact with CIP75. This suggests that although CIP75 can interact with ubiquitinated proteins, its interaction with Cx43 and stimulation of Cx43 proteasomal degradation does not necessarily require ubiquitination (Su et al., 2010).

### UBIQUITINATION AND INTERNALIZATION OF CONNEXINS IN GAP JUNCTIONAL PLAQUES

Laing and Beyer (1995) were the first to describe ubiquitination of Cx43 and ubiquitin-mediated proteasomal degradation. Proteasomal inhibition and inactivation of the E1 ubiquitin activating enzyme resulted in stabilization of Cx43 at the plasma membrane. It was later found that 50% of Cx43 plaques are ubiquitinated, however, ubiquitination is most predominant in older plaques, suggesting that ubiquitination may signal endocytosis of older gap junction from the plasma membrane to the lysosomes for degradation (Laing et al., 1997; Musil et al., 2000; Girao and Pereira, 2003; Rivedal and Leithe, 2005). The role of the proteasomes in endocytosis and degradation of connexins from gap junctional plaques is not clear. Several studies have demonstrated that endocytosis of Cx43 is repressed in the presence of proteasomal inhibitors, suggesting that there may be an intricate interplay between lysosomes and proteasomes as reviewed in (Kjenseth et al., 2010; Falk et al., 2012).

The E3 ubiquitin ligase Nedd4 (neural precursor cell expressed, developmentally downregulated 4) was the first E3 ubiquitin ligase to be shown to interact with connexin (Leykauf et al., 2006). Nedd4 is thought to play an important role in the regulation of connexins in gap junction plaques and ubiquitination by Nedd4 targets connexins for internalization (Leykauf et al., 2006; Girao et al., 2009).

Nedd4 belongs to the HECT family of E3 ubiquitin ligases (Huibregtse et al., 1995) and contains three WW domains. The interaction between Nedd4 and Cx43 takes place between the PY motif of the Cx43 C-terminus (Leykauf et al., 2006; Girao et al., 2009) and the three WW domains of Nedd4 (Leykauf et al., 2006). WW1 and WW2 domains mainly interact with the unphosphorylated form of Cx43, whereas WW3 binds phosphorylated and unphosphorylated forms equally (Leykauf et al., 2006). Only the WW2 domain binds to the PY motif (Leykauf et al., 2006). Other groups have demonstrated interaction of Cx43 with additional E3 ligases, including the other members of the HECT family smad ubiquitination regulatory factor-2 (Smurf2; Fykerud et al., 2012) and WWP1 as well as the RING E3 ligase Tripartite motif-containing protein 2 (TRIM21) as reviewed by Su and Lau (2012).

### EPIDERMAL GROWTH FACTOR MAY STIMULATE UBIQUITINATION OF CONNEXINS IN GAP JUNCTIONAL PLAQUES

Many growth factors, such as EGF and tumor promoters, including TPA inhibits intercellular communication by inducing Cx43

ubiquination followed by endocytosis and degradation (Leithe and Rivedal, 2004a; Leithe et al., 2009; Sirnes et al., 2009). In rat liver epithelial cell lines, application of EGF activates the MAP kinase pathway resulting in Cx43 hyperphosphorylation (Lau et al., 1992; Kanemitsu and Lau, 1993; Leithe and Rivedal, 2004a) on Ser255, 279 and 282 in the C-terminus of Cx43 (Warn-Cramer et al., 1996, 1998). The EGF mediated hyper-phosphorylation of Cx43 was followed by ubiquitination resulting in a rapid transient decrease in intracellular coupling (Leithe and Rivedal, 2004a). However, EGF does not only uncouple gap junctions, they also induce disorganization, endocytosis and degradation of Cx43 plaques (Leithe and Rivedal, 2004a).

Besides stimulating the MAP kinase pathway, EGF activates phospholipase C, resulting in hydrolysis of phosphatidylinositol 4,5-bisphosphate (PIP2) into inositol 1,4,5-trisphosphate (IP3) and diacylglycerol (DAG; van Rheenen et al., 2007). Reduced PIP2 levels inhibit gap junctional coupling in both fibroblasts (van Zeijl et al., 2007) and cardiomyocytes (Hofgaard et al., 2008). Stimulation of cultured cardiomyocytes from neonatal rats with noradrenaline or angiotensin II decrease cell coupling and action potential conduction velocity mediated via a decrease in PIP2 levels (Hofgaard et al., 2008) and in a later study it was demonstrated that noradrenaline induced uncoupling was associated with ubiquitination of Cx43, possibly via Nedd4, and subsequent internalization of Cx43 (Mollerup et al., 2011).

The tumor promoting phorbol ester TPA activates the MAP kinase pathway, as well as PKC (Leithe and Rivedal, 2004a; Sirnes et al., 2009). This in turn induce hyperphosphorylation of Cx43 followed by monoubiquitination at multiple sites (Leithe and Rivedal, 2004b; Leithe et al., 2006). Eps15 is recruited to the membrane to facilitate endocytosis of Cx43 (Girao et al., 2009). Ubiquitination may also be important for the transport from the endosome to the lysosomes, a process facilitated by Hrs and tsg101 (Leithe et al., 2009).

Recently, the role of ubiquitination in regulation of Cx43 gap junction turnover was questioned in a study by Dunn et al. (2012). They demonstrated that a Cx43 construct, where all lysine residues were replaced by arginine residues, behaved similarly to wild-type (Dunn et al., 2012). This is in line with the failure to identify a specific lysine acceptor for ubiquitination on Cx43 and may imply that ubiquitination of Cx43 is not crucial for regulation of Cx43 gap junction turn over. As Cx43 localization is regulated by phosphorylation, the authors hypothesized that another ubiquitinated protein may regulate Cx43 retention or degradation. Since phosphorylation is crucial for localization and activity of Cx43, the effect of inhibitors of the various kinases known to affect Cx43 was tested. These experiments suggests that Akt activity controls gap junction stability through phosphorylation (Dunn et al., 2012). When Akt is activated by phosphorylation it translocates to the plasma membrane, where it phosphorylates membrane proteins, inclusive Cx43 on Ser373 and Ser369 (Park et al., 2007), resulting in stabilization of gap junction plaques (Dunn et al., 2012). Interestingly, Akt is a target for ubiquitination and proteasomal degradation (Yang et al., 2009), which may potentially explain the effect of proteasomal and lysosomal inhibitors on connexin expression.

## SUMOYLATION

Small ubiquitin-like modifier (SUMO) proteins are a small family of proteins that are structurally and functionally related to ubiquitin. In humans, the SUMO protein family consists of 3 members (SUMO1-3). SUMO 2 and 3 show a high degree of similarity (Saitoh and Hinchey, 2000). The structural folding of SUMO proteins is similar to that of ubiquitin, but there is little overlap in the amino acid sequence. The consensus motif for SUMOylation is  $\Psi$ KXD/E where  $\Psi$  is a large hydrophobic residue, K is the acceptor lysine, X is any amino acid followed by an acidic residue (Rodriguez et al., 2001)

Analog to ubiquitination, SUMOylation is controlled by an enzymatic cascade resulting in covalently attachment of SUMO to lysine residues in the target protein (reviewed by Hay, 2005 and Gareau and Lima, 2010). A C-terminal peptide is cleaved from SUMO by sentrin-specific proteases (SENP) to reveal a di-glycine motif. SUMO then becomes bound to an E1 enzyme (or SUMO activating enzyme, SAE). It is then passed to an E2, which is a conjugating enzyme, Ubc9, which is able to directly recognize substrates with a SUMOylation consensus motif (reviewed by Hay, 2005). However, the SUMO moiety can also be transferred to one of a small number of E3 ligating proteins that conjugates SUMO to target proteins. While in ubiquitination an E3 ligating protein is essential for the process, evidence suggests that the E2 is sufficient in SUMOylation, as long as the consensus sequence is present. The SUMO moieties can be removed by SENPs that serve dual functions in the SUMOylation circle (Gareau and Lima, 2010). SUMO2 and SUMO3 contains the SUMOylation consensus motif, which can be utilized to form poly-SUMOylation chains on the target protein (reviewed by Hay, 2005; Gareau and Lima, 2010).

In contrast to ubiquitination, SUMOylation is not used to target proteins for degradation but is rather involved in the regulation of various cellular processes, including transcriptional regulation, protein targeting and stability, response to stress, progression through cell cycle and apoptosis (Geiss-Friedlander and Melchior, 2007).

## CONNEXINS AND SUMOYLATION

Connexins was first described to be regulated by SUMOylation by Kjenseth et al. (2012). In transfected HeLa cells, all three members of the SUMO family increased Cx43 expression and gap junction formation. SUMO2-3 had the strongest effect, resulting in a doubling of Cx43 expression and for Cx43 coexpressed with SUMO3, an increased intracellular communication was demonstrated (Kjenseth et al., 2012).

As previously described, the Cx43 N-terminus contains 3 lysine residues, the intracellular loop 11 and the C-terminus contains 9 residues, but none of these are found in a SUMOylation consensus motif. However, mutational scanning revealed that SUMO1-3 conjugated SUMO groups to Lys144 found in the intracellular loop and Lys237 in the proximal C-terminus of Cx43 (Kjenseth et al., 2012). Lys144 and 237 are evolutionary conserved in Cx43, and interestingly, Lys144 is also conserved in 8 out of 20 human connexins isoforms, including Cx26 and Cx32 (Kjenseth et al., 2012) suggesting that other connexins may also be regulated by SUMOylation. Directly downstream of Lys144 is a large hydrophobic residue and thus this region may function as an inverted

SUMOylation consensus motif as described (Matic et al., 2010). Cx43 proteins, where Lys144 or 237 were replaced by arginine residues, had reduced Cx43 gap junction formation and reduced protein levels (Kjenseth et al., 2012). In addition to lysine 144 and 237, other lysines may be SUMOylated.

For SUMO1 or SUMO2, Cx43 was conjugated to single moieties, whereas for SUMO 3 multiple proteins could be conjugated to Cx43, either as multiple mono-SUMOylation or as poly-SUMOylation (Kjenseth et al., 2012). The majority of the SUMOylated Cx43 was found in the Triton X-100 soluble fraction (Kjenseth et al., 2012), suggesting that Cx43 were not organized in functional gap junctions as gap junction plaques are Triton X-100 insoluble (Musil and Goodenough, 1991; VanSlyke and Musil, 2000). However, gap junctions seem to acquire Triton solubility before internalization (Sirnes et al., 2008) and work in cultured cardiomyocytes show that inhibition of the proteasome and lysosome increase both Triton solubility of Cx43 and intercellular coupling simultaneously, indicating that communicating gap junctions can be part of the soluble fraction (Mollerup et al., 2011).

The molecular mechanism behind the SUMOylation mediated increase in Cx43 protein level is not presently known. It is also unknown, in which subcellular compartment SUMOylation takes place and further studies are needed to determine whether SUMOylation affects intracellular Cx43 trafficking (Kjenseth et al., 2012).

## NITROSYLATION

Recent evidence suggests that S-nitrosylation of cysteine residues may be an important post-translational modification of connexins (Retamal et al., 2006, 2009; Straub et al., 2011). S-nitrosylation is the reversible, covalent addition of NO to the thiol side chain of cysteine and nitrosylation appears to be the major mechanism through which NO exerts its effects on cellular function (Hess et al., 2005; Anand and Stamler, 2012; Hess and Stamler, 2012). The degree of nitrosylation is subject to dynamic regulation through the concerted activity of multiple nitrosylases and denitrosylases, i.e., enzymes that adds or removes NO groups to/from proteins (Hess and Stamler, 2012). Although many proteins contain multiple cysteins, and therefore have many potential sites for nitrosylation, it appears as if only a few of the potential sites are actually subject to nitrosylation, and consequently, that the effects on protein function results from the modification of only one or a few –SH groups in a given protein (Hess and Stamler, 2012). Nitrosylation may directly influence protein function, but interestingly may also have an indirect effect through modification of other post-translational modifications, e.g., phosphorylation, acetylation or ubiquitination (Hess and Stamler, 2012).

## NITROSYLATION OF CONNEXINS

NO has been shown to affect both gap junctions and hemichannels, but only a few studies provides direct evidence showing that the effect is correlated to changes in nitrosylation of the connexins. In the vascular wall the myoendothelial junctions (MEJs) plays an important role in coordinating the activity of EC and vascular smooth muscle cells (VSMC; Sandow et al., 2012). The MEJs form where cellular extensions from the VSMC meet the EC, and heterotypic junctions are formed at the site of contact between

the plasma membranes from the two cell types. In the VSMC, the major connexins present are Cx43 and Cx45, whereas Cx37 and Cx40 are found in the EC (Sandow et al., 2012). Interestingly, the MEJ also appears to have a high content of eNOS coexpressed with the gap junction plaques. Cx43 was found to be constitutively nitrosylated in the MEJ, and denitrosylation induced by addition of phenylephrine resulted in a reduced movement of inositol triphosphate from the VSMC to the EC via the MEJ gap junctions, and this decreased gap junction permeability was associated with an decreased nitrosylation of Cx43 at the Cys271 residue in the intracellular C-terminal part of the protein (Straub et al., 2011). Other data also support the notion that nitrosylation may play role in modifying gap junctions in the vasculature. Two independent studies show that NO donors decrease the permeability between ECs toward small molecules and reduce the electrical coupling of gap junctions composed of Cx37 (Kameritsch et al., 2005; McKinnon et al., 2009). In both cases the effect was independent of the action of NO on cGMP, but none of the studies provided any direct evidence of changes in nitrosylation of the involved proteins. Taken together the studies suggest that nitrosylation of connexins may play an important role in regulation of the intercellular communication in the microcirculation. Intercellular communication is a prerequisite for conducted vasomotor responses, and several conditions like hyperglycemia, hypertension and sepsis is associated with changes in both vascular conduction and NO production, however there is at present no information linking these changes to changes in nitrosylation of the vascular connexins (Gustafsson and Holstein-Rathlou, 1999; McKinnon et al., 2006, 2009; Rai et al., 2008; Rodrigo et al., 2011; Sudano et al., 2011).

Nitrosylation may also play a role in the regulation of hemichannel function. Ischemia and/or hypoxia are associated with an increased production of NO, and at the same time an increase in Cx43 and Cx46 hemichannel permeability has been observed (Retamal et al., 2006, 2009). The increased hemichannel permeability leads to the loss of intracellular ions and small organic compounds, which may contribute to cell death. Retamal et al. (2006) showed that metabolic inhibition of cortical astrocytes resulted in an increased cell permeability as determined by dye uptake. The increased dye uptake was associated with both a dephosphorylation and a nitrosylation of the Cx43 hemichannels. Addition of reducing agents, which decreases nitrosylation, reduced the cellular permeability without having any effects on the phosphorylation level. Since addition of external NO donors also increases cell permeability in the same system, it was concluded that S-nitrosylation play an important role in regulating hemichannel permeability in astrocytes (Retamal et al., 2006). The same group showed that addition of the NO-donor GSNO to Cx46 hemichannels expressed in *Xenopus* oocytes caused an increased voltage sensitivity and current amplitude (Retamal et al., 2009). On the other hand, treatment of the cells by reducing agents reversed the effect of GSNO on hemichannel currents, and mutation of the two cysteine residues in the carboxy-terminal part of Cx46 abolished the effect of GSNO.

## METHYLATION AND ACETYLATION

Although methylation and acetylation are mainly known for their epigenetic regulation of gene transcription by DNA methylation

and histone acetylation, there is emerging evidence that connexins may be directly modified. By mass spectrometry, Cx26 was shown to be both methylated and acetylated (Locke et al., 2009). Five methylated sites were detected, one of which (Arg75) is associated with deafness causing mutations (R75W and R75Q), indicating that methylation of this site plays an important physical role. Several studies show that Cx26 channels carrying the R75W mutation are dysfunctional, and although the channels are trafficked to the membrane, they do not result in electrical or metabolic coupling (Richard et al., 1998; Marziano et al., 2003; Oshima et al., 2003; Thomas et al., 2003b; Chen et al., 2005). The mutant channels even had a dominant negative effect on not only wild type Cx26 (Richard et al., 1998; Marziano et al., 2003; Oshima et al., 2003) but also on Cx30 (Forge et al., 2003; Marziano et al., 2003) with which it coexpresses in the inner ear. Besides disrupting cell to cell communication, mutation of Arg75 also reduced the permeability and macroscopic conductance of Cx26 hemichannels, as well as altered their voltage dependence (Chen et al., 2005; Deng et al., 2006).

Besides methylation, Cx26 is also acetylated on six sites including Lys15 and Lys102 for which disease causing mutations/deletions are known (K15T, del102K; Locke et al., 2009). Acetylation is also described in bovine Cx49 (ortholog of human Cx50) on the N-terminal arginine, a commonly occurring modification (Shearer et al., 2008), which was also reported for Cx26 (Locke et al., 2009). An important physiological role for acetylation was also reported for Cx43 in mdx mice, a model of Duchenne muscle dystrophy (Colussi et al., 2011). Cx43 is acetylated and lateralized in mdx mice and interference with acetylases/deacetylases indicated causality between the two. Furthermore, mutagenesis of three lysines (9, 234 and 264), predicted as acetylation targets, showed that acetyl-mimetic mutations led to intracellular localization, whereas Cx43 with un-acetylatable mutations were resistant to acetylating conditions (Colussi et al., 2011).

The data from Cx26 and Cx43 clearly shows that methylation and acetylation will likely emerge as important PTMs in the regulation of intercellular communication mediated by these and other connexins.

## GLUTAMATE $\gamma$ -CARBOXYLATION

The conversion of glutamic acid to  $\gamma$ -carboxyglutamic acid is a vitamin K dependent PTM, which was originally described for blood clotting proteins (Nelstuen et al., 1974; Stenflo et al., 1974). The mass spectrometry study by Harris and Locke (2009) identified glutamate  $\gamma$ -carboxylations in Glu42 and Glu47 in the extracellular loop (E1), as well as Glu114 in the cytoplasmic loop of Cx26 (Locke et al., 2009).  $\gamma$ -carboxylation is an irreversible modification, which generates a high-affinity  $\text{Ca}^{2+}$  binding site. This indicates that  $\gamma$ -carboxylation of Cx26 may be involved in the regulation of Cx26  $\text{Ca}^{2+}$  sensitivity and, in this context, it is noteworthy that mutations at Glu42 and Glu47

## REFERENCES

- Ai, X., and Pogwizd, S. M. (2005). Connexin 43 downregulation and dephosphorylation in nonischemic heart failure is associated with enhanced colocalized protein phosphatase type 2A. *Circ. Res.* 96, 54–63. doi: 10.1161/01.RES.0000152325.07495.5a
- Anand, P., and Stamler, J. S. (2012). Enzymatic mechanisms regulating protein S-nitrosylation: implications in health and disease. *J. Mol. Med. (Berl.)* 90, 233–244. doi: 10.1007/s00109-012-0878-z
- Axelsen, L. N., Stahlhut, M., Mohammed, S., Larsen, B. D., Nielsen, M. S., Holstein-Rathlou, N.-H., et al. (2006). Identification of ischemia-regulated phosphorylation sites in connexin43: a possible target for the antiarrhythmic peptide analogue rotigapide (ZP123). *J. Mol. Cell Cardiol.* 40,

cause Cx26 dependent deaf mutations (Lee and White, 2009). This implies that glutamate  $\gamma$ -carboxylation of Cx26 may play a physiological role and future studies may reveal if other  $\text{Ca}^{2+}$  sensitive connexins, such as Cx43 and Cx50, are also subject to  $\gamma$ -carboxylation.

## CONCLUSION

The literature clearly shows the importance of PTMs in modifying gap junctional coupling and dependent on the connexin and the PTM type, may either increase or decrease intercellular coupling. This is achieved by regulating connexin function at all levels, including oligomerization, trafficking, channel activity and connexin degradation. The importance of these phenomena is underpinned by the fact that several disease causing mutations affect amino acids known to be PTM sites, as described above.

The large and increasing number of PTMs that regulate connexins comprises a major challenge in unraveling their function and importance. For instance, Cx43 contains at least 24 PTM sites and the number of combinations thereof is overwhelming and their investigation beyond the reach of current methods for studying connexins. Most studies address only one or a few modifications at a time using site directed phosphospecific antibodies or mutagenesis. Such approaches carry the risk of overlooking confounding influence of other modifications and may explain some of the contradicting results in the literature. The field of proteomics is rapidly evolving and may eventually disclose quantitative important PTMs and combinations thereof occurring in physiology and pathophysiology. At present, the published mass spectrometry studies of connexins are limited to determinations of whether a certain modification is detectable or not. The threshold for such detection is undefined and not necessarily linked to the threshold for achieving a significant physiological effect although this is often implied. In some cases, such as for Ser306 in Cx43, one may find a change in phosphorylation that passes the threshold for detection after some intervention, in this case ischemia (Axelsen et al., 2006), and be lucky enough that site phosphorylation is associated with a change in channel function (Procida et al., 2009). The importance of other sites could pass undetected simply because they did not pass threshold. Quantitative proteomics are coming to our rescue and rapidly evolving (Cox and Mann, 2011), but even these techniques may not reveal coupling of PTMs at the single molecule level. In any case, the role of PTMs in regulating intercellular communication, will keep researchers busy for years to come.

## ACKNOWLEDGMENTS

This work was supported by the Danish National Research Foundation, The Novo-Nordisk Foundation and The A. P. Møller Foundation for the Advancement of Medical Science. Lene Nygaard Axelsen was supported by a grant from the Danish Council for Independent Research.

- 790–798. doi: 10.1016/j.jmcc.2006.03.005
- Bao, M., Kanter, E. M., Huang, R. Y. C., Maxeiner, S., Frank, M., Zhang, Y., et al. (2011). Residual Cx45 and its relationship to Cx43 in murine ventricular myocardium. *Channels* 5, 489–499. doi: 10.4161/cham.5.6.18523
- Bao, X., Altenberg, G. A., and Reuss, L. (2004). Mechanism of regulation of the gap junction protein connexin 43 by protein kinase C-mediated phosphorylation. *Am. J. Physiol. Cell Physiol.* 286, C647–C654. doi: 10.1152/ajpcell.00295.2003
- Beardslee, M. A., Lerner, D. L., Tadros, P. N., Laing, J. G., Beyer, E. C., Yamada, K. A., et al. (2000). Dephosphorylation and intracellular redistribution of ventricular connexin43 during electrical uncoupling induced by ischemia. *Circ. Res.* 87, 656–662. doi: 10.1161/01.RES.87.8.656
- Bolon, M. L., Peng, T., Kidder, G. M., and Tyml, K. (2008). Lipopolysaccharide plus hypoxia and reoxygenation synergistically reduce electrical coupling between microvascular endothelial cells by dephosphorylating Connexin40. *J. Cell. Physiol.* 217, 350–359. doi: 10.1002/jcp.21505
- Braun, A. P., and Schulman, H. (1995). The multifunctional calcium/calmodulin-dependent protein kinase: from form to function. *Annu. Rev. Physiol.* 57, 417–445. doi: 10.1146/annurev.ph.57.030195.002221
- Butterweck, A., Gergs, U., Elfang, C., Willecke, K., and Traub, O. (1994). Immunochemical characterization of the gap junction protein connexin45 in mouse kidney and transfected human HeLa cells. *J. Membr. Biol.* 141, 247–256. doi: 10.1007/BF00235134
- Cameron, S. J., Malik, S., Akaike, M., Lerner-Marmarosh, N., Yan, C., Lee, J. D., et al. (2003). Regulation of epidermal growth factor-induced Connexin 43 gap junction communication by big mitogen-activated protein kinase 1/ERK5 but not ERK1/2 kinase activation. *J. Biol. Chem.* 278, 18682–18688. doi: 10.1074/jbc.M213283200
- Chen, V. C., Gouw, J. W., Naus, C. C., and Foster, L. J. (2013). Connexin multi-site phosphorylation: mass spectrometry-based proteomics fills the gap. *Biochim. Biophys. Acta* 1828, 23–34. doi: 10.1016/j.bbamem.2012.02.028
- Chen, Y., Deng, Y., Bao, X., Reuss, L., and Altenberg, G. A. (2005). Mechanism of the defect in gap-junctional communication by expression of a connexin 26 mutant associated with dominant deafness. *FASEB J.* 19, 1516–1518. doi: 10.1096/fj.04-3491fje
- Chung, T. H., Wang, S. M., Chang, Y. C., Chen, Y. L., and Wu, J. C. (2007). 18beta-glycyrrhetic acid promotes src interaction with connexin43 in rat cardiomyocytes. *J. Cell. Biochem.* 100, 653–664. doi: 10.1002/jcb.21018
- Chung, T. H., Wang, S. M., Liang, J. Y., Yang, S. H., and Wu, J. C. (2009). The interaction of estrogen receptor alpha and caveolin-3 regulates connexin43 phosphorylation in metabolic inhibition-treated rat cardiomyocytes. *Int. J. Biochem. Cell Biol.* 41, 2323–2333. doi: 10.1016/j.biocel.2009.06.001
- Colussi, C., Rosati, J., Straino, S., Spallotta, F., Berni, R., Stilli, D., et al. (2011). Nepsilon-lysine acetylation determines dissociation from GAP junctions and lateralization of connexin 43 in normal and dystrophic heart. *Proc. Natl. Acad. Sci. U.S.A.* 108, 2795–2800. doi: 10.1073/pnas.1013124108
- Cooper, C. D., and Lampe, P. D. (2002). Casein kinase 1 regulates connexin-43 gap junction assembly. *J. Biol. Chem.* 277, 44962–44968. doi: 10.1074/jbc.M209427200
- Cox, J., and Mann, M. (2011). Quantitative, high-resolution proteomics for data-driven systems biology. *Annu. Rev. Biochem.* 80, 273–299. doi: 10.1146/annurev-biochem-061308-093216
- Darrow, B. J., Laing, J. G., Lampe, P. D., Saffitz, J. E., and Beyer, E. C. (1995). Expression of multiple connexins in cultured neonatal rat ventricular myocytes. *Circ. Res.* 76, 381–387. doi: 10.1161/01.RES.76.3.381
- Deng, Y., Chen, Y., Reuss, L., and Altenberg, G. A. (2006). Mutations of connexin 26 at position 75 and dominant deafness: essential role of arginine for the generation of functional gap-junctional channels. *Hear. Res.* 220, 87–94. doi: 10.1016/j.heares.2006.07.004
- Diez, J. A., Elvira, M., and Vilalobo, A. (1998). The epidermal growth factor receptor tyrosine kinase phosphorylates connexin32. *Mol. Cell. Biochem.* 187, 201–210. doi: 10.1023/A:1006884600724
- Dikic, I., Wakatsuki, S., and Walters, K. J. (2009). Ubiquitin-binding domains – from structures to functions. *Nat. Rev. Mol. Cell Biol.* 10, 659–671. doi: 10.1038/nrm2767
- Doble, B. W., Dang, X., Ping, P., Fandrich, R. R., Nickel, B. E., Jin, Y., et al. (2004). Phosphorylation of serine 262 in the gap junction protein connexin-43 regulates DNA synthesis in cell-cell contact forming cardiomyocytes. *J. Cell Sci.* 117, 507–514. doi: 10.1242/jcs.00889
- Duffy, H. S., Ashton, A. W., O'Donnell, P., Coombs, W., Taffet, S. M., Delmar, M., et al. (2004). Regulation of connexin43 protein complexes by intracellular acidification. *Circ. Res.* 94, 215–222. doi: 10.1161/01.RES.0000113924.06926.11
- Dunn, C. A., Su, V., Lau, A. F., and Lampe, P. D. (2012). Activation of Akt, not connexin 43 protein ubiquitination, regulates gap junction stability. *J. Biol. Chem.* 287, 2600–2607. doi: 10.1074/jbc.M111.276261
- Duthe, F., Plaisance, I., Sarrouilhe, D., and Hervé, J. C. (2001). Endogenous protein phosphatase 1 runs down gap junctional communication of rat ventricular myocytes. *Am. J. Physiol. Cell Physiol.* 281, C1648–C1656.
- Ek-Vitorin, J. F., King, T. J., Heyman, N. S., Lampe, P. D., and Burt, J. M. (2006). Selectivity of connexin 43 channels is regulated through protein kinase C-dependent phosphorylation. *Circ. Res.* 98, 1498–1505. doi: 10.1161/01.RES.0000227572.45891.2c
- Falk, M. M., Fong, J. T., Kells, R. M., O'Laughlin, M. C., Kowal, T. J., and Thevenin, A. F. (2012). Degradation of endocytosed gap junctions by autophagosomal and endo-/lysosomal pathways: a perspective. *J. Membr. Biol.* 245, 465–476. doi: 10.1007/s00232-012-9464-0
- Forge, A., Marziano, N. K., Casalotti, S. O., Becker, D. L., and Jagger, D. (2003). The inner ear contains heteromeric channels composed of cx26 and cx30 and deafness-related mutations in cx26 have a dominant negative effect on cx30. *Cell Commun. Adhes.* 10, 341–346.
- Fykerud, T. A., Kjenseth, A., Schink, K. O., Sirnes, S., Bruun, J., Omori, Y., et al. (2012). Smad ubiquitination regulatory factor-2 controls gap junction intercellular communication by modulating endocytosis and degradation of connexin43. *J. Cell Sci.* 125, 3966–3976. doi: 10.1242/jcs.093500
- Gareau, J. R., and Lima, C. D. (2010). The SUMO pathway: emerging mechanisms that shape specificity, conjugation and recognition. *Nat. Rev. Mol. Cell Biol.* 11, 861–871. doi: 10.1038/nrm3011
- Geiss-Friedlander, R., and Melchior, F. (2007). Concepts in sumoylation: a decade on. *Nat. Rev. Mol. Cell Biol.* 8, 947–956. doi: 10.1038/nrm2293
- Giepmans, B. N. G., Hengeveld, T., Postma, F. R., and Moolenaar, W. H. (2001). Interaction of c-Src with gap junction protein connexin-43. *J. Biol. Chem.* 276, 8544–8549. doi: 10.1074/jbc.M005847200
- Girao, H., Catarino, S., and Pereira, P. (2009). Eps15 interacts with ubiquitinated Cx43 and mediates its internalization. *Exp. Cell Res.* 315, 3587–3597. doi: 10.1016/j.yexcr.2009.10.003
- Girao, H., and Pereira, P. (2003). Phosphorylation of connexin 43 acts as a stimuli for proteasome-dependent degradation of the protein in lens epithelial cells. *Mol. Vis.* 9, 24–30.
- Gustafsson, F., and Holstein-Rathlou, N.-H. (1999). Conducted vasomotor responses in arterioles: characteristics, mechanisms and physiological significance. *Acta Physiol. Scand.* 167, 11–21. doi: 10.1046/j.1365-201x.1999.00582.x
- Harris, A. L., and Locke, D. (2009). “Permeability of connexin channels,” in *Connexins. A Guide*, eds A. L. Harris and D. Locke (New York: Humana Press), 165–206.
- Haugan, K., Olsen, K. B., Hartvig, L., Petersen, J. S., Holstein-Rathlou, N.-H., Hennan, J., et al. (2005a). The antiarrhythmic peptide analogue ZP123 prevents atrial conduction slowing during metabolic stress. *J. Cardiovasc. Electrophysiol.* 16, 537–545. doi: 10.1111/j.1540-8167.2005.40687.x
- Haugan, K., Kjolby, A. L., Hennan, J. K., and Petersen, J. S. (2005b). Rotigaptide (ZP123) reverts established atrial conduction velocity slowing. *Cell Commun. Adhes.* 12, 271–278. doi: 10.1080/15419060500514135
- Hay, R. T. (2005). SUMO: a history of modification. *Mol. Cell* 18, 1–12. doi: 10.1016/j.molcel.2005.03.012
- Hershko, A., and Ciechanover, A. (1998). The ubiquitin system. *Annu. Rev. Biochem.* 67, 425–479. doi: 10.1146/annurev.biochem.67.1.425
- Hertlein, B., Butterweck, A., Haubrich, S., Willecke, K., and Traub, O. (1998). Phosphorylated carboxy terminal serine residues stabilize the mouse gap junction protein connexin45 against degradation. *J. Membr. Biol.* 162, 247–257. doi: 10.1007/s00239900362
- Hess, D. T., Matsumoto, A., Kim, S. O., Marshall, H. E., and Stamler, J. S. (2005). Protein S-nitrosylation: purview and parameters. *Nat. Rev. Mol. Cell Biol.* 6, 150–166. doi: 10.1038/nrm1569

- Hess, D. T., and Stamler, J. S. (2012). Regulation by S-nitrosylation of protein post-translational modification. *J. Biol. Chem.* 287, 4411–4418. doi: 10.1074/jbc.R111.285742
- Hofgaard, J. P., Banach, K., Mollerup, S., Jorgensen, H. K., Olesen, S. P., Holstein-Rathlou, N.-H., et al. (2008). Phosphatidylinositol-bisphosphate regulates intercellular coupling in cardiac myocytes. *Pflugers Arch.* 457, 303–313. doi: 10.1007/s00424-008-0538-x
- Howarth, F. C., Chandler, N. J., Kharche, S., Tellez, J. O., Greener, I. D., Yamanishi, T. T., et al. (2008). Effects of streptozotocin-induced diabetes on connexin43 mRNA and protein expression in ventricular muscle. *Mol. Cell Biochem.* 319, 105–114. doi: 10.1007/s11010-008-9883-5
- Huang, R. Y., Laing, J. G., Kanter, E. M., Berthoud, V. M., Bao, M., Rohrs, H. W., et al. (2010). Identification of CaMKII phosphorylation sites in connexin43 by high-resolution mass spectrometry. *J. Proteome Res.* 10, 1098–1109. doi: 10.1021/pr1008702
- Huibregtse, J. M., Scheffner, M., Beaudenon, S., and Howley, P. M. (1995). A family of proteins structurally and functionally related to the E6-AP ubiquitin-protein ligase. *Proc. Natl. Acad. Sci. U.S.A.* 92, 5249. doi: 10.1073/pnas.92.11.5249-a
- Ikeda, F., and Dikic, I. (2008). Atypical ubiquitin chains: new molecular signals. ‘Protein modifications: beyond the usual suspects’ review series. *EMBO Rep.* 9, 536–542. doi: 10.1038/embor.2008.93
- Ito, S., Hyodo, T., Hasegawa, H., Yuan, H., Hamaguchi, M., and Senga, T. (2010). PI3K/Akt signaling is involved in the disruption of gap junctional communication caused by v-Src and TNF-alpha. *Biochem. Biophys. Res. Commun.* 400, 230–235. doi: 10.1016/j.bbrc.2010.08.045
- Jeyaraman, M., Tanguy, S., Fandrich, R. R., Lukas, A., and Kardami, E. (2003). Ischemia-induced dephosphorylation of cardiomyocyte connexin-43 is reduced by okadaic acid and calyculin A but not fostriecin. *Mol. Cell. Biochem.* 242, 129–134. doi: 10.1023/A:1021102131603
- Johnson, K. E., Mitra, S., Katoh, P., Kelsey, L. S., Johnson, K. R., and Mehta, P. P. (2013). Phosphorylation on serines 279 and 282 of connexin43 regulates endocytosis and gap junction assembly in pancreatic cancer cells. *Mol. Biol. Cell* 24, 715–733. doi: 10.1091/mbc.E12-07-0537
- Kameritsch, P., Khandoga, N., Nagel, W., Hundhausen, C., Lidington, D., and Pohl, U. (2005). Nitric oxide specifically reduces the permeability of Cx37-containing gap junctions to small molecules. *J. Cell Physiol.* 203, 233–242. doi: 10.1002/jcp.20218
- Kanemitsu, M. Y., and Lau, A. F. (1993). Epidermal growth factor stimulates the disruption of gap junctional communication and connexin43 phosphorylation independent of 12-O-tetradecanoylphorbol 13-acetate-sensitive protein kinase C: the possible involvement of mitogen-activated protein kinase. *Mol. Biol. Cell* 4, 837–848. doi: 10.1091/mbc.4.8.837
- Kanemitsu, M. Y., Loo, L. W., Simon, S., Lau, A. F., and Eckhart, W. (1997). Tyrosine phosphorylation of connexin 43 by v-Src is mediated by SH2 and SH3 domain interactions. *J. Biol. Chem.* 272, 22824–22831. doi: 10.1074/jbc.272.36.22824
- Kelly, S. M., VanSlyke, J. K., and Musil, L. S. (2007). Regulation of ubiquitin-proteasome system mediated degradation by cytosolic stress. *Mol. Biol. Cell* 18, 4279–4291. doi: 10.1091/mbc.E07-05-0487
- Kjenseth, A., Fykerud, T., Rivedal, E., and Leithe, E. (2010). Regulation of gap junction intercellular communication by the ubiquitin system. *Cell. Signal.* 22, 1267–1273. doi: 10.1016/j.cellsig.2010.03.005
- Kjenseth, A., Fykerud, T. A., Sirnes, S., Bruun, J., Yohannes, Z., Kolberg, M., et al. (2012). The gap junction channel protein connexin 43 is covalently modified and regulated by SUMOylation. *J. Biol. Chem.* 287, 15851–15861. doi: 10.1074/jbc.M111.281832
- Komander, D. (2009). The emerging complexity of protein ubiquitination. *Biochem. Soc. Trans.* 37, 937–953. doi: 10.1042/BST0370937
- Kruger, O., Plum, A., Kim, J. S., Winterhager, E., Maxeiner, S., Hallas, G., et al. (2000). Defective vascular development in connexin 45-deficient mice. *Development* 127, 4179–4193.
- Kulathu, Y., and Komander, D. (2012). Atypical ubiquitylation – the unexplored world of polyubiquitin beyond Lys48 and Lys63 linkages. *Nat. Rev. Mol. Cell Biol.* 13, 508–523. doi: 10.1038/nrm3394
- Kumai, M., Nishii, K., Nakamura, K., Takeda, N., Suzuki, M., and Shiba, Y. (2000). Loss of connexin45 causes a cushion defect in early cardiogenesis. *Development* 127, 3501–3512.
- Kwak, B. R., and Jongsma, H. J. (1996). Regulation of cardiac gap junction channel permeability and conductance by several phosphorylating conditions. *Mol. Cell Biochem.* 157, 93–99. doi: 10.1007/BF00227885
- Kwak, B. R., Saez, J. C., Wilders, R., Chanson, M., Fishman, G. I., Hertzberg, E. L., et al. (1995a). Effects of cGMP-dependent phosphorylation on rat and human connexin43 gap junction channels. *Eur. J. Physiol.* 430, 770–778. doi: 10.1007/BF00386175
- Kwak, B. R., van Veen, T. A. B., Analbers, L. J. S., and Jongsma, H. J. (1995b). TPA increases conductance but decreases permeability in neonatal rat cardiomyocyte gap junction channels. *Exp. Cell Res.* 220, 456–463. doi: 10.1006/excr.1995.1337
- Laing, J. G., and Beyer, E. C. (1995). The gap junction protein connexin43 is degraded via the ubiquitin proteasome pathway. *J. Biol. Chem.* 270, 26399–26403. doi: 10.1074/jbc.270.44.26399
- Laing, J. G., Tadros, P. N., Westphale, E. M., and Beyer, E. C. (1997). Degradation of connexin43 gap junctions involves both the proteasome and the lysosome. *Exp. Cell Res.* 236, 482–492. doi: 10.1006/excr.1997.3747
- Lampe, P. D., Cooper, C. D., King, T. J., and Burt, J. M. (2006). Analysis of Connexin43 phosphorylated at S325, S328 and S330 in normoxic and ischemic heart. *J. Cell Sci.* 119, 3435–3442. doi: 10.1242/jcs.03089
- Lampe, P. D., and Lau, A. F. (2000). Regulation of Gap Junctions by Phosphorylation of Connexins. *Arch. Biochem. Biophys.* 384, 205–215. doi: 10.1006/abbi.2000.2131
- Lampe, P. D., TenBroek, E. M., Burt, J. M., Kurata, W. E., and Johnson, R. G. (2000). Phosphorylation of connexin43 on serine368 by protein kinase C regulates gap junctional communication. *J. Cell Biol.* 149, 1503–1512. doi: 10.1083/jcb.149.7.1503
- Lau, A. F., Kanemitsu, M. Y., Kurata, W. E., Danesh, S., and Boynton, A. L. (1992). Epidermal growth factor disrupts gap-junctional communication and induces phosphorylation of connexin43 on serine. *Mol. Biol. Cell* 3, 865–874. doi: 10.1091/mbc.3.8.865
- Lee, J. R., and White, T. W. (2009). Connexin-26 mutations in deafness and skin disease. *Expert Rev. Mol. Med.* 11, e35. doi: 10.1017/S1462399409001276
- Leithe, E., Brech, A., and Rivedal, E. (2006). Endocytic processing of connexin43 gap junctions: a morphological study. *Biochem. J.* 393, 59–67. doi: 10.1042/BJ20050674
- Leithe, E., Kjenseth, A., Sirnes, S., Stenmark, H., Brech, A., and Rivedal, E. (2009). Ubiquitylation of the gap junction protein connexin-43 signals its trafficking from early endosomes to lysosomes in a process mediated by Hrs and Tsg101. *J. Cell Sci.* 122, 3883–3893. doi: 10.1242/jcs.053801
- Leithe, E., and Rivedal, E. (2004a). Epidermal growth factor regulates ubiquitination, internalization and proteasome-dependent degradation of connexin43. *J. Cell Sci.* 117, 1211–1220. doi: 10.1242/jcs.00951
- Leithe, E., and Rivedal, E. (2004b). Ubiquitination and down-regulation of gap junction protein connexin-43 in response to 12-O-tetradecanoylphorbol 13-acetate treatment. *J. Biol. Chem.* 279, 50089–50096. doi: 10.1074/jbc.M402006200
- Leukauf, K., Salek, M., Bomke, J., Frech, M., Lehmann, W. D., Durst, M., et al. (2006). Ubiquitin protein ligase Nedd4 binds to connexin43 by a phosphorylation-modulated process. *J. Cell Sci.* 119, 3634–3642. doi: 10.1242/jcs.03149
- Li, X., Su, V., Kurata, W. E., Jin, C., and Lau, A. F. (2008). A novel connexin43-interacting protein, CIP75, which belongs to the Ubl-UBA protein family, regulates the turnover of connexin43. *J. Biol. Chem.* 283, 5748–5759. doi: 10.1074/jbc.M709288200
- Lin, H., Ogawa, K., Imanaga, I., and Tribulova, N. (2006). Remodeling of connexin 43 in the diabetic rat heart. *Mol. Cell Biochem.* 290, 69–78. doi: 10.1007/s11010-006-9166-y
- Lin, J. S., Fitzgerald, S., Dong, Y. M., Knight, C., Donaldson, P., and Kistler, J. (1997). Processing of the gap junction protein connexin50 in the ocular lens is accomplished by calpain. *Eur. J. Cell Biol.* 73, 141–149.
- Lin, R., Warn-Cramer, B. J., Kurata, W. E., and Lau, A. F. (2001). v-Src phosphorylation of connexin 43 on Tyr247 and Tyr265 disrupts gap-junctional communication. *J. Cell Biol.* 154, 815–828. doi: 10.1083/jcb.200102027
- Locke, D., Bian, S., Li, H., and Harris, A. L. (2009). Post-translational modifications of connexin26 revealed by mass spectrometry. *Biochem. J.* 424, 385–398. doi: 10.1042/BJ20091140
- Locke, D., Koreen, I. V., and Harris, A. L. (2006). Isoelectric points and post-translational modifications of connexin26 and connexin32. *FASEB J.* 20, 1221–1223. doi: 10.1096/fj.05-5309fje
- Loo, L. W., Kanemitsu, M. Y., and Lau, A. F. (1999). In vivo

- association of pp60v-src and the gap-junction protein connexin 43 in v-src-transformed fibroblasts. *Mol. Carcinog.* 25, 187–195. doi: 10.1002/(SICI)1098-2744(199907)25:3<187::AID-MC5>3.0.CO;2-O
- Lorick, K. L., Jensen, J. P., Fang, S., Ong, A. M., Hatakeyama, S., and Weissman, A. M. (1999). RING fingers mediate ubiquitin-conjugating enzyme (E2)-dependent ubiquitination. *Proc. Natl. Acad. Sci. U.S.A.* 96, 11364–11369. doi: 10.1073/pnas.96.20.11364
- Marziano, N. K., Casalotti, S. O., Portelli, A. E., Becker, D. L., and Forge, A. (2003). Mutations in the gene for connexin 26 (GJB2) that cause hearing loss have a dominant negative effect on connexin 30. *Hum. Mol. Genet.* 12, 805–812. doi: 10.1093/hmg/ddg076
- Matic, I., Schimmel, J., Hendriks, I. A., van Santen, M. A., van de Rijke, F., van, D. H., et al. (2010). Site-specific identification of SUMO-2 targets in cells reveals an inverted SUMOylation motif and a hydrophobic cluster SUMOylation motif. *Mol. Cell* 39, 641–652. doi: 10.1016/j.molcel.2010.07.026
- McKinnon, R. L., Bolon, M. L., Wang, H. X., Swarbreck, S., Kidder, G. M., Simon, A. M., et al. (2009). Reduction of electrical coupling between microvascular endothelial cells by NO depends on connexin37. *Am. J. Physiol Heart Circ. Physiol* 297, H93–H101. doi: 10.1152/ajpheart.01148.2008
- McKinnon, R. L., Lidington, D., Bolon, M., Ouellette, Y., Kidder, G. M., and Tyml, K. (2006). Reduced arteriolar conducted vasoconstriction in septic mouse cremaster muscle is mediated by nNOS-derived NO. *Cardiovasc. Res.* 69, 236–244. doi: 10.1016/j.cardiores.2005.09.003
- Mollerup, S., Hofgaard, J. P., Braunstein, T. H., Kjenseth, A., Leithe, E., Rivedal, E., et al. (2011). Norepinephrine inhibits intercellular coupling in rat cardiomyocytes by ubiquitination of connexin43 gap junctions. *Cell Commun. Adhes.* 18, 57–65. doi: 10.3109/15419061.2011.611920
- Musil, L. S., Cunningham, B. A., Edelman, G. M., and Goode-nough, D. A. (1990). Differential phosphorylation of the gap junction protein connexin43 in junctional communication-competent and -deficient cell lines. *J. Cell Biol.* 111, 2077–2088. doi: 10.1083/jcb.111.5.2077
- Musil, L. S., and Goode-nough, D. A. (1991). Biochemical analysis of connexin43 intracellular transport, phosphorylation, and assembly into gap junctional plaques. *J. Cell Biol.* 115, 1357–1374. doi: 10.1083/jcb.115.5.1357
- Musil, L. S., Le, A. C., VanSlyke, J. K., and Roberts, L. M. (2000). Regulation of connexin degradation as a mechanism to increase gap junction assembly and function. *J. Biol. Chem.* 275, 25207–25215. doi: 10.1074/jbc.275.33.25207
- Nelsestuen, G. L., Ztykovicz, T. H., and Howard, J. B. (1974). The mode of action of vitamin K. Identification of gamma-carboxyglutamic acid as a component of prothrombin. *J. Biol. Chem.* 249, 6347–6350.
- Nguyen, J. T., Turck, C. W., Cohen, F. E., Zuckermann, R. N., and Lim, W. A. (1998). Exploiting the basis of proline recognition by SH3 and WW domains: design of N-substituted inhibitors. *Science* 282, 2088–2092. doi: 10.1126/science.282.5396.2088
- Nielsen, M. S., Axelsen, L. N., Sorgen, P. L., Verma, V., Delmar, M., and Holstein-Rathlou, N.-H. (2012). Gap junctions. *Compr. Physiol.* 2, 1981–2035.
- Oshima, A., Doi, T., Mitsuoka, K., Maeda, S., and Fujiyoshi, Y. (2003). Roles of Met-34, Cys-64, and Arg-75 in the assembly of human connexin 26. Implication for key amino acid residues for channel formation and function. *J. Biol. Chem.* 278, 1807–1816. doi: 10.1074/jbc.M207713200
- Pahujaa, M., Anikin, M., and Goldberg, G. S. (2007). Phosphorylation of connexin43 induced by Src: regulation of gap junctional communication between transformed cells. *Exp. Cell Res.* 313, 4083–4090. doi: 10.1016/j.yexcr.2007.09.010
- Park, D. J., Wallick, C. J., Martyn, K. D., Lau, A. F., Jin, C., and Warn-Cramer, B. J. (2007). Akt phosphorylates connexin43 on Ser373, a “mode-1” binding site for 14-3-3. *Cell Commun. Adhes.* 14, 211–226. doi: 10.1080/15419060701755958
- Piehl, M., Lehmann, C., Gumpert, A., Denizot, J. P., Segretain, D., and Falk, M. M. (2007). Internalization of large double-membrane intercellular vesicles by a clathrin-dependent endocytic process. *Mol. Biol. Cell* 18, 337–347. doi: 10.1091/mbc.E06-06-0487
- Plum, A., Hallas, G., Magin, T., Domrowski, F., Hagendorff, A., Schumacher, B., et al. (2000). Unique and shared functions of different connexins in mice. *Curr. Biol.* 10, 1083–1091. doi: 10.1016/S0960-9822(00)00690-4
- Postma, F. R., Hengeveld, T., Alblas, J., Giepmans, B. N. G., Zondag, G. C. M., Jalink, K., et al. (1998). Acute loss of cell-cell communication caused by G protein-coupled receptors: a critical role for c-Src. *J. Cell Biol.* 140, 1199–1209. doi: 10.1083/jcb.140.5.1199
- Procida, K., Jørgensen, L., Schmitt, N., Delmar, M., Taffet, S. M., Holstein-Rathlou, N.-H., et al. (2009). Phosphorylation of connexin43 on serine 306 regulates electrical coupling. *Heart Rhythm* 6, 1632–1638. doi: 10.1016/j.hrthm.2009.07.043
- Puram, K. L., Laird, D. W., and Revel, J. P. (1993). Trapping an intermediate form of connexin43 in the golgi. *Exp. Cell Res.* 206, 85–92. doi: 10.1006/excr.1993.1123
- Qu, J., Volpicelli, F. M., Garcia, L. I., Sandeep, N., Zhang, J., Márquez-Rosado, L., et al. (2009). Gap junction remodeling and spironolactone-dependent reverse remodeling in the hypertrophied heart. *Circ. Res.* 104, 365–371. doi: 10.1161/CIRCRESAHA.108.184044
- Rai, A., Riemann, M., Gustafsson, F., Holstein-Rathlou, N.-H., and Torp-Pedersen, C. (2008). Streptozotocin-induced diabetes decreases conducted vasoconstrictor response in mouse cremaster arterioles. *Horm. Metab. Res.* 40, 651–654. doi: 10.1055/s-0028-1083813
- Remo, B. F., Qu, J., Volpicelli, F. M., Giovannone, S., Shin, D., Lader, J., et al. (2011). Phosphatase-resistant gap junctions inhibit pathological remodeling and prevent arrhythmias. *Circ. Res.* 108, 1459–1466. doi: 10.1161/CIRCRESAHA.111.244046
- Retamal, M. A., Cortes, C. J., Reuss, L., Bennett, M. V., and Saez, J. C. (2006). S-nitrosylation and permeation through connexin 43 hemichannels in astrocytes: induction by oxidant stress and reversal by reducing agents. *Proc. Natl. Acad. Sci. U.S.A.* 103, 4475–4480. doi: 10.1073/pnas.0511118103
- Retamal, M. A., Yin, S., Altenberg, G. A., and Reuss, L. (2009). Modulation of Cx46 hemichannels by nitric oxide. *Am. J. Physiol. Cell Physiol.* 296, C1356–C1363. doi: 10.1152/ajpcell.00054.2009
- Richard, G., White, T. W., Smith, L. E., Bailey, R. A., Compton, J. G., Paul, D. L., et al. (1998). Functional defects of Cx26 resulting from a heterozygous missense mutation in a family with dominant deaf-mutism and palmoplantar keratoderma. *Hum. Genet.* 103, 393–399. doi: 10.1007/s004390050839
- Rivedal, E., and Leithe, E. (2005). Connexin43 synthesis, phosphorylation, and degradation in regulation of transient inhibition of gap junction intercellular communication by the phorbol ester TPA in rat liver epithelial cells. *Exp. Cell Res.* 302, 143–152. doi: 10.1016/j.yexcr.2004.09.004
- Rodrigo, R., Gonzalez, J., and Paoletti, F. (2011). The role of oxidative stress in the pathophysiology of hypertension. *Hypertens. Res.* 34, 431–440. doi: 10.1038/hr.2010.264
- Rodriguez, M. S., Dargemont, C., and Hay, R. T. (2001). SUMO-1 conjugation in vivo requires both a consensus modification motif and nuclear targeting. *J. Biol. Chem.* 276, 12654–12659. doi: 10.1074/jbc.M009476200
- Rucker-Martin, C., Milliez, P., Tan, S., Decrouy, X., Recouvreur, M., Vranckx, R., et al. (2006). Chronic hemodynamic overload of the atria is an important factor for gap junction remodeling in human and rat hearts. *Cardiovasc. Res.* 72, 69–79. doi: 10.1016/j.cardiores.2006.06.016
- Saez, J. C., Nairn, A. C., Czernik, A. J., Fishman, G. I., Spray, D. C., and Hertzberg, E. L. (1997). Phosphorylation of connexin43 and the regulation of neonatal rat cardiac myocyte gap junctions. *J. Mol. Cell Cardiol.* 29, 2131–2145. doi: 10.1006/jmcc.1997.0447
- Saez, J. C., Nairn, A. C., Czernik, A. J., Spray, D. C., Hertzberg, E. L., Greengard, P., et al. (1990). Phosphorylation of connexin 32, a hepatocyte gap-junction protein, by cAMP-dependent protein kinase, protein kinase C and Ca<sup>2+</sup>/calmodulin-dependent protein kinase II. *Eur. J. Biochem.* 192, 263–273. doi: 10.1111/j.1432-1033.1990.tb19223.x
- Saez, J. C., Spray, D. C., Nairn, A. C., Hertzberg, E., Greengard, P., and Bennett, M. V. (1986). cAMP increases junctional conductance and stimulates phosphorylation of the 27-kDa principal gap junction polypeptide. *Proc. Natl. Acad. Sci. U.S.A.* 83, 2473–2477. doi: 10.1073/pnas.83.8.2473
- Saitoh, H., and Hinche, J. (2000). Functional heterogeneity of small ubiquitin-related protein modifiers SUMO-1 versus SUMO-2/3. *J. Biol. Chem.* 275, 6252–6258. doi: 10.1074/jbc.275.9.6252
- Sandow, S. L., Senadheera, S., Bertrand, P. P., Murphy, T. V., and Tare, M. (2012). Myoendothelial contacts, gap junctions, and microdomains: anatomical links to function? *Microcirculation* 19, 403–415. doi: 10.1111/j.1549-8719.2011.00146.x

- Schulman, B. A., and Harper, J. W. (2009). Ubiquitin-like protein activation by E1 enzymes: the apex for downstream signalling pathways. *Nat. Rev. Mol. Cell Biol.* 10, 319–331. doi: 10.1038/nrm2673
- Shah, M. M., Martinez, A. M., and Fletcher, W. H. (2002). The connexin43 gap junction protein is phosphorylated by protein kinase A and protein kinase C: in vivo and in vitro studies. *Mol. Cell Biochem.* 238, 57–68. doi: 10.1023/A:1019902920693
- Shearer, D., Ens, W., Standing, K., and Valdimarsson, G. (2008). Post-translational modifications in lens fiber connexins identified by off-line-HPLC MALDI-quadrupole time-of-flight mass spectrometry. *Invest. Ophthalmol. Vis. Sci.* 49, 1553–1562. doi: 10.1167/iovs.07-1193
- Sirnes, S., Kjenseth, A., Leithe, E., and Rivedal, E. (2009). Interplay between PKC and the MAP kinase pathway in Connexin43 phosphorylation and inhibition of gap junction intercellular communication. *Biochem. Biophys. Res. Commun.* 382, 41–45. doi: 10.1016/j.bbrc.2009.02.141
- Sirnes, S., Leithe, E., and Rivedal, E. (2008). The detergent resistance of Connexin43 is lost upon TPA or EGF treatment and is an early step in gap junction endocytosis. *Biochem. Biophys. Res. Commun.* 373, 597–601. doi: 10.1016/j.bbrc.2008.06.095
- Smith, W. T., Fleet, W. F., Johnson, T. A., Engle, C. L., and Cascio, W. E. (1995). The Ib phase of ventricular arrhythmias in ischemic in situ porcine heart is related to changes in cell-to-cell electrical coupling. Experimental Cardiology Group, University of North Carolina. *Circulation* 92, 3051–3060. doi: 10.1161/01.CIR.92.10.3051
- Solan, J., and Lampe, P. (2007). Key connexin 43 phosphorylation events regulate the gap junction life cycle. *J. Membr. Biol.* 217, 35–41. doi: 10.1007/s00232-007-9035-y
- Solan, J. L., Marquez-Rosado, L., Sorger, P. L., Thornton, P. J., Gafken, P. R., and Lampe, P. D. (2007). Phosphorylation at S365 is a gatekeeper event that changes the structure of Cx43 and prevents down-regulation by PKC. *J. Cell Biol.* 179, 1301–1309. doi: 10.1083/jcb.200707060
- Sovari, A. A., Iravanian, S., Dolmatova, E., Jiao, Z., Liu, H., Zandieh, S., et al. (2011). Inhibition of c-Src tyrosine kinase prevents angiotensin II mediated connexin-43 remodeling and sudden cardiac death. *J. Am. Coll. Cardiol.* 58, 2332–2339. doi: 10.1016/j.jacc.2011.07.048
- Srisakuldee, W., Jeyaraman, M. M., Nickel, B. E., Tangy, S., Jiang, Z. S., and Kardami, E. (2009). Phosphorylation of connexin-43 at serine 262 promotes a cardiac injury-resistant state. *Cardiovasc. Res.* 83, 672–681. doi: 10.1093/cvr/cvp142
- Stenflo, J., Fernlund, P., Egan, W., and Roepstorff, P. (1974). Vitamin K dependent modifications of glutamic acid residues in prothrombin. *Proc. Natl. Acad. Sci. U.S.A.* 71, 2730–2733. doi: 10.1073/pnas.71.7.2730
- Straub, A. C., Billaud, M., Johnstone, S. R., Best, A. K., Yeman, S., Dwyer, S. T., et al. (2011). Compartmentalized connexin 43 S-nitrosylation/denitrosylation regulates heterocellular communication in the vessel wall. *Arterioscler. Thromb. Vasc. Biol.* 31, 399–407. doi: 10.1161/ATVBAHA.110.215939
- Su, V., and Lau, A. F. (2012). Ubiquitination, intracellular trafficking, and degradation of connexins. *Arch. Biochem. Biophys.* 524, 16–22. doi: 10.1016/j.abb.2011.12.027
- Su, V., Nakagawa, R., Koval, M., and Lau, A. F. (2010). Ubiquitin-independent proteasomal degradation of endoplasmic reticulum-localized connexin43 mediated by CIP75. *J. Biol. Chem.* 285, 40979–40990. doi: 10.1074/jbc.M110.170753
- Sudano, I., Roas, S., and Noll, G. (2011). Vascular abnormalities in essential hypertension. *Curr. Pharm. Des.* 17, 3039–3044. doi: 10.2174/138161211798157766
- Takeda, A., Hashimoto, E., Yamamura, H., and Shimazu, T. (1987). Phosphorylation of liver gap junction protein by protein kinase C. *FEBS Lett.* 210, 169–172. doi: 10.1016/S0008-6363(99)00373-9
- TenBroek, E. M., Lampe, P. D., Solan, J. L., Reynhout, J. K., and Johnson, R. G. (2001). Ser364 of connexin43 and the upregulation of gap junction assembly by cAMP. *J. Cell Biol.* 155, 1307–1318. doi: 10.1083/jcb.200102017
- Thomas, M. A., Zosso, N., Scerri, I., Demaurex, N., Chanson, M., and Staub, O. (2003a). A tyrosine-based sorting signal is involved in connexin43 stability and gap junction turnover. *J. Cell Sci.* 116, 2213–2222. doi: 10.1242/jcs.00440
- Thomas, T., Aasen, T., Hodgins, M., and Laird, D. W. (2003b). Transport and function of cx26 mutants involved in skin and deafness disorders. *Cell Commun. Adhes.* 10, 353–358.
- Török, K., Stauffer, K., and Evans, W. H. (1997). Connexin 32 of gap junctions contains two cytoplasmic calmodulin-binding domains. *Biochem. J.* 326, 479–483.
- Totzeck, A., Boengler, K., van de Sand, A., Konietzka, I., Gres, P., Garcia-Dorado, D., et al. (2008). No impact of protein phosphatases on connexin43 phosphorylation in ischemic preconditioning. *Am. J. Physiol. Heart Circ. Physiol.* 295, H2106–H2112. doi: 10.1152/ajpheart.00456.2008
- Toyofuku, T., Akamatsu, Y., Zhang, H., Kuzuya, T., Tada, M., and Hori, M. (2001). c-Src regulates the interaction between connexin-43 and ZO-1 in cardiac myocytes. *J. Biol. Chem.* 276, 1780–1788. doi: 10.1074/jbc.M005826200
- Traub, O., Eckert, R., Lichtenberg-Frate, H., Elfgang, C., Bastide, B., Scheidtmann, K. H., et al. (1994). Immunological and electrophysiological characterization of murine connexin40 and connexin43 in mouse-tissues and transfected human-cells. *Eur. J. Cell Biol.* 64, 101–112.
- van Rheenen, J., Song, X., van Rosmalen, W., Cammer, M., Chen, X., Desmarais, V., et al. (2007). EGF-induced PIP2 hydrolysis releases and activates cofilin locally in carcinoma cells. *J. Cell Biol.* 179, 1247–1259. doi: 10.1083/jcb.200706206
- van Rijen, H. V. M., van Veen, T. A. B., Hermans, M. M. P., and Jongsma, H. J. (2000). Human connexin40 gap junction channels are modulated by cAMP. *Cardiovasc. Res.* 45, 941–951. doi: 10.1016/S0008-6363(99)00373-9
- van Veen, T. A. B., van Rijen, H. V. M., and Jongsma, H. J. (2000). Electrical conductance of mouse connexin45 gap junction channels is modulated by phosphorylation. *Cardiovasc. Res.* 46, 496–510. doi: 10.1016/S0008-6363(00)00047-X
- van Zeijl, L., Ponsioen, B., Giepmans, B. N., Ariaens, A., Postma, F. R., Varnai, P., et al. (2007). Regulation of connexin43 gap junctional communication by phosphatidylinositol 4,5-bisphosphate. *J. Cell Biol.* 177, 881–891. doi: 10.1083/jcb.200610144
- VanSlyke, J. K., Deschenes, S. M., and Musil, L. S. (2000). Intracellular transport, assembly, and degradation of wild-type and disease-linked mutant gap junction proteins. *Mol. Biol. Cell* 11, 1933–1946. doi: 10.1091/mbc.11.6.1933
- VanSlyke, J. K., and Musil, L. S. (2000). Analysis of connexin intracellular transport and assembly. *Methods* 20, 156–164. doi: 10.1006/meth.1999.0933
- VanSlyke, J. K., and Musil, L. S. (2002). Dislocation and degradation from the ER are regulated by cytosolic stress. *J. Cell Biol.* 157, 381–394. doi: 10.1083/jcb.200111045
- Wang, Z., and Schey, K. L. (2009). Phosphorylation and truncation sites of bovine lens connexin 46 and connexin 50. *Exp. Eye Res.* 89, 898–904. doi: 10.1016/j.exer.2009.07.015
- Warn-Cramer, B. J., Cottrell, G. T., Burt, J. M., and Lau, A. F. (1998). Regulation of connexin-43 gap junctional intercellular communication by mitogen-activated protein kinase. *J. Biol. Chem.* 273, 9188–9196. doi: 10.1074/jbc.273.15.9188
- Warn-Cramer, B. J., Lampe, P. D., Kurata, W. E., Kanemitsu, M. Y., Loo, L. W., Eckhart, W., et al. (1996). Characterization of the mitogen-activated protein kinase phosphorylation sites on the connexin-43 gap junction protein. *J. Biol. Chem.* 271, 3779–3786. doi: 10.1074/jbc.271.7.3779
- Waza, A. A., Andrabi, K., and Ul, H. M. (2012). Adenosine-triphosphate-sensitive K<sup>+</sup> channel (Kir6.1): a novel phosphospecific interaction partner of connexin 43 (Cx43). *Exp. Cell Res.* 318, 2559–2566. doi: 10.1016/j.yexcr.2012.08.004
- Weissman, A. M., Shabek, N., and Ciechanover, A. (2011). The predator becomes the prey: regulating the ubiquitin system by ubiquitylation and degradation. *Nat. Rev. Mol. Cell Biol.* 12, 605–620. doi: 10.1038/nrm3173
- Willecke, K., Eiberger, J., Degen, J., Eckardt, D., Romualdi, A., Guldenagel, M., et al. (2002). Structural and functional diversity of connexin genes in the mouse and human genome. *Biol. Chem.* 383, 725–737. doi: 10.1515/BC.2002.076
- Xing, D., Kjolby, A. L., Petersen, J. S., and Martins, J. B. (2005). Pharmacological stimulation of cardiac gap junction coupling does not affect ischemia-induced focal ventricular tachycardia or triggered activity in dogs. *Am. J. Physiol. Heart Circ. Physiol.* 288, H511–H516. doi: 10.1152/ajpheart.00720.2004
- Yang, W. L., Wang, J., Chan, C. H., Lee, S. W., Campos, A. D., Lamothe, B., et al. (2009). The E3 ligase TRAF6 regulates Akt ubiquitination and activation. *Science* 325, 1134–1138. doi: 10.1126/science.1175065
- Yin, X., Gu, S., and Jiang, J. X. (2001). The development-associated cleavage of lens connexin 45.6 by caspase-3-like protease is regulated by casein kinase II-mediated phosphorylation. *J. Biol. Chem.* 276, 34567–34572. doi: 10.1074/jbc.M106073200

Yogo, K., Ogawa, T., Akiyama, M., Ishida, N., and Takeya, T. (2002). Identification and functional analysis of novel phosphorylation sites in Cx43 in rat primary granulosa cells. *FEBS Lett.* 531, 132–136. doi: 10.1016/S0014-5793(02)03441-5

Yogo, K., Ogawa, T., Akiyama, M., Ishida-Kitagawa, N., Sasada, H., Sato, E., et al. (2006). PKA implicated in the phosphorylation of Cx43 induced by stimulation with FSH in rat granulosa cells. *J. Reprod. Dev.* 52, 321–328. doi: 10.1262/jrd.17107

Zhou, L., Kasperek, E. M., and Nicholson, B. J. (1999). Dissection of the molecular basis of pp60v-src induced gating of connexin 43 gap junction channels. *J. Cell Biol.* 144, 1033–1045. doi: 10.1083/jcb.144.5.1033

**Conflict of Interest Statement:** The authors declare that the research was conducted in the absence of any commercial or financial relationships that could be construed as a potential conflict of interest.

Received: 17 April 2013; accepted: 30 September 2013; published online: 22 October 2013.

Citation: Axelsen LN, Calloe K, Holstein-Rathlou N-H and Nielsen MS (2013) Managing the complexity of communication: regulation of gap junctions by post-translational modification. *Front. Pharmacol.* 4:130. doi: 10.3389/fphar.2013.00130

This article was submitted to Pharmacology of Ion Channels and Channelopathies, a section of the journal *Frontiers in Pharmacology*.

Copyright © 2013 Axelsen, Calloe, Holstein-Rathlou and Nielsen. This is an open-access article distributed under the terms of the Creative Commons Attribution License (CC BY). The use, distribution or reproduction in other forums is permitted, provided the original author(s) or licensor are credited and that the original publication in this journal is cited, in accordance with accepted academic practice. No use, distribution or reproduction is permitted which does not comply with these terms.



# Connexin diversity in the heart: insights from transgenic mouse models

Sander Verheule<sup>1\*</sup> and Sven Kaese<sup>2</sup>

<sup>1</sup> Department of Physiology, Faculty of Medicine, Maastricht University, Maastricht, Netherlands

<sup>2</sup> Department of Cardiovascular Medicine, Division of Electrophysiology, University of Muenster, Muenster, Germany

**Edited by:**

Aida Salameh, Heart Centre  
University of Leipzig, Germany

**Reviewed by:**

Mirko Baruscotti, University of  
Milano, Italy

Gregory E. Morley, New York  
University School of Medicine, USA

**\*Correspondence:**

Sander Verheule, Department of  
Physiology, Universiteitssingel 50,  
PO Box 616, 6200 MD, Maastricht,  
Netherlands

e-mail: s.verheule@  
maastrichtuniversity.nl

Cardiac conduction is mediated by gap junction channels that are formed by connexin (Cx) protein subunits. The connexin family of proteins consists of more than 20 members varying in their biophysical properties and ability to combine with other connexins into heteromeric gap junction channels. The mammalian heart shows regional differences both in connexin expression profile and in degree of electrical coupling. The latter reflects functional requirements for conduction velocity which needs to be low in the sinoatrial and atrioventricular nodes and high in the ventricular conduction system. Over the past 20 years knowledge of the biology of gap junction channels and their role in the genesis of cardiac arrhythmias has increased enormously. This review focuses on the insights gained from transgenic mouse models. The mouse heart expresses Cx30, 30.2, 37, 40, 43, 45, and 46. For these connexins a variety of knock-outs, heart-specific knock-outs, conditional knock-outs, double knock-outs, knock-ins and overexpressors has been studied. We discuss the cardiac phenotype in these models and compare Cx expression between mice and men. Mouse models have enhanced our understanding of (patho)-physiological implications of Cx diversity in the heart. In principle connexin-specific modulation of electrical coupling in the heart represents an interesting treatment strategy for cardiac arrhythmias and conduction disorders.

**Keywords:** gap junctions, connexins, mouse models, conduction, arrhythmias, cardiac

## INTRODUCTION

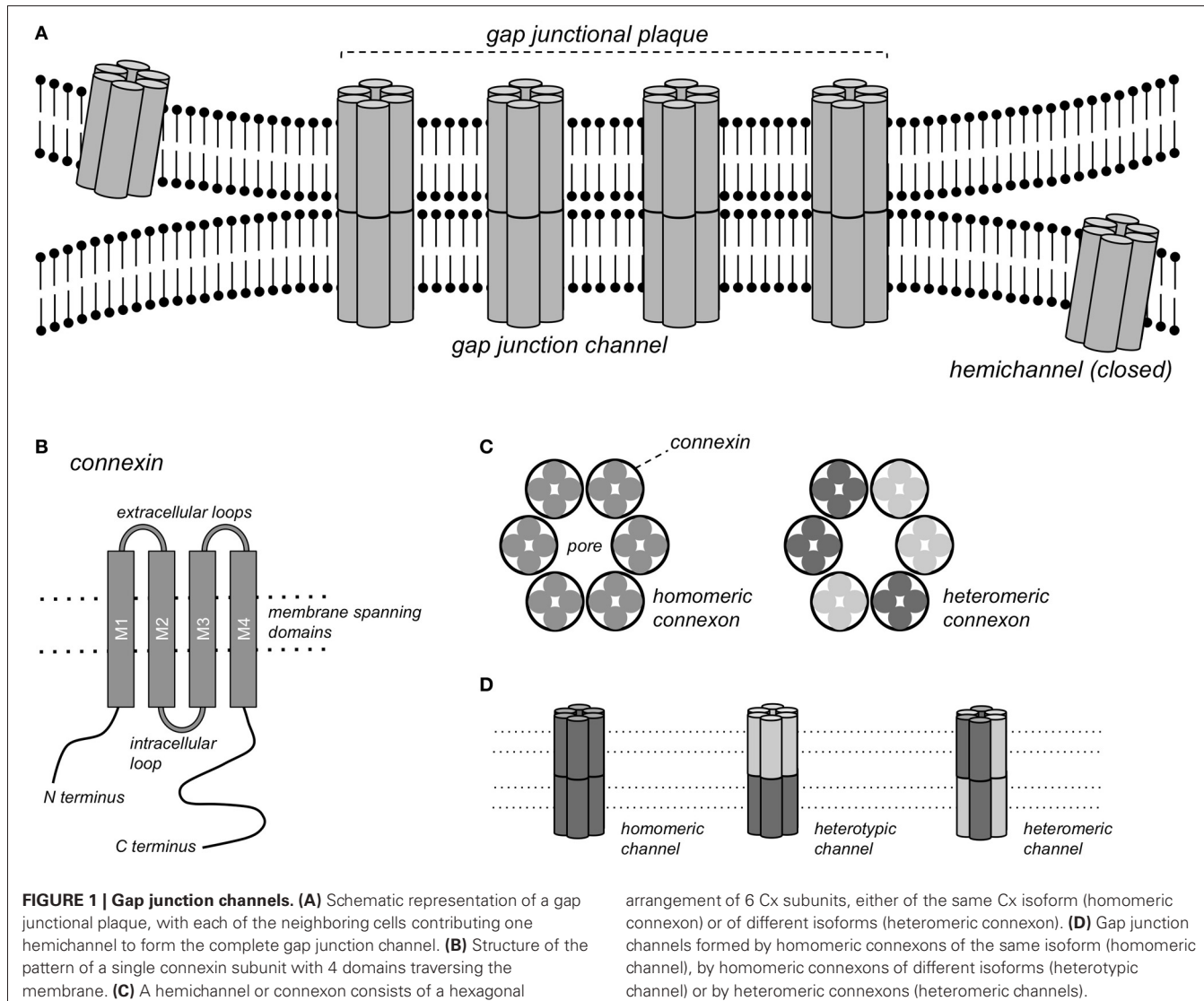
Gap junction channels form continuous pores between the cytoplasms of closely apposed cells that are permeable to ions and molecules <1 kDa, thereby conferring electrical and metabolic coupling between neighboring cells. Gap junction channels consist of connexin (Cx) protein subunits. More than 20 Cx isoforms have been described in both humans and mice and mutations in Cx genes have been implicated in various inheritable diseases (Sohl and Willecke, 2004; Dobrowolski and Willecke, 2009). Complete gap junction channels are formed by the docking of two hemichannels, or connexons, contributed by closely apposed cells (**Figure 1**). Each connexon consists of 6 connexin subunits, and a homomeric gap junction channel consists of 12 Cx proteins of the same isoform. When two homomeric connexons consisting of different connexins are apposed, a heterotypic channel may form if those connexins are compatible. In heteromeric connexons, different isoforms are mixed, and a heteromeric channel may form. Some Cxs also form functional hemichannels, i.e., connexons that can open under certain conditions, causing depolarization of the plasma membrane (John et al., 1999; Bukauskas et al., 2006).

Different regions of the heart show specific profiles of Cx expression, which in mouse and human hearts show many similarities, but also some important differences (**Table 1**). Different parts of the heart also have varying requirements for the degree of electrical coupling. To spread the activation wave rapidly over the ventricles, the large Purkinje myocytes of the specialized ventricular conduction system need to be strongly coupled. To create

a delay between the atrial and ventricular contraction, a very low degree of coupling is required in the atrioventricular (AV) node. Similarly, to allow pacemaker function, pacemaker myocytes in the sinoatrial (SA) node need to be weakly coupled, otherwise the pacemaker (or ectopic focus) would in effect be silenced by the surrounding working myocardium (Joyner and van Capelle, 1986; Joyner et al., 2000).

Cardiac gap junctions are highly dynamic structures, with a Cx43 protein half-life of a few hours and a comparably rapid redistribution in response to e.g., ischemia (Beardslee et al., 1998; Smyth et al., 2012). Connexins interact directly with numerous other cellular proteins, e.g., cytoskeletal components (Herve et al., 2007). Apart from their well-established roles in electrical and metabolic coupling, a number of other functions of Cx proteins are emerging, for example in mechanical adhesion and interactions with voltage-gated membrane channels (Agullo-Pascual and Delmar, 2012) and, in the case of Cx43, in mitochondrial metabolism (Ruiz-Meana et al., 2008). Conversely, electrical coupling may be mediated not only by gap junction channels, but also to some degree by ephaptic coupling, i.e., by electric field effects (Sperelakis, 2002; Lin and Keener, 2010).

Connexins differ in various biophysical properties, such as single channel conductance, permeability to larger (dye) molecules and sensitivity to the cytoplasmic pH and transjunctional potential difference, (see e.g., Elfgang et al., 1995; Gonzalez et al., 2007; Rackauskas et al., 2010). Concerning the latter, gap junction channels may close during prolonged, large voltage differences



between cells, for example when one myocyte fires an action potential while its direct neighbor remains at rest (Lin and Veenstra, 2004; Lin et al., 2005). While such large voltage gradients can be imposed in voltage clamp experiments, they are unlikely to occur in the heart. Even in regions with a relatively low degree of electrical coupling, such as the SA node, transjunctional potential differences  $>10$  mV last only a few milliseconds (Verheule et al., 2001), which would be too short for the slow process of voltage-dependent inactivation of gap junction channels.

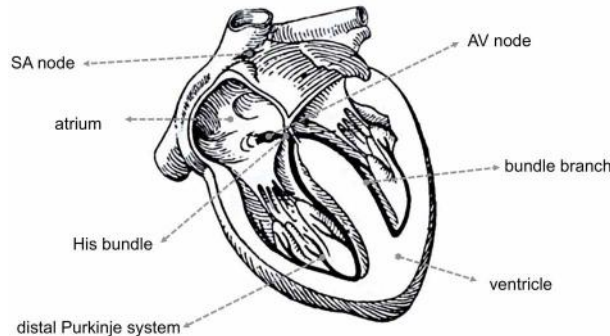
Cx trafficking, degradation, channel gating and permeability can be regulated by phosphorylation of serine and tyrosine residues (Solan and Lampe, 2009). During ischemia, intracellular acidification, release of lipids and channel phosphorylation cause channel closure and redistribution (Dhein, 2006). This response to ischemia allows the confinement of disease from healthy myocardium, thus enabling the myocardium to “heal-over” (de Mello et al., 1969). On the other hand, redistribution of connexins under pathological conditions has

been implicated in arrhythmogenesis (Salameh and Dhein, 2011; Duffy, 2012).

Much of our current knowledge of cardiac connexins stems from studies on mouse models (Table 2). There are numerous similarities, but also some important differences between the hearts of mice and humans (Kaese and Verheule, 2012). In this review, we will discuss evidence from genetically engineered mouse models on the properties and roles of the various cardiac connexins, highlighting both their role during cardiac development and in the adult heart.

## CONNEXIN 30

Cx30 forms channels with a large single channel conductance ( $\gamma_j$ ) of 179 pS (in K-aspartate), a potential of half-maximal inactivation ( $V_{1/2}$ ) of 27 mV and a voltage-independent fraction ( $G_{j, \text{min}}$ ) of 0.15 (Valiunas et al., 1999). Cx30 is expressed at low abundance in the murine SA node (Gros et al., 2010). Interestingly, Cx30-deficient mice have a 9% higher heart rate than wild type (Wt) mice and a lower beat-to-beat variability (Gros et al., 2010). This

**Table 1 | Comparison of Cx regional expression in the mouse and human heart.**

	<b>Mouse</b>	<b>References</b>	<b>Human</b>	<b>References</b>
SA node	Cx45, Cx30.2, (Cx30, Cx46)	Verheijck et al., 2001; Kreuzberg et al., 2005; Chi et al., 2010; Gros et al., 2010	Cx45, Cx40	Davis et al., 1995; Chandler et al., 2009; Kreuzberg et al., 2009
Atria	Cx40, Cx43, ((Cx45))	Delorme et al., 1995, 1997; Alcolea et al., 2004; Miquerol et al., 2004	Cx40, Cx43, (Cx45)	Davis et al., 1995; Vozzi et al., 1999; Kanagaratnam et al., 2002; Kreuzberg et al., 2009; Greener et al., 2011
AV node (compact)	Cx45, Cx30.2	Coppen et al., 2001; Miquerol et al., 2004; Kreuzberg et al., 2006	Cx40, Cx45	Davis et al., 1995; Kreuzberg et al., 2009; Greener et al., 2011
His bundle	Cx40, Cx45, (Cx30.2, Cx46)	Simon et al., 1998; Coppen et al., 1999, 2001; Kreuzberg et al., 2006; Chi et al., 2010	Cx40, Cx43	Hucker et al., 2008; Greener et al., 2011
Bundle branches	Cx40, Cx45, (Cx46)	Simon et al., 1998; Coppen et al., 1999, 2001; van Rijen et al., 2001; Chi et al., 2010	Cx45	Davis et al., 1995; Coppen et al., 2003; Kreuzberg et al., 2009; Greener et al., 2011
Distal Purkinje system	Cx40, Cx43, Cx45, (Cx46)	Coppen et al., 1999; Miquerol et al., 2003; Chi et al., 2010	Cx40, Cx43, (Cx45)	van Kempen et al., 1995; Coppen et al., 2003; Kreuzberg et al., 2009
Ventricles	Cx43, ((Cx45))	Delorme et al., 1997; Stein et al., 2009; Bao et al., 2011	Cx43, (Cx45)	Davis et al., 1995; Vozzi et al., 1999; Dupont et al., 2001; Kreuzberg et al., 2009; Greener et al., 2011

(Cx) and ((Cx)) signify relatively small and trace amounts.

increased rate was still present under autonomic blockade, indicating that Cx30 affects the intrinsic pacemaker frequency. The presence of Cx30 could conceivably enhance electrical coupling between the SA node and the surrounding atrium and thereby decelerate impulse formation within the SA node (Dhein, 2010; Gros et al., 2010). However, it is not known whether Cx30 in the SA node forms heteromeric gap junction channels with the other connexins present (Cx30.2 and Cx45), and whether this would increase or decrease cell-to-cell electrical coupling.

## CONNEXIN 30.2

Cx30.2, the murine ortholog of human Cx31.9 (Belluardo et al., 2001), forms small conductance, weakly voltage-dependent channels [ $\gamma j = 9 \text{ pS}$ ,  $V_{1/2} > 60 \text{ mV}$  (Kreuzberg et al., 2005)]. Cx30.2 is expressed in the murine SA node, AV node and His bundle (Kreuzberg et al., 2005). In transfected HeLa cells, Cx30.2 can form both heterotypic (Kreuzberg et al., 2005) and heteromeric (Gemel et al., 2008) channels with Cx40, Cx43, and Cx45, the major myocardial connexins. Cx30.2 was colocalized with Cx45 in the SA and AV nodes, but not with Cx40 and Cx43 (Kreuzberg et al., 2005). Surprisingly, Cx30.2 deficient mice display accelerated AV nodal conduction, a decrease in AV Wenckebach period

and a higher ventricular rate during atrial fibrillation (Kreuzberg et al., 2006). In addition, whereas deletion of Cx40 slows AV conduction, it is normal in mice deficient for both Cx30.2 and Cx40 (Schrickel et al., 2009), suggesting that the balance between Cx40 and Cx30.2 is an important determinant of AV conduction in mice. Cx30.2 is able to form functional hemichannels (Bukauskas et al., 2006), which in the open state would decrease the membrane resistance and thereby slow conduction, but the role of these hemichannels in the adult heart is uncertain at present. During development, Cx30.2 expression and proper development of the AV conduction system is determined by an enhancer region under the control of Tbx5 and GATA4. Accordingly, the PR interval is shortened in GATA4 $^{+/-}$  mice (Munshi et al., 2009). Moreover, inhibition of Notch signaling during development leads to a loss of Cx30.2 expressing cells, hypoplasia of the AV node and accelerated AV conduction (Rentschler et al., 2011). It is important to note that Cx31.9, the human ortholog of murine Cx30.2, is not expressed in the human SA and AV nodes, ventricular conduction system or working myocardium (Kreuzberg et al., 2009). This indicates that the presence of Cx30.2 may reflect an adaptation in the small mouse heart to allow high activation frequencies and optimize A-V timing. In addition to this difference,

**Table 2 | Overview of genetically engineered mouse models.**

Type	Model	Initial description
Knock-out	Cx30 <sup>-/-</sup>	Gros et al., 2010
	Cx30.2 <sup>-/-</sup>	Kreuzberg et al., 2006
	Cx37 <sup>-/-</sup>	Simon et al., 1997; Munger et al., 2013
	Cx40 <sup>-/-</sup>	Kirchhoff et al., 1998; Simon et al., 1998
	Cx43 <sup>-/-</sup>	Reaume et al., 1995
	Cx45 <sup>-/-</sup>	Kumai et al., 2000
	Cx46 <sup>-/-</sup>	Chi et al., 2010
Conditional Knockout	Cx43 inducible	Eckardt et al., 2004
	Cx43 heart-specific	Gutstein et al., 2001a
	Cx43 chimera	Gutstein et al., 2001b
	Cx45 heart-specific	Frank et al., 2012
Overexpression	Cx43	Ewart et al., 1997
	Cx45	Betsuyaku et al., 2006
Double knock-outs	Cx30.2 <sup>-/-</sup> –Cx40 <sup>-/-</sup>	Schrickel et al., 2009
	Cx30.2 <sup>-/-</sup> –Cx45 <sup>inducible</sup>	Frank et al., 2012
	Cx32 <sup>-/-</sup> –Cx43 <sup>-/-</sup>	Houghton et al., 1999
	Cx37 <sup>-/-</sup> –Cx40 <sup>-/-</sup>	Simon et al., 2004
	Cx40 <sup>-/-</sup> –Cx43 <sup>-/-</sup> and <sup>+/+</sup>	Kirchhoff et al., 2000; Simon et al., 2004
	Cx40 <sup>-/-</sup> –Cx45 <sup>+/+</sup>	Kruger et al., 2006
Knock-ins	Cx40 KI Cx45	Alcolea et al., 2004
	Cx43 KI Cx26	Winterhager et al., 2007
	Cx43 KI Cx31	Zheng-Fischhofer et al., 2006
	Cx43 KI Cx32	Plum et al., 2000
	Cx43 KI Cx40	Plum et al., 2000
	Cx45 KI Cx36	Frank et al., 2010
Mutants	Cx43 K258stop	Maass et al., 2004, 2007
	Cx43 S325/328/330 E or A	Remo et al., 2011
	Cx43 I130T	Kalcheva et al., 2007
	Cx43 G138R	Dobrowolski et al., 2008
	Cx43 G60S	Flenniken et al., 2005; Manias et al., 2008

AV conduction system in the mouse is also electrically connected to the ventricles at the basal part of the septum, leading to a baso-apical activation pattern within the septum (van Rijen et al., 2001).

### CONNEXIN 37

Cx37 forms large conductance channels that are moderately voltage sensitive [ $\gamma j = 200\text{--}250 \mu\text{s}$  in K-glutamate,  $V_{1/2} = 28 \text{ mV}$ ,  $G_{j, \min} = 0.27$  (Reed et al., 1993)]. In the adult heart, Cx37 is expressed by endothelial cells in blood vessels and the endocardial lining of the chambers, although expression has also been observed in parts of the ventricular myocardium during

embryonic development (Haefliger et al., 2000). Cx37<sup>-/-</sup> mice do not develop venous and lymphatic valves (Munger et al., 2013). In addition, mice lacking both Cx37 and Cx40 show a high incidence of atrial and ventricular septal defects at birth (Simon et al., 2004).

### CONNEXIN 40

#### PROPERTIES AND EXPRESSION

Cx40 forms channels with a large single channel conductance and moderate voltage-sensitivity [ $\gamma j = 150 \mu\text{s}$  in KCl,  $V_{1/2} = 44 \text{ mV}$ ,  $G_{j, \min} = 0.5$  (Traub et al., 1994)]. In the developing mouse heart, Cx40 is widely expressed in the ventricles and atria at embryonic day 11. From day 14 onwards, Cx40 becomes restricted to the conduction system in the ventricles, but it remains present in the atrial working myocardium (Delorme et al., 1995). The transcription factors Tbx2 and Tbx3 repress Cx40 expression (Hoogaars et al., 2004; Aanhaanen et al., 2011). Inactivation of Tbx2 leads to the formation of Cx40-expressing accessory pathways and ventricular preexcitation (Aanhaanen et al., 2011). On the other hand, Cx40 expression is increased by Nkx2-5 (Harris et al., 2006) and Tbx5 (Pizard et al., 2005; Arnolds et al., 2012) that delineate the conduction system. In fact, normal development of the ventricular conduction system requires the expression of Cx40 (Sankova et al., 2012).

In the adult mouse heart, Cx40 is expressed by atrial myocytes and ventricular conduction system (His bundle, left and right bundle branches and Purkinje network) (Simon et al., 1998; Miquerol et al., 2004; van Veen et al., 2005b). The selective expression of Cx40 by the conduction system within the ventricle has allowed sophisticated functional studies on conduction within the Purkinje network (Miquerol et al., 2004; Tallini et al., 2007).

#### ATRIA

Information on the effect of Cx40-deficiency on atrial conduction is somewhat contradictory. In the first studies, the P wave duration was significantly prolonged (Kirchhoff et al., 1998; Simon et al., 1998; Hagendorff et al., 1999; Verheule et al., 1999; Bagwe et al., 2005). Some other studies have not reproduced this observation (Bevilacqua et al., 2000; Tamaddon et al., 2000; Vanderbrink et al., 2000). Measurement of P-wave duration in mice is not straightforward, requiring different leads to accurately determine the end of the biphasic P-wave. In two studies that measured atrial conduction directly using direct contact mapping or optical mapping, a reduction in conduction velocity was observed (Verheule et al., 1999; Bagwe et al., 2005). However, a later study used optical mapping to show that deletion of Cx40 did not affect conduction velocity, but did abolish the difference in conduction velocity between the left and right atria (Leaf et al., 2008).

Atrial myocytes express both Cx40 and 43. Based on expression studies in Xenopus oocytes, Cx40 and 43 were originally thought to be incompatible (White and Bruzzone, 1996). However, later studies presented compelling evidence that Cx40 and 43 can form both heterotypic (Valiunas et al., 2000) and heteromeric (He et al., 1999; Cottrell and Burt, 2001) gap junction channels in mammalian cells, including adult atrial myocytes (Elenes et al., 1999). In cultured neonatal mouse atrial myocytes, Cx40

and 43 appear to make equal contributions to total gap junctional conductance (Lin et al., 2010). Intriguingly, a study on cultured strands of atrial myocytes that the Cx40/Cx43 ratio was an important determinant of propagation, with Cx43 increasing and Cx40 decreasing conduction velocity (Beauchamp et al., 2006).

In intact  $Cx40^{-/-}$  mice, episodes of atrial tachyarrhythmias/atrial fibrillation could be induced by transesophageal pacing (Hagendorff et al., 1999) and direct atrial pacing (Verheule et al., 1999; Bevilacqua et al., 2000). In perfused  $Cx40^{-/-}$  mouse hearts studied with optical mapping, atrial ectopic beats and intra-atrial conduction block during pacing at high rates were reported (Bagwe et al., 2005).

### SINOATRIAL NODE

In contrast to larger species, such as rabbits (Verheule et al., 2001), pacemaker myocytes in the central SA node do not express Cx40 (Verheijck et al., 2001; Wiese et al., 2009). However, Cx40-deficiency does cause a modest increase in sinus cycle length (Hagendorff et al., 1999; Verheule et al., 1999; Bevilacqua et al., 2000; de Wit et al., 2003), and an increase in (corrected) SA node recovery time (Hagendorff et al., 1999; Verheule et al., 1999). The effects of Cx40-deficiency on SA node function may be caused either by altered conduction from the SA node to the atrium and/or by the phenomenon that the “atrial pacemaking complex” may be much larger than the area that is classically considered to be the sinus node (Glukhov et al., 2010).

### ATRIOVENTRICULAR CONDUCTION

AV conduction is also affected in  $Cx40^{-/-}$  mice, reflected in a prolonged PR interval, increased QRS duration and a QRS morphology reminiscent of right bundle branch block in humans (Kirchhoff et al., 1998; Simon et al., 1998; Verheule et al., 1999; Bevilacqua et al., 2000; Vanderbrink et al., 2000). In addition, episodes of 2nd and 3rd degree AV block were observed in  $Cx40^{-/-}$  mice (Kirchhoff et al., 1998; Hagendorff et al., 1999). With minor differences between studies, Cx40-deficiency prolongs the AV effective refractory period (ERP), the cycle lengths of A to V Wenckebach and 2:1 block, while the atrial ERP, ventricular ERP, cycle lengths of V to A Wenckebach and 2:1 block are not affected (Hagendorff et al., 1999; Verheule et al., 1999; Bevilacqua et al., 2000; Vanderbrink et al., 2000). Although Cx40 is not expressed in the central AV node (Delorme et al., 1995; Simon et al., 1998; Coppen et al., 1999), the AH interval is prolonged in intact mice (Bevilacqua et al., 2000; Vanderbrink et al., 2000), AV nodal conduction curves are shifted (Vanderbrink et al., 2000) and AV nodal facilitation is reversed (Zhu et al., 2005), indicative of an effect on the AV node itself. However, AV nodal conduction curves recorded in perfused hearts did not differ between WT and  $Cx40^{-/-}$  mice (van Rijen et al., 2001), suggesting a possible role of autonomic activity in the observations in intact mice.

Both the left and right bundle branch normally express high levels of Cx40 (Simon et al., 1998; van Rijen et al., 2001). High resolution mapping has revealed that deletion of Cx40 leads to slower conduction in the left bundle branch and conduction block in the thinner right bundle branch, causing a delayed activation of the right ventricle (Tamaddon et al., 2000; van Rijen et al.,

2001). Interestingly, in mice the common bundle (expressing Cx40 and 45) is electrically connected to the base of the interventricular septum (expressing Cx43) through a small transitional zone expressing Cx43 and 45 (van Rijen et al., 2001; van Veen et al., 2005b). This arrangement results in an activation pattern within the septum from base to apex that is quite different from the pattern in humans (Durrer et al., 1970).

### VENTRICLES

In the ventricular myocardium, which expresses Cx43 but not Cx40, conduction velocity is unaffected by Cx40-deficiency and the inducibility of ventricular arrhythmias under normal conditions was not increased (Verheule et al., 1999; Bevilacqua et al., 2000; Tamaddon et al., 2000), although one study reported an increased inducibility of ventricular tachycardia (VT) in  $Cx40^{-/-}$  mice during infusion of isoproterenol (Bevilacqua et al., 2000), possibly involving the Purkinje system.

In none of the studies mentioned above did heterozygous  $Cx40^{+/-}$  mice display an electrophysiological phenotype that differed from  $Cx40^{+/+}$  mice, indicating that even a substantial reduction in Cx40 protein does not greatly affect cardiac conduction in mice. Moreover, although it differs considerably in its biophysical properties, Cx45 can replace Cx40 almost completely, because cardiac activation in Cx40KICx45 mice is normal, except for a slower conduction velocity in the left atrium and right bundle branch (Alcolea et al., 2004).

Two factors complicate the interpretation of electrophysiological data from  $Cx40^{-/-}$  mice. First, although this was not noted in the earliest studies, Cx40 deficient mice display a high incidence of a variety of cardiac malformations, including ventricular septal defects, tetralogy of Fallot, double-outlet right ventricles, endocardial cushion and aortic arch defects (Kirchhoff et al., 2000; Gu et al., 2003). The occurrence of cardiac malformations is exacerbated in mice in which a homozygous deletion of Cx40 is combined with a heterozygous deletion of either Cx43 (Kirchhoff et al., 2000) or Cx45 (Kruger et al., 2006), leading to neonatal lethality in the former and additional atrial defects and further delayed AV conduction in the latter. Mice that are homozygously deficient for both Cx40 and 43 die much earlier than  $Cx43^{-/-}$  mice, around embryonic day 12, with an abnormal rotation of the ventricles (Simon et al., 2004). Second, apart from expression by atrial myocytes and Purkinje cells, Cx40 is also expressed by endothelial cells (Dahl et al., 1995), together with Cx37. Interestingly, de Wit et al. have reported that in  $Cx40^{-/-}$  mice, arterioles show spontaneous, irregular vasomotion and that blood pressure is greatly increased from 90 to 120 mmHg (de Wit et al., 2003). To what extent hypertension in  $Cx40^{-/-}$  mice is responsible for secondary changes in cardiac pump function, autonomic regulation and electrophysiology (e.g., decreased heart rate and slower AV nodal conduction) is uncertain at present.

## CONNEXIN 43

### PROPERTIES AND EXPRESSION

Cx43 forms channels with a single channel conductance of 120 pS (in CsCl) and a modest voltage dependence ( $V_{1/2} = 60$  mV and  $G_{j, \min} = 0.4$ ) (Elenes et al., 2001).

In the developing mouse heart, Cx43 is specifically present in the trabeculated parts of the ventricle at embryonic day 12.5, but is abundantly expressed by the entire working myocardium later on (Coppen et al., 2003; Miquerol et al., 2003). Cx43 expression is suppressed by the transcription factors Tbx18 (specifying the SA node), Tbx2 and Tbx3 (specifying the AV conduction system) (Christoffels et al., 2004; Bakker et al., 2008; Kapoor et al., 2011; Sizarov et al., 2011).

Cx43<sup>-/-</sup> mice die shortly after birth from respiratory failure caused by a right ventricular outflow tract obstruction (Reaume et al., 1995). Abnormal cardiac development is already visible during the looping phase at embryonic day 10 (Ya et al., 1998). The outflow tract defect can be traced back to the neural crest, where abnormal p53 activation in Cx43<sup>-/-</sup> mice causes apoptosis of primordial germ cells that would otherwise have migrated to the heart (Lo et al., 1997; Francis and Lo, 2006). Both a deficiency and an excess of Cx43 can derail this process (Ewart et al., 1997; Huang et al., 1998), although it does not necessarily depend on Cx43 expression in the neural crest itself (Kretz et al., 2006). In addition to this defect, Cx43<sup>-/-</sup> (and Cx43<sup>+/-</sup>) mice also show abnormal patterning of the main coronary arteries (Li et al., 2002; Walker et al., 2005; Liu et al., 2006).

### VENTRICULAR CONDUCTION

Using optical mapping in Cx43<sup>-/-</sup> mouse embryos, Vaidya et al reported that ventricular conduction velocity was unaffected at embryonic day 12.5, when Cx40 is still present abundantly in the ventricle. At embryonic day 17.5 however, ventricular conduction velocity was greatly reduced and ventricular arrhythmias were frequently observed (Vaidya et al., 2001). Accordingly, gap junctional coupling and conduction velocity are dramatically reduced in cultured neonatal myocytes from Cx43<sup>-/-</sup> mice, which do not show a compensatory increase in Cx40 and 45 (Beauchamp et al., 2004; Vink et al., 2004).

In adult mice, Cx43 is expressed in the atrial and ventricular working myocardium and in the distal Purkinje system (Gourdie et al., 1991; Gros and Jongsma, 1996; van Veen et al., 2005b). Within the ventricular wall, Cx43 expression is lower in the epicardium than in deeper regions (Yamada et al., 2004). Unlike Cx43<sup>-/-</sup> mice, Cx43<sup>+/-</sup> mice survive and age normally (Betsuyaku et al., 2002), although ventricular and atrial level of Cx43 protein are reduced by approximately 50% (Guerrero et al., 1997; Thomas et al., 1998). There has been a debate about to what extent this reduction in expression affects conduction, with one group reporting a 50% reduction in ventricular conduction velocity (Guerrero et al., 1997; Eloff et al., 2001), and another group reporting no change (Morley et al., 2000). The latter result is in better agreement with studies using mathematical models, which predict a weaker dependence of conduction velocity on gap junctional coupling (Shaw and Rudy, 1997; Wiegerinck et al., 2006) and a study on strands of cultured myocytes from Cx43<sup>+/+</sup> and Cx43<sup>+/-</sup> mice, which did not show a difference in conduction velocity (Thomas et al., 2003). Moreover, two later studies in adult mice with conditional deletion of Cx43 showed a reduction of conduction velocity by approximately 40% while Cx43 protein level was decreased by 90% (Gutstein et al., 2001a; van Rijen et al., 2004). Conduction anisotropy and

heterogeneity were increased, especially in the RV. VT was readily induced by pacing, often with a stable reentrant circuit in the RV and fibrillatory conduction in the LV (van Rijen et al., 2004). Telemetric recordings revealed that most mice die from arrhythmic sudden death within weeks of the start of Cx elimination (Gutstein et al., 2001a). By contrast, in a conditional knock-out strain with a 50% reduction in Cx43, no change in conduction velocity was observed and no arrhythmias were inducible (van Rijen et al., 2004).

Similar findings were reported in mice with a cardiac-specific deletion with a gradual postnatal decline in Cx43 expression. At birth, cardiac structure in these mice is normal (Eckardt et al., 2006), but Cx43 protein decreases to 59% of control level at 25 days (without a change in conduction velocity) and 18% at 45 days (with a 50% decrease in conduction velocity). At the latter stage, lethal VTs could be induced in 80% of the mice (Danik et al., 2004). Interestingly, optical mapping during sinus rhythm in this model revealed ectopic sites of ventricular activation caused by a paradoxical increase in conduction across Purkinje-ventricular junctions (Morley et al., 2005). In another approach, chimeric mice were produced with a patchy Cx43 expression pattern in the ventricles. In addition to a depressed pump function, these mice showed heterogeneous ventricular conduction and spontaneous non-sustained VT (Gutstein et al., 2001b, 2005).

### REPLACEMENT OF Cx43

Several studies have assessed whether the role of Cx43 can be taken over by other Cxs, using knock-in mouse models in which Cx43 was replaced by Cx40, 32, 31, or 26. Anatomically, Cx43KI40 hearts showed no abnormalities at birth (apart from mild hypertrophy in some mice), whereas Cx43KI32 hearts showed a mild form of the RV outflow tract abnormalities seen in Cx43<sup>-/-</sup> mice (Plum et al., 2000). ECG intervals in adult Cx43KI32 and Cx43KI40 mice did not differ from those in control mice. However, spontaneous ventricular extrasystoles were observed more frequently in Cx43KI40 mice than in Cx43KI32 and control mice. In Cx43KI31 mice, the RV outflow tract obstruction is severe, cardiac conduction is markedly slow and mice die within days after birth (Zheng-Fischhofer et al., 2006). In this context it is worth noting that Cx31 is highly restricted in its ability to form channels with other Cxs (Elfgang et al., 1995). Neonatal Cx43KI26 mice do not have structurally abnormal hearts, have only slightly decelerated cardiac conduction, but died within weeks because of deficient lactation of their heterozygous mothers (Winterhager et al., 2007). Adult Cx43KI26 mice (reared by foster mothers) showed a small prolongation in His-to-ventricle conduction time and QRS duration. Thus, several connexins are able to replace Cx43 in the developing and healthy adult heart to a large degree. However, the consequences of replacing Cx43 may be more pronounced under pathological conditions (see below for an example in Cx43KI32 mice).

### RESPONSE TO ISCHEMIA

In the ventricles, the closing of gap junction channels in response to ischemia enables the myocardium to “heal-over” (de Mello

et al., 1969), but it is also associated with (phase 1b) arrhythmias occurring 15–60 min after the onset of ischemia (De Groot and Coronel, 2004; Wit and Peters, 2012). During acute ischemia, spontaneous and induced VT occurred more frequently in Cx43<sup>+/−</sup> than in Cx43<sup>+/+</sup> mice (Lerner et al., 2000). However, infarct size in the weeks after coronary occlusion was smaller in Cx43<sup>+/−</sup> mice (Kanno et al., 2003). At those later time points, the incidence of spontaneous and induced VT did not differ between Cx43<sup>+/−</sup> and Cx43<sup>+/+</sup> mice, suggesting that effect of reduced coupling is offset by the smaller infarct size (Betsuyaku et al., 2004).

Cx43 hemichannels are present in the plasma membrane and can open as a non-selective pore in response to metabolic inhibition, which would accelerate cell death (John et al., 1999; Kondo et al., 2000). Gap 19, a peptide that prevents hemichannel opening, without affecting gap junction channels, reduces ischemia/reperfusion damage (Wang et al., 2013).

In addition, Cx43 is located in the nuclear membrane and in subsarcolemmal mitochondria (Rodriguez-Sinovas et al., 2007; Boengler et al., 2009). Ischemic preconditioning increases the levels of mitochondrial Cx43 (Boengler et al., 2005) and accordingly, ischemic preconditioning is lost in Cx43<sup>+/−</sup> mice (Schwanke et al., 2002; Li et al., 2004). Cx43 is involved in mitochondrial K<sup>+</sup> uptake (Miro-Casas et al., 2009) and respiration (Boengler et al., 2012), forming hemichannels in the mitochondrial inner membrane that interact with other proteins (Rodriguez-Sinovas et al., 2007).

The carboxy terminus of the Cx43 protein is an important regulatory domain, involved in e.g., the response to intracellular acidification (Duffy et al., 2004). A mutant with a C terminal truncation shows a redistribution of Cx43 to the periphery of larger, sparser gap junctions (Maass et al., 2007). After ischemia/reperfusion, this mutant has larger infarcts and a higher incidence of induced VT (Maass et al., 2009). Similarly, increased gap junctional coupling by adenoviral transfection of the less pH-sensitive Cx32 increases infarct size in mice with a coronary occlusion (Prestia et al., 2011). Replacement of Cx43 with Cx32 has more complex effects (Rodriguez-Sinovas et al., 2010). Under normal conditions, ATP levels were decreased and lactate levels were increased in the myocardium of these Cx43KI32 mice. Although infarct size following ischemia/reperfusion was smaller, protection by preconditioning was lost, indicating that Cx32 cannot replace Cx43 in its role in mitochondrial metabolism and preconditioning.

### Cx43 MUTATIONS

Several models of mutations in Cx genes have been developed that correspond to inherited diseases in humans, as reviewed in (Dobrowolski and Willecke, 2009) and (Delmar and Makita, 2012). The G60S missense mutation in Cx43 acts in a dominant negative way to cause oculodentodigital dysplasia, including various cardiac manifestations (patent foramen ovale, reduced cardiac function, a large decrease in Cx43 due to impaired trafficking to the intercalated disc, a small decrease in ventricular conduction velocity and a variety of ECG abnormalities, both brady- and tachyarrhythmias) (Flenniken et al., 2005; Kalcheva et al., 2007; Manias et al., 2008; Tuomi et al., 2011). The

G138R (Dobrowolski et al., 2008) and I130T (Kalcheva et al., 2007) mutants show a similar phenotype of oculodentodigital dysplasia, including similar alterations in cardiac structure and function. However, in the case of G138R, Cx43 trafficking seems to be normal, but Cx43 (hemichannel) function is reduced due to a loss of phosphorylation. The importance of Cx43 phosphorylation is also underscored by a study on mice with “phosphatase resistant” Cx43, in which serine residues 325, 328, and 330 are replaced by either phosphomimetic glutamine (S3E) or non-phosphorylatable alanine (S3A) (Remo et al., 2011). S3E mice were resistant to gap junctional remodeling in response to transverse aortic constriction and showed a lower inducibility of VT than wildtype mice. Conversely, in S3A mice Cx43 was lost from the intercalated disc in response to transverse aortic constriction and inducibility of VT was higher than in wildtype mice.

### INTERACTIONS WITH OTHER PROTEINS

Cx43 interacts with a number of other proteins. Whereas the organizations of adherens junctions is not disrupted in the absence of Cx43 (Gutstein et al., 2003), conversely a loss of E-cadherin, N-cadherin, desmin or desmoplakin does greatly decrease Cx43 in intercalated discs (Ferreira-Cornwell et al., 2002; Gard et al., 2005; Kostetskii et al., 2005; Li et al., 2005; Gomes et al., 2012). Among the many changes in gene expression (directly or indirectly) caused by the absence of Cx43 (Iacobas et al., 2005), potassium current also show regional alterations in Cx43<sup>−/−</sup> mice, leading to proarrhythmic shortening of the action potential duration (Danik et al., 2008), whereas sodium channel function may (Desplantez et al., 2012; Jansen et al., 2012a) or may not (Johnson et al., 1999) be affected. Short term (6 h) ventricular pacing causes a decrease in Cx43 gene expression (Kontogeorgis et al., 2008a), while the shift in potassium channel expression in response to pacing was altered in Cx43<sup>+/−</sup> mice (Kontogeorgis et al., 2008b).

Interestingly, inducible deletion of Cx43 leads to increased fibrosis during aging and pressure overload because of enhanced fibroblast activity, with a concomitant increase in conduction heterogeneity and vulnerability to VT (Jansen et al., 2012b). On the other hand, TGF $\beta$ -dependent profibrotic signaling in response to myocardial infarction is blunted in Cx43<sup>+/−</sup> mice compared to Cx43<sup>+/+</sup> mice, leading to a decrease in post-infarct fibrosis (Zhang et al., 2010b), probably because of the difference in Cx43 expression in fibroblasts (Zhang et al., 2010a). With respect to arrhythmogenesis, these and some other studies highlight the clinically relevant conjunction of changes in excitability, electrical coupling and structural remodeling (van Veen et al., 2005a; Stein et al., 2009) that is poorly captured by monogenic alterations in transgenic mouse models.

### CONNEXIN 45

#### PROPERTIES AND EXPRESSION

Cx45 forms channels with small conductance of 30 pS that are the most sensitive to transjunctional voltage of all cardiac Cxs ( $V_{1/2} = 13$  mV,  $G_{j, \text{min}} = 0.12$ ) (Moreno et al., 1995). Cx45 is the connexin expressed earliest in the developing heart, and the only one present before embryonic day 9. Cx45-deficient

mice develop conduction block and a cushion defect caused by impairment of the epithelial-mesenchymal transformation of the cardiac endothelium (Kumai et al., 2000). Mice with cardiac myocyte-specific deletion of Cx45 do not have the cushion defect, but still develop conduction block and also die at around embryonic day 10 from pump failure (Nishii et al., 2003). The function of Cx45 in early cardiac development cannot be replaced by the neuronal connexin Cx36 (Frank et al., 2010).

### PACEMAKER AND CONDUCTION SYSTEM

During later embryonic development, Cx45 becomes increasingly localized to pacemaker and conduction system Alcolea et al., 1999; Coppen et al., 1999. In adult mice, Cx45 is the main connexin in the central SA node, a region apposed by protrusions of Cx40 and 43 positive atrial cells (Verheijck et al., 2001). Nevertheless, the heart rate is unaffected in mice with a heart-specific inducible Cx45 deletion (Frank et al., 2012). Furthermore, Cx45 is expressed along the entire AV conduction system, including the AV node, His bundle, proximal bundle branches and Purkinje system (Coppen et al., 1999; van Veen et al., 2005b). In adult mice, the dependence of AV conduction on the 3 Cxs expressed in the AV node region is complex. As noted above, mice deficient in Cx30.2 and 40 show accelerated and decelerated AV conduction, respectively (Schrickel et al., 2009). Apparently, Cx45 is sufficient for AV conduction, because mice deficient in both Cx30.2 and 40 show normal AV conduction (Schrickel et al., 2009). In mice with a heart-specific, inducible deficiency in Cx45, AV nodal conduction is slower than normal (Frank et al., 2012), whereas atrial and ventricular conduction was not affected (Bao et al., 2011). Interestingly, these mice also displayed a posttranslational reduction of Cx30.2 expression in the conduction system. Combining the inducible deficiency in Cx45 with a deficiency in Cx30.2 further slowed AV nodal conduction (Frank et al., 2012). Although a heterozygous deletion of Cx45 does not prolong the PR interval by itself, it does further increase the observed PR prolongation in Cx40-deficient mice (Kruger et al., 2006).

### WORKING MYOCARDIUM

Cx45 was initially thought to be widely expressed in the mammalian working myocardium (Davis et al., 1994; Verheule et al., 1997). Coppen et al. later showed that this observation was mainly caused by cross-reactivity of a Cx45 antibody with Cx43 (Coppen et al., 1998). Low levels of Cx45 are expressed in the mouse ventricular working myocardium, amounting to 0.3% of total gap junction protein (Bao et al., 2011). Cx45 can form both heterotypic (Elenes et al., 2001) and heteromeric (Desplantez et al., 2004) channels with Cx43. However, co-expression of Cx45 with Cx43 appears to decrease the size of gap junctions (Grikscheit et al., 2008). This phenomenon could be more important under conditions with a higher Cx45/Cx43 ratio, for example in the ventricular epicardium, where Cx43 levels are relatively low (Yamada et al., 2004), or during heart failure, where the expression of Cx45 increases and Cx43 decreases (Yamada et al., 2003). Indeed,

mice overexpressing Cx45 in the heart showed a reduction in gap junctional coupling and an increased inducibility of VT (Betsuyaku et al., 2006).

### CONNEXIN 46

Along with Cx50, Cx46 is the main connexin expressed in the lens, forming channels with a  $\gamma\gamma = 140 \text{ pS}$  in CsCl,  $V_{1/2} = 48 \text{ mV}$ ,  $G_{j, \min} = 0.11$  (Hopperstad et al., 2000). mRNA for Cx46 (and Cx50) has been detected in the adult canine heart (Davis et al., 1994). The localization of Cx46 (and Cx50) protein in the dog heart is unknown, although one study detected minimal Cx46 immunoreactivity between some atrial and ventricular myocytes (Davis et al., 1995). However, in neonatal mice Cx46-positive myocytes were detected in the cardiac conduction system (or more precisely in the atrium, AV canal, intraventricular septum and ventricular subendocardium) (Chi et al., 2010). Cx46-deficient mice displayed a slightly lower heart rate, a prolonged QRS and QT duration and a QRS morphology consistent with bundle branch block (Chi et al., 2010). Cx46 has a propensity to form functional hemichannels (Trexler et al., 1996; Pfahl and Dahl, 1999), but their role in the heart is unknown.

### CONCLUSIONS

The diversity of connexins in the heart allows fine-tuning of electrical coupling depending on the region and on conditions. As therapeutic strategies, both increasing and decreasing gap junctional coupling could in theory be beneficial under certain circumstances. However, a non-specific treatment targeting gap junctions may have beneficial effects in one part of the heart but cause deleterious side effects in another. Several compounds have been developed that can modulate gap junctions (Herve and Dhein, 2010; De Vuyst et al., 2011). Some of these have been successfully tested in animal models. For example, in canine model of heart failure, enhancing gap junctional coupling with rotigaptide can reduce the vulnerability to atrial fibrillation (Guerra et al., 2006). For more selective pharmacological manipulation of gap junction coupling, it is desirable for a treatment to be (1) specific to the heart and/or (2) specific for a particular connexin. In this respect, gap junction blocking “peptidomimetics,” a class of small peptide molecules that have some Cx selectivity, are especially promising (Evans et al., 2012). An enormous amount of knowledge on cardiac connexins has been gathered from genetically engineered mouse models, as described above. There are some important differences in cardiac electrophysiology in general and connexin distribution in particular between murine and human hearts (Kaese and Verheule, 2012). Nevertheless, for the development of connexin-specific treatment strategies, knowledge derived from transgenic mouse models provides a wealth of valuable insights.

### ACKNOWLEDGMENTS

Sven Kaese received a scholarship from the Peter-Osykpa-Foundation. Also supported by the European Union (FP7 Collaborative project EUTRAF, 261057) to Sander Verheule.

## REFERENCES

- Aanhaanen, W. T., Boukens, B. J., Sizarov, A., Wakker, V., De Gier-De Vries, C., Van Ginneken, A. C., et al. (2011). Defective Tbx2-dependent patterning of the atrioventricular canal myocardium causes accessory pathway formation in mice. *J. Clin. Invest.* 121, 534–544. doi: 10.1172/JCI44350
- Agullo-Pascual, E., and Delmar, M. (2012). The noncanonical functions of Cx43 in the heart. *J. Membr. Biol.* 245, 477–482. doi: 10.1007/s00232-012-9466-y
- Alcolea, S., Jarry-Guichard, T., De Bakker, J., Gonzalez, D., Lamers, W., Coppen, S., et al. (2004). Replacement of connexin40 by connexin45 in the mouse: impact on cardiac electrical conduction. *Circ. Res.* 94, 100–109. doi: 10.1161/01.RES.0000108261.67979.2A
- Alcolea, S., Theveniau-Ruissy, M., Jarry-Guichard, T., Marics, I., Tzouanacou, E., Chauvin, J. P., et al. (1999). Downregulation of connexin 45 gene products during mouse heart development. *Circ. Res.* 84, 1365–1379. doi: 10.1161/01.RES.84.12.1365
- Arnolds, D. E., Liu, F., Fahrenbach, J. P., Kim, G. H., Schillinger, K. J., Smemo, S., et al. (2012). TBX5 drives Scn5a expression to regulate cardiac conduction system function. *J. Clin. Invest.* 122, 2509–2518. doi: 10.1172/JCI62617
- Bagwe, S., Berenfeld, O., Vaidya, D., Morley, G. E., and Jalife, J. (2005). Altered right atrial excitation and propagation in connexin40 knockout mice. *Circulation* 112, 2245–2253. doi: 10.1161/CIRCULATIONAHA.104.527325
- Bakker, M. L., Boukens, B. J., Mommersteeg, M. T., Brons, J. F., Wakker, V., Moorman, A. F., et al. (2008). Transcription factor Tbx3 is required for the specification of the atrioventricular conduction system. *Circ. Res.* 102, 1340–1349. doi: 10.1161/CIRCRESAHA.107.169565
- Bao, M., Kanter, E. M., Huang, R. Y., Maxeiner, S., Frank, M., Zhang, Y., et al. (2011). Residual Cx45 and its relationship to Cx43 in murine ventricular myocardium. *Channels (Austin)* 5, 489–499. doi: 10.4161/chan.5.6.18523
- Beardslee, M. A., Laing, J. G., Beyer, E. C., and Saffitz, J. E. (1998). Rapid turnover of connexin43 in the adult rat heart. *Circ. Res.* 83, 629–635. doi: 10.1161/01.RES.83.6.629
- Beauchamp, P., Choby, C., Desplantez, T., De Peyer, K., Green, K., Yamada, K. A., et al. (2004). Electrical propagation in synthetic ventricular myocyte strands from germline connexin43 knockout mice. *Circ. Res.* 95, 170–178. doi: 10.1161/01.RES.0000134923.05174.2f
- Beauchamp, P., Yamada, K. A., Baertschi, A. J., Green, K., Kanter, E. M., Saffitz, J. E., et al. (2006). Relative contributions of connexins 40 and 43 to atrial impulse propagation in synthetic strands of neonatal and fetal murine cardiomyocytes. *Circ. Res.* 99, 1216–1224. doi: 10.1161/01.RES.0000250607.34498.b4
- Belluardo, N., White, T. W., Srinivas, M., Trovato-Salinaro, A., Rippis, H., Mudo, G., et al. (2001). Identification and functional expression of HCx31.9, a novel gap junction gene. *Cell Commun. Adhes.* 8, 173–178. doi: 10.3109/15419060109080719
- Betsuyaku, T., Kanno, S., Lerner, D. L., Schuessler, R. B., Saffitz, J. E., and Yamada, K. A. (2004). Spontaneous and inducible ventricular arrhythmias after myocardial infarction in mice. *Cardiovasc. Pathol.* 13, 156–164. doi: 10.1016/S1054-8807(03)00152-2
- Betsuyaku, T., Kovacs, A., Saffitz, J. E., and Yamada, K. A. (2002). Cardiac structure and function in young and senescent mice heterozygous for a connexin43 null mutation. *J. Mol. Cell. Cardiol.* 34, 175–184. doi: 10.1006/jmcc.2001.1499
- Betsuyaku, T., Nnebe, N. S., Sundset, R., Patibandla, S., Krueger, C. M., and Yamada, K. A. (2006). Overexpression of cardiac connexin45 increases susceptibility to ventricular tachyarrhythmias *in vivo*. *Am. J. Physiol. Heart Circ. Physiol.* 290, H163–H171. doi: 10.1152/ajpheart.01308.2004
- Bevilacqua, L. M., Simon, A. M., Maguire, C. T., Gehrmann, J., Wakimoto, H., Paul, D. L., et al. (2000). A targeted disruption in connexin40 leads to distinct atrioventricular conduction defects. *J. Interv. Card. Electrophysiol.* 4, 459–467. doi: 10.1023/A:1009800328836
- Boengler, K., Dodoni, G., Rodriguez-Sinovas, A., Cabestrero, A., Ruiz-Meana, M., Gres, P., et al. (2005). Connexin 43 in cardiomyocyte mitochondria and its increase by ischemic preconditioning. *Cardiovasc. Res.* 67, 234–244. doi: 10.1016/j.cardiores.2005.04.014
- Boengler, K., Ruiz-Meana, M., Gent, S., Ungefug, E., Soetkamp, D., Miro-Casas, E., et al. (2012). Mitochondrial connexin 43 impacts on respiratory complex I activity and mitochondrial oxygen consumption. *J. Cell. Mol. Med.* 16, 1649–1655. doi: 10.1111/j.1582-4934.2011.01516.x
- Boengler, K., Stahlhofen, S., Van De Sand, A., Gres, P., Ruiz-Meana, M., Garcia-Dorado, D., et al. (2009). Presence of connexin 43 in subsarcolemmal, but not in interfibrillar cardiomyocyte mitochondria. *Basic Res. Cardiol.* 104, 141–147. doi: 10.1007/s00395-009-0007-5
- Bukauskas, F. F., Kreuzberg, M. M., Rackauskas, M., Bukauskienė, A., Bennett, M. V., Verselis, V. K., et al. (2006). Properties of mouse connexin 30.2 and human connexin 31.9 hemichannels: implications for atrioventricular conduction in the heart. *Proc. Natl. Acad. Sci. U.S.A.* 103, 9726–9731. doi: 10.1073/pnas.0603372103
- Chandler, N. J., Greener, I. D., Tellez, J. O., Inada, S., Musa, H., Molenaar, P., et al. (2009). Molecular architecture of the human sinus node: insights into the function of the cardiac pacemaker. *Circulation* 119, 1562–1575. doi: 10.1161/CIRCULATIONAHA.108.804369
- Chi, N. C., Bussen, M., Brand-Arzamendi, K., Ding, C., Olgiv, J. E., Shaw, R. M., et al. (2010). Cardiac conduction is required to preserve cardiac chamber morphology. *Proc. Natl. Acad. Sci. U.S.A.* 107, 14662–14667. doi: 10.1073/pnas.0909432107
- Christoffels, V. M., Hoogaars, W. M., Tessari, A., Clout, D. E., Moorman, A. F., and Campione, M. (2004). T-box transcription factor Tbx2 represses differentiation and formation of the cardiac chambers. *Dev. Dyn.* 229, 763–770. doi: 10.1002/dvdy.10487
- Coppen, S. R., Dupont, E., Rothery, S., and Severs, N. J. (1998). Connexin45 expression is preferentially associated with the ventricular conduction system in mouse and rat heart. *Circ. Res.* 82, 232–243. doi: 10.1161/01.RES.82.2.232
- Coppen, S. R., Gourdie, R. G., and Severs, N. J. (2001). Connexin45 is the first connexin to be expressed in the central conduction system of the mouse heart. *Exp. Clin. Cardiol.* 6, 17–23.
- Coppen, S. R., Kaba, R. A., Halliday, D., Dupont, E., Skepper, J. N., Elneil, S., et al. (2003). Comparison of connexin expression patterns in the developing mouse heart and human foetal heart. *Mol. Cell. Biochem.* 242, 121–127. doi: 10.1023/A:1021150014764
- Coppen, S. R., Severs, N. J., and Gourdie, R. G. (1999). Connexin45 (alpha 6) expression delineates an extended conduction system in the embryonic and mature rodent heart. *Dev. Genet.* 24, 82–90.
- Cottrell, G. T., and Burt, J. M. (2001). Heterotypic gap junction channel formation between heteromeric and homomeric Cx40 and Cx43 connexons. *Am. J. Physiol. Cell Physiol.* 281, C1559–C1567.
- Dahl, E., Winterhager, E., Traub, O., and Willecke, K. (1995). Expression of gap junction genes, connexin40 and connexin43, during fetal mouse development. *Anat. Embryol.* 191, 267–278. doi: 10.1007/BF00187825
- Danik, S. B., Liu, F., Zhang, J., Suk, H. J., Morley, G. E., Fishman, G. I., et al. (2004). Modulation of cardiac gap junction expression and arrhythmic susceptibility. *Circ. Res.* 95, 1035–1041. doi: 10.1161/01.RES.0000148664.33695.2a
- Danik, S. B., Rosner, G., Lader, J., Gutstein, D. E., Fishman, G. I., and Morley, G. E. (2008). Electrical remodeling contributes to complex tachyarrhythmias in connexin43-deficient mouse hearts. *FASEB J.* 22, 1204–1212. doi: 10.1096/fj.07-8974com
- Davis, L. M., Kanter, H. L., Beyer, E. C., and Saffitz, J. E. (1994). Distinct gap junction protein phenotypes in cardiac tissues with disparate conduction properties. *J. Am. Coll. Cardiol.* 24, 1124–1132. doi: 10.1016/0735-1097(94)90879-6
- Davis, L. M., Rodefeld, M. E., Green, K., Beyer, E. C., and Saffitz, J. E. (1995). Gap junction protein phenotypes of the human heart and conduction system. *J. Cardiovasc. Electrophysiol.* 6, 813–822. doi: 10.1111/j.1540-8167.1995.tb00357.x
- De Groot, J. R., and Coronel, R. (2004). Acute ischemia-induced gap junctional uncoupling and arrhythmogenesis. *Cardiovasc. Res.* 62, 323–334. doi: 10.1016/j.cardiores.2004.01.033
- Delorme, B., Dahl, E., Jarry-Guichard, T., Briand, J. P., Willecke, K., Gros, D., et al. (1997). Expression pattern of connexin gene products at the early developmental stages of the mouse cardiovascular system. *Circ. Res.* 81, 423–437. doi: 10.1161/01.RES.81.3.423
- Delorme, B., Dahl, E., Jarry-Guichard, T., Marics, I., Briand, J. P., Willecke, K., et al. (1995). Developmental regulation of connexin 40 gene expression in mouse heart

- correlates with the differentiation of the conduction system. *Dev. Dyn.* 204, 358–371. doi: 10.1002/aja.1002040403
- Delmar, M., and Makita, N. (2012). Cardiac connexins, mutations and arrhythmias. *Curr. Opin. Cardiol.* 27, 236–241. doi: 10.1097/HCO.0b013e328352220e
- de Mello, W. C., Motta, G. E., and Chapeau, M. (1969). A study on the healing-over of myocardial cells of toads. *Circ. Res.* 24, 475–487. doi: 10.1161/01.RES.24.3.475
- Desplantez, T., Halliday, D., Dupont, E., and Weingart, R. (2004). Cardiac connexins Cx43 and Cx45: formation of diverse gap junction channels with diverse electrical properties. *Pflugers Arch.* 448, 363–375. doi: 10.1007/s00424-004-1250-0
- Desplantez, T., McCain, M. L., Beauchamp, P., Rigoli, G., Rothen-Rutishauser, B., Parker, K. K., et al. (2012). Connexin43 ablation in foetal atrial myocytes decreases electrical coupling, partner connexins, and sodium current. *Cardiovasc. Res.* 94, 58–65. doi: 10.1093/cvr/cvs025
- De Vuyst, E., Boengler, K., Antoons, G., Sipido, K. R., Schulz, R., and Leybaert, L. (2011). Pharmacological modulation of connexin-formed channels in cardiac pathophysiology. *Br. J. Pharmacol.* 163, 469–483. doi: 10.1111/j.1476-5381.2011.01244.x
- de Wit, C., Roos, F., Bolz, S. S., and Pohl, U. (2003). Lack of vascular connexin 40 is associated with hypertension and irregular arteriolar vasomotion. *Physiol. Genomics* 13, 169–177.
- Dhein, S. (2006). Cardiac ischemia and uncoupling: gap junctions in ischemia and infarction. *Adv. Cardiol.* 42, 198–212. doi: 10.1159/000092570
- Dhein, S. (2010). Cx30 in the sinus node of murine heart: just one connexin more, or more. Evidence for a construction principle? *Cardiovasc. Res.* 85, 7–8. doi: 10.1093/cvr/cvp351
- Dobrowolski, R., Sasse, P., Schrickel, J. W., Watkins, M., Kim, J. S., Rackauskas, M., et al. (2008). The conditional connexin43G138R mouse mutant represents a new model of hereditary oculodentodigital dysplasia in humans. *Hum. Mol. Genet.* 17, 539–554. doi: 10.1093/hmg/ddm329
- Dobrowolski, R., and Willecke, K. (2009). Connexin-caused genetic diseases and corresponding mouse models. *Antioxid. Redox Signal.* 11, 283–295. doi: 10.1089/ars.2008.2128
- Duffy, H. S. (2012). The molecular mechanisms of gap junction remodeling. *Heart Rhythm* 9, 1331–1334. doi: 10.1016/j.hrthm.2011.11.048
- Duffy, H. S., Ashton, A. W., O'donnell, P., Coombs, W., Taffet, S. M., Delmar, M., et al. (2004). Regulation of connexin43 protein complexes by intracellular acidification. *Circ. Res.* 94, 215–222. doi: 10.1161/01.RES.0000113924.06926.11
- Dupont, E., Matsushita, T., Kaba, R. A., Vozzi, C., Coppen, S. R., Khan, N., et al. (2001). Altered connexin expression in human congestive heart failure. *J. Mol. Cell. Cardiol.* 33, 359–371. doi: 10.1006/jmcc.2000.1308
- Durrer, D., Van Dam, R. T., Freud, G. E., Janse, M. J., Meijler, F. L., and Arzbaecher, R. C. (1970). Total excitation of the isolated human heart. *Circulation* 41, 899–912. doi: 10.1161/01.CIR.41.6.899
- Eckardt, D., Kirchhoff, S., Kim, J. S., Degen, J., Theis, M., Ott, T., et al. (2006). Cardiomyocyte-restricted deletion of connexin43 during mouse development. *J. Mol. Cell. Cardiol.* 41, 963–971. doi: 10.1016/j.jmcc.2006.07.017
- Eckardt, D., Theis, M., Degen, J., Ott, T., van Rijen, H. V., Kirchhoff, S., et al. (2004). Functional role of connexin43 gap junction channels in adult mouse heart assessed by inducible gene deletion. *J. Mol. Cell. Cardiol.* 36, 101–110. doi: 10.1016/j.jmcc.2003.10.006
- Elenes, S., Martinez, A. D., Delmar, M., Beyer, E. C., and Moreno, A. P. (2001). Heterotypic docking of Cx43 and Cx45 connexons blocks fast voltage gating of Cx43. *Biophys. J.* 81, 1406–1418. doi: 10.1016/S0006-3495(01)75796-7
- Elenes, S., Rubart, M., and Moreno, A. P. (1999). Junctional communication between isolated pairs of canine atrial cells is mediated by homogeneous and heterogeneous gap junction channels. *J. Cardiovasc. Electrophysiol.* 10, 990–1004. doi: 10.1111/j.1540-8167.1999.tb01270.x
- Elfgang, C., Eckert, R., Lichtenberg-Frate, H., Butterweck, A., Traub, O., Klein, R. A., et al. (1995). Specific permeability and selective formation of gap junction channels in connexin-transfected HeLa cells. *J. Cell Biol.* 129, 805–817. doi: 10.1083/jcb.129.3.805
- Eloff, B. C., Lerner, D. L., Yamada, K. A., Schuessler, R. B., Saffitz, J. E., and Rosenbaum, D. S. (2001). High resolution optical mapping reveals conduction slowing in connexin43 deficient mice. *Cardiovasc. Res.* 51, 681–690. doi: 10.1016/S0008-6363(01)00341-8
- Evans, W. H., Bultynck, G., and Leybaert, L. (2012). Manipulating connexin communication channels: use of peptidomimetics and the translational outputs. *J. Membr. Biol.* 245, 437–449. doi: 10.1007/s00232-012-9488-5
- Ewart, J. L., Cohen, M. F., Meyer, R. A., Huang, G. Y., Wessels, A., Gourdie, R. G., et al. (1997). Heart and neural tube defects in transgenic mice overexpressing the Cx43 gap junction gene. *Development* 124, 1281–1292.
- Ferreira-Cornwell, M. C., Luo, Y., Narula, N., Lenox, J. M., Lieberman, M., and Radice, G. L. (2002). Remodeling the intercalated disc leads to cardiomyopathy in mice misexpressing cadherins in the heart. *J. Cell. Sci.* 115, 1623–1634.
- Fleniken, A. M., Osborne, L. R., Anderson, N., Ciliberti, N., Fleming, C., Gittens, J. E., et al. (2005). A Gja1 missense mutation in a mouse model of oculodentodigital dysplasia. *Development* 132, 4375–4386. doi: 10.1242/dev.02011
- Francis, R. J., and Lo, C. W. (2006). Primordial germ cell deficiency in the connexin 43 knockout mouse arises from apoptosis associated with abnormal p53 activation. *Development* 133, 3451–3460. doi: 10.1242/dev.02506
- Frank, M., Eiberger, B., Janssen-Bienhold, U., De Sevilla Muller, L. P., Tjarks, A., Kim, J. S., et al. (2010). Neuronal connexin-36 can functionally replace connexin-45 in mouse retina but not in the developing heart. *J. Cell Sci.* 123, 3605–3615. doi: 10.1242/jcs.068668
- Frank, M., Wirth, A., Andrie, R. P., Kreuzberg, M. M., Dobrowolski, R., Seifert, G., et al. (2012). Connexin45 provides optimal atrioventricular nodal conduction in the adult mouse heart. *Circ. Res.* 111, 1528–1538. doi: 10.1161/CIRCRESAHA.112.270561
- Gard, J. J., Yamada, K., Green, K. G., Eloff, B. C., Rosenbaum, D. S., Wang, X., et al. (2005). Remodeling of gap junctions and slow conduction in a mouse model of desmin-related cardiomyopathy. *Cardiovasc. Res.* 67, 539–547. doi: 10.1016/j.cardiores.2005.04.004
- Gemel, J., Lin, X., Collins, R., Veenstra, R. D., and Beyer, E. C. (2008). Cx30.2 can form heteromeric gap junction channels with other cardiac connexins. *Biochem. Biophys. Res. Commun.* 369, 388–394. doi: 10.1016/j.bbrc.2008.02.040
- Glukhov, A. V., Fedorov, V. V., Anderson, M. E., Mohler, P. J., and Efimov, I. R. (2010). Functional anatomy of the murine sinus node: high-resolution optical mapping of ankyrin-B heterozygous mice. *Am. J. Physiol. Heart Circ. Physiol.* 299, H482–H491. doi: 10.1152/ajpheart.00756.2009
- Gomes, J., Finlay, M., Ahmed, A. K., Ciaccio, E. J., Asimaki, A., Saffitz, J. E., et al. (2012). Electrophysiological abnormalities precede overt structural changes in arrhythmicogenic right ventricular cardiomyopathy due to mutations in desmoplakin-A combined murine and human study. *Eur. Heart J.* 33, 1942–1953. doi: 10.1093/eurheartj/ehr472
- Gonzalez, D., Gomez-Hernandez, J. M., and Barrio, L. C. (2007). Molecular basis of voltage dependence of connexin channels: an integrative appraisal. *Prog. Biophys. Mol. Biol.* 94, 66–106. doi: 10.1016/j.pbiomolbio.2007.03.007
- Gourdie, R. G., Green, C. R., and Severs, N. J. (1991). Gap junction distribution in adult mammalian myocardium revealed by an anti-peptide antibody and laser scanning confocal microscopy. *J. Cell Sci.* 99, 41–55.
- Greener, I. D., Monfredi, O., Inada, S., Chandler, N. J., Tellez, J. O., Atkinson, A., et al. (2011). Molecular architecture of the human specialised atrioventricular conduction axis. *J. Mol. Cell. Cardiol.* 50, 642–651. doi: 10.1016/j.jmcc.2010.12.017
- Grikscheit, K., Thomas, N., Bruce, A. F., Rothery, S., Chan, J., Severs, N. J., et al. (2008). Coexpression of connexin 45 with connexin 43 decreases gap junction size. *Cell Commun. Adhes.* 15, 185–193. doi: 10.1080/15419060802013943
- Gros, D., Theveniau-Ruissey, M., Bernard, M., Calmels, T., Kober, F., Sohl, G., et al. (2010). Connexin 30 is expressed in the mouse sino-atrial node and modulates heart rate. *Cardiovasc. Res.* 85, 45–55. doi: 10.1093/cvr/cvp280
- Gros, D. B., and Jongsma, H. J. (1996). Connexins in mammalian heart function. *Bioessays* 18, 719–730. doi: 10.1002/bies.950180907
- Gu, H., Smith, F. C., Taffet, S. M., and Delmar, M. (2003). High incidence of cardiac malformations in connexin40-deficient mice. *Circ. Res.* 93, 201–206. doi: 10.1161/01. RES.0000084852.65396.70
- Guerra, J. M., Everett, T. H. T., Lee, K. W., Wilson, E., and Olglin,

- J. E. (2006). Effects of the gap junction modifier rotigaptide (ZP123) on atrial conduction and vulnerability to atrial fibrillation. *Circulation* 114, 110–118. doi: 10.1161/CIRCULATIONAHA.105.606251
- Guerrero, P. A., Schuessler, R. B., Davis, L. M., Beyer, E. C., Johnson, C. M., Yamada, K. A., et al. (1997). Slow ventricular conduction in mice heterozygous for a connexin43 null mutation. *J. Clin. Invest.* 99, 1991–1998. doi: 10.1172/JCI119367
- Gutstein, D. E., Danik, S. B., Lewiton, S., France, D., Liu, F., Chen, F. L., et al. (2005). Focal gap junction uncoupling and spontaneous ventricular ectopy. *Am. J. Physiol. Heart Circ. Physiol.* 289, H1091–H1098. doi: 10.1152/ajpheart.00095.2005
- Gutstein, D. E., Liu, F. Y., Meyers, M. B., Choo, A., and Fishman, G. I. (2003). The organization of adherens junctions and desmosomes at the cardiac intercalated disc is independent of gap junctions. *J. Cell. Sci.* 116, 875–885. doi: 10.1242/jcs.00258
- Gutstein, D. E., Morley, G. E., Tamaddon, H., Vaidya, D., Schneider, M. D., Chen, J., et al. (2001a). Conduction slowing and sudden arrhythmic death in mice with cardiac-restricted inactivation of connexin43. *Circ. Res.* 88, 333–339. doi: 10.1161/01.RES.88.3.333
- Gutstein, D. E., Morley, G. E., Vaidya, D., Liu, F., Chen, F. L., Stuhlmann, H., et al. (2001b). Heterogeneous expression of gap junction channels in the heart leads to conduction defects and ventricular dysfunction. *Circulation* 104, 1194–1199. doi: 10.1161/hc3601.093990
- Haefliger, J. A., Polikar, R., Schnyder, G., Burdet, M., Sutter, E., Pexieder, T., et al. (2000). Connexin37 in normal and pathological development of mouse heart and great arteries. *Dev. Dyn.* 218, 331–344.
- Hagendorff, A., Schumacher, B., Kirchhoff, S., Luderitz, B., and Willecke, K. (1999). Conduction disturbances and increased atrial vulnerability in Connexin40-deficient mice analyzed by transesophageal stimulation. *Circulation* 99, 1508–1515. doi: 10.1161/01.CIR.99.11.1508
- Harris, B. S., Spruill, L., Edmonson, A. M., Rackley, M. S., Benson, D. W., O'brien, T. X., et al. (2006). Differentiation of cardiac Purkinje fibers requires precise spatiotemporal regulation of Nkx2.5 expression. *Dev. Dyn.* 235, 38–49. doi: 10.1002/dvdy.20580
- He, D. S., Jiang, J. X., Taffet, S. M., and Burt, J. M. (1999). Formation of heteromeric gap junction channels by connexins 40 and 43 in vascular smooth muscle cells. *Proc. Natl. Acad. Sci. U.S.A.* 96, 6495–6500. doi: 10.1073/pnas.96.11.6495
- Herve, J. C., Bourmeyster, N., Sarrouilhe, D., and Duffy, H. S. (2007). Gap junctional complexes: from partners to functions. *Prog. Biophys. Mol. Biol.* 94, 29–65. doi: 10.1016/j.pbiomolbio.2007.03.010
- Herve, J. C., and Dhein, S. (2010). Peptides targeting gap junctional structures. *Curr. Pharm. Des.* 16, 3056–3070. doi: 10.2174/138161210793292528
- Hoogaars, W. M., Tessari, A., Moorman, A. F., De Boer, P. A., Hagoort, J., Soufan, A. T., et al. (2004). The transcriptional repressor Tbx3 delineates the developing central conduction system of the heart. *Cardiovasc. Res.* 62, 489–499. doi: 10.1016/j.cardiores.2004.01.030
- Hopperstad, M. G., Srinivas, M., and Spray, D. C. (2000). Properties of gap junction channels formed by Cx46 alone and in combination with Cx50. *Biophys. J.* 79, 1954–1966. doi: 10.1016/S0006-3495(00)76444-7
- Houghton, F. D., Thonissen, E., Kidder, G. M., Naus, C. C., Willecke, K., and Winterhager, E. (1999). Doubly mutant mice, deficient in connexin32 and -43, show normal prenatal development of organs where the two gap junction proteins are expressed in the same cells. *Dev. Genet.* 24, 5–12.
- Huang, G. Y., Wessels, A., Smith, B. R., Linask, K. K., Ewart, J. L., and Lo, C. W. (1998). Alteration in connexin 43 gap junction gene dosage impairs conotruncal heart development. *Dev. Biol.* 198, 32–44. doi: 10.1016/S0012-1606(98)80027-4
- Hucker, W. J., McCain, M. L., Laughner, J. I., Iaizzo, P. A., and Efimov, I. R. (2008). Connexin 43 expression delineates two discrete pathways in the human atrioventricular junction. *Anat. Rec. (Hoboken)* 291, 204–215. doi: 10.1002/ar.20631
- Iacobas, D. A., Iacobas, S., Li, W. E., Zoidl, G., Dermietzel, R., and Spray, D. C. (2005). Genes controlling multiple functional pathways are transcriptionally regulated in connexin43 null mouse heart. *Physiol. Genomics* 20, 211–223. doi: 10.1152/physiolgenomics.00229.2003
- Jansen, J. A., Noorman, M., Musa, H., Stein, M., De Jong, S., van Der Nagel, R., et al. (2012a). Reduced heterogeneous expression of Cx43 results in decreased Nav1.5 expression and reduced sodium current that accounts for arrhythmia vulnerability in conditional Cx43 knockout mice. *Heart Rhythm* 9, 600–607. doi: 10.1016/j.hrthm.2011.11.025
- Jansen, J. A., van Veen, T. A., De Jong, S., van Der Nagel, R., van Stuijvenberg, L., Driessen, H., et al. (2012b). Reduced Cx43 expression triggers increased fibrosis due to enhanced fibroblast activity. *Circ. Arrhythm. Electrophysiol.* 5, 380–390. doi: 10.1161/CIRCEP.111.966580
- John, S. A., Kondo, R., Wang, S. Y., Goldhaber, J. I., and Weiss, J. N. (1999). Connexin-43 hemichannels opened by metabolic inhibition. *J. Biol. Chem.* 274, 236–240. doi: 10.1074/jbc.274.1.236
- Johnson, C. M., Green, K. G., Kanter, E. M., Bou-Aboud, E., Saffitz, J. E., and Yamada, K. A. (1999). Voltage-gated Na<sup>+</sup> channel activity and connexin expression in Cx43-deficient cardiac myocytes. *J. Cardiovasc. Electrophysiol.* 10, 1390–1401. doi: 10.1111/j.1540-8167.1999.tb00195.x
- Joyner, R. W., and van Capelle, F. J. (1986). Propagation through electrically coupled cells. How a small SA node drives a large atrium. *Biophys. J.* 50, 1157–1164. doi: 10.1016/S0006-3495(86)83559-7
- Joyner, R. W., Wang, Y. G., Wilders, R., Golod, D. A., Wagner, M. B., Kumar, R., et al. (2000). A spontaneously active focus drives a model atrial sheet more easily than a model ventricular sheet. *Am. J. Physiol. Heart Circ. Physiol.* 279, H752–H763.
- Kaese, S., and Verheule, S. (2012). Cardiac electrophysiology in mice: a matter of size. *Front. Physiol.* 3:345. doi: 10.3389/fphys.2012.00345
- Kalcheva, N., Qu, J., Sandeep, N., Garcia, L., Zhang, J., Wang, Z., et al. (2007). Gap junction remodeling and cardiac arrhythmogenesis in a murine model of oculodenotidigital dysplasia. *Proc. Natl. Acad. Sci. U.S.A.* 104, 20512–20516. doi: 10.1073/pnas.0705472105
- Kanagaratnam, P., Rothery, S., Patel, P., Severs, N. J., and Peters, N. S. (2002). Relative expression of immunolocalized connexins 40 and 43 correlates with human atrial conduction properties. *J. Am. Coll. Cardiol.* 39, 116–123. doi: 10.1016/S0735-1097(01)01710-7
- Kanno, S., Kovacs, A., Yamada, K. A., and Saffitz, J. E. (2003). Connexin43 as a determinant of myocardial infarct size following coronary occlusion in mice. *J. Am. Coll. Cardiol.* 41, 681–686. doi: 10.1016/S0735-1097(02)02893-0
- Kapoor, N., Galang, G., Marban, E., and Cho, H. C. (2011). Transcriptional suppression of connexin43 by TBX18 undermines cell-cell electrical coupling in postnatal cardiomyocytes. *J. Biol. Chem.* 286, 14073–14079. doi: 10.1074/jbc.M110.185298
- Kirchhoff, S., Kim, J. S., Hagendorff, A., Thonissen, E., Kruger, O., Lamers, W. H., et al. (2000). Abnormal cardiac conduction and morphogenesis in connexin40 and connexin43 double-deficient mice. *Circ. Res.* 87, 399–405. doi: 10.1161/01.RES.87.5.399
- Kirchhoff, S., Nelles, E., Hagendorff, A., Kruger, O., Traub, O., and Willecke, K. (1998). Reduced cardiac conduction velocity and predisposition to arrhythmias in connexin40-deficient mice. *Curr. Biol.* 8, 299–302. doi: 10.1016/S0960-9822(98)70114-9
- Kondo, R. P., Wang, S. Y., John, S. A., Weiss, J. N., and Goldhaber, J. I. (2000). Metabolic inhibition activates a non-selective current through connexin hemichannels in isolated ventricular myocytes. *J. Mol. Cell. Cardiol.* 32, 1859–1872. doi: 10.1006/jmcc.2000.1220
- Kontogeorgis, A., Kaba, R. A., Kang, E., Feig, J. E., Gupta, P. P., Ponzio, M., et al. (2008a). Short-term pacing in the mouse alters cardiac expression of connexin43. *BMC Physiol.* 8:8. doi: 10.1186/1472-6793-8-8
- Kontogeorgis, A., Li, X., Kang, E. Y., Feig, J. E., Ponzio, M., Kang, G., et al. (2008b). Decreased connexin43 expression in the mouse heart potentiates pacing-induced remodeling of repolarizing currents. *Am. J. Physiol. Heart Circ. Physiol.* 295, H1905–H1916. doi: 10.1152/ajpheart.590.2008
- Kostetskii, I., Li, J., Xiong, Y., Zhou, R., Ferrari, V. A., Patel, V. V., et al. (2005). Induced deletion of the N-cadherin gene in the heart leads to dissolution of the intercalated disc structure. *Circ. Res.* 96, 346–354. doi: 10.1161/01.RES.0000156274.72390.2c
- Kretz, M., Eckardt, D., Kruger, O., Kim, J. S., Maurer, J., Theis, M., et al. (2006). Normal embryonic development and cardiac morphogenesis in mice with Wnt1-Cre-mediated deletion of connexin43. *Genesis* 44, 269–276. doi: 10.1002/dvg.20204
- Kreuzberg, M. M., Liebermann, M., Segschneider, S., Dobrowolski, R., Dobrzynski, H., Kaba, R., et al. (2009). Human connexin31,9,

- unlike its orthologous protein connexin30.2 in the mouse, is not detectable in the human cardiac conduction system. *J. Mol. Cell. Cardiol.* 46, 553–559. doi: 10.1016/j.yjmcc.2008.12.007
- Kreuzberg, M. M., Schrickel, J. W., Ghanem, A., Kim, J. S., Degen, J., Janssen-Bienhold, U., et al. (2006). Connexin30.2 containing gap junction channels decelerate impulse propagation through the atrioventricular node. *Proc. Natl. Acad. Sci. U.S.A.* 103, 5959–5964. doi: 10.1073/pnas.0508512103
- Kreuzberg, M. M., Sohl, G., Kim, J. S., Verselis, V. K., Willecke, K., and Bukauskas, F. F. (2005). Functional properties of mouse connexin30.2 expressed in the conduction system of the heart. *Circ. Res.* 96, 1169–1177. doi: 10.1161/01.RES.0000169271.33675.05
- Kruger, O., Maxeiner, S., Kim, J. S., van Rijen, H. V., De Bakker, J. M., Eckardt, D., et al. (2006). Cardiac morphogenetic defects and conduction abnormalities in mice homozygously deficient for connexin40 and heterozygously deficient for connexin45. *J. Mol. Cell. Cardiol.* 41, 787–797. doi: 10.1016/j.yjmcc.2006.07.005
- Kumai, M., Nishii, K., Nakamura, K., Takeda, N., Suzuki, M., and Shibata, Y. (2000). Loss of connexin45 causes a cushion defect in early cardiogenesis. *Development* 127, 3501–3512.
- Leaf, D. E., Feig, J. E., Vasquez, C., Riva, P. L., Yu, C., Lader, J. M., et al. (2008). Connexin40 imparts conduction heterogeneity to atrial tissue. *Circ. Res.* 103, 1001–1008. doi: 10.1161/CIRCRESAHA.107.168997
- Lerner, D. L., Yamada, K. A., Schuessler, R. B., and Saffitz, J. E. (2000). Accelerated onset and increased incidence of ventricular arrhythmias induced by ischemia in Cx43-deficient mice. *Circulation* 101, 547–552. doi: 10.1161/01.CIR.101.5.547
- Li, J., Patel, V. V., Kostetskii, I., Xiong, Y., Chu, A. F., Jacobson, J. T., et al. (2005). Cardiac-specific loss of N-cadherin leads to alteration in connexins with conduction slowing and arrhythmogenesis. *Circ. Res.* 97, 474–481. doi: 10.1161/01.RES.0000181132.11393.18
- Li, W. E., Waldo, K., Linask, K. L., Chen, T., Wessels, A., Parmacek, M. S., et al. (2002). An essential role for connexin43 gap junctions in mouse coronary artery development. *Development* 129, 2031–2042.
- Li, X., Heinzel, F. R., Boengler, K., Schulz, R., and Heusch, G. (2004). Role of connexin 43 in ischemic preconditioning does not involve intercellular communication through gap junctions. *J. Mol. Cell. Cardiol.* 36, 161–163. doi: 10.1016/j.yjmcc.2003.10.019
- Lin, J., and Keener, J. P. (2010). Modeling electrical activity of myocardial cells incorporating the effects of ephaptic coupling. *Proc. Natl. Acad. Sci. U.S.A.* 107, 20935–20940. doi: 10.1073/pnas.1010154107
- Lin, X., Gemel, J., Beyer, E. C., and Veenstra, R. D. (2005). Dynamic model for ventricular junctional conductance during the cardiac action potential. *Am. J. Physiol. Heart Circ. Physiol.* 288, H1113–H1123. doi: 10.1152/ajpheart.00882.2004
- Lin, X., Gemel, J., Glass, A., Zemlin, C. W., Beyer, E. C., and Veenstra, R. D. (2010). Connexin40 and connexin43 determine gating properties of atrial gap junction channels. *J. Mol. Cell. Cardiol.* 48, 238–245. doi: 10.1016/j.yjmcc.2009.05.014
- Lin, X., and Veenstra, R. D. (2004). Action potential modulation of connexin40 gap junctional conductance. *Am. J. Physiol. Heart Circ. Physiol.* 286, H1726–H1735. doi: 10.1152/ajpheart.00943.2003
- Liu, S., Liu, F., Schneider, A. E., St Amand, T., Epstein, J. A., and Gutstein, D. E. (2006). Distinct cardiac malformations caused by absence of connexin 43 in the neural crest and in the non-crest neural tube. *Development* 133, 2063–2073. doi: 10.1242/dev.02374
- Lo, C. W., Cohen, M. F., Huang, G. Y., Lazatin, B. O., Patel, N., Sullivan, R., et al. (1997). Cx43 gap junction gene expression and gap junctional communication in mouse neural crest cells. *Dev. Genet.* 20, 119–132.
- Maass, K., Chase, S. E., Lin, X., and Delmar, M. (2009). Cx43 CT domain influences infarct size and susceptibility to ventricular tachyarrhythmias in acute myocardial infarction. *Cardiovasc. Res.* 84, 361–367. doi: 10.1093/cvr/cvp250
- Maass, K., Ghanem, A., Kim, J. S., Saathoff, M., Urschel, S., Kirfel, G., et al. (2004). Defective epidermal barrier in neonatal mice lacking the C-terminal region of connexin43. *Mol. Biol. Cell* 15, 4597–4608. doi: 10.1091/mbc.E04-04-0324
- Maass, K., Shibayama, J., Chase, S. E., Willecke, K., and Delmar, M. (2007). C-terminal truncation of connexin43 changes number, size, and localization of cardiac gap junction plaques. *Circ. Res.* 101, 1283–1291. doi: 10.1161/CIRCRESAHA.107.162818
- Manias, J. L., Plante, I., Gong, X. Q., Shao, Q., Churko, J., Bai, D., et al. (2008). Fate of connexin43 in cardiac tissue harbouring a disease-linked connexin43 mutant. *Cardiovasc. Res.* 80, 385–395. doi: 10.1093/cvr/cvn203
- Miquerol, L., Dupays, L., Theveniau-Ruissy, M., Alcolea, S., Jarry-Guichard, T., Abran, P., et al. (2003). Gap junctional connexins in the developing mouse cardiac conduction system. *Novartis Found. Symp.* 250, 80–98. discussion 98–109, 276–279.
- Miquerol, L., Meysen, S., Mangoni, M., Bois, P., van Rijen, H. V., Abran, P., et al. (2004). Architectural and functional asymmetry of the His-Purkinje system of the murine heart. *Cardiovasc. Res.* 63, 77–86. doi: 10.1016/j.cardiores.2004.03.007
- Miro-Casas, E., Ruiz-Meana, M., Agullo, E., Stahlhofen, S., Rodriguez-Sinovas, A., Cabestrero, A., et al. (2009). Connexin43 in cardiomyocyte mitochondria contributes to mitochondrial potassium uptake. *Cardiovasc. Res.* 83, 747–756. doi: 10.1093/cvr/cvp157
- Moreno, A. P., Laing, J. G., Beyer, E. C., and Spray, D. C. (1995). Properties of gap junction channels formed of connexin 45 endogenously expressed in human hepatoma (SKHep1) cells. *Am. J. Physiol.* 268, C356–C365.
- Morley, G. E., Danik, S. B., Bernstein, S., Sun, Y., Rosner, G., Gutstein, D. E., et al. (2005). Reduced intercellular coupling leads to paradoxical propagation across the Purkinje-ventricular junction and aberrant myocardial activation. *Proc. Natl. Acad. Sci. U.S.A.* 102, 4126–4129. doi: 10.1073/pnas.050881102
- Morley, G. E., Vaidya, D., and Jalife, J. (2000). Characterization of conduction in the ventricles of normal and heterozygous Cx43 knockout mice using optical mapping. *J. Cardiovasc. Electrophysiol.* 11, 375–377. doi: 10.1111/j.1540-8167.2000.tb01811.x
- Munger, S. J., Kanady, J. D., and Simon, A. M. (2013). Absence of venous valves in mice lacking Connexin37. *Dev. Biol.* 373, 338–348. doi: 10.1016/j.ydbio.2012.10.032
- Munshi, N. V., McAnally, J., Bezprozvannaya, S., Berry, J. M., Richardson, J. A., Hill, J. A., et al. (2009). Cx30.2 enhancer analysis identifies Gata4 as a novel regulator of atrioventricular delay. *Development* 136, 2665–2674. doi: 10.1242/dev.038562
- Nishii, K., Kumai, M., Egashira, K., Miwa, T., Hashizume, K., Miyano, Y., et al. (2003). Mice lacking connexin45 conditionally in cardiac myocytes display embryonic lethality similar to that of germline knockout mice without endocardial cushion defect. *Cell Commun. Adhes.* 10, 365–369.
- Pfahnl, A., and Dahl, G. (1999). Gating of cx46 gap junction hemichannels by calcium and voltage. *Pflugers Arch.* 437, 345–353. doi: 10.1007/s004240050788
- Pizard, A., Burgon, P. G., Paul, D. L., Bruneau, B. G., Seidman, C. E., and Seidman, J. G. (2005). Connexin 40, a target of transcription factor Tbx5, patterns wrist, digits, and sternum. *Mol. Cell. Biol.* 25, 5073–5083. doi: 10.1128/MCB.25.12.5073-5083.2005
- Plum, A., Hallas, G., Magin, T., Dombrowski, F., Hagendorff, A., Schumacher, B., et al. (2000). Unique and shared functions of different connexins in mice. *Curr. Biol.* 10, 1083–1091. doi: 10.1016/S0960-9822(00)00690-4
- Prestia, K. A., Sosunov, E. A., Anyukhovsky, E. P., Dolmatova, E., Kelly, C. W., Brink, P. R., et al. (2011). Increased cell-cell coupling increases infarct size and does not decrease incidence of ventricular tachycardia in mice. *Front. Physiol.* 2:1. doi: 10.3389/fphys.2011.00001
- Rackauskas, M., Neverauskas, V., and Skeberdis, V. A. (2010). Diversity and properties of connexin gap junction channels. *Medicina (Kaunas)* 46, 1–12.
- Reaume, A. G., De Sousa, P. A., Kulkarni, S., Langille, B. L., Zhu, D., Davies, T. C., et al. (1995). Cardiac malformation in neonatal mice lacking connexin43. *Science* 267, 1831–1834. doi: 10.1126/science.7892609
- Reed, K. E., Westphale, E. M., Larson, D. M., Wang, H. Z., Veenstra, R. D., and Beyer, E. C. (1993). Molecular cloning and functional expression of human connexin37, an endothelial cell gap junction protein. *J. Clin. Invest.* 91, 997–1004. doi: 10.1172/JCI116321
- Remo, B. F., Qu, J., Volpicelli, F. M., Giovannone, S., Shin, D., Lader, J., et al. (2011). Phosphatase-resistant gap junctions inhibit pathological remodeling and prevent arrhythmias. *Circ. Res.* 108, 1459–1466. doi: 10.1161/CIRCRESAHA.111.244046
- Rentschler, S., Harris, B. S., Kuznecoff, L., Jain, R., Manderfield, L.,

- Lu, M. M., et al. (2011). Notch signaling regulates murine atrioventricular conduction and the formation of accessory pathways. *J. Clin. Invest.* 121, 525–533. doi: 10.1172/JCI44470
- Rodriguez-Sinovas, A., Cabestrero, A., Lopez, D., Torre, I., Morente, M., Abellán, A., et al. (2007). The modulatory effects of connexin 43 on cell death/survival beyond cell coupling. *Prog. Biophys. Mol. Biol.* 94, 219–232. doi: 10.1016/j.pbiomolbio.2007.03.003
- Rodriguez-Sinovas, A., Sanchez, J. A., Gonzalez-Loyola, A., Barba, I., Morente, M., Aguilar, R., et al. (2010). Effects of substitution of Cx43 by Cx32 on myocardial energy metabolism, tolerance to ischaemia and preconditioning protection. *J. Physiol.* 588, 1139–1151. doi: 10.1113/jphysiol.2009.186577
- Ruiz-Meana, M., Rodriguez-Sinovas, A., Cabestrero, A., Boengler, K., Heusch, G., and Garcia-Dorado, D. (2008). Mitochondrial connexin43 as a new player in the pathophysiology of myocardial ischaemia-reperfusion injury. *Cardiovasc. Res.* 77, 325–333. doi: 10.1093/cvr/cvm062
- Salameh, A., and Dhein, S. (2011). Adrenergic control of cardiac gap junction function and expression. *Nauyn Schmiedebergs Arch. Pharmacol.* 383, 331–346. doi: 10.1007/s00210-011-0603-4
- Sankova, B., Benes, J. Jr., Krejci, E., Dupays, L., Theveniau-Ruissy, M., Miquerol, L., et al. (2012). The effect of connexin40 deficiency on ventricular conduction system function during development. *Cardiovasc. Res.* 95, 469–479. doi: 10.1093/cvr/cvs210
- Schrickel, J. W., Kreuzberg, M. M., Ghanem, A., Kim, J. S., Linhart, M., Andrie, R., et al. (2009). Normal impulse propagation in the atrioventricular conduction system of Cx30.2/Cx40 double deficient mice. *J. Mol. Cell. Cardiol.* 46, 644–652. doi: 10.1016/j.yjmcc.2009.02.012
- Schwanke, U., Konietzka, I., Duschin, A., Li, X., Schulz, R., and Heusch, G. (2002). No ischemic preconditioning in heterozygous connexin43-deficient mice. *Am. J. Physiol. Heart Circ. Physiol.* 283, H1740–H1742.
- Shaw, R. M., and Rudy, Y. (1997). Ionic mechanisms of propagation in cardiac tissue. Roles of the sodium and L-type calcium currents during reduced excitability and decreased gap junction coupling. *Circ. Res.* 81, 727–741. doi: 10.1161/01.RES.81.5.727
- Simon, A. M., Goodenough, D. A., Li, E., and Paul, D. L. (1997). Female infertility in mice lacking connexin 37. *Nature* 385, 525–529. doi: 10.1038/385525a0
- Simon, A. M., Goodenough, D. A., and Paul, D. L. (1998). Mice lacking connexin40 have cardiac conduction abnormalities characteristic of atrioventricular block and bundle branch block. *Curr. Biol.* 8, 295–298. doi: 10.1016/S0960-9822(98)70113-7
- Simon, A. M., McWhorter, A. R., Dones, J. A., Jackson, C. L., and Chen, H. (2004). Heart and head defects in mice lacking pairs of connexins. *Dev. Biol.* 265, 369–383. doi: 10.1016/j.ydbio.2003.09.036
- Sizarov, A., Devalla, H. D., Anderson, R. H., Passier, R., Christoffels, V. M., and Moorman, A. F. (2011). Molecular analysis of patterning of conduction tissues in the developing human heart. *Circ. Arrhythm. Electrophysiol.* 4, 532–542. doi: 10.1161/CIRCEP.111.963421
- Smyth, J. W., Vogan, J. M., Buch, P. J., Zhang, S. S., Fong, T. S., Hong, T. T., et al. (2012). Actin cytoskeleton rest stops regulate anterograde traffic of connexin 43 vesicles to the plasma membrane. *Circ. Res.* 110, 978–989. doi: 10.1161/CIRCRESAHA.111.257964
- Sohl, G., and Willecke, K. (2004). Gap junctions and the connexin protein family. *Cardiovasc. Res.* 62, 228–232. doi: 10.1016/j.cardiores.2003.11.013
- Solan, J. L., and Lampe, P. D. (2009). Connexin43 phosphorylation: structural changes and biological effects. *Biochem. J.* 419, 261–272. doi: 10.1042/BJ20082319
- Sperelakis, N. (2002). An electric field mechanism for transmission of excitation between myocardial cells. *Circ. Res.* 91, 985–987. doi: 10.1161/01.RES.0000045656.34731.6D
- Stein, M., van Veen, T. A., Remme, C. A., Boulaksil, M., Noorman, M., van Stuijvenberg, L., et al. (2009). Combined reduction of intercellular coupling and membrane excitability differentially affects transverse and longitudinal cardiac conduction. *Cardiovasc. Res.* 83, 52–60. doi: 10.1093/cvr/cvp124
- Tallini, Y. N., Brekke, J. F., Shui, B., Doran, R., Hwang, S. M., Nakai, J., et al. (2007). Propagated endothelial Ca<sup>2+</sup> waves and arteriolar dilation *in vivo*: measurements in Cx40BAC GCaMP2 transgenic mice. *Circ. Res.* 101, 1300–1309. doi: 10.1161/CIRCRESAHA.107.149484
- Tamaddon, H. S., Vaidya, D., Simon, A. M., Paul, D. L., Jalife, J., and Morley, G. E. (2001). Null mutation of connexin43 causes slow propagation of ventricular activation in the late stages of mouse embryonic development. *Circ. Res.* 88, 1196–1202. doi: 10.1161/hh1101.091107
- Valiunas, V., Manthey, D., Vogel, R., Willecke, K., and Weingart, R. (1999). Biophysical properties of mouse connexin30 gap junction channels studied in transfected human HeLa cells. *J. Physiol.* 531, 631–644. doi: 10.1111/j.1469-7793.1999.0631n.x
- Valiunas, V., Weingart, R., and Brink, P. R. (2000). Formation of heterotypic gap junction channels by connexins 40 and 43. *Circ. Res.* 86, E42–E49. doi: 10.1161/01.RES.86.2.e42
- Vanderbrink, B. A., Sellitto, C., Saba, S., Link, M. S., Zhu, W., Homoud, M. K., et al. (2000). Connexin40-deficient mice exhibit atrioventricular nodal and infra-Hisian conduction abnormalities. *J. Cardiovasc. Electrophysiol.* 11, 1270–1276. doi: 10.1046/j.1540-8167.2000.01270.x
- van Kempen, M. J., Ten Velde, I., Wessels, A., Oosthoek, P. W., Gros, D., Jongsma, H. J., et al. (1995). Differential connexin distribution accommodates cardiac function in different species. *Microsc. Res. Tech.* 31, 420–436. doi: 10.1002/jemt.1070310511
- van Rijen, H. V., Eckardt, D., Degen, J., Theis, M., Ott, T., Willecke, K., et al. (2004). Slow conduction and enhanced anisotropy increase the propensity for ventricular tachyarrhythmias in adult mice with induced deletion of connexin43. *Circulation* 109, 1048–1055. doi: 10.1161/01.CIR.0000117402.70689.75
- van Rijen, H. V., van Veen, T. A., Van Kempen, M. J., Wilms-Schopman, F. J., Potse, M., Krueger, O., et al. (2001). Impaired conduction in the bundle branches of mouse hearts lacking the gap junction protein connexin40. *Circulation* 103, 1591–1598. doi: 10.1161/01.CIR.103.11.1591
- van Veen, T. A., Stein, M., Royer, A., Le Quang, K., Charpentier, F., Colledge, W. H., et al. (2005a). Impaired impulse propagation in Scn5a-knockout mice: combined contribution of excitability, connexin expression, and tissue architecture in relation to aging. *Circulation* 112, 1927–1935.
- van Veen, T. A., van Rijen, H. V., Van Kempen, M. J., Miquerol, L., Ophof, T., Gros, D., et al. (2005b). Discontinuous conduction in mouse bundle branches is caused by bundle-branch architecture. *Circulation* 112, 2235–2244.
- Verheijck, E. E., van Kempen, M. J., Veereschild, M., Lurvink, J., Jongsma, H. J., and Bouman, L. N. (2001). Electrophysiological features of the mouse sinoatrial node in relation to connexin distribution. *Cardiovasc. Res.* 52, 40–50. doi: 10.1016/S0008-6363(01)00364-9
- Verheule, S., van Batenburg, C. A., Coenjaerts, E. E., Kirchhoff, S., Willecke, K., and Jongsma, H. J. (1999). Cardiac conduction abnormalities in mice lacking the gap junction protein connexin40.

- J. Cardiovasc. Electrophysiol.* 10, 1380–1389. doi: 10.1111/j.1540-8167.1999.tb00194.x
- Verheule, S., van Kempen, M. J., Postma, S., Rook, M. B., and Jongsma, H. J. (2001). Gap junctions in the rabbit sinoatrial node. *Am. J. Physiol. Heart Circ. Physiol.* 280, H2103–H2115.
- Verheule, S., van Kempen, M. J., Te Welscher, P. H., Kwak, B. R., and Jongsma, H. J. (1997). Characterization of gap junction channels in adult rabbit atrial and ventricular myocardium. *Circ. Res.* 80, 673–681. doi: 10.1161/01.RES.80.5.673
- Vink, M. J., Suadicani, S. O., Vieira, D. M., Urban-Maldonado, M., Gao, Y., Fishman, G. I., et al. (2004). Alterations of intercellular communication in neonatal cardiac myocytes from connexin43 null mice. *Cardiovasc. Res.* 62, 397–406. doi: 10.1016/j.cardiores.2004.01.015
- Vozzi, C., Dupont, E., Coppen, S. R., Yeh, H. I., and Severs, N. J. (1999). Chamber-related differences in connexin expression in the human heart. *J. Mol. Cell. Cardiol.* 31, 991–1003. doi: 10.1006/jmcc.1999.0937
- Walker, D. L., Vacha, S. J., Kirby, M. L., and Lo, C. W. (2005). Connexin43 deficiency causes dysregulation of coronary vasculogenesis. *Dev. Biol.* 284, 479–498. doi: 10.1016/j.ydbio.2005.06.004
- Wang, N., De Vuyst, E., Ponsaerts, R., Boengler, K., Palacios-Prado, N., Wauman, J., et al. (2013). Selective inhibition of Cx43 hemichannels by Gap19 and its impact on myocardial ischemia/reperfusion injury. *Basic Res. Cardiol.* 108, 309. doi: 10.1007/s00395-012-0309-x
- White, T. W., and Bruzzone, R. (1996). Multiple connexin proteins in single intercellular channels: connexin compatibility and functional consequences. *J. Bioenerg. Biomembr.* 28, 339–350. doi: 10.1007/BF02110110
- Wiegerinck, R. F., Verkerk, A. O., Belterman, C. N., van Veen, T. A., Baartscheer, A., Ophof, T., et al. (2006). Larger cell size in rabbits with heart failure increases myocardial conduction velocity and QRS duration. *Circulation* 113, 806–813. doi: 10.1161/CIRCULATIONAHA.105.565804
- Wiese, C., Grieskamp, T., Airik, R., Mommersteeg, M. T., Gardiwal, A., De Gier-De Vries, C., et al. (2009). Formation of the sinus node head and differentiation of sinus node myocardium are independently regulated by Tbx18 and Tbx3. *Circ. Res.* 104, 388–397. doi: 10.1161/CIRCRESAHA.108.187062
- Winterhager, E., Pielsticker, N., Freyer, J., Ghanem, A., Schrickel, J. W., Kim, J. S., et al. (2007). Replacement of connexin43 by connexin26 in transgenic mice leads to dysfunctional reproductive organs and slowed ventricular conduction in the heart. *BMC Dev. Biol.* 7:26. doi: 10.1186/1471-213X-7-26
- Wit, A. L., and Peters, N. S. (2012). The role of gap junctions in the arrhythmias of ischemia and infarction. *Heart Rhythm* 9, 308–311. doi: 10.1016/j.hrthm.2011.09.056
- Ya, J., Erdtsieck-Ernste, E. B., De Boer, P. A., van Kempen, M. J., Jongsma, H., Gros, D., et al. (1998). Heart defects in connexin43-deficient mice. *Circ. Res.* 82, 360–366. doi: 10.1161/01.RES.82.3.360
- Yamada, K. A., Kanter, E. M., Green, K. G., and Saffitz, J. E. (2004). Transmural distribution of connexins in rodent hearts. *J. Cardiovasc. Electrophysiol.* 15, 710–715. doi: 10.1046/j.1540-8167.2004.03514.x
- Yamada, K. A., Rogers, J. G., Sundset, R., Steinberg, T. H., and Saffitz, J. (2003). Up-regulation of connexin45 in heart failure. *J. Cardiovasc. Electrophysiol.* 14, 1205–1212. doi: 10.1046/j.1540-8167.2003.03276.x
- Zhang, Y., Kanter, E. M., and Yamada, K. A. (2010a). Remodeling of cardiac fibroblasts following myocardial infarction results in increased gap junction intercellular communication. *Cardiovasc. Pathol.* 19, e233–e240. doi: 10.1016/j.carpath.2009.12.002
- Zhang, Y., Wang, H., Kovacs, A., Kanter, E. M., and Yamada, K. A. (2010b). Reduced expression of Cx43 attenuates ventricular remodeling after myocardial infarction via impaired TGF-beta signaling. *Am. J. Physiol. Heart Circ. Physiol.* 298, H477–H487. doi: 10.1152/ajpheart.00806.2009
- Zheng-Fischhofer, Q., Ghanem, A., Kim, J. S., Kibschull, M., Schwarz, G., Schwab, J. O., et al. (2006). Connexin31 cannot functionally replace connexin43 during cardiac morphogenesis in mice. *J. Cell. Sci.* 119, 693–701. doi: 10.1242/jcs.02800
- Zhu, W., Saba, S., Link, M. S., Bak, E., Homoud, M. K., Estes, N. A., et al. (2005). Atrioventricular nodal reverse facilitation in connexin40-deficient mice. *Heart Rhythm* 2, 1231–1237. doi: 10.1016/j.hrthm.2005.07.022

**Conflict of Interest Statement:** The authors declare that the research was conducted in the absence of any commercial or financial relationships that could be construed as a potential conflict of interest.

*Received: 15 April 2013; paper pending published: 03 May 2013; accepted: 04 June 2013; published online: 27 June 2013.*

*Citation: Verheule S and Kaese S (2013) Connexin diversity in the heart: insights from transgenic mouse models. Front. Pharmacol. 4:81. doi: 10.3389/fphar.2013.00081*

*This article was submitted to Frontiers in Pharmacology of Ion Channels and Channelopathies, a specialty of Frontiers in Pharmacology.*

*Copyright © 2013 Verheule and Kaese. This is an open-access article distributed under the terms of the Creative Commons Attribution License, which permits use, distribution and reproduction in other forums, provided the original authors and source are credited and subject to any copyright notices concerning any third-party graphics etc.*



# Cyclic nucleotide permeability through unopposed connexin hemichannels

**Virginijus Valiunas\***

Department of Physiology and Biophysics, Stony Brook University, Stony Brook, NY, USA

**Edited by:**

Stefan Dhein, Universitätsklinik Leipzig Herzzentrum Leipzig GmbH, Germany

**Reviewed by:**

John Philip Winpenny, University of East Anglia, UK

Jan Sebastian Schulte, University of Münster, Germany

**\*Correspondence:**

Virginijus Valiunas, Department of Physiology and Biophysics, Stony Brook University, Stony Brook, NY 11794-8661, USA

e-mail: virginijus.valiunas@stonybrook.edu

Cyclic adenosine monophosphate (cAMP) is a well-known intracellular and intercellular second messenger. The membrane permeability of such molecules has potential importance for autocrine-like or paracrine-like delivery. Here experiments have been designed to demonstrate whether gap junction hemichannels, composed of connexins, are a possible entrance pathway for cyclic nucleotides into the interior of cells. HeLa cells stably expressing connexin43 (Cx43) and connexin26 (Cx26) were used to study the cyclic nucleotide permeability of gap junction hemichannels. For the detection of cAMP uptake, the cells were transfected using the cyclic nucleotide-modulated channel from sea urchin sperm (SpiH) as the cAMP sensor. SpiH derived currents ( $I_m$ ) were recorded in whole-cell/perforated patch clamp configuration. Perfusion of the cells in an external K<sup>+</sup> aspartate-(KA<sup>+</sup>) solution containing 500 μM cAMP and no extracellular Ca<sup>2+</sup>, yielded a five to sevenfold increase in the  $I_m$  current level. The SpiH current increase was associated with detectable hemichannel current activity. Depolarization of cells in Ca<sup>2+</sup>-free NaCl perfusate with 500 μM cAMP also induced a SpiH current increase. Elevating extracellular Ca<sup>2+</sup> to mM levels inhibited hemichannel activity. Perfusion with a depolarizing KA<sup>+</sup> solution containing 500 μM cAMP and 2 mM Ca<sup>2+</sup> did not increase SpiH currents. The addition of the gap junction blocker carbenoxolone to the external solution inhibited cAMP uptake. Both cell depolarization and lowered extracellular Ca<sup>2+</sup> increase the open probability of non-junctional hemichannels. Accordingly, the SpiH current augmentation was induced by the uptake of extracellular cAMP via open membrane hemichannels in Cx43 and Cx26 expressing cells. The data presented here show that hemichannels of Cx43 and Cx26 are permeable to cAMP, and further the data suggest that hemichannels are, in fact, a potential pathway for cAMP mediated cell-to-cell signaling.

**Keywords:** connexin43, connexin26, electrophysiology, gap junction, permeability, cyclic AMP

## INTRODUCTION

Hemichannels or connexons are composed of connexins, which are synthesized in the endoplasmic reticulum and assembled into hexameric structures in the Golgi, and subsequently delivered to the plasma membrane via transport vesicles (Segretain and Falk, 2004). Hemichannels are large conductance membrane channels that for many years were thought to be silent or nearly silent subunits. Their function was thought to be only when two such channels, between closely apposed cells, formed an intercellular channel, the gap junction, containing an aqueous pore exclusive of the extracellular space. Once formed, gap junction channels eventually coalesce into aggregates or plaques consisting of hundreds to thousands of channels (Maurer and Weingart, 1987; Bukauskas et al., 2000). However, not all hemichannels are destined to become component parts of a gap junction channel. Rather, many are apparently randomly distributed within the plasma membrane. The presence of hemichannels within plasma membranes has been well-documented *in vitro* (De and Schwartz, 1992; Trexler et al., 1996; Valiunas and Weingart, 2000; Valiunas, 2002) and has prompted speculation about their role in cellular processes like volume regulation (Quist et al., 2000), the influx/efflux of

metabolically relevant solutes such as ATP (Bruzzone et al., 2001; Dahl and Locovei, 2006), and cell death (Plotkin et al., 2002; Kalvelye et al., 2003). The electrophysiological data collected *in vitro* have demonstrated that hemichannels open probability is increased with membrane depolarization in the presence of lowered extracellular calcium. The open probability can be reduced by acidic pH, calcium, trivalent cations, and quinine derivatives (Trexler et al., 1999; Contreras et al., 2002; Eskandari et al., 2002; Stout et al., 2002; Valiunas, 2002; Srinivas et al., 2005).

Cell to cell communication mediated by gap junction channels represents one of two established intercellular pathways for the movement of signaling molecules, metabolites, and siRNA/miRNA from one cell to another (Valiunas et al., 2005; Kanaporis et al., 2008). Exocytosis/endocytosis is another intercellular delivery pathway that utilizes the extracellular volume for autocrine and paracrine mediated signaling. The suggested possible roles for hemichannels, such as volume regulation and/or cell death would also be examples where delivery is via the extracellular space and hence, represents an example of autocrine/paracrine-like delivery. Furthermore, a recent review by Wang et al. (2013) also suggests hemichannels are a significant

source of autocrine and paracrine messengers. When considering the role of hemichannels in such a delivery system it is best to consider the delivery pathway as autocrine-like or paracrine-like because delivery of a solute does not necessarily involve vesicular traffic nor is it necessarily mediated by surface receptors.

Inevitably, an interesting question arises: are hemichannels an alternate autocrine/paracrine-like pathway for delivery of relevant signaling molecules, like adenosine and other related compounds? Two examples focus on cyclic adenosine monophosphate (cAMP) as a signal molecule candidate. The extracellular release of cAMP is known to exert effects such as receptor expression in renal cells (Kuzhikandathil et al., 2011) and inhibition of skeletal muscle inotropism (Duarte et al., 2012). Before addressing further questions, such as if hemichannels are involved in a paracrine-like delivery of cAMP, it is essential to understand the characteristics of hemichannel permeability.

As a first step in assessing hemichannels as a potential delivery pathway, HeLa cells were transfected with cyclic nucleotide sensor SpiH in order to investigate the permeability of cAMP of unopposed connexin43 (Cx43) and connexin26 (Cx26) hemichannels.

## MATERIALS AND METHODS

### CELLS AND CULTURE CONDITIONS

Experiments were carried out on human HeLa cells stably transfected with wild-type mCx43 and hCx26. HeLa cells were grown in Dulbecco's Modified Eagle Medium (DMEM; Gibco BRL), supplemented with 10% fetal calf serum (FCS; Hyclone), 100 mg/mL streptomycin (Gibco BRL), and 100 U/mL penicillin (Gibco BRL). The medium also contained 100 mg/mL hygromycin (Sigma) or 1 mg/mL puromycin (Sigma). The cells were passaged weekly, diluted 1:10, and kept at 37°C in a CO<sub>2</sub> incubator (5% CO<sub>2</sub>/95% ambient air). Culture conditions for these cells have been previously published in complete detail (Valiunas et al., 2000, 2001). Electrophysiological experiments were carried out on single cells cultured for 1–3 days.

### IMMUNOFLUORESCENT LABELING OF CONNEXINS

HeLa cells expressing Cx26 and/or Cx43 were grown on coverslips and stained as described earlier (Laing and Beyer, 1995). Commercially available anti-connexin43 (Sigma) and anti-connexin26 (Zymed Labs) antibodies were used for immunostaining. Alexa Fluor488 conjugated anti-rabbit IgG (Cell Signaling) was used as a secondary antibody. The protein expression and localization was monitored with a 63× oil objective on a Zeiss Axiovert 200 inverted microscope and Axiovision (Zeiss) software.

### ELECTROPHYSIOLOGICAL MEASUREMENTS

Experiments were carried out on single cells using the whole-cell/perforated patch voltage-clamp technique to control the membrane potential and to measure membrane currents of the cell. For electrical recordings, glass coverslips with adherent cells were transferred to an experimental chamber mounted on the stage of an inverted microscope (Olympus-IX71). During experiments, the cells were superfused with depolarizing bath solution (KAsp) at room temperature (~22°C) containing (mM): K<sup>+</sup> aspartate<sup>-</sup> 120; NaCl 10; CaCl<sub>2</sub> 2; HEPES 5 (pH 7.4); glucose 5; 2 mM CsCl, BaCl<sub>2</sub> and TEA<sup>+</sup> Cl<sup>-</sup> were also added. For the

Ca<sup>2+</sup>-free (0 Ca<sup>2+</sup>) bath solution CaCl<sub>2</sub> was omitted. For the regular modified Tyrode external solution (NaCl), K<sup>+</sup> aspartate<sup>-</sup> in the superfuse was replaced with an equal molar concentration of NaCl. The patch pipettes were filled with solution containing (mM): K<sup>+</sup> aspartate<sup>-</sup>, 120; NaCl, 10; MgATP, 3; HEPES, 5 (pH 7.2); EGTA, 10 (pCa ~8); filtered through 0.22 μm pores. In perforated patch experiments, the pipette solution contained 30–50 μM β-escin (Fan and Palade, 1998). The series resistance with β-escin patches measured 11–20 MΩ. Patch pipettes were pulled from glass capillaries (code GC150F; Harvard Apparatus) with a horizontal puller (DMZ-Universal, Zeitz-Instrumente). When filled, the resistance of the pipettes measured 1–4 MΩ.

### cAMP-UPTAKE STUDIES

Cyclic AMP transfer through gap junction hemichannels was investigated using single HeLaCx43 and/or HeLaCx26 cells. For the detection of cAMP uptake, the cells were transfected with the cAMP sensor, a cyclic nucleotide-modulated channel from sea urchin sperm (SpiH; Gauss et al., 1998; Shin et al., 2001; Kanaporis et al., 2008). Production, characterization, culture conditions, staining, and visualization of these cells have been described previously in Kanaporis et al. (2008).

Wild-type, Cx43 and Cx26 transfected cells were incubated in either in NaCl or K<sup>+</sup> aspartate<sup>-</sup> (KAsp) bath solution (with 2 mM Ca<sup>2+</sup> or Ca<sup>2+</sup>-free). For cAMP uptake experiments cAMP (Sigma-Aldrich) was added to the external bath solution to reach a concentration of 500 μM. The SpiH derived currents ( $I_m$ ) were recorded from the single cell expressing SpiH and Cx43 and/or Cx26. In some experiments 50 μM of cAMP was introduced via the patch pipette directly in to the cell. In another series of experiments 500 μM cAMP was also locally introduced to the cell membrane via the external pipette. To prevent cAMP degradation a membrane-permeable phosphodiesterase inhibitor IBMX (200 μM, Sigma-Aldrich) was added to the bath solution. An adenylate cyclase inhibitor, 2',5'-dideoxyadenosine (5 mM, Calbiochem) was added to the pipette and bath solutions to inhibit intracellular cAMP production.

### SIGNAL RECORDING AND ANALYSIS

Voltage and current signals were recorded using patch clamp amplifiers (Axopatch 200). The current signals were digitized with a 16 bit A/D-converter (Digidata 1322A; Molecular Devices) and stored within a personal computer. Data acquisition and analysis were performed with pClamp9 software (Molecular Devices). Statistical analysis was performed using SigmaStat (Jandel Scientific). The Mann–Whitney Rank Sum test was used for all cases unless otherwise noted. The results are presented as means ± SEM.

## RESULTS

### LOCALIZATION OF CONNEXINS WITHIN CELLS

HeLa cells stably transfected with mCx43 and hCx26 were immunostained with anti-Cx43 and anti-Cx26 antibodies, respectively. Immunofluorescent staining verified protein expression and localization of Cx43 and Cx26 within the cells (Figure 1). As shown in Figure 1, typical punctate staining (in green) at the cell to cell contact regions and the cell membranes of single cells indicates

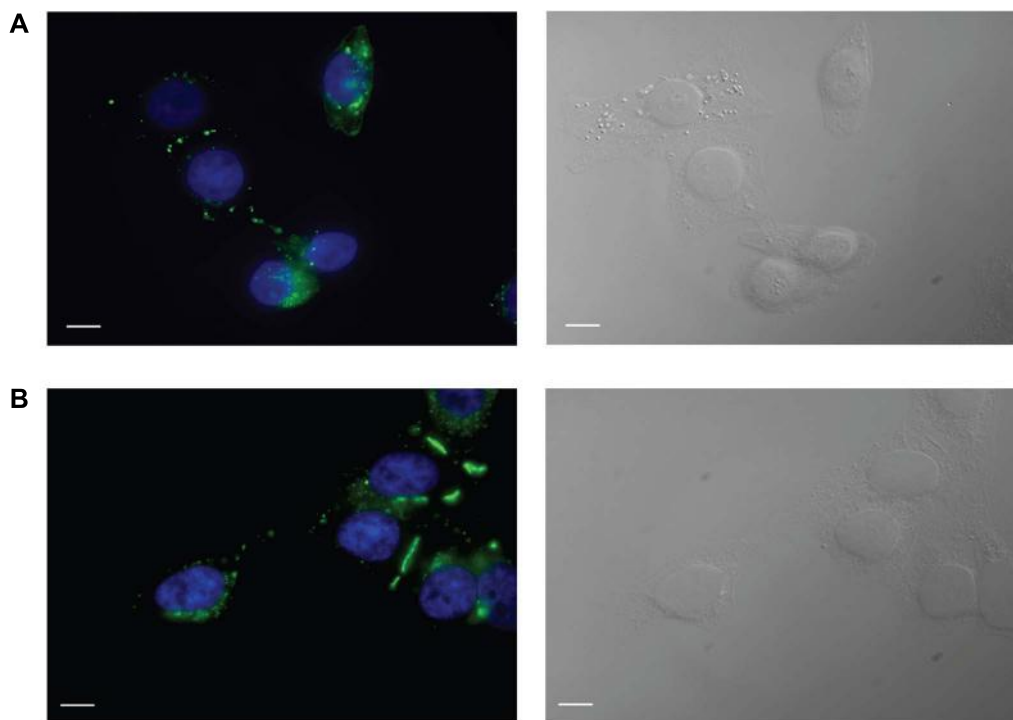


**FIGURE 1 | Immunofluorescent identification of connexin expression in transfected HeLa cells.** HeLa cells expressing Cx43 (A) and Cx26 (B) stained with antibodies to Cx43 and Cx26, respectively, show typical punctate staining of Cx43 and Cx26 gap junction plaques at cell–cell contact areas, as

well as Cx43 and Cx26 localization in the cell membranes of single cells. Green labeling represents staining of connexin proteins, while blue shows DAPI staining of cell nuclei. The right panels show bright field images. Scale bar, 10  $\mu\text{m}$ .

Cx43 (A) and Cx26 (B) expression in HeLa cells stably transfected with Cx43 and Cx26, respectively.

#### PROPERTIES OF cAMP REPORTER CURRENTS

For detecting extracellular cAMP permeation through membrane hemichannels, HeLa cells expressing Cx43 or Cx26 were transfected with the cyclic nucleotide-modulated channel from sea urchin sperm (SpIH; Gauss et al., 1998; Shin et al., 2001) as a cAMP sensor. The activity of SpIH channels in transfected cells was determined using a single cell whole-cell perforated patch clamp. It has been shown that intracellular perfusion with cAMP increased SpIH currents by more than fivefold in a dose-dependent manner (Kanaporis et al., 2008). The cAMP dose-response curve and characterization of SpIH channels derived currents were reported in further detail earlier in Kanaporis et al. (2008).

**Figure 2** shows the voltage protocol ( $V_m$ ) (A) along with the two resultant membrane currents ( $I_m$ ) recorded from the same HeLaCx43 cell transfected with SpIH (B and C). The cell was perfused with the external NaCl (modified Tyrode) solution containing 2 mM  $\text{Ca}^{2+}$  and 500  $\mu\text{M}$  cAMP. **Figure 2B** (left panel) shows whole-cell (perforated patch) currents recorded from a SpIH transfected cell, while the right panel demonstrates experiment conditions. **Figure 2C** (left panel) shows the current recording from the same cell after the second pipette with 50  $\mu\text{M}$  cAMP in whole-cell mode was attached to it (shown in the right panel). Voltage pulses delivered from a holding potential of 0 mV to test potentials between  $-20$  and  $-120$  mV

produced time- and voltage-dependent inward and tail currents ( $V_m = +50$  mV) in SpIH transfected cells. When cAMP was present in the pipette solution, SpIH transfected cells exhibited larger currents. The tail current densities were measured after voltage step to  $V_m = -100$  mV. On average, intracellular application of cAMP increased the peak current level  $\sim$ fivefold, in comparison to the SpIH transfected cells not treated with cAMP ( $31.4 \pm 4.3$  versus  $6.2 \pm 0.9$  pA/pF, **Figure 2D**). These results are consistent with those found in a previous report (Kanaporis et al., 2008).

#### cAMP TRANSFER THROUGH MEMBRANE HEMICHANNELS: MODULATION BY EXTERNAL $\text{Ca}^{2+}$

To examine cAMP permeation through hemichannels within the plasma membrane SpIH transfected HeLa Cx43 and Cx26 cells were incubated in bath solutions (with and without 2 mM  $\text{Ca}^{2+}$ ) containing 500  $\mu\text{M}$  cAMP. The left hand panels in **Figure 3B** show the recorded response of SpIH whole-cell (perforated patch) currents to hyperpolarizing voltage ( $V_m$ ; **Figure 3A**). The recordings were obtained from HeLaCx43 cell perfused with KAsp bath solution with 2 mM  $\text{Ca}^{2+}$ . On average,  $I_m$  measured from 10 preparations yielded  $6.4 \pm 1.1$  pA/pF. **Figure 3C** (left panel) illustrates that the SpIH current increased significantly ( $\sim$ sixfold) in the absence of external  $\text{Ca}^{2+}$  ( $39.5 \pm 5.8$  pA/pF,  $n = 13$ ). The current amplitudes recorded in the presence and absence of external  $\text{Ca}^{2+}$  are summarized in **Figure 3D**. The SpIH current increase is consistent with the opening of Cx43 hemichannels in  $\text{Ca}^{2+}$ -free

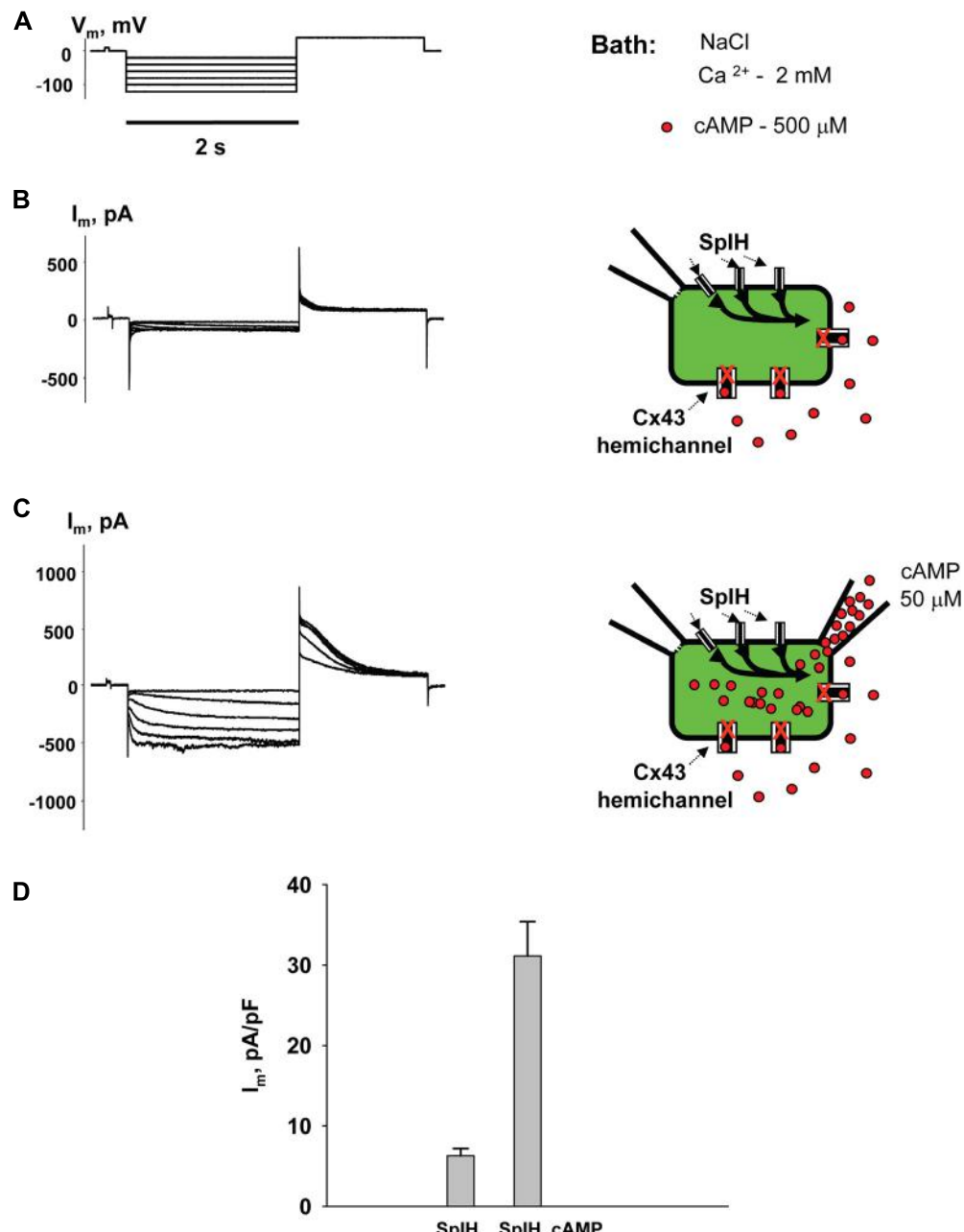


**FIGURE 2 | Properties of SpiH channels. (A)** Voltage protocol ( $V_m$ ) and whole-cell currents ( $I_m$ ) recorded in SpiH transfected HeLaCx43 cells in the absence **(B)** and presence **(C)** of 50  $\mu\text{M}$  cAMP in the pipette solution. Schematics in the right panels illustrate whole-cell recording conditions from

HeLaCx43/SpiH cells. The NaCl external bath solution contained 2 mM  $\text{Ca}^{2+}$  and 500  $\mu\text{M}$  cAMP. **(D)** Average of tail current densities measured after voltage step to  $V_m = -100$  mV in the absence ( $6.2 \pm 0.9$  pA/pF,  $n = 10$  cells) and the presence of intracellular cAMP ( $31.4 \pm 4.3$  pA/pF,  $n = 8$  cells),  $P < 0.001$ .

solution and cAMP flux into the cell following the activation of SpiH channels (Contreras et al., 2003a).

Figure 4 illustrates another series of experiments designed to activate membrane hemichannels by lowering external  $\text{Ca}^{2+}$ . In these experiments cells were first perfused with the external NaCl solution containing 2 mM  $\text{Ca}^{2+}$  and 500  $\mu\text{M}$  cAMP (Figure 4B). When the NaCl external bath solution was replaced with KAsp bath solution with no  $\text{Ca}^{2+}$ , SpiH current increased more than

sevenfold (Figure 4C). An example of the activation of the SpiH current switching from NaCl bath solution with  $\text{Ca}^{2+}$  to the KAsp solution lacking  $\text{Ca}^{2+}$  is shown in Figure 4D. Currents recorded from HeLaCx43 SpiH-expressing cells were derived in response to voltage pulses of  $-100$  mV and returning to a tail potential of +50 mV from a holding potential of 0 mV. At approximately the 30-s time mark, perfusion with  $\text{Ca}^{2+}$ -free KAsp solution was initiated. SpiH currents started to increase over

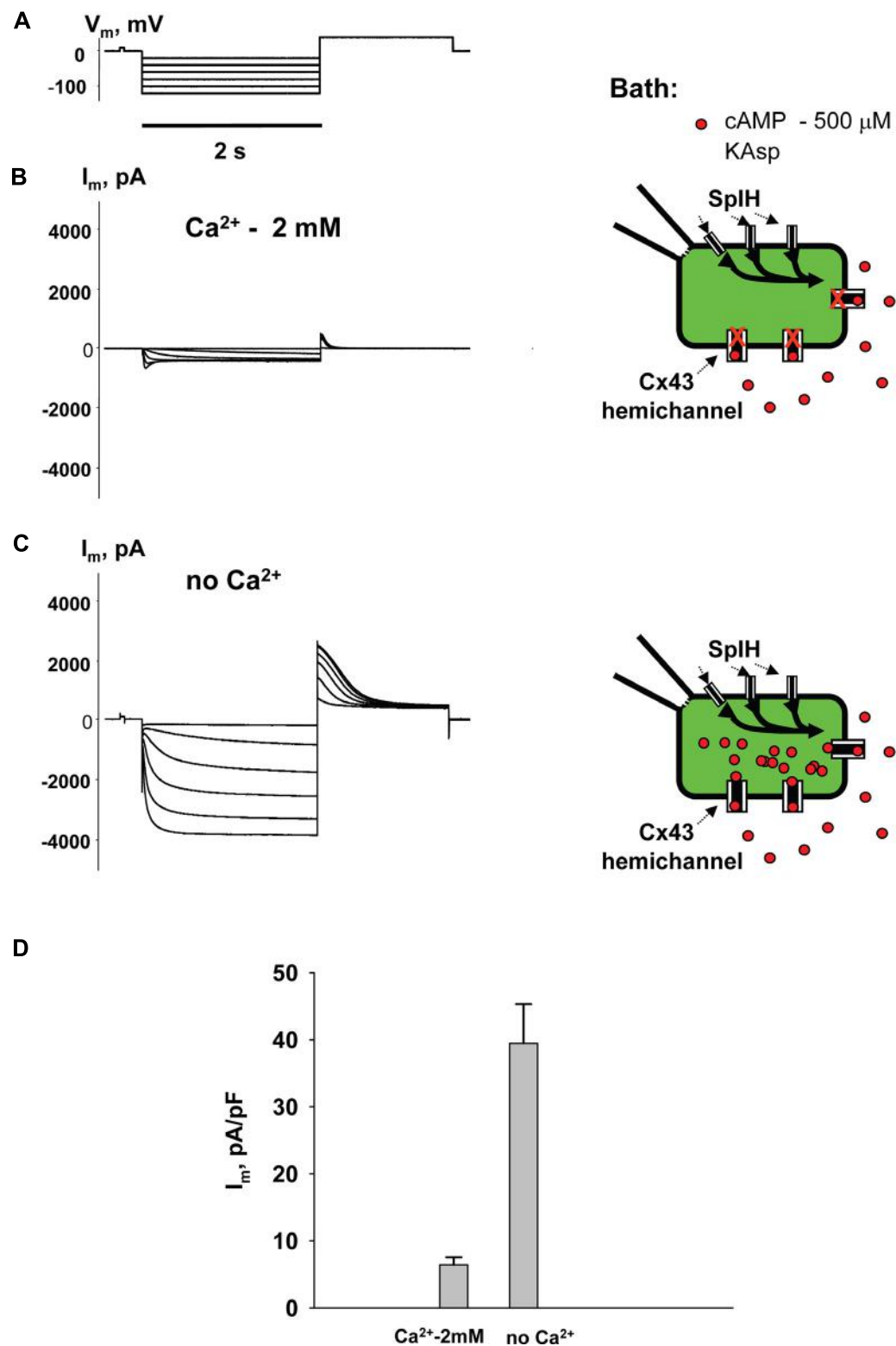


**FIGURE 3 |** cAMP induced activation of SplH channels.  $I_m$  elicited by hyperpolarizing pulses (A) (from  $-20$  to  $-120$  mV) in SplH transfected HeLaCx43 cells in with both  $2\text{ mM}$   $\text{Ca}^{2+}$  (B) and with no added  $\text{Ca}^{2+}$  (C). Schematics in the right panels of (B) and (C) illustrate the experimental conditions. In both cases the external KAsp bath solution contained  $500\text{ }\mu\text{M}$

cAMP.  $I_m$  increased significantly with  $V_m$  and hyperpolarization induced voltage- and time-dependent inward currents when no external  $\text{Ca}^{2+}$  was present. (D) Average of current amplitudes recorded in the presence and in the absence of external  $\text{Ca}^{2+}$ , respectively:  $6.4 \pm 1.1$  pA/pF,  $n = 10$  versus  $39.5 \pm 5.8$  pA/pF,  $n = 13$ ;  $P < 0.001$ .

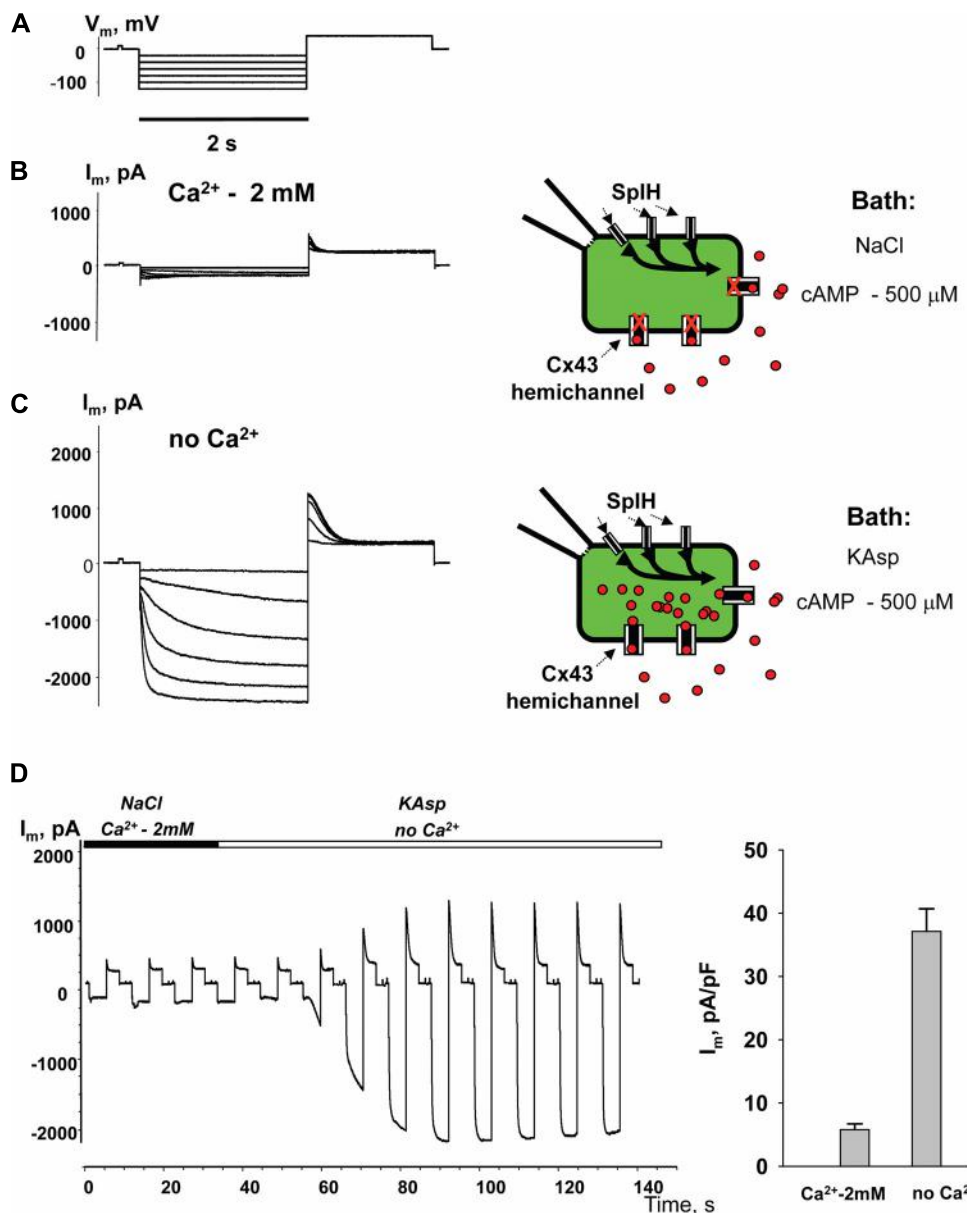


**FIGURE 4 | Detection of intracellular cAMP.** (A) Voltage protocol and  $I_m$  recordings from SpIH transfected HeLaCx43 cells perfused with 2 mM extracellular  $\text{Ca}^{2+}$  (B), as well as after the perfusion solution with no  $\text{Ca}^{2+}$  added (C) (see schematics on the right for the recording conditions of the cells). (D) Current recorded from the HeLaCx43/SpIH cell in response to voltage pulses from a holding potential of 0 to  $-100$  mV, returning to a tail

potential of  $+50$  mV. Over time, perfusion with the  $\text{Ca}^{2+}$ -free KAsp external solution induced a SpIH current increase to a steady-state. (E) Average of current densities measured in the presence of external  $\text{Ca}^{2+}$  and after perfusion with the KAsp solution with no  $\text{Ca}^{2+}$ :  $5.8 \pm 0.9$  pA/pF versus  $37.1 \pm 3.6$ ,  $n = 7$ ,  $P < 0.001$ ,  $t$ -test. 500  $\mu\text{M}$  cAMP was present in the external solution at any time during the experiment.

time to a new steady-state value due to cAMP diffusion from the external bath into the cytoplasm via membrane hemichannels. On average, derived from seven preparations, switching NaCl bath solution with  $\text{Ca}^{2+}$  to the KAsp solution with no  $\text{Ca}^{2+}$ , SpIH currents increased from  $5.8 \pm 0.9$  to  $37.1 \pm 3.6$  pA/pF (Figure 4E).

Experiments performed with HeLaCx43 cells lacking SpIH expression revealed negligible membrane currents in  $\text{Ca}^{2+}$ -free KAsp solution with 500  $\mu\text{M}$  of cAMP (Figure 5A). Figure 5B

shows no current increase when the external NaCl bath solution with 2 mM  $\text{Ca}^{2+}$  was exchanged with  $\text{Ca}^{2+}$ -free KAsp solution, which is in contrast to the considerable current increase when such a procedure was performed on cells expressing SpIH (Figure 4D).

These experiments show that SpIH currents can be activated lowering  $\text{Ca}^{2+}$  in the external solution, because of opening non-junctional hemichannels and following cAMP diffusion into the cell. These observations are consistent with concept that

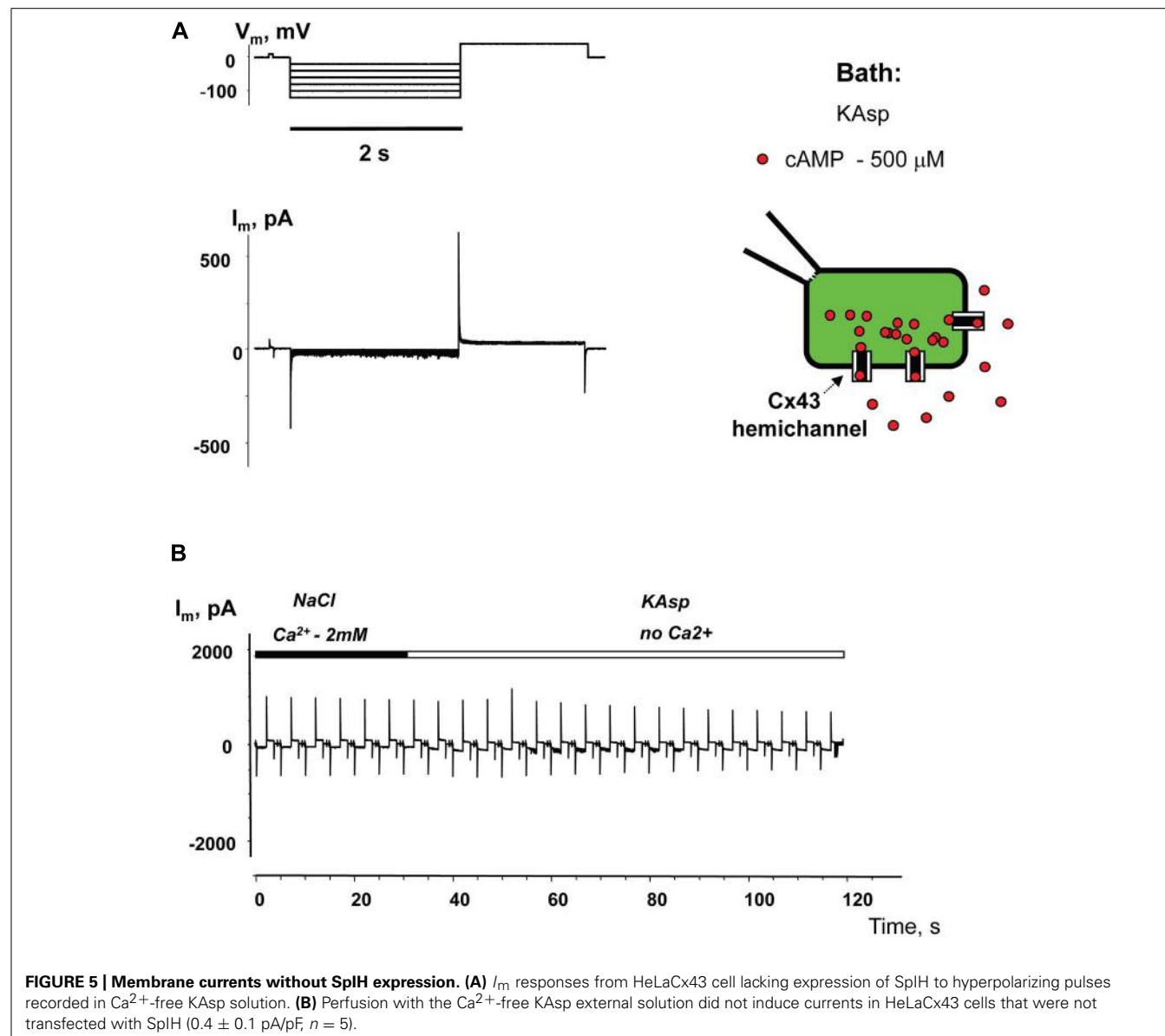


**FIGURE 5 | Membrane currents without SpiH expression. (A)**  $I_m$  responses from HeLaCx43 cell lacking expression of SpiH to hyperpolarizing pulses recorded in Ca<sup>2+</sup>-free KAsp solution. **(B)** Perfusion with the Ca<sup>2+</sup>-free KAsp external solution did not induce currents in HeLaCx43 cells that were not transfected with SpiH ( $0.4 \pm 0.1 \text{ pA/pF}$ ,  $n = 5$ ).

hemichannels activity is regulated by extracellular Ca<sup>2+</sup> (Ebihara et al., 1995; Valiunas and Weingart, 2000; Valiunas, 2002; Contreras et al., 2003b) and HeLa cells expressing Cx43 have been shown to open unopposed Cx43 hemichannels (Contreras et al., 2003a,b).

#### VOLTAGE ENHANCED cAMP UPTAKE

The membrane potential controls hemichannel activity and cell depolarization subsequently triggers the opening of unopposed membrane hemichannels (Ebihara et al., 1995; Valiunas and Weingart, 2000; Valiunas, 2002). An example of depolarization enhanced cAMP uptake is demonstrated in **Figure 6A**. When a single SpiH transfected HeLaCx43 cell was perfused with Ca<sup>2+</sup>-free NaCl solution containing 500  $\mu\text{M}$  cAMP there was a very weak SpiH current increase over the 80 s that the cell was held at +50 mV. However, over time, there was a significant SpiH current increase

with the resulting saturation when the cell membrane was depolarized and held further at +80 mV (~80 s time mark, **Figure 6A**). Cell depolarization from the resting potential (~−40 mV) to 0 and +50 mV similarly enhanced the SpiH currents in three other preparations. Due to the different holding voltages, the SpiH currents in each cell were analyzed individually. However, in each of the four cells, regardless of the holding potential, depolarization yielded a significant SpiH current increase over the time from 2.2 to 5.1-fold (~fourfold on average in four preparations). In contrast, there was no significant SpiH current increase detected when the cells were held at a hyperpolarizing voltage of −40 mV ( $6.3 \pm 3.8$  versus  $6.9 \pm 3.8 \text{ pA/pF}$ ,  $n = 3$ ,  $P = 0.7$ ). Not only did lowered extracellular Ca<sup>2+</sup> increase channel activity, but also depolarization caused activation of hemichannels, i.e., more cAMP flux to the cell and subsequent SpiH current increase. An example of a SpiH current increase and associated detectable

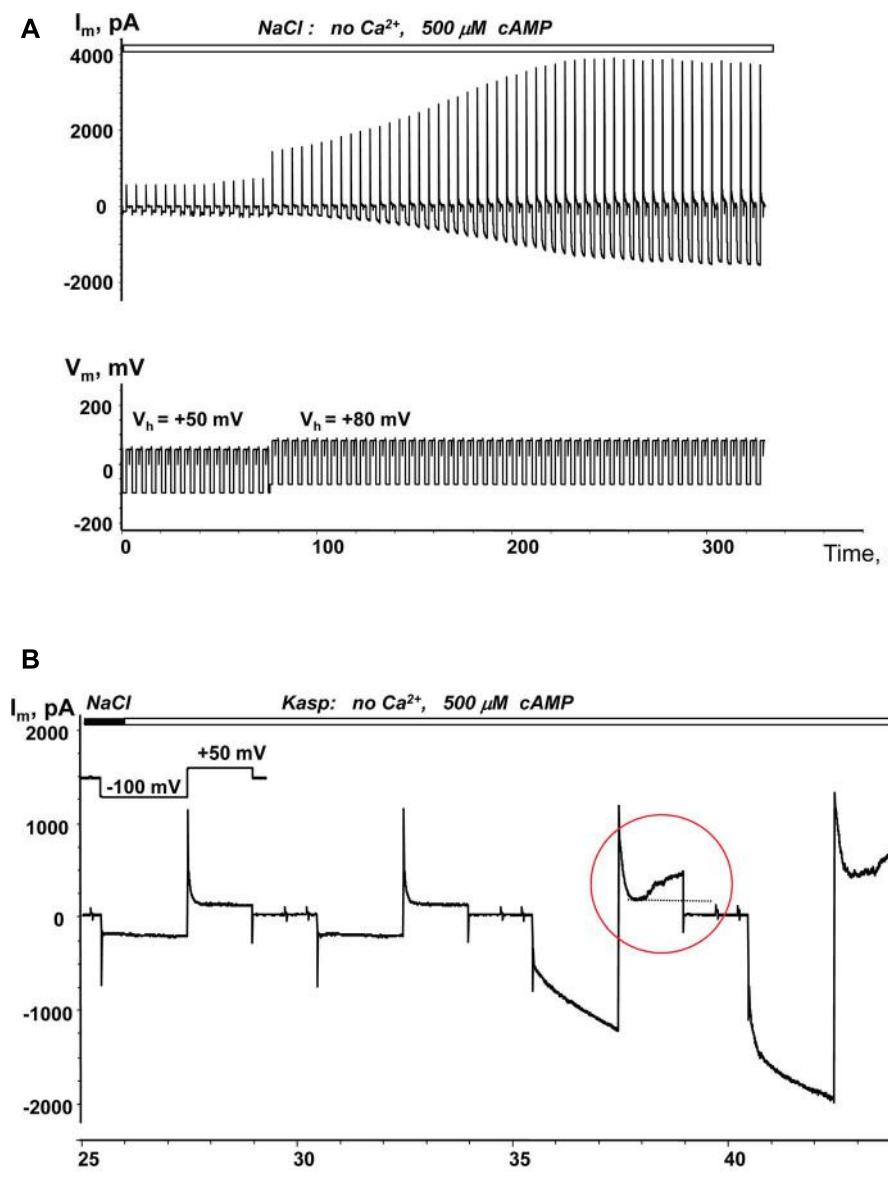


**FIGURE 6 | Depolarization induced cAMP uptake.** (A)  $I_m$  recorded from a HeLaCx43/SpiH cell during perfusion with  $\text{Ca}^{2+}$ -free NaCl solution containing  $500 \mu\text{M}$  cAMP. Initially the cell was held at  $V_h = 0 \text{ mV}$  (not shown in the record). There was a weak (~1.3-fold) current increase over approximately 80 s when the cell was held at  $V_h = +50 \text{ mV}$ . Further cell membrane depolarization to  $V_h = +80 \text{ mV}$  at ~80 s significantly enhanced

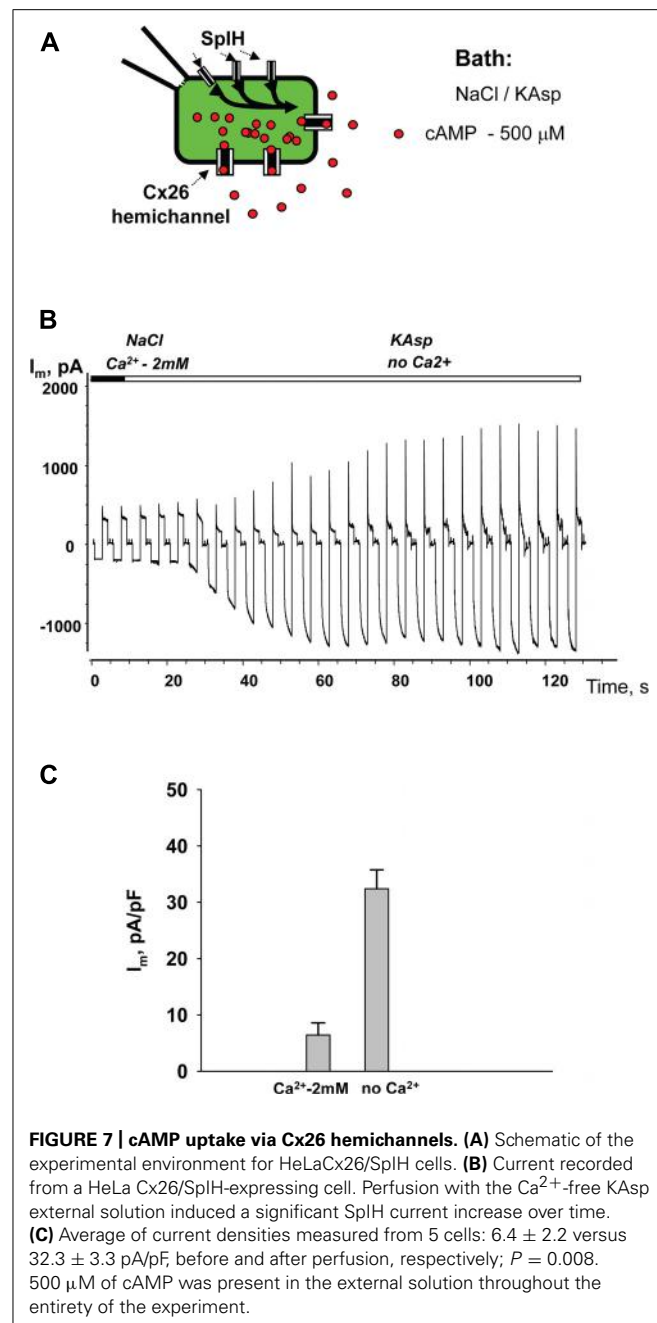
the SpiH current in a time dependent manner by ~threefold (when adjusted to the same  $V_h$ ). (B) SpiH current recorded in a HeLaCx43/SpiH cell during perfusion with  $\text{Ca}^{2+}$ -free KAsp solution. The SpiH current increase was associated with the time-dependent membrane current increase during depolarization (noted by a red circle), typical of hemichannel activity.

Cx43 hemichannel activity is demonstrated in **Figure 6B**, where the area circled in red denotes the time-dependent current increase, which implies activation of hemichannels during depolarization.

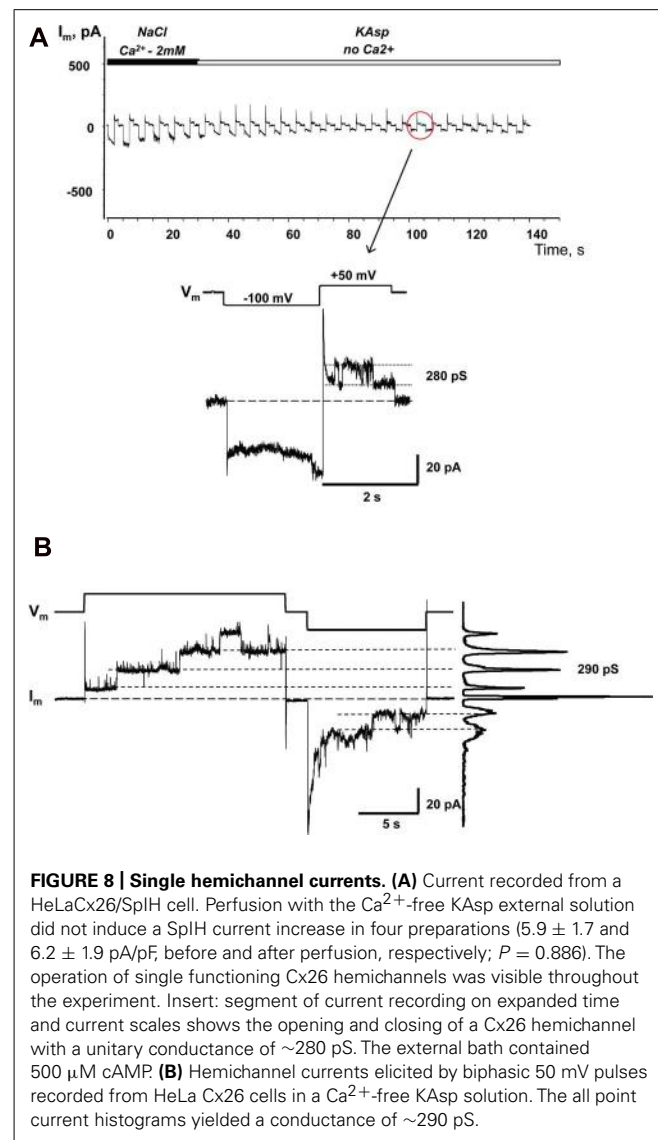
#### cAMP UPTAKE VIA Cx26 HEMICHANNELS

Similar to the HeLaCx43 cells shown in **Figures 2–6**, HeLa cells expressing hCx26 also demonstrated cAMP uptake. **Figure 7** shows a schematic of the experimental conditions (panel A) and SpiH current recordings from a HeLaCx26 cell transfected with

SpiH (panel B). In five preparations SpiH currents increased from  $6.4 \pm 2.2$  to  $32.3 \pm 3.3 \text{ pA/pF}$  when the NaCl external solution with  $2 \text{ mM Ca}^{2+}$  was replaced with  $\text{Ca}^{2+}$ -free KAsp, due to cAMP flux from the external solution through opened membrane hemichannels (**Figure 7C**). In four preparations, some HeLaCx26 cells did not exhibit such SpiH current increases when perfused with  $\text{Ca}^{2+}$ -free KAsp solution containing  $500 \mu\text{M}$  cAMP (**Figure 8A**). Such an absence of a current increase could be explained by the lack of the sufficient numbers of operational non-junctional hemichannels in the cell membrane. It has been reported that homotypic



Cx26 gap junction channels are~7 times less permeable to cAMP than Cx43 channels (Kanaporis et al., 2008). In the recordings shown here (see insert Figure 8A) there are one or two operational hemichannels with~280 pS unitary conductance detectable in the cell. This suggests that cAMP flux through one or two operational hemichannels is not enough to induce a SplH current, in contrast to the example in Figure 7B where presumably there is a much higher number of open hemichannels in  $\text{Ca}^{2+}$ -free solution. Furthermore, phosphodiesterase activity, with such a small number of operational channels, cannot be ruled out completely. Unitary conductance of hemichannels resolved from the record in Figure 8A, i.e., ~280 pS, corresponds to unitary conductance of



Cx26 hemichannels shown in Figure 8B, where the hemichannel current recording was obtained from a HeLaCx26 cell in response to biphasic 50 mV voltage pulses. Discrete steps indicative of the opening (depolarization pulse) and closing (hyperpolarization pulse) of hemichannels are present. The current histograms yielded unitary conductances of 290–300 pS for Cx26 hemichannels, which is in good agreement with Cx26 unitary hemichannel conductance data obtained from *Xenopus* oocytes (Gonzalez et al., 2006; Sanchez et al., 2010).

#### LOCAL ACTIVATION OF MEMBRANE HEMICHANNELS

Perfusion of the cells with  $\text{Ca}^{2+}$ -free KAsp solution activates unopposed hemichannels over the entire surface of the cell membrane. In a series of experiments cAMP was applied locally to a small area of cell membrane through a separate perfusion pipette as illustrated in the Figure 9A experimental schematic. HeLaCx43/SplH cells were bathed in modified Tyrode (NaCl) solution with 2 mM  $\text{Ca}^{2+}$ . The currents were recorded with the patch pipette in

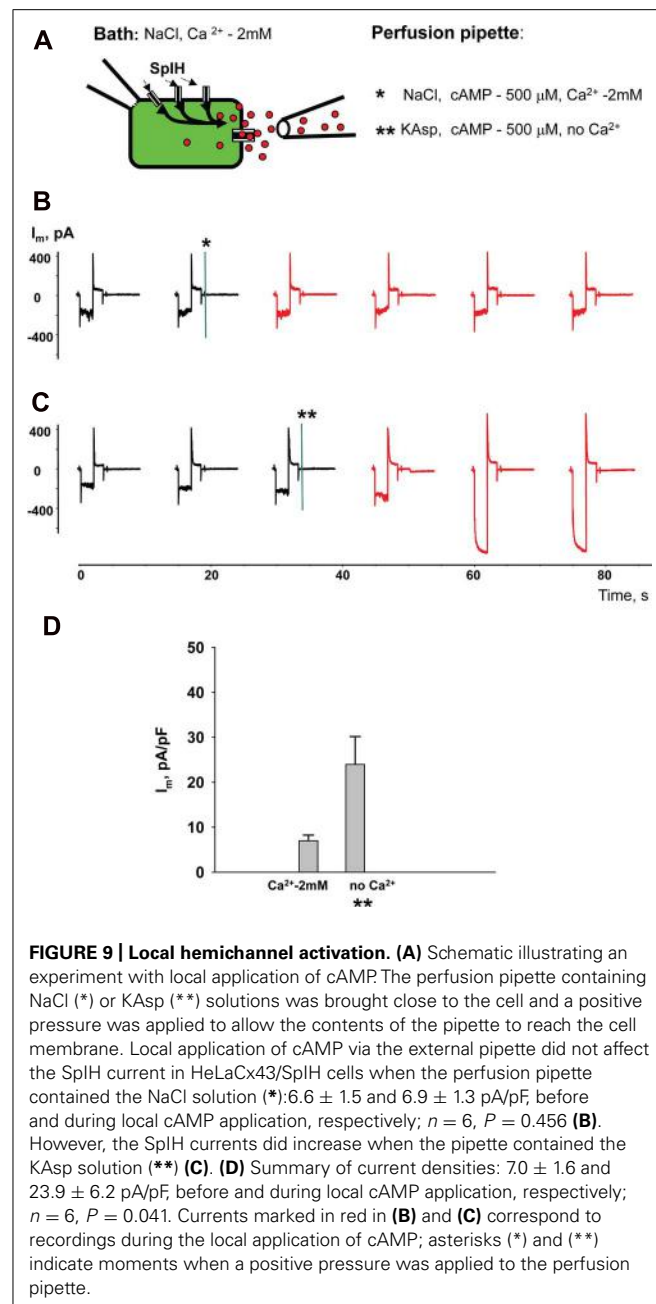


**FIGURE 9 | Local hemichannel activation.** (A) Schematic illustrating an experiment with local application of cAMP. The perfusion pipette containing NaCl (\*) or KAsp (\*\*) solutions was brought close to the cell and a positive pressure was applied to allow the contents of the pipette to reach the cell membrane. Local application of cAMP via the external pipette did not affect the SpiH current in HeLaCx43/SpiH cells when the perfusion pipette contained the NaCl solution (\*):  $6.6 \pm 1.5$  and  $6.9 \pm 1.3$  pA/pF before and during local cAMP application, respectively;  $n = 6$ ,  $P = 0.456$  (B). However, the SpiH currents did increase when the pipette contained the KAsp solution (\*\*) (C). (D) Summary of current densities:  $7.0 \pm 1.6$  and  $23.9 \pm 6.2$  pA/pF, before and during local cAMP application, respectively;  $n = 6$ ,  $P = 0.041$ . Currents marked in red in (B) and (C) correspond to recordings during the local application of cAMP; asterisks (\*) and (\*\*) indicate moments when a positive pressure was applied to the perfusion pipette.

whole-cell mode. The second perfusion pipette was brought in close proximity to the cell and some positive pressure was applied allowing the contents of the pipette to reach the cell membrane. Figure 9B shows the current recording for when the perfusion pipette was filled with NaCl solution containing 2 mM Ca<sup>2+</sup> and 500 μM cAMP. The current amplitude did not change significantly during local perfusion. However, when the perfusion pipette was filled with depolarizing Ca<sup>2+</sup>-free KAsp solution and 500 μM cAMP, SpiH currents increased significantly, indicating a cAMP influx through open hemichannels (Figure 9C). Figure 9D shows averaged current amplitudes recorded before and during local cAMP application.

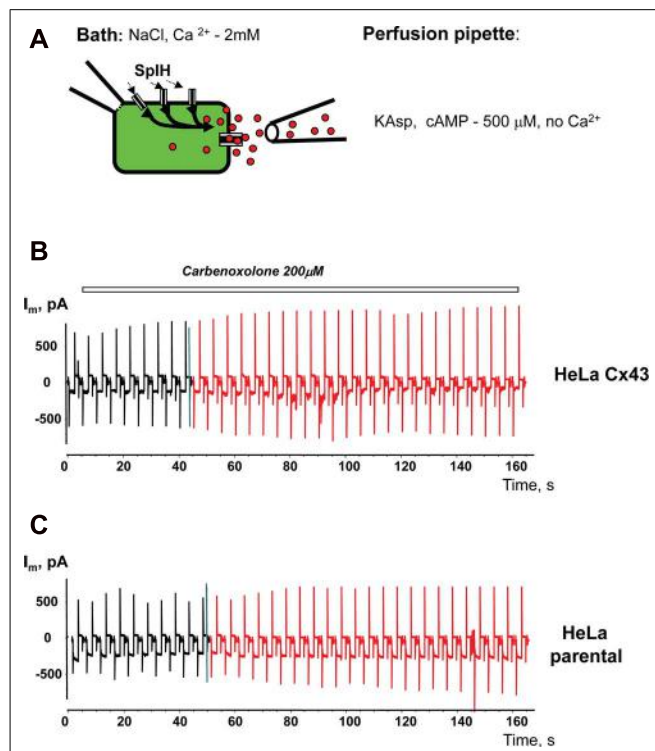


**FIGURE 10 | Modulation of hemichannel activity.** (A) Schematic of the experiment. (B) SpiH current recordings from a HeLaCx43/SpiH cell perfused with Ca<sup>2+</sup>-free KAsp external solution containing 200 μM carbenoxolone. No SpiH current increase was detected during local application of cAMP (red current traces) in five cell preparations ( $6.8 \pm 2.2$  and  $6.6 \pm 2.8$  pA/pF, before and during local application of cAMP, respectively;  $P = 1.0$ ). (C) SpiH current recorded from connexin deficient HeLa parental cells transfected with SpiH during local application of cAMP (red current traces;  $6.8 \pm 1.9$  and  $8.7 \pm 2.8$  pA/pF, before and during local application of cAMP, respectively;  $n = 10$ ,  $P = 0.734$ ).

To prove that cAMP flux is via hemichannels, similar experiments were performed with the presence of the gap junction channel blocker carbenoxolone (200 μM) in the external bath solution. Local perfusion (Figure 10A) with depolarizing KAsp solution (500 μM cAMP, Ca<sup>2+</sup>-free) did not induce a SpiH current rise in HeLaCx43/SpiH cells (Figure 10B). Connexin deficient HeLa parental cells transfected with SpiH likewise did not exhibit a SpiH current increase during local perfusion with cAMP (Figure 10C).

These experiments show that membrane hemichannels can be activated over the small area of the cell membrane and allow passage of cAMP into the cell.

## DISCUSSION

The data presented here show that hemichannels or connexons of Cx43 and Cx26 are permeable to cAMP as demonstrated by the cAMP sensor SpiH. The data address one essential question: are hemichannels to be considered an alternate pathway for autocrine and paracrine delivery? That is, hemichannels are permeable to one signaling molecule known to be involved in paracrine functions utilizing the extracellular pathway (Dahl and Locovei, 2006;

Anselmi et al., 2008; Kanaporis et al., 2008; Kang et al., 2008; Wang et al., 2013).

One issue that has yet to be clearly addressed is the true operational limits of hemichannels. Previous works have often used lowered extracellular  $\text{Ca}^{2+}$  to allow easy demonstration of hemichannel currents. When extracellular  $\text{Ca}^{2+}$  is in the  $\mu\text{M}$  range, macroscopic or multichannel data has revealed that hemichannels have a very high open probability with depolarization (Ebihara et al., 1995; Valiunas and Weingart, 2000; Beahm and Hall, 2002; Valiunas, 2002; Gonzalez et al., 2006).

Ischemia is known to result in membrane depolarization of cardiac myocytes (Kleber et al., 1978; Kleber, 1983) and cells of other aerobic tissues (Al-Mehdi et al., 1998; Calabresi et al., 1999; Dreier, 2011). As such, hemichannels whether activated by altered  $\text{Ca}^{2+}$  levels and/or membrane depolarization have the potential to allow both the influx and efflux of solutes. Consistent with this notion is activation of hCx26 hemichannels at voltages above  $-40\text{ mV}$  (Steffens et al., 2008). In the case of ischemia it is not yet clear whether hemichannel activity is the cause of membrane depolarization or is simply part of the effect. One can speculate that if hemichannels are causal in ischemic depolarization then hemichannels become real therapeutic targets.

The large conductance and permissive selectivity of Cx43 and Cx26 would also allow significant delivery of solutes like cAMP, possibly with even extremely low open probabilities on the order of 0.1–1%. In fact, little is known about the activity of hemichannels when extracellular  $\text{Ca}^{2+}$  is between 1 and 2 mM, the expected range for the interstitial space. What remains to be determined is the open probability of hemichannels versus extracellular  $\text{Ca}^{2+}$  while utilizing conditions to silence other channel types, i.e.,  $\text{K}^+$  channels. For a cell with 10000 hemichannels on its surface and with an imaged open probability of 1% in normal extracellular  $\text{Ca}^{2+}$  the number of functioning channels would be approximately 100 open channels at any instant in time. Assuming the cAMP/ $\text{K}^+$  permeability ratio for Cx43 and Cx26 hemichannels is similar to their respective gap junction channels then the flux per channel is as previously reported (Kanaporis et al., 2008), approximately 6000 molecules/channel/sec for Cx43 and approximately 1800 molecules/channel/sec for Cx26. For 100 functioning channels the total flux per cell would be 0.6 million molecules/sec for Cx43 and 0.18 million for Cx26. Whether such an efflux is sufficient to function as an autocrine/paracrine source of signal molecules like cAMP remains to be seen.

## REFERENCES

- Al-Mehdi, A. B., Zhao, G., and Fisher, A. B. (1998). ATP-independent membrane depolarization with ischemia in the oxygen-ventilated isolated rat lung. *Am. J. Respir. Cell Mol. Biol.* 18, 653–661. doi: 10.1165/ajrccmb.18.5.2834
- Anselmi, F., Hernandez, V. H., Crispino, G., Seydel, A., Ortolano, S., Roper, S. D., et al. (2008). ATP release through connexin hemichannels and gap junction transfer of second messengers propagate  $\text{Ca}^{2+}$  signals across the inner ear. *Proc. Natl. Acad. Sci. U.S.A.* 105, 18770–18775. doi: 10.1073/pnas.0800793105
- Beahm, D. L., and Hall, J. E. (2002). Hemichannel and junctional properties of connexin 50. *Biophys. J.* 82, 2016–2031. doi: 10.1016/S0006-3495(02)75550-1
- Bruzzone, S., Franco, L., Guida, L., Zocchi, E., Contini, P., Bisso, A., et al. (2001). A self-restricted CD38–connexin 43 cross-talk affects NAD $^+$  and cyclic ADP-ribose metabolism and regulates intracellular calcium in 3T3 fibroblasts. *J. Biol. Chem.* 276, 48300–48308. doi: 10.1074/jbc.M107308200
- Bukauskas, F. F., Jordan, K., Bukauskiene, A., Bennett, M. V., Lampe, P. D., Laird, D. W., et al. (2000). Clustering of connexin 43-enhanced green fluorescent protein gap junction channels and functional coupling in living cells. *Proc. Natl. Acad. Sci. U.S.A.* 97, 2556–2561. doi: 10.1073/pnas.050588497
- Calabresi, P., Marfia, G. A., Centonze, D., Pisani, A., and Bernardi, G. (1999). Sodium influx plays a major role in the membrane depolarization induced by oxygen and glucose deprivation in rat striatal spiny neurons. *Stroke* 30, 171–179. doi: 10.1161/01.STR.30.1.171
- Contreras, J. E., Saez, J. C., Bukauskas, F. F., and Bennett, M. V. (2003a). Functioning of cx43 hemichannels demonstrated by single channel properties. *Cell Commun. Adhes.* 10, 245–249. doi: 10.1080/cac.10.4-6.245.249

Understanding the potential role of hemichannels, unrelated to their precursor role in the formation of gap junction channels, as a potential autocrine/paracrine signaling pathway is a real challenge. It is challenging both from a biophysical perspective and the assessment of autocrine and paracrine effects within tissues. Open probability versus calcium is an important biophysical parameter to clearly define, but it is also necessary to test autocrine/paracrine delivery mediated by hemichannels without an endosomal/vesicular background. The latter can be accomplished using drugs that inhibit or block endosomal/vesicular traffic. This study focused on hemichannels composed of connexins but an equally plausible hemichannel construct is a hemichannel composed of pannexins (Wang et al., 2013). Thus, it remains to be seen whether connexins or pannexins are truly able to function as autocrine/paracrine-like delivery systems.

In this study, the SpiH gene, which is a cyclic nucleotide gated channel, was used to assess the permeability of hemichannels to cAMP. This is a useful method, which allows accurate estimates of cyclic nucleotide flux via different membrane hemichannels. In such cases, it is the most suitable approach for quick screening of connexin mutants. Defining the permeability and selectivity properties of hemichannels are important factors in understanding their potential role in normal cell physiology and disease states with connexin mutations.

A final question posed is if there is a role for autocrine and paracrine delivery mediated by hemichannels within the myocardium? Presently autocrine and paracrine functions for hemichannels are open to debate, but there is strong evidence that cAMP influx can act to reduce the sodium current in cardiac myocytes (Hofer and Lefkimiatis, 2007). Autocrine and paracrine-like functions are also a possible explanation for enhanced endothelin expression in response to ischemia or hypertrophy (Drawnel et al., 2013).

A number of reports reviewed in Wang et al. (2013) demonstrated that hemichannels can function as pathways for paracrine messengers, including ATP and prostaglandins. This study now adds an additional potential paracrine-like messenger in the form of cAMP.

## ACKNOWLEDGMENTS

This work was supported by the National Institutes of Health grant GM-088181. The author would like to thank Dr. P. Brink and Dr. T. White for their critical comments on the manuscript, C. Gordon and Dr. Kanaporis for the expert technical assistance.

- Contreras, J. E., Saez, J. C., Bukauskas, F. F., and Bennett, M. V. (2003b). Gating and regulation of connexin 43 (Cx43) hemichannels. *Proc. Natl. Acad. Sci. U.S.A.* 100, 11388–11393. doi: 10.1073/pnas.1434298100
- Contreras, J. E., Sanchez, H. A., Eugenin, E. A., Speidel, D., Theis, M., Willecke, K., et al. (2002). Metabolic inhibition induces opening of unopposed connexin 43 gap junction hemichannels and reduces gap junctional communication in cortical astrocytes in culture. *Proc. Natl. Acad. Sci. U.S.A.* 99, 495–500. doi: 10.1073/pnas.012589799
- Dahl, G., and Locovei, S. (2006). Panxenin: to gap or not to gap, is that a question? *IUBMB Life* 58, 409–419. doi: 10.1080/15216540600794526
- De, V. S. H., and Schwartz, E. A. (1992). Hemi-gap-junction channels in solitary horizontal cells of the catfish retina. *J. Physiol. (Lond.)* 445, 201–230.
- Drawnel, F. M., Archer, C. R., and Roderick, H. L. (2013). The role of the paracrine/autocrine mediator endothelin-1 in regulation of cardiac contractility and growth. *Br. J. Pharmacol.* 168, 296–317. doi: 10.1111/j.1476-5381.2012.02195.x
- Dreier, J. P. (2011). The role of spreading depression, spreading depolarization and spreading ischemia in neurological disease. *Nat. Med.* 17, 439–447. doi: 10.1038/nm.2333
- Duarte, T., Menezes-Rodrigues, F. S., and Godinho, R. O. (2012). Contribution of the extracellular cAMP-adenosine pathway to dual coupling of beta2-adrenoceptors to Gs and Gi proteins in mouse skeletal muscle. *J. Pharmacol. Exp. Ther.* 341, 820–828. doi: 10.1124/jpet.112.192997
- Ebihara, L., Berthoud, V. M., and Beyer, E. C. (1995). Distinct behavior of connexin56 and connexin46 gap junctional channels can be predicted from the behavior of their hemi-gap-junctional channels. *Biophys. J.* 68, 1796–1803. doi: 10.1016/S0006-3495(95)80356-5
- Eskandari, S., Zampighi, G. A., Leung, D. W., Wright, E. M., and Loo, D. D. (2002). Inhibition of gap junction hemichannels by chloride channel blockers. *J. Membr. Biol.* 185, 93–102. doi: 10.1007/s00232-001-0115-0
- Fan, J. S., and Palade, P. (1998). Perforated patch recording with betescin. *Pflugers Arch.* 436, 1021–1023. doi: 10.1007/PL00008086
- Gauss, R., Seifert, R., and Kaupp, U. B. (1998). Molecular identification of a hyperpolarization-activated channel in sea urchin sperm 1. *Nature* 393, 583–587. doi: 10.1038/31248
- Gonzalez, D., Gomez-Hernandez, J. M., and Barrio, L. C. (2006). Species specificity of mammalian connexin-26 to form open voltage-gated hemichannels. *FASEB J.* 20, 2329–2338. doi: 10.1096/fj.06-5828com
- Hofer, A. M., and Lefkimiatis, K. (2007). Extracellular calcium and cAMP: second messengers as “third messengers”? *Physiology (Bethesda)* 22, 320–327. doi: 10.1152/physiol.0019.2007
- Kalvelty, A., Imbrasaita, A., Bukauskienė, A., Verselis, V. K., and Bukauskas, F. F. (2003). Connexins and apoptotic transformation. *Biochem. Pharmacol.* 66, 1661–1672. doi: 10.1016/S0006-2952(03)00540-9
- Kanaporis, G., Mese, G., Valiuniene, L., White, T. W., Brink, P. R., and Valiunas, V. (2008). Gap junction channels exhibit connexin-specific permeability to cyclic nucleotides. *J. Gen. Physiol.* 131, 293–305. doi: 10.1085/jgp.200709934
- Kang, J., Kang, N., Lovatt, D., Torres, A., Zhao, Z., Lin, J., et al. (2008). Connexin 43 hemichannels are permeable to ATP. *J. Neurosci.* 28, 4702–4711. doi: 10.1523/JNEUROSCI.5048-07.2008
- Kleber, A. G. (1983). Resting membrane potential, extracellular potassium activity, and intracellular sodium activity during acute global ischemia in isolated perfused guinea pig hearts. *Circ. Res.* 52, 442–450. doi: 10.1161/01.RES.52.4.442
- Kleber, A. G., Janse, M. J., Van Capelle, F. J., and Durrer, D. (1978). Mechanism and time course of S-T and T-Q segment changes during acute regional myocardial ischemia in the pig heart determined by extracellular and intracellular recordings. *Circ. Res.* 42, 603–613. doi: 10.1161/01.RES.42.5.603
- Kuzhikandathil, E. V., Clark, L., and Li, Y. (2011). The extracellular cAMP-adenosine pathway regulates expression of renal D1 dopamine receptors in diabetic rats. *J. Biol. Chem.* 286, 32454–32463. doi: 10.1074/jbc.M111.268136
- Laing, J. G., and Beyer, E. C. (1995). The gap junction protein connexin43 is degraded via the ubiquitin proteasome pathway. *J. Biol. Chem.* 270, 26399–26403. doi: 10.1074/jbc.270.44.26399
- Maurer, P., and Weingart, R. (1987). Cell pairs isolated from adult guinea pig and rat hearts: effects of  $[Ca^{2+}]_i$  on naxal membrane resistance. *Pflugers Arch.* 409, 394–402. doi: 10.1007/BF00583793
- Plotkin, L. I., Manolagas, S. C., and Bellido, T. (2002). Transduction of cell survival signals by connexin-43 hemichannels. *J. Biol. Chem.* 277, 8648–8657. doi: 10.1074/jbc.M108625200
- Quist, A. P., Rhee, S. K., Lin, H., and Lal, R. (2000). Physiological role of gap-junctional hemichannels. Extracellular calcium-dependent isosmotic volume regulation. *J. Cell Biol.* 148, 1063–1074. doi: 10.1083/jcb.148.5.1063
- Sanchez, H. A., Mese, G., Srinivas, M., White, T. W., and Verselis, V. K. (2010). Differentially altered  $Ca^{2+}$  regulation and  $Ca^{2+}$  permeability in Cx26 hemichannels formed by the A40V and G45E mutations that cause keratitis ichthyosis deafness syndrome. *J. Gen. Physiol.* 136, 47–62. doi: 10.1085/jgp.201010433
- Segretain, D., and Falk, M. M. (2004). Regulation of connexin biosynthesis, assembly, gap junction formation, and removal. *Biochim. Biophys. Acta* 1662, 3–21. doi: 10.1016/j.bbamem.2004.01.007
- Shin, K. S., Rothberg, B. S., and Yellen, G. (2001). Blocker state dependence and trapping in hyperpolarization-activated cation channels: evidence for an intracellular activation gate 8. *J. Gen. Physiol.* 117, 91–101. doi: 10.1085/jgp.117.2.91
- Srinivas, M., Kronengold, J., Bukauskas, F. F., Bargiello, T. A., and Verselis, V. K. (2005). Correlative studies of gating in Cx46 and Cx50 hemichannels and gap junction channels. *Biophys. J.* 88, 1725–1739. doi: 10.1529/biophys.104.054023
- Steffens, M., Gopel, F., Negezahayo, A., Zeilinger, C., Ernst, A., and Kolb, H. A. (2008). Regulation of connexons composed of human connexin26 (hCx26) by temperature. *Biochim. Biophys. Acta* 1778, 1206–1212. doi: 10.1016/j.bbamem.2008.01.016
- Stout, C. E., Costantin, J. L., Naus, C. C., and Charles, A. C. (2002). Intercellular calcium signaling in astrocytes via ATP release through connexin hemichannels. *J. Biol. Chem.* 277, 10482–10488. doi: 10.1074/jbc.M109902200
- Trexler, E. B., Bennett, M. V., Bargiello, T. A., and Verselis, V. K. (1996). Voltage gating and permeation in a gap junction hemichannel. *Proc. Natl. Acad. Sci. U.S.A.* 93, 5836–5841. doi: 10.1073/pnas.93.12.5836
- Trexler, E. B., Bukauskas, F. F., Bennett, M. V., Bargiello, T. A., and Verselis, V. K. (1999). Rapid and direct effects of pH on connexins revealed by the connexin46 hemichannel preparation. *J. Gen. Physiol.* 113, 721–742. doi: 10.1085/jgp.113.5.721
- Valiunas, V. (2002). Biophysical properties of connexin-45 gap junction hemichannels studied in vertebrate cells. *J. Gen. Physiol.* 119, 147–164. doi: 10.1085/jgp.119.2.147
- Valiunas, V., Gemel, J., Brink, P. R., and Beyer, E. C. (2001). Gap junction channels formed by coexpressed connexin40 and connexin43. *Am. J. Physiol. Heart Circ. Physiol.* 281, H1675–H1689.
- Valiunas, V., Polosina, Y. Y., Miller, H., Potapova, I. A., Valiuniene, L., Doronin, S., et al. (2005). Connexin-specific cell-to-cell transfer of short interfering RNA by gap junctions. *J. Physiol.* 568, 459–468. doi: 10.1113/jphysiol.2005.090985
- Valiunas, V., and Weingart, R. (2000). Electrical properties of gap junction hemichannels identified in transfected HeLa cells. *Pflugers Arch.* 440, 366–379. doi: 10.1007/s004240000294
- Valiunas, V., Weingart, R., and Brink, P. R. (2000). Formation of heterotypic gap junction channels by connexins 40 and 43. *Circ. Res.* 86, E42–E49. doi: 10.1161/01.RES.86.2.e42
- Wang, N., De Bock, M., Decrock, E., Bol, M., Gadicherla, A., Vinken, M., et al. (2013). Paracrine signaling through plasma membrane hemichannels. *Biochim. Biophys. Acta* 1828, 35–50. doi: 10.1016/j.bbamem.2012.07.002

**Conflict of Interest Statement:** The author declares that the research was conducted in the absence of any commercial or financial relationships that could be construed as a potential conflict of interest.

*Received: 14 February 2013; accepted: 22 May 2013; published online: 06 June 2013.*

*Citation: Valiunas V (2013) Cyclic nucleotide permeability through unopposed connexin hemichannels. Front. Pharmacol. 4:75. doi: 10.3389/fphar.2013.00075*

*This article was submitted to Frontiers in Pharmacology of Ion Channels and Channelopathies, a specialty of Frontiers in Pharmacology.*

*Copyright © 2013 Valiunas. This is an open-access article distributed under the terms of the Creative Commons Attribution License, which permits use, distribution and reproduction in other forums, provided the original authors and source are credited and subject to any copyright notices concerning any third-party graphics etc.*



# Connexin expression and gap-junctional intercellular communication in ES cells and iPS cells

Masahito Oyamada<sup>1\*</sup>, Kumiko Takebe<sup>1</sup>, Aya Endo<sup>1</sup>, Sachiko Hara<sup>1</sup> and Yumiko Oyamada<sup>2</sup>

<sup>1</sup> Department of Food Science and Human Nutrition, Faculty of Human Life Sciences, Fuji Women's University, Ishikarishi, Japan

<sup>2</sup> Department of Surgical Pathology, Tonan Hospital, Sapporo, Japan

**Edited by:**

Stefan Dhein, Herzzentrum Leipzig  
GmbH – Universitätsklinik, Germany

**Reviewed by:**

Olga Zegarra-Moran, Istituto  
Giannina Gaslini, Italy  
Marc Chanson, University of  
Geneva, Switzerland

**\*Correspondence:**

Masahito Oyamada, Department of  
Food Science and Human Nutrition,  
Faculty of Human Life Sciences, Fuji  
Women's University, Hanakawa  
Minami 4-jou 5-choume, Ishikarishi,  
Hokkaido 061-3204, Japan  
e-mail: oyamada@fujijoshi.ac.jp

Pluripotent stem cells, i.e., embryonic stem (ES) and induced pluripotent stem (iPS) cells, can indefinitely proliferate without commitment and differentiate into all cell lineages. ES cells are derived from the inner cell mass of the preimplantation blastocyst, whereas iPS cells are generated from somatic cells by overexpression of a few transcription factors. Many studies have demonstrated that mouse and human iPS cells are highly similar but not identical to their respective ES cell counterparts. The potential to generate basically any differentiated cell types from these cells offers the possibility to establish new models of mammalian development and to create new sources of cells for regenerative medicine. ES cells and iPS cells also provide useful models to study connexin expression and gap-junctional intercellular communication (GJIC) during cell differentiation and reprogramming. In 1996, we reported connexin expression and GJIC in mouse ES cells. Because a substantial number of papers on these subjects have been published since our report, this Mini Review summarizes currently available data on connexin expression and GJIC in ES cells and iPS cells during undifferentiated state, differentiation, and reprogramming.

**Keywords:** connexins, gap-junctional intercellular communication, ES cells, iPS cells, differentiation, reprogramming, pluripotency

## INTRODUCTION

Gap junctions are cell–cell communicating junctions that consist of multimeric proteins called connexins and mediate the exchange of low-molecular-weight metabolites and ions between contacting cells (Oyamada et al., 2013). Gap-junctional intercellular communication (GJIC) has long been hypothesized to play a crucial role in the maintenance of homeostasis, morphogenesis, cell differentiation, and growth control in multicellular organisms. Discoveries of human genetic disorders due to mutations in connexin genes and experimental data on connexin knockout mice provide direct evidence that gap junctional intercellular communication is essential for tissue functions and organ development and that its dysfunction causes diseases. Connexin-related signaling also involves extracellular signaling (hemichannels) and non-channel intracellular signaling.

GJIC during embryonal development has been demonstrated by using microelectrode impalements to monitor the cell-to-cell movement of ions (ionic coupling) and by microinjection of small-molecular-weight fluorescent dyes such as Lucifer yellow into a single cell and observation of the subsequent dye spread into the surrounding cells (dye coupling) (Lo and Gilula, 1979; Kalimi and Lo, 1988, 1989). It has been revealed that in many instances, GJIC is established within the first few cleavages and results in the entire embryo becoming interconnected as a syncytium. As development progresses, however, dye coupling delineates boundaries defining restrictions in GJIC that effectively segregate the developing embryo or tissue into a number of “communication compartment” domains. Thus, cells

lying within a communication compartment are well coupled, exhibiting both ionic and dye coupling, whereas there is little or no coupling between cells situated across a compartment border. Such restriction of GJIC and the segregation of cells into communication compartment domains are almost always associated with embryogenesis and development.

Pluripotent stem cells, which include embryonic stem (ES) cells and induced pluripotent stem (iPS) cells, possess the ability to proliferate indefinitely without commitment *in vitro* and also differentiate into all cell lineages belonging to the three embryonic germ layers (Evans and Kaufman, 1981; Thomson et al., 1998; Takahashi and Yamanaka, 2006; Takahashi et al., 2007). ES cells are derived from the inner cell mass of the preimplantation blastocyst, whereas iPS cells are generated from many different types of somatic cells by overexpression of only a few pluripotency-related transcription factors. Many studies have demonstrated that mouse and human iPS cells are highly similar but not identical to their respective ES cell counterparts morphologically, functionally, and molecularly at the level of transcription and genome-wide distribution of chromatin modification. The potential to generate basically any differentiated cell types from ES cells and iPS cells offers the possibility to establish new models of mammalian development and to create new sources of cells for regenerative medicine (Robinton and Daley, 2012).

The *in vitro* differentiation system using ES cells and iPS cells also provides a useful model to study connexin expression and GJIC during the early stage of cell differentiation (Wong et al.,

2008; Sharovskaya, 2011). In addition, the importance of understanding the regulation of connexin expression in differentiating pluripotent cells is recognized in regenerative medicine.

In 1996, we first reported the expression of connexin genes and GJIC during *in vitro* cardiomyocyte differentiation of mouse ES cells (Oyamada et al., 1996). Because a substantial number of papers on these subjects have been published since our first report, this Mini Review summarizes currently available data on connexin expression and GJIC in ES cells and iPS cells during undifferentiated state, differentiation, and reprogramming.

## QUESTIONS ABOUT CONNEXIN EXPRESSION AND GAP-JUNCTIONAL INTERCELLULAR COMMUNICATION IN ES/IPS CELLS

Main questions about connexin expression and GJIC in ES/iPS cells that have been addressed thus far can be summarized as below:

1. What kinds of connexins are expressed in undifferentiated ES/iPS cells?
2. To what extent do undifferentiated ES/iPS cells communicate with each other via gap junctions?
3. What changes in connexin expression and GJIC occur during differentiation of ES/iPS cells?
4. What roles do connexin expression and/or GJIC play in maintenance of pluripotency in ES/iPS cells?
5. What changes in connexin expression and GJIC occur during induction of pluripotency in somatic cells (reprogramming)?
6. What roles do connexin expression and/or GJIC play in reprogramming?

## CURRENTLY AVAILABLE DATA ON CONNEXIN EXPRESSION AND GAP-JUNCTIONAL INTERCELLULAR COMMUNICATION IN ES CELLS

**Table 1** summarizes results of published papers concerning connexin expression and GJIC in ES cells.

## CONNEXIN EXPRESSION AND GAP-JUNCTIONAL INTERCELLULAR COMMUNICATION IN iPS CELLS

**Table 2** summarizes results of published papers concerning connexin expression and GJIC in iPS cells.

Using human iPS cells, Sharovskaya et al. (2012) reported that GJIC is re-established during reprogramming to pluripotency: GJIC in incompletely reprogrammed cells was markedly decreased compared with that in the parental somatic cells, but GJIC in completely reprogrammed cells exceeded that in the parental somatic cells and was comparable to that in human ES cells. They drew an analogy between dramatic reduction of GJIC among the cells undergoing early reprogramming and weak GJIC or lack thereof among epithelial stem cells, such as keratinocyte stem cells, breast epithelial, and neural-glial stem cells, suggesting that changes in GJIC during early reprogramming might be associated with mesenchymal-to-epithelial transition (MET). They also showed that the opposite process of cell differentiation from the pluripotent state leads to the disruption of GJIC between pluripotent and differentiated cell subsets. However, GJIC is subsequently re-established *de novo* within each differentiated

cell type *in vitro*, forming communication compartments within a histotype. Human iPS cells they utilized were derived from human umbilical vein endothelial cells (HUVECs) by lentiviral transfection with four transcription factors: KLF4, OCT4, SOX2, and C-MYC. To evaluate changes in GJIC during late stages of reprogramming, incompletely reprogrammed endo-iPSC10 cells at passage 6 and completely reprogrammed cells of the same line at passage 26 were studied. Incompletely reprogrammed iPS cells were characterized by residual expression of endothelial-specific genes including Cx37 and reduced expression of pluripotency-related genes. In addition, they compared expression of connexins in HUVEC, endo-iPS-10, 12, and human ES cells and found that only Cx37 and Cx43 expression varied significantly in the examined cell types. In incompletely reprogrammed iPS cells, Cx37 and Cx43 were expressed at the level similar to HUVEC. In faithfully reprogrammed iPS cells, cells lacked characteristics of parental HUVEC Cx37 expression, whereas Cx43 expression increased three- to five-fold.

Ke et al. (2013) demonstrated that Cx43 is specifically and highly enriched in undifferentiated human iPS cell lines during and after the reprogramming process. They also showed that iPS cells display functional GJIC and that Cx43 expression is gradually upregulated (~4.5-fold increase) during the reprogramming process. They observed that the Cx43 protein level increased gradually along with the expression of the pluripotency marker NANOG. Because Cx43 has been identified as a downstream target of the key pluripotency transcription factors OCT4, SOX2 and NANOG (Boyer et al., 2005), Cx43 expression might be upregulated by the key factors during reprogramming. They also found that the ectopic expression of Cx43 enhances the reprogramming efficiency (~3-fold increase), whereas the knockdown of endogenous Cx43 expression by RNAi reduces the efficiency, possibly by affecting the MET process, as reported by changes in E-cadherin expression. In addition, they showed that pharmacological GJIC inhibitors, CBX, 18-a-GA and the Cx43 mimetic peptide GAP27, did not affect the efficiency of iPS cell generation, suggesting that the effect of Cx43 on the efficiency of iPS cell generation may be attributed to the Cx43 protein itself but not to the function of GJIC, i.e., through a GJIC-independent pathway.

Taken together, these results suggest that Cx43 may represent a pluripotency marker of iPS cells and may play an important role in the reprogramming process.

Lundy et al. (2013) recently have developed a cell culture protocol capable of generating and maintaining highly purified human ES cell- and iPS cell-derived cardiomyocytes for several months *in vitro*. They have shown that these human ES cell- and iPS cell-derived cardiomyocytes are capable of maturing to a phenotype that more closely resembles adult cardiomyocytes in both structure and function. A robust induction of key cardiac structural markers including Cx43 has been demonstrated in late-stage ES cell- and iPS cell-derived cardiomyocytes. These findings suggest that ES cell- and iPS cell-derived cardiomyocytes are capable of slowly maturing to more closely resemble the phenotype of adult cardiomyocytes and may eventually possess the potential to regenerate the lost myocardium with robust *de novo* force-producing tissue.

**Table 1 | Connexin expression and GJIC in ES cells.**

<b>ES cell lines</b>	<b>Connexin expression in undifferentiated cells</b>	<b>GJIC in undifferentiated cells</b>	<b>Differentiation from ES cells</b>	<b>Connexin expression during differentiation</b>	<b>GJIC during differentiation</b>	<b>Methods used to determine the final phenotype of differentiated cells</b>	<b>References</b>
Mouse ES cells (J1)	Cx43 <sup>1</sup> , Cx45 <sup>1</sup> Not detected: Cx40 <sup>1</sup>	Present <sup>3</sup>	Cardiomyocytes	Cx40 <sup>1</sup> , Cx43 <sup>1,2</sup> , Cx45 <sup>1</sup>	Present <sup>3</sup> . Restricted to neighboring beating cells	Contraction, Ca <sup>2+</sup> -imaging, cardiac-specific gene expression	Oyamada et al., 1996
Mouse ES cells (D3)			Cardiomyocytes	Cx43 <sup>2</sup>	Present <sup>3</sup>	Contraction, EM	Westfall et al., 1997
Mouse Cx43 <sup>-/-</sup> ES cells (R1)	Cx45 <sup>1</sup> . No compensatory upregulation of Cx40 <sup>1</sup> and Cx45 <sup>1</sup>	Very low GJIC <sup>3</sup>	Cardiomyocytes. Cx43 knockout did not significantly change either the time course, frequency of cardiomyocytic differentiation, or expression of cardiac-specific genes	Upregulation of Cx40 <sup>1</sup>	Very low GJIC <sup>3</sup>	Contraction, cardiac-specific gene expression	Oyamada et al., 2000
Mouse ES cells (D3)	Cx43 <sup>1,2</sup>		Cardiomyocytes	Increases in Cx40 <sup>2</sup> and Cx43 <sup>2</sup> during cardiac differentiation		Contraction, cardiac-specific gene expression, electrophysiology	Van Kempen et al., 2003
Mouse ES cells (HM1)			Cardiomyocytes	Upregulation of Cx40 <sup>2</sup> at a peak around day 3 (hanging drop period) + 14		Cardiac-specific gene expression, ANEPPS fluorescence, electrophysiology	Fijnvandraat et al., 2003
Mouse ES cells (CCE)	Cx43 <sup>1,2</sup> , Cx45 <sup>1,2</sup> No or very low expression: Cx37 <sup>1</sup> , Cx40 <sup>1</sup>		Cardiomyocytes (irregular contractions in Cx45 <sup>-/-</sup> cells)	Cx37 <sup>1</sup> , Cx40 <sup>1</sup> , Cx43 <sup>1,2</sup> , Cx45 <sup>1</sup>		Contraction, Ca <sup>2+</sup> -imaging, multielectrode array, cardiac-specific gene expression, EM	Egashira et al., 2004
Human ES cells (H1, H7, H9, H14)	Cx43 <sup>1,2</sup> , Cx45 <sup>1</sup>	Present <sup>3</sup>					Carpenter et al., 2004
Human ES cells (GE01, GE09, BG01, BG02, TE06)	Cx43 <sup>1</sup> , Cx45 <sup>1</sup>						Bhattacharya et al., 2004

(Continued)

**Table 1 | Continued**

<b>ES cell lines</b>	<b>Connexin expression in undifferentiated cells</b>	<b>GJIC in undifferentiated cells</b>	<b>Differentiation from ES cells</b>	<b>Connexin expression during differentiation</b>	<b>GJIC during differentiation</b>	<b>Methods used to determine the final phenotype of differentiated cells</b>	<b>References</b>
Human ES cells (HES-3, HES-4)	Cx43 <sup>1</sup> (As one of the candidate human ES marker genes)						Richards et al., 2004
Human ES cells (HES-3, HES-4)	Cx43 <sup>1,2</sup> , Cx45 <sup>1,2</sup>	Present <sup>3</sup>					Wong et al., 2004, 2006
Mouse ES cells (Royan B1)			Cardiomyocytes		Presence of gap junctions in 21-day cardiomyocytes by EM	Cardiac-specific gene expression, EM, pharmacological reagents	Baharvand et al., 2005
Mouse ES cells (DBA/1 LacJ)			Cardiomyocytes	Cx43 <sup>1</sup> , Cx45 <sup>1</sup>		Contraction, Ca <sup>2+</sup> -imaging, cardiac-specific gene expression, EM	Chaudhary et al., 2006
Human ES cells (BG01, H1)	Cx43 <sup>1,2</sup> , Cx40 <sup>1,2</sup> , Cx45 <sup>1,2</sup> , Cx25 <sup>1</sup> , Cx26 <sup>1</sup> , Cx30 <sup>1</sup> , Cx30.2 <sup>1</sup> , Cx30.3 <sup>1</sup> , Cx31 <sup>1</sup> , Cx31.1 <sup>1</sup> , Cx31.9 <sup>1</sup> , Cx32 <sup>1</sup> , Cx36 <sup>1</sup> , Cx37 <sup>1</sup> , Cx46 <sup>1</sup> , Cx47 <sup>1</sup> , Cx59 <sup>1</sup> , Cx62 <sup>1</sup> Not detected: Cx40.1 <sup>1</sup> , Cx50 <sup>1</sup>	Presence of GJIC <sup>3,5</sup> and hemichannels Extremely rare dye coupling between ES cells and feeder cells			Contraction, electrophysiology, cardiac-specific gene expression, EM, pharmacological reagents	Huettnet et al., 2006	
Cynomolgus monkey ES cells (CMK-6)	Cx43 <sup>1</sup>		Embryoid bodies (EBs)		Suppression of Cx43 mRNA expression during EB differentiation		Yamamoto et al., 2007
Human ES cells (HES2, HES-3, ENVY)	Cx43 <sup>2</sup>			Presence of GJIC mediated transport of shRNA			Wolvetaang et al., 2007
Mouse ES cells (D3)	Cx43 <sup>1,2</sup>		Present <sup>3</sup> . Cx43 silencing inhibited GJIC, induced a loss of pluripotent state, and decreased in the proliferation rate	EBs GJIC blockers and Cx43-siRNA inhibited the formation of EBs from ES cells			Todorova et al., 2008

(Continued)

**Table 1 | Continued**

ES cell lines	Connexin expression in undifferentiated cells	GJIC in undifferentiated cells	Differentiation from ES cells	Connexin expression during differentiation	GJIC during differentiation	Methods used to determine the final phenotype of differentiated cells	References
Mouse ES cells (HM1)	Cx43 <sup>1, 2</sup> , Cx45 <sup>1, 2</sup> , Cx31 <sup>1, 2</sup> , Cx26 <sup>1</sup> , Cx30 <sup>31</sup> , Cx32 <sup>1</sup> , Cx37 <sup>1</sup>	Present <sup>3, 4</sup> Reduction of GJIC by decreased expression of Cx31 or Cx45 via RNA interference in Cx26 <sup>2</sup> , Cx29 <sup>1</sup> , Cx30 <sup>1</sup> , Cx30 <sup>21</sup> , Cx31 <sup>11</sup> , Cx32 <sup>2</sup> , Cx33 <sup>1</sup> , Cx36 <sup>1</sup> , Cx37 <sup>2</sup> , Cx40 <sup>1</sup> , Cx46 <sup>1</sup> , Cx47 <sup>1</sup> , Cx50 <sup>1</sup> , Cx57 <sup>1</sup>	Neuroectodermal cells Cx43 <sup>-/-</sup> ES cells showed a failure of oligodendrocyte development and an amplification of astrocytic cells	Wild-type ES cells showed "two-tailed" Cx43 expression with a maximum at day 7	Sox1-promoter-GFP, neuronal lineage-specific gene expression	Parekkadan et al., 2008	
Mouse ES cells (D3): Sox1-promoter-GFP + ES cells and Cx43 <sup>-/-</sup> ES cells	Cx43 <sup>1</sup>	Not characterized	Present but attenuated <sup>3</sup> Restricted to differentiated cells Absence of GJIC between pluripotent and differentiating cells	Present but attenuated <sup>3</sup> Restricted to differentiated cells Absence of GJIC between pluripotent and differentiating cells	Sharovskaya et al., 2009		
Human ES cells (hESM01)	Present <sup>3</sup>						
Mouse ES cells (R1)	Cardiomyocytes	Cx43 <sup>2</sup> expression in cell sheets of mouse ES cell-derived cardiomyocytes	Cardiac-specific gene expression, multielectrode array	Matsuura et al., 2011			

<sup>1</sup>mRNA level; <sup>2</sup>Protein level; <sup>3</sup>dye coupling (Lucifer yellow etc.); <sup>4</sup>neurobiotin tracer coupling; <sup>5</sup>electrical coupling; EM, electron microscopy.

**Table 2 | Connexin expression and GJIC in iPS cells.**

iPS cell lines	Connexin expression in undifferentiated cells	GJIC in undifferentiated cells	Differentiation from iPS cells	Connexin expression during differentiation	GJIC during differentiation	Methods used to determine the final phenotype of differentiated cells	References
Mouse iPS cells (O9), Mouse ES cells (E14.11)			Cardiomyocytes differentiated from iPS and ES cells with the use of a standard EB-based protocol	Cx43 in iPS cell- and ES cell-derived cardiomyocytes on day 22		Contraction, cardiac-specific gene expression, Ca <sup>2+</sup> -imaging, multielectrode array	Mauritz et al., 2008
Human iPS cells reprogrammed from primary keratinocytes	Cx43 <sup>2</sup>						Aasen et al., 2008
Mouse iPS cells (O9, N10), Mouse ES cells (R1, D3)			Cardiomyocytes	Cx43 in iPS cell- and ES cell-derived cardiomyocytes		Contraction, cardiac-specific gene expression, multielectrode array, electrophysiology, pharmacological reagents	Pfannkuché et al., 2009
Mouse iPS cells reprogrammed without c-MYC			<i>In vivo</i> 3 germ layer differentiation, i.e., endoderm, ectoderm, and mesoderm. <i>In vitro</i> cardiomyocyte differentiation	Cx43 in iPS cell-derived cardiomyocytes <i>in vivo</i> and <i>in vitro</i>		Contraction, cardiac-specific gene expression, Ca <sup>2+</sup> -imaging, electrophysiology, EM	Martinez-Fernandez et al., 2009
Human iPS cells reprogrammed from HUVECs	Cx43 <sup>1</sup> , Cx45 <sup>1</sup> Not detected: Cx37 <sup>1</sup>	GJIC <sup>3</sup> is re-established during reprogramming to pluripotency		HUVECs express Cx43 <sup>1</sup> , Cx37 <sup>1</sup> , and Cx45 <sup>1</sup>	Low GJIC in HUVECs		Sharovskaya et al., 2012
Human iPS cells reprogrammed from human embryonic fibroblasts	Cx43 <sup>1, 2</sup> , Cx25 <sup>1</sup> , Cx26 <sup>1</sup> , Cx30 <sup>1</sup> , Cx30.2 <sup>1</sup> , Cx30.3 <sup>1</sup> , Cx31 <sup>1</sup> , Cx31.1 <sup>1</sup> , Cx31.9 <sup>1</sup> , Cx37 <sup>1</sup> , Cx40 <sup>1</sup> , Cx45 <sup>1</sup> , Cx46 <sup>1</sup> , Cx47 <sup>1</sup> , Cx59 <sup>1</sup> , Cx62 <sup>1</sup> . Cx43 increases during reprogramming	Present <sup>3</sup>		Human embryonic fibroblasts express Cx43 <sup>1, 2</sup> at low levels			Ké et al., 2013
Human iPS cell line (iMR90)			Cardiomyocytes differentiated from iPS and ES cells using a long-term (over 150 days) culture protocol		Significant increase in Cx43 <sup>1, 2</sup> expression in late-stage (80–120 days) cardiomyocytes vs. early stage (20–40 days) counterparts	Optical contraction analysis, electrophysiology, Ca <sup>2+</sup> -imaging, cardiac-specific gene expression, EM	Lundy et al., 2013
Human ES cell lines (H7, RuES-2)							

<sup>1</sup>mRNA level; <sup>2</sup>protein level; <sup>3</sup>dye coupling (*lucifer yellow etc.*); EM, electron microscopy.

## CONCLUSIONS: CURRENT ANSWERS TO THE QUESTIONS ON CONNEXIN EXPRESSION AND GAP-JUNCTIONAL INTERCELLULAR COMMUNICATION IN ES/iPS CELLS

It seems reasonable to conclude that mRNAs encoding almost all of the connexins are expressed in ES/iPS cells. At protein level, however, expression of only a few connexins, such as Cx43, Cx45, Cx31, and Cx40, has been confirmed. Many studies have shown that undifferentiated ES/iPS cells communicate with each other via gap junctions at a high level. Several studies using Cx43 RNAi demonstrated that Cx43 contributes substantially to a high level of GJIC in undifferentiated ES/iPS cells.

Concerning changes in connexin expression and GJIC during differentiation of ES/iPS cells, it has been shown that expression of tissue-related connexins, such as Cx40, Cx43, Cx45, and Cx37 in the cardiomyocyte, is upregulated and that GJIC between pluripotent and differentiated cells is disrupted, resulting in formation of “communication compartments.” Regarding changes in connexin expression and GJIC during induction of pluripotency in somatic cells, the studies mentioned here have demonstrated that GJIC is re-established and Cx43 expression is upregulated during reprogramming to pluripotency.

## REFERENCES

- Aasen, T., Raya, A., Barrero, M. J., Garreta, E., Consiglio, A., Gonzalez, F., et al. (2008). Efficient and rapid generation of induced pluripotent stem cells from human keratinocytes. *Nat. Biotechnol.* 26, 1276–1284. doi: 10.1038/nbt.1503
- Baharvand, H., Azarnia, M., Parivar, K., and Ashtiani, S. K. (2005). The effect of extracellular matrix on embryonic stem cell-derived cardiomyocytes. *J. Mol. Cell. Cardiol.* 38, 495–503. doi: 10.1016/j.yjmcc.2004.12.011
- Bhattacharya, B., Miura, T., Brandenberger, R., Mejido, J., Luo, Y., Yang, A. X., et al. (2004). Gene expression in human embryonic stem cell lines: unique molecular signature. *Blood* 103, 2956–2964. doi: 10.1182/blood-2003-09-3314
- Boyer, L. A., Lee, T. I., Cole, M. F., Johnstone, S. E., Levine, S. S., Zucker, J. P., et al. (2005). Core transcriptional regulatory circuitry in human embryonic stem cells. *Cell* 122, 947–956. doi: 10.1016/j.cell.2005.08.020
- Carpenter, M. K., Rosler, E. S., Fisk, G. J., Brandenberger, R., Ares, X., Miura, T., et al. (2004). Properties of four human embryonic stem cell lines maintained in a feeder-free culture system. *Dev. Dyn.* 229, 243–258. doi: 10.1002/dvdy.10431
- Chaudhary, K. W., Barrezueta, N. X., Bauchmann, M. B., Milici, A. J., Beckius, G., Stedman, D. B., et al. (2006). Embryonic stem cells in predictive cardiotoxicity: laser capture microscopy enables assay development. *Toxicol. Sci.* 90, 149–158. doi: 10.1093/toxsci/kfj078
- Egashira, K., Nishii, K., Nakamura, K., Kumai, M., Morimoto, S., and Shibata, Y. (2004). Conduction abnormality in gap junction protein connexin45-deficient embryonic stem cell-derived cardiac myocytes. *Anat. Rec. A Discov. Mol. Cell Evol. Biol.* 280, 973–979. doi: 10.1002/ar.a.20110
- Evans, M. J., and Kaufman, M. H. (1981). Establishment in culture of pluripotential cells from mouse embryos. *Nature* 292, 154–156. doi: 10.1038/292154a0
- Fijnvandraat, A. C., Van Ginneken, A. C., Schumacher, C. A., Boheler, K. R., Lekanne Deprez, R. H., Christoffels, V. M., et al. (2003). Cardiomyocytes purified from differentiated embryonic stem cells exhibit characteristics of early chamber myocardium. *J. Mol. Cell. Cardiol.* 35, 1461–1472. doi: 10.1016/j.yjmcc.2003.09.011
- Huettnner, J. E., Lu, A., Qu, Y., Wu, Y., Kim, M., and McDonald, J. W. (2006). Gap junctions and connexon hemichannels in human embryonic stem cells. *Stem Cells* 24, 1654–1667. doi: 10.1634/stemcells.2005-0003
- Kalimi, G. H., and Lo, C. W. (1988). Communication compartments in the gastrulating mouse embryo. *J. Cell Biol.* 107, 241–255. doi: 10.1083/jcb.107.1.241
- Kalimi, G. H., and Lo, C. W. (1989). Gap junctional communication in the extraembryonic tissues of the gastrulating mouse embryo. *J. Cell Biol.* 109, 3015–3026. doi: 10.1083/jcb.109.6.3015
- Ke, Q., Li, L., Cai, B., Liu, C., Yang, Y., Gao, Y., et al. (2013). Connexin 43 is involved in the generation of human-induced pluripotent stem cells. *Hum. Mol. Genet.* 22, 2221–2233. doi: 10.1093/hmg/ddt074
- Lo, C. W., and Gilula, N. B. (1979). Gap junctional communication in the preimplantation mouse embryo. *Cell* 18, 399–409. doi: 10.1016/0092-8674(79)90059-X
- Lundy, S. D., Zhu, W. Z., Regnier, M., and Laflamme, M. A. (2013). Structural and functional maturation of cardiomyocytes derived from human pluripotent stem cells. *Stem Cells Dev.* doi: 10.1089/scd.2012.0490. [Epub ahead of print].
- Martinez-Fernandez, A., Nelson, T. J., Yamada, S., Reyes, S., Alekseev, A. E., Perez-Terzic, C., et al. (2009). iPS programmed without c-MYC yield proficient cardiogenesis for functional heart chimerism. *Circ. Res.* 105, 648–656. doi: 10.1161/CIRCRESAHA.109.203109
- Matsuura, K., Masuda, S., Haraguchi, Y., Yasuda, N., Shimizu, T., Hagiwara, N., et al. (2011). Creation of mouse embryonic stem cell-derived cardiac cell sheets. *Biomaterials* 32, 7355–7362. doi: 10.1016/j.biomaterials.2011.05.042
- Mauritz, C., Schwanke, K., Reppel, M., Neef, S., Katsirntaki, K., Maier, L. S., et al. (2008). Generation of functional murine cardiac myocytes from induced pluripotent stem cells. *Circulation* 118, 507–517. doi: 10.1161/CIRCULATIONAHA.108.778795
- Oyamada, M., Oyamada, Y., Komatsu, K., Mori, M., and Takamatsu, T. (2000). *In vitro* cardiomyocytic differentiation of mouse embryonic stem cells deficient in gap junction protein connexin43. *Card. Vasc. Regen.* 1, 54–64.
- Oyamada, M., Takebe, K., and Oyamada, Y. (2013). Regulation of connexin expression by transcription factors and epigenetic mechanisms. *Biochim. Biophys. Acta* 1828, 118–133. doi: 10.1016/j.bbamem.2011.12.031
- Oyamada, Y., Komatsu, K., Kimura, H., Mori, M., and Oyamada, M. (1996). Differential regulation of gap junction protein (connexin) genes during cardiomyocytic differentiation of mouse embryonic stem cells *in vitro*. *Exp. Cell Res.* 229, 318–326. doi: 10.1006/excr.1996.0377

- Parekkadan, B., Berdichevsky, Y., Irimia, D., Leeder, A., Yarmush, G., Toner, M., et al. (2008). Cell-cell interaction modulates neuroectodermal specification of embryonic stem cells. *Neurosci. Lett.* 438, 190–195. doi: 10.1016/j.neulet.2008.03.094
- Pfannkuche, K., Liang, H., Hannes, T., Xi, J., Fatima, A., Nguemo, F., et al. (2009). Cardiac myocytes derived from murine reprogrammed fibroblasts: intact hormonal regulation, cardiac ion channel expression and development of contractility. *Cell Physiol. Biochem.* 24, 73–86. doi: 10.1159/000227815
- Richards, M., Tan, S. P., Tan, J. H., Chan, W. K., and Bongso, A. (2004). The transcriptome profile of human embryonic stem cells as defined by SAGE. *Stem Cells* 22, 51–64. doi: 10.1634/stemcells.22-1-51
- Robinton, D. A., and Daley, G. Q. (2012). The promise of induced pluripotent stem cells in research and therapy. *Nature* 481, 295–305. doi: 10.1038/nature10761
- Sharovskaya, Y. Y. (2011). Intercellular interactions through gap junctions in embryonic stem cells. *Biophysics* 56, 86–89. doi: 10.1134/S0006350911010192
- Sharovskaya, Y. Y., Lagarkova, M. A., Kiselev, S. L., and Chailakhyan, L. M. (2009). Gap junctional intercellular communication in human embryonic stem cells during spontaneous differentiation. *Dokl. Biol. Sci.* 427, 387–390.
- Sharovskaya, Y. Y., Philonenko, E. S., Kiselev, S. L., and Lagarkova, M. A. (2012). *De novo* reestablishment of gap junctional intercellular communications during reprogramming to pluripotency and differentiation. *Stem Cells Dev.* 21, 2623–2629. doi: 10.1089/scd.2011.0707
- Takahashi, K., Tanabe, K., Ohnuki, M., Narita, M., Ichisaka, T., Tomoda, K., et al. (2007). Induction of pluripotent stem cells from adult human fibroblasts by defined factors. *Cell* 131, 861–872. doi: 10.1016/j.cell.2007.11.019
- Takahashi, K., and Yamanaka, S. (2006). Induction of pluripotent stem cells from mouse embryonic and adult fibroblast cultures by defined factors. *Cell* 126, 663–676. doi: 10.1016/j.cell.2006.07.024
- Thomson, J. A., Itskovitz-Eldor, J., Shapiro, S. S., Waknitz, M. A., Swiergiel, J. J., Marshall, V. S., et al. (1998). Embryonic stem cell lines derived from human blastocysts. *Science* 282, 1145–1147. doi: 10.1126/science.282.5391.1145
- Todorova, M. G., Soria, B., and Quesada, I. (2008). Gap junctional intercellular communication is required to maintain embryonic stem cells in a non-differentiated and proliferative state. *J. Cell. Physiol.* 214, 354–362. doi: 10.1002/jcp.21203
- Van Kempen, M., Van Ginneken, A., De Grijt, I., Mutsaers, N., Ophof, T., Jongsma, H., et al. (2003). Expression of the electrophysiological system during murine embryonic stem cell cardiac differentiation. *Cell Physiol. Biochem.* 13, 263–270. doi: 10.1159/000074541
- Westfall, M. V., Pasik, K. A., Yule, D. I., Samuelson, L. C., and Metzger, J. M. (1997). Ultrastructure and cell-cell coupling of cardiac myocytes differentiating in embryonic stem cell cultures. *Cell Motil. Cytoskeleton* 36, 43–54.
- Wolvetang, E. J., Pera, M. F., and Zuckerman, K. S. (2007). Gap junction mediated transport of shRNA between human embryonic stem cells. *Biochem. Biophys. Res. Commun.* 363, 610–615. doi: 10.1016/j.bbrc.2007.09.035
- Wong, R. C. B., Dottori, M., Koh, K. L. L., Nguyen, L. T. V., Pera, M. F., and Pebay, A. (2006). Gap junctions modulate apoptosis and colony growth of human embryonic stem cells maintained in a serum-free system. *Biochem. Biophys. Res. Commun.* 344, 181–188. doi: 10.1016/j.bbrc.2006.03.127
- Wong, R. C., Pebay, A., Nguyen, L. T., Koh, K. L., and Pera, M. F. (2004). Presence of functional gap junctions in human embryonic stem cells. *Stem Cells* 22, 883–889. doi: 10.1634/stemcells.22-6-883
- Wong, R. C. B., Pera, M. F., and Pebay, A. (2008). Role of gap junctions in embryonic and somatic stem cells. *Stem Cell Rev.* 4, 283–292. doi: 10.1007/s1205-008-9038-9
- Worsdorfer, P., Maxiner, S., Markopoulos, C., Kirfel, G., Wulf, V., Auth, T., et al. (2008). Connexin expression and functional analysis of gap junctional communication in mouse embryonic stem cells. *Stem Cells* 26, 431–439. doi: 10.1634/stemcells.2007-0482
- Yamamoto, M., Tase, N., Okuno, T., Kondo, Y., Akiba, S., Shimoza, N., et al. (2007). Monitoring of gene expression in differentiation of embryoid bodies from cynomolgus monkey embryonic stem cells in the presence of bisphenol A. *J. Toxicol. Sci.* 32, 301–310. doi: 10.2131/jts.32.301

**Conflict of Interest Statement:** The authors declare that the research was conducted in the absence of any commercial or financial relationships that could be construed as a potential conflict of interest.

*Received: 21 April 2013; accepted: 13 June 2013; published online: 03 July 2013.*

*Citation: Oyamada M, Takebe K, Endo A, Hara S and Oyamada Y (2013) Connexin expression and gap-junctional intercellular communication in ES cells and iPS cells. Front. Pharmacol. 4:85. doi: 10.3389/fphar.2013.00085*

*This article was submitted to Frontiers in Pharmacology of Ion Channels and Channelopathies, a specialty of Frontiers in Pharmacology.*

*Copyright © 2013 Oyamada, Takebe, Endo, Hara and Oyamada. This is an open-access article distributed under the terms of the Creative Commons Attribution License, which permits use, distribution and reproduction in other forums, provided the original authors and source are credited and subject to any copyright notices concerning any third-party graphics etc.*



# Connexin 43 impacts on mitochondrial potassium uptake

Kerstin Boengler<sup>1</sup>, Elvira Ungefug<sup>1</sup>, Gerd Heusch<sup>2</sup>, Luc Leybaert<sup>3</sup> and Rainer Schulz<sup>1\*</sup>

<sup>1</sup> Physiologisches Institut, Justus-Liebig-Universität Giessen, Giessen, Germany

<sup>2</sup> Institut für Pathophysiologie, Universitätsklinikum Essen, Essen, Germany

<sup>3</sup> Department of Basic Medical Sciences, Ghent University, Ghent, Belgium

**Edited by:**

Aida Salameh, Heart Centre  
University of Leipzig, Germany

**Reviewed by:**

Klaus Groschner, University of Graz,  
Austria

Aida Salameh, Heart Centre  
University of Leipzig, Germany

**\*Correspondence:**

Rainer Schulz, Physiologisches  
Institut, Justus-Liebig-Universität  
Giessen, Aufweg 129, 35392 Giessen,  
Germany  
e-mail: rainer.schulz@physiologie.  
med.uni-giessen.de

In cardiomyocytes, connexin 43 (Cx43) forms gap junctions and unopposed hemichannels at the plasma membrane, but the protein is also present at the inner membrane of subsarcolemmal mitochondria (SSM). Both inhibition and genetic ablation of Cx43 reduce ADP-stimulated complex 1 respiration. Since mitochondrial potassium influx impacts on oxygen consumption, we investigated whether or not inhibition or ablation of mitochondrial Cx43 alters mitochondrial potassium uptake. SSM were isolated from rat left ventricular myocardium and loaded with the potassium-sensitive dye PBFI (potassium-binding benzofuran isophthalate). Intramitochondrial potassium was replaced by tetraethylammonium. Mitochondria were incubated under control conditions or treated with 250 μM Gap19, a peptide that specifically inhibits Cx43-based hemichannels at plasma membranes. Subsequently, 140 mM KCl was added and the slope of the increase in PBFI fluorescence over time was calculated. The slope of the PBFI fluorescence of the control mitochondria was set to 100%. In the presence of Gap19, the mitochondrial potassium influx was reduced from 100 ± 11.6% in control mitochondria to 65.5 ± 10.7% ( $n = 6$ ,  $p < 0.05$ ). In addition to the pharmacological inhibition of Cx43, potassium influx was studied in mitochondria isolated from conditional Cx43 knockout mice. Here, the ablation of Cx43 was achieved by the injection of 4-hydroxytamoxifen (4-OHT; Cx43<sup>Cre-ER(T)/fl</sup> + 4-OHT). The mitochondria of the Cx43<sup>Cre-ER(T)/fl</sup> + 4-OHT mice contained 3 ± 1% Cx43 ( $n = 6$ ) of that in control mitochondria (100 ± 11%,  $n = 8$ ,  $p < 0.05$ ). The ablation of Cx43 ( $n = 5$ ) reduced the velocity of the potassium influx from 100 ± 11.2% in control mitochondria ( $n = 9$ ) to 66.6 ± 5.5% ( $p < 0.05$ ). Taken together, our data indicate that both pharmacological inhibition and genetic ablation of Cx43 reduce mitochondrial potassium influx.

**Keywords:** connexin 43, mitochondria, potassium uptake, Gap19, PBFI

## INTRODUCTION

Connexin 43 (Cx43) forms gap junctions between adjacent cardiomyocytes and is thus essential for cell–cell communication. Six Cx43 proteins at the plasma membrane assemble into a hemichannel, and hemichannels open during ischemia and thereby contribute to cell injury (Shintani-Ishida et al., 2007; Clarke et al., 2009). Additionally, Cx43 is present at the inner membrane of cardiomyocyte mitochondria, and cross-linking studies suggest the presence of Cx43-hemichannels within cardiomyocyte mitochondria (Miro-Casas et al., 2009). However, not all cardiomyocyte mitochondria contain Cx43. In contrast to subsarcolemmal mitochondria (SSM), interfibrillar mitochondria (IFM) lack Cx43 (Boengler et al., 2009). An analysis of the impact of Cx43 on mitochondrial function revealed reduced oxygen consumption in mitochondria in which Cx43 was either inhibited by 18α-glycyrrhetic acid (18αGA) or Cx43-mimetic peptides or in which Cx43 was deleted by conditional knockout (Boengler et al., 2012).

Since mitochondrial potassium fluxes are important for the cardioprotection by ischemic pre- and postconditioning (O’Rourke, 2004; Boengler et al., 2011) and ischemic preconditioning depends on Cx43 (Schwanke et al., 2002), the impact of Cx43 on mitochondrial potassium uptake was studied. In permeabilized wild-type mouse cardiomyocytes, mitochondrial potassium influx

was reduced by 18αGA. Also, the replacement of Cx43 by Cx32 – a connexin which forms channels with lower potassium conductance (Harris, 2002) – decreased the potassium influx into permeabilized murine cardiomyocytes (Miro-Casas et al., 2009). In astrocytes, which also contain mitochondrial Cx43, the administration of the Cx43 inhibitors carbenoxolone and 18αGA reduced mitochondrial potassium uptake (Kozoriz et al., 2010).

In the present study, we investigated the importance of Cx43 for potassium uptake in isolated cardiac mitochondria rather than in intact cardiomyocytes. We studied potassium influx in isolated wild-type mouse mitochondria that were treated with Gap19, a novel peptide which specifically targets Cx43-based hemichannels. In addition, mitochondria isolated from conditional Cx43 knockout mice were investigated.

## MATERIALS AND METHODS

### ANIMALS

The present study was performed with approval by the Bioethical Committee of the State of Nordrhein-Westfalen, Germany. It conforms to the *Guide for the Care and Use of Laboratory Animals* published by the US National Institutes of Health (NIH publication No. 85-23, revised 1996).

A dose of 3 mg 4-hydroxytamoxifen (4-OHT) was injected daily for five consecutive days in Cx43<sup>Cre-ER(T)/fl</sup> mice in which one Cx43 allele had been replaced by the tamoxifen-inducible Cre recombinase. The mice were sacrificed on day 11 after the first injection and mitochondria were isolated from the left ventricles. 4-OHT-treated Cx43<sup>fl/fl</sup> mice served as a control for potassium measurements, and untreated Cx43<sup>fl/fl</sup> mice were used as a control for Western blot analysis.

Experiments on the effects of Gap19 on potassium uptake were performed in SSM and IFM from C57/Bl6 mice.

### ISOLATION OF MITOCHONDRIA

Subsarcolemmal mitochondria were isolated as previously described (Boengler et al., 2005). In brief, ventricles were minced in isolation buffer [in mM: sucrose 250; 4-(2-hydroxyethyl)-1-piperazineethanesulfonic acid (HEPES) 10; ethylene glycol tetraacetic acid (EGTA) 1; 0.5% bovine serum albumin (BSA); pH 7.4], homogenized with an Ultra Turrax, and centrifuged at 700 g for 10 min. The resulting supernatant was centrifuged at 10,780 g for 10 min, and the mitochondrial sediment was re-suspended in isolation buffer without BSA and centrifuged at 7,650 g for 10 min. The protein concentration of the isolated mitochondria was determined using the Dc protein assay (Bio-Rad, Hercules, CA, USA) with BSA as standard. For Western blot analysis, the mitochondria were further purified by Percoll gradient ultracentrifugation (30% Percoll in isolation buffer, 34,000 g, 30 min).

Subsarcolemmal mitochondria and IFM were isolated as already described (Boengler et al., 2009). Ventricular tissue was washed in buffer A [in mM: KCl 100, 3-(N-morpholino)-propanesulfonic acid (MOPS) 50, MgSO<sub>4</sub> 5, ATP 1, EGTA 1, pH 7.4] and weighed. Ventricles were minced in 10 ml/g buffer B (buffer A + 0.04% BSA). The homogenate was centrifuged for 10 min at 800 g and the resulting supernatant (for SSM isolation) for 10 min at 8,000 g. The sediment was re-suspended in buffer A, washed, and re-suspended in a small volume of buffer A. The sediment of the first centrifugation (used for isolation of IFM) was re-suspended in buffer B (10 ml/g tissue). Nagarse (8 U/g) was added and incubated for 1 min on ice. The tissue was homogenized and centrifuged for 10 min at 800 g. The supernatant was centrifuged for 10 min at 8,000 g. The mitochondria in the sediment were re-suspended, washed in buffer A, and finally re-suspended in a small volume of buffer A.

### MITOCHONDRIAL POTASSIUM INFLUX

Mitochondria were loaded with 10 μM PBFI-AM [acetoxymethyl ester of PBFI (potassium-binding benzofuran isophthalate); Sigma-Aldrich, Heidenheim, Germany] diluted 2:1 with 20% pluronic F127 for 10 min at 25°C according to the protocol by Costa et al. (2006). Three volumes of tetraethylammonium (TEA) buffer (in mM: sucrose 175, TEA-Cl 50, HEPES 10, pyruvate 5, malate 5, succinate 5, P<sub>i</sub> 5, EGTA 0.1, and MgCl<sub>2</sub> 0.5 for experiments with conditional Cx43 knockout mitochondria; TEA-Cl 120, HEPES 10, succinate 10, Na<sub>2</sub>HPO<sub>4</sub> 5, EGTA 0.1, MgCl<sub>2</sub> 0.5, rotenone 5 μM, oligomycin 0.67 μM, pH 7.2 for experiments with Gap19) were added, and the mitochondria were incubated for 2 min. Subsequently, the mitochondria were washed twice in isolation buffer and the protein concentration was measured using

the Dc protein assay (Bio-Rad, Hercules, CA, USA). A sample of 200 μg mitochondrial proteins (SSM and IFM) was incubated for 30 min at 4°C with 250 μM of the Cx43-hemichannel blocking peptide Gap19 or under control conditions. In addition, untreated mitochondria from Cx43<sup>fl/fl</sup> and Cx43<sup>Cre-ER(T)/fl</sup> + 4-OHT mice (SSM) were studied. Mitochondria (100 μg/ml) were added to isolation buffer supplemented with 1 μg/ml oligomycin (inhibits the ATP synthase), 50 μM glibenclamide (blocks the mitochondrial ATP-dependent potassium channel; control and conditional Cx43 knockout mice), and 1 μM cyclosporin A (inhibits opening of the mitochondrial permeability transition pore; Gap19 experiments). The uptake of potassium into the mitochondria was induced by adding 140 mM KCl. The PBFI fluorescence was measured in a Cary Eclipse Fluorescence Spectrophotometer (Varian, Mulgrave, Australia) at alternating excitation wavelengths of 340 (maximum potassium sensitivity of the probe) and 380 nm (isosbestic point of the probe), respectively, and an emission wavelength of 500 nm at 25°C. The maximal slope of the PBFI fluorescence after the KCl pulse was determined, and the maximal slope for the control mitochondria was set to 100%.

### WESTERN BLOTTING ANALYSIS

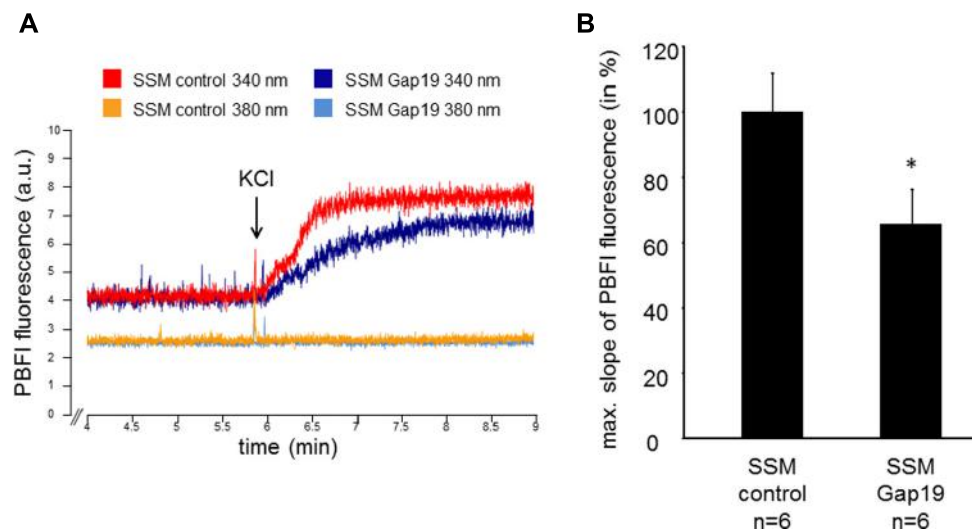
Mitochondrial proteins were extracted in 1 × Cell Lysis Buffer [Cell Signaling, Beverly, MA, USA, containing in mM: Tris 20, NaCl 150, ethylenediaminetetraacetic acid (EDTA) 1, EGTA 1, sodium pyrophosphate 2.5, β-glycerophosphate 1, Na<sub>3</sub>VO<sub>4</sub> 1, phenylmethanesulfonyl fluoride (PMSF) 1, 1 μg/ml leupeptin, 1% Triton X-100, pH 7.5, supplemented with complete protease inhibitors (Roche, Basel, Switzerland)]. After centrifugation at 13,000 g for 10 min at 4°C the supernatants were collected, and the protein concentrations were determined using the Dc protein assay (Bio-Rad, Hercules, CA, USA). Right ventricular or mitochondrial proteins (20 μg) were electrophoretically separated on 10% SDS-PAGE (sodium dodecyl sulfate-polyacrylamide gel electrophoresis) and transferred to nitrocellulose membranes. After blocking, the membranes were incubated with rabbit polyclonal anti-rat Cx43 (Invitrogen, Carlsbad, CA, USA) or rabbit-polyclonal anti-human manganese superoxide dismutase (MnSOD, Upstate, Lake Placid, NY, USA). After incubation with the respective secondary antibodies, immunoreactive signals were detected by chemiluminescence (SuperSignal West Femto Maximum Sensitivity Substrate, Pierce, Rockford, IL, USA) and quantified with the Scion Image software (Frederick, MD, USA).

### STATISTICS

Data are presented as mean values ± SEM. Western blot data and the velocities of mitochondrial potassium uptake were compared by Student's *t*-test.

### RESULTS

The velocity of the mitochondrial potassium influx was measured in wild-type SSM under control conditions and after incubation with 250 μM Gap19, a peptide that specifically inhibits Cx43-based hemichannels at plasma membranes, at excitation wavelengths of 340 and 380 nm, respectively (Figure 1). In the presence of Gap19, the velocity of the mitochondrial potassium influx (340 nm) was reduced from 100 ± 11.6% in control



mitochondria to  $65.5 \pm 10.7\%$  ( $n = 6$ ,  $p < 0.05$ ). At 380 nm excitation, which represents the isosbestic point, the addition of KCl did not affect the PBFI fluorescence ( $6.5 \pm 0.8\%$  control vs.  $7.8\% \pm 1.0\%$  Gap19 treatment,  $n = 6$ ,  $p = \text{ns}$ ). In IFM, which do not contain Cx43, Gap19 treatment had no influence on the velocity of the mitochondrial potassium uptake ( $100 \pm 11.8\%$  IFM control vs.  $106.2 \pm 22.2\%$  IFM Gap19-treated,  $n = 5$ ,  $p = \text{ns}$ ).

The Cx43 content in SSM was determined in  $\text{Cx}43^{\text{Cre-ER(T)}/\text{fl}}$  mice treated with 4-OHT and in  $\text{Cx}43^{\text{fl}/\text{fl}}$  control mice (Figures 2A,B). Western blot analysis demonstrated a reduction in mitochondrial Cx43 from  $100 \pm 10.7\%$  in  $\text{Cx}43^{\text{fl}/\text{fl}}$  mice ( $n = 8$ ) to  $3.2 \pm 1.1\%$  in  $\text{Cx}43^{\text{Cre-ER(T)}/\text{fl}} + 4\text{-OHT}$  mice ( $n = 6$ ,  $p < 0.05$ ). To exclude effects of 4-OHT treatment on mitochondrial function,

potassium influx was measured in mitochondria isolated from 4-OHT-treated  $\text{Cx}43^{\text{fl}/\text{fl}}$  and  $\text{Cx}43^{\text{Cre-ER(T)}/\text{fl}}$  mice. The reduction of the mitochondrial Cx43 content was associated with a reduction in the maximal slope of the PBFI fluorescence from  $100 \pm 11.2\%$  in  $\text{Cx}43^{\text{fl}/\text{fl}} + 4\text{-OHT}$  mitochondria ( $n = 9$ ) to  $66.6 \pm 5.5\%$  in  $\text{Cx}43^{\text{Cre-ER(T)}/\text{fl}} + 4\text{-OHT}$  mitochondria ( $n = 5$ ,  $p < 0.05$ , Figure 2C).

## DISCUSSION

The present study addressed the role of Cx43 in mitochondrial potassium uptake and demonstrated that both inhibition and genetic ablation of mitochondrial Cx43 reduce the velocity of the mitochondrial potassium influx specifically in SSM.

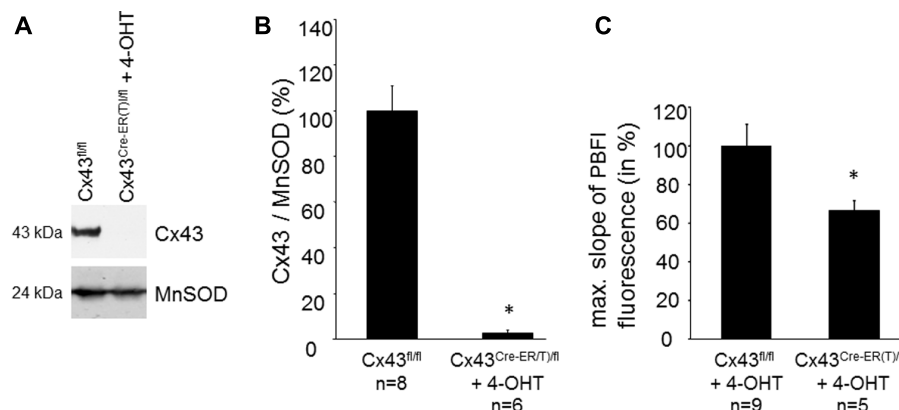


**FIGURE 2 | Genetic ablation of Cx43 reduces mitochondrial potassium uptake.** **(A)** Western blot analysis was performed for Cx43 and the mitochondrial marker protein MnSOD on proteins isolated from SSM of  $\text{Cx}43^{\text{fl}/\text{fl}}$  and  $\text{Cx}43^{\text{Cre-ER(T)}/\text{fl}} + 4\text{-OHT}$  mice. **(B)** Bar graphs represent the mitochondrial Cx43 content normalized to MnSOD in

$\text{Cx}43^{\text{fl}/\text{fl}}$  control mice, which were set to 100%, and 4-OHT-treated  $\text{Cx}43^{\text{Cre-ER(T)}/\text{fl}}$  mice. \* $p < 0.05$ . **(C)** Bar graphs represent the maximal slope of the PBFI fluorescence at 340 nm excitation and 500 nm emission of 4-OHT-treated  $\text{Cx}43^{\text{fl}/\text{fl}}$  and  $\text{Cx}43^{\text{Cre-ER(T)}/\text{fl}}$  mitochondria. \* $p < 0.05$ .

The electrochemical gradient drives an inward potassium flux into mitochondria. For cardiac mitochondria, the ATP-dependent potassium (mitoK<sub>ATP</sub>) channel is of major importance. This channel is activated by pharmacological agents such as diazoxide, whereas glibenclamide and ATP inhibit mitoK<sub>ATP</sub> channel activity. The molecular identity of the mitoK<sub>ATP</sub> channel has not yet been definitely established. However, data suggest mitochondrial localization of sarcolemmal potassium channel subunits (Ye et al., 2009), and, most recently, the contribution of the ROMK (renal outer medullary potassium channel) to the mitoK<sub>ATP</sub> channel (Foster et al., 2012).

Opening of the mitoK<sub>ATP</sub> channel is important for the cardioprotection afforded by ischemic preconditioning (O'Rourke, 2004; Ardehali and O'Rourke, 2005), presumably via the formation of low amounts of reactive oxygen species that function as signaling molecules (Pain et al., 2000). Cx43 is involved in the cardioprotection conferred by mitoK<sub>ATP</sub> channel opening, since reactive oxygen species formation and subsequent infarct size reduction by diazoxide are lost in Cx43-deficient mice (Heinzel et al., 2005).

The present study addressed the contribution of mitochondrial Cx43 to potassium influx. Experiments were performed in the presence of glibenclamide in order to allow the analysis of putative Cx43-based channels and separate them from effects of Cx43 on mitoK<sub>ATP</sub> channels.

Previous data showed that in permeabilized mouse cardiomyocytes Cx43 contributes to mitochondrial potassium uptake (Miro-Casas et al., 2009). In this study, the Cx43 inhibitor 18αGA was employed, and cardiomyocytes were used in which Cx43 had been replaced by Cx32. The aim of the present study was to investigate the importance of Cx43 for mitochondrial potassium refilling in more detail. Therefore, isolated mitochondria from control and conditional Cx43 knockout mice were used. The ablation of Cx43 was achieved by the administration of 4-OHT, which may impact on mitochondrial function, especially on mitochondrial calcium homeostasis (Lobaton et al., 2005). However, previous data demonstrated that the 4-OHT treatment used here has no influence on mitochondrial oxygen consumption (Boengler et al., 2012). To exclude putative effects of 4-OHT on mitochondrial potassium uptake, data obtained in mitochondria from conditional Cx43 knockout mice were compared to those obtained from 4-OHT-treated control mice. Our data demonstrate that mitochondria that contain only minimal amounts of Cx43 (about 3% of the amount of control mitochondria) have a reduced velocity of potassium refilling. Therefore, our data confirm the importance of Cx43 for mitochondrial potassium uptake.

In addition to the chronic scenario of the Cx43 knockout mice, the acute situation was analyzed in which mitochondrial Cx43 was inhibited by Gap19. Gap19 is a peptide derived from nine

amino acids of the Cx43 cytoplasmic loop. This peptide inhibits single channel Cx43-hemichannel currents at plasma membranes but has no effect on gap junction channels or Cx40/pannexin-1-dependent hemichannels as determined by calcium-induced ATP release. Gap19 binds to the carboxy terminus of Cx43 and thereby prevents interactions between the carboxy terminus and the cytoplasmic loop (Wang et al., 2013). In isolated cardiomyocytes, Gap19 reduced cell swelling and cell death following simulated ischemia/reperfusion and reduced infarct size in mouse hearts *in vivo* (Wang et al., 2013). The specificity of Gap19 for Cx43-based hemichannels makes this peptide an excellent tool to study the role of Cx43 in mitochondrial potassium uptake. Since the carboxy terminus of mitochondrial Cx43 is directed toward the intermembrane space (Boengler et al., 2009), Gap19 does not have to enter the mitochondrial matrix in order to interact with Cx43.

In SSM isolated from wild-type mice, Gap19 induced a decrease in the velocity of mitochondrial potassium influx. In IFM, which do not contain Cx43 (Boengler et al., 2009), Gap19 had no effect, demonstrating the specificity of the peptide for Cx43.

The present experiments were performed in the presence of glibenclamide, which inhibits potassium fluxes through mitoK<sub>ATP</sub> channels (Inoue et al., 1991; Paucek et al., 1992); therefore, it is unlikely that the delayed potassium influx in Cx43-deficient and Gap19-treated mitochondria is due to effects of Cx43 on these channels. However, several other channels also contribute to the mitochondrial potassium cycle, among them calcium-dependent potassium channels, the mitochondrial Kv1.3 potassium channel, and the two-pore potassium channel TASK-3 (for review, see Szabo et al., 2012). Since in the present study only total mitochondrial potassium fluxes were measured, it was not possible to distinguish whether mitochondrial potassium influx occurs through putative Cx43-based hemichannels or through an indirect modulation of the above mentioned potassium channels. Whether or not mitochondrial Cx43 forms a channel similar to those at the plasma membrane remains to be established. However, cross-linking studies of mitochondrial proteins with subsequent Western blot analysis for Cx43 revealed immunoreactive signals at a molecular weight typical for Cx43-based hexamers (Miro-Casas et al., 2009).

Taken together, both the genetic ablation of Cx43 in conditional knockout mice and the acute inhibition of mitochondrial Cx43 by Gap19 demonstrate reduced velocities of mitochondrial potassium uptake. These findings substantiate the impact of Cx43 on mitochondrial potassium fluxes.

## ACKNOWLEDGMENT

This study was supported by the German Research Foundation (Schu 843/7-2).

## REFERENCES

- Ardehali, H., and O'Rourke, B. (2005). Mitochondrial K(ATP) channels in cell survival and death. *J. Mol. Cell. Cardiol.* 39, 7–16. doi: 10.1016/j.yjmcc.2004.12.003
- Boengler, K., Dodoni, G., Rodriguez-Sinovas, A., Cabestrero, A., Ruiz-Meana, M., Gres, P., et al. (2005). Connexin 43 in cardiomyocyte mitochondria and its increase by ischemic preconditioning. *Cardiovasc. Res.* 67, 234–244. doi: 10.1016/j.cardiores.2005.04.014
- Boengler, K., Heusch, G., and Schulz, R. (2011). Mitochondria in postconditioning. *Antioxid. Redox Signal.* 14, 863–880. doi: 10.1089/ars.2010.3309
- Boengler, K., Ruiz-Meana, M., Gent, S., Ungefug, E., Soetkamp, D., Miro-Casas, E., et al. (2012). Mitochondrial connexin 43 impacts on respiratory complex I activity and mitochondrial oxygen consumption. *J. Cell. Mol. Med.* 16, 1649–1655. doi: 10.1111/j.1582-4934.2011.01516.x
- Boengler, K., Stahlhofen, S., Van De Sand, A., Gres, P., Ruiz-Meana, M., Garcia-Dorado, D., et al. (2009). Presence of connexin 43 in subsarcolemmal, but not in interfibrillar cardiomyocyte mitochondria. *Basic Res. Cardiol.* 104, 141–147. doi: 10.1007/s00395-009-0007-5

- Clarke, T. C., Williams, O. J., Martin, P. E., and Evans, W. H. (2009). ATP release by cardiac myocytes in a simulated ischaemia model: inhibition by a connexin mimetic and enhancement by an antiarrhythmic peptide. *Eur. J. Pharmacol.* 605, 9–14. doi: 10.1016/j.ejphar.2008.12.005
- Costa, A. D., Quinlan, C. L., Andrukhliv, A., West, I. C., Jaburek, M., and Garlid, K. D. (2006). The direct physiological effects of mitoK(ATP) opening on heart mitochondria. *Am. J. Physiol. Heart Circ. Physiol.* 290, H406–H415. doi: 10.1152/ajpheart.00794.2005
- Foster, D. B., Ho, A. S., Rucker, J., Garlid, A. O., Chen, L., Sidor, A., et al. (2012). Mitochondrial ROMK channel is a molecular component of mitoK(ATP). *Circ. Res.* 111, 446–454. doi: 10.1161/CIRCRESAHA.112.266445
- Harris, A. L. (2002). Voltage-sensing and substrate rectification: moving parts of connexin channels. *J. Gen. Physiol.* 119, 165–169. doi: 10.1085/jgp.119.2.165
- Heinzel, F. R., Luo, Y., Li, X., Boengler, K., Buechert, A., Garcia-Dorado, D., et al. (2005). Impairment of diazoxide-induced formation of reactive oxygen species and loss of cardioprotection in connexin 43 deficient mice. *Circ. Res.* 97, 583–586. doi: 10.1161/01.RES.0000181171.65293.65
- Inoue, I., Nagase, H., Kishi, K., and Higuti, T. (1991). ATP-sensitive K<sup>+</sup> channel in the mitochondrial inner membrane. *Nature* 352, 244–247. doi: 10.1038/352244a0
- Kozoriz, M. G., Church, J., Ozog, M. A., Naus, C. C., and Krebs, C. (2010). Temporary sequestration of potassium by mitochondria in astrocytes. *J. Biol. Chem.* 285, 31107–31119. doi: 10.1074/jbc.M109.082073
- Lobaton, C. D., Vay, L., Hernandez-Sanmiguel, E., Santodomingo, J., Moreno, A., Montero, M., et al. (2005). Modulation of mitochondrial Ca<sup>2+</sup> uptake by estrogen receptor agonists and antagonists. *Br. J. Pharmacol.* 145, 862–871. doi: 10.1038/sj.bjp.0706265
- Miro-Casas, E., Ruiz-Meana, M., Agullo, E., Stahlhofen, S., Rodriguez-Sinovas, A., Cabestrero, A., et al. (2009). Connexin43 in cardiomyocyte mitochondria contributes to mitochondrial potassium uptake. *Cardiovasc. Res.* 83, 747–756. doi: 10.1093/cvr/cvp157
- O'Rourke, B. (2004). Evidence for mitochondrial K<sup>+</sup> channels and their role in cardioprotection. *Circ. Res.* 94, 420–432. doi: 10.1161/01.RES.0000117583.66950.43
- Pain, T., Yang, X. M., Critz, S. D., Yue, Y., Nakano, A., Liu, G. S., et al. (2000). Opening of mitochondrial K(ATP) channels triggers the preconditioned state by generating free radicals. *Circ. Res.* 87, 460–466. doi: 10.1161/01.RES.87.6.460
- Paucek, P., Mironova, G., Mahdi, F., Beavis, A. D., Woldegiorgis, G., and Garlid, K. D. (1992). Reconstitution and partial purification of the glibenclamide-sensitive, ATP-dependent K<sup>+</sup> channel from rat liver and beef heart mitochondria. *J. Biol. Chem.* 267, 26062–26069.
- Schwanke, U., Konietzka, I., Duschin, A., Li, X., Schulz, R., and Heusch, G. (2002). No ischemic preconditioning in heterozygous connexin43-deficient mice. *Am. J. Physiol. Heart Circ. Physiol.* 283, H1740–H1742. doi: 10.1152/ajpheart.00442.2002
- Shintani-Ishida, K., Uemura, K., and Yoshida, K. (2007). Hemichannels in cardiomyocytes open transiently during ischemia and contribute to reperfusion injury following brief ischemia. *Am. J. Physiol. Heart Circ. Physiol.* 293, H1714–H1720. doi: 10.1152/ajpheart.00022.2007
- Szabo, I., Leanza, L., Gulbins, E., and Zoratti, M. (2012). Physiology of potassium channels in the inner membrane of mitochondria. *Pflugers Arch.* 463, 231–246. doi: 10.1007/s00424-011-1058-7
- Wang, N., De Vuyst, E., Ponsaerts, R., Boengler, K., Palacios-Prado, N., Wauman, J., et al. (2013). Selective inhibition of Cx43 hemichannels by Gap19 and its impact on myocardial ischemia/reperfusion injury. *Basic Res. Cardiol.* 108, 309. doi: 10.1007/s00395-012-0309-x
- Ye, B., Kroboth, S. L., Pu, J. L., Sims, J. J., Aggarwal, N. T., McNally, E., et al. (2009). Molecular identification and functional characterization of a mitochondrial sulfonylurea receptor 2 splice variant generated by intraexonic splicing. *Circ. Res.* 105, 1083–1093. doi: 10.1161/CIRCRESAHA.109.195040

**Conflict of Interest Statement:** The authors declare that the research was conducted in the absence of any commercial or financial relationships that could be construed as a potential conflict of interest.

Received: 04 March 2013; paper pending published: 25 March 2013; accepted: 17 May 2013; published online: 06 June 2013.

Citation: Boengler K, Ungefug E, Heusch G, Leybaert L and Schulz R (2013) Connexin 43 impacts on mitochondrial potassium uptake. *Front. Pharmacol.* 4:73. doi: 10.3389/fphar.2013.00073

This article was submitted to Frontiers in Pharmacology of Ion Channels and Channelopathies, a specialty of Frontiers in Pharmacology.

Copyright © 2013 Boengler, Ungefug, Heusch, Leybaert and Schulz. This is an open-access article distributed under the terms of the Creative Commons Attribution License, which permits use, distribution and reproduction in other forums, provided the original authors and source are credited and subject to any copyright notices concerning any third-party graphics etc.



# Interfering amino-terminal peptides and functional implications for heteromeric gap junction formation

Eric C. Beyer<sup>1</sup>, Xianming Lin<sup>2†</sup> and Richard D. Veenstra<sup>2\*</sup>

<sup>1</sup> Department of Pediatrics, University of Chicago, Chicago, IL, USA

<sup>2</sup> Department of Pharmacology, State University of New York Upstate Medical University, Syracuse, NY, USA

**Edited by:**

Aida Salameh, Heart Centre  
University of Leipzig, Germany

**Reviewed by:**

Motohiro Nishida, Kyushu University,  
Japan

Stefan Dhein, Universitätsklinik  
Leipzig Herz-Zentrum Leipzig GmbH,  
Germany

**\*Correspondence:**

Richard D. Veenstra, Department of  
Pharmacology, State University of  
New York Upstate Medical University,  
750 East Adams Street, Syracuse,  
NY 13210, USA.

e-mail: veenstr@upstate.edu

**†Present address:**

Xianming Lin, Leon H. Charney  
Division of Cardiology, New York  
University School of Medicine,  
New York, NY 10016, USA.

Connexin43 (Cx43) is widely expressed in many different tissues of the human body. In cells of some organs, Cx43 is co-expressed with other connexins (Cx), including Cx46 and Cx50 in lens, Cx40 in atrium, Purkinje fibers, and the blood vessel wall, Cx45 in heart, and Cx37 in the ovary. Interactions with the co-expressed connexins may have profound functional implications. The abilities of Cx37, Cx45, Cx46, and Cx50 to function in heteromeric gap junction combinations with Cx43 are well documented. Different studies disagree regarding the ability of Cx43 and Cx40 to produce functional heteromeric gap junctions with each other. We review previous studies regarding the heteromeric interactions of Cx43. The possibility of negative functional interactions between the cytoplasmic pore-forming amino-terminal (NT) domains of these connexins was assessed using pentameric connexin sequence-specific NT domain [interfering NT (iNT)] peptides applied to cells expressing homomeric Cx40, Cx37, Cx45, Cx46, and Cx50 gap junctions. A Cx43 iNT peptide corresponding to amino acids 9–13 (Ac-KLLDK-NH<sub>2</sub>) specifically inhibited the electrical coupling of Cx40 gap junctions in a transjunctional voltage ( $V_j$ )-dependent manner without affecting the function of homologous Cx37, Cx46, Cx50, and Cx45 gap junctions. A Cx40 iNT (Ac-EFLEE-OH) peptide counteracted the  $V_j$ -dependent block of Cx40 gap junctions, whereas a similarly charged Cx50 iNT (Ac-EEVNE-OH) peptide did not, suggesting that these NT domain interactions are not solely based on electrostatics. These data are consistent with functional Cx43 heteromeric gap junction formation with Cx37, Cx45, Cx46, and Cx50 and suggest that Cx40 uniquely experiences functional suppressive interactions with a Cx43 NT domain sequence. These findings present unique functional implications about the heteromeric interactions between Cx43 and Cx40 that may influence cardiac conduction in atrial myocardium and the specialized conduction system.

**Keywords:** connexin43, connexin40, gap junction, heteromeric channel, spermine

## INTRODUCTION

Gap junctions facilitate the metabolic, biochemical, and electrical integration of component cells into functional tissues, because they contain intercellular channels that link them while excluding access to the extracellular milieu. The task of coupling the cells of the various tissues in the body is accomplished by 20 different connexin (Cx) proteins. Although the requirement for so many different connexins is not well understood and there are some functional redundancies, there are significant differences in functional properties among the channels formed of different connexins (including conductance, permeability, and gating).

Essentially all mammalian tissues (and most of the cells within them) contain more than one connexin. The expression of multiple connexins provides the opportunity for interactions with each other to form heteromeric and heterotypic channels. The properties of the resulting hetero-oligomeric channels can have a diversity of functional properties determined by their different subunits, the interactions of those subunits, and the stoichiometries of the interactions.

In previous studies, we have particularly focused on Cx43 and its interactions with other co-expressed connexins. Cx43 is one of

the most widely expressed connexins. It has been found in some cells in most organs of the body, and it has been implicated in significant functions in smooth muscle, myocardium, astrocytes, lens epithelium, endothelium, etc. Many of these cells also contain other connexins. Cx43 is most commonly found with the other connexins that have the most similar sequences including Cx37, Cx40, Cx46, and Cx50 (that are members of the  $\alpha$  sub-family of connexins encoded by the gap junction alpha (GJA) group of genes; Kumar and Gilula, 1992; Beyer and Berthoud, 2009).

The functional interactions of Cx43 with other connexins have been extensively studied by expression of the connexins in *Xenopus* oocytes or in transfected communication-deficient cells. Such studies have consistently shown that Cx43 will form functional heteromeric and/or heterotypic gap junction channels with three  $\alpha$ -connexins, Cx37, Cx46, Cx50, and with Cx45 (now classified as a  $\gamma$ -connexin), but not with the  $\beta$  sub-family connexins, Cx26 and Cx32 (White et al., 1994, 1995; Elfgang et al., 1995; Brink et al., 1997; Berthoud et al., 2001; Martinez et al., 2002; Gemel et al., 2004). These functional interactions between Cx43 and other connexins may have significant functional consequences, like generation of a large variety of different channel sizes (Brink et al.,

1997) or alteration of permeability, gating, and phosphorylation-dependent regulation (Elenes et al., 2001; Martinez et al., 2002). Some of these studies are supported by biochemical data showing the co-isolation of the co-expressed connexin with Cx43 in hexamers.

The ability of Cx43 and Cx40 to form functional interactions within mixed channels is controversial. Initial reports of studies conducted using *Xenopus* oocytes or HeLa cell transfectants concluded that this pair of connexins could not make functional heterotypic channels (Bruzzone et al., 1993; Elfgang et al., 1995; White et al., 1995; Haubrich et al., 1996). However, these observations were contradicted by subsequent reports of functional Cx43–Cx40 heterotypic interactions in pairs of neuro 2a (N2a) cells (Valiunas et al., 2000) and rat insulinoma (RIN) cells (Cottrell and Burt, 2001). When Veenstra and colleagues paired Cx43 with a Cx40 mutant containing substitutions of two charged residues (Musa et al., 2004), they observed symmetrically convergent alterations of voltage-dependent gating, arguing for Cx43–Cx40 heterotypic interactions (Lin et al., 2011; and unpublished results). But, in contrast, a study of connexins tagged with fluorescent proteins at their C-termini concluded that Cx40 and Cx43 only appeared to make heterotypic gap junctions when Cx45 (which could interact with either connexin) was co-expressed (Rackauskas et al., 2006).

However, the issue of heterotypic interactions between these connexins should only have importance in the rare case of a cell producing only Cx40 contacting another expressing only Cx43. In contrast, the possible heteromeric interaction of these connexins may occur frequently in cells (such as atrial myocytes and some endothelial cells) that co-express both connexins.

Several studies have supported the abilities of Cx40 and Cx43 to form functional heteromers. Mixed heteromers of these two connexins were identified by affinity purification or co-immunoprecipitation studies performed using co-expressing cells (He et al., 1999; Valiunas et al., 2001). In transfected N2A cells, Valiunas et al. (2001) observed a rather low total conductance in pairs of cells expressing both Cx40 and Cx43, with only a rather small variation in single channel conductances and alterations of voltage-dependent gating; they suggested that Cx40–Cx43 heteromers might form inefficiently and many might be non-functional. Burt and colleagues have extensively studied the consequences of Cx40 and Cx43 co-expression in A7r5 and RIN cells, including pairs of cells with different relative expression ratios (Cottrell and Burt, 2001; Cottrell et al., 2002; Burt and Steele, 2003; Heyman et al., 2009). Their data suggest that these two connexins readily form heteromeric channels and that the composition of these channels influences many properties including gating, conductance, permeability, charge selectivity, and response to platelet-derived growth factor (PDGF).

The domains within the connexin protein that influence oligomerization between subunits to form a hexamer and between different connexins to form a heteromeric hexamer have not been clearly defined. However, various biochemical and mutagenesis studies have implicated residues within the amino-terminal (NT) and within the first and third transmembrane domains (Lagree et al., 2003; Maza et al., 2005; Martinez et al., 2011). The NT has also been implicated in contributing to various channel properties

including voltage-dependent gating, unitary conductance, and perm-selectivity (Oh et al., 2000, 2004; Veenstra, 2003; Musa et al., 2004; Dong et al., 2006; Gemel et al., 2006; Tong and Ebihara, 2006; Veenstra and Lin, 2006).

Some gap junction channels are very sensitive to block by polyamines like spermine and spermidine (Musa et al., 2001; Musa and Veenstra, 2003). However, this block is selective among connexins with Cx40 being very sensitive and Cx43 insensitive (Musa and Veenstra, 2003). Mutagenesis studies suggest that this connexin-specific difference is imparted by N-terminal amino acids (Musa et al., 2004; Gemel et al., 2006; Lin et al., 2006). Specifically, replacement of two negatively charged residues (E9 and E13) in Cx40 with the corresponding positively charged residues (K9 and K13) of Cx43 abolished spermine block (Musa et al., 2004). This also suggested that the block of Cx40 (but not Cx43) channels by spermine might involve interaction with these NT residues.

Polyamines (including putrescine, spermidine, and spermine) are ubiquitous polybasic molecules that interact with a wide variety of cellular molecules including nucleic acids, nucleotide triphosphates, phospholipids, and acidic proteins and influence gene transcription and translation, signaling pathways, enzyme activities, and ion channel function essential to eukaryotic cell growth and mammalian development (Igarashi and Kashiwagi, 2000; Pegg, 2009). Thus connexin channels are only one of many intracellular targets that may be modulated by cytoplasmic polyamines.

The NT domain of the connexins consists of their first 22–23 amino acids. Some of the amino acids within the NT are highly conserved, while others are variable and contribute to different properties. (The NT domains of several connexins are shown in alignment in **Figure 1**.) The structure of the NT domain was initially investigated by studying synthetic peptides using circular dichroism and nuclear magnetic resonance (Purnick et al., 2000; Arita et al., 2006; Kalmatsky et al., 2009; Kyle et al., 2009). Each of these studies showed that much of the beginning of the NT is  $\alpha$ -helical, although they differ in the exact helical region; Purnick et al. (2000) concluded that the  $\alpha$ -helix in Cx26 extended from position 1 to 10 while Kyle et al. (2009) suggested that it extended between amino acids 5 and 15 in Cx37. When Maeda et al. (2009) determined the structure of a Cx26 channel at 3.5 Å resolution, they observed that the NT regions of the six subunits lined the pore entrance and formed a “funnel,” which restricts the diameter at the entrance of the pore. The beginning of the NT is located deep within the pore. The NT helix extends beyond the cytoplasmic side of the membrane and then forms a loop (including the highly conserved amino acids corresponding to the serine and threonine at positions 18 and 19 in **Figure 1**) that bends back to the membrane where TM1 begins. Although all of the connexins may have homologies, their NT domains do not necessarily assume identical configurations. The  $\beta$ -connexins were proposed to have a “glycine hinge” including and following amino acids 12 and 13 (Purnick et al., 2000; that correspond to amino acids 13 and 14 in the  $\alpha$ -connexins); however, insertion of the SG/GG ( $\beta$ -connexin) motif into Cx40 or Cx43 NT abolishes  $V_j$ -gating, suggesting a structural/functional disparity between the sub-families (Gemel et al., 2006).

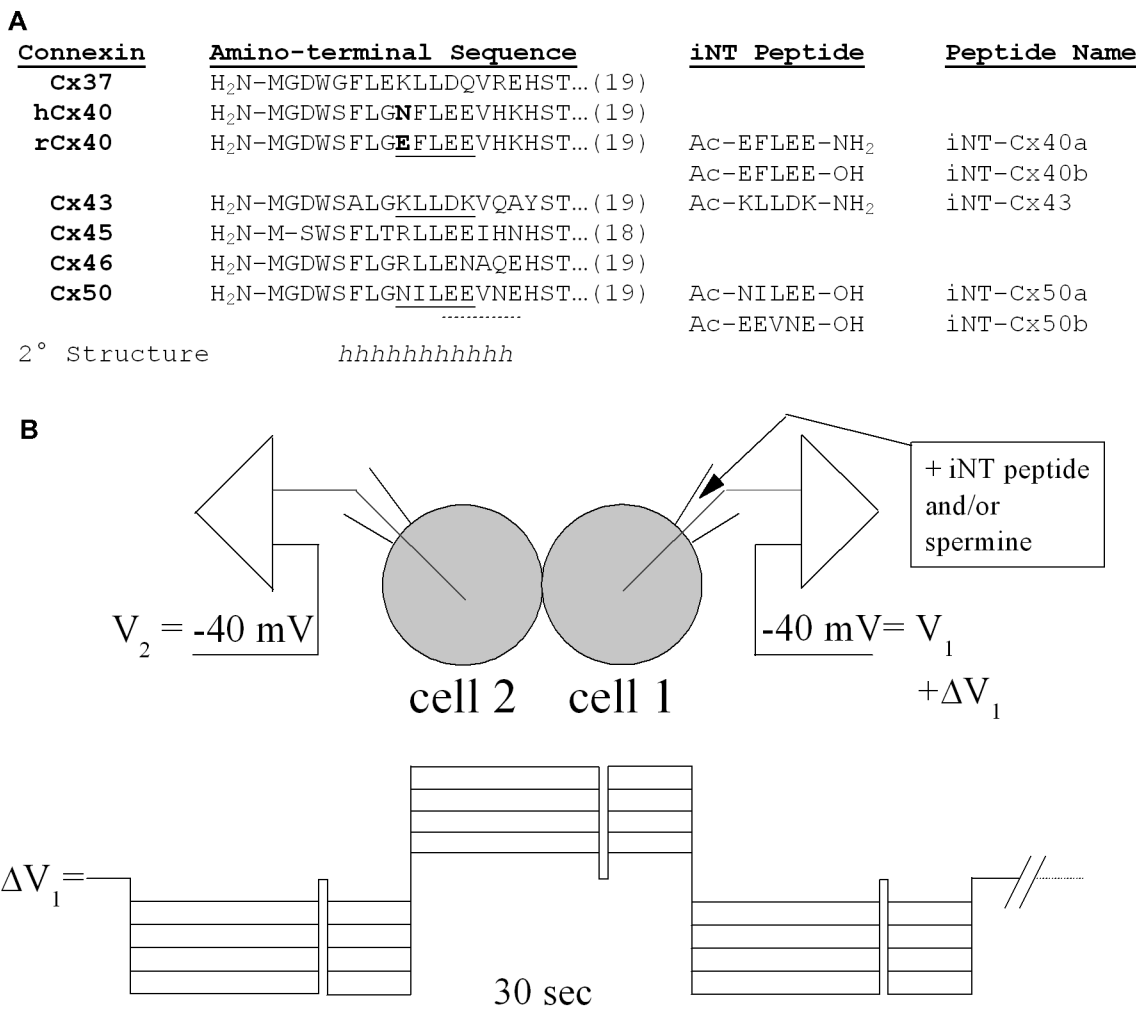


**FIGURE 1 | (A)** The amino acid sequences of the first 18 or 19 amino acids are shown for six different connexins and aligned with each other. The sequences in this NT region are identical for the homologous connexins in rodents or humans except for Cx40 (which differs at position 9 as shown in bold). A substantial part of the NT domain is likely to form  $\alpha$ -helices (h) based on consensus secondary structure predictions (Veenstra and Lin, 2006), nuclear magnetic resonance studies (Kyle et al., 2009), and homology modeling to the X-ray structure of Cx26 (Maeda et al., 2009).

Synthetic pentameric NT domain peptides corresponding to underlined (continuous or dotted) connexin sequences are also shown along with their peptide names. These interfering NT (iNT) peptides were protected by amino-terminal acetylation (Ac-) and carboxy-terminal amidation ( $-\text{NH}_2$ ) or hydroxylation ( $-\text{OH}$ ). **(B)** Diagram of the N2a cell pair configuration for the iNT peptide and/or spermine block experiments and the voltage step protocol used to apply the  $V_j$  gradients across the connexin-specific gap junctions.

In the current study, we examined the possibility of differential regulation of channels made of different connexins through interactions of their NT domains. Based on their inhibition by spermine, we hypothesized that Cx40 channels might be blocked by short peptides that contained similarly spaced positively charged residues, like the Cx43 sequence from residues 9–13 (KLLDK as shown in Figure 1). We synthesized this potentially interfering peptide (designated Cx43iNT1) and tested its ability to inhibit gap junction channel formed of various  $\alpha$ -connexins. Because Cx37, Cx45, Cx46, and Cx50 all contain multiple glutamate residues (like Cx40 as shown in Figure 1), we hypothesized that they might also be susceptible to block by spermine or Cx43iNT1. In the study presented below, we tested this peptide against the different  $\alpha$ -connexin channels and tested additional

“interfering” NT (iNT) peptides based on the sequences of other connexins (Figure 1).

The data presented suggest that corresponding sequences of acidic and basic amino acid residues within NT domains of Cx43, Cx37, Cx40, Cx45, Cx46, and Cx50 may influence connexin-specific interactions and their abilities to function as heteromeric channels.

## MATERIALS AND METHODS

### N2a CELL CULTURES AND CONNEXIN EXPRESSION

Stable N2a cell clones expressing human Cx37, Cx40 (hCx40), or rat Cx40 (rCx40) were prepared and cultured as previously described (Veenstra et al., 1994; Lin and Veenstra, 2007; Xu et al., 2012). Mouse Cx45 (mCx45), Cx46, and Cx50 were

transiently expressed in N2a cells using the pTracer<sup>TM</sup> vector (Chen et al., 2011).

### CONNEXIN iNT PEPTIDE PRODUCTION

Connexin-specific NT domain peptides were synthesized in 5 mg quantities, high-performance liquid chromatography (HPLC) purified to >95%, and stored ( $-20^{\circ}\text{C}$ ) as lyophilized powder until needed (Anaspec, San Jose, CA, USA). The peptides were dissolved in diethylpyrocarbonate (DEPC)-treated sterile distilled water to create a stock concentration of 10 mM, stored at  $-20^{\circ}\text{C}$ , and 40  $\mu\text{l}$  aliquots were diluted with 140 mM KCl internal pipette solution (IPS) as needed for daily patch clamp experiments. The relevant connexin NT domain and peptide sequences are provided in **Figure 1A**. The amino and carboxyl termini of two peptides (iNT-Cx43 and iNT-Cx40b) were acetylated (amino) and amidated (carboxyl) to protect them from hydrolysis in aqueous solution. Pentameric iNT peptides for Cx43, Cx40, and Cx50 were prepared and tested in dual whole cell patch clamp experiments on homotypic Cx37, Cx40, Cx43, Cx45, Cx46, and Cx50 gap junctions expressed in N2a cells.

### GAP JUNCTION CONDUCTANCE ( $g_j$ ) MEASUREMENTS

Dual whole patch clamp experiments were performed on connexin-transfected N2a cell pairs using established procedures (Veenstra, 2001). The connexin iNT peptides were added to the patch pipette receiving the  $\pm\Delta V_j$  voltage clamp step for quantitative  $g_j$  measurements and calculation of the fraction of unblocked junctional current ( $I_j$ ) using the previously developed spermine block  $V_j$  step protocol (Musa and Veenstra, 2003; Lin and Veenstra, 2007). Equimolar spermine concentrations were added along with the iNT peptide in some experiments to assess the ability of the peptide to antagonize the  $V_j$ -dependent spermine block of Cx40 gap junctions. For the peptide–spermine competition experiments, iNT peptides and spermine were added at reduced concentrations (500  $\mu\text{M}$ ) to conserve the amount of equimolar iNT peptide added to the patch pipette. The  $V_j$ -dependent spermine block still achieved 70% inhibition of rCx40  $g_j$ , sufficient to assess the action of the iNT peptides on the block by spermine.

Patch pipettes (4–5  $M\Omega$  to patch break) were filled with a KCl IPS [in mM: KCl, 140; MgCl<sub>2</sub>, 1.0; CaCl<sub>2</sub>, 3.0; BAPTA (1,2-bis(o-aminophenoxy)ethane-N,N,N',N'-tetraacetic acid), 5.0; HEPES (4-(2-hydroxyethyl)-1-piperazineethanesulfonic acid), 25; pH titrated to 7.4 using 1 N KOH]. The bath saline contained (in mM): NaCl, 142; KCl, 1.3; CsCl, 4; tetraethylammonium chloride (TEACl), 2; MgSO<sub>4</sub>, 0.8; NaH<sub>2</sub>PO<sub>4</sub>, 0.9; CaCl<sub>2</sub>, 1.8; dextrose, 5.5; HEPES, 10; pH 7.4 with 1 N NaOH. The osmolarity of both external and internal solutions was adjusted to 310 mOsm/L. Connexin iNT and/or spermine were added to one patch pipette at the indicated concentrations. Both N2a cells were held at  $-40$  mV resting potential ( $V_j = 0$  mV) and the cell (1) receiving the iNT peptides and/or spermine was stepped ( $\Delta V_1$ ) to varying membrane potentials to produce a  $V_j$  gradient [ $V_2 - (V_1 + \Delta V_1)$ ]. Junctional conductance was calculated according to the equation:

$$g_j = -\Delta I_2 / [(V_2 - R_{el2} \cdot I_2) - (V_1 - R_{el1} \cdot I_1)],$$

where  $\Delta I_2$  ( $= -I_j$ ) is the change in whole cell 2 current ( $I_2$ ) during the  $\Delta V_1$  step,  $R_{el1}$  and  $R_{el2}$  are the respective whole cell patch

electrode resistances, and  $I_1$  and  $I_2$  correspond to the respective whole cell currents (Veenstra, 2001). To determine the fraction of  $I_j$  block induced by the iNT-Cx43 peptide or spermine,  $\Delta V_1$  was alternately stepped negative, positive, and negative to the common holding potential ( $-40$  mV) in 5 mV increments from 5 to 50 mV (**Figure 1B**). The duration of each  $-/+/- \Delta V_1$  sequence was 90 s with a 500-ms step to  $-40$  mV occurring 20 s into each 30 s  $-/+/-$  interval, as an internal  $I_j = 0$  pA ( $V_j = 0$  mV) baseline control measurement, followed by a 30-s rest interval. The fraction of unblocked  $I_j = (\Delta I_2(\text{at positive } V_j)) / (\Delta I_2(\text{at negative } V_j))$ . Only those experiments where the  $I_j = 0$  baseline remained stable throughout the total 20 min duration of the cation block protocol were used in the final analysis.

### STATISTICAL ANALYSIS

Raw data ( $N \geq 3$ ) from each experimental group was tested for normality by the Shapiro–Wilk test ( $p$ -value  $< 0.05$ ) and then subjected to one-way ANOVA analysis ( $f$ -value  $< 0.05$ ) in Origin 8.6.

## RESULTS

### Cx43 iNT PEPTIDE SELECTIVELY INHIBITS Cx40 GAP JUNCTION CHANNELS

The iNT-Cx43 peptide had some structural similarity to spermine: namely terminal amino groups separated by at least 10 C–C or C–N bonds. Therefore, we initially tested whether iNT-Cx43 peptide possessed any inhibitory activity toward rCx40 gap junctions. The Cx43 iNT peptide was a potent  $V_j$ -dependent inhibitor of junctional conductance ( $g_j$ ) in cells expressing rCx40; indeed, equivalent block was observed at peptide concentrations of 10  $\mu\text{M}$ , 100  $\mu\text{M}$ , and 1 mM (**Figures 2A,C**).

Although Glu-9 contributes to the spermine block of rat Cx40 channels (Musa et al., 2004), this residue is replaced with an asparagine (N9) in human Cx40 (hCx40). Therefore, we hypothesized that hCx40 might show a different effect of iNT-Cx43 peptide. Surprisingly, we found that 100  $\mu\text{M}$  iNT-Cx43 peptide showed a similar inhibition of both human and rat Cx40 gap junctions (**Figures 2B,D**).

This unexpected result led us to test the ability of the Cx43 iNT peptide to interfere with the function of other connexins that also contain an ExxxE or ExxxD motif in their N-termini (**Figure 1**), Cx37, Cx46, and Cx50, or with Cx45 (which possesses only an ...EE... motif). In contrast to its effects on both rat and human isoforms of Cx40, 100  $\mu\text{M}$  iNT-Cx43 peptide did not affect the conductance of Cx37, Cx45, Cx46, or Cx50 gap junctions (**Figure 3**).

### Cx43iNT1 PEPTIDE EFFECTS DO NOT CORRELATE WITH SPERMINE BLOCK

Since rCx40 (but not Cx43) exhibits  $V_j$ -dependent spermine block (Musa and Veenstra, 2003; Musa et al., 2004; Lin et al., 2006; Lin and Veenstra, 2007), we tested the possible relationship of iNT-Cx43 block to spermine block by examining the effects of unilateral application of 2 mM spermine on the other five connexins. Not surprisingly, hCx40  $g_j$  was reduced in a  $V_j$ -dependent manner by 2 mM spermine (**Figure 4A**, black squares).

Interestingly, spermine also caused at least some inhibition of each of the other connexins. The spermine inhibition curve for

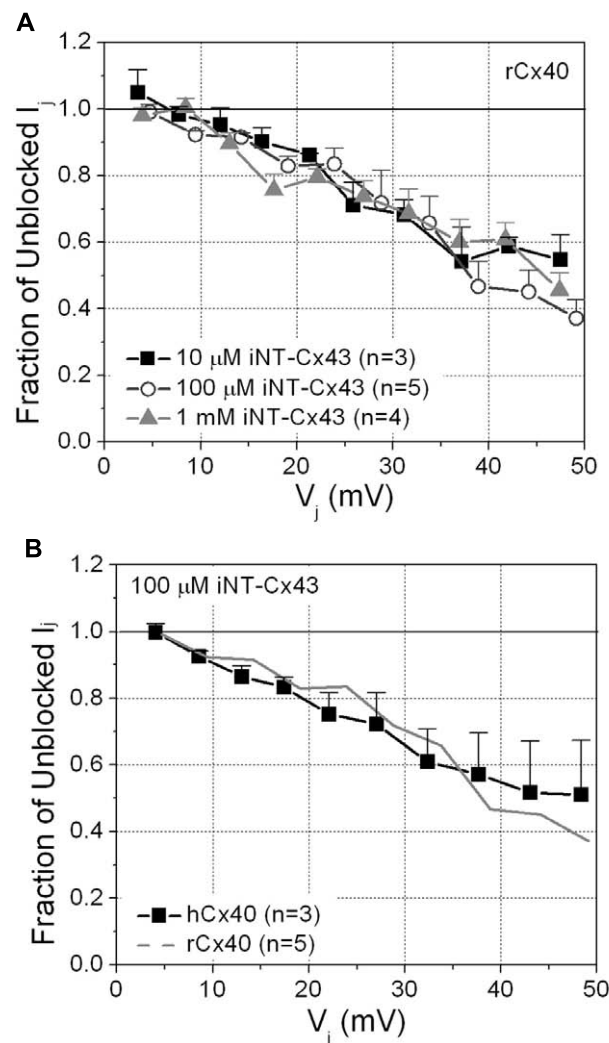
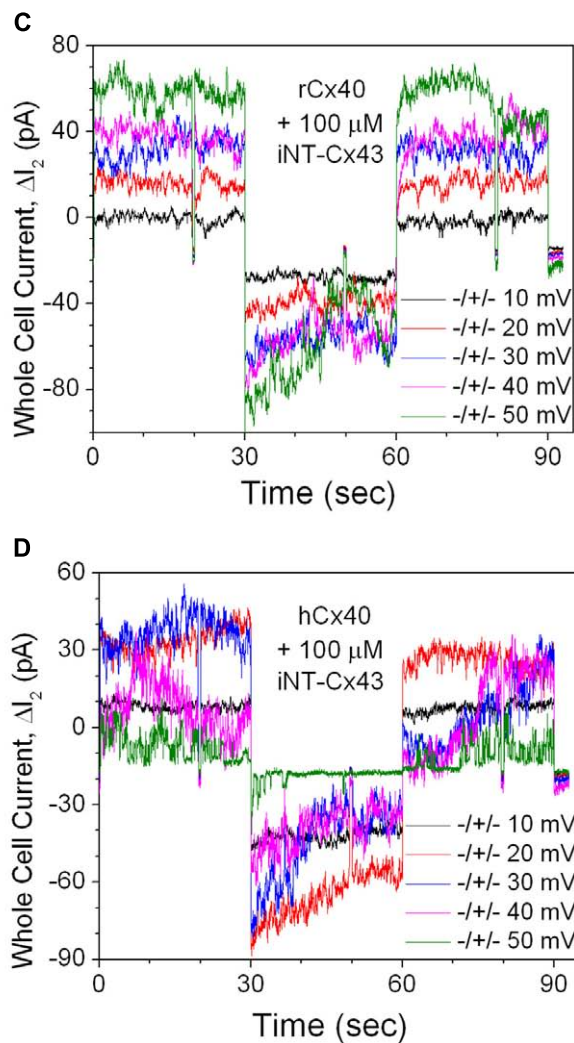


**FIGURE 2 | (A)** The inhibition of rCx40 gap junction currents ( $I_j$ ) by unilateral addition of 10  $\mu$ M (■), 100  $\mu$ M (○), or 1 mM (△) iNT-Cx43 peptide increased in a transjunctional voltage ( $V_j$ )-dependent manner. There was no statistical difference between the three curves based on comparison of the means at each  $V_j$  value. **(B)** The  $V_j$ -dependent blockade of hCx40 gap junctions (■) by 100  $\mu$ M iNT-Cx43 peptide was not significantly different from rCx40 (continuous gray line). **(C)** Whole cell current traces recorded from cell 2 of a rat Cx40 cell pair with 100  $\mu$ M iNT-Cx43 peptide added to cell 1 during



the  $\Delta V_1$  cation block voltage clamp protocol diagrammed in **Figure 1B**. The  $\Delta I_2$  current ( $= -I_j$ ) decrease during the  $+V_1$  voltage steps (only 10 mV incremental steps shown) illustrates the block induced by the iNT-Cx43 peptide. **(D)** Actual  $\Delta I_2$  current recordings from a hCx40 cell pair during an iNT-Cx43 peptide experiment illustrating a similar  $V_j$ -dependent block of hCx40 gap junction currents. Gap junction channel currents are visible at  $\pm 50$  mV with reduced open probability during the positive (blocking)  $V_j$  step.

Cx50 appeared similar to that of hCx40, and the maximum inhibition of Cx50  $g_j$  was ~80% (**Figure 4A**, gray circles). Cx46  $g_j$  achieved 60% inhibition (**Figure 4A**, open circles). Cx37  $g_j$  was reduced by >70% at low  $V_j$  values and then plateaued at ~50% inhibition (**Figure 4A**, gray open diamonds). Spermine inhibited Cx45  $g_j$  by <50% (data not shown).

Thus, the selective ability of iNT-Cx43 peptide to inhibit Cx40, but not other connexin channels, does not correlate with spermine inhibition.

#### iNT PEPTIDE ANTAGONISM OF SPERMINE BLOCK

Since Cx40 gap junctions were inhibited by both the Cx43iNT1 peptide and spermine, we examined whether iNT peptides based

on the NT sequences of Cx40 or Cx50 (containing the ExxEE motif) could antagonize the spermine block of Cx40 gap junctions. Spermine block experiments were performed with or without the addition of iNT peptides.

The first Cx40 iNT peptide (iNT-Cx40a) was acetylated and amidated like the iNT-Cx43 peptide (**Figure 1**). iNT-Cx40a peptide was partially effective at reversing the 500  $\mu$ M spermine block (**Figure 4B**, compare gray circles to spermine alone curve indicated with solid black squares). A second Cx40 iNT peptide containing the EFLEE sequence, iNT-Cx40b, 9–13 peptide was synthesized where the carboxy-terminus was hydroxylated instead of amidated to prevent the neutralization of the terminal glutamic acid group (**Figure 1**). The iNT-Cx40b peptide totally prevented the

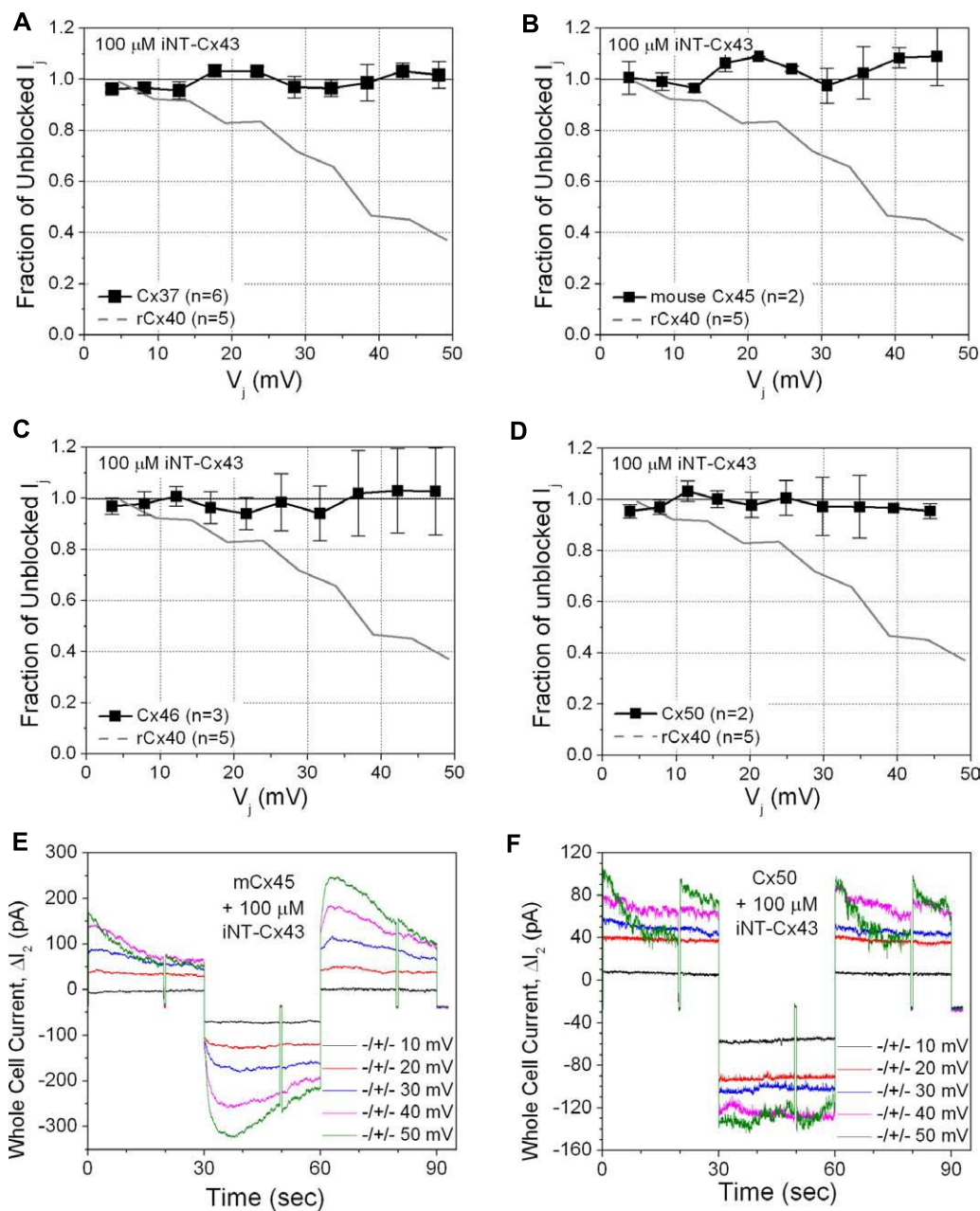


**FIGURE 3 |**The ability of the iNT-Cx43 peptide to inhibit Cx37 (A), Cx45 (B), Cx46 (C), and Cx50 (D) gap junctions was tested using the same  $V_j$ -dependent block protocol as in Figure 2. As a reference, the blockade of rCx40  $I_j$  (continuous gray line) is illustrated in each panel. Unlike rCx40, none of these four connexin gap junctions were significantly inhibited by 100  $\mu$ M iNT-Cx43 peptide. Actual  $\Delta I_2$  current traces from Cx45 (E) and Cx50 (F) cell pair iNT-Cx43 peptide experiments illustrating the lack of  $I_j$  current block

during the  $+ \Delta V_1 (\equiv V_j)$  step, in contrast to the Cx40 experiments shown in Figure 2. Cx45 and Cx50 gap junctions are more  $V_j$ -dependent than Cx40 (half inactivation  $V_j = V_0$  or  $V_{1/2} \equiv \pm 30, \pm 40$ , or  $\pm 49$  mV, respectively; Lin et al., 2006; Gonzalez et al., 2007). mCx45 gap junctions prominently display contingent hemichannel gating upon  $V_j$  polarity reversal, proposed by Harris et al. (1981), owing to the increased  $V_j$ -dependence and lack of fast  $V_j$ -gating kinetics of these gap junctions.

block of rCx40 by 500  $\mu$ M spermine (Figures 4B–D, dark gray circles).

These findings suggested the hypothesis that block might result from the electrostatic interaction of the ExxEE sequence. To test this hypothesis, a hydroxylated peptide corresponding to residues 12–16 of Cx50 (EEVNE), iNT-Cx50b (Figure 1), was synthesized.

iNT-Cx50b had no detectable effect on the block of rCx40 gap junctions by 500  $\mu$ M spermine (Figure 4E, gray circles). However, in contrast, a second hydroxylated Cx50 iNT peptide, iNT-Cx50a, corresponding to amino acids 9–13 (NILEE; Figure 1) effectively eliminated the  $V_j$ -dependent spermine block of rCx40 gap junctions (Figure 4F). This suggested a structural requirement for

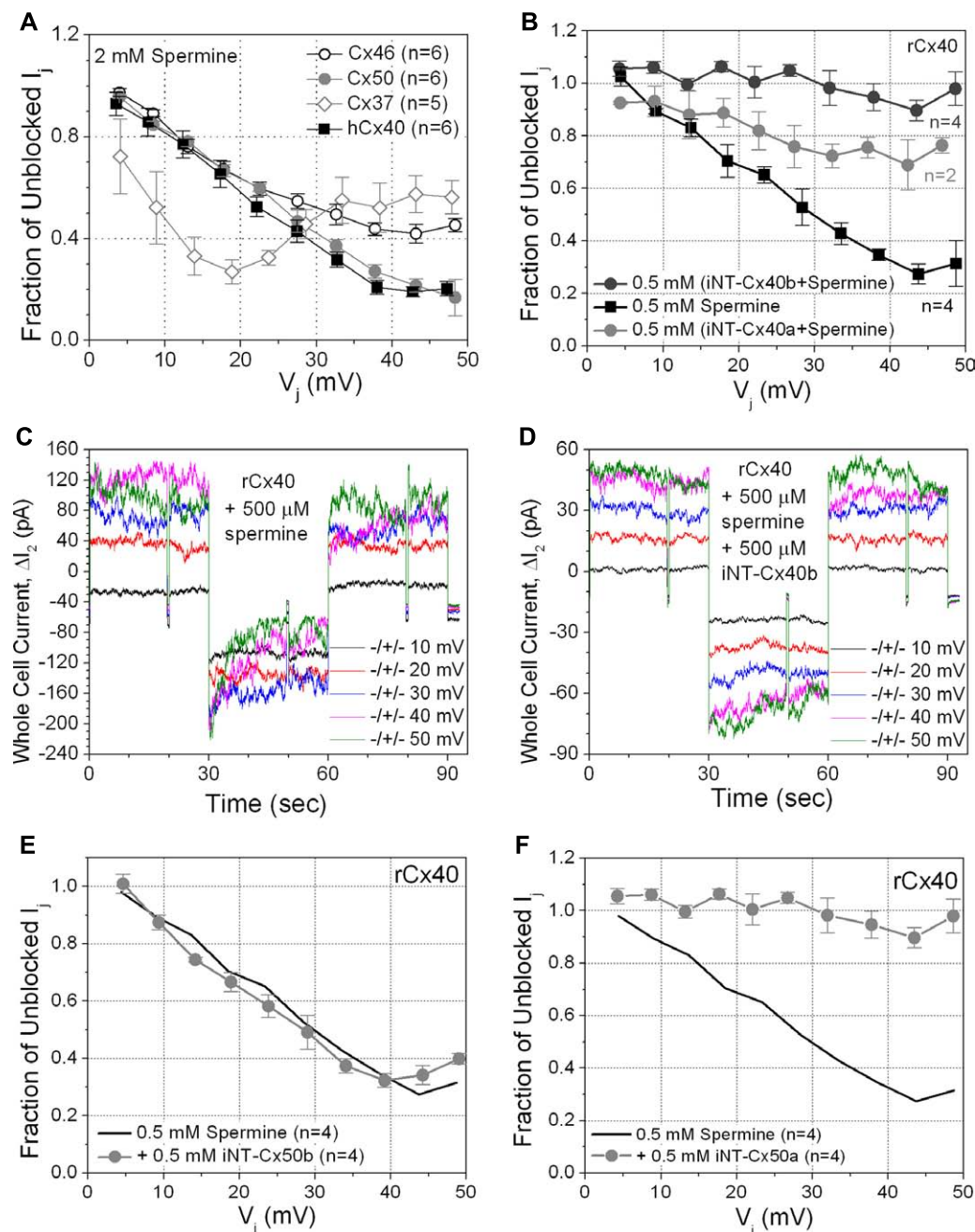


**FIGURE 4 | (A)** The sensitivity of four connexin-specific gap junctions was tested using the 2 mM spermine block assay. Human Cx40 (hCx40, ■) displayed similar  $V_j$ -dependent sensitivity to spermine as rCx40 despite the N9 substitution. Cx37 (◊), Cx46 (○), and Cx50 (●) gap junctions were all  $\geq 60\%$  inhibited by spermine. The maximum inhibition of Cx37  $g_j$  occurred at  $\pm 20$  mV, half the  $V_j$  required for maximal block of any other known connexin-specific gap junction. **(B)** The ability of iNT-Cx40 peptides to interfere with spermine block was tested by adding 500  $\mu$ M spermine and iNT-Cx40a or iNT-Cx40b peptides to one patch pipette. The carboxyl-terminal hydroxylated ( $-OH$ ,  $z = -4$ ) form of the Cx40 peptide (Cx40b) effectively abolished the  $V_j$ -dependent spermine block, while the amidated form (Cx40a,  $-NH_2$ ,  $z = -3$ ) was only partially effective (ANOVA,  $f$ -value  $< 0.05$ ). **(C)**  $\Delta I_2$  current traces from an rCx40 cell pair with 500  $\mu$ M spermine added to cell 1.  $I_j$  decreased during the positive 30, 40, and 50 mV  $V_j$  pulses and returned to prepulse levels during subsequent negative  $V_j$

pulses. This illustrates the time- and  $V_j$ -dependent spermine block and unblock of rCx40 gap junctions. **(D)**  $I_2$  current traces from an rCx40 cell pair experiment with 500  $\mu$ M spermine and the iNT-Cx40b peptide added to cell 1. Accounting for the occurrence of  $V_j$ -dependent gating at  $V_j \geq \pm 40$  mV, instantaneous and steady state  $I_2$  increased in a stepwise (ohmic) fashion with increasing  $V_j$  amplitude, indicative of a lack of spermine block. **(E)** A negatively charged ( $z = -4$ ) iNT-Cx50b peptide failed to significantly prevent the 500  $\mu$ M spermine block of rCx40 gap junctions, suggesting that the bimolecular interactions between the rCx40 NT domain, spermine, and iNT peptides are not purely based on electrostatic forces. **(F)** An iNT-Cx50a peptide (based on amino acids 9–13 and possessing a carboxyl-terminal valence ( $z$ ) of  $-3$ ) significantly reduced the 500  $\mu$ M spermine block of rCx40 gap junctions, suggesting a structural requirement for the interactions of iNT-Cx peptides with NT domains or spermine molecules.

the abilities of these pentameric peptides to oppose the spermine block of rCx40 gap junctions.

## DISCUSSION

We began this series of experiments with a relatively simple rationale: Cx40 channels which contain the sequence ExxxE in their N-termini are inhibited by the polyamine, spermine, and might also be inhibited by a pentameric peptide derived from the NT of Cx43 which has the motif KxxxK. Indeed, we observed potent block of rCx40 channels by iNT-Cx43. The block occurred in a transjunctional voltage ( $V_j$ )-dependent manner that resembled spermine block. However, the simple model of electrostatic interaction between this peptide and the connexin NT is dispelled by several other observations. The human Cx40 channel was also blocked by iNT-Cx43 despite the neutralization of the 9th residue in the human isoform (substitution of N for E). Moreover, iNT-Cx43 peptide had no effect on Cx37, Cx46, or Cx50 gap junctions, despite the presence of a similar (ExxxE or ExxxD) motif in these connexins. There also appears to be a structural requirement for the iNT effects. While a Cx50 iNT peptide containing similarly spaced negative charges had no effect, a Cx50 iNT peptide representing amino acids 9–13 antagonized spermine block of rCx40.

Our data support a selective inhibitory interaction between the NT domains of Cx40 and Cx43. iNT-Cx43 only blocked Cx40 channels. This interaction appears to have a rather high affinity, since equivalent block was achieved with 10  $\mu\text{M}$  peptide to that produced by higher concentrations. This putative selective NT interaction parallels the observed functional heteromeric interactions among this group of connexins. The Cx43 iNT peptide exhibited no effect on Cx37, Cx45, Cx46, or Cx50 gap junctions, but blocked Cx40 channels. Similarly, functional heteromeric

interactions between Cx43 and Cx37, Cx45, Cx46, and Cx50 have been extensively supported in the literature. We might have anticipated a reciprocal interaction of the Cx40 NT domain with Cx43 channels; however, we observed no effect when an iNT-Cx40 peptide was prepared and applied to Cx43 gap junctions (data not shown). This negative result might have been anticipated by the lack of effect of spermine on Cx43 gap junctions (Musa and Veenstra, 2003). The lack of direct reciprocity between Cx40 and Cx43 amino termini with alternately charged sequences implies that there is a structural difference between these two NT domains beyond their oppositely charged amino acids at positions 9 and 13.

Our iNT peptide data support the conclusion that Cx40 and Cx43 can form heteromeric channels, but most (if not all) of them will be non-functional (closed) due to the interactions of their amino termini. It is likely that a single Cx43 subunit is sufficient to nullify the function of a heteromeric Cx40-Cx43 hemichannel (connexon), based on the stoichiometric study of N2D and N2E mutant Cx32\*Cx43E1 hemichannels showing that a single NT domain is sufficient to induce  $V_j$ -dependent closure of a connexin hemichannel (Oh et al., 2000).

Finally, the connexin-specific effects of these iNT peptides also suggest the possibility of designing drugs that serve as gap junction agonists or antagonists by altering modulatory  $V_j$  or chemical gating interactions involving unique connexin domains. For instance, the Cx43 iNT peptide may antagonize the aberrant function of mutant Cx40 hemi- or gap junction channels associated with atrial fibrillation (Gollob et al., 2006; Yang et al., 2010).

## ACKNOWLEDGMENTS

The project was supported by NIH grants HL-042220 to Richard D. Veenstra and HL-059199 to Eric C. Beyer and Richard D. Veenstra.

## REFERENCES

- Arita, K., Akiyama, M., Aizawa, T., Umetsu, Y., Segawa, I., Goto, M., et al. (2006). A novel N14Y mutation in connexin26 in keratitis-ichthyosis-deafness syndrome: analyses of altered gap junctional communication and molecular structure of N terminus of mutated connexin26. *Am. J. Pathol.* 169, 416–423.
- Berthoud, V. M., Montegna, E. A., Atal, N., Aithal, N. H., Brink, P. R., and Beyer, E. C. (2001). Heteromeric connexons formed by the lens connexins, connexin43 and connexin56. *Eur. J. Cell Biol.* 80, 11–19.
- Beyer, E. C., and Berthoud, V. M. (2009). “The family of connexin genes,” in *Connexins: A Guide*, eds A. Harris and D. Locke (New York: Humana Press), 3–26.
- Brink, P. R., Cronin, K., Banach, K., Peterson, E., Westphale, E. M., Seul, K. H., et al. (1997). Evidence for heteromeric gap junction channels formed from rat connexin43 and human connexin37. *Am. J. Physiol. Cell Physiol.* 273, C1386–C1396.
- Bruzzone, R., Haefliger, J. A., Gimlich, R. L., and Paul, D. L. (1993). Connexin40, a component of gap junctions in vascular endothelium, is restricted in its ability to interact with other connexins. *Mol. Biol. Cell* 4, 7–20.
- Burt, J. M., and Steele, T. D. (2003). Selective effect of PDGF on connexin43 versus connexin40 comprised gap junction channels. *Cell Commun. Adhes.* 10, 287–291.
- Chen, Y., Zhou, Y., Lin, X., Wong, H. C., Xu, Q., Jiang, J., et al. (2011). Molecular interaction and functional regulation of connexin50 gap junctions by calmodulin. *Biochem. J.* 435, 711–722.
- Cottrell, G. T., and Burt, J. M. (2001). Heterotypic gap junction channel formation between heteromeric and homomeric Cx40 and Cx43 connexons. *Am. J. Physiol. Cell Physiol.* 281, C1559–C1567.
- Cottrell, G. T., Wu, Y., and Burt, J. M. (2002). Cx40 and Cx43 expression ratio influences heteromeric/heterotypic gap junction channel properties. *Am. J. Physiol. Cell Physiol.* 282, C1469–C1482.
- Dong, L., Liu, X., Li, H., Vertel, B. M., and Ebihara, L. (2006). Role of the N-terminus in permeability of chicken connexin45.6 gap junctional channels. *J. Physiol.* 576, 787–799.
- Elenes, S., Martinez, A. D., Delmar, M., Beyer, E. C., and Moreno, A. P. (2001). Heterotypic docking of cx43 and cx45 connexons blocks fast voltage gating of cx43. *Biophys. J.* 81, 1406–1418.
- Elfgang, C., Eckert, R., Lichtenberg-Fratre, H., Butterweck, A., Traub, O., Klein, R. A., et al. (1995). Specific permeability and selective formation of gap junction channels in connexin-transfected HeLa cells. *J. Cell Biol.* 129, 805–817.
- Gemel, J., Lin, X., Veenstra, R. D., and Beyer, E. C. (2006). N-terminal residues in Cx43 and Cx40 determine physiological properties of gap junction channels, but do not influence heteromeric assembly with each other or with Cx26. *J. Cell Sci.* 119, 2258–2268.
- Gemel, J., Valiunas, V., Brink, P. R., and Beyer, E. C. (2004). Connexin43 and connexin26 form gap junctions, but not heteromeric channels in co-expressing cells. *J. Cell Sci.* 117, 2469–2480.
- Gollob, D. A., Jones, D. L., Krahn, A. D., Danis, L., Gong, X.-Q., Shao, Q., et al. (2006). Somatic mutations in the connexin 40 gene (GJA5). *N. Engl. J. Med.* 354, 2677–2688.
- Gonzalez, D., Gomez-Hernandez, J. M., and Barrio, L. C. (2007). Molecular basis of voltage dependence of connexin channels: an integrative appraisal. *Prog. Biophys. Mol. Biol.* 94, 66–106.
- Harris, A. L., Spray, D. C., and Bennett, M. V. (1981). Kinetic properties of a voltage-dependent junctional conductance. *J. Gen. Physiol.* 77, 95–117.
- Haubrich, S., Schwartz, H.-J., Bukauskas, F., Lichtenberg-Fratre, H., Traub, O., Weingart, R., et al. (1996). Incompatibility of connexin 40 and 43 hemichannels in gap junctions between mammalian cells is determined by intracellular domains. *Mol. Biol. Cell* 7, 1995–2006.
- He, D. S., Jiang, J. X., Taffet, S. M., and Burt, J. M. (1999). Formation

- of heteromeric gap junction channels by connexins 40 and 43 in vascular smooth muscle cells. *Proc. Natl. Acad. Sci. U.S.A.* 96, 6495–6500.
- Heyman, N. S., Kurjaka, D. T., Ek Vitorin, J. F., and Burt, J. M. (2009). Regulation of gap junctional charge selectivity in cells coexpressing connexin 40 and connexin 43. *Am. J. Physiol. Heart Circ. Physiol.* 297, H450–H459.
- Igarashi, K., and Kashiwagi, K. (2000). Polyamines: mysterious modulators of cellular functions. *Biochem. Biophys. Res. Commun.* 271, 559–564.
- Kalmatsky, B. D., Bhagan, S., Tang, Q., Bargiello, T. A., and Dowd, T. L. (2009). Structural studies of the N-terminus of connexin 32 using <sup>1</sup>H-NMR spectroscopy. *Arch. Biochem. Biophys.* 490, 9–16.
- Kumar, N. M., and Gilula, N. B. (1992). Molecular biology and genetics of gap junction channels. *Semin. Cell Biol.* 3, 3–16.
- Kyle, J. W., Berthoud, V. M., Kurutz, J., Minogue, P. J., Greenspan, M., Hanck, D. A., et al. (2009). The N terminus of connexin37 contains an α-helix that is required for channel function. *J. Biol. Chem.* 284, 20418–20427.
- Lagree, V., Brunschwig, K., Lopez, P., Gilula, N. B., Richard, G., and Falk, M. M. (2003). Specific amino-acid residues in the N-terminus and TM3 implicated in channel function and oligomerization compatibility of connexin43. *J. Cell Sci.* 116, 3189–3201.
- Lin, X., Fenn, E., and Veenstra, R. D. (2006). An amino-terminal lysine residue of rat connexin40 that is required for spermine block. *J. Physiol.* 570, 251–269.
- Lin, X., and Veenstra, R. D. (2007). Effect of transjunctional KCl gradients on the spermine inhibition of connexin40 gap junctions. *Biophys. J.* 93, 483–495.
- Lin, X., Xu, Q., and Veenstra, R. D. (2011). Formation of heterotypic gap junctions by connexins -40 and -43,” in *International Gap Junction Conference Proceedings*, abstract # 1.7.
- Maeda, S., Nakagawa, S., Suga, M., Yamashita, E., Oshima, A., Fujiyoshi, Y., et al. (2009). Structure of the connexin 26 gap junction channel at 3.5 Å resolution. *Nature* 458, 597–602.
- Martinez, A. D., Hayrapetyan, V., Moreno, A. P., and Beyer, E. C. (2002). Connexin43 and connexin45 form heteromeric gap junction channels in which individual components determine permeability and regulation. *Circ. Res.* 90, 1100–1107.
- Martinez, A. D., Maripillan, J., Acuna, R., Minogue, P. J., Berthoud, V. M., and Beyer, E. C. (2011). Different domains are critical for oligomerization compatibility of different connexins. *Biochem. J.* 436, 35–43.
- Maza, J., Das, S. J., and Koval, M. (2005). Defining a minimal motif required to prevent connexin oligomerization in the endoplasmic reticulum. *J. Biol. Chem.* 280, 21115–21121.
- Musa, H., Fenn, E., Crye, M., Gemel, J., Beyer, E. C., and Veenstra, R. D. (2004). Amino terminal glutamate residues confer spermine sensitivity and affect voltage gating and channel conductance of rat connexin40 gap junctions. *J. Physiol.* 557, 863–878.
- Musa, H., Gough, J. D., Lees, W. J., and Veenstra, R. D. (2001). Ionic blockade of the rat connexin40 gap junction channel by large tetraalkylammonium ions. *Biophys. J.* 81, 3253–3274.
- Musa, H., and Veenstra, R. D. (2003). Voltage-dependent blockade of connexin40 gap junctions by spermine. *Biophys. J.* 84, 205–219.
- Oh, S., Abrams, C. K., Verselis, V. K., and Bargiello, T. A. (2000). Stoichiometry of transjunctional voltage-gating polarity reversal by a negative charge substitution in the amino terminus of a connexin32 chimera. *J. Gen. Physiol.* 116, 13–32.
- Oh, S., Rivkin, S., Tang, Q., Verselis, V. K., and Bargiello, T. A. (2004). Determinants of gating polarity of a connexin 32 hemichannel. *Biophys. J.* 87, 912–928.
- Pegg, A. E. (2009). Mammalian polyamine metabolism and function. *IUBMB Life* 61, 880–894.
- Purnick, P. E., Benjamin, D. C., Verselis, V. K., Bargiello, T. A., and Dowd, T. L. (2000). Structure of the amino terminus of a gap junction protein. *Arch. Biochem. Biophys.* 381, 181–190.
- Rackauskas, M., Kreuzberg, M. M., Pranenvicius, M., Willecke, K., Verselis, V. K., and Bukauskas, F. F. (2006). Gating properties of heterotypic gap junction channels formed of connexins 40, 43 and 45. *Biophys. J.* 92, 1952–1965.
- Tong, J. J., and Ebihara, L. (2006). Structural determinants for the differences in voltage gating of chicken Cx56 and Cx45.6 gap-junctional hemichannels. *Biophys. J.* 91, 2142–2154.
- Valiunas, V., Gemel, J., Brink, P. R., and Beyer, E. C. (2001). Gap junction channels formed by coexpressed connexin40 and connexin43. *Am. J. Physiol. Heart Circ. Physiol.* 281, H1675–H1689.
- Valiunas, V., Weingart, R., and Brink, P. R. (2000). Formation of heterotypic gap junction channels by connexins 40 and 43. *Circ. Res.* 86, E42–E49.
- Veenstra, R. D. (2001). Voltage clamp limitations of dual whole-cell gap junction current and voltage recordings. I. Conductance measurements. *Biophys. J.* 80, 2231–2247.
- Veenstra, R. D. (2003). Towards gap junction channel structure. *Recent Res. Dev. Biophys.* 2, 65–94.
- Veenstra, R. D., and Lin, X. (2006). More on the pore of gap junction channels. *Recent Res. Dev. Biophys.* 5, 1–35.
- Veenstra, R. D., Wang, H. Z., Beyer, E. C., and Brink, P. R. (1994). Selective dye and ionic permeability of gap junction channels formed by connexin45. *Circ. Res.* 75, 483–490.
- White, T. W., Bruzzone, R., Wolfram, S., Paul, D. L., and Goodenough, D. A. (1994). Selective interactions among the multiple connexin proteins expressed in the vertebrate lens: the second extracellular domain is a determinant of compatibility between connexins. *J. Cell Biol.* 125, 879–892.
- White, T. W., Paul, D. L., Goodenough, D. A., and Bruzzone, R. (1995). Functional analysis of selective interactions among rodent connexins. *Mol. Biol. Cell* 6, 459–470.
- Xu, Q., Kopp, R. F., Chen, Y., Yang, J. J., Roe, M. W., and Veenstra, R. D. (2012). Gating of connexin 43 gap junctions by a cytoplasmic loop calmodulin binding domain. *Am. J. Physiol. Cell Physiol.* 302, C1548–C1556.
- Yang, Y.-Q., Liu, X., Zhang, X.-L., Wang, X.-H., Tan, H.-W., Shi, H.-F., et al. (2010). Novel connexin40 missense mutations in patients with familial atrial fibrillation. *Europace* 12, 1421–1427.

**Conflict of Interest Statement:** The authors declare that the research was conducted in the absence of any commercial or financial relationships that could be construed as a potential conflict of interest.

*Received: 19 February 2013; paper pending published: 04 March 2013; accepted: 29 April 2013; published online: 21 May 2013.*

*Citation: Beyer EC, Lin X and Veenstra RD (2013) Interfering amino-terminal peptides and functional implications for heteromeric gap junction formation. *Front. Pharmacol.* 4:67. doi: 10.3389/fphar.2013.00067*

*This article was submitted to Frontiers in Pharmacology of Ion Channels and Channelopathies, a specialty of Frontiers in Pharmacology.*

*Copyright © 2013 Beyer, Lin and Veenstra. This is an open-access article distributed under the terms of the Creative Commons Attribution License, which permits use, distribution and reproduction in other forums, provided the original authors and source are credited and subject to any copyright notices concerning any third-party graphics etc.*



# Together and apart: inhibition of DNA synthesis by connexin-43 and its relationship to transforming growth factor $\beta$

**Maya M. Jeyaraman<sup>1,2</sup>, Robert R. Fandrich<sup>1,3</sup> and Elissavet Kardami<sup>1,2,3\*</sup>**

<sup>1</sup> Institute of Cardiovascular Sciences, St. Boniface Research Centre, University of Manitoba, Winnipeg, MB, Canada

<sup>2</sup> Department of Physiology, University of Manitoba, Winnipeg, MB, Canada

<sup>3</sup> Department of Human Anatomy and Cell Sciences, University of Manitoba, Winnipeg, MB, Canada

**Edited by:**

Stefan Dhein, Universitätsklinik Leipzig Herzzentrum Leipzig GmbH, Germany

**Reviewed by:**

Marc Chanson, University of Geneva, Switzerland

Stefan Dhein, Universitätsklinik Leipzig Herzzentrum Leipzig GmbH, Germany

**\*Correspondence:**

Elissavet Kardami, Institute of Cardiovascular Sciences, St. Boniface Research Centre, University of Manitoba, 351 Taché Avenue, Winnipeg, MB R2H 2A6, Canada  
e-mail: ekardami@sbsrc.ca

The membrane and channel protein connexin-43 (Cx43), as well as the cytokine transforming growth factor (TGF)  $\beta$ , suppress proliferative growth in cardiomyocytes and other cell types. Previously we showed that the inhibitory effect of Cx43 is canceled when Cx43 becomes phosphorylated at serine (S) 262 in response to mitogen stimulation. We have now asked if the TGF $\beta$ -triggered inhibition of DNA synthesis is associated with changes in Cx43 phosphorylation at S262. Conversely, we investigated if inhibition of DNA synthesis by overexpressed Cx43 is dependent on engaging TGF $\beta$  signal transduction. We report that TGF $\beta$  acutely prevented mitogen-induced Cx43 phosphorylation at S262, while chronic inhibition of TGF $\beta$  signal transduction raised baseline levels of endogenous phospho-S262-Cx43 without affecting total Cx43. Inhibition of baseline TGF $\beta$  signal transduction through (a) inhibiting TGF $\beta$  receptor I (TGF $\beta$ RI) with SB431542, (b) inhibiting TGF $\beta$  receptor II (TGF $\beta$ RII) by overexpressing dominant-negative (DN) TGF $\beta$ RII, (c) inhibiting the downstream signaling mediator Smad2 by overexpressing DN Smad2, each separately increased baseline cardiomyocyte DNA synthesis, but could not reverse DNA synthesis inhibition by overexpressed Cx43. It is suggested that inhibition of cardiomyocyte DNA synthesis by TGF $\beta$ /TGF $\beta$ RI/II/phospho-Smad2 signaling is mediated, at least in part, by reducing endogenous phospho-S262-Cx43 levels.

**Keywords:** connexin-43, phosphorylation, cell proliferation, transforming growth factor  $\beta$ , cardiomyocytes

## INTRODUCTION

Cardiomyocytes, the contractile functional units of the heart pump, are proliferative during the embryonic and early neonatal stages. Subsequently cardiac increases in mass and size occur mainly by increased size of individual myocytes (hypertrophy) rather than cell proliferation (Ahuja et al., 2007). Ischemic heart disease and myocardial infarction cause damage and loss of functional myocardium, which is replaced mainly by scar tissue, resulting in maladaptive remodeling and heart failure. Endogenous capacity for regeneration after extensive injury resulting in cell death is inadequate to replace lost cardiac tissue; nevertheless, a small percentage of adult cardiomyocytes maintain the capacity to enter the cell cycle (Bergmann et al., 2009), and this percentage increases after myocardial infarction (Senyo et al., 2013), indicative of an attempt for a regenerative response. To improve cardiac regeneration after injury it is important to identify factors and mechanisms stimulating or inhibiting cardiomyocyte proliferation. This understanding can provide strategies for stimulating or dis-inhibiting cardiomyocyte proliferation as may be needed during cardiac repair after myocardial infarction.

Overexpression as well as knock-down studies have shown that the membrane and gap junction channel phosphoprotein connexin-43 (Cx43) inhibits DNA synthesis in cardiomyocytes and several other cell types (Doble et al., 2004; Kardami et al.,

2007; Zhang et al., 2008; Matsuyama and Kawahara, 2009). The mechanism by which Cx43 affects cell proliferation includes significant effects on gene expression; and does not require the channel-forming ability of the molecule (Kardami et al., 2007). It is important to note that the ability of Cx43 to inhibit cell proliferation is regulatable: mitogen-induced phosphorylation of Cx43, or the C-terminal of Cx43 (Cx43-CT) at S262, was shown to cancel their inhibitory effect on DNA synthesis (Doble et al., 2004; Dang et al., 2006). Mitogens such as fibroblast growth factor 2 (FGF-2) stimulate cardiomyocyte proliferation, as well as Cx43 phosphorylation at S262.

The proliferative action of FGF-2 is counteracted by another multifunctional protein, transforming growth factor (TGF)  $\beta$ , which inhibits cardiomyocyte proliferation (Kardami, 1990; Sheikh et al., 2004). Proliferative growth suppression by Cx43 may be linked to TGF $\beta$  signaling: Cx43 was reported to potentiate TGF $\beta$  signaling in the atria-derived cardiomyocyte cell line HL-1, by competing with the downstream mediator of TGF $\beta$  signal transduction, Smad2, for binding to tubulin (Dai et al., 2007). This competitive binding released Smad2 from microtubules, thus making it available for phosphorylation by TGF $\beta$  receptor I (TGF $\beta$ RI), followed by nuclear translocation, and activation of TGF $\beta$  responsive genes (Dai et al., 2007). In addition, TGF $\beta$  is known to upregulate Cx43 expression in a number of

cell types including epithelial cells and vascular smooth muscle cells, and this upregulation may contribute to inhibition of DNA synthesis (Rama et al., 2006; Tacheau et al., 2008).

In the present study, we addressed the potential relationship between Cx43 and TGF $\beta$ -mediated inhibition of cardiomyocyte DNA synthesis. Our data showed that TGF $\beta$  signaling inhibited the growth factor-induced phosphorylation of endogenous Cx43 at S262. On the other hand, inhibition of cardiomyocyte DNA synthesis by overexpressed Cx43 did not require downstream activation of TGF $\beta$ -related signals such as TGF $\beta$ RI, TGF $\beta$ RII, or Smad2. Overall our data suggest that Cx43-mediated inhibition is downstream of early TGF $\beta$  signal transduction, and that the mechanism of TGF $\beta$ -triggered inhibition of cardiomyocyte DNA synthesis includes downregulation of endogenous pS262-Cx43.

## MATERIALS AND METHODS

### ANIMALS

One-day-old Sprague Dawley rat pups were obtained from the Central Animal Care Facility at the University of Manitoba. This study was carried out in strict accordance with the recommendations in the Guide for the Care and Use of Laboratory Animals by the US National Institutes of Health (NIH Publication No. 85-23, revised 1996). Approval for use of rat pups was obtained by the Protocol Management and Review Committee of the University of Manitoba.

### REAGENTS

Rabbit polyclonal antibodies recognizing: (i) total Cx43 (phosphorylated as well as unphosphorylated), were raised in-house against a synthetic peptide containing Cx43 residues 367–382; the immune serum was used at 1:10,000 dilution for western blotting, (ii) anti-phospho-(p) 262-Cx43 antibodies were purchased from Santa Cruz Biotechnology (CA, USA), as a 200- $\mu$ g/ml solution, and were used at 1:1000 dilution. These antibodies have been characterized and described previously (Doble et al., 2004; Srisakuldee et al., 2009). Anti-bromodeoxyuridine (BrdU) antibodies (GE Biosciences) were used at 1:1000 dilution. Anti-phospho-(p)Smad2(Ser465/467), or anti-Smad2 antibodies were purchased from Upstate or Cell Signaling Technology (MA, USA), respectively and used at 1:1000 dilution. Mouse monoclonal anti- $\alpha$ -actinin (1:200) and rabbit anti-actin (1:1000) antibody were from Sigma (USA). Goat anti-mouse and anti-rabbit HRP (horse radish peroxidase) secondary antibodies, were obtained from Bio-Rad (CA, USA) and used as per manufacturer's instructions. The TGF $\beta$ RI inhibitor SB431542 was purchased from Tocris Bioscience (Bristol, UK). TGF $\beta$ 1 was purchased from R&D Systems (USA), and used at 5 ng/ml. Recombinant 18 kDa FGF-2 was produced in-house as we have described (Jiang et al., 2002, 2004), and used at 10 ng/ml. Adenoviral vectors expressing wild type-Cx43, mutant S262A-Cx43 or truncated Cx43-CT (residues 247–382), have been described previously (Doble et al., 2004; Kardami et al., 2007), and were used at low titers (2 m.o.i; multiplicity of infection), achieving modest overexpression, namely a two- to threefold increase in total Cx43 (Srisakuldee et al., 2009). The adenoviral vector expressing TGF $\beta$ RII-dominant-negative (DN) has been described (Sheikh et al., 2004) and was used at 50 m.o.i. Adenoviral vectors expressing DN Smad2-DN, or Smad3-DN have been described in

(Uemura et al., 2005) and were generous gifts from Dr. Rebecca Wells (University of Pennsylvania School of Medicine, PA, USA); they were used at 100 m.o.i.

### WESTERN BLOTTING ANALYSIS

Lysates were analyzed on 10% polyacrylamide gels, at 10  $\mu$ g protein/lane, as described previously (Srisakuldee et al., 2009). Broad range (6.5–200 kDa) molecular mass standards (Bio-Rad) were used in all analyses. Protein concentration was determined by the bicinchoninic acid (BCA) protein assay reagent (Pierce) followed by spectrophotometry. The proteins on the gel were electrophoretically transferred to polyvinylidene difluoride membranes. Antigen–antibody complexes were visualized using enhanced chemiluminescence (ECLplus), from Amersham Pharmacia. Densities of western blot bands were determined using the Bio-Rad Model GS-800 densitometer with Molecular Analyst software (Bio-Rad). Band densities were adjusted based on the density of corresponding loading controls.

### NEONATAL RAT VENTRICULAR MYOCYTE CULTURES

Cardiomyocytes were isolated from the ventricles of 1-day-old rat pups according to standard procedures (Doble et al., 1996). For studies on DNA synthesis, myocytes were plated on collagen-coated coverslips at 400,000 cells/35 mm well, in the presence of 10% bovine calf serum supplemented with FGF-2 (10 ng/ml) and routinely maintained in this type of medium in experiments using adenoviral vector gene transfer. In some experiments, myocytes were placed in a low serum medium (0.5% bovine calf serum supplemented with 0.5% bovine serum albumin (BSA), 1% penicillin/streptomycin, 0.04% vitamin C, 0.1% insulin, 0.1% transferrin/selenium) for 48 h, followed by stimulation with FGF-2 (10 ng/ml, 30 min) in the presence or absence of 15 min pre-treatment with TGF $\beta$  (5 ng/ml).

### BROMODEOXYURIDINE LABELING INDEX

As described previously (Doble et al., 2004). Briefly, cardiomyocytes cultured on coverslips were incubated with BrdU (3  $\mu$ g/ml) for 8–12 h prior to the termination of various experiments. Coverslips were then fixed with 1% paraformaldehyde for 15 min in the cold, and then treated with 0.07 M NaOH for 2 min at room temperature. Labeling for sarcomeric  $\alpha$ -actinin (exclusively cytosolic as well as cardiomyocyte-specific), for BrdU (to identify nuclei synthesizing DNA), and Cx43 (to ascertain Cx43 overexpression after transfection) was achieved using mouse monoclonal antibodies against  $\alpha$ -actinin, against BrdU, and rabbit polyclonal antibodies against Cx43. Coverslips were also counterstained for DNA, with Hoechst 33342. A minimum of 24 randomly selected visual fields, distributed in three coverslips, were observed under epifluorescence optics, photographed, and individually scored for numbers of BrdU-positive cardiomyocyte nuclei, over total cardiomyocyte nuclei (BrdU labeling index).

### STATISTICS

The GraphpadStat and SigmaStat software programs were used for data analysis. Data are presented as mean  $\pm$  SEM (standard error of the mean). Statistical analysis was performed using either one-way ANOVA to compare more than two groups or two-way

ANOVA to compare more than two groups with two independent variables.  $P < 0.05$  was considered statistically significant.  $P < 0.01$  was considered statistically very significant.

## RESULTS

### EFFECT OF TGF $\beta$ ON RELATIVE CARDIOMYOCYTE pS262-Cx43 LEVELS

Our previous studies have demonstrated that cardiomyocytes maintained in culture under growth-stimulating conditions, are nevertheless subjected to a degree of mitotic suppression by "baseline TGF $\beta$ ," representing TGF $\beta$  present in serum, and/or made by myocytes and the small amount of contaminating fibroblasts, in culture. Inhibiting this baseline TGF $\beta$  signaling potentiated the ability of growth factors such as FGF-2 to stimulate cardiomyocyte proliferation (Doble et al., 2004; Sheikh et al., 2004). As we have found a positive relationship between growth factor-induced Cx43 phosphorylation at S262, and the ability of growth factors to

stimulate cardiomyocyte proliferation, we asked whether inhibition of baseline TGF $\beta$  signal transduction would influence levels of endogenous pS262-Cx43, in culture.

Primary cultures of neonatal cardiac myocytes, placed under conditions stimulating proliferative growth (10% bovine calf serum, plus 10 ng/ml FGF-2) were exposed to a pharmacological inhibitor of TGF $\beta$ RI (SB431542), or subjected to overexpression of DN versions of either TGF $\beta$ RII or Smad2, through adenovirally mediated transient gene transfer. One day following these manipulations cell lysates were analyzed for total as well as pS262-Cx43 by western blotting. Two types of control cultures were used: in the first, cells were kept in growth medium without any treatment, while in the second cells were treated with an empty adenoviral vector. As shown in Figure 1, both types of controls elicited signals of similar intensity for pS262-Cx43, as well as total Cx43, indicating that the adenoviral vector had no effect on Cx43. Treatment

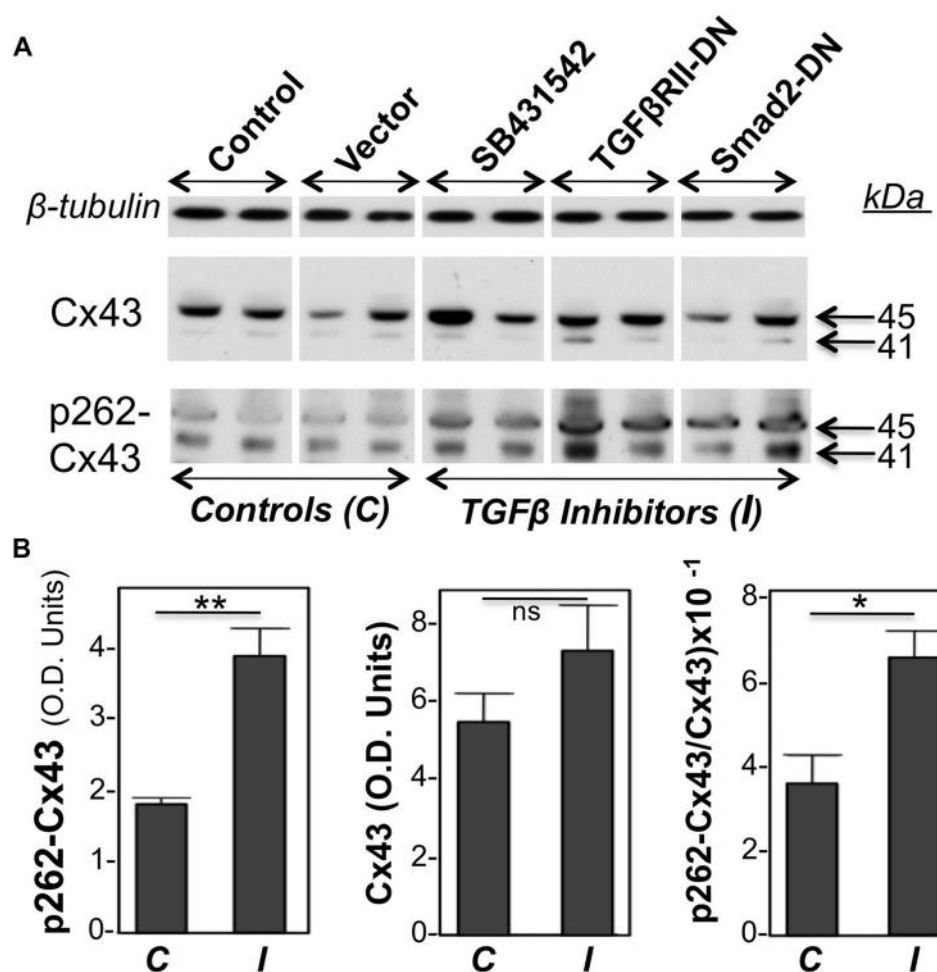


**FIGURE 1 |** Inhibition of TGF $\beta$  signaling increases baseline cardiomyocyte Cx43 phosphorylation at S262. (A) Western blots of cardiomyocyte lysates probed for total Cx43 (Cx43), pS262-Cx43, and  $\beta$ -tubulin (loading control), as indicated. Samples shown represent five groups, including two types of controls (C), such as myocytes subjected to no treatment (Control), or exposed to an empty adenoviral vector (Vector); the two controls produced similar data. The remaining three groups were treated with TGF $\beta$  signaling

inhibitors (I), such as SB431542 (20  $\mu$ M) and adenoviral vectors expressing TGF $\beta$ RII-DN or Smad2-DN, as indicated. All three groups showed increased signal for pS262-Cx43, compared to control groups. (B) Combined densitometry data (optical density, OD units) comparing relative pS262-Cx43, total Cx43, or the ratio of pS262-Cx43/total Cx43 between control, C ( $n = 4$ ), and I-treated groups ( $n = 6$ ). \*\*, \*, and ns denote  $P < 0.01$ ,  $P < 0.05$ , and  $P < 0.05$ .

of cardiomyocytes with inhibitors of TGF $\beta$  signal transduction elicited a significant increase in pS262-Cx43 (**Figure 1**), but had no significant effect on total Cx43.

Probing with antibodies recognizing total Cx43 showed that the majority of Cx43 migrated at 45 kDa, representing extensively phosphorylated Cx43, with a faint signal near 41 kDa, representing unphosphorylated or minimally phosphorylated Cx43. This pattern is typical for cardiomyocytes (Doble et al., 2004; Srisakuldee et al., 2009). Probing with anti-pS262-Cx43 detected bands migrating near 41 as well as 45 kDa, indicating that, under “growth stimulation” conditions, phosphorylation at the S262 site can occur, respectively, on Cx43 that lacks substantial phosphorylation at other sites, as well as on Cx43 extensively phosphorylated at other sites. Please note that any shift in motility that might be caused by phosphorylation at a single site (S262) would not be detectable by standard one-dimensional electrophoresis as used here. Inhibition of TGF $\beta$  signal transduction upregulated both the faster and slower migrating pS262-Cx43 bands. **Figure 1B** is showing densitometric results representing the sum of Cx43 or pS262-Cx43 bands.

In another experiment, we tested the effect of TGF $\beta$  on the acute FGF-2-induced stimulation of Cx43 phosphorylation at S262. To minimize baseline protein kinase C (PKC) activity, and thus baseline levels of pS262-Cx43, cardiomyocytes were kept in low serum (0.5% fetal bovine serum) for 48 h before stimulation, as described previously (Doble et al., 2004). Myocytes were then subjected or not to a brief 15-min pre-incubation with TGF $\beta$  (5 ng/ml), and then stimulated with FGF-2 (10 ng/ml) for 30 min. FGF-2 significantly increased the anti-pS262-Cx43 signal, migrating at 45 kDa, in the absence of TGF $\beta$  pre-treatment, as expected from previous studies (Doble et al., 2004); **Figure 2**. The stimulatory effect of FGF-2 was, however, completely prevented in cells pre-treated with TGF $\beta$ ; **Figure 2**. The faster migrating pS262-Cx43 observed in the previous experiment (**Figure 1**) was not detectable in cultures kept in low serum and may be a characteristic of cultures grown under conditions promoting proliferative growth.

### EFFECT OF INHIBITION OF TGF $\beta$ SIGNAL TRANSDUCTION ON GROWTH SUPPRESSION BY OVEREXPRESSED Cx43

To examine the hypothesis that growth suppression by Cx43 is mediated by downstream activation of TGF $\beta$  signal transduction, cardiomyocyte cultures were subjected to Cx43 or Cx43-CT overexpression, in a background of pharmacological (SB431542) TGF $\beta$ RI inhibition. BrdU labeling index (proportion of cardiomyocyte nuclei incorporating BrdU, over total number of cardiomyocyte nuclei) was determined 2 days later, as a measure of relative DNA synthesis ability. We have established in previous studies that cardiomyocyte labeling index determinations are mirrored by, and are therefore representative of, cell number determinations (Kardami, 1990; Pasumarthi et al., 1996). The BrdU labeling index of control groups, maintained in growth-stimulating conditions (FGF-2-supplemented serum), varied between 0.25 and 0.30 in different primary cardiomyocyte preparations.

**Figure 3A** compares normalized BrdU labeling index between the various groups, where the value for the control group, subjected to treatment with an empty adenoviral vector (Vector),

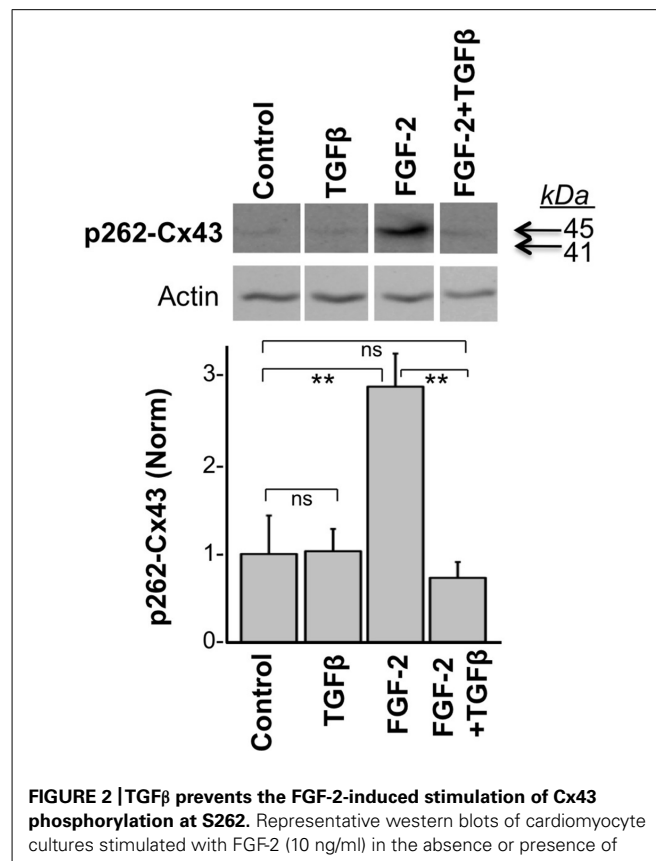


**FIGURE 2 | TGF $\beta$  prevents the FGF-2-induced stimulation of Cx43 phosphorylation at S262.** Representative western blots of cardiomyocyte cultures stimulated with FGF-2 (10 ng/ml) in the absence or presence of TGF $\beta$  pre-treatment for 15 min, as indicated. Corresponding normalized densitometry-based data are also included. \*\* and ns correspond to  $P < 0.01$ , or  $P > 0.05$ ;  $n = 3$ .

was arbitrarily defined as 1. In the absence of Cx43 or Cx43-CT overexpression, inhibition of TGF $\beta$ RI by SB431542 elicited a significant increase in BrdU incorporation ( $P < 0.05$ ), as anticipated from successful inhibition of baseline TGF $\beta$  signal transduction (Sheikh et al., 2004). In the absence of SB431542, overexpression of Cx43, or Cx43-CT elicited a robust inhibition of cardiomyocyte BrdU labeling index, compared to Vector-treated controls, in agreement with our previous report that inhibition of cardiomyocyte DNA synthesis by Cx43 does not require the channel-forming portion of the molecule (Kardami et al., 2007). The presence of SB431542 was unable to reverse/prevent the inhibitory effects of Cx43, or Cx43-CT overexpression, indicating that suppression of DNA synthesis by Cx43, or Cx43-CT overexpression does not depend on activation of TGF $\beta$ RI. In fact it would appear that Cx43, or Cx43-CT, overexpression, blocked the ability of SB431542 to increase baseline cardiomyocyte DNA synthesis. This suggested the possibility that Cx43 overexpression may have somehow blunted the ability of SB431542 to inhibit TGF $\beta$ RI. If that were the case, SB431542 would not be able to prevent the downstream phosphorylation and activation of Smad2 (pSmad2). We therefore tested the status of Smad2 activation (pSmad2, phosphorylated at serines 465/467) in response to SB431542, Cx43-, Cx43-CT, and a Cx43 phosphorylation mutant (S262A-Cx43). Representative data are shown in **Figure 3B**. SB431542 eliminated baseline Smad2/3 activation under control

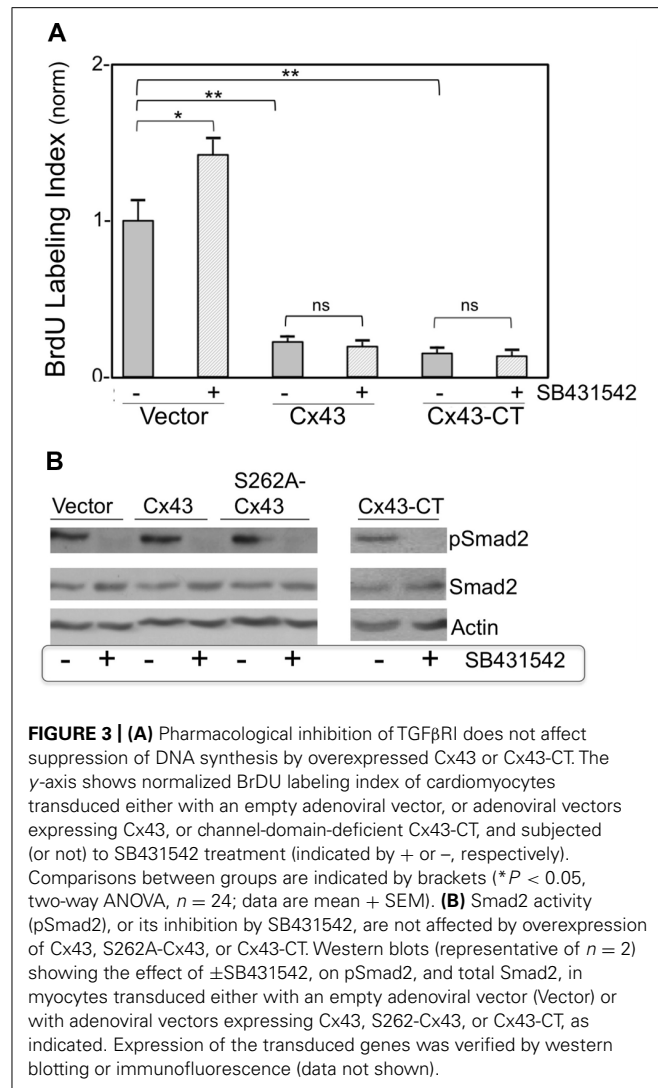


**FIGURE 3 | (A)** Pharmacological inhibition of TGF $\beta$ RI does not affect suppression of DNA synthesis by overexpressed Cx43 or Cx43-CT. The y-axis shows normalized BrdU labeling index of cardiomyocytes transduced either with an empty adenoviral vector, or adenoviral vectors expressing Cx43, or channel-domain-deficient Cx43-CT, and subjected (or not) to SB431542 treatment (indicated by + or -, respectively). Comparisons between groups are indicated by brackets (\* $P < 0.05$ , two-way ANOVA,  $n = 24$ ; data are mean  $\pm$  SEM). **(B)** Smad2 activity (pSmad2), or its inhibition by SB431542, are not affected by overexpression of Cx43, S262A-Cx43, or Cx43-CT. Western blots (representative of  $n = 2$ ) showing the effect of  $\pm$ SB431542, on pSmad2, and total Smad2, in myocytes transduced either with an empty adenoviral vector (Vector) or with adenoviral vectors expressing Cx43, S262A-Cx43, or Cx43-CT, as indicated. Expression of the transduced genes was verified by western blotting or immunofluorescence (data not shown).

conditions, validating its ability to block downstream TGF $\beta$ -TGF $\beta$ RI signal transduction. The ability of SB431542 to prevent baseline Smad2/3 activation was maintained in the presence of Cx43, Cx43-CT, and S262A-Cx43 overexpression. Furthermore, none of the overexpressed proteins (Cx43, Cx43-CT, S262A-Cx43) appeared to affect baseline levels of pSmad2/3; no discernible changes were observed in total Smad2/3 in any of the groups tested.

The effect of directly inhibiting Smad2 (by expressing a cDNA for Smad2-DN) on cardiomyocyte BrdU labeling index, in the absence or presence of Cx43 or S262A-Cx43 overexpression, was also examined. Expression of Smad2-DN significantly increased cardiomyocyte labeling index over control cells (Figure 4A). As expected, expression of S262A-Cx43 decreased BrdU incorporation significantly compared to controls; expression of wild type Cx43 exerts a similar inhibitory effect (Figure 3A). The effect of S262A-Cx43, as well as wild type Cx43 remained unchanged in the presence of Smad2-DN (Figure 4A and unpublished observations). The inability of Smad2-DN to reverse the inhibitory effect of S262A-Cx43 may be linked to the inability of the mutant

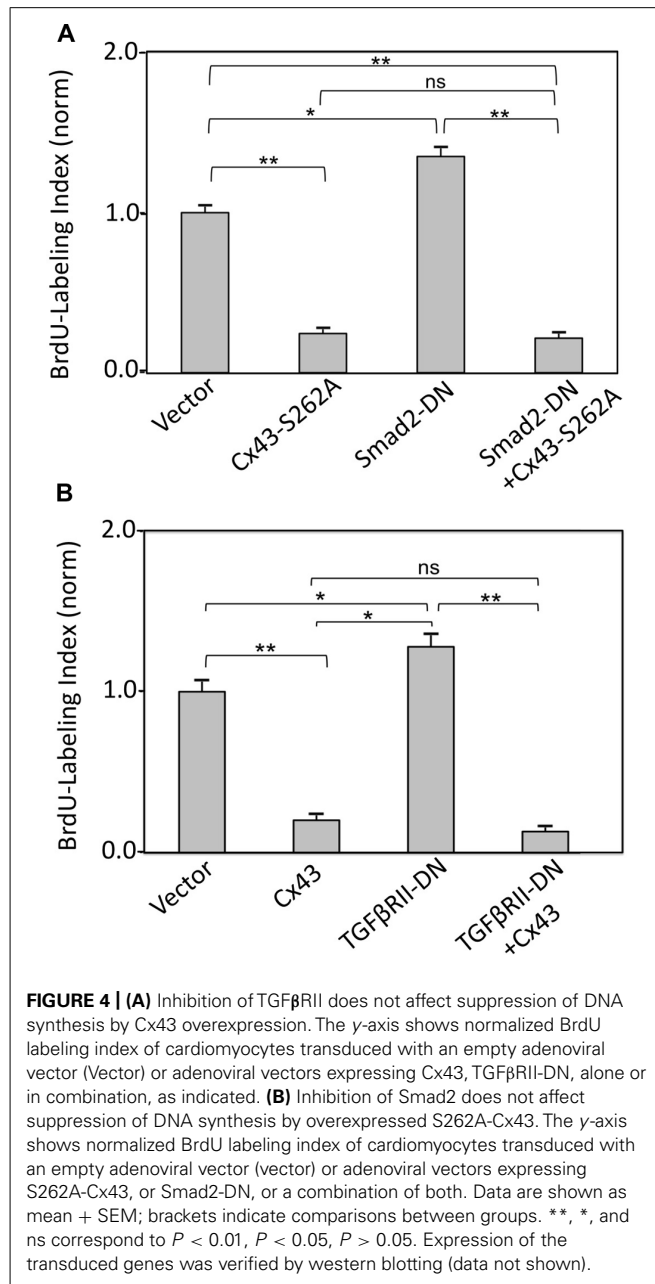


**FIGURE 4 | (A)** Inhibition of TGF $\beta$ RII does not affect suppression of DNA synthesis by Cx43 overexpression. The y-axis shows normalized BrdU labeling index of cardiomyocytes transduced with an empty adenoviral vector (Vector) or adenoviral vectors expressing Cx43, S262A-Cx43, or Smad2-DN, alone or in combination, as indicated. Data are shown as mean  $\pm$  SEM; brackets indicate comparisons between groups. \*\*, \*, and ns correspond to  $P < 0.01$ ,  $P < 0.05$ ,  $P > 0.05$ . Expression of the transduced genes was verified by western blotting (data not shown).

Cx43 to become phosphorylated at amino-acid 262, providing an irreversible signal.

Inhibition of TGF $\beta$ RII by overexpressing TGF $\beta$ RII-DN significantly increased BrdU labeling index in cardiomyocytes, as we reported previously (Sheikh et al., 2004). This effect was prevented in the presence of Cx43 overexpression (Figure 4B).

Taken together, our findings with inhibitors of early TGF $\beta$  signal transduction are consistent with a scenario where Cx43-mediated growth suppression occurs downstream of TGF $\beta$ /TGF $\beta$ RII/TGF $\beta$ RI/pSmad2 signaling.

Finally we asked if inhibition of cardiomyocyte DNA synthesis by Cx43 was additive to that by TGF $\beta$ . As shown in Figure 5, addition of TGF $\beta$  or overexpression of Cx43, both exerted a

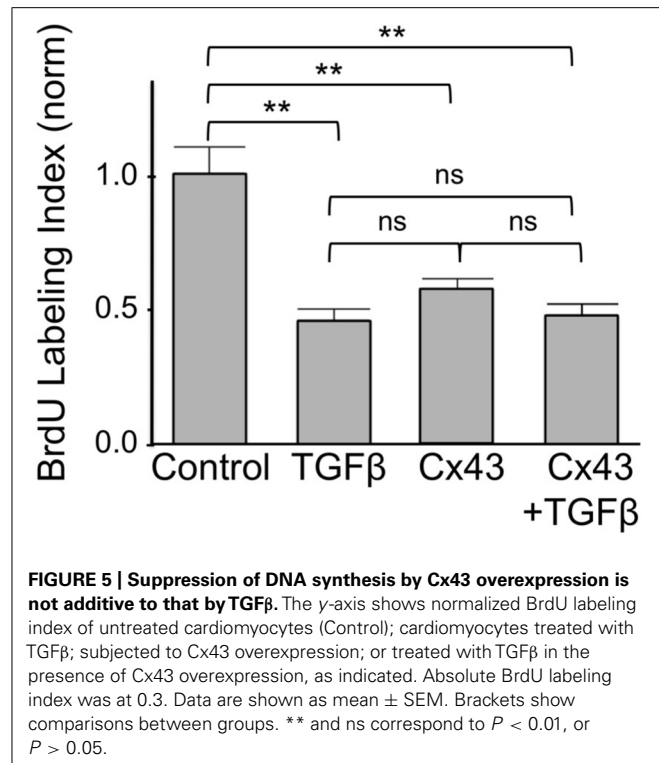


**FIGURE 5 | Suppression of DNA synthesis by Cx43 overexpression is not additive to that by TGF $\beta$ .** The y-axis shows normalized BrdU labeling index of untreated cardiomyocytes (Control); cardiomyocytes treated with TGF $\beta$ ; subjected to Cx43 overexpression; or treated with TGF $\beta$  in the presence of Cx43 overexpression, as indicated. Absolute BrdU labeling index was at 0.3. Data are shown as mean  $\pm$  SEM. Brackets show comparisons between groups. \*\* and ns correspond to  $P < 0.01$ , or  $P > 0.05$ .

significant inhibitory effect on BrdU labeling index, assessed 1 day after treatment. The degree of inhibition by TGF $\beta$  was not significantly different to that by Cx43. The extent of inhibition of BrdU incorporation by combined use of TGF $\beta$  and Cx43 overexpression was not significantly different to that of either inhibitor alone. The absence of an additive effect on DNA synthesis inhibition suggests that TGF $\beta$ -triggered signals, and Cx43-mediated signals, are components of the same pathway, where, as indicated by our results shown in the previous Figures (1–5), Cx43-triggered signals are downstream of early TGF $\beta$  signal transduction.

Experimental evidence presented here in combination with previous work pointed to a hypothetical scenario where phosphorylation of Cx43 at S262 allows this protein to act as a switch between pro-mitotic and anti-mitotic signaling, as illustrated in Figure 6.

## DISCUSSION

Connexin-43 is constitutively phosphorylated at multiple sites, ensuring correct trafficking of this protein to the plasma membrane as well as assembly of connexons and channel functionality (Solan and Lampe, 2009). In addition to the constitutively phosphorylated sites, specific sites at the C-terminal tail of Cx43 can become phosphorylated in response to growth factor- or oncogene-linked signaling, preventing Cx43 from suppressing cell proliferation. For example, the src-targeted tyrosines 247 and 265 can affect the ability of Cx43 to inhibit proliferation of glioma cells (Herrero-Gonzalez et al., 2010); serines 255, 262, 279, 282 are reported as targets of mitogen-activated protein kinase pathways, and, their phosphorylation allows for platelet-derived growth factor-triggered mitotic stimulation of vascular smooth

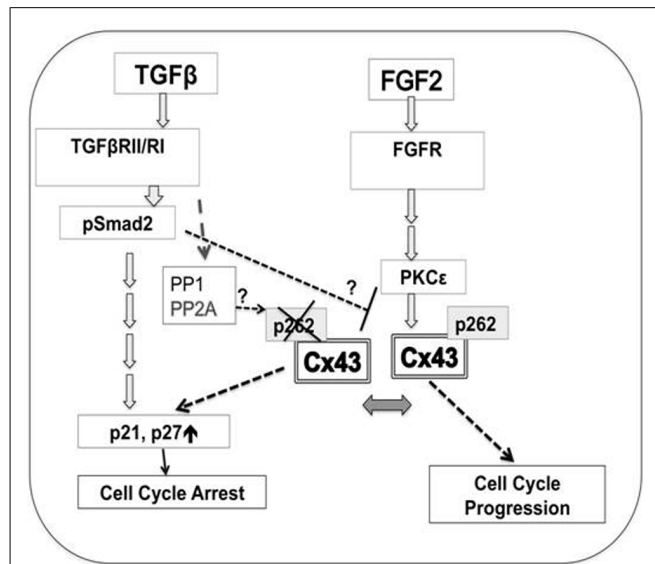


**FIGURE 6 | A hypothetical model for the regulation of cardiomyocyte proliferation by Cx43 phosphorylation at S262.** Mitogen (FGF-2)-triggered signaling includes activation of cognate receptor (FGFR, fibroblast growth factor receptors), downstream activation of PKC $\epsilon$ , followed by increased interaction between PKC $\epsilon$  and Cx43, and phosphorylation of Cx43 at S262. This phosphorylation event blocks the ability of Cx43 to act as a suppressor of DNA synthesis, and allows FGF-2 signaling to promote cell cycle progression. Early TGF $\beta$ -triggered signaling including TGF $\beta$ RII/RI and Smad2/3 activation results in decreased levels of pS262-Cx43, allowing Cx43 to act as a growth suppressor. TGF $\beta$  signaling may: activate phosphatases such as PP1, or PP2A, to affect Cx43 dephosphorylation; prevent the FGF-2-induced PKC $\epsilon$  activation, and/or prevent PKC $\epsilon$ /Cx43 interaction and thus Cx43 phosphorylation. These possibilities are indicated by question marks. Cx43-, as well as TGF $\beta$ -mediated inhibition of cell proliferation is achieved via downstream activation of cell cycle inhibitors p21/p27.

muscle cells (Johnstone et al., 2012). In cardiomyocytes, the FGF-2-induced mitotic stimulation is accompanied by increased phosphorylation of Cx43 at S262, mediated by PKC $\epsilon$  (Doble et al., 2000, 2004). To understand the role of phosphorylation at S262 on the ability of Cx43 to suppress growth, in previous studies we used Cx43 phosphorylation mutants to simulate either constitutive phosphorylation (S262-to-aspartate (D) substitution) or lack of phosphorylation (S262A) at the S262 site. The ability of Cx43 to suppress DNA synthesis was found to be maximal in cells expressing S262A-Cx43 but absent in cells expressing S262D-Cx43 (Doble et al., 2004; Dang et al., 2006). Overall our previous work indicated that pS262-Cx43 is “permissive” for DNA synthesis, allowing cells to progress through the cell cycle in response to growth factor stimulation. One may therefore consider the notion that conditions and factors known to inhibit cell proliferation may actively prevent the phosphorylation of Cx43 at specific sites. TGF $\beta$  is one such factor, known for its cytostatic properties in many situations (Massague, 2000). Because TGF $\beta$  signaling counteracts the stimulatory effect of FGF-2 on cardiomyocytes DNA synthesis (Kardami, 1990), we hypothesized that TGF $\beta$  may promote the “growth inhibitory” state of Cx43, by preventing its phosphorylation at S262. This question was addressed in both an acute as well as a more “chronic” setting, in culture.

In the acute setting, a brief pre-treatment with TGF $\beta$  rendered cardiomyocytes incapable of responding to FGF-2 as shown by their blunted ability to upregulate pS262-Cx43; the acute response has “chronic” consequences as it is accompanied by a blunted DNA synthesis and cell proliferation response (Kardami, 1990); see also **Figure 5**. In a more “chronic” scenario, we tested the consequences of inhibiting constitutive TGF $\beta$  signal transduction on endogenous pS262-Cx43 levels. The biological effects of TGF $\beta$  are transduced by binding to plasma membrane receptors, TGF $\beta$ RII and TGF $\beta$ RI, downstream activation/phosphorylation of the regulatory Smads (Smad2 and Smad3), their interaction with Smad4, nuclear translocation and activation of specific gene expression (Massague and Wotton, 2000; Heldin et al., 2009). Inhibition at the level of TGF $\beta$ RI was achieved through the use of SB431542, which inhibits TGF $\beta$ RI (ALK5) by acting as a competitive ATP binding site kinase inhibitor (Inman et al., 2002). In cardiomyocytes, which express ALK5, SB431542 is effective in preventing downstream activation (phosphorylation) of Smad2 as shown by (Waghabi et al., 2002), and confirmed here. To specifically target the activity of TGF $\beta$ RII, which acts as a co-receptor with TGF $\beta$ RI, we overexpressed a kinase-deficient TGF $\beta$ RII which has been shown to be effective in inhibiting endogenous TGF $\beta$ RII in a DN fashion (Sheikh et al., 2004). Finally, Smad2 activation (phosphorylation) was prevented by overexpressing Smad2-DN. All of these inhibitors increased endogenous levels of pS262-Cx43, without affecting total Cx43 protein levels, indicating that early TGF $\beta$  signal transduction (engaging the activity of TGF $\beta$ RII and TGF $\beta$ RI and resulting in Smad2 phosphorylation) downregulates pS262-Cx43. This may occur by: directly preventing the FGF-2-induced activation of PKC $\epsilon$  which acts as an upstream phosphorylating kinase for Cx43; by preventing Cx43 interaction and/or phosphorylation by the PKC $\epsilon$ ; by activating phosphatase(s) that would cause Cx43 dephosphorylation. There is evidence to support the latter possibility: TGF $\beta$  signaling activates protein phosphatase (PP)-2A (Petritsch et al., 2000), which has been reported to target Cx43 for dephosphorylation (Ai et al., 2011). Other potential phosphatases implicated in Cx43 dephosphorylation include PP1 and PP2B (Jeyaraman et al., 2003). There is at present limited information as to potential effects of TGF $\beta$  on PKC $\epsilon$  activity or expression, or on the PKC $\epsilon$ /Cx43 interaction. It is of interest, however, that PKC $\epsilon$  is promoting the proliferation of cells, including cardiomyocytes (Kardami et al., 2003), and has an antithetical relationship with TGF $\beta$  regarding the control of CD4 $^{+}$  T-lymphocyte proliferation (Mirandola et al., 2011).

In parallel to increasing endogenous pS262-Cx43, inhibition of constitutive TGF $\beta$  signal transduction increased cardiomyocyte DNA synthesis, providing further validation to the notion that Cx43 phosphorylation at S262 is permissive for mitogenic stimulation. It should, however, be noted that inhibition of constitutive TGF $\beta$  signal transduction was unable to reverse the inhibitory effects of overexpressed Cx43. It is possible that overexpressed Cx43 (or Cx43-CT) overwhelm the endogenous cellular machinery (kinases/phosphatases) affected by inhibition of baseline TGF $\beta$  signaling. In broad agreement with this notion, we have previously observed that only a small fraction of overexpressed Cx43, or Cx43-CT, become phosphorylated at S262 under normal culture conditions, requiring stimulation with a highly potent PKC

activator, phorbol-12-myristate-13-acetate, for Cx43 to become mostly phosphorylated at that site (Dang et al., 2006). A likely explanation therefore for the apparent discrepancy of our findings with endogenous versus overexpressed Cx43 is that any signals (kinases/phosphatases) activated or dis-inhibited by blocking baseline TGF $\beta$  signaling may be inadequate to promote or sustain substantial phosphorylation at S262 when Cx43 is present at above-normal levels.

Previous studies using a cardiac cell line, atria-derived HL-1, indicated that Cx43, of unknown phosphorylation status, activated TGF $\beta$  transcriptional activity, by activating TGF $\beta$ RI, and promoting Smad2/3 phosphorylation and nuclear translocation; it was suggested that Cx43-dependent suppression of cardiomyocyte proliferative growth reflected downstream activation of Smad2/3 (Dai et al., 2007). This would position Cx43 expression upstream of TGF $\beta$ RI-pSmad2 signal transduction, in apparent contrast to findings presented here. We showed that ectopic expression of Cx43 inhibited DNA synthesis regardless of the status of TGF $\beta$ RI or Smad2/3 activation; in addition neither Cx43 nor Cx43-CT overexpression had any discernible effect on relative pSmad2 levels in our system. Our data therefore suggested that Cx43-mediated inhibition of DNA synthesis is not mediated by downstream activation of TGF $\beta$  signals. It is possible that these differences may reflect differences between experimental approaches (gain-of-function in the case of overexpression versus loss-of-function in knock-down studies) and/or cell types, namely the mouse atrial HL-1 cell line versus rat primary ventricular cardiomyocytes used here. Also, as Dai et al. (2007) used TGF $\beta$  transcriptional activation as their end-point, there was no information as to how the observed Smad2/3 and/or Cx43 expression changes affected DNA synthesis in their system.

The precise molecular mechanism by which Cx43 and pS262-Cx43 affect proliferative growth remains to be determined. The role of subcellular localization of Cx43 is not clear: Cx43-CT, which, unlike Cx43, localizes to the cytosol and nucleus, retains inhibitory activity (Dang et al., 2003; Kardami et al., 2007), suggesting that localization at cell–cell contact sites and/or gap junction function are not crucial determinants of growth inhibitory activity. Furthermore, phosphorylation at S262 (simulated by expression of S262D-Cx43, or -Cx43-CT) blocked the inhibitory properties of not only Cx43 but also Cx43-CT, without affecting their respective distinct localizations, at plasma membrane versus cytosolic/nuclear sites, in HEK293 cells; unpublished observations and as shown previously (Dang et al., 2003, 2006). It is of interest, however, that Cx43 (Boengler et al., 2005) as well as a C-terminal containing fragment of Cx43 (Kardami et al., 2007) have also been detected in cardiac mitochondria. Mitochondria play an important role in cell cycle regulation (Antico Arciuch et al., 2012), and therefore future studies should examine whether mitochondrial Cx43, and its potential phosphorylation at S262, modulate mitochondrial function in this context.

In conclusion, our studies suggest the following model to describe the relationship between TGF $\beta$  and Cx43-mediated growth suppression in cardiomyocytes; **Figure 6**. TGF $\beta$ -triggered early signal transduction, involving activation of TGF $\beta$ RII/RI and phosphorylation of Smad2, reduces relative levels of pS262-Cx43, by either preventing the growth factor-induced PKC $\epsilon$  activation,

or PKC $\epsilon$ /Cx43 interaction, and/or by activating Cx43-targeting phosphatase(s). Cx43 lacking phosphorylation at S262 possesses growth inhibitory activity, blocks growth factor (FGF-2) signals from stimulating cell cycle progression, and mediates or at least contributes to inhibition of DNA synthesis by TGF $\beta$ . It has been established that both TGF $\beta$ -, and Cx43-, mediated suppression of cell proliferation are achieved by upregulating the cyclin-dependent kinase inhibitors p21/p27 which control cell cycle arrest (Sanchez-Alvarez et al., 2006; Abbas and Dutta, 2009; Bauer et al., 2012), and thus these signals are proposed to be activated downstream of Cx43 lacking phosphorylation at S262. Mitogens, such as FGF-2, overcome/attenuate inhibition of DNA synthesis by Cx43 by promoting activation of PKC $\epsilon$  which interacts with, and phosphorylates Cx43 at S262. The ability of FGF-2 to

overcome the growth inhibitory effect of Cx43 on cardiomyocytes is likely to depend on expression of appropriate levels of signal-transducing machinery [FGF-2 receptors, active PKC $\epsilon$ , inactive phosphatase(s)] to achieve and/or sustain phosphorylation of endogenous Cx43 at S262.

## ACKNOWLEDGMENTS

This work was funded (to Elissavet Kardami) by the Heart and Stroke Foundation of Manitoba, and the Canadian Institutes for Health Research (FRN 74733). Maya M. Jeyaraman had a studentship award from the Heart and Stroke Foundation of Canada. We thank Dr. Rebecca G. Wells (University of Pennsylvania School of Medicine, PA, USA) for her generous gift of adenoviral vectors expressing DN versions of Smad2 and Smad3.

## REFERENCES

- Abbas, T., and Dutta, A. (2009). p21 in cancer: intricate networks and multiple activities. *Nat. Rev. Cancer* 9, 400–414. doi: 10.1038/nrc2657
- Ahuja, P., Sdeh, P., and Maclellan, W. R. (2007). Cardiac myocyte cell cycle control in development, disease, and regeneration. *Physiol. Rev.* 87, 521–544. doi: 10.1152/physrev.00032.2006
- Ai, X., Jiang, A., Ke, Y., Solaro, R. J., and Pogwizd, S. M. (2011). Enhanced activation of p21-activated kinase 1 in heart failure contributes to dephosphorylation of connexin 43. *Cardiovasc. Res.* 92, 106–114. doi: 10.1093/cvr/crv163
- Antico Arciuch, V. G., Elguero, M. E., Poderoso, J. J., and Carreras, M. C. (2012). Mitochondrial regulation of cell cycle and proliferation. *Antioxid. Redox Signal.* 16, 1150–1180. doi: 10.1089/ars.2011.4085
- Bauer, J., Sporn, J. C., Cabral, J., Gomez, J., and Jung, B. (2012). Effects of activin and TGF $\beta$  on p21 in colon cancer. *PLoS ONE* 7:e39381. doi: 10.1371/journal.pone.0039381
- Bergmann, O., Bhardwaj, R. D., Bernard, S., Zdunek, S., Barnabe-Heider, F., Walsh, S., et al. (2009). Evidence for cardiomyocyte renewal in humans. *Science* 324, 98–102. doi: 10.1126/science.1164680
- Boengler, K., Dodoni, G., Rodriguez-Sinovas, A., Cabestrero, A., Ruiz-Meana, M., Gres, P., et al. (2005). Connexin 43 in cardiomyocyte mitochondria and its increase by ischemic preconditioning. *Cardiovasc. Res.* 67, 234–244. doi: 10.1016/j.cardiores.2005.04.014
- Dai, P., Nakagami, T., Tanaka, H., Hitomi, T., and Takamatsu, T. (2007). Cx43 mediates TGF-beta signaling through competitive Smads binding to microtubules. *Mol. Biol. Cell* 18, 2264–2273. doi: 10.1091/mbc.E06-12-1064
- Dang, X., Doble, B. W., and Kardami, E. (2003). The carboxytail of connexin-43 localizes to the nucleus and inhibits cell growth. *Mol. Cell. Biochem.* 242, 35–38. doi: 10.1023/A:1021152709313
- Dang, X., Jeyaraman, M., and Kardami, E. (2006). Regulation of connexin-43-mediated growth inhibition by a phosphorylatable amino-acid is independent of gap junction-forming ability. *Mol. Cell. Biochem.* 289, 201–207. doi: 10.1007/s11010-006-9162-2
- Doble, B. W., Chen, Y., Bosc, D. G., Litchfield, D. W., and Kardami, E. (1996). Fibroblast growth factor-2 decreases metabolic coupling and stimulates phosphorylation as well as masking of connexin43 epitopes in cardiac myocytes. *Circ. Res.* 79, 647–658. doi: 10.1161/01.RES.79.4.647
- Doble, B. W., Dang, X., Ping, P., Fandrich, R. R., Nickel, B. E., Jin, Y., et al. (2004). Phosphorylation of serine 262 in the gap junction protein connexin-43 regulates DNA synthesis in cell-cell contact forming cardiomyocytes. *J. Cell Sci.* 117, 507–514. doi: 10.1242/jcs.00889
- Doble, B. W., Ping, P., and Kardami, E. (2000). The epsilon subtype of protein kinase C is required for cardiomyocyte connexin-43 phosphorylation. *Circ. Res.* 86, 293–301. doi: 10.1161/01.RES.86.3.293
- Heldin, C. H., Landstrom, M., and Moustakas, A. (2009). Mechanism of TGF-beta signaling to growth arrest, apoptosis, and epithelial-mesenchymal transition. *Curr. Opin. Cell Biol.* 21, 166–176. doi: 10.1016/j.celbi.2009.01.021
- Herrero-Gonzalez, S., Gangoso, E., Giaume, C., Naus, C. C., Medina, J. M., and Tabernero, A. (2010). Connexin43 inhibits the oncogenic activity of c-Src in C6 glioma cells. *Oncogene* 29, 5712–5723. doi: 10.1038/onc.2010.299
- Inman, G. J., Nicolas, F. J., Callahan, J. F., Harling, J. D., Gaster, L. M., Reith, A. D., et al. (2002). SB-431542 is a potent and specific inhibitor of transforming growth factor-beta superfamily type I activin receptor-like kinase (ALK) receptors ALK4, ALK5, and ALK7. *Mol. Pharmacol.* 62, 65–74. doi: 10.1124/mol.62.1.65
- Jeyaraman, M., Tanguy, S., Fandrich, R. R., Lukas, A., and Kardami, E. (2003). Ischemia-induced dephosphorylation of cardiomyocyte connexin-43 is reduced by okadaic acid and calyculin A but not fostriecin. *Mol. Cell. Biochem.* 242, 129–134. doi: 10.1023/A:1021102131603
- Jiang, Z. S., Padua, R. R., Ju, H., Doble, B. W., Jin, Y., Hao, J., et al. (2002). Acute protection of ischemic heart by FGF-2: involvement of FGF-2 receptors and protein kinase C. *Am. J. Physiol. Heart Circ. Physiol.* 282, H1071–H1080.
- Jiang, Z. S., Srisakuldee, W., Soulet, F., Bouche, G., and Kardami, E. (2004). Non-angiogenic FGF-2 protects the ischemic heart from injury, in the presence or absence of reperfusion. *Cardiovasc. Res.* 62, 154–166. doi: 10.1016/j.cardiores.2004.01.009
- Johnstone, S. R., Kroncke, B. M., Straub, A. C., Best, A. K., Dunn, C. A., et al. (2012). MAPK phosphorylation of connexin 43 promotes binding of cyclin E and smooth muscle cell proliferation. *Circ. Res.* 111, 201–211. doi: 10.1161/CIRCRESAHA.112.272302
- Kardami, E. (1990). Stimulation and inhibition of cardiac myocyte proliferation in vitro. *Mol. Cell. Biochem.* 92, 129–135. doi: 10.1007/BF00218130
- Kardami, E., Banerji, S., Doble, B. W., Dang, X., Fandrich, R. R., Jin, Y., et al. (2003). PKC-dependent phosphorylation may regulate the ability of connexin43 to inhibit DNA synthesis. *Cell Commun. Adhes.* 10, 293–297.
- Kardami, E., Dang, X., Iacobas, D. A., Nickel, B. E., Jeyaraman, M., Srisakuldee, W., et al. (2007). The role of connexins in controlling cell growth and gene expression. *Prog. Biophys. Mol. Biol.* 94, 245–264. doi: 10.1016/j.pbiomolbio.2007.03.009
- Massague, J. (2000). How cells read TGF-beta signals. *Nat. Rev. Mol. Cell Biol.* 1, 169–178. doi: 10.1038/35043051
- Massague, J., and Wotton, D. (2000). Transcriptional control by the TGF-beta/Smad signaling system. *EMBO J.* 19, 1745–1754. doi: 10.1093/embj/19.8.1745
- Matsuyama, D., and Kawahara, K. (2009). Proliferation of neonatal cardiomyocytes by connexin43 knockdown via synergistic inactivation of p38 MAPK and increased expression of FGF1. *Basic Res. Cardiol.* 104, 631–642. doi: 10.1007/s00395-009-0029-z
- Mirandola, P., Gobbi, G., Masselli, E., Micheloni, C., Di Marcantonio, D., Queirolo, V., et al. (2011). Protein kinase C epsilon regulates proliferation and cell sensitivity to TGF-1beta of CD4 $^{+}$  T lymphocytes: implications for Hashimoto thyroiditis. *J. Immunol.* 187, 4721–4732. doi: 10.4049/jimmunol.1003258
- Pasumarthi, K. B., Kardami, E., and Cattini, P. A. (1996). High and low molecular weight fibroblast growth factor-2 increase proliferation of neonatal rat cardiac myocytes but have differential effects on binucleation and nuclear morphology. Evidence for both paracrine and intracrine actions of fibroblast growth factor-2. *Circ. Res.* 78, 126–136. doi: 10.1161/01.RES.78.1.126
- Petritsch, C., Beug, H., Balmain, A., and Oft, M. (2000). TGF-beta inhibits p70 S6 kinase via protein phosphatase 2A to induce G(1) arrest. *Genes Dev.* 14, 3093–3101. doi: 10.1101/gad.854200
- Rama, A., Matsushita, T., Charolidi, N., Rothery, S., Dupont, E., and

- Severs, N. J. (2006). Up-regulation of connexin43 correlates with increased synthetic activity and enhanced contractile differentiation in TGF-beta-treated human aortic smooth muscle cells. *Eur. J. Cell Biol.* 85, 375–386. doi: 10.1016/j.ejcb.2005.11.007
- Sanchez-Alvarez, R., Paineo, T., Herrero-Gonzalez, S., Medina, J. M., and Tabernero, A. (2006). Tolbutamide reduces glioma cell proliferation by increasing connexin43, which promotes the up-regulation of p21 and p27 and subsequent changes in retinoblastoma phosphorylation. *Glia* 54, 125–134. doi: 10.1002/glia.20363
- Senyo, S. E., Steinhauser, M. L., Pizimenti, C. L., Yang, V. K., Cai, L., Wang, M., et al. (2013). Mammalian heart renewal by pre-existing cardiomyocytes. *Nature* 493, 433–436. doi: 10.1038/nature11682
- Sheikh, F., Hirst, C. J., Jin, Y., Bock, M. E., Fandrich, R. R., Nickel, B. E., et al. (2004). Inhibition of TGF $\beta$  signaling potentiates the FGF-2-induced stimulation of cardiomyocyte DNA synthesis. *Cardiovasc. Res.* 64, 516–525. doi: 10.1016/j.cardiores.2004.08.009
- Solan, J. L., and Lampe, P. D. (2009). Connexin43 phosphorylation: structural changes and biological effects. *Biochem. J.* 419, 261–272. doi: 10.1042/BJ20082319
- Srisakuldee, W., Jeyaraman, M. M., Nickel, B. E., Tangy, S., Jiang, Z. S., and Kardami, E. (2009). Phosphorylation of connexin-43 at serine 262 promotes a cardiac injury-resistant state. *Cardiovasc. Res.* 83, 672–681. doi: 10.1093/cvr/cvp142
- Tacheau, C., Fontaine, J., Loy, J., Mauviel, A., and Verrecchia, F. (2008). TGF- $\beta$  induces connexin43 gene expression in normal murine mammary gland epithelial cells via activation of p38 and PI3K/AKT signaling pathways. *J. Cell. Physiol.* 217, 759–768. doi: 10.1002/jcp.21551
- Uemura, M., Swenson, E. S., Gaca, M. D., Giordano, F. J., Reiss, M., and Wells, R. G. (2005). Smad2 and Smad3 play different roles in rat hepatic stellate cell function and alpha-smooth muscle actin organization. *Mol. Biol. Cell* 16, 4214–4224. doi: 10.1091/mbc.E05-02-0149
- Waghabi, M. C., Coutinho, C. M., Soeiro, M. N., Pereira, M. C., Feige, J. J., Keramidas, M., et al. (2002). Increased *Trypanosoma cruzi* invasion and heart fibrosis associated with high transforming growth factor beta levels in mice deficient in alpha(2)-macroglobulin. *Infect. Immun.* 70, 5115–5123. doi: 10.1128/IAI.70.9.5115-5123.2002
- Zhang, Y., Kanter, E. M., Laing, J. G., Aprhys, C., Johns, D. C., Kardami, E., et al. (2008). Connexin43 expression levels influence intercellular coupling and cell proliferation of native murine cardiac fibroblasts. *Cell Commun. Adhes.* 15, 289–303. doi: 10.1080/15419060802198736
- Conflict of Interest Statement:** The authors declare that the research was conducted in the absence of any commercial or financial relationships that could be construed as a potential conflict of interest.
- Received: 12 April 2013; accepted: 28 June 2013; published online: 19 July 2013.*
- Citation: Jeyaraman MM, Fandrich RR and Kardami E (2013) Together and apart: inhibition of DNA synthesis by connexin-43 and its relationship to transforming growth factor  $\beta$ . *Front. Pharmacol.* 4:90. doi: 10.3389/fphar.2013.00090*
- This article was submitted to Frontiers in Pharmacology of Ion Channels and Channelopathies, a specialty of Frontiers in Pharmacology.
- Copyright © 2013 Jeyaraman, Fandrich and Kardami. This is an open-access article distributed under the terms of the Creative Commons Attribution License, which permits use, distribution and reproduction in other forums, provided the original authors and source are credited and subject to any copyright notices concerning any third-party graphics etc.



# Histone deacetylase inhibition reduces cardiac connexin43 expression and gap junction communication

**Qin Xu<sup>1</sup>, Xianming Lin<sup>1,2</sup>, Laura Andrews<sup>1</sup>, Dakshesh Patel<sup>1</sup>, Paul D. Lampe<sup>3</sup> and Richard D. Veenstra<sup>1,4\*</sup>**

<sup>1</sup> Department of Pharmacology, State University of New York Upstate Medical University, Syracuse, NY, USA

<sup>2</sup> Leon H. Charney Division of Cardiology, New York University School of Medicine, New York, NY, USA

<sup>3</sup> Fred Hutchinson Cancer Research Center, Seattle, WA, USA

<sup>4</sup> Department of Cell and Developmental Biology, State University of New York Upstate Medical University, Syracuse, NY, USA

**Edited by:**

Aida Salameh, Heart Centre  
University of Leipzig, Germany

**Reviewed by:**

Kerstin Boenigler,  
Justus-Liebig-Universität Giessen,  
Germany

Thomas Seidel, Nora Eccles Harrison  
Cardiovascular Research and Training  
Institute, University of Utah, USA

**\*Correspondence:**

Richard D. Veenstra, Department of  
Pharmacology, State University of  
New York Upstate Medical University,  
750 East Adams Street, Syracuse,  
NY 13210, USA.

e-mail: veenstr@upstate.edu

Histone deacetylase inhibitors (HDACIs) are being investigated as novel therapies for cancer, inflammation, neurodegeneration, and heart failure. The effects of HDACIs on the functional expression of cardiac gap junctions (GJs) are essentially unknown. The purpose of this study was to determine the effects of trichostatin A (TSA) and vorinostat (VOR) on functional GJ expression in ventricular cardiomyocytes. The effects of HDAC inhibition on connexin43 (Cx43) expression and functional GJ assembly were examined in primary cultured neonatal mouse ventricular myocytes. TSA and VOR reduced Cx43 mRNA, protein expression, and immunolocalized Cx43 GJ plaque area within ventricular myocyte monolayer cultures in a dose-dependent manner. Chromatin immunoprecipitation experiments revealed altered protein interactions with the Cx43 promoter. VOR also altered the phosphorylation state of several key regulatory Cx43 phospho-serine sites. Patch clamp analysis revealed reduced electrical coupling between isolated ventricular myocyte pairs, altered transjunctional voltage-dependent inactivation kinetics, and steady state junctional conductance inactivation and recovery relationships. Single GJ channel conductance was reduced to 54 pS only by maximum inhibitory doses of TSA ( $\geq 100$  nM). These two hydroxamate pan-HDACIs exert multiple levels of regulation on ventricular GJ communication by altering Cx43 expression, GJ area, post-translational modifications (e.g., phosphorylation, acetylation), gating, and channel conductance. Although a 50% downregulation of Cx43 GJ communication alone may not be sufficient to slow ventricular conduction or induce arrhythmias, the development of class-selective HDACIs may help avoid the potential negative cardiovascular effects of pan-HDACI.

**Keywords:** gap junctions, connexin43, phosphorylation, connexin40, trichostatin A, vorinostat

## INTRODUCTION

Histone acetyltransferases (HATs) and deacetylases (HDACs) regulate the nuclear protein acetylation–deacetylation cycle that modulates gene expression by altering chromatin condensation and transcription factor [e.g., MEF2 (myocyte enhancer factor-2), p53] activities (Kouzarides, 2000; Yang and Grégoire, 2007; Yang and Seto, 2008; Haberland et al., 2009). Several cytosolic proteins have been identified as substrates for the HAT/HDAC protein acetylation cycle (e.g., tubulin; Piperno et al., 1987; Yang and Grégoire, 2007). There are 11 highly homologous mammalian HDACs containing Zn<sup>2+</sup>-dependent catalytic deacetylase (DAC) domains, subdivided into three classes based on their divergent amino- and carboxyl-terminal domains. The class I HDACs (HDAC1–3 and 8) consist primarily of a single DAC with short amino and carboxyl-termini, as does the class IV HDAC (HDAC11; Yang and Seto, 2008). The class IIa HDACs (HDAC4, 5, 7, and 9) possess amino-terminal MEF2 and 14-3-3 protein binding motifs and shuttle between the nucleus and cytosol in a phosphorylation-dependent manner (McKinsey et al., 2000; Zhou et al., 2000; Little et al., 2007). Phosphorylation of HDAC4, 5, and 9 promotes the expression of cardiac prohypertrophic genes and their deletion

increases susceptibility to stress-induced hypertrophy (Little et al., 2007; Yang and Seto, 2008; Haberland et al., 2009). HDAC4 is implicated in the regulation of cardiac contractility via muscle LIM protein (MLP) acetylation (Gupta et al., 2008). The class IIb HDAC6 is unique in that it possesses two DAC domains and deacetylates tubulin along with sirtuins (SIRT2) (SIRT1–7 are the NAD-dependent class III HDACs; Hubert et al., 2002; Haberland et al., 2009). The function of the class IIb HDAC10 is poorly understood.

Histone DAC inhibitors (HDACIs) are known to induce diverse biological responses including apoptosis and cell-cycle arrest (Rasheed et al., 2007). HDACI chemical subgroups include, in order of potency, hydroxamic acids, cyclic peptides, benzamides, electrophilic ketones, and short chain fatty acids. Trichostatin A (TSA) is a biological hydroxamate compound with antibacterial, antifungal, and antiproliferative activities attributed to its HDAC inhibitory activity (Yoshida et al., 1990). Two HDACIs have received FDA approval for treating cutaneous T cell lymphoma (CTCL) and there are >140 ongoing HDACI clinical trials as novel therapeutics for numerous diseases including other forms of cancer, neurodegeneration, inflammation, and heart failure

([www.clinicaltrials.gov](http://www.clinicaltrials.gov); Marks and Breslow, 2007; Rasheed et al., 2007; Kazantsev and Thompson, 2008; Haberland et al., 2009; Ryan, 2009; Shakespear et al., 2011; McKinsey, 2012). Vorinostat [VOR, suberoylanilide hydroxamic acid (SAHA), Zolinza<sup>TM</sup>] and romidepsin (depsipeptide, FK-228, Istodax<sup>TM</sup>) are relatively non-selective pan-HDACIs despite possessing differential inhibitory potencies for class IIa HDACs (Rasheed et al., 2007; Bradner et al., 2010). Their broad spectrum HDACI profiles produce dose limiting toxicities such as fatigue, thrombocytopenia, gastrointestinal toxicity, and QT interval prolongation (Rasheed et al., 2007; McKinsey, 2011). Dose-dependent toxicities and increased susceptibility to ventricular arrhythmias associated with some HDACI therapies have emphasized the need to develop isoform selective HDACIs (Shah et al., 2006; McKinsey, 2011).

Vorinostat reduced the occurrence of restraint-induced ventricular arrhythmias in Duchenne muscular dystrophic (mdx) mice (Colussi et al., 2010). However, mdx mouse hearts exhibit reduced cardiac sodium channel (Nav1.5) expression and connexin43 (Cx43) lateralization owing to a hyperacetylated condition that was reversed by VOR (Colussi et al., 2010, 2011). In wild-type (wt) mouse hearts, VOR increased Cx43 acetylation and lateralization, consistent with observations from the mdx mouse that increased protein acetylation leads to Cx43 dissociation from N-cadherin (Ncad), zonula occludens-1 (ZO-1), and cardiac intercalated disks, and increased c-Src-dependent Y265 phosphorylation, molecular events known to downregulate Cx43-mediated gap junction (GJ) communication (Colussi et al., 2011). Functional assessment of ventricular electrical coupling is difficult to perform in intact heart, but is directly quantifiable by dual whole cell patch clamp analysis in isolated cardiomyocyte cell pairs (Lin et al., 2005, 2008a, 2010).

This study was performed to examine the functional effects of TSA and VOR on ventricular Cx43 GJs. Previous preliminary findings suggested that Cx43 is acetylated and that treatment of primary neonatal mouse ventricular myocyte cultures with TSA reduced electrical coupling by nearly 50% (Hertzberg and Spektor, 2004; Lin et al., 2008b). We assessed the ability of TSA and VOR to inhibit total ventricular HDAC activity using a fluorimetric assay; measured Cx43 and Ncad mRNA and protein levels; determined the phospho-serine (pSer) state of Cx43; quantified the Cx43 GJ plaque area; and measured the GJ conductance ( $g_j$ ), transjunctional voltage ( $V_j$ ) gating, and single ventricular GJ channel conductance ( $\gamma_j$ ) properties in ventricular cardiomyocyte cultures by patch clamp techniques. These results provide the first direct evidence for the functional downregulation of Cx43 GJ-mediated electrical coupling between normal ventricular myocytes by pan-HDAC inhibition. These effects presumably result from indirect and direct effects of HDACI-induced increased protein acetylation on Cx43 expression, GJ assembly, and function.

## MATERIALS AND METHODS

### CELL CULTURE

Newborn C57Bl/6 mice were anesthetized with isoflurane and the hearts excised in accordance with procedures approved by the institution's Committee for the Humane Use of Animals. Neonatal murine atrial and ventricular tissues were dissociated separately in a  $\text{Ca}^{2+}$ - and  $\text{Mg}^{2+}$ -free collagenase balanced salt solution

(dulbecco's modified saline [DMS<sub>8</sub>], in mM: NaCl, 116; KCl, 5.4,  $\text{Na}_2\text{PO}_4$ , 1.0; and dextrose, 5.5) containing  $\approx$ 1 mg/ml of purified collagenase (type II), 5.5  $\mu\text{g}/\text{ml}$  deoxyribonuclease I (Worthington Biochemical Corp., Lakewood, NJ, USA), and 1 mg/ml bovine serum albumin (BSA, fraction V, Sigma Chemical Corp., St. Louis, MO, USA; Lin et al., 2005, 2008a, 2010). A total of five 10-min dissociation cycles at 37°C were performed using 5 ml of dissociation solution/cycle. The supernatant from the first cycle was discarded and the supernatant from the remaining four cycles were filtered through a 70- $\mu$  cell strainer (Falcon, Franklin Lakes, NJ, USA) into 5 ml of M199 cell culture media supplemented with 10% fetal bovine serum (FBS; Atlanta Biologicals) and 100 U/ml penicillin/streptomycin (Invitrogen). Cell pellets were produced by low speed centrifugation (500 rpm, 5 min) and resuspended in M199/FBS media. The primary cell cultures were enriched for cardiomyocytes by a 30-min differential cell adhesion step. The cell media was collected, pelleted by low speed centrifugation, and resuspended in approximately 1 ml of media per dissociated heart ventricles. Approximately 0.1 ml of the ventricular myocyte cell suspension was added to each 35 mm diameter culture dish for patch clamp electrophysiology experiments. The remainder of the ventricular cell suspension was divided between two 35-mm culture dishes or four 12-wells containing fibronectin-coated coverslips for real-time (RT)-PCR, immunoblotting, immunoprecipitation, or immunostaining procedures. Exact cell counts were obtained with a hemocytometer for plating cells in 96-well plates for fluorimetric HDAC activity assays. The media was exchanged daily and 200  $\mu\text{M}$  bromodeoxyuridine (BrDU) was added on culture day 2 to the high density myocyte cultures to inhibit fibroblast proliferation. Stable transfectants of HeLa cells with rat Cx43 (HeLa-Cx43 cells) were prepared and cultured as described for mouse Neuro2a (N2a) cells (Lin et al., 2003).

### HDAC ACTIVITY ASSAYS

Aliquots of  $6 \times 10^{15}$  ventricular myocytes or HeLa cells per well (96-well plate) were grown in 200  $\mu\text{l}$  of 200  $\mu\text{M}$  BrDU/M199 or N2a culture media, exchanged daily. Cell densities were counted with a hemocytometer. Cell wells were incubated with 2,000 pmol of the acetylated Fluor-de-Lys<sup>®</sup> substrate for 6 h during HDAC inhibition. Cell, media, and standard curve deacetylated substrate sample wells were developed according to manufacturer's directions and background subtracted relative fluorescence unit (RFU) counts were acquired with a BIO-TEK Synergy plate reader (360 nm excitation, 460 nm emission). A standard curve was generated using serial 1:10 dilutions of the deacetylated Fluor-de-Lys standard and developer supplied with the BML-AK503 HDAC fluorimetric cellular activity assay kit (Figure 1D; Enzo Life Sciences). TSA was purchased from Calbiochem or Enzo Life Sciences. VOR (SAHA, Zolinza<sup>TM</sup>) was initially obtained from Merck HDAC Research, LLC via a Material Transfer Agreement (MTA) for *in vitro* use only and was subsequently purchased commercially from Selleck Chemicals, LLC.

### REAL-TIME PCR

Total atrial or ventricular RNA was isolated with Qiagen RNeasy<sup>®</sup> mini kit, quantified by UV absorption, and 500 ng reverse-transcribed with QuantiTect<sup>®</sup> Reverse Transcription kit

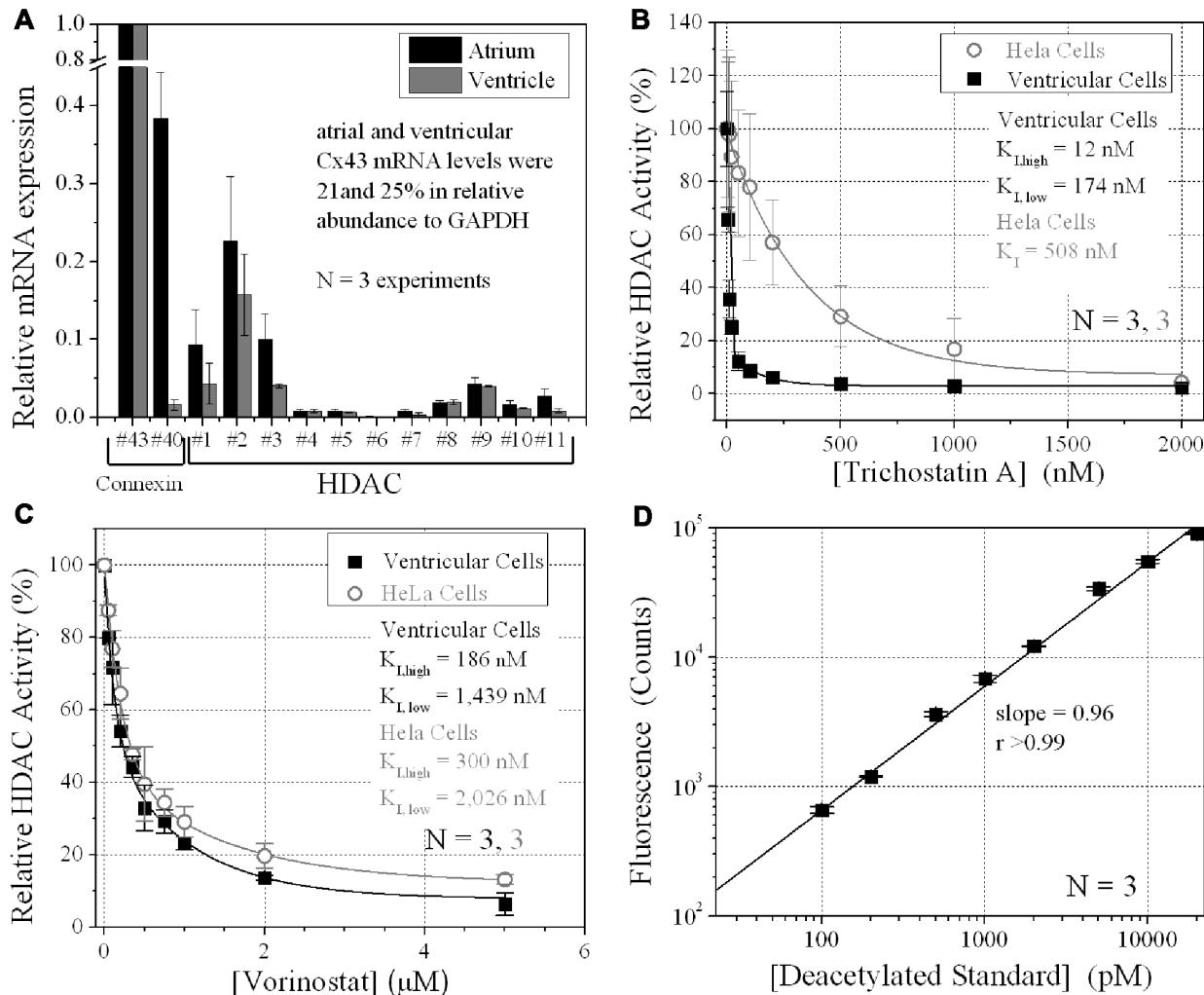


**FIGURE 1 | Ventricular HDAC expression and inhibition.** **(A)** The mRNA expression levels for all 11 mammalian HDACs and two connexins, Cx43 and Cx40, were detected by real-time PCR using the SYBR® GreenER™ qPCR SuperMix (Invitrogen) and custom-designed forward and reverse primers. The data was averaged from three experiments. **(B,C)** Total HDAC activity was measured in ventricular myocyte and stable Cx43-transfected HeLa cell (HeLa-Cx43) cultures by deacetylated Fluor-de-Lys® fluorescence during trichostatin A (TSA) **(B)** or vorinostat (VOR) inhibition **(C)**. All data were normalized to the background subtracted maximum relative fluorescence of the control well. The data from three experiments were averaged and fitted

with a second-order exponential decaying function in Origin7.5 and the equilibrium inhibition constants ( $K_I$ ) were calculated from the expression  $K_I = 0.693/[HDAC]_{\text{decay}}$  constant. **(D)** A series of 1:10 dilutions of the deacetylated Fluor-de-Lys substrate were combined with the developer and fluorescence counts were obtained with the BIO-TEK Synergy plate reader in conjunction (i.e., parallel) with the cell-based HDAC activity assays. The background (empty well) subtracted fluorescence emission at 460 nm increased linearly with the concentration of the deacetylated substrate. The experiments were performed in triplicate (mean  $\pm$  SEM).

(Qiagen). Fifty nanograms of the cDNA reaction mix was combined with equal (nM) amounts of custom forward (5'-3') and reverse (3'-5') RT-PCR primers, Superscript® enzyme mix, and SYBR® GreenER™ dye in a 200- $\mu$ l PCR tube (rxn volume = 25  $\mu$ l). All RT-PCR reagents were from Invitrogen and the samples were run for 40 cycles in a 96-well plate. All results were expressed relative to glyceraldehyde 3-phosphate dehydrogenase (GAPDH) and a cellular RNA sample without reverse transcription was run as a negative control to test for genomic DNA.  $cT$  values were determined by the apparatus and the quality of the PCR product was confirmed by analyzing the melt-curve. RT-PCR primers were custom-designed for all murine 11 HDAC

genes based on the mouse gene sequences according to published rat HDAC RT primers (Morrison et al., 2006), *Gja1*, *Gja5*, *Gapdh*, and *Cdh2* (*Ncad*) murine genes (Lin et al., 2010). RT-PCR primers were designed to span exon-intron regions of the gene of interest or by custom ordering primer sets from realtimeprimers.com.

Oligonucleotide primer sequences for the RT-PCR assays of murine HDAC1-11, Cx43, Cx40, Ncad, and GAPDH gene expression were: *Hdac1*, forward 5'-TGGGGCTGGCAAAGG CAA-3', reverse 5'-TGGGGCAGCATCCTCAAGTCC-3'; *Hdac2*, forward 5'-CGGACAAAAG AATTTCATTCTG-3', reverse 5'-CAATGTCTCAAACAGGGAAAG-3'; *Hdac3*, forward 5'-CCGCT-TCCATTCTGAGGACTAC-3', reverse 5'-GACCCGGTCAGTGA-

GGTAGAAG-3'; *Hdac4*, forward 5'-GTTCCAGCGTCAACATGA-G-3', reverse 5'-GTTGAGAACAAACTCCTG CAGCT-3'; *Hdac5*, forward 5'-GCCAGCACCGAGGTAAGGCT-3', reverse 5'-TTAC-GGAGG GGAAAGTCATCA-3'; *Hdac6*, forward 5'-ACCACCTC-TCTGGAGGCTT-3', reverse 5'-TGG GGTACACAGCATAAAATA-CATC-3'; *Hdac7*, forward 5'-AACTTCGGCAACTTCTCAATAA-3', reverse 5'-GGGTGTGCTGCTACTACTGGG-3'; *Hdac8*, forward 5'-ATGCCACCTCCA CACTG-3', reverse 5'-CTTGCA-TGATGCCACCCCTC-3'; *Hdac9*, forward 5'-ATGCCTGTGG TGG-ATCCTGT-3', reverse 5'-AGAGGAGGAAGCTGCTGCTC-3'; *Hdac10*, forward 5'-TGG CACCGCTATGAGCAT-3', reverse 5'-GACACCAGCACCAACTCAGG-3'; *Hdac11*, forward 5'-GGCAGCGAAGGTAACATCTA-3', reverse 5'-CACATCCTCTT-ACCCCTGTG-3'; *Gja1*, forward 5'-GAGAGCCGAACCTCTCCT-TT-3', reverse 5'-TGGAGTAGGCTTGGACCTTG-3'; *Gja5*, forward 5'-CAGAGCCTGAAGAAGCCAAC-3', reverse 5'-GCAAC-CAGGCTGAATG GTAT-3'; *Cdhc2*, forward 5'-TATGTGATGAC-GGTCACTGC-3', reverse 5'-GAAAGGCCAT AAGTGGGATT-3'; and *Gapdh*, forward 5'-TGCCACTCAGAAGACTGTGG-3', reverse 5'-AGGAATGGGAGTTGCTGTTG-3'.

#### WESTERN BLOTTING

Ventricular myocytes were cultured at high density in 35 mm culture dishes for 4 days in 3 ml of BrDU/M199 media, harvested, and lysed with 1% Triton X-100 extraction buffer (50 mM Tris pH 8.0, 150 mM NaCl, 0.02% sodium azide, 1.0 mM phenylmethanesulfonylfluoride (PMSF), 1 µg/ml aprotinin, 1% Triton X-100, 1 mM Na<sub>3</sub>VO<sub>4</sub>, 50 mM sodium fluoride (NaF) with protease inhibitors (Roche). One dish from each primary culture served as a control sample and a second dish was treated with either TSA or VOR for 24 h prior to harvesting. Sonicated samples (three 30-s pulses) were incubated on ice for 30 min, centrifuged at 14,000 rpm (10 min at 4°C), transferred to new tubes, and protein concentrations were measured using the coomassie blue protein assay (Bio-Rad). Fifteen micrograms of total protein/sample was heated (55°C) and loaded onto an SDS-PAGE (sodium dodecyl sulfate polyacrylamide gel electrophoresis) gel and electrophoresed for 90 min at 110 V in 4× NuPAGE sampling buffer and 10× NuPAGE reducing buffer (Invitrogen). The protein gels were transferred onto polyvinylidene difluoride (PVDF) membranes for 90 min at 4°C (110 V), blocked with 5% non-fat milk for 1 h at room temperature, and incubated overnight at 4°C with Cx43, Ncad, α-tubulin, or α-actin primary antibodies in phosphate-buffered saline (PBS) with Tween 20 (PBS-T) with 5% non-fat milk. The membranes were washed 5 min × 4 with PBS-T, incubated with horseradish peroxidase (HRP)-labeled secondary antibody (1:5000) at room temperature in PBS-T with 5% non-fat milk for 30 min, washed again 5 min × 4 with PBS-T, and developed using the ECL™ Western Blot Detection Reagents (Bio-Rad). The image was taken by exposing light sensitive films (Midsci) to the PVDF membrane and developing the films using the Auto-developer (Kodak) in a dark room. The density of the bands was quantified using ImageJ. Primary antibodies used in this study include rabbit anti-Cx43 (Chemicon), mouse anti-Cx43 (Zymed), mouse anti-Cx40 (Zymed), mouse anti-α-tubulin (Sigma), rabbit anti-acetylated-α-tubulin (Enzo), mouse anti-α-actin antibody (Sigma), rabbit anti-acetylated lysine antibody (Abcam), and Ncad

(Sigma). pSer-specific Cx43 antibodies were produced as previously described including rabbit anti-pS255 (Santa Cruz; Sirnes et al., 2009), rabbit anti-pS262 (Santa Cruz; Sriskuldee et al., 2006), rabbit anti-pS279/282 (Santa Cruz; Arnold et al., 2005; Solan and Lampe, 2008), rabbit anti-pS325/328/330 (Lampe et al., 2006), rabbit anti-pS365 (Solan et al., 2007), rabbit anti-pS368 (R&D; Solan et al., 2007), and rabbit anti-pS373 (P. D. Lampe, personal communication, manuscript in preparation).

#### IMMUNOSTAINING, IMAGING, AND ANALYSIS

Ventricular myocytes were cultured at high density on 10 µg/ml fibronectin-coated 18 mm diameter glass coverslips in 12-well plates with 1 ml of BrDU/M199 media for 4 days. Control and TSA- or VOR-treated myocyte cultures were fixed with 4% paraformaldehyde, permeabilized with 1% Triton X-100 in PBS, and blocked by the addition of 2% goat serum at room temperature for 15 min. Primary mouse anti-Cx43 antibody (Invitrogen) was diluted 1:500 in 2% goat serum/1% Triton X-100/PBS, 250 µl added to each coverslip, and incubated overnight at 4°C according to previously published procedures (Lin et al., 2010). Coverslips were washed three times with PBS, incubated in the dark with Alexa Fluor546 goat anti-mouse secondary antibodies (1:1500 dilution) for 3 h at room temperature, washed three times with PBS, stained with 4',6-diamidino-2-phenylindole (DAPI) for 5–10 min, rinsed twice with PBS and finally with distilled, deionized water and mounted onto glass slides with the Prolong Gold antifade medium (Invitrogen).

Confocal fluorescence micrographs for the TSA experiments were acquired using the Zeiss LSM 510 META confocal microscope core facility and viewed using the Zeiss LSM Image Browser V3.5 software. Confocal fluorescence micrographs for the VOR experiments were acquired using the Perkin-Elmer UltraView Vox dual spinning disk confocal microscope facility located in the Cell and Developmental Biology Department of State University of New York Upstate Medical University. Optical sections were acquired with 0.5 µm resolution ( $\approx 1\lambda$  since fluorophore is Alexa Fluor546 (nm) and one section from the center of the Z-stack representing the highest GJ area was exported as a TIF file, imported into ImageJ, converted to 8-bit red color, background subtracted using the fluorescence intensity histogram (10–25%, average  $\approx 10\%$ ), and converted to black-on-white bitmaps of Cx43 immunofluorescent regions in ImageJ based on the methods of Hunter et al. (2005). Only confluent ventricular cell monolayer regions were imaged and five regions per coverslip were sampled. Each experiment was repeated three times, resulting in 15 analyzed images per [TSA] or [VOR] experiment. GJ area was expressed as the % of immunolocalized Cx43 area per total area of each image and each experiment was performed on cultured glass coverslips treated with 0, 20, 50, or 100 nM TSA or 0, 0.2, 0.5, 1.0, or 5.0 µM VOR prepared from the same ventricular myocyte primary culture.

#### CHROMATIN IMMUNOPRECIPITATION ASSAY

Ventricular myocytes were seeded at high density in 35 mm culture dishes, cultured for 4 days in BrDU/M199 media, treated overnight with 2 µM VOR, fixed with 1% formaldehyde, collected and stored in –80°C for chromatin immunoprecipitation (ChIP) assay. ChIP assays were carried out using the ChIP Assay kit (Millipore Catalog

#17-295) according to the manufacturer's procedures. The cells were lysed with SDS lysis buffer (1% SDS, 10 mM ethylenediaminetetraacetic acid (EDTA), 50 mM Tris, 1 mM PMSF, 1 µg/ml aprotinin, and 1 µg/ml pepstatin A, pH 8.1, sonicated to shear the chromatin DNA to 400–1000 bp, diluted 10-fold in ChIP dilution buffer (0.01% SDS, 1.1% Triton X-100, 1.2 mM EDTA, 16.7 mM Tris-HCl, 167 mM NaCl, 1 mM PMSF, 1 µg/ml aprotinin, and 1 µg/ml pepstatin A, pH 8.1), and pre-cleared with 50 µl protein A agarose/salmon sperm DNA (supplied with the kit) for 30 min at 4°C. The pre-cleared cell lysis was immunoprecipitated with 10 µg of rabbit anti-HDAC1 antibody (Enzo Life Sciences), rabbit anti-HDAC2 antibody (Enzo Life Sciences), rabbit anti-Sp1 antibody (Santa Cruz), rabbit anti-RNA Pol II antibody (Santa Cruz), or normal rabbit IgG (Sigma) overnight (4°C). 50 µl of protein A agarose/salmon sperm DNA was added the next morning and incubated for 1 h at 4°C. The agarose was pelleted by centrifugation at 1000 rpm for 1 min, the pellets were washed with low salt buffer (0.1% SDS, 1% Triton X-100, 2 mM EDTA, 20 mM Tris-HCl, 150 mM NaCl pH 8.1), high salt buffer (0.1% SDS, 1% Triton X-100, 2 mM EDTA, 20 mM Tris-HCl, 500 mM NaCl pH 8.1), LiCl buffer (0.25 M LiCl, 1% IGEPAL-CA630, 1% deoxycholic acid, 1 mM EDTA, 10 mM Tris, pH 8.1), and TE buffer (1 mM EDTA, 10 mM Tris, pH 8.0). The agarose/protein/DNA complex was eluted with 250 µl elution buffer (0.1 M NaHCO<sub>3</sub>, 1% SDS), at room temperature for 15 min and the elution step was repeated once. Twenty microliters of 5 mol/l NaCl was added to the 500 µl elution solution, and heated for 4 h at 65°C to reverse protein-DNA crosslinks. Ten microliters of 0.5 M EDTA, 20 µl of 1 M Tris-HCl (pH 6.5), and 2 µl of 10 mg/ml proteinase K was added to the elution solution and incubated 1 h at 45°C. The DNA in the elution was purified with GENECLEAN® II Kit (MP) and tested by PCR amplification for 26 cycles. Primers specific for the mouse Cx43 promoter were: primer set-1 of 5'-TCCCCATGCCACCAGCCTT-3' (sense) and 5'-TGCAGGGCTGTGACTCCTCA-3' (antisense) corresponding to nucleotide positions –511 to –492 bp and –225 to –206 bp; primer set-2 of 5'-TGAGGAGTCACAGCCCCGCA-3' (sense) and 5'-TCCCTCACGCCCTTCCCCCA-3' (antisense) corresponding to nucleotide positions –225 to –206 bp and +65 to +84 bp, with respect to the transcription start site of Cx43.

## ELECTROPHYSIOLOGY

Dual whole cell patch clamp experiments were performed on isolated ventricular myocyte cell pairs as previously described (Lin et al., 2005, 2008a, 2010). The initial GJ conductance ( $g_j$ ) was measured immediately upon establishment of the dual whole cell patch clamp configuration from the linear slope portion of a 2-s –100 to +100 mV transjunctional voltage ( $V_j$ ) ramp. Ventricular GJ channel activity was recorded during 30-s  $V_j$  pulses ranging from ±20 to ±60 mV. All points current amplitude histograms were produced from each junctional current ( $I_j$ ) recording and fitted with Gaussian distributions in Origin7.5 to determine the mean GJ channel current ( $i_j$ ) amplitudes. The linear slope of the cumulative  $i_j$ - $V_j$  relationship from three experiments was used to calculate the single GJ channel conductance ( $\gamma_j$ ). Steady state  $V_j$ -dependent inactivation (increasing  $V_j$ ) and recovery (decreasing  $V_j$ ) normalized junctional conductance–voltage

( $G_j$ - $V_j$ ) curves were obtained using a 200 ms/mV, ±120 mV voltage ramp protocol. Quantitative junctional voltage series resistance errors were corrected for each patch electrode by the expression (Veenstra, 2001):

$$g_j = \frac{-\Delta I_2}{V_1 - (I_1 \cdot R_{el1}) - V_2 + (I_2 \cdot R_{el2})}, \quad (1)$$

where  $V_1$  and  $V_2$  are the command potentials applied to cells 1 and 2,  $I_1$  and  $I_2$  are the corresponding whole cell currents,  $R_{el1}$  and  $R_{el2}$  are the corresponding whole cell patch electrode resistances, and  $-\Delta I_2$  is the change in  $I_2$  recorded with constant  $V_2$  during a voltage step applied to  $V_1$  ( $\Delta V_1$ ; Veenstra, 2001).  $I_j$  is assumed to originate from the  $\Delta V_1$  pulse with the same polarity, therefore  $I_j = I_2 - \Delta I_2$ . The resultant inactivation and recovery  $G_j$ - $V_j$  curves were fit with the Boltzmann equation:

$$G_j^{ss} = \left[ \frac{G_{max}^{ss} \cdot [\exp(A \cdot (V_j - V_{1/2}))] + G_{min}^{ss}}{1 + [\exp(A \cdot (V_j - V_{1/2}))]} \right], \quad (2)$$

where  $G_j^{ss} = g_j/g_{j,max}$ ,  $G_{max}^{ss}$  = the maximum value of  $g_j/g_{j,max} = 1$ ,  $G_{min}^{ss}$  = the minimum value of  $g_j/g_{j,max}$ ,  $A$  = the slope factor for the Boltzmann curve (= zF/RT at 20°C), and  $V_{1/2}$  = the half-inactivation voltage. The actual  $g_{j,max}$  value is determined from the linear slope conductance of the  $I_j$ - $V_j$  relationship for each experiment. The  $I_j$ - $V_j$  relationship is typically linear between ±10 and ±25 mV. Curve-fitting procedures were performed using Clampfit software (pClamp version 8.2, Axon Instruments, Inc.) and final graphs were prepared using Origin version 7.5 software (Origin-Lab Corporation, Northampton, MA, USA). Tetrodotoxin (30 µM TTX, Sigma) was added to the bath saline (mM: NaCl 142, KCl 1.3; CsCl 4, TEACl 2, MgSO<sub>4</sub> 0.8, NaH<sub>2</sub>PO<sub>4</sub> 0.9, CaCl<sub>2</sub> 1.8, dextrose 5.5, 4-(2-hydroxyethyl)-1-piperazineethanesulfonic acid (HEPES) 10, pH 7.4 with 1 N NaOH) of each dish to prevent activation of the sodium current during the dual whole cell patch clamp experiments. Patch pipettes measuring 4–5 MΩ before patch break were filled with a KCl internal pipette solution (IPS KCl, in mM: KCl, 140; MgCl<sub>2</sub>, 1.0; CaCl<sub>2</sub>, 3.0; 1,2 bis(*o*-amino-phenoxy)ethane-*N,N,N',N'*-tetra acetic acid (BAPTA), 5.0; HEPES, 25; pH titrated to 7.4 using 1 N KOH). The osmolarity of both external and internal solutions was adjusted to 310 mOsm/l.

## STATISTICAL ANALYSIS

One-way ANOVA was performed on multiple experimental datasets in Origin7.5 with the Levene's test for equal variance and the Bonferroni means comparison test. Actual *p* values are shown in the figures when statistically significant (*p* < 0.05).

## RESULTS

### HDAC EXPRESSION AND INHIBITION IN CULTURED VENTRICULAR MYOCYTES

The relative expression of all 11 HDACs in neonatal mouse ventricular myocyte cultures was examined by RT-PCR. HDAC mRNA levels ranged from 1 to 16% relative to Cx43 mRNA levels (Figure 1A). Cx40 mRNA levels were 1.6 ± 0.7% (mean ± SEM) relative to Cx43, indicative of contributions from the ventricular conduction system and coronary endothelial cells. The

same relative HDAC mRNA expression pattern was found in atrial cardiomyocyte cultures wherein the Cx40 mRNA level was  $38.4 \pm 5.9\%$ , consistent with the contribution of Cx40 to atrial myocardial GJs (Figure 1A; Lin et al., 2010). TSA, the prototypical hydroxamic acid pan-HDACI, suppressed ventricular HDAC activity with apparent inhibitory equilibrium constants ( $K_1$ ) of 12 and 174 nM (Figure 1B). HeLa cells exogenously expressing Cx43 (stable HeLa-Cx43 cells) exhibited a single  $K_1$  of 510 nM. VOR, by comparison, inhibited ventricular cardiac HDAC activity with approximately 10-fold higher  $K_1$ s of 186 and 1440 nM (Figure 1C). HeLa-Cx43 cell inhibition by VOR also exhibited a dual affinity profile with  $K_1$ s of 300 nM and 2  $\mu$ M. Ventricular cardiomyocyte total HDAC activity declined to a minimum of 2–6% with TSA or VOR inhibition.

#### TRICHOSTATIN A AND VORINOSTAT AFFECT Cx43 mRNA AND PROTEIN EXPRESSION

Since protein acetylation is known to alter gene expression, we examined the effect of HDAC inhibition by TSA and VOR on Cx43 mRNA and protein expression levels by RT-PCR and western blot analyses. The lowest doses of TSA and VOR tested did not significantly change Cx43 mRNA expression, though further increases in [TSA] or [VOR] produced a progressive decline in Cx43 mRNA levels to a minimum of 13% relative to untreated control values (Figures 2A,B). One micromolar VOR reduced the Cx43 mRNA expression levels by 54%. The transcriptional effects of HDACI by TSA or VOR were verified at the translational level by western blot analysis of Cx43 (Figures 2C–F). Acetylated  $\alpha$ -tubulin levels increased with both TSA and VOR. Densitometry scans of three HDACI western blot experiments confirm a gradual dose-dependent reduction in the amount of Cx43 protein to a minimum of 5–12% of control levels by TSA and VOR. The recommended therapeutic dose of 1  $\mu$ M VOR reduced Cx43 protein levels by an average of  $60 \pm 3\%$ . Ncad mRNA and protein levels were reduced by  $\approx 30\%$  (Figures 3A,B; Kerr et al., 2010). This dose of VOR also reduced atrial cardiomyocyte Cx40 protein expression by  $64 \pm 6\%$  (Figures 3C,D). The Cx43 and Cx40 levels relative to the  $\alpha$ -tubulin loading controls were similar,  $1.26 \pm 0.30$  for Cx43 ( $n = 3$ , mean  $\pm$  SEM) and  $1.26 \pm 0.26$  for Cx40 ( $n = 4$ ). We further examined whether ventricular HDAC inhibition by 1  $\mu$ M VOR could affect the phosphorylation state of Cx43 using custom and commercially available pSer-specific Cx43 antibodies. Western blot analysis of seven identified Cx43 pSer sites revealed altered protein kinase-dependent Cx43 phosphorylation content relative to control levels. Since total Cx43 was downregulated by HDACI treatment, the phospho/total Cx43 ratios of the treated samples were normalized to the phospho/total ratios of the control samples to analyze the changes of pSer levels by VOR. The results indicated additional down-regulation of phosphorylation at S255 (pS255) by  $57.9 \pm 4.9\%$ . Conversely, the phosphorylation of S325/328/330 was upregulated by  $48.5 \pm 19.8\%$  in presence of 1  $\mu$ M VOR. The pS262, pS279/282, pS365, pS368, and pS373 levels were not significantly altered (Figures 4A,B).

#### HDACI ALTERS PROTEIN BINDING TO THE Cx43 PROMOTER REGION

To examine whether VOR induced repression of Cx43 (*Gja1*) gene expression by altering protein binding to the proximal promoter

of Cx43 in heart, ChIP assays were performed to examine the association of Sp1 (specificity protein 1) and RNA polymerase II (RNA Pol II) with the *Gja1* promoter. Up to 0.5 kb of the *Gja1* promoter containing one TATA and several GC boxes was examined by PCR using two sets of primers (Figure 5A). Primer set-1 specifically amplified the –511 to –206 bp and primer set-2 specifically recognized –225 to +65 bp of the *Gja1* promoter region. The results indicate that 2  $\mu$ M VOR decreased association of Sp1 and RNA Pol II with the Cx43 promoter (Figures 5B,C). *Gja1* promoter association with Sp1 was detected by primer set-1 while only primer set-2 detected RNA Pol II association. The association of HDAC1 and 2 with the *Gja1* promoter was increased by VOR treatment (Figures 5D,E). The expression of HDAC1, 2, Sp1, and RNA Pol II were not altered by VOR.

#### HDACI DECREASES Cx43 GAP JUNCTION AREA

Since TSA and VOR reduced Cx43 mRNA and protein levels, we examined whether HDACI also affected the formation of Cx43 GJs between cultured ventricular myocytes. Cx43 was immunolocalized in cardiomyocytes after culturing on glass coverslips for 3 days and overnight TSA or VOR treatments. Five micrographs of confluent fields from each coverslip were imaged on a confocal microscope and the Cx43 immunolabeled area was quantified using ImageJ (Figures 6A–H). Each [TSA] and [VOR] experiment was repeated three times and the maximum % of Cx43 GJ area was tabulated for each HDACI concentration. Again, the lowest dose of TSA or VOR produced a modest increase in Cx43 GJ area followed by a progressive dose-dependent decrease in GJ area to a minimum of 25% relative to control values (Figures 6I,J).

#### FUNCTIONAL CONSEQUENCES OF HDAC INHIBITION ON VENTRICULAR GAP JUNCTIONS

##### *Gap junction conductance*

To examine whether the downregulation of Cx43 expression and GJ assembly by pan-HDACI translates into functional alterations of electrical coupling, the effects of TSA and VOR on functional Cx43-mediated GJ electrical coupling was studied in dual whole cell patch experiments of isolated ventricular myocyte cell pairs. The GJ conductance ( $g_j$ ) was measured at the onset of dual whole patch clamp recordings of junctional current ( $I_j$ ) in ventricular myocyte cultures treated overnight with TSA or VOR (Figures 6K,L). Increasing concentrations of TSA produced a progressive decline in electrical coupling between ventricular cardiomyocytes that achieved statistical significance above 35 nM. VOR produced a slight increase in electrical coupling at 200 nM followed by a gradual decrease in ventricular  $g_j$ . The recommended therapeutic dose of 1  $\mu$ M VOR reduced ventricular  $g_j$  by 20% ( $p < 0.05$ ). Maximal HDAC inhibition by TSA ( $\geq 100$  nM) or VOR (5  $\mu$ M) produced significant 40–50% decreases in ventricular  $g_j$ .

##### *Transjunctional voltage gating*

We previously described the steady state transjunctional voltage ( $V_j$ ) gating of ventricular GJs using continuous 24 s,  $\pm 120$  mV  $V_j$  staircase and reported the phenomenon of a higher slope  $g_j$  during the return (declining) phase of the  $V_j$  staircase termed facilitation (Figure 7A; Lin et al., 2005). TSA reduced the amplitude of this increased  $G_j$  during the recovery phase in a

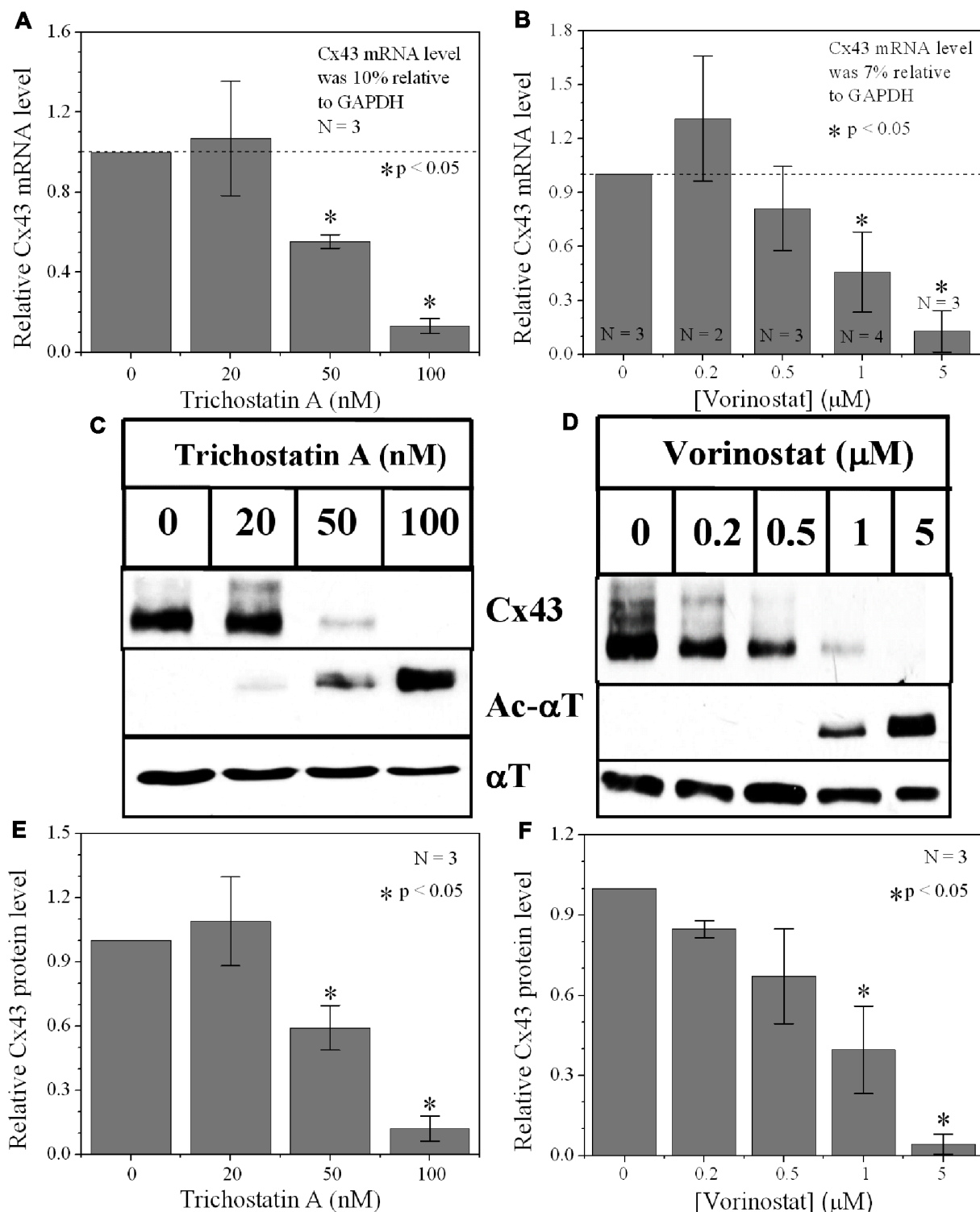


**FIGURE 2 | Dose-dependent alteration of Cx43 expression by pan-HDACI.**  
**(A,B)** Real-time PCR results of Cx43 mRNA expression levels after overnight inhibition by increasing [TSA] (A) and [VOR] (B) relative to control (untreated) values. Experiments were performed in triplicate and the lowest dose of both pan-HDACI produced an insignificant increase in average Cx43 mRNA levels and a significant reduction in Cx43 mRNA levels at the highest doses. **(C,D)** Representative Cx43 western blots of

ventricular cell lysates from TSA (C) or VOR (D) treated cultures. **(E,F)** Statistical analysis of the protein densitometry scans from three experiments reveal significant dose-dependent reductions in Cx43 protein content. Cx43 protein levels were normalized to a control sample from each experiment with  $\alpha$ -tubulin ( $\alpha$ T) expression used as an internal control and acetylated  $\alpha$ -tubulin (Ac- $\alpha$ T) as a positive indicator for HDAC inhibition.

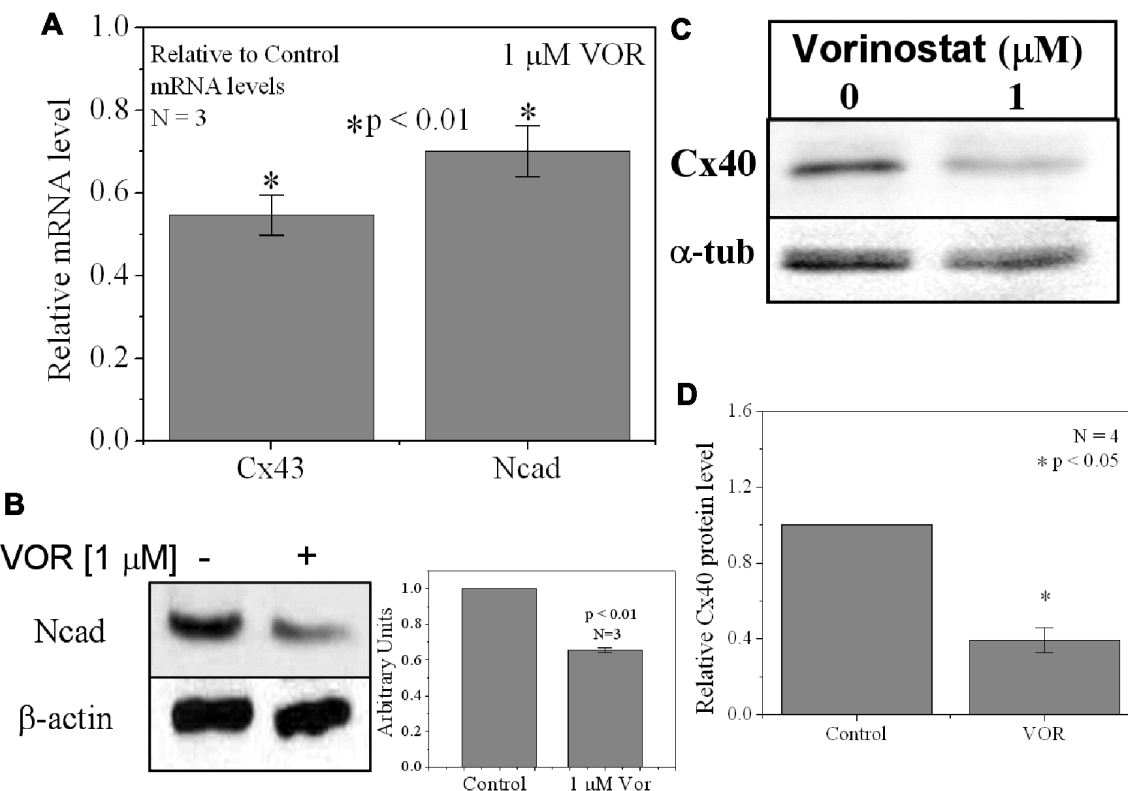


**FIGURE 3 | Reduction of Cx40 and N-cadherin expression by HDACi.** (A) Overnight (18 h) treatment with 1 μM VOR significantly reduced Cx43 and N-cadherin mRNA levels by  $45 \pm 5$  and  $30 \pm 6\%$ , respectively. Experimental mean values were statistically different from control values ( $p$ -value  $< 0.05$ , one-way ANOVA). (B) Immunoblots were also performed for Ncad and β-actin (internal control). Total Ncad levels from three experiments were decreased by 1 μM VOR relative to control (untreated)

samples. (C) Representative Cx40 western blots of atrial cell lysates from control or 1 μM VOR-treated cultures. (D) Statistical analysis of the protein densitometry scans from four experiments reveals a significant reduction in Cx40 protein content. Cx40 protein levels were normalized to a control sample from each experiment with α-tubulin expression used as an internal control and acetylated α-tubulin (Ac-αT) as a positive indicator for HDAC inhibition.

dose-dependent manner, eliminating any increase in recovery  $G_j$  when  $[TSA] \geq 100$  nM (Figures 7B,C). VOR also abolished  $G_j$  facilitation in a dose-dependent manner (Figures 7G,H). TSA and VOR also slightly altered the  $V_{1/2}$ -dependent inactivation properties of ventricular GJs. TSA increased the half-inactivation voltage ( $V_{1/2}$ ) of the inactivation and recovery  $G_j$ - $V_j$  curves by 10–15 mV with a slight reduction in the  $V_j$ -insensitive  $G_j$  component ( $G_{min}$ ) from 0.40 to 0.25 (Table 1). VOR also shifted the  $V_{1/2}$  values outward by 5–10 mV. The kinetics of time-dependent inactivation were examined for varying [TSA] by exponentially fitting the  $I_j$  curves to determine the fast and slow decay time constants ( $\tau_{fast}$  and  $\tau_{slow}$ ; Figures 7D–F). The fast and slow inactivation on-rates ( $K_{fast}$  and  $K_{slow}$ ) were calculated using the equation  $K = (1 - P_{open})/\tau_{decay}$ . The  $K_{fast}$  and  $K_{slow}$  values increased exponentially every  $20.9 \pm 1.4$  or  $20.0 \pm 1.2$  mV, respectively, and were not altered by TSA. However, the amplitude of the  $K_{slow}$  inactivation component decreased progressively with increasing TSA concentrations.

#### Single gap junction channel conductance

From twenty 100-nM TSA ventricular cell pair recordings, single GJ channel currents could be resolved in only three poorly coupled

ventricular myocyte cell pairs. GJ channel current ( $i_j$ ) amplitudes corresponding to low (30–50 pS), intermediate (60–80 pS), and high (90–110 pS) channel conductance ( $\gamma_j$ ) states were observed in untreated cardiomyocyte cell pairs, consistent with previous observations for Cx43 and ventricular GJ channels (Moreno et al., 1994). In the three 100-nM TSA experiments, ventricular  $\gamma_j$  was reduced to 54 pS, corresponding to only the low  $\gamma_j$  state of Cx43 GJ channels. The 80 pS state was still evident in the presence of 5 μM VOR (Figure 8).

#### DISCUSSION

Our results show that the atrial and ventricular myocardial HDAC expression pattern is similar. Therefore, any differential effects of a particular HDACi on atrial or ventricular excitability and contractility will depend primarily on the expression of ion channels, transporter, junctional, and contractile proteins unique to the specialized regions of the mammalian heart. The cell-based HDAC activity assay also indicates that VOR inhibits total myocardial HDAC activity with two apparent affinities of approximately 200 nM and 1.4 μM (Figure 1C). The nanomolar higher capacity site falls within the recommended serum therapeutic range for VOR of  $\leq 1$  μM (400 mg/day) and likely corresponds to inhibition

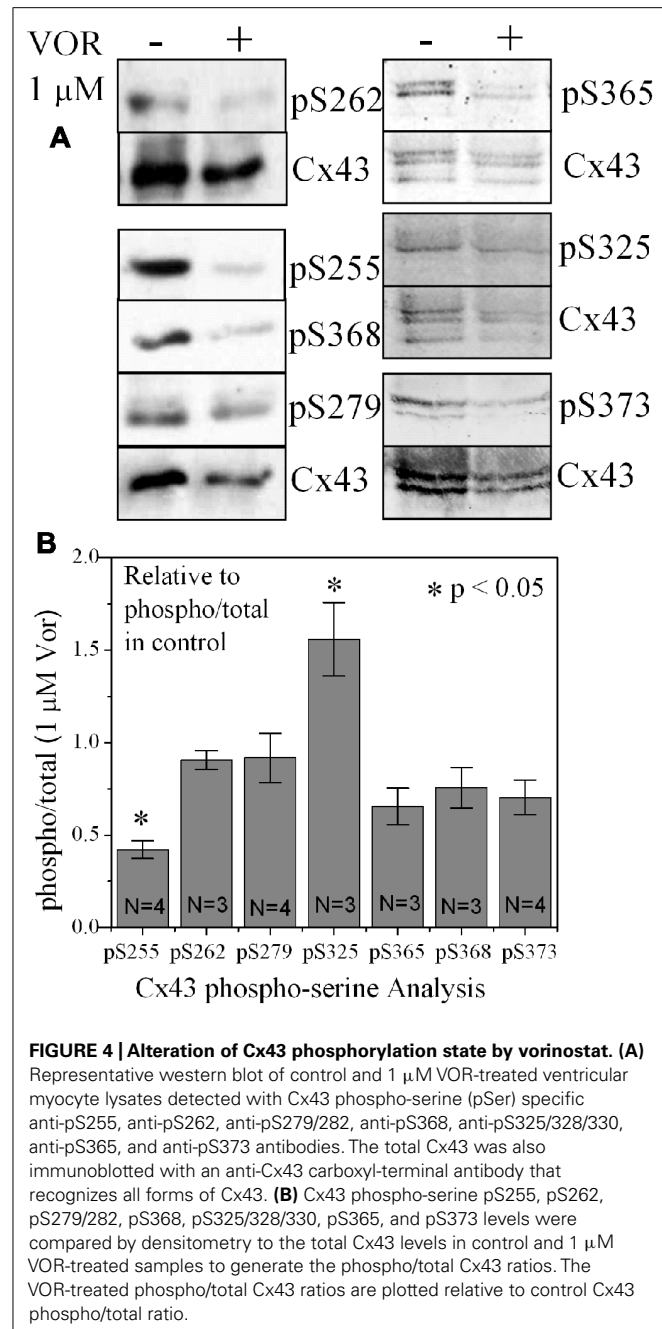


**FIGURE 4 | Alteration of Cx43 phosphorylation state by vorinostat. (A)** Representative western blot of control and 1  $\mu$ M VOR-treated ventricular myocyte lysates detected with Cx43 phospho-serine (pSer) specific anti-pS255, anti-pS262, anti-pS279/282, anti-pS368, anti-pS325/328/330, anti-pS365, and anti-pS373 antibodies. The total Cx43 was also immunoblotted with an anti-Cx43 carboxyl-terminal antibody that recognizes all forms of Cx43. **(B)** Cx43 phospho-serine pS255, pS262, pS279/282, pS368, pS325/328/330, pS365, and pS373 levels were compared by densitometry to the total Cx43 levels in control and 1  $\mu$ M VOR-treated samples to generate the phospho/total Cx43 ratios. The VOR-treated phospho/total Cx43 ratios are plotted relative to control Cx43 phospho/total ratio.

of the class I HDACs (HDAC1–3 and 8) and the class IIb HDAC6 (Bradner et al., 2010; Kerr et al., 2010). This is important because the reductions in ventricular Cx43 expression and electrical coupling observed in our experiments are not significant until the concentration of VOR meets or exceeds this 1  $\mu$ M therapeutic value. This dose of VOR lowered Ncad protein content by 33%, Cx43 protein content by approximately 50%, GJ area by 33%, and ventricular  $g_j$  by less than 20% (Figures 2, 3, and 6). The significant reduction in Ncad and functional Cx43 GJ expression may result from occupying the micromolar affinity HDAC site, which could correlate with inhibition of the class IIa HDACs (HDAC4,

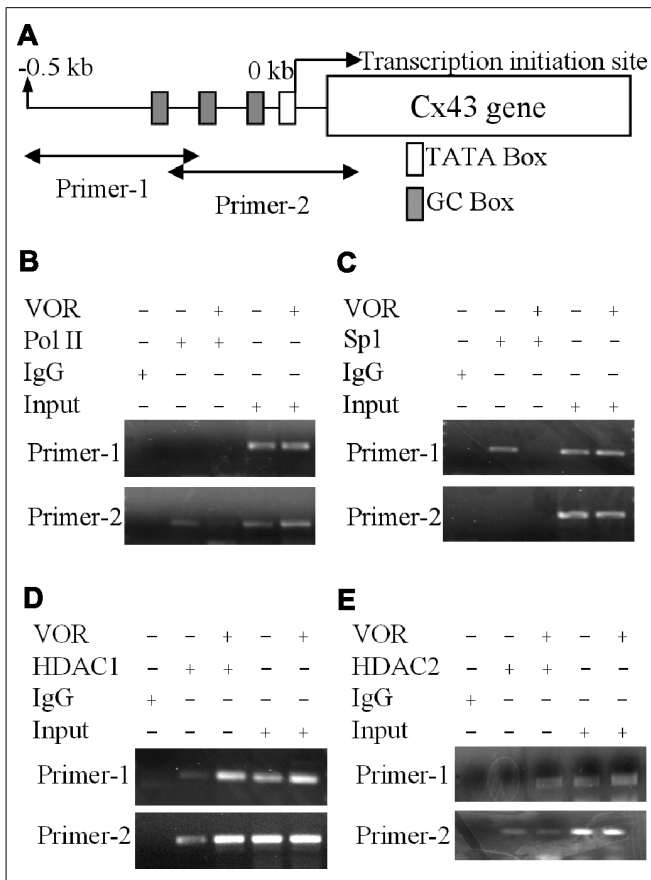


**FIGURE 5 | Alteration of Cx43 promoter associated proteins by vorinostat. (A)** Illustration of the Cx43 promoter region up to  $-0.5$  kb from the Cx43 gene (*Gja1*) transcription start site of Cx43 with TATA and GC boxes indicated. Two primer sets were designed from  $-511$  to  $-206$  and  $-225$  to  $+65$  bp of the Cx43 promoter region. **(B,C)** Chromatin immunoprecipitation assays illustrate the reduced binding of RNA polymerase II (RNA Pol II) and specific protein 1 (Sp1) to the promoter region of Cx43 after overnight exposure to 2  $\mu$ M VOR. **(D,E)** A chromatin immunoprecipitation assay was performed with rabbit IgG and rabbit anti-HDAC1 or anti-HDAC2 antibodies to assess the binding of HDAC1 (**D**) and HDAC2 (**E**) to the promoter region of the Cx43 gene (*Gja1*). Overnight treatment with 2  $\mu$ M VOR enhanced the association of HDAC1 and HDAC2 to the *Gja1* promoter.

5, 7, and 9) since the  $K_1$  of VOR for these HDACs is nearly 10-fold higher (Bradner et al., 2010). We intend to study the differential effects of specific class I, IIb, and IIa HDAC inhibition on myocardial expression and function using class-selective HDACIs like MS-275 or MGCD-0103, tubastatin, and MC-1568, respectively (Mai et al., 2005; Rasheed et al., 2007; Bradner et al., 2010; Butler et al., 2010).

These reductions in cardiac intercalated disk adhesion and communicating junctions may not affect conduction velocity or promote arrhythmias since a 50% global loss of Cx43 content minimally alters myocardial conduction velocity or the incidence of sustained ventricular tachycardias (Danik et al., 2004). However, heterogeneous loss of  $>80\%$  of Cx43 expression leads to ventricular systolic dysfunction and increased susceptibility to lethal ventricular arrhythmias (Gutstein et al., 2001). Chronic

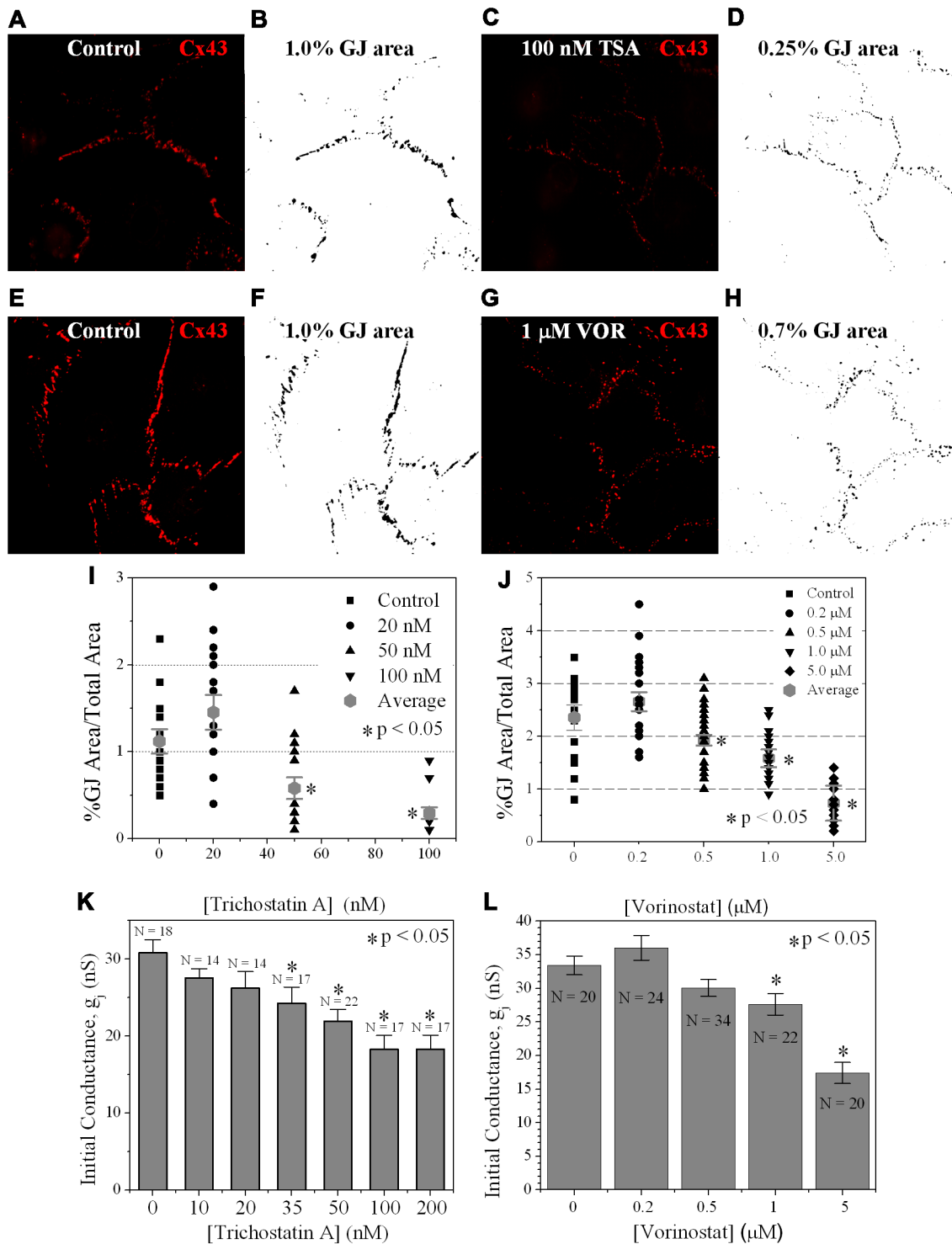


**FIGURE 6 | Measurement of Cx43 GJ area and ventricular electrical coupling.** **(A–H)** Representative confocal images of mouse primary anti-Cx43 and goat anti-mouse Alexa Fluor 546 secondary antibody immunolocalized Cx43 gap junction plaques from 4-day ventricular myocyte cultures (**A,C,E,G**) and their corresponding black-on-white bitmaps of the Cx43-positive pixels (**B,D,F,H**). The total GJ area was calculated relative to the total image area of the confluent monolayer cardiomyocyte cluster. Five clusters were imaged per coverslip and each experiment was repeated in triplicate for each [TSA]

and [VOR]. **(I,J)** Statistical analysis of the average Cx43 GJ area values ( $\pm$ SEM,  $n = 15$ ) at each pan-HDACI concentration revealed a significant decrease in GJ area for [TSA]  $\geq$  50 nM and [VOR]  $\geq$  1  $\mu$ M. **(K,L)** Initial gap junction conductance ( $g_j$ ) measurements, upon establishment of the dual whole cell patch clamp configuration, from numerous ( $n = 14$ –34) cell pairs revealed a dose-dependent maximum decrease in ventricular  $g_j$  of 40–50% by pan-HDACI. The decline in ventricular  $g_j$  was statistically significant for [TSA]  $\geq$  35 nM and [VOR]  $\geq$  1  $\mu$ M.

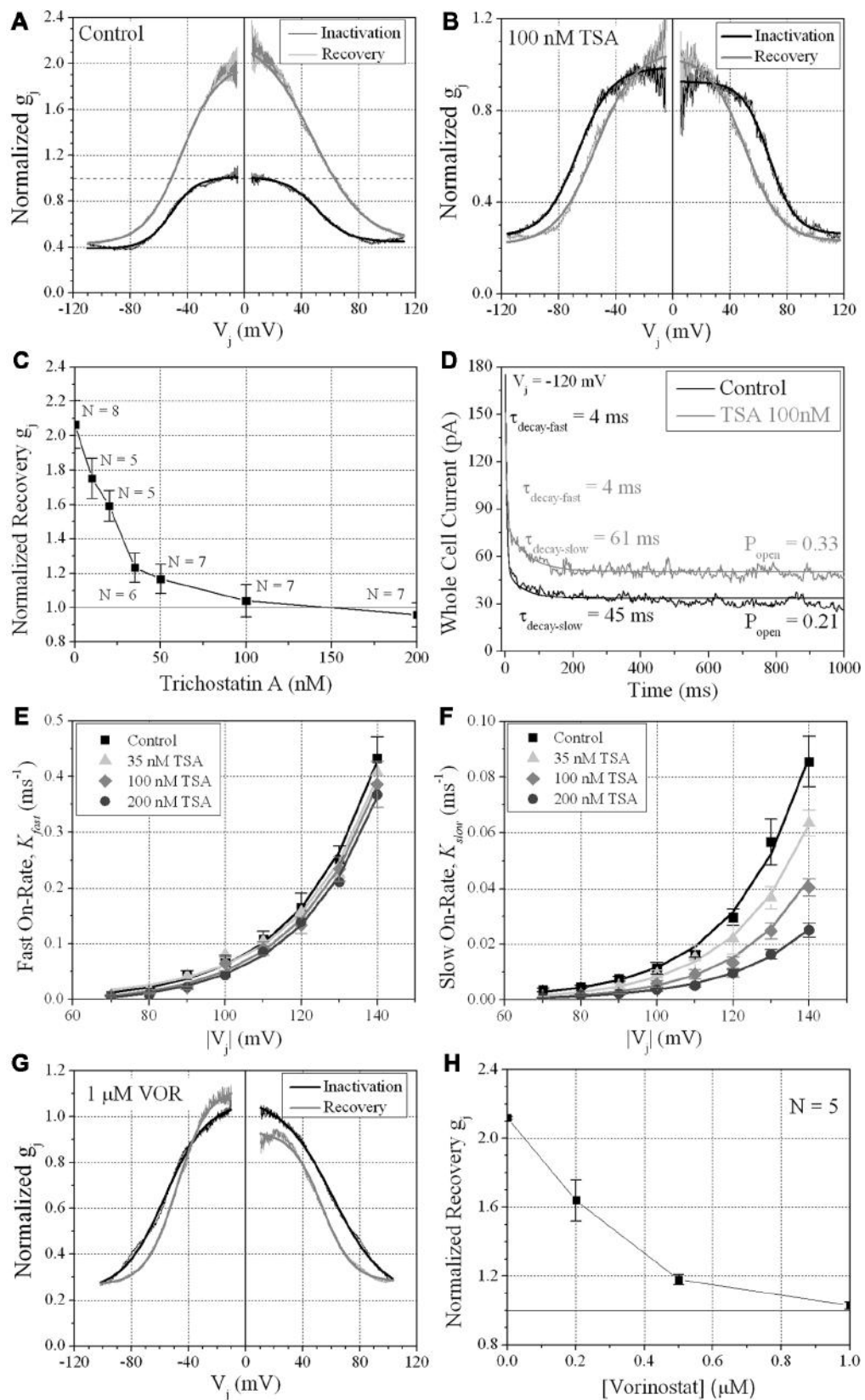


FIGURE 7 | Continued

**FIGURE 7 | Continued**

**V<sub>j</sub>-dependent gating of ventricular gap junctions during HDAC inhibition.** A 200 ms/mV V<sub>j</sub> ramp from 0 to  $\pm 120$  mV was applied to patch clamped ventricular myocyte pairs and V<sub>j</sub> was returned to 0 mV by ramp reversal to produce the normalized junctional conductance–voltage (G<sub>j</sub>–V<sub>j</sub>) inactivation and recovery curves. The black line represents the normalized g<sub>j</sub> during the increasing V<sub>j</sub> (inactivation) ramp and the gray line is the G<sub>j</sub>–V<sub>j</sub> curve obtained during the decreasing V<sub>j</sub> (recovery) ramp. The facilitated recovery of g<sub>j</sub> was observed as an increase in the normalized g<sub>j</sub> (G<sub>j</sub>) of the recovery curve relative to the initial slope g<sub>j</sub> of the ventricular gap junctions during the increasing (inactivation) phase of the V<sub>j</sub> ramp (inactivation curve normalized slope g<sub>j</sub> = 1.0). The smooth black and gray lines are Boltzmann equation fits of the ventricular G<sub>j</sub>–V<sub>j</sub> curves obtained from five to six experiments from control myocytes (**A**), 100 nM TSA-treated myocytes (**B**), or 1  $\mu$ M VOR (**G**). The parameters for the Boltzmann fits of the 100 nM TSA and 1  $\mu$ M VOR G<sub>j</sub>–V<sub>j</sub> inactivation and recovery curves are listed in **Table 1**. (**C**) The slope G<sub>j</sub> of the recovery G<sub>j</sub>–V<sub>j</sub> curves was increased in normal ventricular myocytes and abolished by TSA treatments in a dose-dependent manner. (**D**) The inactivation kinetics were determined in control and TSA-treated ventricular myocyte pairs by ensemble averaging the I<sub>j</sub> from 5 to 10 V<sub>j</sub> pulses from  $-70$  to  $-140$  mV. The ensemble averaged I<sub>j</sub> trace was fitted with a second-order decaying function and the fast and slow inactivation rates were calculated from the expression  $k_{on} = (1 - P_{open})/\tau_{decay}$ . One example is shown for a control (black line) and 100 nM TSA-treated (gray line) myocyte pair in response to a train of  $-120$  mV V<sub>j</sub> pulses. (**E,F**) The fast (**E**) and slow (**F**) on-rates for hypothesized inactivation particles were plotted relative to the absolute value of the V<sub>j</sub> pulses and fitted with first-order exponential increasing functions. The fast inactivation rates were not affected by TSA while the amplitude, but not the V<sub>j</sub>-dependence, of the slow inactivation rates were progressively reduced by increasing TSA concentrations. (**G**) The smooth black and gray lines are Boltzmann equation fits of the ventricular G<sub>j</sub>–V<sub>j</sub> curves obtained from five 1.0  $\mu$ M VOR-treated myocyte pairs (see **Table 1**). (**H**) The slope G<sub>j</sub> of the recovery G<sub>j</sub>–V<sub>j</sub> curves, increased under normal conditions, was abolished by VOR treatments in a dose-dependent manner.

heart failure (CHF) and myocardial infarction (MI) also reduces Cx43 content and remodels GJ connections, potentially predisposing the myocardium to reentrant arrhythmias (Luke and Saffitz, 1991; Kostin et al., 2003). There are no reports of QT interval prolongation or cardiac arrhythmias occurring with VOR (Rasheed et al., 2007), even with single dose administration of twice (i.e., 800 mg/day) the normal therapeutic dose of VOR in 24 patients with advanced malignancies (Munster et al., 2009). QT interval prolongation and associated risk for torsades de pointes (TdP) ventricular tachyarrhythmias were reported in clinical trials with two hydroxamic acid-derived HDACIs, LAQ-824 and LBH-589 (Rasheed et al., 2007). Romidepsin, a tricyclic peptide HDACI, has resulted in corrected QT (QTc) interval prolongation and sudden cardiac death from probable fatal ventricular arrhythmias (Shah et al., 2006; Rasheed et al., 2007). The mechanistic basis for these cardiac arrhythmias remains essentially unknown since preliminary studies suggest that human ether-a-go-go potassium channel (Kv11.1) protein (HERG) blockade develops only in the supra micromolar range for LBH-589 and VOR (Giles et al., 2006; Kerr et al., 2010).

In general, HDACI is thought to improve Cx43 GJ intercellular communication (GJIC) between cancer cells (Ogawa et al., 2005; Hernandez et al., 2006). However, HDACIs do not necessarily increase connexin expression and GJIC, owing to different HDACI activities and fundamental differences between immortalized cancer cell lines and primary cell cultures (e.g., hepatocytes, cardiomyocytes; Vinken et al., 2007). The TSA-induced

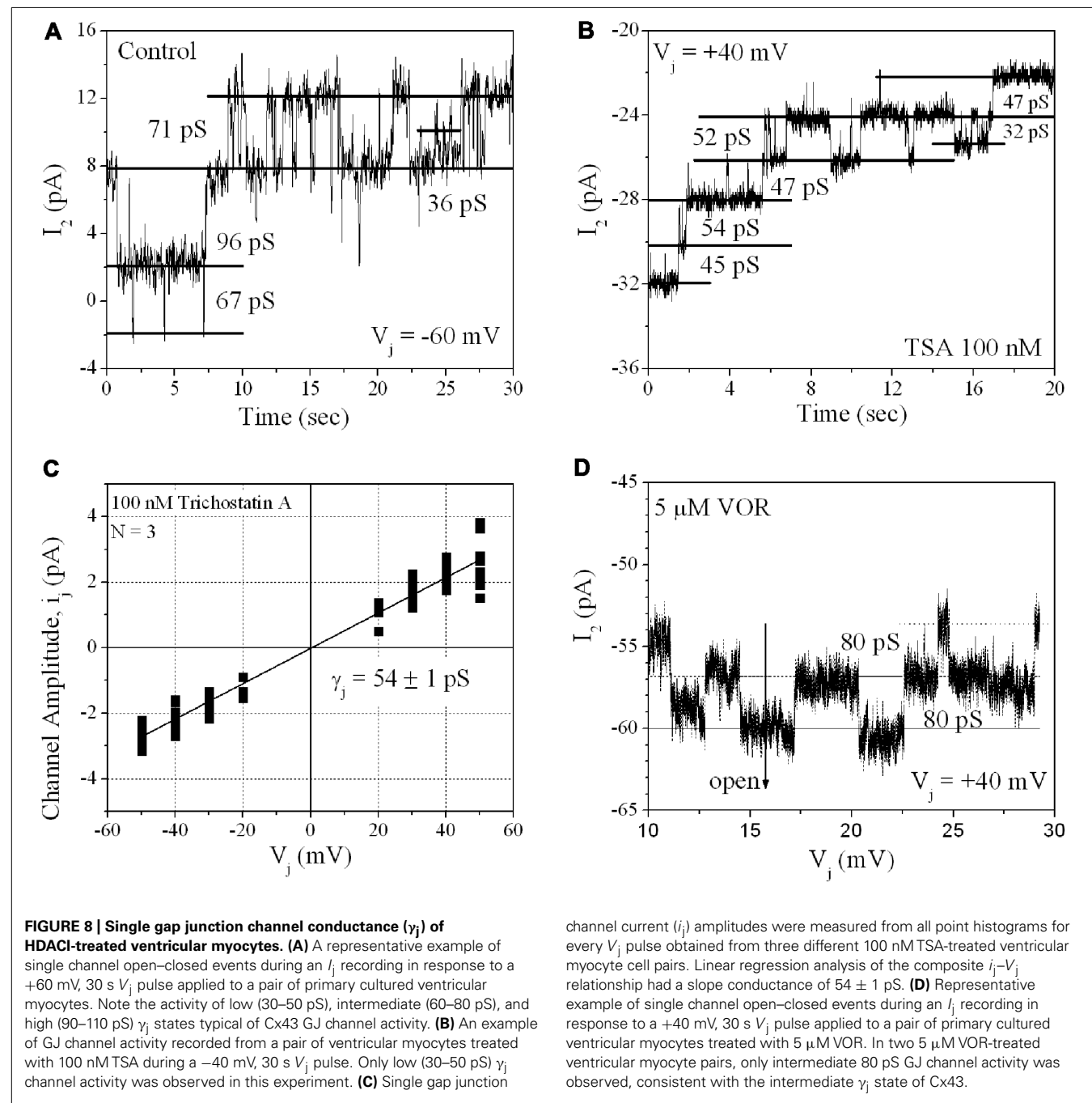
increased transcription of Cx43 (*Gja1*) gene expression requires positive cooperation between Ap1 and Sp1 elements and is associated with hyperacetylated HDAC4 within the 2.4 kb gene promoter region (Hernandez et al., 2006). We analyzed the proximal 500 bp of the *Gja1* gene promoter sequence via ChIP assay (**Figure 5**), inclusive of the Sp1 and four Ap1 sites, and found decreased Sp1 and RNA Pol II and increased HDAC1 and 2 association within this promoter region in the presence of 2  $\mu$ M VOR. Lower doses of VOR (e.g., 200 nM) were not tested. The altered RNA Pol II and HDAC1 and 2 associations with the *Gja1* gene promoter sequence were not previously described. The HAT P300/CBP associated factor (PCAF), and HDAC3, 4, and 5 reportedly co-localize with Cx43 in the cytosol (Colussi et al., 2011). Precise control of *Gja1* gene transcription by HDAC and HDACI activities requires further investigation using class-specific HDACIs and/or HDAC gene knockout or RNAi knockdown strategies. Again, class-specific HDAC inhibition with second generation HDACIs such as MGCD-0103 or MS-275, tubastatin, and MC-1568 will further delineate the effects of HDACI on *Gja1* gene expression. Preliminary results from our laboratory with sodium phenylbutyrate, a low affinity HDACI with class I/IIa activities, conversely showed an increase in Cx43 protein expression (data not shown). Mice with germline deletion of the class IIa/b HDACs 4–10 are viable while class I HDAC1–3 knockout mice are embryonic lethal and require conditional knockout strategies to be studied further. The impact of pan- and class-selective HDACI or HDAC gene deletion/knockdown on connexin expression should be studied in primary tissues to understand the effects of these emerging HDACI clinical therapies on normal physiology (e.g., cardiac electrophysiology) in addition to the therapeutics effects under pathophysiological conditions in cancerous and other diseased tissues.

Colussi et al. (2010, 2011) did not directly compare the Cx43 expression levels in wt mouse hearts treated with VOR for 96 h although Cx43 levels were reportedly unchanged in wt or mdx mouse hearts. Our *in vitro* results indicate that TSA and VOR first produce a negligible change in Cx43 expression and function followed by a progressive diminution of Cx43 (and Cx40) expression and GJIC with increasing concentrations of pan-HDACI. Increased protein acetylation associated with the mdx mouse or induced by HDACI treatment of wt mice correlated with Cx43 dissociation from cardiac intercalated disk proteins (e.g., ZO-1, Ncad) and lateralization (Colussi et al., 2010, 2011). Cx43 lateralization occurs during ischemia and is associated with dephosphorylation of Cx43, particularly S325/328/330 and S364/365 sites (Lampe et al., 2006; Solan et al., 2007; Solan and Lampe, 2009), and is thought to represent functional GJ downregulation. Colussi et al. (2011) demonstrated that Cx43 is acetylated and that c-Src-dependent Y265 phosphorylation is increased while S255 and S262 phosphorylation of Cx43 is decreased in mdx mouse hearts. They did not examine the effects of VOR on wt hearts. Phosphorylation of Cx43 S262 has been associated with p34<sup>cdc42</sup>, protein kinase C (PKC), mitogen-activated protein kinase (MAPK), and v-Src kinase activity (Solan and Lampe, 2005). Our results indicate that VOR increases phosphorylated S325/328/330 and decreases phosphorylated S255 content while decreasing total ventricular Cx43

**Table 1 |***V<sub>j</sub>-gating properties of ventricular gap junctions.*

Parameter*	G <sub>j,max</sub> (-V <sub>j</sub> )	G <sub>j,min</sub> (-V <sub>j</sub> )	V <sub>½</sub> (mV)	z (q)	G <sub>j,max</sub> (+V <sub>j</sub> )	G <sub>j,min</sub> (+V <sub>j</sub> )	V <sub>½</sub> (mV)	z (q)	Correlation coefficient
Inactivation control ( <i>n</i> = 5)	1.011 ± 0.002	0.387 ± 0.001	-51.4 ± 0.1	-2.80 ± 0.03	1.011 ± 0.002	0.445 ± 0.001	+50.9 ± 0.1	+2.28 ± 0.02	0.98
Inactivation TSA ( <i>n</i> = 6)	0.987 ± 0.001	0.252 ± 0.002	-66.7 ± 0.1	-2.13 ± 0.02	0.926 ± 0.002	0.262 ± 0.002	+67.5 ± 0.1	+2.73 ± 0.04	0.97
Inactivation VOR ( <i>n</i> = 5)	1.064 ± 0.002	0.240 ± 0.003	-56.5 ± 0.1	-1.71 ± 0.02	1.088 ± 0.002	0.216 ± 0.003	+60.9 ± 0.1	+1.40 ± 0.01	0.96
Recovery control ( <i>n</i> = 5)	1.995 ± 0.005	0.427 ± 0.002	-44.3 ± 0.1	-1.97 ± 0.02	2.242 ± 0.009	0.451 ± 0.005	+47.9 ± 0.2	+1.38 ± 0.02	0.99
Recovery TSA ( <i>n</i> = 6)	1.058 ± 0.003	0.216 ± 0.002	-54.4 ± 0.2	-1.81 ± 0.02	1.037 ± 0.003	0.230 ± 0.002	+50.7 ± 0.1	+2.00 ± 0.02	0.98
Recovery VOR ( <i>n</i> = 5)	1.127 ± 0.002	0.267 ± 0.001	-48.1 ± 0.1	-2.30 ± 0.02	0.936 ± 0.002	0.281 ± 0.002	+53.5 ± 0.1	+2.36 ± 0.02	0.96
									0.97

\*Parameters were determined by curve-fitting the G<sub>j</sub>-V<sub>j</sub> curves with Eq. 2.



expression (Figure 4). Cx43 Y265 phosphorylation was not examined in our study and should be considered since Y265, S255, S262, and S368 phosphorylation downregulate while S325/328/330 and S364/365 phosphorylation increase Cx43 GJ function (Lampe et al., 2006; Solan et al., 2007; Solan and Lampe, 2009). Cancer cells may downregulate Cx43 GJIC by reducing expression and/or c-Src and MAPK phosphorylation of Cx43 and altering the phosphorylation state of Cx43 is another mechanism by which HDACI may improve GJIC in malignant tissues.

Direct acetylation may also alter the localization of Cx43 since a triple K-to-Q acetyl-mimetic mutant of Cx43 was predominantly

maintained in the cytoplasm whereas the K-to-A acetylation-resistant mutant Cx43 readily formed GJ plaques of unknown function (Colussi et al., 2011). We are presently studying the biophysical GJ gating and channel properties of the putative Cx43 K9, K234, and K264 acetyl-mimetic and -resistant mutations, individually and in combination, to determine the possible effects of Cx43 N<sup>e</sup>-lysine acetylation on Cx43 GJ formation and function. Our ventricular myocyte patch clamp experiments revealed concentration-dependent decreases in functional GJ coupling and altered  $V_j$ -dependent gating properties with TSA and VOR (Figure 7; Table 1). Ventricular  $\gamma_j$  was reduced only by high doses

of TSA (**Figure 8**), perhaps because of the higher potency TSA for class IIa inhibition relative to VOR (Bradner et al., 2010). The pan-HDACI-induced decrease in ventricular  $g_j$  probably results from the decreased Cx43 expression and GJ area, which results in a reduced number of GJ channels ( $N$ ), since the channel open probability ( $P_o$ ) was only slightly affected by the changes in  $V_j$ -dependent gating.  $\gamma_j$  was reduced only by high doses of TSA, and  $g_j = N \cdot P_o \cdot \gamma_j$ . We hypothesize that the acetylation-induced changes in  $\gamma_j$  and  $V_j$ -gating may be due to direct acetylation of Cx43 amino-terminal (K9) and carboxyl-terminal (K234, K264) lysine residues since these cytoplasmic domains have been implicated in these respective GJ channel functions (Moreno et al., 2002; Musa et al., 2004). Post-translational acetylation may affect the Cx43 half-life since lysine ubiquitination is a major degradation pathway for Cx43 GJIC (Kjenseth et al., 2010).

Limitations of the present study include the lack of correlative *in vivo* Cx43 expression and GJ localization results, not normalizing the immunolabeled Cx43 GJ area to cell membrane area by co-staining with fluorescently conjugated wheat germ agglutinin, and no assessment of pan-HDACI effects on myocardial conduction velocity or susceptibility to arrhythmias. Our supply of VOR for these initial functional GJ studies was restricted to *in vitro* use only by the terms of the MTA agreement. Future HDACI studies will include *in vivo* expression and electrocardiogram parameter (e.g., heart rate, QT interval) monitoring. *In vitro* conduction velocity measurements were not possible because we do not presently have access to a multi-electrode array (MEA) system. We hope to provide functional correlates like conduction velocity and the occurrence of spontaneous ventricular contractions, tachycardias, or arrhythmias in future investigations.

## REFERENCES

- Arnold, J. M., Phipps, M. W., Chen, J., and Phipps, J. (2005). Cellular sublocalization of Cx43 and the establishment of functional coupling in IMR-32 neuroblastoma cells. *Mol. Carcinog.* 42, 159–169.
- Bradner, J. E., West, N., Grachan, M. L., Greenberg, E. F., Haggarty, S. J., Warnow, T., et al. (2010). Chemical phylogenetics of histone deacetylases. *Nat. Chem. Biol.* 6, 238–243.
- Butler, K. V., Kalin, J., Brochier, C., Vistoli, G., Langley, B., and Kozikowski, A. P. (2010). Rational design and simple chemistry yield a superior, neuroprotective HDAC6 inhibitor, tubastatin A. *J. Am. Chem. Soc.* 132, 10842–10846.
- Colussi, C., Berni, R., Rosati, J., Straino, S., Vitale, S., Spallotta, F., et al. (2010). The histone deacetylase inhibitor suberoylanilide hydroxamic acid reduces cardiac arrhythmias in dystrophic mice. *Cardiovasc. Res.* 87, 73–82.
- Colussi, C., Rosati, J., Straino, S., Spallotta, F., Berni, R., Stilli, D., et al. (2011). N<sup>ε</sup>-lysine acetylation determines dissociation from gap junctions and lateralization of connexin 43 in normal and dystrophic heart. *Proc. Natl. Acad. Sci. U.S.A.* 108, 2795–2800.
- Danik, S. B., Liu, F., Zhang, J., Suk, H. J., Morley, G. E., Fishman, G. I., et al. (2004). Modulation of cardiac gap junction expression and arrhythmic susceptibility. *Circ. Res.* 95, 1035–1041.
- Giles, F., Fischer, T., Cortes, J., Garcia-Manero, G., Beck, J., Ravandi, F., et al. (2006). A phase I study of intravenous LBH589, a novel cinnamycin hydroxamic acid analogue histone deacetylase inhibitor, in patients with refractory hematologic malignancies. *Clin. Cancer Res.* 12, 4628–4635.
- Gupta, M. P., Samant, S. A., Smith, S. H., and Shroff, S. G. (2008). HDAC4 and PCAF bind to cardiac sarcomeres and play a role in regulating myofilament contractile activity. *J. Biol. Chem.* 283, 10135–10146.
- Gutstein, D. E., Morley, G. E., Vaidya, D., Liu, F., Chen, F. L., Stuhmann, H., et al. (2001). Heterogeneous expression of gap junction channels in the heart leads to conduction defects and ventricular dysfunction. *Circulation* 104, 1194–1199.
- Haberland, M., Montgomery, R. L., and Olsen, E. N. (2009). The many roles of histone deacetylases in development and physiology: implications for disease and therapy. *Nat. Rev. Genet.* 10, 32–42.
- Hernandez, M., Shao, Q., Yang, X.-J., Luh, S.-P., Kandouz, M., Batist, G., et al. (2006). A histone deacetylation-dependent mechanism for transcriptional repression of the gap junction gene Cx43 in prostate cancer cells. *Prostate* 66, 1151–1161.
- Hertzberg, E. L., and Spektor, A. (2004). Acetylation: a novel and important connexin modification with connexin-specific effects. *Mol. Biol. Cell* 15(Suppl.), Abstract #1024.
- Hubbert, C., Guardiola, A., Shao, R., Kawaguchi, Y., Ito, A., Nixon, A., et al. (2002). HDAC6 is a microtubule-associated deacetylase. *Nature* 417, 455–458.
- Hunter, A. W., Barker, R. J., Zhu, C., and Gourdie, R. G. (2005). Zonula occludens-1 alters connexin43 gap junction size and organization by influencing channel accretion. *Mol. Biol. Cell* 16, 5686–5698.
- Kazantsev, A. G., and Thompson, L. M. (2008). Therapeutic application of histone deacetylase inhibitors for central nervous system disorders. *Nat. Rev. Drug Discov.* 7, 854–868.
- Kerr, J. S., Galloway, S., Lagrutta, A., Armstrong, M., Miller, T., Richon, V. M., et al. (2010). Nonclinical safety assessment of the histone deacetylase inhibitor vorinostat. *Int. J. Toxicol.* 29, 3–19.
- Kjenseth, A., Fykerud, T., Rivedal, E., and Leithe, E. (2010). Regulation of gap junction intercellular communication by the ubiquitin system. *Cell. Signal.* 22, 1267–1273.
- Kostin, S., Rieger, M., Dammer, S., Hein, S., Richter, M., Klövekorn, W. P., et al. (2003). Gap junction remodeling and altered connexin43 expression in the failing heart. *Mol. Cell. Biochem.* 242, 135–144.
- Kouzarides, T. (2000). Acetylation: a regulatory modification to rival phosphorylation? *EMBO J.* 19, 1176–1179.
- Lampe, P. D., Cooper, C. D., King, T. J., and Burt, J. M. (2006). Analysis of phosphorylation of connexin43 at S325/S328/S330 in normoxic and ischemic heart. *J. Cell Biol.* 119, 3435–3442.

In conclusion, the present study demonstrates, for the first time, that pan-HDAC inhibition produces dose-dependent reductions in *Gja1* transcription, Cx43 protein content, Cx43 pSer content, Cx43 GJ area, and functional electrical coupling in normal mammalian ventricular myocardium with lesser effects on  $V_j$ -dependent gating and  $\gamma_j$  properties. These inhibitory effects on ventricular  $g_j$  correlate with VOR inhibition of myocardial HDAC activity in the micromolar range and suggest inhibition of class IIa HDACs in combination with class I and IIb HDACs may be responsible for these potentially adverse effects. VOR therapy is not associated with the induction of cardiac arrhythmias observed in clinical trials with three different pan-HDACIs, but these results suggest that more potent pan-HDAC inhibitory profiles may be more likely to cause adverse cardiac effects, including reduced myocardial electrical communication, that may predispose the heart to potentially fatal arrhythmias. Further investigations of class-selective HDACIs are necessary to understand the underlying mechanisms for arrhythmogenic adverse cardiac effects and improved cardiac safety profiles for this emerging class of novel therapeutics with diverse beneficial clinical indications.

## ACKNOWLEDGMENTS

We thank Dr. Steve Taffet, Department of Microbiology and Immunology, and Wanda Coombs, Department of Pharmacology, for helpful methodological western blot, real-time PCR, and ChIP assay discussions. This project was supported by NIH grant HL-042220 to Richard D. Veenstra and GM55632 to Paul D. Lampe.

- Lin, X., Crye, M., and Veenstra, R. D. (2003). Regulation of connexin43 gap junctional conductance by ventricular action potentials. *Circ. Res.* 93, e63–e73.
- Lin, X., Gemel, J., Beyer, E. C., and Veenstra, R. D. (2005). A dynamic model for ventricular junctional conductance during the cardiac action potential. *Am. J. Physiol. Heart Circ. Physiol.* 288, H1113–H1123.
- Lin, X., Zemlin, C., Hennan, J., Petersen, J. S., and Veenstra, R. D. (2008a). Enhancement of ventricular gap junction coupling by rotigaptide. *Cardiovasc. Res.* 79, 416–426.
- Lin, X., Gemel, J., Beyer, E. C., and Veenstra, R. D. (2008b). Histone deacetylase inhibition reduces gap junction coupling. *Mol. Biol. Cell* 19(Suppl.), Abstract #1680.
- Lin, X., Gemel, J., Glass, A., Zemlin, C. W., Beyer, E. C., and Veenstra, R. D. (2010). Connexin40 and connexin43 determine gating properties of atrial gap junction channels. *J. Mol. Cell. Cardiol.* 48, 238–245.
- Little, G. H., Bai, Y., Williams, T., and Poizat, C. (2007). Nuclear calcium/calmodulin-dependent protein kinase II $\delta$  preferentially transmits signals to histone deacetylase 4 in cardiac cells. *J. Biol. Chem.* 282, 7219–7231.
- Luke, R. A., and Saffitz, J. E. (1991). Remodeling of ventricular conduction pathways in healed canine infarct border zones. *J. Clin. Invest.* 87, 1594–1602.
- Mai, A., Massa, S., Pezzi, R., Simeoni, S., Rotili, D., Nebbiosi, A., et al. (2005). Class II (IIa)-selective histone deacetylase inhibitors. I. Synthesis and biological evaluation of novel (aryloxopropenyl)pyrrolyl hydroxyamides. *J. Med. Chem.* 48, 3344–3353.
- Marks, P. A., and Breslow, R. (2007). Dimethyl sulfoxide to vorinostat: development of this histone deacetylase inhibitor as an anticancer drug. *Nat. Biotechnol.* 25, 84–90.
- McKinsey, T. A. (2011). Isoform-selective HDAC inhibitors: closing in on translational medicine for the heart. *J. Mol. Cell. Cardiol.* 51, 491–496.
- McKinsey, T. A. (2012). Therapeutic potentials for HDAC inhibitors in the heart. *Annu. Rev. Pharmacol. Toxicol.* 52, 303–319.
- McKinsey, T. A., Zhang, C.-L., Lu, J., and Olson, E. N. (2000). Signal-dependent nuclear export of a histone deacetylase regulates muscle differentiation. *Nature* 408, 106–111.
- Moreno, A. P., Chanson, M., Elenes, S., Anumonwo, J., Scerri, I., Gu, H., et al. (2002). Role of the carboxyl terminal of connexin43 in transjunctional fast voltage gating. *Circ. Res.* 90, 450–457.
- Moreno, A. P., Sáez, J. C., Fishman, G. I., and Spray, D. C. (1994). Human connexin43 gap junction channels. Regulation of unitary conductances by phosphorylation. *Circ. Res.* 74, 1050–1057.
- Morrison, B. E., Majdzadeh, N., Zhang, X., Lyles, A., Bassel-Duby, R., Olson, E. N., et al. (2006). Neuroprotection by histone deacetylase-related protein. *Mol. Cell. Biol.* 26, 3550–3564.
- Munster, P. N., Rubin, E. H., Van Belle, S., Friedman, E., Patterson, J. K., Van Dyck, K., et al. (2009). A single supratherapeutic dose of vorinostat does not prolong QTc interval in patients with advanced cancer. *Clin. Cancer Res.* 15, 7077–7084.
- Musa, H., Fenn, E., Crye, M., Gemel, J., Beyer, E. C., and Veenstra, R. D. (2004). Amino terminal glutamate residues confer spermine sensitivity and affect voltage gating and channel conductance of rat connexin40 gap junctions. *J. Physiol.* 557, 863–878.
- Ogawa, T., Hayashi, T., Tokunou, M., Nakachi, K., Trosko, J. E., Chang, C. C., et al. (2005). Suberoylanilide hydroxamic acid enhances gap junctional intercellular communication via acetylation of histone containing connexin43 gene locus. *Cancer Res.* 65, 9771–9778.
- Piperno, G., LeDizet, M., and Chang, X. J. (1987). Microtubules containing acetylated  $\alpha$ -tubulin in mammalian cells. *J. Cell Biol.* 104, 289–302.
- Rasheed, W. K., Johnstone, R. W., and Price, H. M. (2007). Histone deacetylase inhibitors in cancer therapy. *Expert Opin. Invest. Drugs* 16, 659–678.
- Ryan, Q. (2009). FDA Review of Romidepsin (Istodax<sup>TM</sup>). *Efficacy and Safety in Single Arm Trials.* 2009 UCM192189. Available at: www.fda.gov
- Shah, M. H., Binkley, P., Chan, K., Xiao, J., Arbogast, D., Collamore, M., et al. (2006). Cardiotoxicity of histone deacetylase inhibitor depsipeptide in patients with metastatic neuroendocrine tumors. *Clin. Cancer Res.* 12, 3997–4003.
- Shakespear, M. R., Halili, M. A., Irvine, K. M., Fairlie, D. P., and Sweet, M. J. (2011). Histone deacetylases as regulators of inflammation and immunity. *Trends Immunol.* 32, 335–343.
- Sirnes, S., Kjeneseth, A., Leithe, E., and Rivedal, E. (2009). Interplay between PKC and the MAP kinase pathway in connexin43 phosphorylation and inhibition of gap junction intercellular communication. *Biochem. Biophys. Res. Commun.* 382, 41–45.
- Solan, J. L., and Lampe, P. D. (2005). Connexin phosphorylation as a regulatory event linked to gap junction channel assembly. *Biochim. Biophys. Acta* 1711, 154–163.
- Solan, J. L., and Lampe, P. D. (2008). Connexin43 in LA-25 cells with active v-src is phosphorylated on Y247, Y265, S262, S279/282, and S368 via multiple signaling pathways. *Cell Commun. Adhes.* 15, 75–84.
- Solan, J. L., and Lampe, P. D. (2009). Connexin43 phosphorylation: structural changes and biological effects. *Biochem. J.* 419, 261–272.
- Solan, J. L., Marquez-Rosado, L., Sorger, P. L., Thornton, P. J., Gafken, P. R., and Lampe, P. D. (2007). Phosphorylation at S365 is a gatekeeper event that changes the structure of Cx43 and prevents down-regulation by PKC. *J. Cell Biol.* 179, 1301–1309.
- Srisakuldee, W., Nickel, B. E., Fan-drich, R. R., Jiang, Z.-S., and Kardmi, E. (2006). Administration of FGF-2 to the heart stimulates connexin-43 phosphorylation at protein kinase C target sites. *Cell Commun. Adhes.* 13, 13–19.
- Veenstra, R. D. (2001). Voltage clamp limitations of dual whole-cell gap junction current and voltage recordings. I. Conductance measurements. *Biophys. J.* 80, 2231–2247.
- Vinken, M., Henkens, T., Snykers, S., Lukaszuk, A., Tourwé, D., Rogiers, V., et al. (2007). The novel histone deacetylase inhibitor 4-Me2N-BAVAH differentially affects cell junctions between primary hepatocytes. *Toxicology* 236, 92–102.
- Yang, X.-J., and Grégoire, S. (2007). Metabolism, cytoskeleton and cellular signaling in the grip of protein N<sup>ε</sup>- and O-acetylation. *EMBO Rep.* 8, 556–562.
- Yang, X.-J., and Seto, E. (2008). The Rpd3/Had1 family of lysine deacetylases: from bacteria and yeast to mice and men. *Nat. Rev. Mol. Cell Biol.* 9, 206–218.
- Yoshida, M., Kijima, M., Akita, M., and Beppu, T. (1990). Potent and specific inhibition of mammalian histone deacetylase both in vivo and in vitro by trichostatin A. *J. Biol. Chem.* 265, 17174–17179.
- Zhou, X., Richon, V. M., Wang, A. H., Yang, X. J., Rifkind, R. A., and Marks, P. A. (2000). Histone deacetylase 4 associates with extracellular signal-regulated kinases 1 and 2, and its cellular localization is regulated by oncogenic Ras. *Proc. Natl. Acad. Sci. U.S.A.* 97, 14329–14333.

**Conflict of Interest Statement:** The authors declare that the research was conducted in the absence of any commercial or financial relationships that could be construed as a potential conflict of interest.

**Received:** 14 February 2013; **paper pending published:** 04 March 2013; **accepted:** 27 March 2013; **published online:** 15 April 2013.

**Citation:** Xu Q, Lin X, Andrews L, Patel D, Lampe PD and Veenstra RD (2013) Histone deacetylase inhibition reduces cardiac connexin43 expression and gap junction communication. *Front. Pharmacol.* 4:44. doi: 10.3389/fphar.2013.00044

This article was submitted to Frontiers in Pharmacology of Ion Channels and Channelopathies, a specialty of Frontiers in Pharmacology.

Copyright © 2013 Xu, Lin, Andrews, Patel, Lampe and Veenstra. This is an open-access article distributed under the terms of the Creative Commons Attribution License, which permits use, distribution and reproduction in other forums, provided the original authors and source are credited and subject to any copyright notices concerning any third-party graphics etc.



# The effects of the histone deacetylase inhibitor 4-phenylbutyrate on gap junction conductance and permeability

**Joshua Kaufman, Chris Gordon, Roberto Bergamaschi, Hong Z. Wang, Ira S. Cohen, Virginijus Valiunas and Peter R. Brink\***

Department of Physiology and Biophysics, Stony Brook University, Stony Brook, NY, USA

**Edited by:**

Stefan Dhein, Universitätsklinik  
Leipzig Herz-Zentrum Leipzig GmbH,  
Germany

**Reviewed by:**

Stefan Dhein, Universitätsklinik  
Leipzig Herz-Zentrum Leipzig GmbH,  
Germany  
Klaus Willecke, University of Bonn,  
Germany

**\*Correspondence:**

Peter R. Brink, Department of  
Physiology and Biophysics, Stony  
Brook University, Stony Brook,  
NY 11794-8661, USA  
e-mail: peter.brink@stonybrook.edu

Longitudinal resistance is a key factor in determining cardiac action potential propagation. Action potential conduction velocity has been shown to be proportional to the square root of longitudinal resistance. A major determinant of longitudinal resistance in myocardium is the gap junction channel, comprised connexin proteins. Within the ventricular myocardium connexin43 (Cx43) is the dominantly expressed connexin. Reduced numbers of gap junction channels will result in an increase in longitudinal resistance creating the possibility of slowed conduction velocity while increased numbers of channels would potentially result in an increase in conduction velocity. We sought to determine if inhibition of histone deacetylase (HDAC) by 4-phenylbutyrate (4-PB), a known inhibitor of HDAC resulted in an increase in junctional conductance and permeability, which is not the result of changes in single channel unitary conductance. These experiments were performed using HEK-293 cells and HeLa cells stably transfected with Cx43. Following treatment with increasing concentrations of 4-PB up-regulation of Cx43 was observed via Western blot analysis. Junctional ( $g_j$ ) conductance and unitary single channel conductance were measured via whole-cell patch clamp. In addition intercellular transfer of lucifer yellow (LY) was determined by fluorescence microscopy. The data in this study indicate that 4-PB is able to enhance functional Cx43 gap junction coupling as indicated by LY dye transfer and multichannel and single channel data along with Western blot analysis. As a corollary, pharmacological agents such as 4-PB have the potential, by increasing intercellular coupling, to reduce the effect of ischemia. It remains to be seen whether drugs like 4-PB will be effective in preventing cardiac maladies.

**Keywords:** connexin43, 4-phenylbutyrate, gap junction, conductance, permeability

## INTRODUCTION

In multicellular organisms, the direct communication between adjacent cells is mediated via protein structures known as gap junctions (Sohl and Willecke, 2004). Connexins belong to a family of integral membrane proteins that form the underlying structure of gap junctions (Pointis, 2006). Various compounds including metabolites, ions, and fluorescent dyes can be exchanged from cell to cell via passive diffusion through these protein channels. Gap junctions consist of two smaller hemichannels called connexons, which are each composed of six smaller subunits called connexins. These protein channels are responsible for coordinating cellular activity in most biological systems including the myocardium, brain, and vascular endothelium.

The present study is focused on the role of connexin43 (Cx43) found predominantly in ventricular myocardium. In the myocardium, gap junctions create an electrical conduit between adjacent cells that is vital to normal cardiac function. The result is a synchronized propagating action potential and subsequent muscle contraction that starts in the sinoatrial (SA) node and ends within the cells of the ventricular myocardium. The conduction velocity of the cardiac action potential is linked to the longitudinal

resistance arising from cytoplasm and gap junctional membranes (Rudy, 2001; Donahue and Laurita, 2011) where conduction velocity,  $\theta$ , is inversely proportional to the square root of longitudinal resistance,  $R_l$  or  $(\theta \propto 1/\sqrt{R_l})$ ; Hodgkin and Huxley, 1952).

Under pathological conditions such as cardiac ischemia rapid changes in ionic homeostasis often cause irreparable cellular damage that can affect gap junction distribution within myocytes (Saffitz et al., 2007). Ischemia also induced uncoupling in myocytes and has been linked to the induction of reentrant currents seen during ventricular tachycardia (VT; Xing et al., 2003).

4-Phenylbutyrate (4-PB) belongs to a group of agents known as histone deacetylase (HDAC) inhibitors, and is currently used as a promising anti-cancer drug (Khan et al., 2007). In previous studies, the drug 4-PB has been reported to increase Cx43 expression (Asklund et al., 2004; Khan et al., 2007). HDACs are able to induce histone hyper-acetylation, altered chromatin structure, and modulations in gene expression that allow for increased mRNA transcription. By causing DNA to lose its affinity to histone proteins, exposure of portions of DNA allow for increased mRNA transcription that codes for increased Cx43 translation.

The aim of this study was to investigate the role of 4-PB with regards to its ability to induce increases in junctional conductance and correlate it with up-regulation of Cx43. It was hypothesized that those cells that were exposed to 4-PB would express increased levels of Cx43, as previously reported (Asklund et al., 2004; Khan et al., 2007) and result in an increased number of gap junction channels. Following treatment with increasing concentrations of 4-PB, up-regulation of Cx43 was observed via Western blot analysis consistent with previous studies (Asklund et al., 2004; Khan et al., 2007). Junctional conductance ( $g_j$ ) and intercellular transfer of lucifer yellow (LY) were measured via the whole cell patch clamp and by fluorescence microscopy. Demonstration that 4-PB can increase gap junction conductance and reduce longitudinal resistance allows for its potential use as an agent to reduce life-threatening conduction abnormalities, including reentrant ventricular arrhythmias.

## MATERIALS AND METHODS

### CELLS AND CULTURE CONDITIONS

Experiments were performed on HeLa cells stably transfected with mCx43 or HEK-293 cells that were endogenously expressing Cx43. Production and characterization of these cells, culture conditions, and staining methods for identification of specific cells have been described previously (Valiunas et al., 2000, 2001, 2004; Gemel et al., 2004). Experimental groups of cells were cultured with a medium containing 5 mM of 4-PB. Both the control and experimental groups of cells were plated onto glass coverslips 1–3 days prior to experimentation and were stored in a CO<sub>2</sub> incubator (5% CO<sub>2</sub>, 95% ambient air at 37°C). Electrophysiological measurements and dye flux studies were carried out on cell pairs and linear arrays triplets, respectively.

### ELECTROPHYSIOLOGICAL MEASUREMENTS

These experiments were preformed on HEK-293 and HeLa Cx43 cell pairs. A dual voltage clamp method and whole cell recording were used to control the membrane potential of both cells and to measure currents. For electrical recordings, glass coverslips with adherent cells were transferred to an experimental chamber mounted on the stage of an inverted microscope (Olympus IMT-2) equipped with epi-fluorescence imaging. The chamber was perfused at room temperature (RT; 22°C) with bath solution containing (in mM) NaCl, 150; KCl, 10; CaCl<sub>2</sub>, 2; HEPES, 5 (pH 7.4); glucose, 5; 2 mM CsCl and BaCl<sub>2</sub> were added. The patch pipettes were filled with solution containing (in mM) K<sup>+</sup> aspartate<sup>-</sup>, 120; NaCl, 10; MgATP, 3; HEPES, 5 (pH 7.2); EGTA, 10 ( $pCa \sim 8$ ); filtered through 0.22-μm pores. Patch pipettes were pulled from glass capillaries (code GC150F-10; Harvard Apparatus) with a horizontal puller (Sutter Instruments).

### DYE FLUX STUDIES

Experiments were performed on HeLa Cx43 cell triplets that were linearly coupled, using the direct dye injection technique. LY (Molecular Probes) was dissolved in the pipette solution to reach a concentration of 2 mmol/L. The donor cell was attached to a patch pipette connected to a micromanipulator (Narishige International), and an amplifier (Axopatch 200B) so that the membrane

potential could be observed to help obtain the whole cell patch. The use of the whole cell patch clamp was used to ensure delivery of dye intracellularly without leakage into the bathing solution. Fluorescent dye cell-to-cell spread was monitored using the digital charge-coupled diode (CCD) camera PixelFly (12-bit; The Cooke). LY concentration is directly proportional to fluorescence intensity. A picture of the cell triplet's fluorescence was taken every 60 s over a period of 10 min (CamWare v2.10). Fluorescence intensity of each cell was measured and recorded every minute. The background intensity was subtracted from the respective images.

### WESTERN BLOT

HEK-293 cells were collected from 35 mm plates by scraping. Cell suspensions were centrifuged at 14000 rpm at RT for 5 min (calculated  $g = 13148$ ), supernatants were removed, and the pellets were re-suspended in cold 1× phosphate-buffered saline (PBS). The pellets were centrifuged, supernatants removed, pellets then re-suspended in cold radio-immuno precipitation assay (RIPA) buffer (R0278, Sigma), protease inhibitor cocktail (AEBSF, aprotinin, bestatin hydrochloride, E-64, EDTA, leupeptin; P2714, Sigma), sodium orthovanadate (S-6508, Sigma), and PMSF (P-7626, Sigma). Samples were then centrifuged at 4°C, 14000 rpm ( $g = 13148$ ) for 10 min, supernatants were transferred to pre-chilled microtubes. Protein concentration of each sample was determined by the Bradford assay. Volumes containing 30 μg of total protein of each lysate were mixed with equal volumes of Laemmli sample buffer (161-0737, Bio-Rad) containing β-mercaptoethanol and boiled for 5 min at 95°C. All samples were centrifuged for 1 min at 14000 rpm ( $g = 13148$ ) at RT before being loaded on a SDS-polacrylamide gel (4% stacking gel, 10% separating gel). Prestained Protein Ladder (SM0671, Fermentas) or MagicMark XP Protein Standard (LC5602, Invitrogen) was loaded along with the samples. After separation by electrophoresis, proteins were transferred to Immobilon-P membrane (Millipore) by electrophoresis in tris-glycine/methanol buffer. Non-specific antibody binding was blocked for 1 h at RT in 5% Blotting Grade Blocker non-fat dry milk (Bio-Rad) dissolved in 1× TBST (mixture of Tris-buffered saline and Tween 20). A 43-kDa protein was probed for by incubating the membrane with the Anti-Connexin 43 antibody (C 6219, Sigma) at 1:8000 in 1% milk for 1 h at RT. After washing the membrane well the membrane was incubated with goat anti-rabbit IgG-HRP (sc-2004, Santa Cruz) at 1:10000 in 1% milk. After washing the secondary antibody was detected using SuperSignal West Femto Maximum Sensitivity Substrate (34095, Pierce) and images obtained by exposing the membrane to HyBlot CL Autoradiography Film (E3012, Denville Scientific).

As a loading control for normalization a 55 kDa protein was probed for by incubating the membrane for 1 h at RT with Anti-α Tubulin (sc-8035) at 1:1000 in 1% milk. After washing the membrane well with 1× TBST the membrane was incubated for 1 h at RT with goat anti-mouse IgG-HRP (sc-2005) at 1:10000 in 1% milk. After washing the membrane well with 1× TBST the secondary antibody was detected using SuperSignal West Femto Maximum Sensitivity Substrate (34095, Pierce) and images obtained by exposing the membrane to HyBlot CL

Autoradiography Film. ImageJ software (NIH) was used for analysis and quantification of Western blot data.

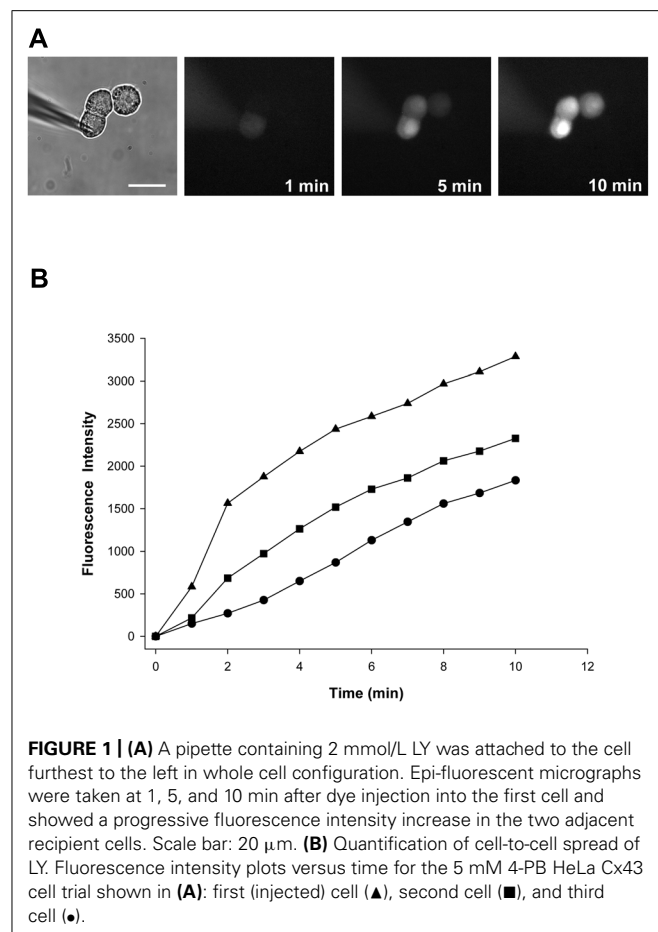
## SIGNAL RECORDING AND ANALYSIS

Voltage and current signals were recorded using patch clamp amplifiers (Axopatch 200b). The current signals were digitized with a 16-bit A/D-converter (Digidata 1322A; Molecular Devices) and stored with a personal computer. Data acquisition and analysis were performed with pClamp9 software (Molecular Devices). Curve fitting and statistical analyses were performed using SigmaPlot and SigmaStat, respectively (Jandel Scientific). The Mann–Whitney rank sum test was used for all cases unless otherwise noted,  $p < 0.05$  was considered to indicate significant changes. The results are presented as means  $\pm$  SEM.

## RESULTS

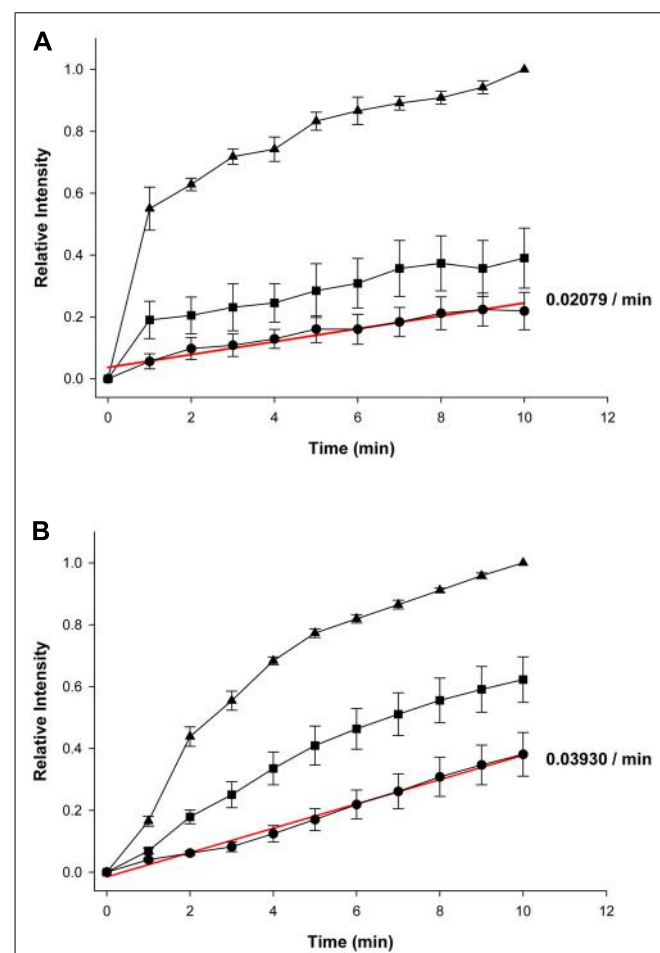
### LY DYE TRANSFER

We compared the LY dye spread in control cells and in cells exposed to 4-PB for 48 h. All trials were performed using HeLa Cx43 cell triplets. The amount of LY transfer was determined over time by epi-fluorescence microscopy. One such experiment is depicted in **Figure 1A**. As time elapses, the concentration of LY within a given cell increases due to diffusion of LY from electrode to the first source cell then to adjacent cell through gap junction channels. In this case, three time points are shown



(1, 5, and 10 min) after dye injection. Once a linearly coupled cell triplet was identified, the patch pipette containing LY was attached to the donor or source cell in the whole cell mode. Fluorescence intensity was subsequently determined at 1-min time intervals for each experiment in all cells of the triplet. **Figure 1B** shows fluorescence intensity data for the experiment seen in **Figure 1A**.

**Figures 2A,B** summarize the fluorescence intensity data obtained from six experiments in HeLa Cx43 control cells and four experiments with 5 mM 4-PB exposed cells, respectively. This data shows the relative fluorescent intensities for the first (source) cell ( $\blacktriangle$ ), second cell ( $\blacksquare$ ), and third cell ( $\bullet$ ). The maximum (steady state) intensity attained in the source cell represents the equivalent of the concentration in the pipette. Fluorescence intensity in each cell increased with time in both the control and 5 mM 4-PB exposed cells. The increases in fluorescence intensity were normalized in both groups of experiments. There was a marked difference, between control and 5 mM 4-PB cells, in dye transfer to the third



cell. In control cells, the third cell was able to reach  $\sim 21\%$  of the concentration reached by the loading cell compared to the  $\sim 39\%$ , which was achieved in the 5 mM 4-PB group (**Figures 2A,B**) in the same time period (10 min).

Because dye transfer between each adjacent cell occurred through Cx43 comprised gap junction channels, comparing the increase in LY fluorescence intensity in the third cell correlates to the amount of Cx43 channels present between adjacent cells. Linear fits of the third cell data to first-order regression (red lines, **Figures 2A,B**) yielded the following slopes:  $0.02079 \pm 0.001752/\text{min}$  and  $0.03930 \pm 0.001233/\text{min}$  for control and 4-PB treated cells, respectively. Comparison of the regression lines by analysis of covariance (GraphPad Prism) revealed that the difference between the slopes was significant ( $p < 0.001$ ).

These findings point to an increase of dye permeation upon exposure to 4-PB. Previous studies (Asklund et al., 2004; Khan et al., 2007) have also shown enhanced dye spread with exposure to 4-PB. This can be explained by an increase in the number of functioning channels resulting from increased expression. It is also possible that an increase in junctional conductance might arise from an increase of unitary channel conductance/permeability of Cx43 gap junction channels upon exposure to 5 mM 4-PB. In addition, changes in channel open probability would be predicted to affect junctional conductance. Does 4-PB affect any of these parameters?

#### MACROSCOPIC AND UNITARY CONDUCTANCES of Cx43 GAP JUNCTIONS

An important experiment was to determine the effect of 4-PB on macroscopic gap junction conductance. Gap junction currents in HEK-293 cells were recorded using the double whole cell patch clamp. **Figure 3A** shows the voltage protocol ( $V_1$ ,  $V_2$ ) and junctional currents recorded from control cells (left panel) and cells treated with 5 mM 4-PB (right panel). Starting from a holding voltage,  $V_h$  of 0 mV, bipolar pulses of 400 ms were delivered to the one cell of a pair to establish  $V_j$  gradient of identical amplitude with either polarity from  $\pm 10$  to  $\pm 110$  mV in increments of 20 mV (top panel, **Figure 3A**). In both groups junctional currents exhibited voltage dependent gating typical to Cx43 gap junction channels. The junctional conductances measured in control cells and cells treated with 4-PB are summarized in **Figure 3B**. The average junctional conductances in the control and 5 mM 4-PB groups were  $16.9 \pm 1.8 \text{ nS}$  ( $n = 32$ ) and  $22.7 \pm 1.7 \text{ nS}$  ( $n = 31$ ), respectively. These data indicate a statistically significant ( $p = 0.011$ ) increase in gap junction conductance between these two groups of cells. Previous experiments have suggested that increases in Cx43 expression and number of Cx43 comprised gap junctions are reflected by enhanced gap junctional conductance in double cell patch clamp experiments (Dhein, 2004).

The effect of 4-PB on unitary conductance of Cx43 gap junction channels was determined in selected pairs where only one or two operational channels were observable.

The pulse protocol involved an inversion of  $V_j$  polarity but of equal magnitude. **Figure 4A** shows single channel currents recorded from a 4-PB (5 mM) treated HeLa Cx43 cell pair (middle panel) and control HeLa Cx43 cell pair (lower panel). The

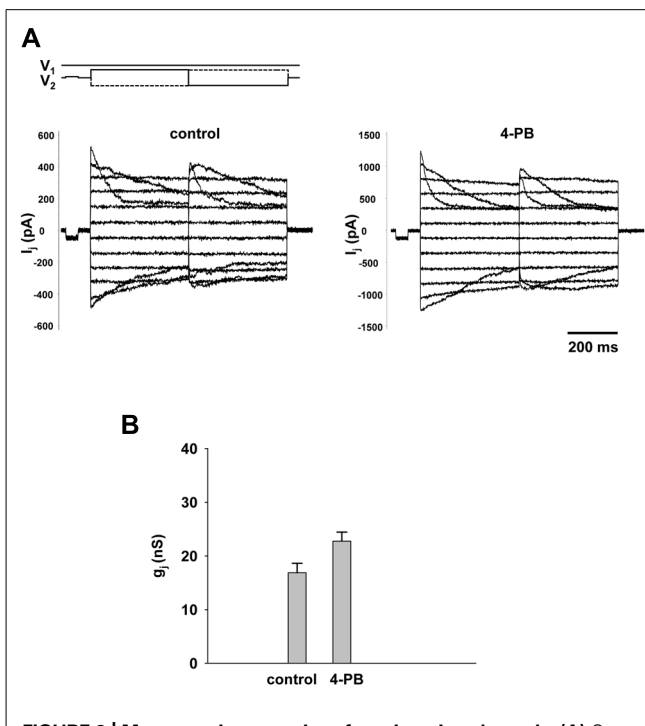
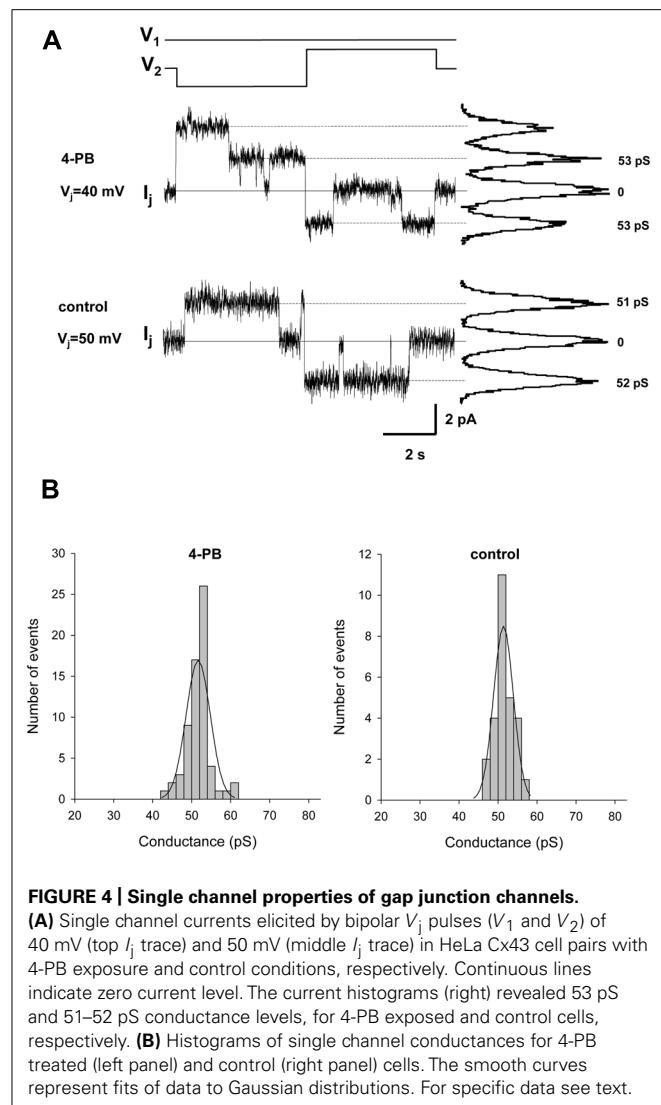


**FIGURE 3 | Macroscopic properties of gap junction channels. (A)** Gap junction currents ( $I_j$ ) elicited from HEK-293 cells by bipolar  $V_j$  pulses ( $V_1$  and  $V_2$ ; top panel) in control pairs (left panel) and cell pairs with 4-PB exposure (right panel). **(B)** Average of gap junction conductance for 4-PB treated ( $22.7 \pm 1.7 \text{ nS}$ ,  $n = 31$  cell pairs) and control ( $16.9 \pm 1.8 \text{ nS}$ ,  $n = 32$  cell pairs),  $p = 0.011$ .

histograms in **Figure 4B** summarizes the data collected from five HeLa Cx43 cell pairs treated with 5 mM 4-PB (left panel) and four control HeLa Cx43 cell pairs. Both data groups were fitted with a Gaussian (solid lines). The 4-PB treated cells yielded a mean value of  $51.7 \pm 3.1 \text{ pS}$  ( $n = 66$ ) and control cells revealed unitary conductance of  $51.4 \pm 2.5 \text{ pS}$  ( $n = 27$ ),  $p = 0.386$ . The unitary conductance values correspond to the previously reported Cx43 unitary conductances in  $120 \text{ mM K}^+$  aspartate<sup>-</sup> solution (Valiunas et al., 2002). These data indicate that 4-PB does not affect the unitary conductance of Cx43 gap junction channels. The long duration open times are similar for the records shown and are consistent with the notion that 4-PB did not significantly affect open probability (Brink et al., 1996).

#### WESTERN BLOT ANALYSIS

The gap junction protein Cx43 was detected in cell cultures by Western blot analysis using a commercially available, polyclonal, anti-Cx43 antibody (C 6219, Sigma). 4-PB was exposed to cells in concentrations of: 0, 1, 2, and 5 mM. The observed changes in the Cx43 expression are shown in **Figure 5**. The Western blots qualitatively demonstrate that the total Cx43 content in HEK-293 and HeLa Cx43 cells increases upon exposure of cells to 4-PB as compared to cells not exposed to 4-PB. The quantification of the Western blots data shown in **Figure 5A** using ImageJ software yielded the following: the amount of Cx43 with 5 mM 4-PB exposure was  $\sim 70\%$  greater in HEK-293 cells and  $\sim 40\%$  greater in HeLa Cx43 cells in comparison to control cells. Anti- $\alpha$  tubulin



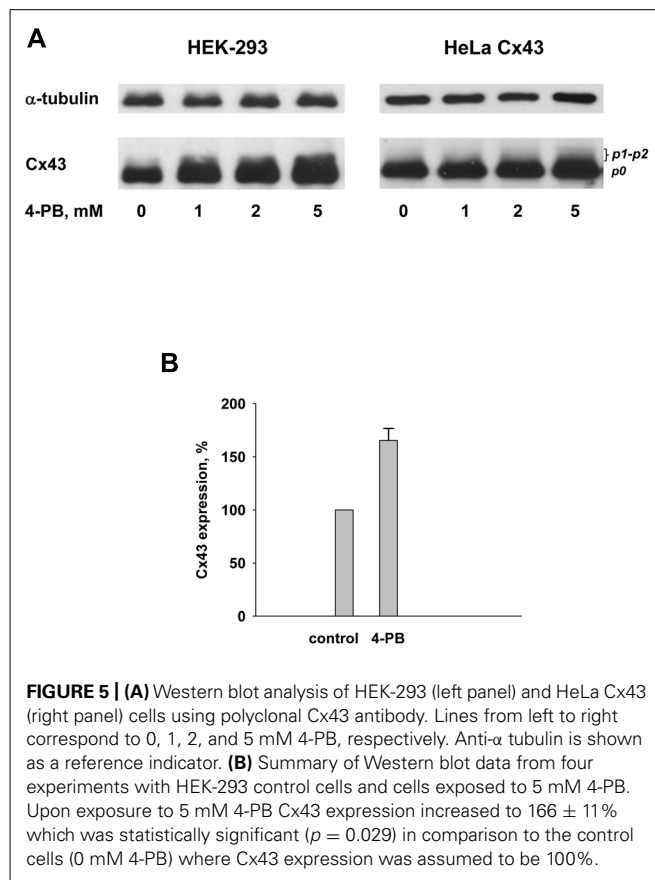
is shown, as a reference indicating that 4-PB was the modulated variable in each of the dose experiments. Both cell types showed increased expression of Cx43 with 4-PB. The data with 5 mM 4-PB from four different experiments with HEK-293 cells are summarized in **Figure 5B**. The 4-PB treated cells exhibited statistical significant increase ( $p = 0.029$ ) in the Cx43 expression in comparison to the control cells (166  $\pm$  11 versus 100%, respectively).

These data are consistent with previously published studies showing 4-PB increase the expression of Cx43 and manifest in Western blot (Asklund et al., 2004; Khan et al., 2007; Dovzhanskiy et al., 2012).

## DISCUSSION

### GAP JUNCTION COMMUNICATION

The increased rate of LY dye transfer and junctional conductance seen in cells exposed to 5 mM 4-PB for 24 h indicates that there are more Cx43 gap junction channels functioning as a consequence of increased connexin expression. The conclusion that



4-PB increased expression and subsequently resulted in more functional channels is supported by the fact the single channel unitary conductance is unaffected by 4-PB along with no apparent change in open probability (Brink et al., 1996). Consistent with this conclusion is the increased expression of Cx43 as demonstrated by Western blot analysis (Asklund et al., 2004; Khan et al., 2007). The data support the notion that 4-PB enhances transcription of Cx43 mRNA, which ultimately results in an increase in the number of active channels.

However, the 4-PB induced Cx43 expression or protein abundance and functional coupling do not necessarily follow a one to one relationship. In fact previous studies have provided evidence that expression exceeds the number of functional channels (Asklund et al., 2004; Khan et al., 2007). Another confounding factor is the number of functioning channels within a junctional plaque. Bukauskas et al. (2000) demonstrated that only a small fraction (~10%) of channels function at any instant in time with a given plaque.

Histone deacetylase inhibitors are potent regulators of gene expression through their effect on the acetylation of core histones (Asklund et al., 2004). Comparison of **Figures 2A,B** indicates that cells exposed to 5 mM 4-PB allowed for greater dye transfer across the three cell liner arrays so that the cell furthest away from the source cell was able to obtain a much greater level of LY dye over a 10-min time interval. There was a marked difference in dye distribution among the three adjacent cells when comparing the

control and 5 mM 4-PB groups. In the control cells, less dye was able to diffuse into the second and third cells. This is opposed to the cells exposed to 5 mM 4-PB, which exhibited a much more even distribution of dye across all three of the adjacent cells. This is consistent with a 4-PB induced increase in gap junctions resulting in a more effective diffusive pathway. In other words an increased number of Cx43 gap junction channels allows for better dye transfer between each of the cells. In the control cells, fewer Cx43 gap junction channels caused the dye to pool mostly in the first cell with a decreased transfer between cells. Hence, 4-PB was able to enhance functional intercellular communication. This finding has several implications, as LY can be substituted for any number of different drugs or second messenger molecules.

### CONNEXINS AND CARDIAC DYSFUNCTION

Currently, VT and ventricular fibrillation (VF) are two of the leading causes of death in the United States (Xing et al., 2003). Previous studies have provided evidence that abnormal functioning of gap junctions in cardiac tissue may play an important role in the induction of both VF and VT (Xing et al., 2003). In the heart, normal cardiac function relies on the electrical syncytium between adjacent cells in the myocardium. The spread of an electrical impulse is highly coordinated and any blockage that disrupts cell-to-cell communication has immediate and harmful consequences (Xing et al., 2003). A period of acute ischemia causes gap junction channels to close, leading to an uncoupling of all adjacent cells. Similarly, a prolonged period of ischemia is correlated to a non-uniform down regulation of Cx43 (Xing et al., 2003). The closure of gap junction channels combined with a decrease in Cx43 translation leaves the heart particularly susceptible to reentrant ventricular

circuits and subsequently, VT or VF. The disruption of impulse propagation through the ventricular myocardium causes an irregular contraction of the ventricles. Instead of the action potential traveling normally throughout the ventricle, a decrease in gap junctions causes the electrical signal to propagate more slowly allowing for reentrant arrhythmias. This causes sporadic contraction of different parts of the ventricle known as VF. The incidence of VF has been directly related to decreased connexin levels (Xing et al., 2003). Because the drug 4-PB can induce connexin mRNA transcription, it is possible that the drug could effectively trigger renewed channel formation reduced by cardiac ischemia. Thus, the findings in this study suggest that drugs such as 4-PB which enhance gap junction coupling, might be implicated in the prevention of ischemia induced VT or VF as earlier has been shown with the anti-arrhythmic peptide ZP123 (Xing et al., 2003). In addition, another related study has shown that 4-PB significantly enhanced coupling and action potential propagation between rodent cardiomyocytes (Jia et al., 2012) suggesting that cardiac cells may be responsive to HDAC inhibitors and, hence potentially useful as a cardiac therapy.

However, it remains to be seen whether drugs like 4-PB will be effective in preventing ischemia induced cardiac maladies. Yet more thorough studies have to be done in arrhythmia models to test 4-PB potential to act as anti-arrhythmic gap junction modulator similar to anti-arrhythmic peptides AAP10 and ZP123 (Dhein et al., 2003).

### ACKNOWLEDGMENTS

This work was supported by NIH grants GM RO1 088180 to Peter R. Brink and GM RO1 088181 to Virginijus Valiunas and HL 094410 to Ira S. Cohen.

### REFERENCES

- Asklund, T., Appelskog, I., Appelskog, I. B., Ammerpohl, O., Ekstrom, T. J., and Almqvist, P. M. (2004). Histone deacetylase inhibitor 4-phenylbutyrate modulates glial fibrillary acidic protein and connexin 43 expression and enhances gap junction communication, in human glioblastoma cells. *Eur. J. Cancer* 40, 1073–1081. doi: 10.1016/j.ejca.2003.11.034
- Brink, P., Ramanan, S., and Christ, G. (1996). Human connexin 43 gap junction channel gating: evidence for mode shifts and/or heterogeneity. *Am. J. Physiol.* 271, 321–331.
- Bukauskas, F. F., Jordan, K., Bukauskiene, A., Bennett, M. V. L., Lampe, P. D., Laird, D. W., et al. (2000). Clustering of connexin 43-enhanced green fluorescent protein gap junction channels and functional coupling in living cells. *Proc. Natl. Acad. Sci. U.S.A.* 97, 2556–2561. doi: 10.1073/pnas.050588497
- Dhein, S. (2004). Pharmacology of gap junctions in the cardiovascular system. *Cardiovasc. Res.* 62, 287–298. doi: 10.1016/j.cardiores.2004.01.019
- Dhein, S., Larsen, B. D., Petersen, J. S., and Mohr, F. W. (2003). Effects of the new antiarrhythmic peptide ZP123 on epicardial activation and repolarization pattern. *Cell Commun. Adhes.* 10, 371–378. doi: 10.1080/cac.10.4-6.371.378
- Donahue, J. K., and Laurita, K. R. (2011). "Trachyarrhythmia therapies: approaches to atrial fibrillation and postinfarction ventricular arrhythmias," in *Regenerating the Heart: Stem Cells and the Cardiovascular System*, eds I. S. Cohen and G. Gaudette (New York, NY: Springer), 349–378.
- Dovzhanskiy, D. I., Hartwig, W., Lazar, N. G., Schmidt, A., Felix, K., Straub, B. K., et al. (2012). Growth inhibition of pancreatic cancer by experimental treatment with 4-phenylbutyrate is associated with increased expression of connexin43. *Oncol. Res.* 20, 103–111. doi: 10.3727/096504012X13477145152959
- Gemel, J., Valiunas, V., Brink, P., and Beyer, E. (2004). Connexin43: and connexin26 for gap junctions, but not heteromeric channels in co-expressing cells. *J. Cell Sci.* 117, 2469–2480. doi: 10.1242/jcs.01084
- Hodgkin, A. L., and Huxley, A. F. (1952). A quantitative description of membrane current and its application to conduction and excitation in nerve. *J. Physiol.* 117, 500–544.
- Jia, Z., Bien, H., Shiferaw, Y., and Entcheva, E. (2012). Cardiac cellular coupling and the spread of early instabilities in intracellular  $\text{Ca}^{2+}$ . *Biophys. J.* 102, 1294–1302. doi: 10.1016/j.bpj.2012.02.034
- Khan, Z., Akhtar, M., Asklund, T., Juliusson, B., Almqvist, P., and Ekstrom, T. (2007). HDAC inhibition amplifies gap junction communication in neural progenitors: potential for cell mediated enzyme prodrug therapy. *Exp. Cell Res.* 313, 2958–2967. doi: 10.1016/j.yexcr.2007.05.004
- Pointis, G. (2006). Connexin43: emerging role in erectile function. *Int. J. Biochem. Cell Biol.* 38, 1642–1646. doi: 10.1016/j.biocel.2006.03.007
- Rudy, Y. (2001). The ionic mechanisms of conduction in cardiac tissue. *J. Electrocardiol.* 34, 65–68. doi: 10.1054/jelc.2001.28831
- Saffitz, J. E., Hames, K. Y., and Kanno, S. (2007). Remodeling of gap junctions in ischemic and nonischemic forms of heart disease. *J. Membr. Biol.* 218, 65–71. doi: 10.1007/s00232-007-9031-2
- Sohl, G., and Willecke, K. (2004). Gap junctions and the connexin protein family. *Cardiovasc. Res.* 62, 228–232. doi: 10.1016/j.cardiores.2003.11.013
- Valiunas, V., Beyer, E., and Brink, P. (2002). Cardiac gap junction channels show quantitative differences in selectivity. *Circ. Res.* 91, 104–111. doi: 10.1161/01.RES.0000025638.24255.AA
- Valiunas, V., Gemel, J., Brink, P., and Beyer, E. (2001). Gap junction channels formed by coexpressed connexin40 and connexin43. *Am. J. Physiol. Heart Circ. Physiol.* 281, 1675–1689.
- Valiunas, V., Mui, R., McLachlan, E., Valdimarsson, G., Brink, P., and Beyer, E. (2003). Gap junctions formed by coexpressed connexin40 and connexin43 in rat heart. *Am. J. Physiol. Heart Circ. Physiol.* 284, H1675–H1689.

and White, T. (2004). Biophysical characterization of zebra fish connexin35 hemichannels. *Am. J. Physiol. Cell Physiol.* 287, 1596–1604. doi: 10.1152/ajpcell.00225.2004

Valiunas, V., Weingart, R., and Brink, P. (2000). Formation of heterotypic gap junction channels by connexins 40 and 43. *Circ. Res.* 86, 42–49. doi: 10.1161/01.RES.86.2.e42

Xing, D., Kjolby, A., Nielsen, M., Petersen, J., Harlow, K., Rathlou, N., et al. (2003). ZP123

increases gap junctional conductance and prevents reentrant ventricular tachycardia during myocardial ischemia in open chest dogs. *J. Cardiovasc. Electrophysiol.* 14, 510–520. doi: 10.1046/j.1540-8167.2003.02329.x

**Conflict of Interest Statement:** The authors declare that the research was conducted in the absence of any commercial or financial relationships that could be construed as a potential conflict of interest.

Received: 13 February 2013; accepted: 14 August 2013; published online: 03 September 2013.

Citation: Kaufman J, Gordon C, Bergamaschi R, Wang HZ, Cohen IS, Valiunas V and Brink PR (2013) The effects of the histone deacetylase inhibitor 4-phenylbutyrate on gap junction conductance and permeability. *Front. Pharmacol.* 4:111. doi: 10.3389/fphar.2013.00111

This article was submitted to Pharmacology of Ion Channels and Channelopathies, a section of the journal *Frontiers in Pharmacology*.

Copyright © 2013 Kaufman, Gordon, Bergamaschi, Wang, Cohen, Valiunas and Brink. This is an open-access article distributed under the terms of the Creative Commons Attribution License (CC BY). The use, distribution or reproduction in other forums is permitted, provided the original author(s) or licensor are credited and that the original publication in this journal is cited, in accordance with accepted academic practice. No use, distribution or reproduction is permitted which does not comply with these terms.



# The oligodendroglial precursor cell line Oli-neu represents a cell culture system to examine functional expression of the mouse gap junction gene connexin29 (Cx29)

Goran Söhl<sup>\*†</sup>, Sonja Hombach<sup>†</sup>, Joachim Degen<sup>†</sup> and Benjamin Odermatt<sup>†</sup>

Abteilung Molekulargenetik, Institut für Genetik, Universität Bonn, Bonn, Germany

**Edited by:**

Stefan Dhein, Universitätsklinik Leipzig Herz-Zentrum Leipzig GmbH, Germany

**Reviewed by:**

Raúl Estévez, Universidad Autónoma de Barcelona, Spain  
Christian Giaume, Collège de France, France

**\*Correspondence:**

Goran Söhl, Department of Development and Quality Management, University of Applied Science, RheinAhrCampus, Joseph-Rovan-Allee 2, Remagen 53424, Germany  
e-mail: soehl@rheinahr-campus.de; soehl@hs-koblenz.de

**†Present address:**

Goran Söhl, Abteilung für Hochschulentwicklung und Qualitätsmanagement (HEQM), Hochschule Koblenz, Remagen, Germany  
Sonja Hombach, Fakultät für Biologie und Vorklinische Medizin, Institut für Biochemie, Genetik und Mikrobiologie, Universität Regensburg, Regensburg, Germany  
Joachim Degen, LIMES Institut, Universität Bonn, Bonn, Germany  
Benjamin Odermatt, Anatomisches Institut, Universität Bonn, Bonn, Germany

## INTRODUCTION

Oligodendrocytes do myelinate neuronal axons in the CNS to allow fast nerve conduction as well as guidance and care for neuronal networks (cf. Kandel et al., 2000). Oligodendroglial progenitor cells (O-2A) can be divided in two different lineages developing from neuro-epithelial precursors in the wall of the embryonic neural tube around mouse embryonic day E12 (Richardson et al., 2000). In the CNS, O-2A cells exist in two subpopulations with different maturation profiles: O-2A<sup>perinatal</sup> cells are up-regulated in the rat postnatally, providing myelination during this period, but disappear about 6 weeks after birth (Wolswijk and Noble, 1989); O-2A<sup>adult</sup> cells exist in the adult

The potential gap junction forming mouse connexin29 (Cx29) protein is concomitantly expressed with connexin32 (Cx32) in peripheral myelin forming Schwann cells and together with both Cx32 and connexin47 (Cx47) in oligodendrocytes of the CNS. To study the genomic structure and functional expression of Cx29, either primary cells or cell culture systems might be selected, from which the latter are easier to cultivate. Both structure and expression of Cx29 is still not fully understood. In the mouse sciatic nerve, brain and the oligodendroglial precursor cell line Oli-neu the Cx29 gene is processed in two transcript isoforms both harboring a unique reading frame. In contrast to Cx32 and Cx47, only Cx29 protein is abundantly expressed in undifferentiated as well as differentiated Oli-neu cells but the absence of EtBr dye transfer after microinjection concealed the function of Cx29-mediated gap junction communication between those cells. Although HeLa cells stably transfected with Cx29 or Cx29-eGFP neither demonstrated any permeability for Lucifer yellow nor for neurobiotin, blocking of EtBr uptake from the media by gap junction blockers does suppose a role of Cx29 in hemi-channel function. Thus, we conclude that, due to its high abundance of Cx29 expression and its reproducible culture conditions, the oligodendroglial precursor cell line Oli-neu might constitute an appropriate cell culture system to study molecular mechanisms or putative extracellular stimuli to functionally open Cx29 channels or hemi-channels.

**Keywords:** gap junction, connexin, Cx29, oligodendroglial precursor cell-line Oli-neu, HeLa cells, dye transfer

brain with a limited capacity for remyelination (Zhang et al., 1999). Murine oligodendroglial cells express NGFs, which are important for oligodendrocyte-neuron interactions, essential for neuronal survival, redifferentiation, and remyelination (Byravan et al., 1994). In order to study such cell-cell interactions, O-2A progenitor cells were stably transfected with the *t-neu* tyrosine kinase (Jung et al., 1995). The resulting Oli-neu cell line can be induced to differentiate *in vitro* after application of dibutyryl cAMP. In the presence of demyelinated lesions, Oli-neu cells engage with demyelinated axons but do not differentiate further to wrap the axons (Jung et al., 1995).

In the present study, expression of the myelin-related connexins Cx29, Cx32, and Cx47 (Kleopa et al., 2004; Li et al., 2004) was analyzed in differentiated and undifferentiated Oli-neu cells. Connexins are the subunits of gap junctions, which are formed by docking of two hemi-channels (connexons), each comprised of 6 connexins in adjacent cells. Today, at least 21 connexin genes

**Abbreviations:** RT-PCR, polymerase chain reaction after reverse transcription; Cx, connexin; UTR, untranslated region; CNS, central nervous system; PNS, peripheral nervous system; EtBr, ethidiumbromide; eGFP, enhanced green fluorescence protein; NGF, nerve growth factor; CMTX, Charcot-Marie-Tooth disease X-chromosomal.

are described in the murine and human genome, most of which are orthologs (Söhl and Willecke, 2003; Sonntag et al., 2009). Targeted disruption of mouse connexin genes revealed functional consequences often coinciding with pathological situations in patients suffering from mutations in the respective orthologous connexin (Willecke et al., 2002). Ablation of the connexin32 (Cx32) protein (Nelles et al., 1996) resulted in a demyelinating peripheral neuropathy (Anzini et al., 1997; Scherer et al., 1998) reverted by transgenic expression of human Cx32 in myelinating mouse Schwann cells (Scherer et al., 2005). Although abnormalities caused by Cx32 mutations found in CNS myelin are largely subtle, they fall into the category of patients suffering from the inherited peripheral neuropathy CMTX mostly caused by point mutations of the Cx32 gene (Scherer et al., 1998). Targeted deletion of the connexin47 (Cx47) gene revealed subtle vacuolization of CNS nerve fibers (Menichella et al., 2003; Odermatt et al., 2003). Cx32/Cx47-double deficient mice, however, develop a more severe CNS vacuolization coinciding with action tremor and death around 7 weeks after birth (Odermatt et al., 2003). This is reminiscent to nystagmus, progressive spasticity, and ataxia found in some patients with a mutated Cx47 gene suffering from Pelizaeus–Merzbacher-Like disease (Uhlenberg et al., 2004; Tress et al., 2011).

Connexin29 (Cx29) transcription was shown to be postnatally up-regulated in the mouse CNS concomitantly with Cx32 and Cx47 (Söhl et al., 2001a). In the CNS, Cx29 was detectable at the internodal and juxtaparanodal regions of small myelin sheaths (Altevogt et al., 2002) but did not co-localize with any of the two other oligodendroglial (Cx32 and Cx47) or the prominent astroglial connexins (Cx30 and Cx43), supposed to form an astroglial, if not panglial syncytium (Altevogt and Paul, 2004; cf. Theis et al., 2005). In the PNS, Cx29 protein was only found in the innermost layer of mouse sciatic nerve myelin (Li et al., 2002), the (juxta) paranodes, the inner mesaxon and together with Cx32 within the incisures (Altevogt et al., 2002). Cx29 hemi-channels were suggested due to their subcellular distribution in peripheral Schwann cells at the innermost layer of myelin apposing axonal Shaker-type K<sup>+</sup> channels (Altevogt et al., 2002), in cochlear Schwann cells (Tang et al., 2006), and in oligodendrocytes that myelinate small caliber fibers (cf. Kleopa et al., 2010). However, transfection of Cx29 as well as its human ortholog Cx31.3 into HeLa wild-type cells neither produced significant junctional conductance nor formed functional intercellular channels or hemi-channels (Altevogt et al., 2002; Ahn et al., 2008; Sargiannidou et al., 2008). Recently, a missense mutation (E269D) in the human ortholog of Cx29 supposed to contribute to non-syndromic hearing impairment (NSHI) at least disturbed the formation of gap junctions in HeLa cell transfectants (Hong et al., 2010) although targeted deletion of the Cx29 coding region in mice does not result in any obvious phenotypical alterations or abnormalities (Altevogt and Paul, 2004; Eiberger et al., 2006).

Here we report the presence and gene structure of Cx29 in mouse sciatic nerve and brain as well as in cultured Oli-neu cells. The spliced transcript isoform contains Exon1 (442 bp), which is separated by a 4.8 kb intron from Exon2 (~3.8 kb), comprising the complete coding region. Since both the splice acceptor and

the consensus motif for translational initiation partially overlap, translation efficacy is altered after splicing. Unexpectedly, out of three characterized myelin-related connexin genes Cx29, Cx32, and Cx47, only Cx29 is abundantly transcribed and translated in differentiated as well as undifferentiated Oli-neu cells. Their homologous coupling does not promote the transfer of neuropeptidyl, whereas immunofluorescence analyses and dye uptake measurements suggest Cx29 protein in hemi-channels. Similarly, Cx29 HeLa cell transfectants express Cx29 transcript and protein highly abundant but only show a very limited tracer coupling and dye uptake around background when compared to HeLa wild-type control.

## MATERIALS AND METHODS

### SEQUENCE DATA ACQUISITION AND ANALYSIS

Current sequence information about the Cx29 gene is provided by the *Entrez Gene* platform of the NCBI-mediated genome browser under the GeneID: 118446. A locus tag [MGI: 2153041] of the gap junction membrane channel protein epsilon1 is provided by Mouse Genome Informatics. A genomic sequence contig [acc. no. NC\_000071 or ENSMUSG00000056966] from 135358446 to 135349315 is presented which shows graphically aligned transcripts [NM\_0800450] and the polypeptide sequence [Q921C1] of 258 amino acids. Furthermore, a predicted polypeptide sequence [NP\_536698] of 269 amino acids is annotated to the genomic contig. This polypeptide additionally contains 11 amino acids (MLLLELPKCR) attached to the N-terminus of Cx29 (Söhl et al., 2001a; Altevogt et al., 2002) and translation was predicted to start on exon1 supposed to be spliced to exon2 usually harboring the ATG start codon. This prediction was confirmed after applying the cross-linked *Ensembl Contig View*, the *UCSC Browser*, or the *NCBI Map Viewer*.

Two different but interrupted Cx29 cDNA clones (accession nos. AW495262 and BB644041) containing additional and overlapping sequence information at the 5'-region (5'-UTR) of the Cx29 reading frame (accession no. AJ297318) have been identified. A detailed search in the Celera's mouse genomic database [[www.celera.com](http://www.celera.com)] yielded one contiguous Celera clone [GA\_X5J8B7W67DU: 8500001::8737182], including the whole Cx29 gene. This sequence segment is quite similar to the above mentioned genomic sequence contig [acc. no. NC\_000071], thus we have considered both as a common sequence segment. In order to implement an unequivocally system for position numbers of important sites (i.e., translational start site, splice donor, and acceptor sites) or primer annealing sites, we have decided to assign the A of the actual ATG start codon on exon2 with +1. Consecutive numbering further downstream will be positive in contrast to consecutive negative numbering further upstream.

Functional implications on translational efficacies of each consensus motif of translational initiation in RNA transcripts have been calculated according to the criteria of (Iida and Masuda, 1996).

### RT-PCR ANALYSIS

Reverse transcription of total RNA from mouse brain, sciatic nerve, and Oli-neu cell lines was performed according to Söhl et al. (1998). Aliquots of the transcribed cDNA [1/25 from tissue

and cells ( $\sim 0.1$  ng)] were amplified using different combinations of Cx29 specific primers listed in **Table 1** and depicted in **Figure 1B**. Reaction mixtures (50  $\mu$ l) contained 20 mM Tris-HCl (pH 8.4), 250  $\mu$ M dNTPs, 1.25 mM MgCl<sub>2</sub>, 50 mM KCl, 2  $\mu$ M of each primer and 1 unit Taq DNA-polymerase (Promega, Madison, WI, USA). PCR was carried out for 40 cycles using a PTC-200 Thermal Cycler (MJ Research, Watertown, MA, USA) with the following program: first denaturing step at 94°C for 3 min, denaturing at 94°C for 1 min, annealing at 65°C for 1 min, elongation at 72°C for 2 min, and final elongation for 7 min. After gel electrophoresis in a 1% agarose gel Etbr stained fragments were documented (Sambrook and Russel, 2001). The integrity of all primer combinations was verified before with appropriate Cx29 genomic mouse 129/SvJ plasmid controls (Eiberger et al., 2006). Fragments of interest were excised from the gel, purified by using the QIAquick purification procedure for PCR-fragments (Qiagen, Hilden, Germany) and finally subcloned into the pGEM-T<sub>easy</sub> vector system suited for cloning PCR-fragments (Promega). Fragments were commercially sequenced by AGOWA, Berlin, Germany.

#### NORTHERN BLOTTING ANALYSIS

Total RNA from mouse brain (C57BL/6NCrl)), from HeLa as well as Oli-neu cells was prepared with TRIzol®-reagent (GibcoBRL) according to the manufacturer. RNA (20  $\mu$ g) was electrophoresed (Sambrook and Russel, 2001) and transferred to HybondN nylon membrane (Amersham International, Amersham, Bucks, UK) by capillary diffusion in 20× SSC. Northern membrane was probed by using corresponding hybridization fragments of mouse Cx29, Cx32, Cx45, and Cx47 (described in (Söhl et al., 2001a)) subsequently. Probes were <sup>32</sup>P labeled, using the random primed labeling method (multiprime labelling Kit, Amersham) to a specific activity of 0.5 to 1.0  $\times 10^9$  cpm/ $\mu$ g DNA and added to fresh QuikHyb hybridization solution (Stratagene, La Jolla, CA, USA) at 1.25  $\times 10^6$  cpm/ml. Hybridization at high stringency was carried out for 1 h at 68°C. Filters were

finally washed for 30 min in 0.1× SSC/0.1% SDS at 60°C and exposed to XAR X-ray film (Eastman Kodak, Rochester, NY, USA) with intensifying screen at -80°C. The amounts of total RNA on the Northern blot were roughly standardized by determination of the intensities of the Etbr stained 18S- and 28S rRNA. The densitometric analysis was carried out with the Biometra Scan Package (Version 4.0), Göttingen, Germany.

#### IMMUNOBLOTTING

Protein extracts from Oli neu cell lines and cultured HeLa cells were obtained after homogenizing by sonification in 1× Complete® protease inhibitor (Roche, Mannheim, Germany). Protein concentrations were determined after using the bicinchoninic acid protein determination kit (Sigma, Deisenhofen, Germany), according to the instructions of the manufacturer. Aliquots of 50  $\mu$ g protein per lane were separated by polyacrylamide gel electrophoresis, transferred to nitrocellulose membranes (Sambrook and Russel, 2001), blocked with 1× RotiBlock® (Roth, Karlsruhe, Germany) for 1 h and incubated for 2 h at room temperature with a 1:600 dilution of polyclonal Cx29 antibodies (Zymed; Cat. No 34-4200) diluted in 1× RotiBlock. After washing (2× for 5 min and 2× for 10 min) in 1× RotiBlock immune-complexes were analyzed using <sup>125</sup>I-labeled protein A.

#### IMMUNOCYTOCHEMISTRY

HeLa cells and Oli-neu cells were seeded on coverslips, cultivated for 3 days and washed twice in PBS for 5 min. Cells were fixed in absolute ethanol (-20°C) for 5 min, washed twice in PBS for 5 min and pre-incubated for 45 min in blocking reagent (PBS containing 4% BSA and 0.1% Triton X-100). Cryosections (12  $\mu$ m) of whole C57BL/6N mouse adult brain were fixed in absolute ethanol (-20°C) for 10 min, washed twice in PBS for 5 min, and pre-incubated for 45 min in blocking reagent (PBS containing 4% BSA and 0.1% Triton X-100). For detection of Cx29, slides were incubated for 2 h with

**Table 1 | Description of primers used to determine the genomic structure of mCx29.**

Name	Sequence	Position	5'-linker
Ex1 USP1	5'-gag ccg tac gag ttc tcc act gag	-5498 to -5475	-
Ex1 USP2	5'-agg cag ctc atc cct aga caa ggg	-5259 to -5236	-
Ex1 USP3	5'-act ttc cag aga tcg cgg ctt gag	-5046 to -5023	-
Ex1 USP4	5'-cca gtg tga aga ttc ctt ttg g	-4889 to -4868	HindIII
Intron USP	5'-act gga gct cag tgt cat gtg	-626 to -608	KpnI
TATA USP1	5'-aat ctg tgc tgt gct att tgg	-259 to -239	HindIII
TATA USP2	5'-agt aaa gat gga taa agt gtg	-157 to -137	HindIII
Ex2 USP1	5'-tac aaa gtt tct aag gag agg	+891 to +911	KpnI
Ex2 USP2	5'-gca gat ctc cca gag cac tgg	+2520 to +2540	KpnI
Ex2 DSP1	5'-ggg gga gtg ctg gct ctc ctg	+54 to +34	BamHI
Ex2 DSP2	5'-gga aag aaa aat tag aag tgg	+1829 to +1809	BamHI
Ex2 DSP3	5'-cac caa aca gag aca cca ttg	+3715 to +3695	BamHI

Position numbers refer to the genomic sequence of mCx29 available from the NCBI database available under [acc. no. NC\_000071 or ENSMUSG00000056966]. Some primer additionally contain 5'-linkers with appropriate restriction sites designed according to the technical references of New England Biolabs Inc. (NEB) 2001, page 210–211.

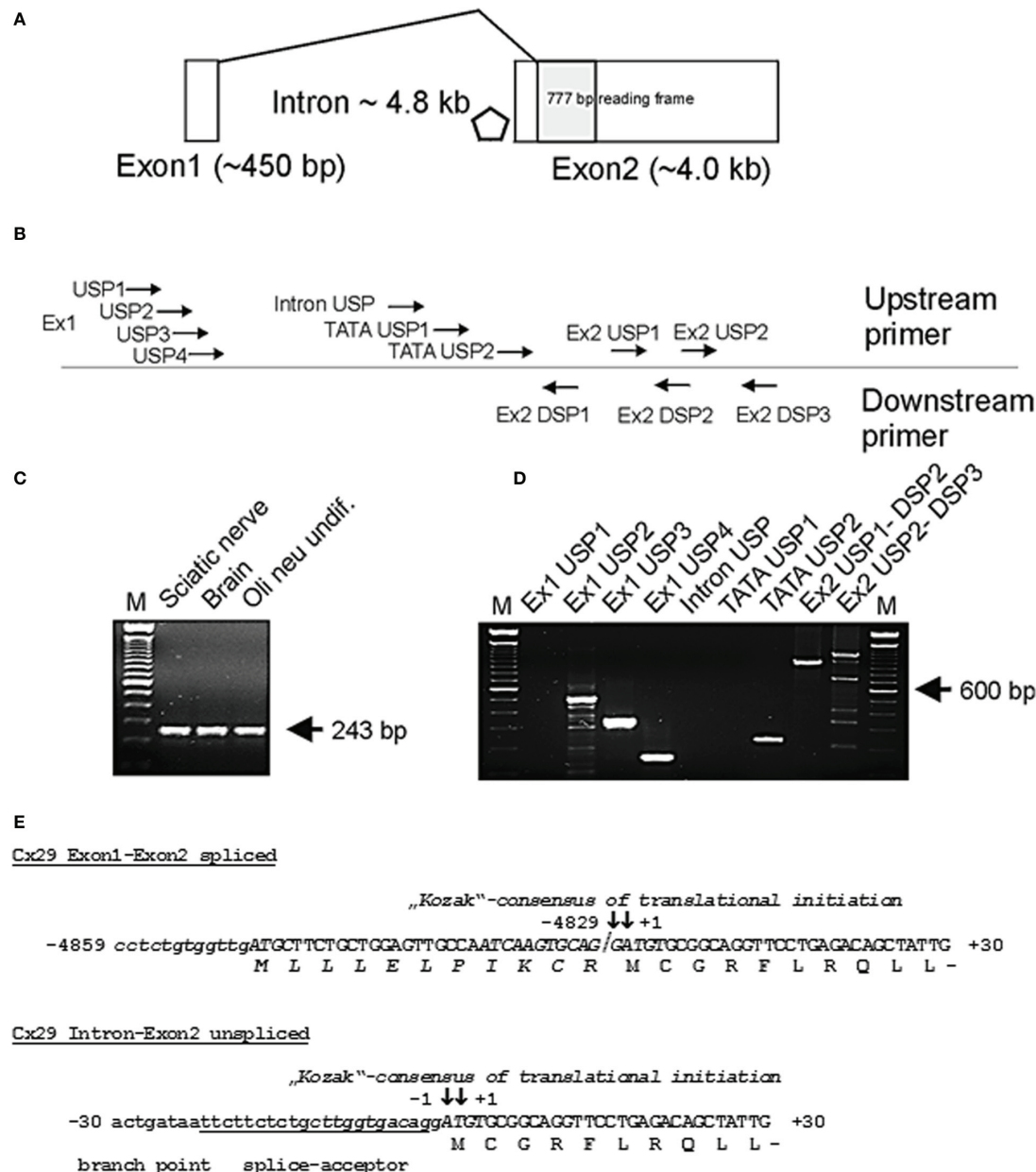


**FIGURE 1 | (A)** Genomic structure of mouse connexin29 (Schematic drawing). Exons are indicated by boxes. Shaded box represents the open reading frame (ORF) of 777 base pairs (bp) encoding for 258 amino acid residues (aa). Rhombus indicates a TATA-box motif within the 4.8 kb intron (position -194 to -189). Exon1 is spliced directly to the ATG start codon. **(B)** Rough delineation of primers used for subsequent RT-PCR analyses. Primer sequences, their position and orientation in the genomic sequence of Cx29 are listed in **(A)**. **(C)** RT-PCR with primers for β-actin (De Sousa et al., 1993) amplifying a single 243 bp amplicon of mouse β-actin cDNA without genomic DNA (330 bp). M = 100 bp ladder (Gibco-BRL). **(D)** RT-PCR using different primer combinations, delineated in **(B)**, and mRNA from Oli-neu cells. Seven upstream primers (Ex1 USP 1–4, Intron USP, and TATA USP 1–2) were subsequently combined with downstream primer Ex2 DSP1 to verify splicing of Exon1 to Exon2 and to roughly determine gene extension. Amplicons of 497, 284, and 127 bp (lane 2 to 4 from the left) indicate that Exon1 at least comprises 442 bp and is spliced to Exon2. The amplicon (210 bp) generated by

upstream primer TATA USP2 suggests transcriptional activity downstream of a TATA-box motif (position -194 to -189). Exon2 derived primer combinations Ex2 USP1-DSP2 and Ex2 USP2-DSP3 generated fragments of 938 bp and 1195 bp extending the 3' untranslated region (3'-UTR) of Exon2 to about 3 kb. Primer DSP3 also amplified unspecific fragments under PCR conditions selected. M = 100 bp ladder (Gibco-BRL). **(E)** Partial sequences of the spliced (Exon1 and Exon2) and of the unspliced (Intron and Exon2) Cx29 transcript isoforms containing the start codon (ATG) numbered according to (+1) for the A of the ATG and (-1) for the adjacent base upstream. The coding nucleotide sequence (capital letters) is aligned to its deduced amino acid sequence. The consensus motifs of translational initiation are written in *italics*. ATG codons in use are in bold capital letters and boxed. The splice junction between exon1 and exon2 is separated by a slash. Note that a hypothetical N-terminus (gray shaded italic letters) is suggested to start at the boxed ATG on exon1. The putative branch point (boxed) and splice acceptor (underlined) overlap with the consensus initiation region of translation (Kozak, 1989; Iida and Masuda, 1996).

a 1:200 dilution of the affinity-purified polyclonal anti-Cx29 antibodies (Zymed; Cat. No 34-4200) at room temperature. After three washes in PBS for 5 min, respectively, tissue samples were stained for 45 min with a 1:2000 dilution of the secondary antibody Alexa (488)-conjugated goat anti-rabbit [# A11037] (MoBiTec, Göttingen, Germany). After incubation, samples were washed three times in PBS for 5 min, stained with Hoechst 33528 (Roche) and mounted in fluorescence mounting solution (DAKO, Hamburg, Germany). Fluorescent signals were recorded by using a Zeiss Axiophot photomicroscope equipped with a  $63\times$  oil immersion objective and appropriate filters.

## PLASMIDS

For stable transfection of HeLa cells, the translational initiation optimized Exon2 coding region of mouse Cx29 was PCR amplified from phage DNA and cloned into the expression vector pMJ green, consisting of an *AsnI/StuI* fragment (2570 bp) descending from the pEGFP-N1 vector (Clontech, Palo Alto, CA, USA), which was cloned into the *NotI/ClaI* opened pBEHpac18 vector ( $\sim$ 3700 bp; Horst and Hasilik, 1991) in order to construct a fusion protein of the Cx29 sequence with the enhanced green fluorescent protein at its C-terminus. The primers had a *XhoI* site at the N-terminus (primer XhoATG: 5'-CCG CTC GAG CGG CCA CCA TGT GCG GCA GGT TCC TG-3') and a *PstI* site behind the stop codon of the connexin gene (primer PstSTOP: 5'-CGA ATG CAT TGG CTG CAG TTC AAA ATG GCT CTT TTG C-3') or, in case of the fusion protein, a *PstI*-site instead of the stop codon of the Cx29 gene (primer PstGO: 5'-CGA ATG CAT TGG CTG CAG TTT AAA TGG CTC TTT TGC-3'). The PCR products were cloned with *XhoI* and *PstI* into the pMJ green and sequenced; the resulting expression plasmids were named pCx29 and pCx29eGFP.

## HeLa CELL CULTURE AND TRANSFECTION

Human cervix carcinoma HeLa cells (ATCC CCL1; American Type Culture Collection, Rockville, MD, USA) were cultured in Dulbecco's modified Eagles medium (DMEM) low glucose, 2 mM glutamine, 10% fetal calf serum, 100 U/ml penicillin, and 100  $\mu$ g/ml streptomycin (all from Life Technologies). HeLa transflectants were maintained in standard medium containing puromycin (0.5 mg/ml; Sigma) being cultivated in a 37°C incubator in a moist atmosphere of 10% CO<sub>2</sub>. HeLa cells were transfected with 20  $\mu$ g of the linearized pMJ green plasmid vector containing either the pCx29 and pCx29eGFP plasmids using the calcium phosphate transfection protocol employed routinely by Elfgang et al. (1995). In brief, between 24 and 48 h after exposure to DNA, puromycin was added to the medium. Clones were picked after 3 weeks and grown under selective conditions. Alternatively, cells have been transfected using the Tfx20-reagent (Promega). Resistant clones were isolated after 2 weeks of selection with 1  $\mu$ g/ml Puromycin (Sigma), and tested for Cx29EGFP expression by microscopy with an excitation wavelength of 488 nm. Microinjection of dyes like Lucifer yellow, propidium iodide, EtBr, or DAPI as well as of the tracer neurobiotin was done iontophoretically in close accordance to Elfgang et al. (1995).

## Oli-Neu CELL CULTURE CONDITIONS

Oli-neu cells were incubated in SATO medium containing 1% horse serum, gentamycin and 1 mM dibutyryl cAMP (dbcAMP; Sigma, Heidelberg, Germany) for differentiation during a period of at least 10–20 days at 37°C (Jung et al., 1995). Cells were plated in 35 mm Petri dishes or six-well plates on poly-L-lysine coated coverslips (Nunc, Wiesbaden, Germany), and stained for indirect immunofluorescence.

## DYE TRANSFER MEASUREMENTS

HeLa or Oli-neu cells were grown on 35 mm dishes for 2–3 days. Glass micropipettes were pulled from capillary glass (World Precision Instruments, Berlin, Germany) with a horizontal pipette puller (Model P-97, Sutter Instruments, Novato, CA) and backfilled with dye solution (see below). Dyes were injected iontophoretically (Iontophoresis Programmer model 160; World Precision Instruments) and cell-to-cell transfer was monitored using an inverted microscope (IM35; Zeiss) equipped with fluorescent illumination. Cell culture dishes were kept on a heated block at 37°C. Lucifer Yellow CH (Molecular Probes) at 4% (w/v) in 1 M LiCl was injected by applying hyperpolarizing currents for 10 s ( $I = 20$  nA). Cell to cell transfer was evaluated 30 min after dye injection. Neurobiotin (N-2(2-aminoethyl)-biotinamide hydrochloride; Vector Lab, Burlingame, CA) and rhodamine 3-isothiocyanate dextrane 10S (Sigma) at concentrations of 6 and 0.4% (w/v), respectively, in 0.1 M Tris-Cl (pH 7.6) were injected by applying depolarizing currents for 10 s ( $I = 20$  nA). Thirty minutes after injection, cells were washed twice with phosphate buffered saline (PBS), fixed for 10 min in 1% glutaraldehyde in PBS, washed twice with PBS, incubated in 2% Triton X-100 in PBS over night at 4°C, washed three times with PBS, incubated with horseradish peroxidase-avidinD complex (Vecor Lab) diluted 1:1000 in PBS for 90 min, washed three times with PBS, and incubated in 0.05% diaminobenzidine, 0.003% hydrogen peroxide solution for 30 s. The staining reaction was stopped by washing three times with PBS. Cell-to-cell transfer was quantified by counting the number of stained cells neighboring the microinjected cell.

## DYE UPTAKE IN Oli-Neu CELLS

Stock solutions of fluorescence dyes were prepared in 150 mM LiCl [110  $\mu$ M Lucifer Yellow CH (LY)] or in PBS (5 mM or 12.5 mM Etbr). For visualization of dye uptake, 0.5  $\mu$ l of stock solutions were applied at room temperature through a glass micropipette over the area of the culture plate to be evaluated, and 2 min later, the dye was washed away and replaced with recording medium (SATO). Alternatively, 2.5  $\mu$ l Etbr (1 mg/ml) was added directly to a 6 cm culture dish, incubated for 4 min, washed and subsequently replaced by fresh medium. The former described local application of the dye, however, produced only little background and was thus preferred. The gap junction blocker heptanol and octanol have been applied for 5 min, 1 mM just before dye application. In permeabilized cells, Etbr labelling was detectable as fluorescence of the nuclei. The retained dye was monitored using an inverted microscope (IM35; Zeiss) equipped with fluorescent illumination and documented by a Powershot G50 digital camera (Canon). For time-lapse recordings of dye

uptake, the fluorescence exposure times were usually 5–10 s, with 15 s between each fluorescence image. This procedure was already and successfully applied to cultured astrocytes (Contreras et al., 2002) and thus adapted for Oli-neu cells.

## RESULTS

### GENOMIC STRUCTURE OF MOUSE CONNEXIN29

Untranslated sequence information (5'-UTR) of two interrupted Cx29 cDNA clones have been aligned in the genomic Cx29 sequence from position –5049 to –4829 (see sequence data acquisition and analysis), representing a putative untranslated Exon1 of 220 bp with a splice-donor site (CAG↓GTAAAT) at its 3'-end, that contains all criteria of canonical splice-donor sites (Padgett et al., 1986). It is separated by an intron of about 4.8 kb from the coding region (shaded box; **Figure 1A**). RT-PCR primer sequences and template positions to verify functional splicing of Cx29 Exon1 to Exon2 are listed in **Table 1** and schematically delineated in **Figure 1B**.

Quality of cDNA pools generated from total RNA of mouse sciatic nerve, brain and Oli-neu cells have been tested using a specific primer combination to amplify β-actin (De Sousa et al., 1993). No residual genomic DNA contamination was detectable (330 bp) whereas the 243 bp cDNA β-actin amplicon implied proper cDNA synthesis (**Figure 1C**).

A subset of upstream primers covering Exon1 (220 bp) and the genomic region further upstream, was combined with intron-spanning Exon2-specific downstream primer Ex2 DSP1 (see **Table 1** and **Figure 1B**) to produce a distinct pattern of amplicons, enabling a rough estimation of the putative Exon 1 size (**Figure 1D**). The shortest amplicon of 127 bp (lane 4) was subcloned, sequenced, and confirmed the anticipated splice pattern deduced from both cDNA clones. Thus, Exon1 of Cx29 is functionally expressed and spliced to Exon2 in at least mouse sciatic nerve, mouse brain as well as in Oli-neu cells (undifferentiated) (**Figure 1D**). Larger amplicons of about 284 and 497 bp (lane 2 and 3; **Figure 1D**) let extend Exon1 to at least 442 bp (see also **Figure 1A**).

A further objective was to determine the approx. 5'-extention of Cx29 Exon2, since the corresponding splice acceptor site and

the consensus motif of translational initiation (Kozak, 1989) nearly coincide in a sequence of 12 bp (depicted in *italics* in **Figure 1E**).

Therefore, three upstream primers (**Table 1**) should anneal between Exon 1 and 2 (two of them enframe a putative TATA-box motif), which were combined with downstream primer Ex2 DSP1 (see **Figure 1B** and **Table 1**). Unexpectedly, the intron-derived primer (TATA USP2) downstream of the TATA-box motif (rhombus; **Figure 1A**) was able to generate an amplicon of 210 bp, suggesting the initiation of transcription. Cloning and sequencing identified the genomic sequence containing the native splice acceptor site (**Figure 1E**). Thus, an additional unspliced transcript isoform might be expressed from the Cx29 gene. The fact that the consensus motif of the splice acceptor site is in such a proximity to the ATG start codon leaves only the base guanine in front of the ATG unchanged after splicing, which, however, does not severely decrease (only 12%) the efficacy of translational initiation compared to the unspliced Cx29 transcript isoform (**Figure 1E**, **Table 2**). An alternative ATG in frame within exon1, suspected to initiate translation of an elongated Cx29 protein with additional 11 N-terminal amino acid residues [NP\_536698] is covered by a consensus motif of a very low translational efficacy (1.7) inappropriate to initiate translation (Iida and Masuda, 1996; Kozak, 1997). Instead, translation (efficacy 3.3) is more likely to start with the ATG located further upstream (**Table 2**) but being out of frame. Conclusively, these data confirm that either the spliced or the unspliced consensus motif around the ATG at position (+1) will sustainably initiate translation of the Cx29 protein (**Figure 1E**).

Two independent primer combinations located in the putative 3'-untranslated region (3'-UTR) of exon2 should determine the downstream extension of the Cx29 transcript. PCR-fragments of calculated sizes (**Figure 1D**) indicated that about 3 kb might be considered as the (3'-UTR) of Exon2. Therefore, a predicted tandem termination region containing totally four polyA-signals (AAUAAA) from position +4283 to +4415 is likely to be used (Genescan tool/HUSAR/Heidelberg). Finally, one can estimate the size of both Cx29 transcript isoforms. Each contains an exon2 of about 4.3 kb, but one additionally obtains a spliced exon1 of

**Table 2 | An evaluation matrix suggested by Iida and Masuda (1996) helps to calculate the hypothetical efficacy of suspected translational initiation sites, termed more generally consensus motifs for translational initiation.**

Consensus motif of translation	Sequence	Position	Efficacy	% efficacy
High impact motif	[ccagggacaacATGg]	–	6.7	100
Cx29 unspliced motif	[cttggtgacaggATGt]	–12 to +4	5.0	75
Cx29 spliced motif (Ex1 to Ex2)	[atcaagtgcaggATGt]	–4839 to +4	4.2	63
Cx29 exon1 motif (out of frame)	[agcctgccaggaaATGa]	–4975 to –4960	3.8	57
Cx29 exon1 motif (in frame) see <b>Figure 1E</b>	[cctctgtggtgATGc]	–4850 to –4835	1.7	27
Cx29 intron motif	[ctttgcagaccATGg]	–102 to –87	3.3	50
Most inappropriate motif	[tggtttaggtgtATGc]	–	0.3	0

Sixteen bases around the bold ATG of the genomic sequence of connexin29 [acc. no. NC\_000071 or ENSMUSG00000056966] are included, each. Both consensus motifs, which confer the highest (6.7) and the lowest (0.3) absolute efficacy in terms of translational initiation are included in order to determine relative (%) efficacies. Note the relatively low efficacy (1.7) of the consensus motif around the in-frame ATG of exon1 which is suggested to initiate translation of a connexin29 protein harboring eleven additional amino acid residues at its N-terminus (MLLLELPKCR).

440 bp, and the other merely will contain an upstream extension of 160 bp.

#### NORTHERN AND IMMUNOBLOTH HYBRIDIZATION

Northern blot hybridizations using probes against Cx29, -32, -45, and -47 underscored only an abundant Cx29 expression in both types of differentiated as well as undifferentiated Oli-neu cells. Interestingly, expression of Cx47 is not present and Cx32 was only found weakly in undifferentiated Oli-neu cells (**Figure 2A**). This was, however, unexpected since Cx32 and Cx47 are connexin genes characterized to occur in oligodendrocytes (Kleopa et al., 2004; Li et al., 2004).

The absence of any signal in the lanes of the established rat adrenal pheochromocytoma cell line (PC12), having a neuronal background (Greene and Tischler, 1976) and used as control, underlined that glial connexins are absent from this cell type. RNA from HeLa wild-type and HeLa Cx45 transfectants was additionally blotted in order to exclude possible cross reactions of the Cx47 hybridization probe due to high sequence similarities with connexins45 (Teubner et al., 2001). As expected, hybridization probe against Cx45 only gave a signal with Cx45 transfected HeLa cells, coinciding well to the current opinion that Cx45 is expressed in neurons (Maxeiner et al., 2003) but not in PC12 cells. Concerning Cx29, however, two hybridization signals (4.4 kb and ~10 kb) have been

detected. Whereas the shorter fragment could be readily explained by summing up both exons amplified by RT-PCR (~4.6 kb), the larger signal is likely to represent the unspliced heteronuclear RNA of the Cx29 transcript, containing still the 4.8 kb intron.

Immunoblotting of lysates harvested from stably transfected Cx29 HeLa cells and from undifferentiated Oli-neu cells identified two different protein fractions of about 30 and 56 kDa (**Figure 2B**). This pattern is quite similar to results obtained after using homogenates from mouse sciatic nerves and lysates of transiently transfected Cx29 HeLa cells (Li et al., 2002), except that a third immunosignal of about 70 kDa was not detectable in our blots. Stably transfected HeLa cells expressing a fusion protein of Cx29 and eGFP instead showed a shift in both signals to 50 and 110 kDa. Thus, both HeLa cell lines express highly abundantly either the proper Cx29 protein or the fusion protein consisting of Cx29 and eGFP.

#### Cx29 IMMUNOFUORESCENCE ANALYSES OF STABLY TRANSFECTED HE LA CELLS

HeLa cells have already been transiently transfected with Cx29 cDNAs in order to establish cultured cells and protein lysates serving for positive controls to test the manufactured polyclonal antibodies against Cx29 (Zymed). Immunosignals have been detected in the cytoplasm and the periphery of these

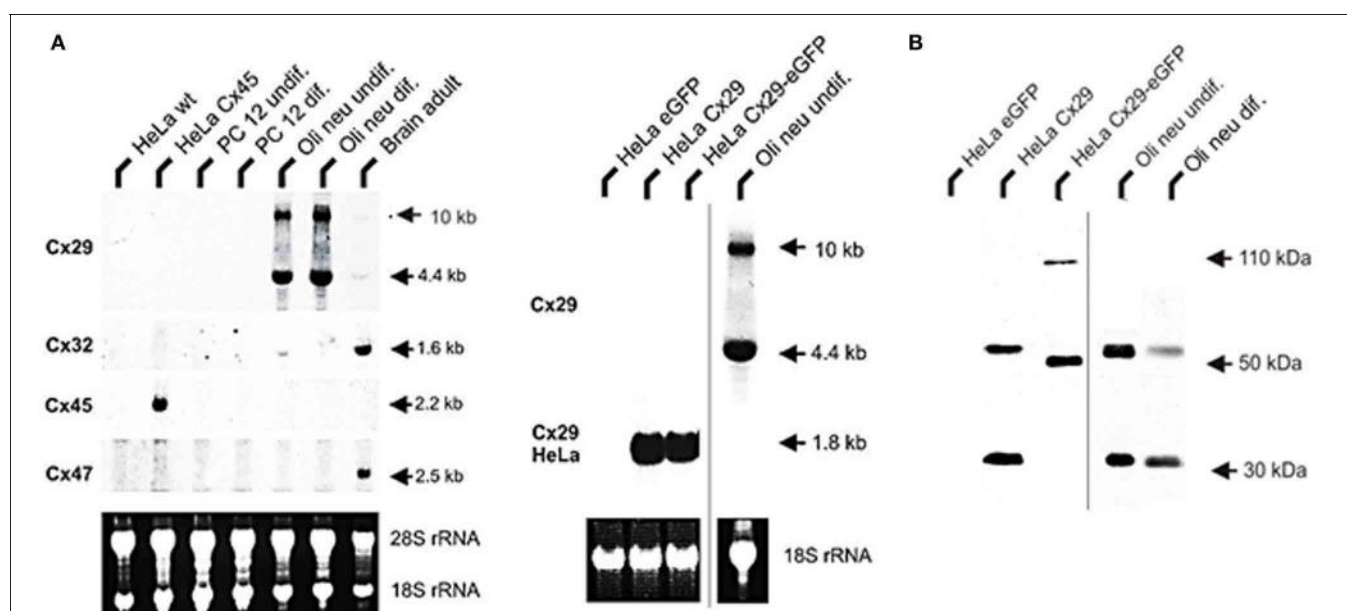


**FIGURE 2 |** Northern blot analysis of total RNA from HeLa, PC12, Oli-neu cells, and mouse adult brain. **(A)** A 4.4 kb signal representing Cx29 expression was detected highly abundant in undifferentiated as well as differentiated Oli-neu cells and weakly in brain. A 1.6 kb signal of Cx32 expression is distinctly visible in RNA from adult brain (100%) as control but is hardly detectable (3 vs. 14%) in Oli-neu cells (diff. and undif.), respectively. Cx47 expression (2.5 kb) is also evident in adult brain but missing in Oli-neu cells. No signals of oligodendroglial connexins were seen in HeLa wild type (wt), HeLa Cx45 transfectants, and PC12 cells (diff. or undif.). Additional hybridization signals at about 10 kb are visible after hybridizing the Cx29 probe against RNA of Oli-neu cells as well as from

adult brain. HeLa cells stably transfected with the tandem cloned connexin29 and eGFP reading frames (both of ~800 bp) either separated by a stop-codon or directly fused, yielded hybridization signals of the expected 1.8 kb. The blot was standardized by measuring the intensities of both the EtBr stained 18S- and 28S-rRNA. All signals have been documented after 3 weeks of exposure. **(B)** Immunoblot analysis of Cx29 and Cx29-eGFP stably transfected HeLa cells and Oli-neu cells (dif. and undif.) using the Cx29 polyclonal antibodies (Zymed). Two signals of about 30 and 56 kDa were prominent in Cx29 HeLa cells and Oli-neu cells. In the Cx29-eGFP HeLa cells, however, both signals seemed to be shifted to about 50 and 110 kDa due to the appended eGFP coding region.

transfectants. However, no functional dye or tracer transfer studies have been undertaken then (Li et al., 2002).

Distribution of Cx29 protein in stably transfected Cx29- and Cx29-eGFP cells is shown in **Figure 3**. The Cx29 protein is transferred to the membrane of the transfected HeLa cells forming gap junction like plaques between neighboring cells (**Figure 3F**). The Cx29-eGFP fusion protein, however, is only partially transported into the plasma membrane while aggregates also remained within the cytoplasm (see **Figures 3A,B,D**) indicated by the red immunofluorescence (**Figure 3B**) of Cx29 protein, that completely overlap with the green fluorescence evoked by the eGFP protein after merging both fluorescence signals (**Figure 3A**). Here, gap junction plaques seem less abundant compared to the Cx29 transfected HeLa cells, omitting eGFP. These results indicate that both transfected HeLa cell lines (Cx29 and Cx29-eGFP) express and process Cx29 protein to their membranes so that gap

junction like plaques can be formed between adjacent cells. It cannot be excluded that the observed aggregation of the Cx29-eGFP fusion protein might be induced by the eGFP protein. Therefore, Cx29-eGFP HeLa transfectants were omitted from further functional studies.

#### DYE AND TRACER INJECTIONS INTO Cx29 HeLa CELLS

To examine if molecules can pass through Cx29-mediated gap junction channels, permeability was investigated after injection of Lucifer Yellow ( $M_r$  488, net charge -2) or neurobiotin ( $M_r$  287, net charge +1) into one cell of a cluster. Neither HeLa wild-type cells nor Cx29 stably-transfected HeLa cells showed dye transfer after injection with Lucifer Yellow (**Figure 4A**). Cx43 stably-transfected HeLa cells used as control demonstrated the frequently described abundant spread of Lucifer Yellow (around 80% of first order neighboring cells surrounding the injected one;

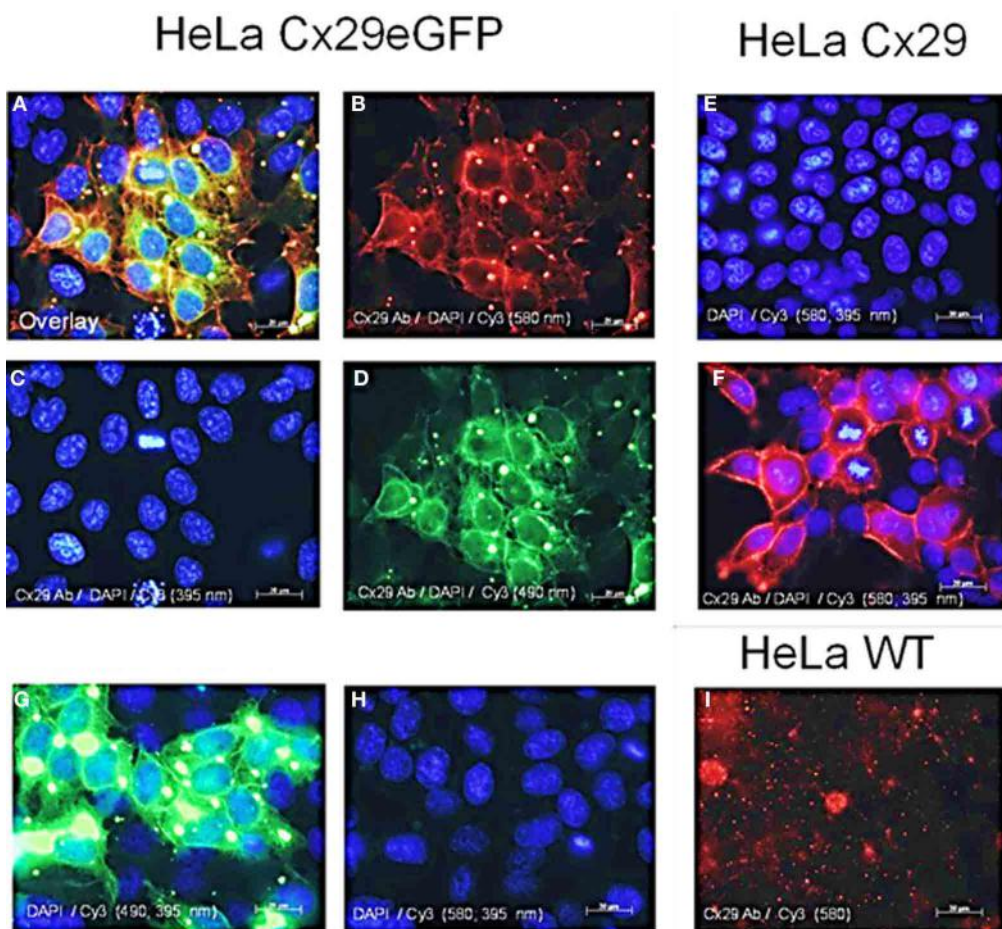


**FIGURE 3 | Immunofluorescence analysis of stably transfected Cx29-HeLa cells. (A–D)** HeLa cells transfected with a construct coding for Cx29-eGFP fusion protein. **(A)** Merged picture of **(B–D)**. **(B)** Immunofluorescence after applying the Cy3 filter (580 nm) indicating Cx29 antibody distribution. **(C)** Staining of the cellular nuclei of the Cx29-eGFP transfectants with DAPI. **(D)** Green fluorescence of the eGFP reflects the distribution of the Cx29-eGFP fusion protein. **(E)** Staining of the cellular nuclei of the Cx29 transfectants with DAPI. Application of single secondary Cy3 antibody excludes cross-reactivity of

the secondary antibody. **(F)** Distribution of the Cx29 protein and cellular nuclei after a double staining with Cx29 antibodies, DAPI, and Cy3. **(G,H)** Cy3 and filter control. Omitting the primary Cx29 antibody but instead applying DAPI and Cy3 allows to control if the intense green signals detectable through the FITC filter (490 nm) in **(G)** also pass, at least in traces, through the Cy3 filter (580 nm), thus mimicking Cx29 signals. Furthermore, the Cy3 secondary antibody does not cross react. **(I)** No cross reactivity is seen with HeLa wild type cells, neither with Cx29 antibodies nor with secondary Cy3 antibodies.

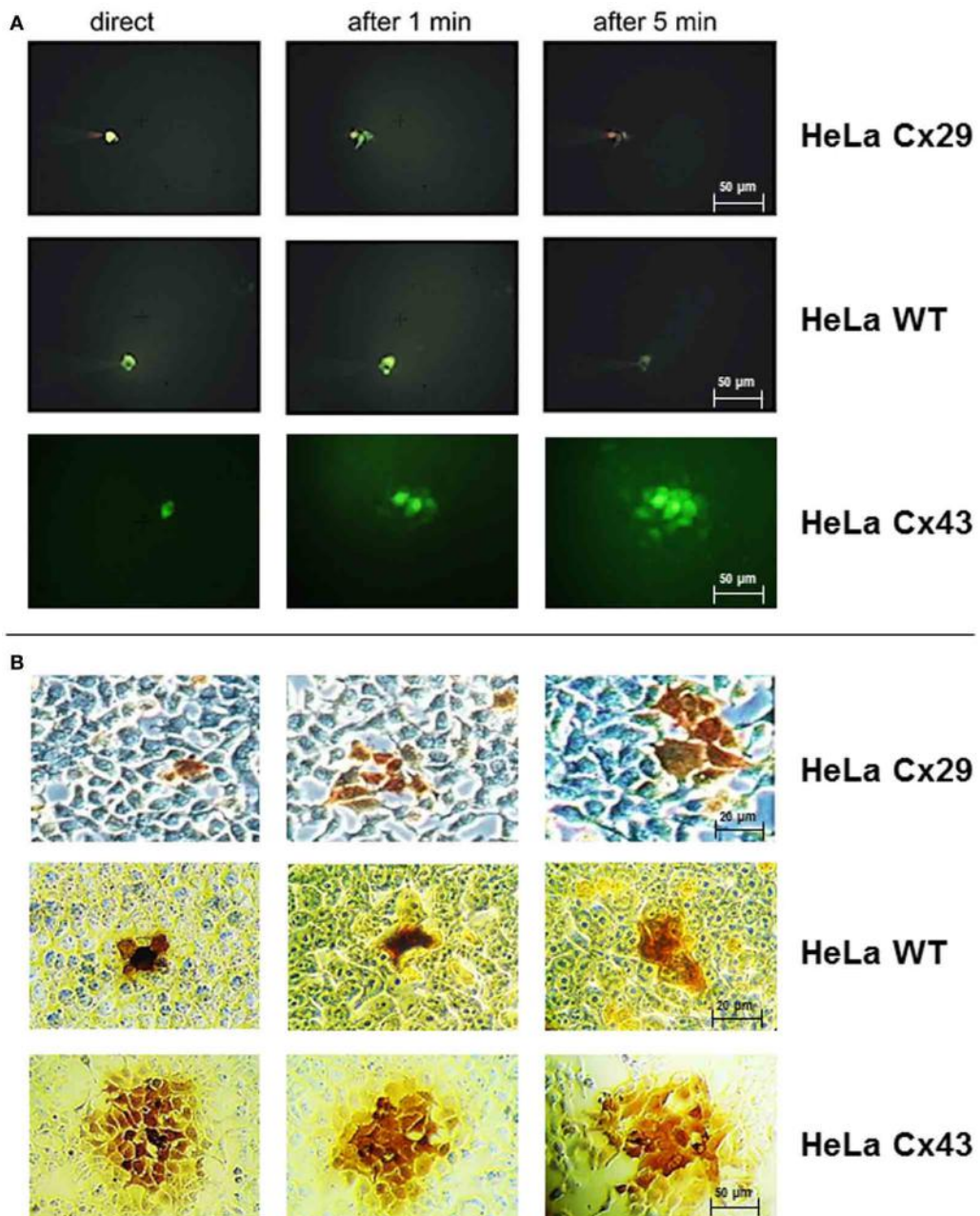


**FIGURE 4 |** Dye and tracer injections into Cx29-transfected HeLa cells, untransfected HeLa wild-type cells, and Cx43-transfected HeLa cells.

(A) Absence of any spreading of microinjected Lucifer Yellow into neighboring cells in both HeLa wild type as well as Cx29-transfected cells indicated the impermeability of Cx29 gap junction channels for this dye. In contrast, Lucifer Yellow spreads readily into neighboring Cx43-transfected HeLa cells after

injection. (B) Corresponding three single neurobiotin microinjections in Cx29-transfected, wild-type, and Cx43-transfected HeLa cells fixed and stained after 30 min. The transfer of neurobiotin into an average of 2.4 of about 7 next neighboring cells is similar after injection of HeLa wild-type and Cx29-transfected HeLa cells and in contrast to Cx43-transfected HeLa cells. In these cells tracer commonly spreads into the third order of neighboring cells.

$n = 15$ ; see Elfgang et al., 1995), that have been measured after 5 min.

The transfer of the tracer molecule neurobiotin was examined up to 30 min after injection. In both HeLa wild type cells ( $n = 27$ ) and Cx29 stably-transfected HeLa cells ( $n = 15$ ) only about 35% of the first order neighboring cells were stained (Figure 4B), probably due to a background spread after the

long incubation time after injection. Additionally, tracer transfer to higher order surrounding cells was always negligible and shorter incubation times as well as changing to EtBr or Propidium iodide (data not shown) revealed no difference between stably-transfected and wild-type cells. As control, transfer between Cx43 stably-transfected HeLa cells ( $n = 15$ ) was about 82% of first order neighboring cells, 99 and 53% of second, respectively third

order neighboring cells after 5 min. Thus, there is no coupling measurable between Cx29 stably-transfected HeLa cells.

#### Cx29 IMMUNOFLUORESCENCE ANALYSES OF Oli-Neu CELLS

Northern blot as well as immunoblot results suggested that Cx29 is highly expressed in both undifferentiated as well as in differentiated Oli-neu cells. In order to determine the subcellular distribution of Cx29 protein, immunofluorescence analyses have been performed with differentiated Oli-neu cells (and as a completion with undifferentiated Oli-neu cells, see **Figure A2**). Immunofluorescence signals of antibodies against

Cx29 (**Figure 5A**) implied that the Cx29 protein is transported properly into their plasma membranes, regardless if cells are isolated or clustered in small groups. Omitting the primary antibody leads to an absence of any immunofluorescence signal, excluding cross reactivity of the secondary antibody Cy3 (**Figure 5B**). Furthermore, due to stronger signals between closely attached cells, it became apparent, that there might be an accumulation of Cx29 resulting upon formation of gap junction plaques between adjacent cells. Thus, under cell culture conditions differentiated Oli-neu cells might constitute a cell line to study functional Cx29 gap junction coupling. Long-term culture procedures will hence

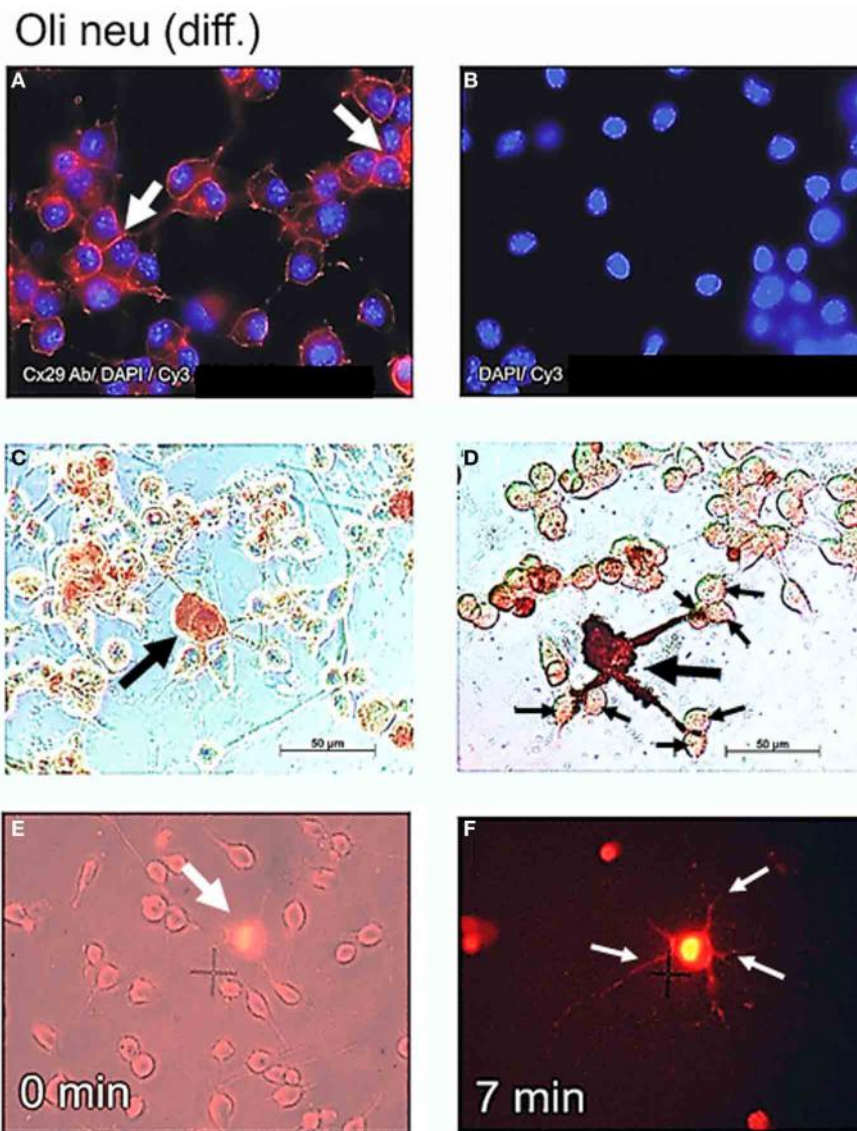


**FIGURE 5 | Cx29 immunofluorescence analyses and microinjections of differentiated Oli-neu cells.** (A) Distribution of the Cx29 protein mostly in plasma membranes (arrows) applying Cx29-specific and Cy3 coupled secondary antibodies in relation to the cellular nuclei after DAPI staining. (B) Omitting primary Cx29 antibodies excluded cross reactivity of Cy3 antibodies with Oli-neu cells. (C and D) Two examples of Oli-neu cells microinjected with neurobiotin and stained thereafter (arrow) (C) No

neurobiotin transfer into both cells directly attached below was detectable. (D) After filling one cell (large arrow), neurobiotin readily spreads into the three protrusions but did not migrate further into adjacent cells at their ends (small arrows). (E) Combined UV light- and trans-illumination identified the Etbr-microinjected Oli-neu cell (arrow). (F) Only the Etbr filled soma and the protrusions of the injected cell are faintly visible after 7 min (arrows).

support the attachment of growing cells, whereas culturing for a shorter period might allow examination of hemi-channel activity within separated cells.

### MEASUREMENT OF DIRECT GAP JUNCTION COUPLING BETWEEN Oli-Neu CELLS

Highly abundant subcellular distribution of Cx29 protein in the plasma membranes of differentiated Oli-neu cells (see **Figure 5A**) suggested direct coupling between closely attached cell bodies or their developed protrusions. However, after microinjection of Lucifer yellow and neurobiotin into differentiated Oli-neu cells, either adjacent to neighboring cells (**Figure 5C**) or linked by protrusions to its neighbors (**Figure 5D**) these tracers were kept within the injected cells and did never spread into attached or connected cells. **Figure 5D** underlines that neurobiotin is only accumulated within the injected cell and its protrusions. These results could be confirmed after microinjection of Etbr into differentiated Oli-neu cells (**Figures 5E,F**). From totally 20 Etbr injections only two exceptions of Etbr spread into the next neighbor cells was found. Microinjected cells had an average of 0.7 next neighbors and about 6 cells to which protrusions are forwarded.

### DYE UPTAKE MEASUREMENTS OF Oli-Neu CELLS

The high abundance of Cx29 protein in the plasma membranes of differentiated Oli-neu cells might implicate the formation of hemi-channels. In order to functionally determine detached hemi-channels, we applied Etbr to differentiated Oli-neu cells in culture and also tried to inhibit putative dye uptake by applying commonly used gap junction blockers like heptanol and octanol. This procedure was established by Contreras et al. (2002) with cultured cortical astrocytes. The authors demonstrated that an induced opening of distant connexin43 gap junction hemi-channels by inhibition of glycolytic and oxidative metabolism could be blocked significantly i.e., by octanol. In our study, we omitted metabolic inhibition of the cultured Oli-neu cells in order to initially analyze Cx29 hemi-channel function under normal physiological conditions. In 12 independent applications Etbr was directly added to the culture media on the top of the cells in the visible field and an average of 4.9 presumably cellular artifacts showed an immediate dye uptake after ~55 s, whereas an average of 20.5 cells in the visual field weakly took up the dye just after 2 min. To reduce background staining of Etbr in culture media, cells have been washed and documented after 4 min (**Figure 6A**). Application of octanol to the cell culture 5 min before dye application ( $n = 13$ ) completely blocked the uptake of Etbr in about 19.9 cells of the visual field, whereas the 4.8 presumably cellular artifacts showed staining already after ~30 s (**Figure 6B**). To increase the sensitivity of the uptake measurement the concentration of the applied Etbr was five-fold decreased. Again, Etbr uptake ( $n = 6$ ) without gap junction blocker was seen on average in 7.6 presumably cellular artifacts after ~20 s and in all 22.8 cells of the field after ~4 min (**Figure 6C**). Application of octanol before the release of Etbr ( $n = 2$ ) again completely blocked the uptake of dye in all 16 cells whereas 5 cellular artifacts on average readily took up the dye after 15 s (**Figure 6D**). We additionally applied the gap junction blocker heptanol in a serial trial of four micropipette applications of Etbr at a higher concentration (12.5 mM). In no

case dye uptake could be monitored in at least 20 visible cells but the mean 2 putative cellular artifacts had already incorporated the dye after 3.6 s (not shown). The results of the dye uptake measurements can be summarized accordingly: (1) Although Cx29 protein is prominent in the plasma membrane of single Oli-neu cells, the uptake of the extracellular dye Etbr remains dispensable. (2) The subtle uptake of the dye after, at least 4 min could clearly be prevented by gap junction hemi-channel blockers like octanol or heptanol.

It is now tempting to speculate, whether putative hemi-channels are largely closed in the plasma membrane of Oli-neu cells under normal culture conditions. A presumed transfer through these hemi-channels (Li et al., 1996) would allow a subtle uptake of Etbr that could be prevented after application of commonly used gap junction blockers. Already before, there have been no indications of functional hemi-channels of mouse Cx29 (Altevogt et al., 2002) and its human ortholog Cx31.3 (Sargiannidou et al., 2008) in transfected HeLa cells.

## DISCUSSION

### GENE STRUCTURE OF MOUSE CONNEXIN29

A close genomic characterization implied that a spliced as well as unspliced transcript isoform can be expressed from mouse Cx29 locus. Because both the splice acceptor and consensus motif for translational initiation nearly overlap, these isoforms indeed differ in their respective motifs but only with negligible effect on translational efficacy (Iida and Masuda, 1996). Northern blot hybridization revealed a prominent 4.4 and 10 kb band comprising the expression of both transcript isoforms that coincides in sciatic nerve and brain as well as in Oli-neu cells. This is reminiscent of the expression of different Cx32 transcript isoforms in sciatic nerve (Neuhaus et al., 1996; Söhl et al., 2001b).

Calculation of translational efficacies of various consensus motifs let it appear implausible that the prominent but predicted ATG start codon on exon1 [NP\_536698], being in frame with the coding region on exon2 after splicing, is used *in vivo*. However, if cell-type specific factors might support initiation of translation at least partially at this ATG on exon1, then Cx29 proteins are likely to contain additional N-terminal amino acids (MLLELPIKCR) unusual to other connexin proteins.

### EXPRESSION OF MOUSE CONNEXIN29

Zymed anti-Cx29 antisera gave similar and intense results when applied to Oli-neu cells in culture or to Oli-neu lysates in immunoblots, respectively. Mouse brain regions enriched of myelinated oligodendrocytes also showed intense immunofluorescent signals after antibody application (see **Figure A1**). Stable Cx29-transfected HeLa cells yielded a punctuated staining pattern in their membranes. Immunoblotting of lysates from stable Cx29-transfected HeLa cells also detected two different protein fractions of about 30 and 56 kDa, comparable with lysates of either Oli-neu cells or tissue homogenates collected from sciatic nerve (Li et al., 2002). The specificity of the applied Cx29-antibodies was finally proven after targeted deletion of the Cx29 gene from the mouse genome. This also unraveled the fact that the 56 kDa protein fraction must be related to Cx29, possibly a stable dimer form of Cx29, since it disappeared like the 30 kDa signal after

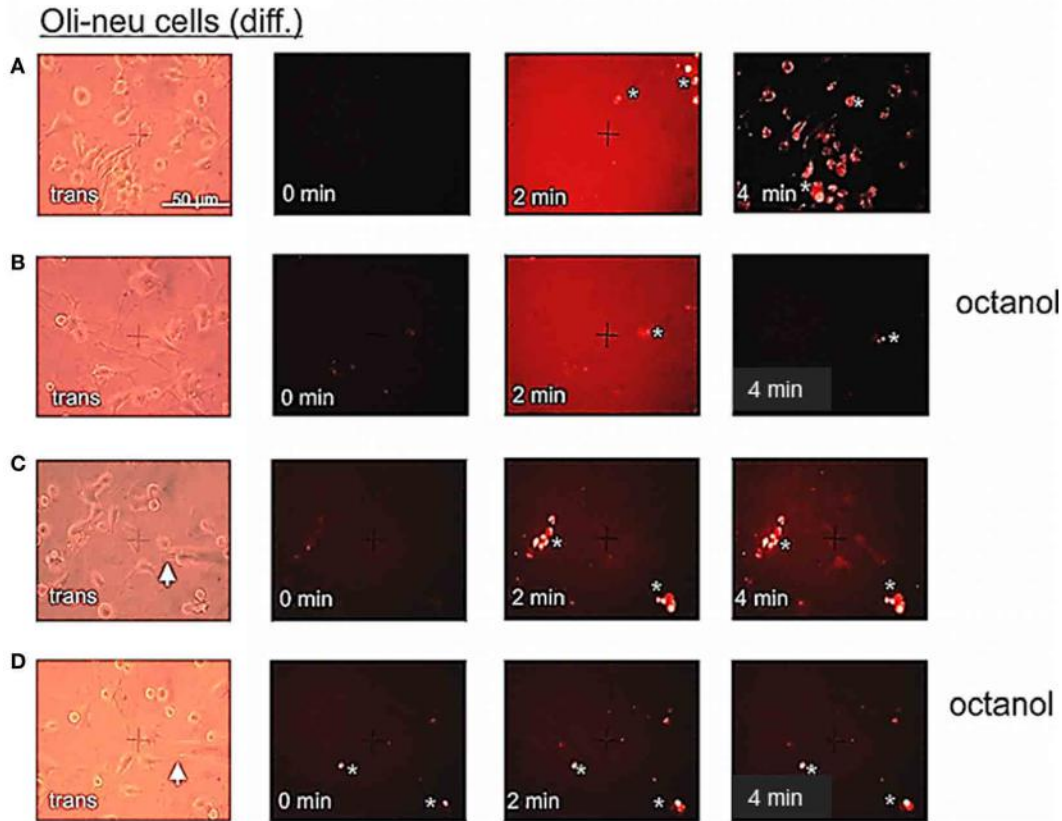


**FIGURE 6 |** Etbr uptake by differentiated Oli-neu cells can be blocked by octanol. **(A)** Phase contrast image (trans) of a culture dish sector before application of 2.5 µl Etbr (1 mg/ml) directly to the medium (0 min). After 4 min, cells were briefly washed in PBS and photographed thereafter. Oli-neu cells of a different sector are slightly stained with Etbr. **(B)** Cells have been incubated with 1 mM octanol 5 min before dye application (0 min). After 4 min, cells have been washed and the same sector has

been photographed. **(C)** Direct application (0 min) of 0.5 µl Etbr (5 mM) by a micropipette (white arrow) to the cultured cells. After 4 min, a faint Etbr staining of all cells next to the pipette tip is visible. **(D)** Cells have been incubated with 1 mM octanol 5 min before dye application. After 4 min very faint Etbr staining of cells in the vicinity of the pipette tip was detectable. Presumably cellular artifacts are directly stained after application of Etbr in **(A,B,C)** and **(D)**.

immunoblotting of brain and sciatic nerve homogenates from Cx29 ( $-/-$ ) mice (Eiberger et al., 2006). Even the intense (often cytoplasmic) immunofluorescence labeling within presumably oligodendroglial cells of the CNS from wild-type animals was absent in Cx29 deficient mice (Eiberger et al., 2006). It became evident that these cytoplasmic signals do not reflect an unspecific cross-reactivity of the antibody to myelin, but represent Cx29 protein processed or stored within oligodendroglial cells. Therefore, the strong immunofluorescence signals in Oli-neu cell and the immunoblot signals of their lysates might reflect high abundant Cx29 protein expression. Conclusively, the Oli-neu cell culture system contains a high abundance of Cx29 mRNA and protein, thus facilitating the analysis of transcript structures as well as protein localization.

#### LOCALIZATION AND FUNCTION OF MOUSE CONNEXIN29

In contrast to Cx32 and Cx47, only little is known about the precise position and function of Cx29 protein within myelin. Cx29 seems to be located at the internodal and juxtaparanodal regions of small myelin sheaths (Altevogt et al., 2002) but does not co-localize with the two other oligodendroglial connexins

(Altevogt and Paul, 2004). Homotypic Cx29 channels within intracellular membranes of myelin or hemi-channels are suspected to allow glial uptake of K<sup>+</sup> from the small, extracellular space between axon and Schwann cells (Brophy, 2001) or likewise between axon and oligodendrocyte (Altevogt and Paul, 2004). With respect to their immunolocalization, Cx29 (hemi)-channels might exist in close vicinity to Kv 1.1 and Kv 1.2 potassium channels, also predicted in juxtaparanodal axonal membranes (Arroyo and Scherer, 2000; Altevogt et al., 2002).

However, disruption of the Cx29 gene leads to no obvious phenotypical alteration or abnormalities. Cx29 ( $-/-$ ) mice are viable, healthy, and fertile (Altevogt and Paul, 2004; Eiberger et al., 2006). Both studies speculated that the function of Cx29 is either dispensable or compensated by redundancy of both the other oligodendroglial connexins Cx32 and Cx47, but the sub-cellular detachment of Cx29 to Cx32 and Cx47 is obscuring this hypothesis. Nevertheless, replacement of the Cx29 coding region by a LacZ reporter gene identified novel Cx29 expressing cell types and tissues, like Bergmann glia cell of the cerebellum (Altevogt and Paul, 2004) or the postnatal cochlea (Eiberger et al., 2006). Interestingly, at least one missense mutation (E269D) in

the human ortholog of Cx29 is discussed to contribute to NSHI. This mutation disturbs, at least, the formation of gap junctions after co-transfections in the HeLa cell culture system (Hong et al., 2010).

Here we have expanded the unexpected expression profile of Cx29 on Oli-neu cells, which derived from stably *t-neu* tyrosine kinase transfected O-2A cells that provide a developmental state comparable to neonatal oligodendroglial precursor cells *in vivo* (Jung et al., 1995). This extended our Northern blot result with RNA from different perinatal stages of mouse total brain, implying that Cx29 is not up-regulated before postnatal day 7 (Söhl et al., 2001a). Thus, it might be possible that high abundance of Cx29 expression reflects an auspicious side effect due to transfection of the *t-neu* tyrosine kinase. In this case, differentiated Oli-neu cells might serve as a suitable cell culture system to study the function of Cx29, since both the other oligodendroglial connexins Cx32 and Cx47, are rather absent from these cells. Interestingly, induction of differentiation with dibutyryl cAMP continuously suppressed Cx32 and Cx47. This is in contrast to the co-cultivation of Oli-neu cells with non-touching astrocytes, which have a significant impact on the expression levels of genes supporting myelination. Both Cx29 and Cx47 have been among these genes, being up-regulated due to the proximity of astrocytes (Iacobas and Iacobas, 2010).

Cx29 gap junction channels remain closed between neighboring Cx29, Cx29-eGFP HeLa cell transfectants, between undifferentiated and differentiated Oli-neu and their protrusions, respectively. This outcome is in accordance to other studies (Altevogt et al., 2002; Ahn et al., 2008). Although the oligodendroglial precursor cell line Oli-neu has, compared to stably-transfected HeLa cells, advantages like proper cytoplasmic

conditions enriched with putative co-factors for channel function or the native genomic vicinity around the Cx29 gene, it rather has no impact on Cx29 channel opening. Despite a more convenient environment, selective signals for opening still seem to be needed, yet. Again, proximity of astrocytes (Iacobas and Iacobas, 2010) might support Oli-neu cells with distinct signals for channel opening. Co-cultures of Oli-neu cells with neurons *in vitro* and *in vivo* are likely to produce also important extracellular signals.

In accordance to the localization of Cx29 protein in the plasma membrane of single Oli-neu cells, we cannot exclude Cx29 to form hemi-channels. However, dye-uptake studies after application of two different hemi-channel blockers suggested that putative hemi-channels are largely closed under recommended cell culture conditions, which might diverge from physiological condition *in vivo*. Even though extracellular calcium (Hofer and Dermietzel, 1998) or metabolic stress (Contreras et al., 2002) have been reported to induce Cx43 hemi-channel opening in astrocytes, the physiological signals to open Cx29 hemi-channels under non stressed conditions remain to be discovered. Therefore, this Oli-neu cell culture system might represent a well suited tool to functionally explore these signals.

## ACKNOWLEDGMENTS

We thank Prof. J. Trotter for kindly providing the Oli-neu cell line to our laboratory. Furthermore, we thank Gerda Hertig and Joana Stegemann (former Fischer) both from Bonn for their excellent technical assistance. Work was done in the Institute of Molecular Genetics in Bonn, Germany. This study was supported by the German Research Foundation through the Collaborative Research Centre (SFB-645), project Z3 to Joachim Degen.

## REFERENCES

- Ahn, M., Lee, J., Gustafsson, A., Enriquez, A., Lancaster, E., Sul, J. Y., et al. (2008). Cx29 and Cx32, two connexins expressed by myelinating glia, do not interact and are functionally distinct. *J. Neurosci. Res.* 86, 992–1006. doi: 10.1002/jnr.21561
- Altevogt, B. M., Kleopa, K. A., Postma, F. R., Scherer, S. S., and Paul, D. L. (2002). Connexin29 is uniquely distributed within myelinating glial cells of the central and peripheral nervous systems. *J. Neurosci.* 22, 6458–6470.
- Altevogt, B. M., and Paul, D. L. (2004). Four classes of intercellular channels between glial cells in the CNS. *J. Neurosci.* 24, 4313–4323.
- Anzini, P., Neuberg, D. H., Schachner, M., Nelles, E., Willecke, K., Zielasek, J., et al. (1997). Structural abnormalities and deficient maintenance of peripheral nerve myelin in mice lacking the gap junction protein connexin 32. *J. Neurosci.* 17, 4545–4551.
- Arroyo, E. J., and Scherer, S. S. (2000). On the molecular architecture of myelinated fibers. *Histochem. Cell Biol.* 113, 1–18.
- Brophy, P. J. (2001). Axoglial junctions: separate the channels or scramble the message. *Curr. Biol.* 11, R555–R557. doi: 10.1016/S0960-9822(01)00341-4
- Byravan, S., Foster, L. M., Phan, T., Verity, A. N., and Campagnoni, A. T. (1994). Murine oligodendroglial cells express nerve growth factor. *Proc. Natl. Acad. Sci. U.S.A.* 91, 8812–8816. doi: 10.1073/pnas.91.19.8812
- Contreras, J. E., Sanchez, H. A., Eugenin, E. A., Speidel, D., Theis, M., Willecke, K., et al. (2002). Metabolic inhibition induces opening of unapposed connexin 43 gap junction hemichannels and reduces gap junctional communication in cortical astrocytes in culture. *Proc. Natl. Acad. Sci. U.S.A.* 99, 495–500. doi: 10.1073/pnas.012589799
- De Sousa, P. A., Valdimarsson, G., Nicholson, B. J., and Kidder, G. M. (1993). Connexin trafficking and the control of gap junction assembly in mouse preimplantation embryos. *Development* 117, 1355–1367.
- Eiberger, J., Kibschull, M., Strenzke, N., Schober, A., Büssow, H., Wessig, C., et al. (2006). Expression pattern and functional characterization of connexin29 in transgenic mice. *Glia* 53, 601–611. doi: 10.1002/glia.20315
- Elfgang, C., Eckert, R., Lichtenberg-Frate, H., Butterweck, A., Traub, O., Klein, R. A., et al. (1995). Specific permeability and selective formation of gap junction channels in connexin-transfected HeLa cells. *J. Cell Biol.* 129, 805–817. doi: 10.1083/jcb.129.3.805
- Greene, L. A., and Tischler, A. S. (1976). Establishment of a noradrenergic clonal line of rat adrenal pheochromocytoma cells which respond to nerve growth factor. *Proc. Natl. Acad. Sci. U.S.A.* 73, 2424–2428. doi: 10.1073/pnas.73.7.2424
- Hofer, A., and Dermietzel, R. (1998). Visualization and functional blocking of gap junction hemichannels (connexons) with antibodies against external loop domains in astrocytes. *Glia* 24, 141–154. doi: 10.1002/(SICI)1098-1136(199809)24:1<141::AID-GLIA>3.0.CO;2-R
- Hong, H. M., Yang, J. J., Su, C. C., Chang, J. Y., Li, T. C., and Li, S. Y (2010). A novel mutation in the connexin 29 gene may contribute to nonsyndromic hearing loss. *Hum. Genet.* 127, 191–199. doi: 10.1007/s00439-009-0758-y
- Horst, M., and Hasilik, A. (1991). Expression and maturation of human cathepsin D in baby hamster kidney cells. *Biochem. J.* 273, 355–361.
- Iacobas, S., and Iacobas, D. A. (2010). Astrocyte proximity modulates the myelination gene fabric of oligodendrocytes. *Neuron Glia Biol.* 5, 1–13.
- Iida, Y., and Masuda, T. (1996). Strength of translation initiation signal sequence of mRNA as studied by quantification method: effect of nucleotide substitutions upon translation efficiency in rat pre-pro-insulin mRNA. *Nucleic Acids Res.* 24, 3313–3316. doi: 10.1093/nar/24.17.3313

- Jung, M., Kramer, E., Grzenkowski, M., Tang, K., Blakemore, W., Aguzzi, A., et al. (1995). Lines of murine oligodendroglial precursor cells immortalized by an activated neu tyrosine kinase show distinct degrees of interaction with axons *in vitro* and *in vivo*. *Eur. J. Neurosci.* 7, 1245–1265. doi: 10.1111/j.1460-9568.1995.tb01115.x
- Kandel, E. R., Schwartz, J. H., and Jessell, T. M. (2000). *Principles of Neural Science, Chapter 3, 4th Edn.* New York, NY: McGraw-Hill, Inc.
- Kleopa, K. A., Orthmann, J. L., Enriquez, A., Paul, D. L., and Scherer, S. S. (2004). Unique distributions of the gap junction proteins connexin29, connexin32, and connexin47 in oligodendrocytes. *Glia* 47, 346–357. doi: 10.1002/glia.20043
- Kleopa, K. A., Orthmann-Murphy, J., and Sargiannidou, I. (2010). Gap junction disorders of myelinating cells. *Rev. Neurosci.* 21, 397–419. doi: 10.1515/REVNEURO.2010.21.5.397
- Kozak, M. (1989). The scanning model for translation: an update. *J. Cell Biol.* 108, 229–241. doi: 10.1083/jcb.108.2.229
- Kozak, M. (1997). Recognition of AUG and alternative initiator codons is augmented by G in position +4 but is not generally affected by the nucleotides in positions +5 and +6. *EMBO J.* 16, 2482–2492. doi: 10.1093/emboj/16.9.2482
- Li, X., Ionescu, A. V., Lynn, B. D., Lu, S., Kamasawa, N., Morita, M., et al. (2004). Connexin47, connexin29 and connexin32 co-expression in oligodendrocytes and Cx47 association with zonula occludens-1 (ZO-1) in mouse brain. *Neuroscience* 126, 611–630. doi: 10.1016/j.neuroscience.2004.03.063
- Li, H., Liu, T. F., Lazrak, A., Peracchia, C., Goldberg, G. S., Lampe, P. D., et al. (1996). Properties and regulation of gap junctional hemichannels in the plasma membranes of cultured cells. *J. Cell Biol.* 134, 1019–1030. doi: 10.1083/jcb.134.4.1019
- Li, X., Lynn, B. D., Olson, C., Meier, C., Davidson, K. G., Yasumura, T., et al. (2002). Connexin29 expression, immunocytochemistry and freeze-fracture replica immunogold labelling (FRIL) in sciatic nerve. *Eur. J. Neurosci.* 16, 795–806. doi: 10.1046/j.1460-9568.2002.02149.x
- Maxeiner, S., Krüger, O., Schilling, K., Traub, O., Urschel, S., and Willecke, K. (2003). Spatiotemporal transcription of connexin45 during brain development results in neuronal expression in adult mice. *Neuroscience* 119, 689–700. doi: 10.1016/S0306-4522(03)00077-0
- Menichella, D. M., Goodenough, D. A., Sirkowski, E., Scherer, S. S., and Paul, D. L. (2003). Connexins are critical for normal myelination in the CNS. *J. Neurosci.* 23, 5963–5973.
- Nelles, E., Bützler, C., Jung, D., Temme, A., Gabriel, H. D., Dahl, U., et al. (1996). Defective propagation of signals generated by sympathetic nerve stimulation in the liver of connexin32-deficient mice. *Proc. Natl. Acad. Sci. U.S.A.* 93, 9565–9570. doi: 10.1073/pnas.93.18.9565
- Neuhaus, I. M., Bone, L., Wang, S., Ionasescu, V., and Werner, R. (1996). The human connexin32 gene is transcribed from two tissue-specific promoters. *Biosci. Rep.* 16, 239–248. doi: 10.1007/BF01207338
- Odermatt, B., Wellershaus, K., Wallraff, A., Seifert, G., Degen, J., Euwens, C., et al. (2003). Connexin 47 (Cx47)-deficient mice with enhanced green fluorescent protein reporter gene reveal predominant oligodendrocytic expression of Cx47 and display vacuolized myelin in the CNS. *J. Neurosci.* 23, 4549–4559.
- Padgett, R. A., Grabowski, P. J., Konarska, M. M., Seiler, S., and Sharp, P. A. (1986). Splicing of messenger RNA precursors. *Annu. Rev. Biochem.* 55, 1119–1150.
- Richardson, W. D., Smith, H. K., Sun, T., Pringle, N. P., Hall, A., and Woodruff, R. (2000). Oligodendrocyte lineage and the motor neuron connection. *Glia* 29, 136–142. doi: 10.1002/(SICI)1098-1136(20000115)29:2<136::AID-GIA6>3.0.CO;2-G
- Sambrook, J., and Russel, D. W. (2001). *Molecular Cloning: A laboratory Manual, 3rd Edn.* Cold Spring Harbor, NY: Cold Spring Harbor Laboratory Press.
- Sargiannidou, I., Ahn, M., Enriquez, A. D., Peinado, A., Reynolds, R., Abrams, C., et al. (2008). Human oligodendrocytes express Cx31.3: function and interactions with Cx32 mutants. *Neurobiol. Dis.* 30, 221–233. doi: 10.1016/j.nbd.2008.01.009
- Scherer, S. S., Xu, Y. T., Messing, A., Willecke, K., Fischbeck, K. H., and Jeng, L. J. (2005). Transgenic expression of human connexin32 in myelinating Schwann cells prevents demyelination in connexin32-null mice. *J. Neurosci.* 25, 1550–1559. doi: 10.1523/JNEUROSCI.3082-04.2005
- Scherer, S. S., Xu, Y. T., Nelles, E., Fischbeck, K., Willecke, K., and Bone, L. J. (1998). Connexin32-null mice develop demyelinating peripheral neuropathy. *Glia* 24, 8–20. doi: 10.1002/(SICI)1098-1136(199809)24:1<8::AID-GLIA2>3.0.CO;2-3
- Söhl, G., Degen, J., Teubner, B., and Willecke, K. (1998). The murine gap junction gene connexin36 is highly expressed in mouse retina and regulated during brain development. *FEBS Lett.* 428, 27–31.
- Söhl, G., Eiberger, J., Jung, Y. T., Kozak, C. A., and Willecke, K. (2001a). The mouse gap junction gene connexin29 is highly expressed in sciatic nerve and regulated during brain development. *Biol. Chem.* 382, 973–978. doi: 10.1515/BC.2001.122
- Söhl, G., Theis, M., Hallas, G., Brambach, S., Dahl, E., Kidder, G., et al. (2001b). A new alternatively spliced transcript of the mouse connexin32 gene is expressed in embryonic stem cells, oocytes, and liver. *Exp. Cell Res.* 266, 177–186. doi: 10.1006/excr.2001.5209
- Söhl, G., and Willecke, K. (2003). An update on connexin genes and their nomenclature in mouse and man. *Cell Commun. Adhes.* 10, 173–180. doi: 10.1080/cac.10.4-6.173.180
- Sonntag, S., Söhl, G., Dobrowolski, R., Zhang, J., Theis, M., Winterhager, E., et al. (2009). Mouse lens connexin23 (Gje1) does not form functional gap junction channels but causes enhanced ATP release from HeLa cells. *Eur. J. Cell Biol.* 88, 65–77. doi: 10.1016/j.ejcb.2008.08.004
- Tang, W., Zhang, Y., Chang, Q., Ahmad, S., Dahlke, I., Yi, H., et al. (2006). Connexin29 is highly expressed in cochlear Schwann cells, and it is required for the normal development and function of the auditory nerve of mice. *J. Neurosci.* 26, 1991–1999. doi: 10.1523/JNEUROSCI.5055-05.2006
- Teubner, B., Odermatt, B., Güldenagel, M., Söhl, G., Degen, J., Bukauskas, F., et al. (2001). Functional expression of the new gap junction gene connexin47 transcribed in mouse brain and spinal cord neurons. *J. Neurosci.* 21, 1117–1126.
- Theis, M., Söhl, G., Eiberger, J., and Willecke, K. (2005). Emerging complexities in identity and function of glial connexins. *Trends Neurosci.* 28, 188–195. doi: 10.1016/j.tins.2005.02.006
- Tress, O., Maglione, M., Zlomuzica, A., May, D., Dicke, N., Degen, J., et al. (2011). Pathologic and phenotypic alterations in a mouse expressing a connexin47 missense mutation that causes Pelizaeus-Merzbacher-like disease in humans. *PLoS Genet.* 7:e1002146. doi: 10.1371/journal.pgen.1002146
- Uhlenberg, B., Schuelke, M., Ruschendorf, F., Ruf, N., Kaindl, A. M., Henneke, M., et al. (2004). Mutations in the gene encoding gap junction protein alpha 12 (connexin 46.6) cause Pelizaeus-Merzbacher-like disease. *Am. J. Hum. Genet.* 75, 251–260. doi: 10.3410/f.1022277.253682
- Willecke, K., Eiberger, J., Degen, J., Eckardt, D., Romualdi, A., Güldenagel, M., et al. (2002). Structural and functional diversity of connexin genes in the mouse and human genome. *Biol. Chem.* 383, 725–737.
- Wolswijk, G., and Noble, M. (1989). Identification of an adult-specific glial progenitor cell. *Development* 105, 387–400.
- Zhang, S. C., Ge, B., and Duncan, I. D. (1999). Adult brain retains the potential to generate oligodendroglial progenitors with extensive myelination capacity. *Proc. Natl. Acad. Sci. U.S.A.* 96, 4089–4094. doi: 10.1073/pnas.96.7.4089

**Conflict of Interest Statement:** The authors declare that the research was conducted in the absence of any commercial or financial relationships that could be construed as a potential conflict of interest.

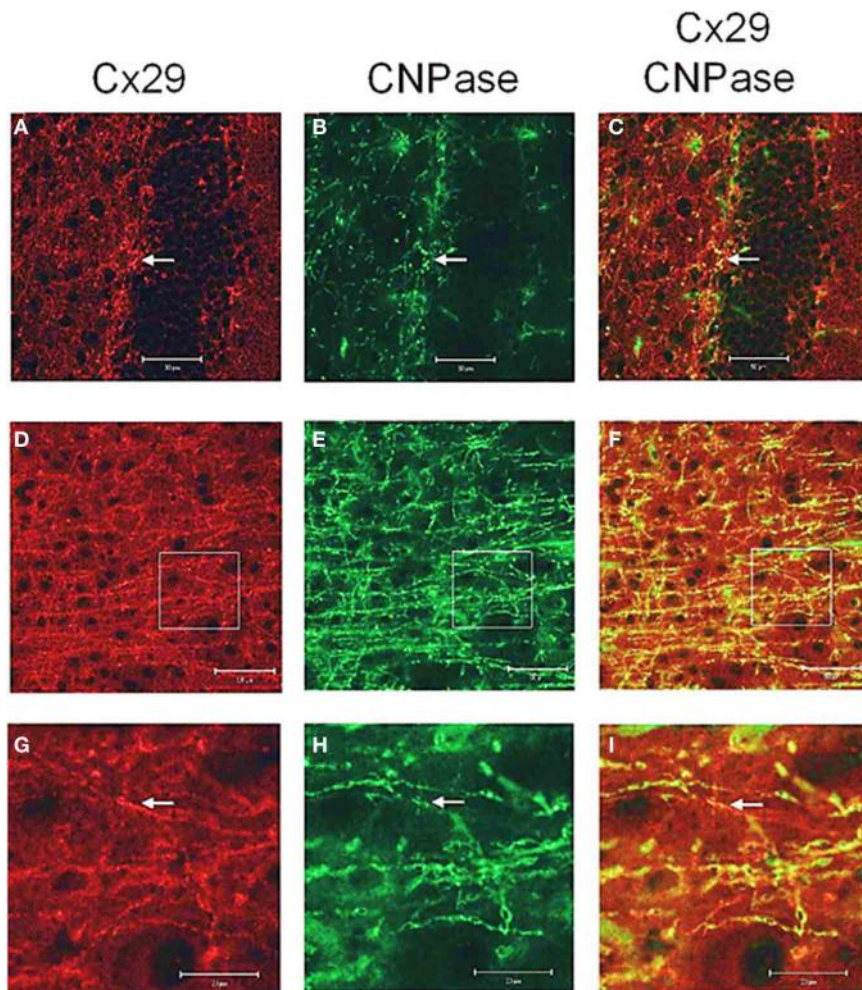
*Received: 14 February 2013; accepted: 10 June 2013; published online: 28 June 2013.*

*Citation: Söhl G, Hombach S, Degen J and Odermatt B (2013) The oligodendroglial precursor cell line Oli-neu represents a cell culture system to examine functional expression of the mouse gap junction gene connexin29 (Cx29). Front. Pharmacol. 4:83. doi: 10.3389/fphar.2013.00083*

*This article was submitted to Frontiers in Pharmacology of Ion Channels and Channelopathies, a specialty of Frontiers in Pharmacology.*

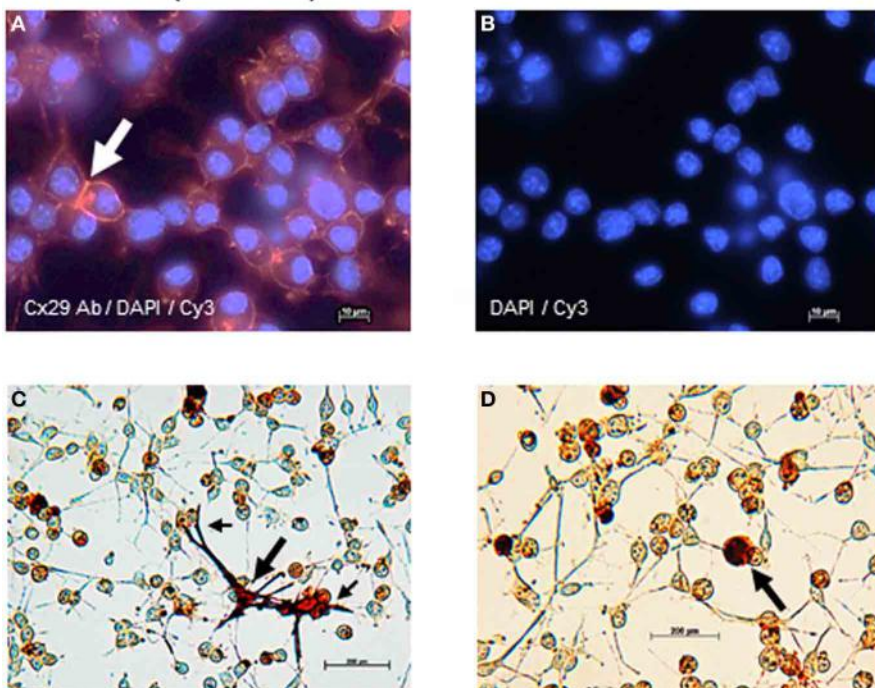
*Copyright © 2013 Söhl, Hombach, Degen and Odermatt. This is an open-access article distributed under the terms of the Creative Commons Attribution License, which permits use, distribution and reproduction in other forums, provided the original authors and source are credited and subject to any copyright notices concerning any third-party graphics etc.*

## APPENDIX



**FIGURE A1 |** Laser scan microscopy immunofluorescence analyses of Cx29 protein expression in the hippocampus (A–C) and in the neocortex (D–I) of the adult mouse brain. Pictures (G–I) represent enlargements of the white squares present in pictures (D–F), respectively. Cx29 immunofluorescence signals (A,D,G) co-localize with myelin-associated CNPase (2', 3'-cyclic nucleotide 3'-phosphodiesterase). CNPase is present in the plasma membrane of oligodendrocytes and their processes, in periaxonal membranes and the inner mesaxons, the outer processes, the paranodal

myelin loops, and the “incisure-like” membranes (B,E,H). Merged pictures are (C,F,I). Arrows in (A,B,C) indicate co-localization of Cx29 and CNPase in the soma of an oligodendrocyte. Arrows in (G,H,I) point to a co-localization of Cx29 and CNPase in myelinated fibers. However, Cx29 is hardly co-localized but present in the same neural structures as the myelin associated CNPase. This expression profile strengthened the credibility of the used Cx29 antibodies (Zymed), which was tested on tissue sections of Cx29 ( $-/-$ ) deficient mice (Eiberger et al., 2006).

**Oli neu (undiff.)**

**FIGURE A2 | Cx29 immunofluorescence analyses and microinjections of undifferentiated Oli-neu cells.** **(A)** Distribution of the Cx29 protein mostly in plasma membranes (arrow) applying Cx29-specific and Cy3 coupled secondary antibodies in relation to the cellular nuclei after DAPI staining. **(B)** Omitting primary Cx29 antibodies excluded cross reactivity of Cy3 antibodies with Oli-neu

cells. **(C,D)** Two examples of Oli-neu cells microinjected with neurobiotin and stained thereafter (arrow). **(C)** After filling one cell (large arrow), neurobiotin readily spreads into the various protrusions but did not pour into the attached cells at the ends (small arrows). **(D)** No neurobiotin transfer into the next neighboring could be demonstrated.



# An *Escherichia coli* strain for expression of the connexin45 carboxyl terminus attached to the 4th transmembrane domain

Jennifer L. Kopanic, Mona Al-Mugotir, Sydney Zach, Srustidhar Das, Rosslyn Grosely and Paul L. Sorgen\*

Department of Biochemistry and Molecular Biology, University of Nebraska Medical Center, Omaha, NE, USA

**Edited by:**

Stefan Dhein, Universitätsklinik Leipzig Herzzentrum Leipzig GmbH, Germany

**Reviewed by:**

Steven M. Taffet, SUNY Upstate Medical University, USA

Gina Sosinsky, University of California at San Diego, USA

**\*Correspondence:**

Paul L. Sorgen, Department of Biochemistry and Molecular Biology, University of Nebraska Medical Center, 985870 Nebraska Medical Center, Omaha, NE 68198-5870, USA  
e-mail: psorgen@unmc.edu

A major problem for structural characterization of membrane proteins, such as connexins, by nuclear magnetic resonance (NMR) occurs at the initial step of the process, the production of sufficient amounts of protein. This occurs because proteins must be expressed in minimal based media. Here, we describe an expression system for membrane proteins that significantly improves yield by addressing two common problems, cell toxicity caused by protein translation and codon bias between genomes. This work provides researchers with a cost-effective tool for NMR and other biophysical studies, to use when faced with little-to-no expression of eukaryotic membrane proteins in *Escherichia coli* expression systems.

**Keywords:** membrane protein expression, rare codons, connexins, NMR, minimal media

## INTRODUCTION

Membrane proteins play a fundamental role in human disease and constitute a major portion of drug targets; lacking is sufficient structural and functional information compared to soluble proteins (Drew et al., 2003; Molina et al., 2008). The limitations can be traced to difficulties in expression, optimizing purification procedures, and reconstituting the proper fold in a lipid environment. Yield is a major problem because only a few membrane proteins are expressed in large-enough quantities to be collected from natural sources. Strategies developed to overcome this problem include engineering vectors to express membrane proteins in *S. cerevisiae* yeast, Sf9 insect, and *Escherichia coli* bacteria cell expression systems (Bernaudat et al., 2011).

*Escherichia coli* is a widely used host for the production of heterologous proteins due to its ability to grow rapidly at high density and in inexpensive substrates (Molina et al., 2008). The *E. coli* strain BL21 is extensively used for protein expression because it is deficient in lon and ompT proteases (Ratelade et al., 2009). The BL21(DE3) version carries a chromosomal copy of the T7 RNA polymerase gene under control of the lacUV5 promoter, suitable for protein production from target genes cloned into any T7 vector (e.g., pET) by induction with isopropyl-β-D-thiogalactopyranoside (IPTG; Studier and Moffatt, 1986; Unger et al., 1999). However, problems still arise because bacteria have difficulties folding membrane proteins and expression can be toxic (Miroux and Walker, 1996; Laible et al., 2004). Derivatives of BL21(DE3) called the Walker strains, C41(DE3) and C43(DE3), were therefore created with an enhanced ability to express otherwise toxic membrane proteins (Miroux and Walker, 1996). C41(DE3) was derived from the BL21(DE3)

strain through natural selection to survive expression of the oxoglutarate-malate carrier protein from mitochondrial membranes. C41(DE3) has at least one uncharacterized mutation, enabling membrane protein expression into inclusion bodies without toxic effects (Miroux and Walker, 1996). Because expression of other membrane proteins were still toxic in the C41(DE3) strain, C43(DE3) was derived from C41(DE3) by selecting resistance to the F-ATPase b subunit gene. Thus, C43(DE3) can express a different set of toxic membrane proteins than C41(DE3).

Eukaryotic protein expression by *E. coli* is also strongly affected by codon bias. The genetic code contains 64 possible nucleotide combinations, which encode 20 amino acids and three codons that terminate translation. The frequencies with which different codons are used, which correlates with the amount of their corresponding tRNAs, vary between organisms (Gouy and Gauquier, 1982). For example, eukaryotes commonly use the AGG codon for Arginine, which is rarely used in *E. coli* (Novy et al., 2001; Gustafsson et al., 2004). Expressing an eukaryotic gene with numerous rare codons in bacteria can impact expression through premature termination of translation, translational stalling, frame shifting, and mis-incorporation of amino acids (Kurland and Gallant, 1996). This problem can be solved by exchanging rare codons in the target gene for more frequently used codons in *E. coli* or by expressing the rare tRNAs. The latter has been implemented through creation of the BL21(DE3)-derived Rosetta (Novagen) and BL21(DE3)-CodonPlus (Agilent Technologies) strains. These strains contain a plasmid to express eukaryotic tRNAs rarely used in *E. coli*. For example, the pLysS plasmid within the Rosetta 2(DE3)pLysS strain carries tRNA genes that encode for seven rare codons, including AGG (Novy et al., 2001). Many studies

have shown that protein expression is enhanced in these strains (Kane, 1995).

Every membrane protein is unique in the challenges needed to obtain a sample viable for structural studies. The increased number of possible methodologies at each step will help save researcher's time and money, and more importantly may provide ideas for future improvements. Previous Cx43 studies from our laboratory identified that tethering of the CT domain to TM4 was necessary to elicit a change in secondary structure in response to factors known to regulate gap junction channels (Kellezi et al., 2008; Grosely et al., 2013). Therefore, our studies were extended to test the expression of other connexin carboxyl-terminal domains when attached to their 4th transmembrane domain (TM4-CxCT; Cx26, Cx32, Cx37, Cx40, Cx45, and Cx50). This is the first critical step toward structural characterization of their CT domains. These isoforms were chosen for investigation because of their known functional significance and involvement in human disease (for review, see Laird, 2010; Zoidl and Dermietzel, 2010). The protocol developed for TM4-Cx45CT expression will be described in detail, as an example of the TM4-CxCT domains. Cx45 is highlighted because of the unique expression requirements in comparison to the other isoforms. Cx45 is the first cardiac connexin expressed during embryonic development and plays an important role in propagating the action potential from the conduction system to the working myocardium (Severs et al., 2006; Palacios-Prado et al., 2010). Cx45 gap junction channels close when the membrane potential becomes negative, which has been suggested to prevent retrograde conduction from the myocardium to the conduction system (Palacios-Prado et al., 2010). Cx45 has limited expression in normal, working ventricular myocytes; however, in failing heart tissue, an up-regulation of Cx45 reduces the cell-to-cell coupling while promoting arrhythmogenesis, especially when superimposed on the down-regulation of Cx43 (Yamada et al., 2003; Betsuyaku et al., 2005).

Development of the methods described herein has resulted in protein yields that are at the levels necessary for biophysical characterization (e.g., circular dichroism (CD), isothermal calorimetry, etc.), including structural analysis by nuclear magnetic resonance (NMR). This methodology will be of general usage for other intrinsically ordered domains from membrane proteins.

## MATERIALS AND METHODS

### GENERATION OF THE TM4-CxCT CONSTRUCTS

TM4-CxCT domains used in this study were from the Cx50, Cx45, Cx43, Cx40, Cx37, Cx32, and Cx26 isoforms. **Table 1** provides the amino acid sequence and species used for each TM4-CT domain to clone and ligate into the pET-14b expression vector (N-terminal 6× His-tag, ampicillin resistance; Novagen). Each construct includes 10 residues prior to their predicted TM4 domain (e.g., TM4-Cx45CT, **Figure 1**). All plasmid sequences were verified at the University of Nebraska Medical Center DNA Sequencing Core Facility.

### PURIFICATION OF THE TM4-Cx45CT

Purification of the TM4-Cx45CT was based on the protocol developed for the TM4-Cx43CT domain (Kellezi et al., 2008). Cells were resuspended in 1× PBS buffer containing a bacterial protease inhibitor cocktail (250 μL/4 L cells; Sigma-Aldrich) and 1 mM β-mercaptoethanol. Cells were then lysed with an Emulsiflex-C3 (Avestin) for three passages at 15,000 psi. Cell debris was removed with centrifugation (4,000 rpm, 1 h) and a pellet containing the inclusion bodies was collected by centrifugation (18,000 rpm, 1 h). The pellet was resuspended in 50 mL Buffer A (6 M urea, 1× PBS, 20 mM imidazole, and 1 mM β-mercaptoethanol, 1% Triton X-100, pH 8.0) and rocked overnight at 4°C. The suspension was centrifuged again (18,500 rpm, 1 h), and the supernatant was loaded onto an ÄKTA FPLC using a HisTrap HP column (GE Healthcare). Protein elution was accomplished using a step gradient (4, 8, 10, 30, and 50%) of Buffer B (6 M urea, 1× PBS, 1 M imidazole, 1 mM β-mercaptoethanol, and 1% Triton X-100, pH 8.0). Fractions that contained the 22 kDa His-tagged TM4-Cx45CT protein (verified by SDS-PAGE and Western blot analyses) were pooled and dialyzed overnight at 4°C using a 10,000 MW cut off Slide-A-Lyzer dialysis cassette (Pierce) against buffer C [1 M urea, 1 mM dithiothreitol (DTT), 1 mM EDTA, and 1% Triton X-100]. The precipitate was collected and centrifuged (4,000 rpm, 5 min), washed twice with water then buffer D (20 mM MES buffer, 1 mM DTT, 1 mM EDTA, and 50 mM NaCl, pH 5.8). The washed precipitate was then solubilized in buffer E (20 mM MES, 1 mM DTT, 8% 1-palmitoyl-2-hydroxy-sn-glycerol-3-[phospho-RAC-(1-glycerol)] (LPPG; Avanti Lipids), and 1 mM

**Table 1 | Conditions used to produce NMR samples for each TM4-CxCT construct.**

Connexin isoform	Species	Optimal cell line	LB media <sup>‡</sup>	M63 minimal media <sup>‡</sup>
TM4-Cx26CT (D179-V226)	<i>Homo sapiens</i>	C41	1.5	6
TM4-Cx32CT (D178-C283)	<i>Rattus norvegicus</i>	C41, C41Rt, R2	1.5	6
TM4-Cx37CT (D197-V333)	<i>Mus musculus</i>	C41, C41Rt	6	8
TM4-Cx40CT (N194-V356)	<i>Rattus norvegicus</i>	C41	10	12
TM4-Cx43CT (D197-I382)	<i>Rattus norvegicus</i>	C41	12	12
TM4-Cx45CT (D219-I396)	<i>Mus musculus</i>	C41Rt	10	8*
TM4-Cx50CT (D200-I440)	<i>Mus musculus</i>	C41, C41Rt, BL21	1	2

Abbreviations used for *E. coli* competent cell stains: C41, C41(DE3); R2, Rosetta2(DE3)pLysSRARE2; C41Rt, C41(DE3)pLys; BL21, BL21(DE3).

\*Liters of bacterial culture required to produce a 300 μL sample at 1 mM concentration.

\*\*ISOGRO required for TM4-Cx45CT expression in minimal media.

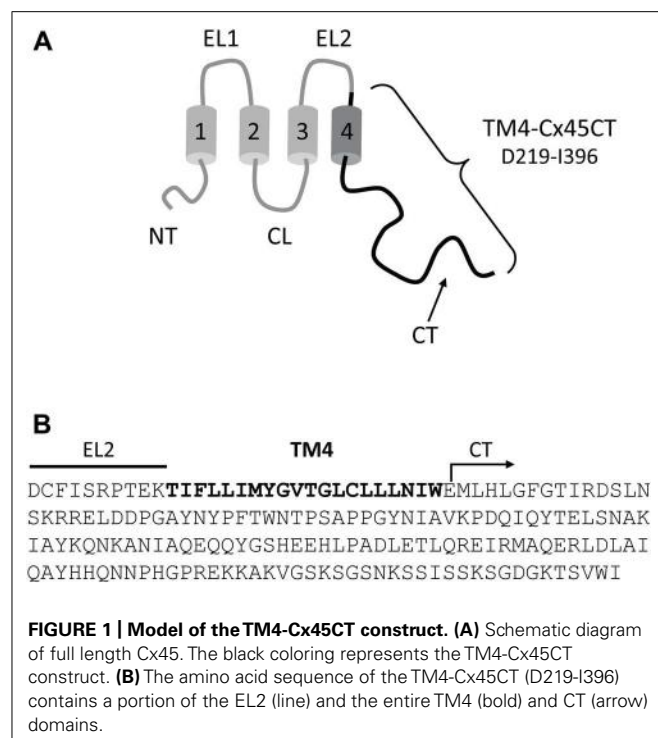


**FIGURE 1 | Model of the TM4-Cx45CT construct. (A)** Schematic diagram of full length Cx45. The black coloring represents the TM4-Cx45CT construct. **(B)** The amino acid sequence of the TM4-Cx45CT (D219-I396) contains a portion of the EL2 (line) and the entire TM4 (bold) and CT (arrow) domains.

EDTA) and incubated at 42°C for 30 min. Buffer E was used for all TM4-Cx45CT experiments.

#### WESTERN BLOTTING ANALYSIS

Protein samples were separated on 15% SDS-PAGE gels and transferred to a 0.45 µ polyvinylidene difluoride membrane (Millipore) equilibrated in transfer buffer (192 mM glycine, 25 mM Tris, 0.05% SDS, 10% methanol) using an electrophoretic transfer cell for 90 min at 100 V. After incubation with 5% non-fat milk in 1× PBS for 2.5 h, membranes were incubated with either mouse monoclonal anti-Cx45 (1:2,000, Cx45CR1 clone P3C9, Fred Hutchinson Cancer Center) or anti-His (1:2,000, His-Tag 27E9, Cell Signaling Technology, gift from Dr. Surinder Batra) for 16 h, 4°C. Membranes were washed four times at room temperature with washing buffer (0.1% Tween-20 in 1× PBS) for 10 min. Membranes were then incubated with goat anti-mouse IgG secondary antibody horseradish peroxidase conjugates (1:12,000, 12-349, Millipore) for 1 h, 25°C, then washed again. Bound antibodies were visualized using SuperSignal West Femto (Thermo Scientific).

#### NUCLEAR MAGNETIC RESONANCE SPECTROSCOPY

All NMR data were acquired using a 600 MHz Varian INOVA NMR Spectrometer outfitted with a cryo-probe at the University of Nebraska Medical Center's NMR Facility. NMR spectra were processed and phased using NMRPipe and NMRDraw (Delaglio et al., 1995) and analyzed using NMRView (Johnson, 2004). Gradient-enhanced two-dimensional <sup>15</sup>N-HSQC experiments were acquired with 1,024 complex points in the direct dimension and 256 complex points in the indirect dimension (Kay

et al., 1992). Sweep widths were 10,000 Hz in the <sup>1</sup>H dimension and 2,430.6 Hz in the <sup>15</sup>N dimension.

#### CIRCULAR DICHROISM SPECTROSCOPY

Circular dichroism experiments were performed using a Jasco J-815 spectrophotometer fitted with a Peltier temperature control system. For each sample, five scans (wavelength range: 300–190 nm; response time: 1 s; scan rate: 50 nm/min; bandwidth 1.0 nm) were collected using a 0.01 cm quartz cell and processed using Spectra Analysis (Jasco). Each spectrum is shown as the mean residue ellipticity (MRE; deg cm<sup>2</sup> dmol<sup>-1</sup>) as a function of wavelength and average of five scans. All spectra were corrected by subtracting the solvent spectrum. Protein concentrations were determined using a NanoDrop 1000 (Thermo Scientific) or Biospec 1601 UV-VIS spectrophotometer (Shimadzu) at 280 nm. Analyses of spectra were accomplished using the Provencher and Glöckner method with the SP175 reference set on the online program DichroWeb (Provencher and Glöckner, 1981; Whitmore and Wallace, 2004; Lees et al., 2006).

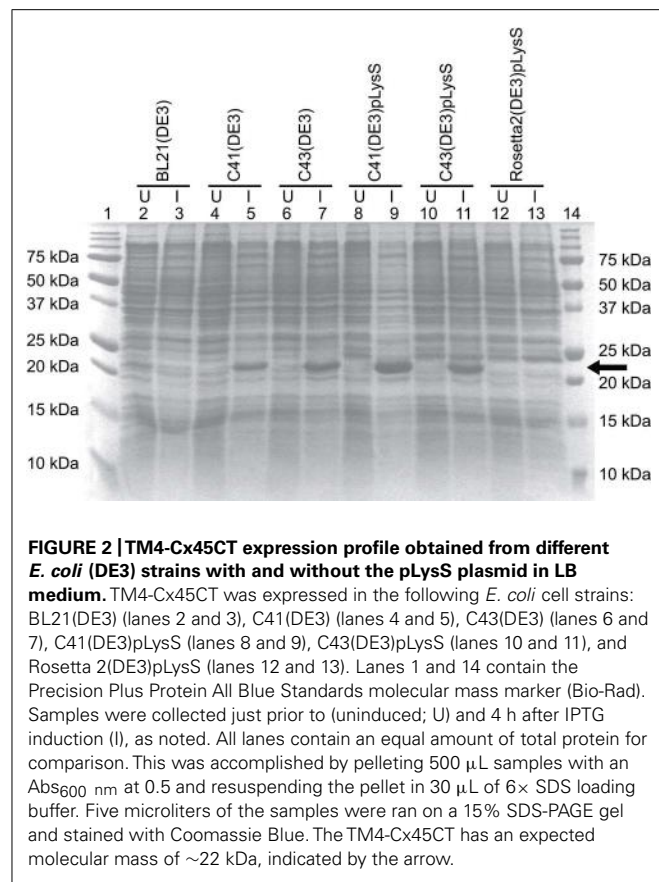
## RESULTS

#### BACTERIAL STRAINS USED FOR PROTEIN EXPRESSION

The *E. coli* strains BL21(DE3), C41(DE3), C43(DE3), and Rosetta 2(DE3)pLysS (chloramphenicol resistance) were transformed with the TM4-Cx45CT plasmid and incubated in lysogeny broth (LB) medium at 37°C, 250 rpm. Rosetta 2(DE3)pLysS expresses seven rare codons (Arg, AGA, AGG, CGA, CGG; Ile, AUA; Pro, CCC, Leu, CUA) in comparison to the BL21-Codon Plus(DE3)-RIPL strain (contains the most amount of tRNA genes in the BL21-Codon Plus series), which contains only five tRNA genes (Arg, AGA, AGG; Ile, AUA; Pro, CCC, Leu, CUA). The TM4-Cx45CT contains five Arg rare codons, including two CGA, which the BL21-Codon Plus(DE3)-RIPL strain does not have the corresponding tRNA. Therefore, Rosetta 2(DE3)pLysS was chosen as the representative strain that expresses rare codons for this study. Protein expression was induced by the addition of 1.0 mM IPTG (final concentration; Bioexpress) at an optical density of 0.6 at 600 nm. The electrophoretic profile of total cellular proteins obtained 4 h after induction indicated that only C41(DE3) and C43(DE3) expressed TM4-Cx45CT (Figure 2, lanes 5 and 7, respectively). However, this protein yield is not optimal as significantly less protein per liter was produced than what was needed for the TM4-Cx43CT NMR structural studies (Kellezi et al., 2008). Upon examination of the TM4-Cx45CT gene sequence, 14 rare codons were identified; of these, eight (two in tandem) translate to the amino acid with the greatest codon bias, Arg (Table 2). Even though the Rosetta 2(DE3)pLysS strain was unable to express TM4-Cx45CT (Figure 2, lane 13), we hypothesized that expression would be enhanced by combining the pLysS plasmid with the C41(DE3) or C43(DE3) strains.

#### EXPRESSION OF TM4-Cx45CT WITH THE pLysS PLASMID

The pLysS (also referred to as pLysSRARE2) plasmid was isolated from Rosetta 2(DE3)pLysS cells using the QIAprep Spin Miniprep Kit (Qiagen) and co-transformed with the TM4-Cx45CT plasmid into the C41(DE3) and C43(DE3) strains. The cells were grown and induced as described above. The electrophoretic profile of



total cellular proteins obtained 4 h after induction showed that TM4-Cx45CT expression in C43(DE3) was similar with and without transformation of the pLysS plasmid (**Figure 2**, lanes 7 and 11, respectively). Conversely, TM4-Cx45CT expression was significantly increased in the C41(DE3)pLysS strain as compared to C41(DE3) alone (**Figure 2**, lanes 9 and 5, respectively). The expression was quantified by densitometry and revealed that the addition of the pLysS plasmid increased TM4-Cx45CT expression by 70% in C41(DE3). The expression of TM4-Cx45CT was confirmed by Western blot analyses using anti-His6 and anti-Cx45 antibodies (**Figure 3**).

Expression using the C41(DE3)pLysS strain was tested in isotope-labeled M63 minimal medium, which allows the control of nitrogen and carbon sources needed for NMR structural studies. The TM4-Cx45CT expression level decreased 84% in M63 as compared to LB (**Figure 4**, lanes 6 and 3, respectively). However, expression was restored to LB level when M63 was supplemented with <sup>15</sup>N-ISOGRO (1 g/L, Isotec; **Figure 4**, lane 9). ISOGRO is an algal lysate-derived complex labeling medium that provides cells a metabolic boost that often decreases lag time, facilitates the attainment of growth saturation, and promotes recombinant protein production. ISOGRO helps cultures conserve cellular energy by limiting the requirement for *de novo* synthesis of cellular machinery and metabolic precursors; permitting more cellular resources to be direct toward recombinant protein expression. At this expression level, 8 L of growth is necessary to obtain

**Table 2 | Rare codon usage for each TM4-CxCT domain.**

Connexin isoform	Number of rare codons <sup>‡</sup>					
	Arginine	Isoleucine	Leucine	Proline	Total	Tandem
TM4-Cx26CT (D179-V226)	0 AGG 1 AGA 0 CGA	0	1 CTA	2 CCC	4	No
TM4-Cx32CT (D178-C283)	0 AGG 1 AGA 1 CGA	1 ATA	0	3 CCC	5	No
TM4-Cx37CT (D197-V333)	1 AGG 2 AGA 3 CGA	1 ATA	0	8 CCC	15	No
TM4-Cx40CT (N194-V356)	2 AGG 0 AGA 1 CGA	0	1 CTA	4 CCC	8	No
TM4-Cx43CT (D197-I382)	1 AGG 3 AGA 1 CGA	0	0	2 CCC	7	No
TM4-Cx45CT (D219-I396)	2 AGG 2 AGA 2 CGA	1 ATA	3 CTA	4 CCC	14	Yes
TM4-Cx50CT (D200-I440)	5 AGG 1 AGA 0 CGA	2 ATA	1 CTA	3 CCC	12	No

<sup>‡</sup>Number of rare codons was determined using the Rare Codon Calculator (<http://nihserver.mbi.ucla.edu/RACC/>).

a 1 mM at 300  $\mu$ L volume (“gold standard” concentration and volume for NMR structural studies; **Table 1**). This is in contrast to the 54 or 180 L would be necessary in M63 without <sup>15</sup>N-ISOGRO or without <sup>15</sup>N-ISOGRO and the pLysS plasmid, respectively.

Another advantage of using the pLysS plasmid is the suppression of T7 RNA polymerase expression prior to induction with IPTG. The phenotypes observed from “leaky” expression (before IPTG induction) of a membrane protein that is toxic to *E. coli* are a slow growth rate, low cell density, and in some cases, cell death. The TM4-Cx45CT expression was not toxic to the *E. coli* strains tested as the growth rates and final cell densities were identical with and without the pLysS plasmid (**Figure 5**), indicating that the benefit gained from the pLysS plasmid was solely the tRNAs expression.

## EXPRESSION OF OTHER TM4-CxCT CONSTRUCTS

Outlined in **Table 1** are the results from the other six connexin isoforms. With the exception of the TM4-Cx45CT, all of the constructs were able to grow in C41(DE3) cells. When comparing the primary sequences of the connexin isoforms, they all contain rare codons (**Table 2**). However, TM4-Cx45CT is the only construct that contains rare codons in tandem, which is known

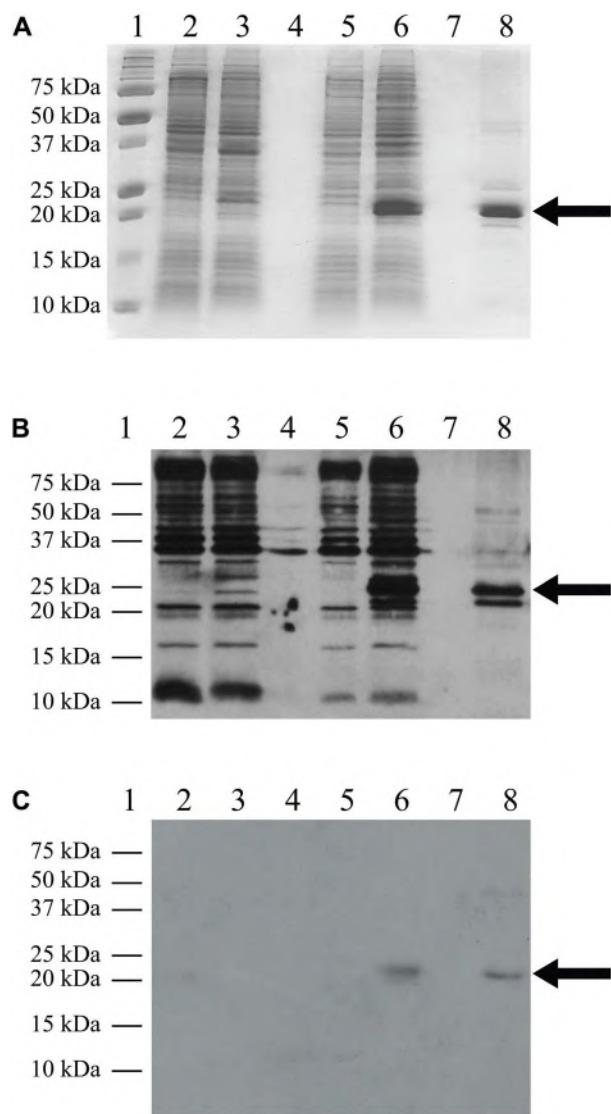


**FIGURE 3 | Western blot analysis.** C41(DE3)pLysS transformed with the empty pET-14b vector (lanes 2 and 3) or the TM4-Cx45CT plasmid (lanes 5 and 6). Lane 8 contains the TM4-Cx45CT after purification. Lane 1 contains the Precision Plus Protein All Blue Standards molecular mass marker (Bio-Rad) and lanes 4 and 7 are blank. Samples were collected just prior to (lanes 2 and 5) and 4 h after IPTG induction (lanes 3 and 6). A total of 500  $\mu$ L samples with an Abs<sub>600 nm</sub> at 0.5 were pelleted and resuspended in 30  $\mu$ L of 6x SDS loading buffer. Equal amounts of total protein (7  $\mu$ L) were ran on a 15% SDS-PAGE gel. **(A)** Coomassie Blue stained gel is shown as a reference. Western blot analyses were performed using either **(B)** anti-His6, or **(C)** anti-Cx45 primary antibodies. The expected molecular mass of the TM4-Cx45CT is ~22 kDa, which is indicated by the arrow. Of note, in **(B)** lane 8, the anti-His6 primary antibody also reacted with a ~20 Da protein. Although not present in the **(A)** 15% SDS-PAGE gel or reactive with the **(C)** anti-Cx45 primary antibody, we speculate the doublet is caused by proteolysis of the TM4-Cx45CT.

to inhibit protein expression (Kim and Lee, 2006). In addition, the TM4-Cx32CT, TM4-Cx37CT, and TM4-Cx50CT constructs were also able to grow in the C41(DE3)pLysS strain. In general, the TM4-CxCT constructs produced more protein in LB media

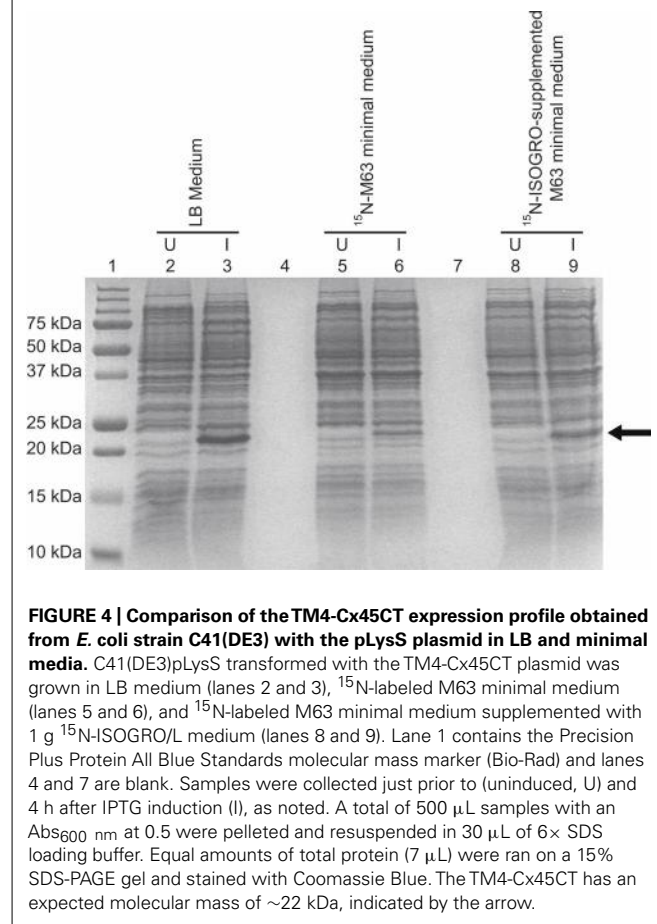
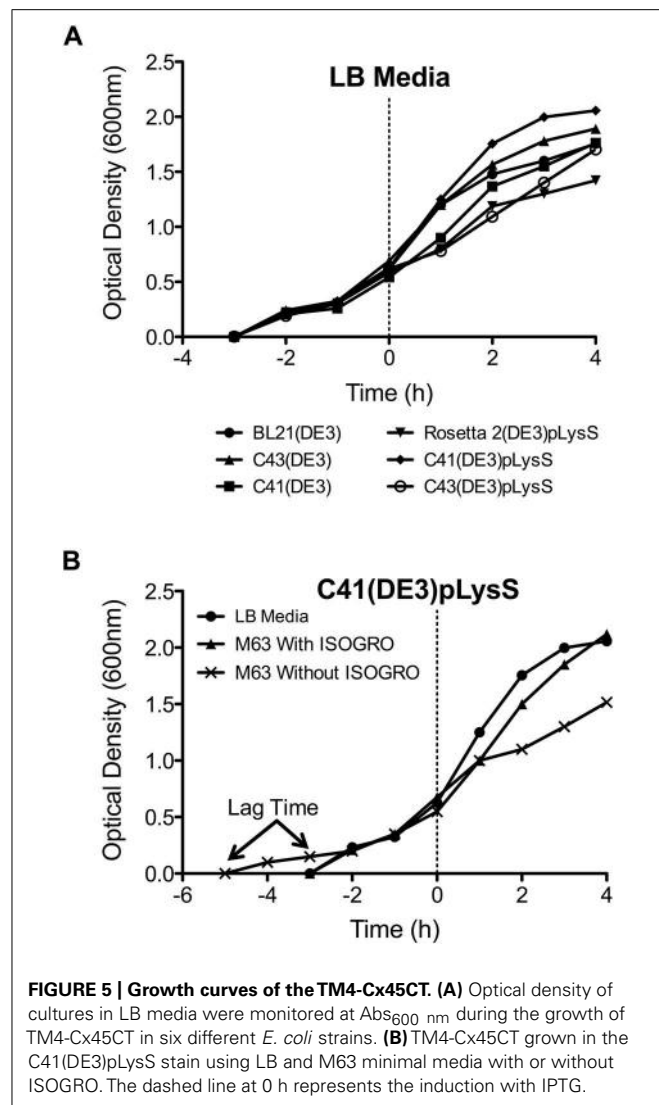


**FIGURE 4 | Comparison of the TM4-Cx45CT expression profile obtained from *E. coli* strain C41(DE3) with the pLysS plasmid in LB and minimal media.** C41(DE3)pLysS transformed with the TM4-Cx45CT plasmid was grown in LB medium (lanes 2 and 3), <sup>15</sup>N-labeled M63 minimal medium (lanes 5 and 6), and <sup>15</sup>N-labeled M63 minimal medium supplemented with 1 g <sup>15</sup>N-ISOGRO/L medium (lanes 8 and 9). Lane 1 contains the Precision Plus Protein All Blue Standards molecular mass marker (Bio-Rad) and lanes 4 and 7 are blank. Samples were collected just prior to (uninduced, U) and 4 h after IPTG induction (I), as noted. A total of 500  $\mu$ L samples with an Abs<sub>600 nm</sub> at 0.5 were pelleted and resuspended in 30  $\mu$ L of 6x SDS loading buffer. Equal amounts of total protein (7  $\mu$ L) were ran on a 15% SDS-PAGE gel and stained with Coomassie Blue. The TM4-Cx45CT has an expected molecular mass of ~22 kDa, indicated by the arrow.

(e.g., for CD, ITC, etc.) as compared with minimal media (i.e., for NMR). The only differences were the TM4-Cx43CT isoform grew equally as well and the TM4-Cx45CT grew better in minimal media, which is caused by the addition of <sup>15</sup>N-ISOGRO to the media.

#### CHARACTERIZATION OF THE TM4-Cx45CT SECONDARY STRUCTURE

Combining a plasmid that expresses rare tRNAs with an *E. coli* strain selected to express toxic membrane proteins improved the yield of TM4-Cx45CT to levels that are cost-effective and now feasible for NMR structural studies. Using the expression protocol developed herein, the TM4-Cx45CT was purified and reconstituted into detergent micelles (LPPG) using techniques developed previously for the TM4-Cx43CT construct (Kellezi et al., 2008). The purity of the TM4-Cx45CT was verified by SDS-PAGE and Western blot analyses (Figure 3, Lane 8). Next, a <sup>15</sup>N-HSQC spectrum was collected to evaluate the sample properties of the TM4-Cx45CT. The <sup>15</sup>N-HSQC is a two-dimensional NMR experiment in which each amino acid except proline gives one signal, or chemical shift, that corresponds to the N–H amide group. Figure 6A shows the <sup>15</sup>N-HSQC for TM4-Cx45CT collected in 20 mM MES, 1 mM DTT, 8% LPPG, and 1 mM EDTA. Unexpectedly, the spectra quality is poor, and only approximately 50% of the expected cross peaks are present. Previous studies identified that a soluble version of the Cx45CT (K265-I396) was in a dimer



conformation that could be disrupted by acetonitrile (Kopanic and Sorgen, 2012). Therefore, a  $^{15}\text{N}$ -HSQC spectrum was collected in the presence of 30% acetonitrile (Figure 6B), which shows the total number (168) of expected amide cross peaks corresponding to the non-proline residues of the TM4-Cx45CT. Additionally, the number of Gly residues (12, circled and numbered) matches the number found in the primary sequence and indicates that the TM4-Cx45CT construct is in a single conformation. Altogether, this demonstrates the feasibility of solving the monomeric TM4-Cx45CT structure.

Circular dichroism was used to gain insight into the TM4-Cx45CT secondary structure before obtaining an atomic level structure. Intracellular acidification is a major consequence of tissue ischemia during a myocardial infarction, which leads to closure and degradation of gap junction channels and can be a substrate for malignant ventricular arrhythmias (Lau, 2005). Therefore, data were collected at either physiological (pH 7.5) or ischemic (pH 5.8) conditions (Figure 7). The TM4-Cx45CT (without acetonitrile) has a small increase in  $\alpha$ -helical content under acidic conditions

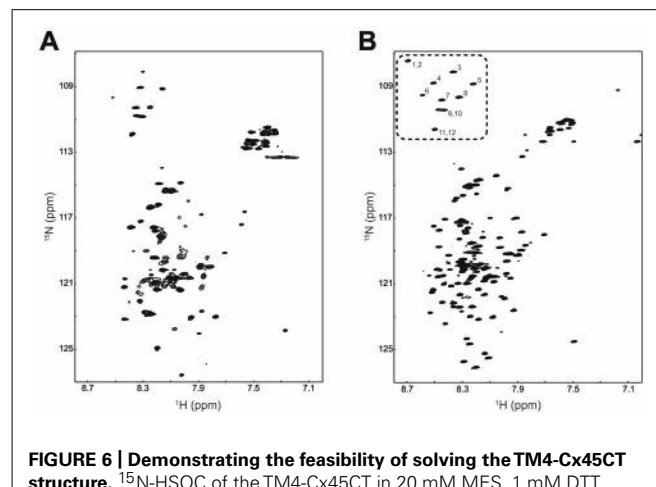


**FIGURE 6 | Demonstrating the feasibility of solving the TM4-Cx45CT structure.**  $^{15}\text{N}$ -HSQC of the TM4-Cx45CT in 20 mM MES, 1 mM DTT, 1 mM EDTA, and 8% 1-palmitoyl-2-hydroxy-sn-glycero-3-[phospho-RAC-(1-glycerol)] detergent micelles (A) alone or (B) in the presence of 30% deuterated acetonitrile. Highlighted are the 12 Gly residues in the TM4-Cx45CT (dotted rectangle, numbered).

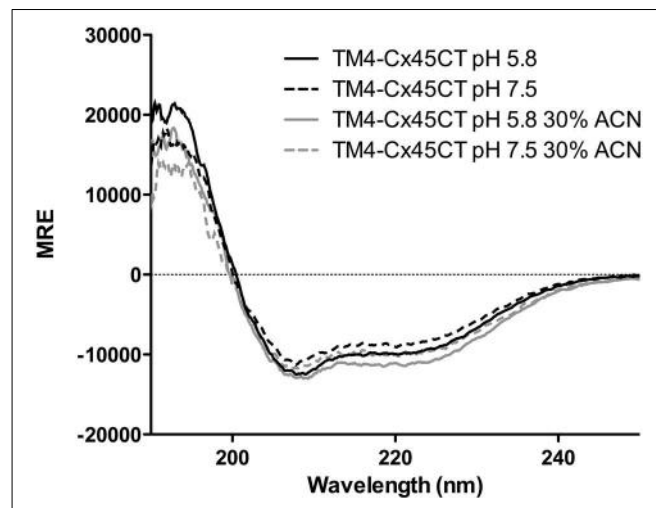


**FIGURE 7 | Secondary structure of the TM4-Cx45CT.** Circular dichroism of the TM4-Cx45CT in 20 mM MES, 1 mM DTT, 1 mM EDTA, and 8% 1-palmitoyl-2-hydroxy-sn-glycero-3-[phospho-RAC-(1-glycerol)] detergent micelles alone (black) or in presence of 30% acetonitrile (gray) at pH 7.5 (solid lines) and 5.8 (dashed lines).

(pH 7.5, 25%; pH 5.8, 28%). This pH-effect is similar in the presence of 30% acetonitrile with a small increase in overall  $\alpha$ -helical content (pH 7.5 28%; pH 5.8, 32%). The pH-induced increase in  $\alpha$ -helical content for the TM4-Cx45CT (3–4%) is smaller than observed for the TM4-Cx43CT (16%; Kellezi et al., 2008; Grosely et al., 2012).

## DISCUSSION

Even though the soluble versions of connexin CT domains have proven to be useful for describing mechanisms involved in gap junction regulation, several results indicate that these constructs may not be optimal. For example, the cryo-electron microscopy

structure of the Cx43 mutant (truncated at residue T263) suggested that the N-terminal region of the CT domain (S255-T263) contains  $\alpha$ -helical structure (Unger et al., 1999). In contrast, the NMR data for the soluble Cx43CT (S255-I382) identified these same residues as weak resonances, suggesting an exchange between an unstructured and  $\alpha$ -helical conformations (Sorgen et al., 2004). Additionally, not all of the expected NOEs were observed in the two dynamic  $\alpha$ -helical regions of the soluble CT structure. The TM4-tethered Cx43CT protein (D219-I382) solubilized in detergent micelles offers a more native-like construct for structural studies (Kellezi et al., 2008). CD and NMR data indicated that the TM4-Cx43CT has more  $\alpha$ -helical content than can be attributed to solely the addition of the TM4 domain to the soluble CT domain (Kellezi et al., 2008; Grosely et al., 2012). In addition, the TM4-Cx43CT is also structurally

responsive to the changes in pH and phosphorylation, unlike the soluble Cx43CT, indicating that this construct is a better model for the investigation of structural-based mechanisms behind gap junction channel regulation (Kellezi et al., 2008; Grosely et al., 2012). Extending this study to other connexin isoforms, such as Cx45, will allow future structural studies to characterize mechanisms of gap junction regulation. The motivation behind this study is that a better understanding of the similarities and differences in structure between connexin CT domains when attached to the TM4 can be exploited to aid in the design of chemical modifiers.

## ACKNOWLEDGMENT

This work was supported by United States Public Health Service Grant GM072631.

## REFERENCES

- Bernaudat, F., Frelet-Barrand, A., Pochon, N., Dementin, S., Hivin, P., Boutigny, S., et al. (2011). Heterologous expression of membrane proteins: choosing the appropriate host. *PLoS ONE* 6:e29191. doi: 10.1371/journal.pone.0029191
- Betsuyaku, T., Nnebe, N. S., Sundset, R., Patibandla, S., Krueger, C. M., and Yamada, K. A. (2005). Overexpression of cardiac connexin45 increases susceptibility to ventricular tachyarrhythmias in vivo. *Am. J. Physiol. Heart Circ. Physiol.* 290, H163–H171. doi: 10.1152/ajpheart.01308.2004
- Delaglio, F., Grzesiek, S., Vuister, G. W., Zhu, G., Pfeifer, J., and Bax, A. (1995). NMRPipe: multidimensional spectral processing system based on UNIX pipes. *J. Biomol. NMR* 6, 277–293. doi: 10.1007/BF00197809
- Drew, D., Fröderberg, L., Baars, L., and de Gier, J.-W. L. (2003). Assembly and overexpression of membrane proteins in *Escherichia coli*. *Biochim. Biophys. Acta* 1610, 3–10. doi: 10.1016/S0005-2736(02)00707-1
- Gouy, M., and Gautier, C. (1982). Codon usage in bacteria: correlation with gene expressivity. *Nucleic Acids Res.* 10, 7055–7074. doi: 10.1093/nar/10.22.7055
- Grosely, R., Kieken, F., and Sorgen, P. L. (2012). (1)H, (13)C, and (15)N backbone resonance assignments of the connexin43 carboxyl terminal domain attached to the 4th transmembrane domain in detergent micelles. *Biomol. NMR Assign.* doi: 10.1007/s12104-012-9432-8 [Epub ahead of print].
- Grosely, R., Kopanic, J. L., Nabors, S., Kieken, F., Spagnol, G., Al-Mugotir, M., et al. (2013). Effects of phosphorylation on the structure and backbone dynamics of the intrinsically disordered Connexin43 carboxyl-terminal domain. *J. Biol. Chem.* doi: 10.1074/jbc.M113.454389 [Epub ahead of print].
- Gustafsson, C., Govindarajan, S., and Minshull, J. (2004). Codon bias and heterologous protein expression. *Trends Biotechnol.* 22, 346–353. doi: 10.1016/j.tibtech.2004.04.006
- Johnson, B. A. (2004). Using NMRView to visualize and analyze the NMR spectra of macromolecules. *Methods Mol. Biol.* 278, 313–352. doi: 10.1385/1-59259-809-9:313
- Kane, J. F. (1995). Effects of rare codon clusters on high-level expression of heterologous proteins in *Escherichia coli*. *Curr. Opin. Biotechnol.* 6, 494–500. doi: 10.1016/0958-1669(95)80082-4
- Kay, L., Keifer, P., and Saarinen, T. (1992). Pure absorption gradient enhanced heteronuclear single quantum correlation spectroscopy with improved sensitivity. *J. Am. Chem. Soc.* 114, 10663–10665. doi: 10.1021/ja00052a088
- Kellezi, A., Grosely, R., Kieken, F., Borgstahl, G. E. O., and Sorgen, P. L. (2008). Purification and reconstitution of the connexin43 carboxyl terminus attached to the 4th transmembrane domain in detergent micelles. *Protein Expr. Purif.* 59, 215–222. doi: 10.1016/j.pep.2008.01.023
- Kim, S., and Lee, S. B. (2006). Rare codon clusters at 5'-end influence heterologous expression of archaeal gene in *Escherichia coli*. *Protein Expr. Purif.* 50, 49–57. doi: 10.1016/j.pep.2006.07.014
- Kopanic, J. L., and Sorgen, P. L. (2012). Chemical shift assignments of the connexin45 carboxyl terminal domain: monomer and dimer conformations. *Biomol. NMR Assign.* doi: 10.1007/s12104-012-9431-9 [Epub ahead of print].
- Kurland, C., and Gallant, J. (1996). Errors of heterologous protein expression. *Curr. Opin. Biotechnol.* 7, 489–493. doi: 10.1016/S0958-1669(96)80050-4
- Laible, P. D., Scott, H. N., Henry, L., and Hanson, D. K. (2004). Towards higher-throughput membrane protein production for structural genomics initiatives. *J. Struct. Funct. Genomics* 5, 167–172. doi: 10.1023/B:JSFG.0000029201.33710.46
- Laird, D. W. (2010). The gap junction proteome and its relationship to disease. *Trends Cell Biol.* 20, 92–101. doi: 10.1016/j.tcb.2009.11.001
- Lau, A. F. (2005). c-Src: bridging the gap between phosphorylation- and acidification-induced gap junction channel closure. *Sci. STKE* 2005, pe33. doi: 10.1126/stke.2912005pe33
- Lees, J. G., Miles, A. J., Wien, F., and Wallace, B. A. (2006). A reference database for circular dichroism spectroscopy covering fold and secondary structure space. *Bioinformatics* 22, 1955–1962. doi: 10.1093/bioinformatics/btl327
- Miroux, B., and Walker, J. E. (1996). Over-production of proteins in *Escherichia coli*: mutant hosts that allow synthesis of some membrane proteins and globular proteins at high levels. *J. Mol. Biol.* 260, 289–298. doi: 10.1006/jmbi.1996.0399
- Molina, D. M., Cornvik, T., Eshagh, S., Haeggström, J. Z., Nordlund, P., and Sabet, M. I. (2008). Engineering membrane protein overproduction in *Escherichia coli*. *Protein Sci.* 17, 673–680. doi: 10.1110/ps.073242508
- Novy, R., Drott, D., Yaeger, K., and Mierendorf, R. (2001). Overcoming the codon bias of *E. coli* for enhanced protein expression. *Innovations* 12, 1–3.
- Palacios-Prado, N., Briggs, S. W., Skeberdis, V. A., Pranevicius, M., Studier, F. W., and Moffatt, B. A. (1986). Use of bacteriophage T7 RNA polymerase to direct selective high-level expression of cloned genes. *J. Mol. Biol.* 189, 113–130. doi: 10.1016/0022-2836(86)90385-2
- Unger, V. M., Kumar, N. M., Gilula, N. B., and Yeager, M. (1999). Three-dimensional structure of a

- recombinant gap junction membrane channel. *Science* 283, 1176–1180. doi: 10.1126/science.283.5405.1176
- Whitmore, L., and Wallace, B. A. (2004). DICHROWEB, an online server for protein secondary structure analyses from circular dichroism spectroscopic data. *Nucleic Acids Res.* 32, W668–W673. doi: 10.1093/nar/gkh371
- Yamada, K. A., Rogers, J. G., Sundset, R., Steinberg, T. H., and Safitz, J. E. (2003). Up-regulation of connexin45 in heart failure. *J. Cardiovasc. Electrophysiol.* 14, 1205–1212. doi: 10.1046/j.1540-8167.2003.03276.x
- Zoidl, G., and Dermietzel, R. (2010). Gap junctions in inherited human disease. *Pflugers Archiv.* 460, 451–466. doi: 10.1007/s00424-010-0789-1
- Conflict of Interest Statement:** The authors declare that the research was conducted in the absence of any commercial or financial relationships that could be construed as a potential conflict of interest.
- Received: 14 May 2013; accepted: 07 August 2013; published online: 23 August 2013.
- Citation: Kopanic JL, Al-Mugotir M, Zach S, Das S, Grosely R and Sorgen PL (2013) An Escherichia coli strain for expression of the connexin45 carboxyl terminus attached to the 4th transmembrane domain. *Front. Pharmacol.* 4:106. doi: 10.3389/fphar.2013.00106
- This article was submitted to Pharmacology of Ion Channels and Channelopathies, a section of the journal Frontiers in Pharmacology.
- Copyright © 2013 Kopanic, Al-Mugotir, Zach, Das, Grosely and Sorgen. This is an open-access article distributed under the terms of the Creative Commons Attribution License (CC BY). The use, distribution or reproduction in other forums is permitted, provided the original author(s) or licensor are credited and that the original publication in this journal is cited, in accordance with accepted academic practice. No use, distribution or reproduction is permitted which does not comply with these terms.



# Promises and pitfalls of a Pannexin1 transgenic mouse line

**Regina Hanstein<sup>1</sup>, Hiromitsu Negoro<sup>1,2</sup>, Naman K. Patel<sup>1</sup>, Anne Charollais<sup>3</sup>, Paolo Meda<sup>3</sup>, David C. Spray<sup>1</sup>, Sylvia O. Suadicani<sup>1,2</sup> and Eliana Scemes<sup>1\*</sup>**

<sup>1</sup> Dominick P. Purpura Department of Neuroscience, Albert Einstein College of Medicine, Yeshiva University, New York, NY, USA

<sup>2</sup> Department of Urology, Albert Einstein College of Medicine, Yeshiva University, New York, NY, USA

<sup>3</sup> Department of Cell Physiology and Metabolism, Medical School, University of Geneva, Geneva, Switzerland

**Edited by:**

Aida Salameh, Heart Centre  
University of Leipzig, Germany

**Reviewed by:**

Marc Chanson, University of  
Geneva, Switzerland  
Georg Zoidl, York University, Canada

**\*Correspondence:**

Eliana Scemes, Dominick P. Purpura  
Department of Neuroscience, Albert  
Einstein College of Medicine,  
1410 Pelham Parkway South,  
Kennedy Center, Room 203,  
Bronx, New York, NY 10461, USA.  
e-mail: eliana.scemes@  
einstein.yu.edu

Gene targeting strategies have become a powerful technology for elucidating mammalian gene function. The recently generated knockout (KO)-first strategy produces a KO at the RNA processing level and also allows for the generation of conditional KO alleles by combining FLP/FRT and Cre/loxP systems, thereby providing high flexibility in gene manipulation. However, this multipurpose KO-first cassette might produce hypomorphic rather than complete KOs if the RNA processing module is bypassed. Moreover, the generation of a conditional phenotype is also dependent on specific activity of Cre recombinase. Here, we report the use of an efficient molecular biological approach to test pannexin1 (*Panx1*) mRNA expression in global and conditional Panx1 KO mice derived from the KO-first mouse line, *Panx1*<sup>tm1a(KOMP)Wtsi</sup>. Using qRT-PCR, we demonstrate that tissues from wild-type (WT) mice show a range of *Panx1* mRNA expression levels, with highest expression in trigeminal ganglia, bladder and spleen. Unexpectedly, we found that in mice homozygous for the KO-first allele, *Panx1* mRNA expression is not abolished but reduced by 70% compared to that of WT tissues. Thus, Panx1 KO-first mice present a hypomorphic phenotype. Crosses of Panx1 KO-first with FLP deleter mice generated Panx1<sup>f/f</sup> mice. Further crosses of the latter mice with mGFAP-Cre or NFH-Cre mice were used to generate astrocyte- and neuron-specific Panx1 deletions, respectively. A high incidence of ectopic Cre expression was found in offspring of both types of conditional Panx1 KO mice. Our study demonstrates that *Panx1* expression levels in the global and conditional Panx1 KO mice derived from KO-first mouse lines must be carefully characterized to ensure modulation of *Panx1* gene expression. The precise quantitation of *Panx1* expression and its relation to function is expected to provide a foundation for future efforts aimed at deciphering the role of Panx1 under physiological and pathological conditions.

**Keywords:** qPCR, cell-specific deletion, Cre-recombinase, hypomorphism, pannexin

## INTRODUCTION

Pannexins are a group of proteins that share some sequence homology with the invertebrate gap junctions, the innexins, and because of that are considered to be members of this family. Three Pannexins (Panx1, Panx2, and Panx3) are present in mammalian tissues (Panchin et al., 2000). They have no sequence homologies with the chordate gap junction proteins, connexins, but membrane topology predicts similar four transmembrane domains with cytosolic N- and C- termini. Panx1 is ubiquitously expressed while Panx2 is restricted to the CNS and Panx3 is mainly found in cartilage and dermis (Baranova et al., 2004; Barbe et al., 2006; Penuela et al., 2007). Of the three, Panx1 is best characterized, forming high conductance plasma membrane channels with a maximal conductance of 500 pS that are permeable to ATP and modulated by intracellular signaling molecules (calcium, tyrosine kinase, caspases) (Bao et al., 2004; Locovei et al., 2006a; Pelegrin and Surprenant, 2006; Iglesias et al., 2008;

Sandilos and Bayliss, 2012). Panx1 channel activity can be modulated by mechanical stretch, membrane potential, cytoplasmic Ca<sup>2+</sup> concentration (Bao et al., 2004; Locovei et al., 2006b), and by ATP directly or via purinergic receptors (Locovei et al., 2006b, 2007; Pelegrin and Surprenant, 2006; Qiu and Dahl, 2009). Panx1 channels are permeable to ATP (Bao et al., 2004; Locovei et al., 2006a) and thus contribute to purinergic signaling including that involved in the propagation of intercellular calcium waves between astrocytes (Scemes et al., 2007; Suadicani et al., 2012), communication between taste bud cells (Huang et al., 2007), neutrophil activation and immune defense (Chen et al., 2010), and vascular tone (Billaud et al., 2012). Several studies indicate the involvement of Panx1 in certain pathophysiological conditions (ischemia, seizures, innate immune response, ATP-induced cell death, HIV infection, etc.) [reviewed in Scemes et al., 2009; Dahl and Keane, 2012].

Over the last few years at least four different transgenic mouse lines have been generated to knockdown Panx1 expression: the Monyer (single and double Panx1 and Panx2 KO (Bargiotas et al., 2011), the Knockout Mouse Project (KOMP; www.KOMP.org), the Genentech (www.genentech.com), and the Miami (Romanov

**Abbreviations:** Panx1, pannexin1; CNS, central nervous system; PNS, peripheral nervous system; RT-PCR, reverse transcription-polymerase chain reaction; qRT-PCR, quantitative real time RT-PCR; GFAP, glial fibrillary acidic protein; NFH, neurofilament H; WT, wild-type; KO, knockout.

et al., 2012) mice. While the former mice were generated by introducing a lacZ and a neomycin cassette within exon 1 of *Panx1* (Bargiotas et al., 2011), hence disrupting the gene transcription, the other three Panx1-null mice were designed using approaches that allow for both global deletion as well as cell-specific deletion. The Genentech and the Miami mouse lines were generated using the “conditional first” strategy, which relies on the creation of a conditional allele which when crossed with a Cre-deleter or a promoter specific-Cre mouse removes the loxP flanked region for transmission of the knockout (KO) or conditional allele. The KOMP mouse is based on the KO-first strategy (Testa et al., 2004) involving the insertion of a cassette into the first intron of *Panx1* that produces a KO at the transcript level, due to the presence of a splice acceptor in the cassette that captures the transcript. Thus, mice homozygous for the KO-first cassette are Panx1-null; however, a hypomorphic phenotype may result if the KO function of the RNA processing module is bypassed. For cell-specific KO, the KO-first allele was designed with two FRT sites flanking the cassette containing the splice acceptor and loxP sites flanking *Panx1* exon 2. Conditional KO mice can be generated by crossing Panx1 KO-first mice with flippase deleter mice, hereby inducing excision of the cassette at the FRT sites. This restores gene function and leaves *Panx1* exon 2 flanked by 2 loxP sites. The use of appropriate Cre expressing mouse lines then allows for a cell-type specific *Panx1* gene deletion.

Here we provide a molecular biological approach that allows for the evaluation of the state of knockdown of *Panx1* in the global and conditional Panx1 KO mice from KOMP. Our results indicate that global Panx1 KO mice (homozygous KO-first alleles) have a hypomorphic phenotype, with about 70% reduction of *Panx1* mRNA in 10 tissues that were analyzed. In the conditional Panx1 KO, our study indicates significant ectopic expression of Cre recombinase when using either mGFAP or the mNFH promoters to generate glia- and neuron-specific deletion of *Panx1*, respectively. We also describe a useful tail qRT-PCR method to readily detect such ectopic activity.

## MATERIALS AND METHODS

### ANIMALS

The Panx1-null mouse line (*Panx1*<sup>tm1a(KOMP)Wtsi</sup>), generated by KOMP ([www.KOMP.org](http://www.KOMP.org)) in the C57BL/6 background, uses a construct that introduces a floxed locus so that cell-type specific KO can be achieved through breeding with a Cre recombinase mouse. KOMP mice are maintained in our animal facility at Albert Einstein College of Medicine as global Panx1 knockout (Panx1 KO-first) and wild-type (WT) Panx1 (*Panx1*<sup>+/+</sup>). Panx1<sup>f/f</sup> mice were generated by crossing Panx1 KO-first with flippase deleter mice (B6.ACTFLPe/J) to allow targeted knockdown of Panx1 in either astrocytes or neurons after crossing with cell-type specific Cre mice. For that, mGFAP-Cre (B6.Cg-Tg(Gfap-cre)73.12Mvs/J) and mNFH-Cre (Tg(Nefh-cre)12Kul/J) mice in the C57BL/6 background were purchased from Jackson laboratory and were used to generate mGFAP-Cre:Panx1<sup>f/f</sup> and mNFH-Cre:Panx1<sup>f/f</sup> mice that are maintained in our animal facility. For some studies, we also used the Panx1<sup>-/-</sup> mouse line (Bargiotas et al., 2011), which was maintained at the animal facility of the University of Geneva. All studies were performed

following protocols approved by the Albert Einstein Animal Care and Use Committee.

### GENOTYPING

As previously described (Santiago et al., 2011), Panx1 KO-first mice were genotyped by tail PCR using two forward (F1a, F1b) and two reverse (R1a, R1b) primers (F1a: GAGAT GGCGAACGCAATTAAAT; R1a: CTGGCTCTCATAATTCTT GCCCTG; F1b: CTGTATCACACAACCACATTCAATAG3; R1b: GAGCTGACCCCTTCATTCAATAG3). The WT *Panx1* allele was targeted by primers F1a and R1a and identified as a 579 bp amplicon, while the transgene was targeted by primers F1b and R1b and identified as a 381 bp amplicon (Figure 1).

### TISSUE PREPARATION

Six month old WT and Panx1 KO-first mice were anesthetized with isoflurane and exsanguinated by intracardiac perfusion with ice-cold phosphate buffered saline, pH 7.4. The tissues were immediately removed, transferred to vials with RNAlater solution (Ambion, Life Technologies, Grand Island, NY), and stored at 4°C until processing for qRT-PCR analysis. Tissue samples were collected from tail tips, nervous system (cortex, hippocampus, cerebellum, trigeminal ganglia), heart (apex region), bone (calvaria), spleen, urinary bladder, liver (middle lobe), and kidney (cortical and medullar regions).

### RT-PCR

Primers used for *Panx1* mRNA coding region were F: ATGGCCA TCGCCCCACTTG R: GCAGGACGGATTCAAGGCC (1278 bp). Reaction mixtures using Multiplex PCR kit (Qiagen) with targeted cDNA were denatured at 95°C for 10 min, followed by 40 PCR cycles. Each cycle consisted of the following three steps: 94°C for 30 s, 55°C for 30 s, and 72°C for 90 s. Final extension was set at 72°C for 10 min.

### qRT-PCR

Tissues of adult mice (Panx1 WT, Panx1 KO-first, Panx1<sup>f/f</sup>, GFAP-Cre:Panx1<sup>f/f</sup>, and NFH-Cre:Panx1<sup>f/f</sup>) were used to quantify the levels of *Panx1* transcripts. Tissues were minced and homogenized with a Bullet Blender (Next Advance Inc.) and total RNA was extracted using the RNeasy fibrous tissue or plus mini kits (Qiagen) according to the manufacturer’s protocol. Complementary DNA was synthesized from 1 μg/10 μl of RNA, using a Superscript VILO cDNA Synthesis Kit (Invitrogen). Primers used are Pannexin1 (F: AGCCAGAGACTGGAGTTCA AAGA; R: CATTAGCAGGACGGATTCAAGAA) and 18S ribosomal RNA (F: CACGGCCGGTACAGTGAAAC; R: AGAGGAGC GAGCGACCAAA). GAPDH primers (F: CAAGGCTGTGGGCA AGGTCA; R: CATCATACTTGGCAGGTTTC). GAPDH and 18S were used as house-keeping genes for normalization. Real-time RT-PCR was performed using SYBR Green PCR Master Mix with 7300 Fast Real-Time PCR system (Applied Biosystems). Reaction mixtures were denatured at 95°C for 10 min, followed by 40 PCR cycles. Each cycle consisted of the following three steps: 94°C for 15 s, 57°C for 15 s, and 72°C for 1 min. Each sample was normalized against internal controls (18S ribosomal or GAPDH RNAs); the relative values for target abundance was extrapolated from standard curves generated from the reference standard.

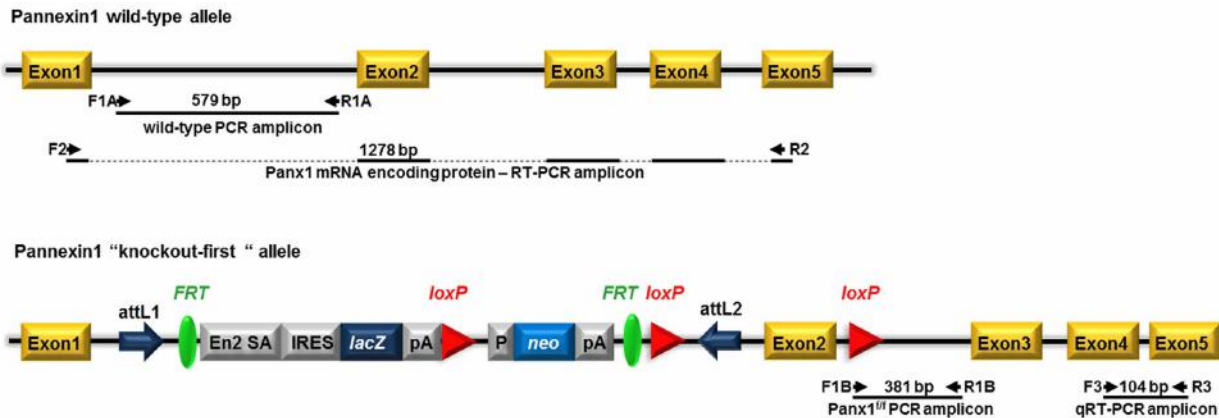


**FIGURE 1 | Schematic view of the Panx1 wild-type allele and the “knockout-first” conditional allele of Panx1<sup>tm1a(KOMP)Wtsi</sup> mice.** Pannexin1 (*Panx1*) gene consists of 5 exons. Panx1 “knockout-first” allele was generated by KOMP through insertion of the L1L2\_Bact\_P cassette into the mouse *Panx1* gene at position 15010456 of Chromosome 9. The cassette is composed of 2 FRT sites flanking an IRES:*lacZ* trapping cassette and a floxed human beta actin promoter-driven *neo* cassette inserted into the intron 1 of *Panx1* and an additional third loxP site downstream, at position 15009768, of *Panx1* exon 2, the critical exon. This “knockout-first” allele is designed to generate a Panx1 null allele through splicing exon 1 to a *lacZ* trapping element and disrupting

*Panx1* mRNA expression. The trapping cassette also includes the mouse En2 splice acceptor (En2 SA) and the SV40 polyadenylation sequences. Position of primers used for genotyping (two primer sets: F1a—R1a and F1b—R1b), for RT-PCR (primer set F2—R2), and for qRT-PCR (primer set F3—R3) with expected amplicon length are indicated. *attL1* and *attL2*: sites for site-specific recombination of the entry clone. FRT: sites for flippase activity. EN2-SA: splice acceptor of mouse engrail (En2) exon 2. IRES, internal ribosome entry site; *lacZ*, gene encoding β-galactosidase; pA, polyadenylation signal; *neo*, neomycin phosphotransferase; loxP sites (triangles); target sites for Cre recombinase. Adapted from [www.KOMP.org](http://www.KOMP.org).

## IMMUNOHISTOCHEMISTRY

Trigeminal ganglia from WT, Panx1 KO-first, Panx1<sup>f/f</sup> and conditional Panx1 KO (GFAP-Cre:Panx1<sup>f/f</sup> and NFH-Cre:Panx1<sup>f/f</sup>) mice were removed from animals anesthetized with isoflurane and sacrificed by decapitation. Isolated trigeminal ganglia were then fixed in 4% p-formaldehyde overnight and incubated in 30% sucrose for 48 h. Tissues were then embedded in O.C.T., cryosectioned (12 μm), incubated with blocking solution containing 0.4% Triton-X, and immunostained with a Panx1 antibody and with neuronal (NeuN) or glial (glutamine synthase) markers. The primary antibodies used were: chicken anti-Panx1 (1:500; extracellular loop epitope: VQQKSSLQSES; Aves Lab #6358); mouse anti-NeuN (1:100; Millipore); goat anti-glutamine synthase (1:200; Santa Cruz). Secondary Alexa conjugated antibodies (1:2000) were: goat anti-chicken, goat anti-mouse, and donkey anti-goat. Images were acquired using an Olympus Fluoview 300 confocal laser scanning microscope equipped with a 40× water-immersion lens (0.80 NA), and FITC, TRITC, and UV filter sets.

## RESULTS

### PRESENCE OF PANNEXIN1 mRNA IN PANNEXIN1 KO-FIRST MICE

The Panx1 transgenic mice generated by KOMP using the KO-first strategy (Testa et al., 2004) result from the insertion into intron 1 of the *Panx1* gene of a cassette containing a splice acceptor that captures the nascent RNA and a polyadenylation signal that truncates the transcript downstream of the cassette (Figure 1). Depending on the intron, this type of construct can yield either a KO or a hypomorphic allele, in case of alternative splicing or the presence of a downstream promoter.

Heterozygous Panx1 KO-first purchased from KOMP were bred to obtain homozygous WT and Panx1 KO-first mice

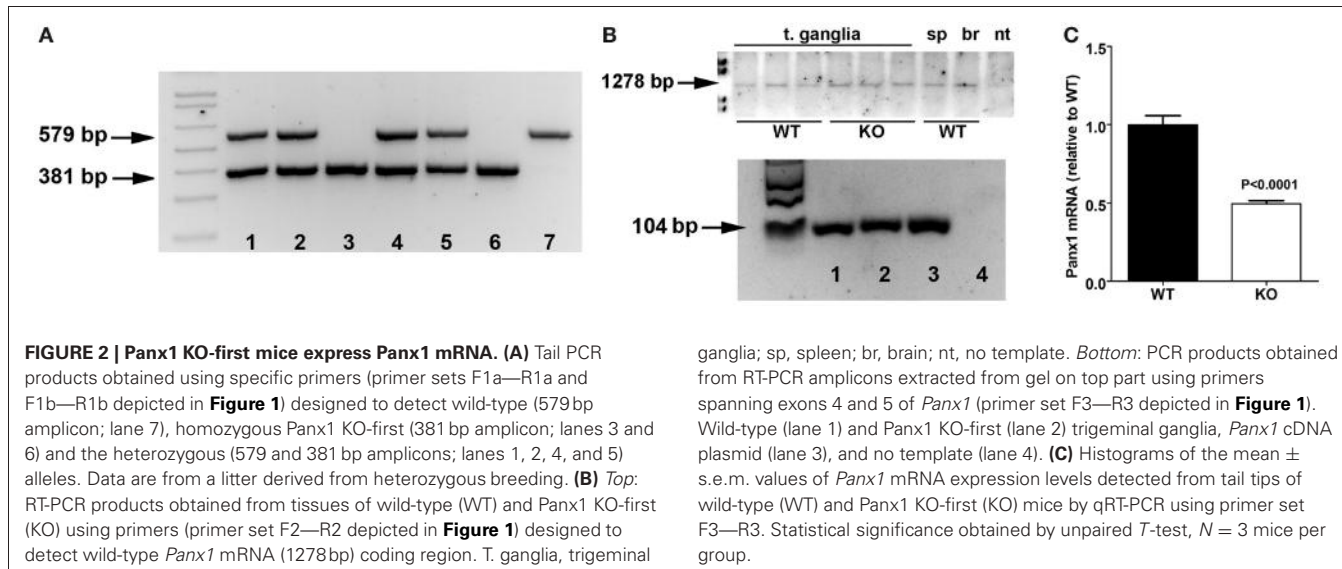
(Figure 2A). To evaluate whether Panx1 KO-first mice represent a complete KO or a hypomorphic phenotype with residual *Panx1* transcript, we designed RT-PCR primers (set F2—R2 in Figure 1) to detect *Panx1* mRNA coding region in tissues of WT and Panx1 KO-first adult mice. As shown in Figure 2B, Panx1 KO-first mice displayed amplicons corresponding to the entire *Panx1* mRNA region (1278 bp) similar to WT (C57Bl/6N and C57Bl/6J) mice, confirming that the KO-first strategy did not completely prevent *Panx1* transcription. In addition, extraction of bands from the RT-PCR gel for further amplification, using primer sets spanning exons 4 and 5 of *Panx1*, confirmed that the KO-first trapping cassette could be bypassed (Figure 2B, bottom), allowing for transcription of the entire *Panx1* mRNA in the Panx1 KO-first mice. Note, in Figure 2B *Panx1* mRNA expression is shown qualitatively, but not quantitatively. To quantify the extent of *Panx1* deletion (i.e., efficiency of the KO-first trapping cassette), we performed qRT-PCR using primers (set F3—R3 in Figure 1; downstream of the trapping cassette) and tail tip samples from 3 WT and 3 KO-first adult mice.

After normalization of ct values of *Panx1* to those obtained for control 18S, *Panx1* mRNA expression levels recorded from Panx1 KO-first were compared to those obtained from WT samples. As indicated in Figure 2C, we measured about 50% reduction of *Panx1* mRNA in tail tips of Panx1 KO-first relative to that of WT.

Thus, our results indicate that transcription of *Panx1* mRNA is only partially ablated in the Panx1 KO-first mouse.

### HYPOMORPHIC PHENOTYPE OF PANNEXIN1 KO-FIRST MICE

Pannexin1 is ubiquitously expressed, but its expression levels in different tissues have not previously been quantified. We therefore measured *Panx1* mRNA levels in various tissues of three WT mice by qRT-PCR using primers (set F3—R3 in Figure 1) spanning



exons 4 and 5. Comparison of *Panx1* mRNA expression levels (normalized to 18S) identified highest *Panx1* levels in trigeminal ganglia of the PNS (t. ganglia; 17.12e-005), followed by bladder (14.05e-005) and spleen (10.94e005) (**Figure 3A**). *Panx1* mRNA expression levels were 4–10 times lower in the CNS compared to t. ganglia and differed in various brain regions (cortex: 4.772e-005, hippocampus: 6.28 e-005, cerebellum: 1.705e-005). Similar results were obtained when *Panx1* mRNA were normalized to GAPDH (data not shown).

We next evaluated by qPCR whether down-regulation of *Panx1* transcript occurred in a homogeneous fashion across different tissues from Panx1 KO-first mice. Tissues of at least 3 mice per genotype were used; no siblings were used and not all tissues were from the same set of animals. We found that *Panx1* mRNA expression was similarly reduced by 70% in all Panx1 KO-first tissues analyzed compared to their respective tissue in WT mice. **Figure 3B** shows *Panx1* mRNA levels in Panx1 KO-first mice normalized to those of WT mice, which are (mean ± s.e.m.): cortex (WT: 1.0 ± 0.11; KO: 0.34 ± 0.06), hippocampus (WT: 1.0 ± 0.22; KO: 0.31 ± 0.008), cerebellum (WT: 1.0 ± 0.02; KO: 0.25), trigeminal ganglia (WT: 1.0 ± 0.02; KO: 0.34 ± 0.008), calvaria (WT: 1.0 ± 0.09; KO 0.33 ± 0.034), heart (WT: 1.0 ± 0.15; KO 0.3 ± 0.18), bladder (WT: 1.0 ± 0.22; KO: 0.46 ± 0.05), spleen (WT: 1.0 ± 0.12; KO: 0.34 ± 0.22), kidney (WT: 1.0 ± 0.07; KO: 0.35 ± 0.03), and liver (WT: 1.0 ± 0.08; KO: 0.28 ± 0.03).

These results indicate that the KO-first cassette leads to a similar reduction of *Panx1* mRNA in all tissues tested, and that, for any given tissue, the variability between animals was low, as evaluated by the s.e.m. values.

Using this same set of primers and qPCR conditions, we evaluated *Panx1* levels in another transgenic mouse line, the Panx1<sup>−/−</sup> (Bargiotas et al., 2011). Compared to Panx1 KO-first, *Panx1* mRNA levels measured from hippocampi of Panx1<sup>−/−</sup> mice was markedly reduced (Panx1<sup>+/+</sup>: 0.99 ± 0.12; Panx1<sup>−/−</sup>: 0.01 ± 0.003; **Figure 3C**), further confirming the hypomorphic phenotype of the Panx1 KO-first.

Immunohistochemistry performed on trigeminal ganglia isolated from WT and Panx1 KO-first indicated that the remaining 30% Panx1 mRNA in the KO-first tissue did not result in detectable Panx1 protein (**Figures 3D,E**).

#### CONDITIONAL, CELL-SPECIFIC Panx1 KO MICE: GFAP-Cre:Panx1<sup>f/f</sup> AND NFH-Cre:Panx1<sup>f/f</sup>

One of the advantages of the KO-first strategy is the possibility of generating conditional deletion of the gene of interest. By crossing Panx1 KO-first with flipase deleter mice, the KO-first cassette flanked by FRT sites is removed, and *Panx1* gene function is restored, leaving 2 loxP sites flanking exon 2 of *Panx1*. Crossing these floxed Panx1 mice with mice expressing Cre recombinase under cell-specific promoters allows for the generation of conditional KO mice (**Figure 4**).

To evaluate the extent to which *Panx1* mRNA expression was restored after removal of the KO-first cassette, we performed qRT-PCR on tail tip samples of Panx1<sup>f/f</sup> and compared that to WT samples. As shown in **Figure 5**, we found that in 26 Panx1<sup>f/f</sup> mice *Panx1* mRNA was 1.22 ± 0.08 fold that of WT mice.

We then generated conditional astrocyte- and neuron-specific Panx1 KO mice by crossing Panx1<sup>f/f</sup> with either mGFAP-Cre or mNFH-Cre mice, respectively. Cre-recombinase displays high incidence of ectopic activity, leading to non-cell-type specific target deletion (Schmidt-Suprian and Rajewsky, 2007). We therefore developed a strategy to detect ectopic Cre activity in the tail of GFAP-Cre:Panx1<sup>f/f</sup> and NFH-Cre:Panx1<sup>f/f</sup> mice using qRT-PCR to determine *Panx1* mRNA expression levels. We considered that if mice showed tail levels of *Panx1* mRNA expression level less than 80% that of Panx1<sup>+/+</sup> mice, they were likely to exhibit ectopic Cre expression, since reduced *Panx1* mRNA expression in the tail would most likely be due to off target deletion of *Panx1*. Based on this consideration, we found that 16.7% (4/24) NFH-Cre:Panx1<sup>f/f</sup> and 52.6% (10/19) GFAP-Cre:Panx1<sup>f/f</sup> offspring from Panx1<sup>f/f</sup> females and Cre:Panx1<sup>f/f</sup> males had less than 80% *Panx1* mRNA compared

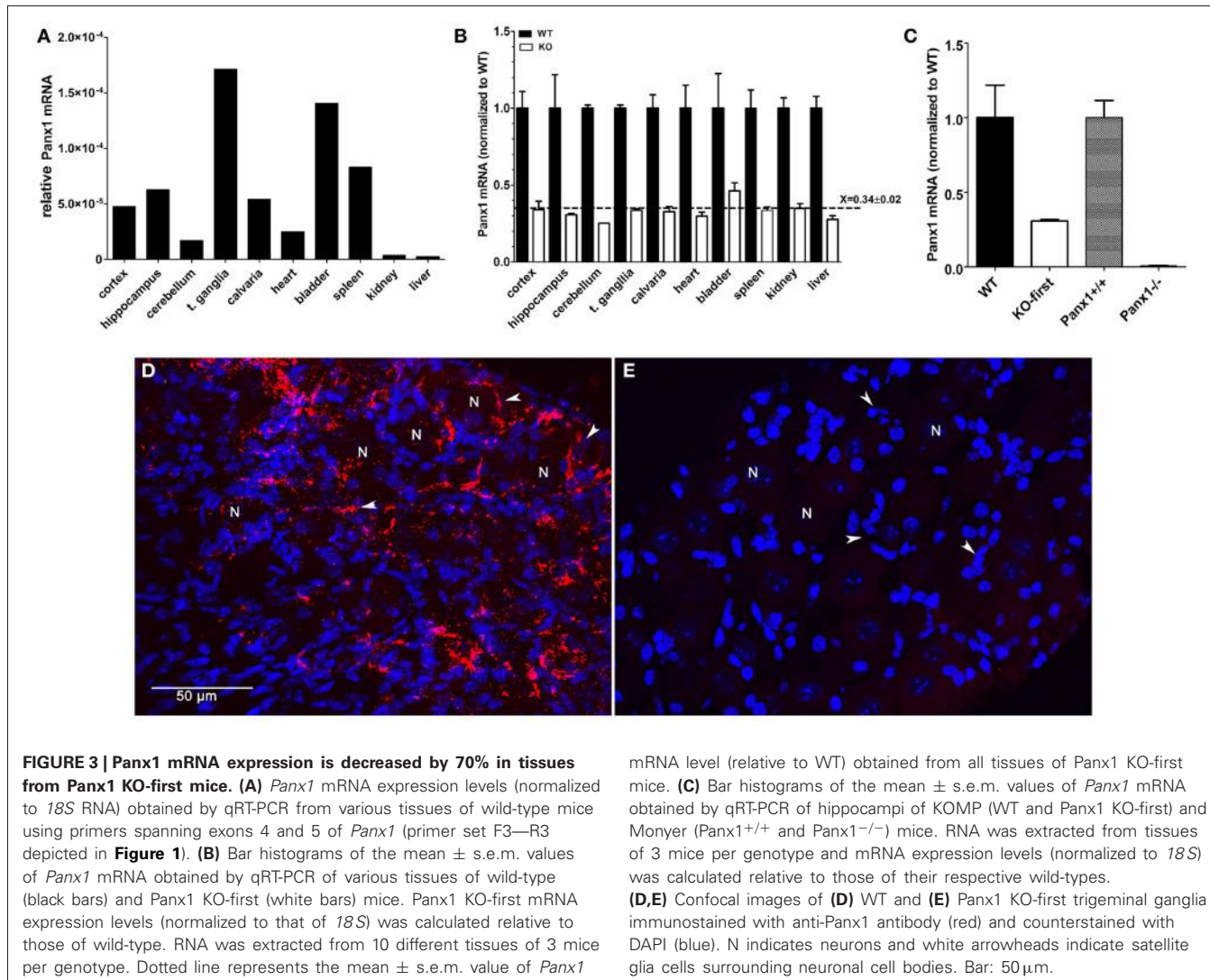


**FIGURE 3 |** *Panx1* mRNA expression is decreased by 70% in tissues from *Panx1* KO-first mice. **(A)** *Panx1* mRNA expression levels (normalized to 18S RNA) obtained by qRT-PCR from various tissues of wild-type mice using primers spanning exons 4 and 5 of *Panx1* (primer set F3—R3 depicted in Figure 1). **(B)** Bar histograms of the mean  $\pm$  s.e.m. values of *Panx1* mRNA obtained by qRT-PCR of various tissues of wild-type (black bars) and *Panx1* KO-first (white bars) mice. *Panx1* KO-first mRNA expression levels (normalized to that of 18S) was calculated relative to those of wild-type. RNA was extracted from 10 different tissues of 3 mice per genotype. Dotted line represents the mean  $\pm$  s.e.m. value of *Panx1*

mRNA level (relative to WT) obtained from all tissues of *Panx1* KO-first mice. **(C)** Bar histograms of the mean  $\pm$  s.e.m. values of *Panx1* mRNA obtained by qRT-PCR of hippocampi of KOMP (WT and *Panx1* KO-first) and Monyer (*Panx1*<sup>+/+</sup> and *Panx1*<sup>-/-</sup>) mice. RNA was extracted from tissues of 3 mice per genotype and mRNA expression levels (normalized to 18S) was calculated relative to those of their respective wild-types.

**(D,E)** Confocal images of **(D)** WT and **(E)** *Panx1* KO-first trigeminal ganglia immunostained with anti-*Panx1* antibody (red) and counterstained with DAPI (blue). N indicates neurons and white arrowheads indicate satellite glial cells surrounding neuronal cell bodies. Bar: 50 μm.

to WT controls (Figure 5). We found that about 34% *Panx1*<sup>f/f</sup> littermates (offspring of *Panx1*<sup>f/f</sup> and mNFH-Cre:*Panx1*<sup>f/f</sup> or mGFAP-Cre:*Panx1*<sup>f/f</sup>) had lower *Panx1* mRNA expression in tail tip samples ( $0.69 \pm 0.03$  fold;  $N = 11$  mice) compared to WT mice. No significant differences in 18S RNA levels were detected among these samples. This reduced expression of *Panx1* mRNA in *Panx1*<sup>f/f</sup> (littermates of conditional *Panx1* KO mice) compared to those detected from offspring of *Panx1*<sup>f/f</sup> and *Panx1*<sup>f/f</sup> mice, most likely relates to the transient expression of Cre in the germlines of *Panx1*<sup>f/f</sup> derived from GFAP-Cre or mNFH-Cre crosses.

Mice that did not show ectopic Cre activity were then evaluated for *Panx1* deletion in glia and neuronal cells using trigeminal ganglia processed for immunohistochemistry. As shown in Figure 6, *Panx1* expression in satellite glial cells (Figures 6B,E) and in neurons (Figures 6C,F) was significantly reduced in the trigeminal ganglia of GFAP-Cre and NFH-Cre:*Panx1*<sup>f/f</sup> mice, respectively, compared to that found in *Panx1*<sup>f/f</sup> ganglia (Figures 6A,D).

## DISCUSSION

Here we characterized *Panx1* expression in WT and transgenic *Panx1* mice developed by KOMP. Although *Panx1* is ubiquitously expressed in WT mice, we detected different levels of *Panx1* mRNA in distinct tissues, with highest *Panx1* levels in trigeminal ganglia, bladder and spleen. Transgenic *Panx1* mice from KOMP were generated using a KO-first approach, which allows generation of global KO or conditional KO mice. We found that *Panx1* KO-first mice represent a hypomorphic phenotype, and not a complete KO. Moreover, *Panx1* mRNA was similarly reduced by 70% in all tissues derived from *Panx1* KO-first mice compared to the level of each respective WT tissue. Mice with conditional deletion of *Panx1* in astrocytes and neurons, which we generated from *Panx1* KO-first mice using FLP deleter and cell-type specific Cre mice, are shown to exhibit ectopic Cre expression with non-specific *Panx1* downregulation in the tail of 16.7% NFH-Cre:*Panx1*<sup>f/f</sup> and 52.6% GFAP-Cre:*Panx1*<sup>f/f</sup>. This indicates the importance of careful monitoring of transgenic *Panx1* mice for colony stability. To this end,

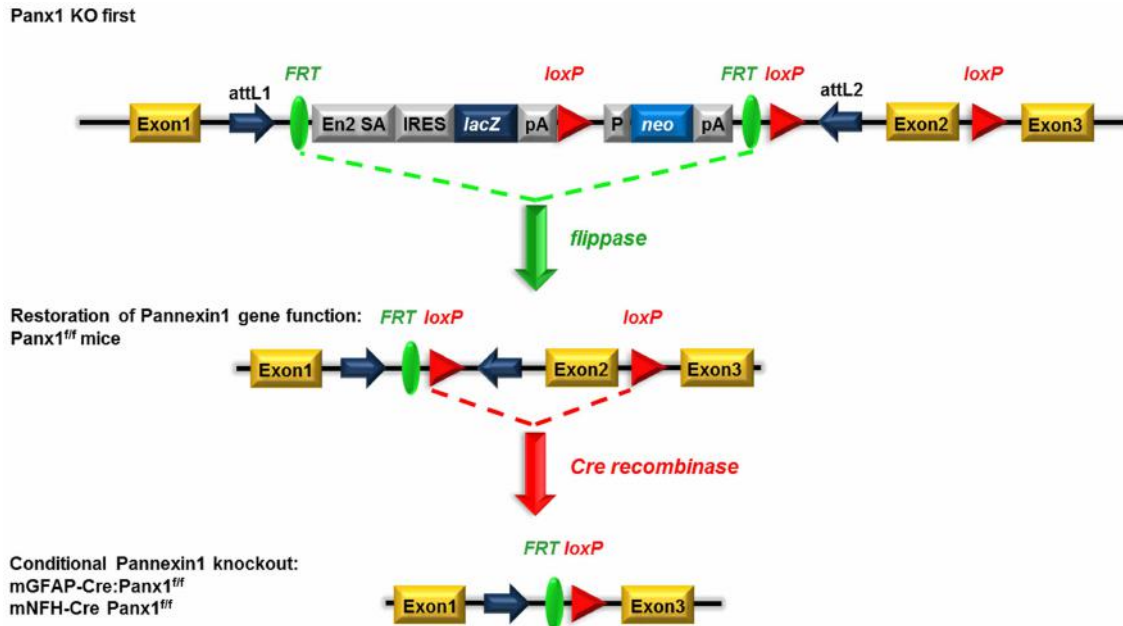
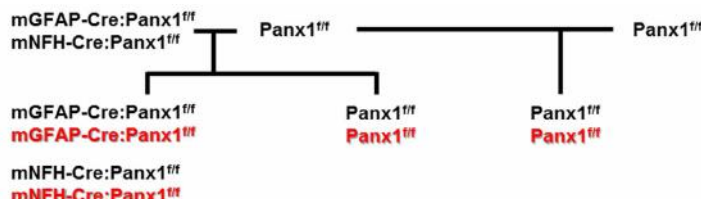


**FIGURE 4 | Schematic view of the generation of conditional GFAP-Cre and NFH-Cre Panx1<sup>tm1a(KOMP)Wtsi</sup> mice.** Mice homozygous for the “knockout-first” allele are expected to have a null phenotype due to the splicing of exon 1 to a *lacZ* trapping element and disruption of *Panx1* mRNA expression. The insertion cassette is flanked by FRT recombination sites that allow flippase recombinase to remove the gene-trapping cassette, hereby

converting the “knockout-first” allele to a conditional allele (loxP sites flanking exon 2) and restoring *Panx1* gene expression/activity. Upon removal of the floxed exon 2 with Cre recombinases, transcription of this *Panx1* allele generates a frameshift mutation and premature stop codon, which triggers nonsense mediated decay of the transcript. Adapted from [www.KOMP.org](http://www.KOMP.org).



Panx1 expression relative to Panx1 WT	Panx1 WT	Panx1 KO first	Panx1 <sup>t/t</sup> from f/f x f/f	mGFAP-Cre:Panx1 <sup>t/t</sup> from Cre x f/f	mNFH-Cre:Panx1 <sup>t/t</sup> from Cre x f/f	Panx1 <sup>t/t</sup> from Cre x f/f
Panx1 level ( $\geq 0.80$ )	1		1.22 $\pm$ 0.08	0.96 $\pm$ 0.03	1.04 $\pm$ 0.03	0.99 $\pm$ 0.04
Panx1 level ( $< 0.80$ )		0.43 $\pm$ 0.02	0.73	0.72 $\pm$ 0.01	0.68 $\pm$ 0.06	0.69 $\pm$ 0.03
incidence of reduced Panx1 expression			3.7% (1 of 27)	52.63% (10 of 19)	16.67% (4 of 24)	34.4% (11 of 32)

**FIGURE 5 | Ectopic activity of Cre recombinase. (Top)** Breeding scheme of Panx1<sup>f/f</sup> mice and conditional Panx1 knockout mice (mGFAP-Cre:Panx1<sup>t/t</sup> and NFH-Cre-Panx1<sup>t/t</sup>) used to evaluate *Panx1* mRNA expression.

**(Bottom)** Table showing *Panx1* expression determined by tail qPCR of

conditional Panx1 knockout and in Panx1<sup>f/f</sup> mice, which were generated as shown in top part. Animals were considered to have ectopic Cre activity if they showed less than 80% of *Panx1* mRNA expression compared to that found in WT mice.

we provide a useful molecular biological approach using tail biopsies.

In contrast to standard KO designs using targeted deletion, the KO-first approach leaves the *Panx1* gene intact and *Panx1* mRNA truncation depends on splicing *Panx1* exon1 to a trapping element consisting of splice acceptor and polyadenylation

site contained in the targeting cassette (International Mouse Knockout Consortium et al., 2007). However, the function of this RNA processing module can be bypassed through alternative splicing due to inefficiency in the splice acceptor-polyA module or the presence of additional, downstream regulatory elements. This inefficiency is likely the cause of the hypomorphic phenotype that

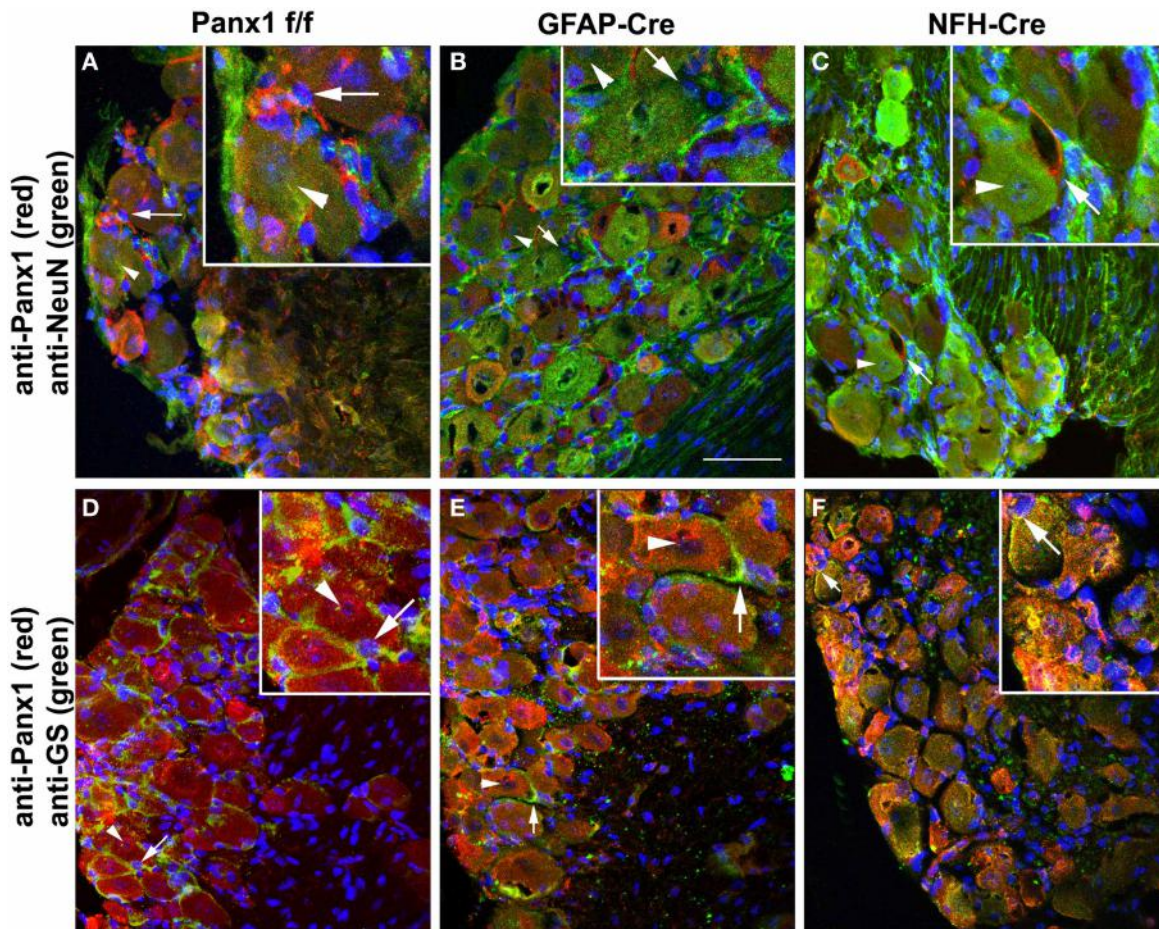


**FIGURE 6 | Conditional deletion of Panx1.** Confocal images of trigeminal ganglia showing expression of Panx1 in satellite glial cells and neurons in Panx1<sup>f/f</sup> (**A,D**), GFAP-Cre:Panx1<sup>f/f</sup> (**B,E**) and NFH-Cre:Panx1<sup>f/f</sup> (**C,F**) mice. The cell-specific markers NeuN and glutamine synthase (GS) were used to identify neurons (arrowheads) and glial cells (arrows), respectively. Panx1 immunostaining is evident in both neurons and glial cells of Panx1<sup>f/f</sup> mouse ganglion (**A,D**). In GFAP-Cre:Panx1<sup>f/f</sup> mice Panx1 immunoreactivity (red) is observed in neurons and not in glial cells (**B,E**). Conversely, in

NFH-Cre:Panx1<sup>f/f</sup> mice Panx1 immunoreactivity (red) is observed in glial cells and not in neurons (**C,F**). Note in panel (**F**) the faint immunoreactivity for Panx1 that colocalizes with neurons but actually corresponds to Panx1 expression in glial cells enwrapping the neuronal cell bodies. Images were obtained with a Olympus Fluoview 300 confocal laser scanning microscope equipped with 40× water-immersion lens (0.80 NA), U.V., and laser lines and appropriate filter sets. Bar: 50 μm; magnification in insets 2× that in main panels.

we report in Panx1 KO-first mice which featured a residual 30% *Panx1* mRNA in several tissues. Such hypomorphic phenotype has been previously described for other targeted genes (Meyers et al., 1998; Nagy et al., 1998).

The remaining Panx1 transcripts present in the KO-first tissues is not sufficient to revert the KO to a WT phenotype. Indeed, immunohistochemistry of trigeminal ganglia, a tissue that displays high levels of Panx1 mRNA, did not reveal the presence of Panx1 protein in the KO-first mice (Figure 3). Similarly, previous studies reported the absence of Panx1 protein in distinct tissues and cells (hippocampus, kidney, astrocytes, microglia, erythrocytes, airway epithelia cells) derived from these Panx1 KO-first mice (Seminario-Vidal et al., 2011; Qiu et al., 2011; Santiago et al., 2011; Hanner et al., 2012; Rigato et al., 2012; Suadicani et al., 2012). However, concerns regarding antibody specificity were raised in a study in which another

Panx1 KO mouse line was investigated (Bargiolas et al., 2011). In that study, only one out of four Panx1 antibodies tested indicated absence of a ~47 kDa band on western blots of Panx1 KO brain tissues (Bargiolas et al., 2011). In contrast to that report, a reduction or lack of Panx1 bands on western blots of tissues from two mouse lines (KOMP and Genentech) was recently reported using five different antibodies (Cone et al., 2013). Importantly, Cone et al. (2013) provided clear evidence that differences in patterns and intensities of bands are not restricted to the antibody sources, but is also found between Panx1 KO mouse lines and between tissues of the same transgenic mouse.

At present it is premature to conclude whether or not Panx1 protein is still present in the KO-first mice or even in other Panx1 KO mouse lines. Still, even if low levels of Panx1 protein would be present, the KOMP mice are

functional Panx1 KOs. Evidence of such are our recent report showing no significant differences in animal behavior, tissue and cell physiology, and even protein expression between the Panx1 KO-first and the Panx1<sup>-/-</sup> mice (Santiago et al., 2011). Taking into consideration the similarities between these two mouse lines together with our present findings showing that Panx1 KO-first express significantly higher levels of Panx1 transcripts than Panx1<sup>-/-</sup> mice (**Figure 2**), 70% knock down of Panx1 transcript appears sufficient to produce a functional KO.

As global deletions of single genes might lead to premature lethality, conditional gene disruption offers the possibility to investigate the role of a protein in specific cell-types during development. The Cre/lox system is a simple two component genetic tool, whereby under the control of a defined promoter Cre recombinase can be restricted to a specific tissue or cell-type (Nagy, 2000). However, recent reports show that Cre expression is not often strictly confined to the desired cells, often leading to spontaneously ectopic Cre activity (Eckardt et al., 2004). Furthermore, the efficiency of Cre recombination is variable and may be lost. Also, Cre expression may result in pleiotropic effects (Lee et al., 2006; Schulz et al., 2007; Wellershaus et al., 2008), including cell toxicity (Schmidt-Suprian and Rajewsky, 2007; Requardt et al., 2009). These reports showing non-homogeneity in cell-type specific target gene disruption, may have major impact on the experimental outcome. Therefore, individual mice with non-cell-type specific recombination (ectopic Cre activity) or reduced Cre activity have to be identified and discarded and the extent of the Cre-mediated gene ablation, here *Panx1*, must be correlated with phenotypic alterations.

As previously reported for the hGFAP-Cre: Cx43<sup>f/f</sup> mice (Requardt et al., 2009), we reveal a limitation of GFAP-Cre:Panx1<sup>f/f</sup> and NFH-Cre:Panx1<sup>f/f</sup> mice, spontaneous ectopic *Panx1* gene disruption, that requires a rigorous quality control. We have observed ectopic GFAP-Cre and NFH-Cre mediated recombination, which might be caused by spontaneous transgene rearrangements (Schulz et al., 2007), or other epigenetic mechanisms suggested to lead to evolutionary selection against Cre activity (Lee et al., 2006; Requardt et al., 2009). Individual genotyping PCR to detect Cre on the DNA level does not necessarily indicate the presence or absence of gene disruption in a specific cell-type, and analyses of the efficacy of disruption is required. We suggest tail-biopsy qRT-PCR for quality control to pre-experimentally ensure that *Panx1* expression levels in the tail are unaffected by GFAP- or NFH-Cre directed Cre activity. This simple control monitors ectopic Cre activity. The Cre recombination status in the colony must be properly monitored by routine testing of the offspring obtained from all breeding pairs, to ensure cell-specific Cre activity and *Panx1* gene disruption. Otherwise, unfortunate choice of parental animals with ectopic or non-functional Cre may increase the number of these mice in the colony during the following generations. For experimental animals, a good strategy to validate cell-specific *Panx1* gene disruption is the post-experimental confirmation of cell-specific Cre activity and *Panx1* deletion using immunohistochemical approaches in every

individual mouse and to correlate the index of gene inactivation with phenotypical alterations. Indeed, our immunohistochemical studies indicated significant reduction of Panx1 expression in satellite glial cells and neurons of the trigeminal ganglia of GFAP-Cre:Panx1<sup>f/f</sup> and NFH-Cre:Panx1<sup>f/f</sup> mice which did not show ectopic Cre expression. The lack of complete cell-type specific deletion of Panx1 in these conditional KO mice may be related to the efficiency of GFAP and NFH recombination which could be checked using a reporter mouse line. Using such an approach, we estimated that 80% astrocytes and 70% pyramidal neurons of the hippocampus are recombined when using the mGFAP-Cre and NFH-Cre lines (data not shown). These values are in accordance with previous reports using these Cre mouse lines (Hirasawa et al., 2001; Garcia et al., 2004).

Panx1 has been shown to be a major ATP release channel, which is expressed in all cells releasing ATP (Dahl and Keane, 2012). Panx1 channels also interact with other proteins, such as the purinergic receptor P2X<sub>7</sub> and possibly inflammasome components involved in the innate immune response and associated secondary cell death (Pelegrin and Surprenant, 2006; Locovei et al., 2007; Silverman et al., 2009), thus responsible for amplification of the primary lesion in CNS trauma, stroke and epilepsy (Bergfeld and Forrester, 1992; De Rivero Vaccari et al., 2009; Santiago et al., 2011). Recently, it has been shown that Panx1 is involved in the fusion of T cell membrane with the human immunodeficiency virus (Seror et al., 2011). In all these processes Panx1-mediated ATP release is an early signal event in which Panx1 acts as a signal amplifier and is therefore an obvious target for the development of innovative therapeutic approaches. Advantages of Panx1 as a drug target are that it is accessible to drugs and Panx1 inhibitors are already available and FDA approved, such as the anti-malaria drug mefloquine and the gouty arthritis drug probenecid. However, more research is required to identify whether Panx1 has additional roles under physiological and pathological conditions in order to avoid undesirable side effects when targeting it.

We conclude that mice with *Panx1* modulation, specifically the multi-purpose Panx1 KO-first mice, represent a suitable model to investigate these questions. However, in this model and in many others using this strategy, the expression levels of the genes of interest must be carefully monitored to allow for a correct interpretation of the experimental findings.

## ACKNOWLEDGMENTS

We greatly appreciate the assistance of Dr. Eno E. Ebong with cryosections and the use of the Image Core Facility of the Rose F. Kennedy Intellectual and Developmental Disabilities Research Center, supported by the Eunice Kennedy Shriver National Institute of Child Health and Human Development of the National Institutes of Health (1P30HD071593-01). The US group was supported by the National Institutes of Health, National Institute of Neurological Disorders and Stroke [Grants NS052245 (to Eliana Scemes) and NS041282 (to David C. Spray)], National Institute of Diabetes and Digestive and Kidney Disease [Grant DK081435 (to Sylvia O. Suadicani)],

and the National Institute of Arthritis and Musculoskeletal and Skin Diseases [Grant AR057139 (to David C. Spray)]. The Geneva team was supported by grants from the Swiss National Science Foundation (310000-109402, CR32I3\_129987,

IZ73Z0\_127935), the Juvenile Diabetes Research Foundation (40-2011-11, 99-2012-775), and the European Union (BETAIMAGE 222980; IMIDIA, C2008-T7, BETATRAIN, 289932).

## REFERENCES

- Bao, L., Locovei, S., and Dahl, G. (2004). Pannexin membrane channels are mechanosensitive conduits for ATP. *FEBS Lett.* 572, 65–68.
- Baranova, A., Ivanov, D., Petrush, N., Pestova, A., Skoblov, M., Kelmanson, I., et al. (2004). The mammalian pannexin family is homologous to the invertebrate innexin gap junction proteins. *Genomics* 83, 706–716.
- Barbe, M. T., Monyer, H., and Bruzzone, R. (2006). Cell-cell communication beyond connexins: the pannexin channels. *Physiology (Bethesda)* 21, 103–114.
- Bargiolas, P., Krenz, A., Hormuzdi, S. G., Ridder, D. A., Herb, A., Barakat, W., et al. (2011). Pannexins in ischemia-induced neurodegeneration. *Proc. Natl. Acad. Sci. U.S.A.* 108, 20772–20777.
- Bergfeld, G. R., and Forrester, T. (1992). Release of ATP from human erythrocytes in response to a brief period of hypoxia and hypercapnia. *Cardiovasc. Res.* 26, 40–47.
- Billaud, M., Sandilos, J. K., and Isakson, B. E. (2012). Pannexin 1 in the regulation of vascular tone. *Trends Cardiovasc. Med.* 22, 68–72.
- Chen, Y., Yao, Y., Sumi, Y., Li, A., To, U. K., Elkhal, A., et al. (2010). Purinergic signaling: a fundamental mechanism in neutrophil activation. *Sci. Signal.* 3:ra45. doi: 10.1126/scisignal.2000549
- Cone, A. C., Ambrosi, C., Scemes, E., Martone, M. E., and Sosinsky, G. E. (2013). A comparative antibody analysis of pannexin1 expression in four rat brain regions reveals varying subcellular localizations. *Front. Pharmacol.* 4:6. doi: 10.3389/fphar.2013.00006
- Dahl, G., and Keane, R. W. (2012). Pannexin: from discovery to bedside in 11+/-4 years? *Brain Res.* 1487, 150–159.
- De Rivero Vaccari, J. P., Lotocki, G., Alonso, O. F., Bramlett, H. M., Dietrich, W. D., and Keane, R. W. (2009). Therapeutic neutralization of the NLRP1 inflammasome reduces the innate immune response and improves histopathology after traumatic brain injury. *J. Cereb. Blood Flow Metab.* 29, 1251–1261.
- Eckardt, D., Theis, M., Doring, B., Speidel, D., Willecke, K., and Ott, T. (2004). Spontaneous ectopic recombination in cell-type-specific Cre mice removes loxP-flanked marker cassettes *in vivo*. *Genesis* 38, 159–165.
- Garcia, A. D., Doan, N. B., Imura, T., Bush, T. G., and Sofroniew, M. V. (2004). GFAP expressing progenitors are the principal source of constitutive neurogenesis in adult mouse forebrain. *Nat. Neurosci.* 7, 1233–1241.
- Hirasawa, M., Cho, A., Sreenath, T., Sauer, B., Julien, J. P., and Kulkarni, A. B. (2001). Neuron-specific expression of Cre during the late phase of brain development. *Neurosci. Res.* 40, 125–132.
- Hanner, F., Lam, L., Nguyen, M. T., Yu, A., and Peti-Peterdi, J. (2012). Intrarenal localization of the plasma membrane ATP channel pannexin1. *Am. J. Physiol. Renal Physiol.* 303, F1454–F1459.
- Huang, Y. J., Maruyama, Y., Dvoryanchikov, G., Pereira, E., Chaudhari, N., and Roper, S. D. (2007). The role of pannexin 1 hemichannels in ATP release and cell-cell communication in mouse taste buds. *Proc. Natl. Acad. Sci. U.S.A.* 104, 6436–6441.
- Iglesias, R., Locovei, S., Roque, A., Alberto, A. P., Dahl, G., Spray, D. C., et al. (2008). P2X7 receptor-Pannexin1 complex: pharmacology and signaling. *Am. J. Physiol. Cell Physiol.* 295, C752–C760.
- International Mouse Knockout Consortium, Collins, F. S., Rossant, J., and Wurst, W. (2007). A mouse for all reasons. *Cell* 128, 9–13.
- Lee, Y., Su, M., Messing, A., and Brenner, M. (2006). Astrocyte heterogeneity revealed by expression of a GFAP-LacZ transgene. *Glia* 53, 677–687.
- Locovei, S., Bao, L., and Dahl, G. (2006a). Pannexin 1 in erythrocytes: function without a gap. *Proc. Natl. Acad. Sci. U.S.A.* 103, 7655–7659.
- Locovei, S., Wang, J., and Dahl, G. (2006b). Activation of pannexin 1 channels by ATP through P2Y receptors and by cytoplasmic calcium. *FEBS Lett.* 580, 239–244.
- Locovei, S., Scemes, E., Qiu, F., Spray, D. C., and Dahl, G. (2007). Pannexin1 is part of the pore forming unit of the P2X(7) receptor death complex. *FEBS Lett.* 581, 483–488.
- Meyers, E. N., Lewandoski, M., and Martin, G. R. (1998). An Fgf8 mutant allelic series generated by Cre- and Flp-mediated recombination. *Nat. Genet.* 18, 136–141.
- Nagy, A. (2000). Cre recombinase: the universal reagent for genome tailoring. *Genesis* 26, 99–109.
- Nagy, A., Moens, C., Ivanyi, E., Pawling, J., Gertsenstein, M., Hadjantonakis, A. K., et al. (1998). Dissecting the role of N-myc in development using a single targeting vector to generate a series of alleles. *Curr. Biol.* 8, 661–664.
- Panchin, Y., Kelmanson, I., Matz, M., Lukyanov, K., Usman, N., and Lukyanov, S. (2000). A ubiquitous family of putative gap junction molecules. *Curr. Biol.* 10, R473–R474.
- Pelegrin, P., and Surprenant, A. (2006). Pannexin-1 mediates large pore formation and interleukin-1beta release by the ATP-gated P2X7 receptor. *EMBO J.* 25, 5071–5082.
- Penuela, S., Bhalla, R., Gong, X. Q., Cowan, K. N., Celetti, S. J., Cowan, B. J., et al. (2007). Pannexin 1 and pannexin 3 are glycoproteins that exhibit many distinct characteristics from the connexin family of gap junction proteins. *J. Cell. Sci.* 120, 3772–3783.
- Qiu, F., and Dahl, G. (2009). A permeant regulating its permeation pore: inhibition of pannexin 1 channels by ATP. *Am. J. Physiol. Cell Physiol.* 296, C250–C255.
- Qiu, F., Wang, J., Spray, D. C., Scemes, E., and Dahl, G. (2011). Two non-vesicular ATP release pathways in the mouse erythrocyte membrane. *FEBS Lett.* 585, 3430–3435.
- Requardt, R. P., Kaczmarczyk, L., Dublin, P., Wallraff-Beck, A., Mikeska, T., Degen, J., et al. (2009). Quality control of astrocyte-directed Cre transgenic mice: the benefits of a direct link between loss of gene expression and reporter activation. *Glia* 57, 680–692.
- Rigato, C., Swinnen, N., Buckinx, R., Couillin, I., Mangin, J. M., Rigo, J. M., et al. (2012). Microglia proliferation is controlled by P2X7 receptors in a Pannexin-1-independent manner during early embryonic spinal cord invasion. *J. Neurosci.* 32, 11559–11573.
- Romanov, R. A., Bystrova, M. F., Rogachevskaia, O. A., Sadovnikov, V. B., Shestopalov, V. I., and Kolesnikov, S. S. (2012). The ATP permeability of Pannexin 1 channels in a heterologous system and in mammalian taste cells is dispensable. *J. Cell Sci.* 125, 5514–5523.
- Sandilos, J. K., and Bayliss, D. A. (2012). Physiological mechanisms for the modulation of pannexin 1 channel activity. *J. Physiol.* 590, 6257–6266.
- Santiago, M. F., Veliskova, J., Patel, N. K., Lutz, S. E., Caille, D., Charollais, A., et al. (2011). Targeting pannexin1 improves seizure outcome. *PLoS ONE* 6:e25178. doi: 10.1371/journal.pone.0025178
- Scemes, E., Spray, D. C., and Meda, P. (2009). Connexins, pannexins, innexins: novel roles of “hemichannels”. *Pflugers Arch.* 457, 1207–1226.
- Scemes, E., Suadicani, S. O., Dahl, G., and Spray, D. C. (2007). Connexin and pannexin mediated cell-cell communication. *Neuron Glia Biol.* 3, 199–208.
- Schmidt-Suprian, M., and Rajewsky, K. (2007). Vagaries of conditional gene targeting. *Nat. Immunol.* 8, 665–668.
- Schulz, T. J., Glaubitz, M., Kuhlwein, D., Thierbach, R., Birringer, M., Steinberg, P., et al. (2007). Variable expression of Cre recombinase transgenes precludes reliable prediction of tissue-specific gene disruption by tail-biopsy genotyping. *PLoS ONE* 2:e1013. doi: 10.1371/journal.pone.0001013
- Seminario-Vidal, L., Okada, S. F., Sesma, J. I., Kreda, S. M., van Heusden, C. A., Zhu, Y., et al. (2011). Rho signaling regulates pannexin 1-mediated ATP release from airway epithelia. *J. Biol. Chem.* 286, 26277–26286.
- Seror, C., Melki, M. T., Subra, F., Raza, S. Q., Bras, M., Saidi, H., et al. (2011). Extracellular ATP acts on P2Y2 purinergic receptors to facilitate HIV-1 infection. *J. Exp. Med.* 208, 1823–1834.
- Silverman, W. R., De Rivero Vaccari, J. P., Locovei, S., Qiu, F., Carlsson, S. K., Scemes, E., et al. (2009).

The pannexin 1 channel activates the inflammasome in neurons and astrocytes. *J. Biol. Chem.* 284, 18143–18151.

Suadicani, S. O., Iglesias, R., Wang, J., Dahl, G., Spray, D. C., and Scemes, E. (2012). ATP signaling is deficient in cultured Pannexin1-null mouse astrocytes. *Glia* 60, 1106–1116.

Testa, G., Schaft, J., Van Der Hoeven, F., Glaser, S., Anastasiadis, K., Zhang, Y., et al. (2004). A reliable lacZ expression reporter cassette for multipurpose,

knockout-first alleles. *Genesis* 38, 151–158.

Wellershaus, K., Degen, J., Deuchars, J., Theis, M., Charollais, A., Caille, D., et al. (2008). A new conditional mouse mutant reveals specific expression and functions of connexin36 in neurons and pancreatic beta-cells. *Exp. Cell Res.* 314, 997–1012.

**Conflict of Interest Statement:** The authors declare that the research was conducted in the absence of any

commercial or financial relationships that could be construed as a potential conflict of interest.

Received: 28 January 2013; paper pending published: 27 February 2013; accepted: 20 April 2013; published online: 09 May 2013.

Citation: Hanstein R, Negoro H, Patel NK, Charollais A, Meda P, Spray DC, Suadicani SO and Scemes E (2013) Promises and pitfalls of a Pannexin1 transgenic mouse line. *Front. Pharmacol.* 4:61. doi: 10.3389/fphar.2013.00061

This article was submitted to Frontiers in Pharmacology of Ion Channels and Channelopathies, a specialty of Frontiers in Pharmacology.

Copyright © 2013 Hanstein, Negoro, Patel, Charollais, Meda, Spray, Suadicani and Scemes. This is an open-access article distributed under the terms of the Creative Commons Attribution License, which permits use, distribution and reproduction in other forums, provided the original authors and source are credited and subject to any copyright notices concerning any third-party graphics etc.



# Connexin and pannexin hemichannels in brain glial cells: properties, pharmacology, and roles

**Christian Giaume<sup>1,2,3\*</sup>, Luc Leybaert<sup>4</sup>, Christian C. Naus<sup>5</sup> and Juan C. Sáez<sup>6,7</sup>**

<sup>1</sup> Collège de France, Center for Interdisciplinary Research in Biology/Centre National de la Recherche Scientifique, Unité Mixte de Recherche 7241/Institut National de la Santé et de la Recherche Médicale U1050, Paris, France

<sup>2</sup> University Pierre et Marie Curie, Paris, France

<sup>3</sup> MEMOLIFE Laboratory of Excellence and Paris Science Lettre Research University, Paris, France

<sup>4</sup> Physiology Group, Department of Basic Medical Sciences, Faculty of Medicine and Health Sciences, Ghent University, Ghent, Belgium

<sup>5</sup> Department of Cellular and Physiological Sciences, Life Sciences Institute, Faculty of Medicine, University of British Columbia, Vancouver, BC, Canada

<sup>6</sup> Departamento de Fisiología, Pontificia Universidad Católica de Chile, Santiago, Chile

<sup>7</sup> Instituto Milenio, Centro Interdisciplinario de Neurociencias de Valparaíso, Valparaíso, Chile

## Edited by:

Aida Salameh, Heart Centre  
University of Leipzig, Germany

## Reviewed by:

Gregory E. Morley, New York  
University School of Medicine, USA

Roger J. Thompson, University of  
Calgary, Canada

Panagiotis Bargiolas, University of  
Heidelberg, Germany

## \*Correspondence:

Christian Giaume, Collège de France,  
Center for Interdisciplinary Research  
in Biology/Centre National de la  
Recherche Scientifique, Unité Mixte  
de Recherche 7241/Institut National  
de la Santé et de la Recherche  
Médicale U1050, 11 Place Marcelin  
Berthelot, 75231 Paris Cedex 05,  
France  
e-mail: christian.giaume@college-de-  
france.fr

Functional interaction between neurons and glia is an exciting field that has expanded tremendously during the past decade. Such partnership has multiple impacts on neuronal activity and survival. Indeed, numerous findings indicate that glial cells interact tightly with neurons in physiological as well as pathological situations. One typical feature of glial cells is their high expression level of gap junction protein subunits, named connexins (Cxs), thus the membrane channels they form may contribute to neuroglial interaction that impacts neuronal activity and survival. While the participation of gap junction channels in neuroglial interactions has been regularly reviewed in the past, the other channel function of Cxs, i.e., hemichannels located at the cell surface, has only recently received attention. Gap junction channels provide the basis for a unique direct cell-to-cell communication, whereas Cx hemichannels allow the exchange of ions and signaling molecules between the cytoplasm and the extracellular medium, thus supporting autocrine and paracrine communication through a process referred to as "gliotransmission," as well as uptake and release of metabolites. More recently, another family of proteins, termed pannexins (Panxs), has been identified. These proteins share similar membrane topology but no sequence homology with Cxs. They form multimeric membrane channels with pharmacology somewhat overlapping with that of Cx hemichannels. Such duality has led to several controversies in the literature concerning the identification of the molecular channel constituents (Cxs versus Panxs) in glia. In the present review, we update and discuss the knowledge of Cx hemichannels and Panx channels in glia, their properties and pharmacology, as well as the understanding of their contribution to neuroglial interactions in brain health and disease.

**Keywords:** astrocytes, oligodendrocytes, microglia, gap junctions, neuroglial interactions

## INTRODUCTION

For a long time, it has been taken as dogma that connexin (Cx) proteins can only function as gap junction channels. Indeed, before the aggregation of Cxs at the junctional plaque and subsequent formation of gap junctions, hexameric rings of Cxs, termed connexons, were initially assumed to remain closed. An obvious reason for this occlusion was that, as gap junction channels are "poorly" selective for ions and permeable to low molecular weight molecules (<1 to 1.2 kDa), if once at the membrane connexons could open, the cell would lose its integrity or at least would have to spend substantial energy to maintain this energetically unfavorable condition. Such statements began to be challenged when evidence for "functional hemichannels," a term proposed to substitute for plasma membrane connexons, were reported in the early 1990s. In these pioneering studies, Cx hemichannels were opened either by large depolarization in *Xenopus* oocytes (Paul et al., 1991) or by lowering the extracellular calcium ion ( $\text{Ca}^{2+}$ ) concentration in horizontal cells (DeVries and Schwartz, 1992). Later on, the

occurrence of functional hemichannels (i.e., hemichannels that can be turned into the open state) composed of Cx43 was demonstrated in primary cultures of astrocytes in the absence of external  $\text{Ca}^{2+}$  (Hofer and Dermietzel, 1998). This observation was followed by the demonstration that metabolic inhibition performed in the presence of normal external  $\text{Ca}^{2+}$  concentrations (1–2 mM) induced cell permeabilization, due to Cx43 hemichannel opening, before loss of membrane integrity (Contreras et al., 2002). More recently, hemichannel opening in astrocytes was triggered either by treatment with pro-inflammatory cytokines or selective lipopolysaccharide (LPS) stimulation of microglia co-cultured with astrocytes, again in the presence of external  $\text{Ca}^{2+}$  (Retamal et al., 2007a). The opening of Cx43 hemichannels in astrocytes was also demonstrated to occur in experiments designed to decipher the mechanism of intercellular  $\text{Ca}^{2+}$  wave propagation in astrocytes to which both gap junction channels and hemichannels contribute (Scemes and Giaume, 2006; Leybaert and Sanderson, 2012). In this case, the release of ATP through Cx43 hemichannels

turned out to play a key role in  $\text{Ca}^{2+}$  wave propagation mediated by an extracellular paracrine signaling component (Cotrina et al., 1998; Arcuino et al., 2002). All these initial experiments on Cx hemichannels utilized astrocytes as a cell model giving to these cells new roles in neuroglial interaction (Bennett et al., 2003).

At the turn of the century another membrane channel family, the pannexins (Panxs), was identified (Panchin et al., 2000) and demonstrated to be orthologs of innexins, the gap junction proteins expressed in invertebrates (Baranova et al., 2004). So far, there are no reports of gap junctional communication supported by native Panxs, although over expression of Panx1 enhances gap junctional coupling in glioma cells (Lai et al., 2007). They form membrane channels contributing to membrane permeabilization, similar to Cx hemichannels, and they are expressed in glial cells (Orellana et al., 2009; Scemes, 2012). The aim of the present review is to summarize what is actually known about Cx hemichannels and Panx channels in glia (mainly astrocytes and microglia) and to discuss their contribution to neuroglial interactions taken in the normal and pathological context. An overview of methods and approaches to investigate Cx hemichannels and Panx channels has recently been published (Giaume et al., 2012); we refer the reader to this paper for a more detailed discussion of methodological aspects.

## CONNEXIN AND PANNEXIN EXPRESSION IN GLIAL CELLS

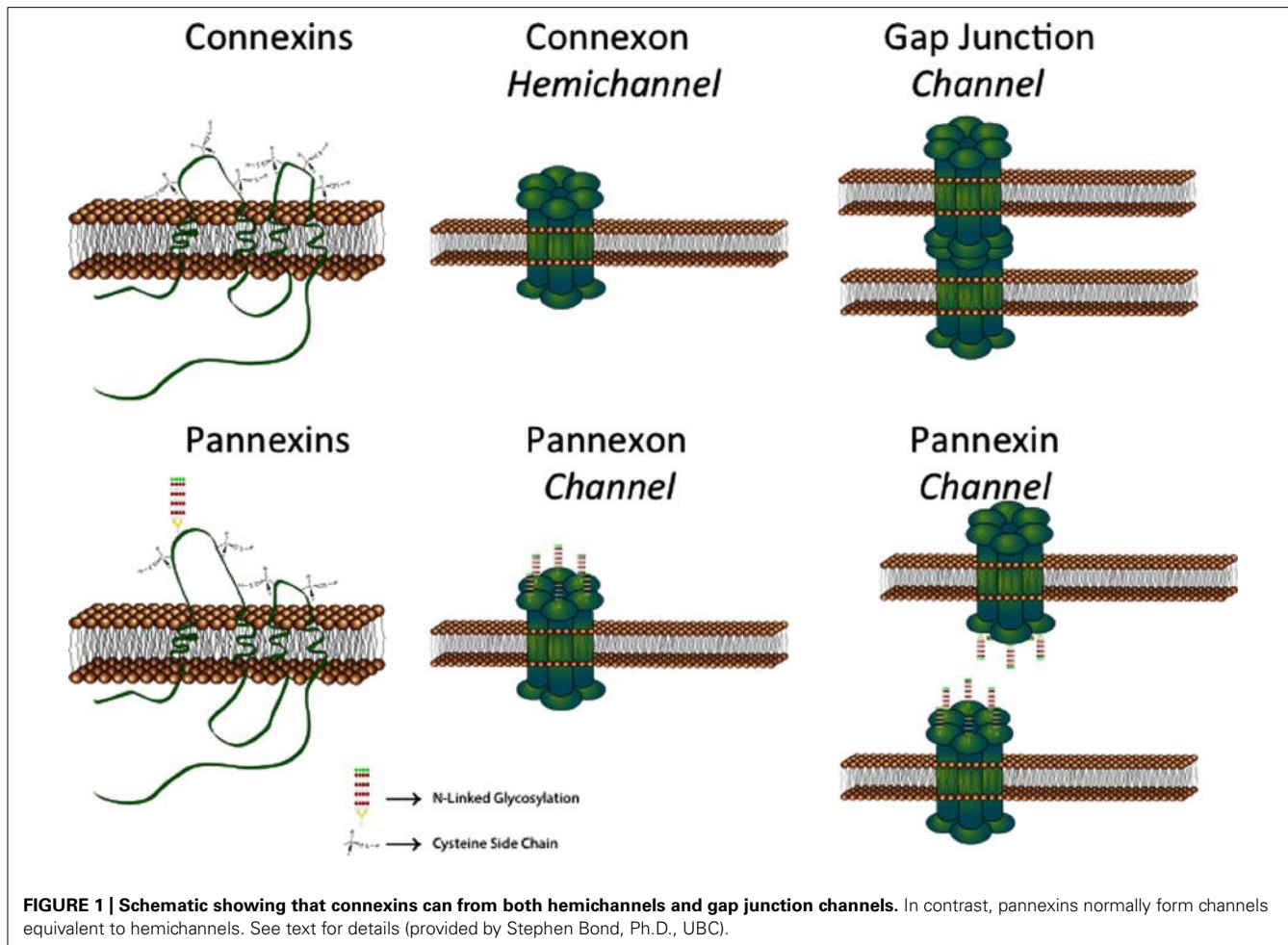
Gap junctions provide a unique direct conduit between cells, influencing crucial cellular processes through activities including electrical conductance and metabolic cooperation, mediated by the passage of ions, amino acids, glucose, glutathione, ATP, and small signaling molecules (reviewed in Sohl and Willecke, 2004), as well as microRNAs (Katakowski et al., 2010). When one considers Cx expression in the brain (Theis et al., 2005), it is evident that they are most abundant in glia, namely the astrocytes, oligodendrocytes, and microglia (Rouach et al., 2002). With the genomic characterization of Cx (Willecke et al., 2002) and Panx (Baranova et al., 2004) gene families, it has been determined that there are at least 10 Cxs and 2 Panxs expressed in the brain (see below). There is also a temporal (i.e., developmental) and spatial (i.e., cell type and brain region) pattern regarding this expression and localization. Furthermore, these channel proteins can have different roles in different cell types, either as the canonical gap junction intercellular channel or as a hemichannel (Goodenough and Paul, 2003; **Figure 1**). Cx hemichannels and Panx1 channels mediate the release of ATP that activates P2 receptors, promoting rises in intracellular  $\text{Ca}^{2+}$  concentrations; gap junction channels mediate the intercellular transfer of second messenger propagated calcium signal (Suadicani et al., 2004; Anselmi et al., 2008; Leybaert and Sanderson, 2012). Under pathological conditions, Panx1 channels have been proposed to mediate activation of the inflammasome both in neurons and astrocytes (Iglesias et al., 2009; Silverman et al., 2009), whereas Cx43 hemichannels are involved in acceleration of astrogliosis and neuronal cell death triggered by hypoxia-reoxygenation in high glucose (Orellana et al., 2010) and  $\beta$ -amyloid peptide, respectively (Orellana et al., 2011b,c). A further level of complexity can be envisioned in the context of Cxs, where the heteromeric assembly of different Cx proteins into a single channel can result in distinct differences in biophysical properties

(Bevans et al., 1998; Harris, 2007). This feature is also true for Panxs since Panx1 can form both homomeric and heteromeric channels with Panx2 (Bruzzone et al., 2005). Thus for specific cellular functions, the complement of Cxs and Panxs expressed is important in the physiological or pathological context being considered. While other “non-channel” functions are emerging for Cxs (Vinken et al., 2012) and Panxs (MacVicar and Thompson, 2010), this review will be limited to channel-related functions and properties.

While this review will focus on gap junction channels and hemichannels in brain glial cells, it is important to note that gap junction proteins have also been identified in brain neurons (Andrew et al., 1981; Söhl et al., 2005). These include Cx26, Cx30.2, Cx36, Cx45, and Cx57 (Rouach et al., 2002). Neurons also express Panx1 *in vivo* (Bruzzone et al., 2003), and recently it has been reported that neural progenitors in the adult rodent hippocampus express Panx2 (Swayne et al., 2010). It is thus possible, and has been reported in some situations, that neurons form gap junctions with astrocytes since some of the same Cxs are expressed in both cell types (Fróes et al., 1999; Alvarez-Maubecin et al., 2000). Astrocytes express multiple Cxs, including Cx43, Cx26, Cx30, Cx40, Cx45, and Cx46 (Giaume et al., 2012), as well as Panx1 (Iglesias et al., 2009) and Panx2 (Zappala et al., 2007). Non-treated microglia express Cx43 (Eugenín et al., 2001; Garg et al., 2005), Cx36 (Dobrenis et al., 2005), and Cx32 (Maezawa and Jin, 2010), as well as Panx1 (Orellana et al., 2011b). Finally, oligodendrocytes express Cx32, Cx47, and Cx29 *in vivo* (Altevogt et al., 2002; Wasseff and Scherer, 2011). The complexity of Cxs and Panxs functioning as gap junction channels/hemichannels and channels, respectively, in these various cell types can be viewed as providing a background level of activity to support and modulate the complex neural activity mediated *via* gliotransmission.

The expression profiles noted have been associated with mature neurons and glial cell types. However, these various cell types arise developmentally from neuronal and glial precursors. Several studies have demonstrated changes in expression of Cxs and Panxs during brain development (reviewed in Vogt et al., 2005; Belousov and Fontes, 2013). Given that several reports have described disturbed neural development when expression of some Cxs is modified through the use of gene knockdown or knockout strategies, gap junction channels and hemichannels are likely to play significant roles in processes including cell proliferation, migration, and differentiation (Fushiki et al., 2003; Elias et al., 2007; Wiencken-Barger et al., 2007; Cina et al., 2009; Liu et al., 2012).

Initial studies on Cx functions in neural cells in culture and in brain slices focused on their expected role in forming gap junction channels, confirming their function *via* electrophysiological analysis or methods using low molecular weight dye tracers, which can pass from cell to cell through these intercellular channels (Giaume et al., 1991). Therefore, many of the phenotypic changes observed when enhancing or decreasing Cx expression were attributed to changes in gap junctional communication. With the recognition that Cxs can also form hemichannels, the consequences of Cx expression began to be considered in a new way (Contreras et al., 2004), and appropriate methods developed to assess their presence and activity (Giaume and Theis, 2010). Cx hemichannels and Panx channels are more typical of most membrane channels, like ion



channels, in their direct communication between intracellular and extracellular space. However, they are unique in their pore size and conductance properties (Thompson and Macvicar, 2008).

The formation of gap junction channels and hemichannels by Cxs can help explain some contradictory effects of altering Cx expression. For example, enhanced Cx43 expression in brain glial cells, in culture and *in vivo*, has been shown to be both neuroprotective and neurodestructive in ischemic and excitotoxic situations (reviewed in Orellana et al., 2009; Kozoric and Naus, 2013). Recent studies have indicated that gap junction channels formed by Cx43 can be neuroprotective, while Cx43 hemichannels may be more detrimental to neuronal survival. The following sections of this review provide further insight into the distinct properties of hemichannels and how these impact the progression of neurological disorders.

### Cx HEMICHANNEL AND Panx CHANNEL PROPERTIES IN GLIA BIOPHYSICS

Today, most Cxs expressed in rodent glial cells, including Cx26, Cx30, Cx32, Cx43, and Cx45, have been shown to form functional hemichannels in endogenous and/or exogenous expression systems (Bennett et al., 2003). Nevertheless, it remains unknown if this is also the case for Cx29 and Cx47 found in

oligodendrocytes. In exogenous expression systems, Cx30, Cx32, Cx43, and Cx45 hemichannels show a very low open probability at resting membrane potential and normal concentration of the extracellular divalent cations,  $\text{Ca}^{2+}$  and  $\text{Mg}^{2+}$ . For Cx26 hemichannels, these properties are species-specific; human and sheep but not rat Cx26 forms hemichannels that at resting membrane potential and normal concentration of extracellular divalent cations show opening activity but the rat protein is characterized by a single evolutionary amino acid change (D159N) that limits this feature (González et al., 2006).

Opening of Cx hemichannels studied so far can be promoted by positive transmembrane voltages and reduced concentrations of extracellular divalent cations (Bennett et al., 2003). These conditions have been most frequently used to gain knowledge on biophysical features of hemichannels, including permeability properties (see below), identification of voltage sensitivity, unitary conductance, kinetic properties, and polarity of closure. However, other gating mechanisms can also promote opening of hemichannels, as described below (see Regulation). In general, hemichannels show a time- and voltage-dependent macroscopic current, activating with depolarization and inactivating with hyperpolarization. However, this feature is not equal in hemichannels formed by different Cxs. For example, the voltage dependency is strong

for mouse Cx30 hemichannels (Valiunas and Weingart, 2000) but detectable only at very high positive potentials for rat Cx43 hemichannels (Contreras et al., 2003). For Cx32 hemichannels, the conductance is determined by charges dispersed over the pore pathway (Oh et al., 2008). Hemichannels formed by human Cx26 or rat Cx43 show bipolar voltage behavior (Contreras et al., 2003; González et al., 2006); however, this appears to be less well established for Cx43, for which unitary current events were found to monotonically rise in the voltage range of +30 to +90 mV (Wang et al., 2012). Hemichannels present two distinct voltage-gating mechanisms, which are called loop- (slow) and V(j)- (fast) gating, respectively (Contreras et al., 2003; Oh et al., 2008). For Cx32 hemichannels the loop-gate is mediated by a conformational change that reduces the pore diameter in a region located close to the first transmembrane domain and first extracellular loop (Bargiello et al., 2012). It was recently also proposed that the intracellular pore entrance narrows from 15 to 10 Å with loop-gated but not with V(j)-gated channel closure. Moreover, it was shown that the extracellular entrance does not undergo evident large conformational changes with either voltage-gating mechanisms (Kwon et al., 2013). The unitary conductance is characteristic for hemichannels with specific Cx composition; the fully open state for Cx26 hemichannels is characterized by ~320 pS unitary conductance (González et al., 2006), for Cx32 hemichannels this is ~90 pS, for Cx43 hemichannels ~220 pS (Contreras et al., 2003; Retamal et al., 2007a; Wang et al., 2012) and for Cx45 hemichannels ~57 pS (Valiunas, 2002). They also present conductance substates as a result of an inactivation mechanism that hinders complete activation of hemichannels under prolonged depolarization (Valiunas, 2002; Contreras et al., 2003; Gómez-Hernández et al., 2003). The most general features mentioned above have been useful to demonstrate and understand the involvement of hemichannels in different physiologic functions and also to identify hemichannels with specific Cx composition in glial cells (Orellana et al., 2011c). However, much more remains to be investigated since Cxs are post-translationally modified and thus, their biophysical features might be affected according to the metabolic state of the cell.

The biophysical properties of Panx channels are much less documented than those of Cx hemichannels, possibly as a result of their more recent discovery. Panx1 channels have been so far demonstrated to be present in microglia, astrocytes, and oligodendrocytes (Iglesias et al., 2009; Domercq et al., 2010; Orellana et al., 2011a), whereas Panx2 is expressed in post-ischemic astrocytes (Zappala et al., 2007). The open state of Panx1 channels is promoted by positive membrane voltages and elevation of intracellular free Ca<sup>2+</sup> concentration. Voltage clamp experiments have indicated widely divergent unitary conductances for Panx1 channels, varying from 68 to 550 pS (Locovei et al., 2006; Kienitz et al., 2011; Ma et al., 2012). This controversy in the single channel conductance of Panx1 channels has not been resolved yet and might be explained in part by differences in recording conditions or solutions, cell type, phenotypic differences, and post-translational modifications. It could be partially explained by simultaneous opening of channels and thus, high conductance values might represent multiples of a single channel with a lower conductance value. An issue to keep in mind is that biophysical properties

of exogenously expressed Panx channels might be different from those expressed simultaneously with all membrane and intracellular proteins (e.g., P2X receptors) that might interact with them in endogenous expression systems.

## PERMEABILITY

In addition to selective ion channels or transporters, other channels can alter the permeability of the cell membrane under physiological and pathological conditions (Schalper et al., 2009). The origin of these permeability changes could be Cx- and Panx-based channels located at the cell surface. However, other membrane channels might also be involved in drastic changes in membrane permeability [e.g., P2X<sub>7</sub> receptors, transient receptor potential (TRP) channels and calcium homeostasis modulator 1 (CALHM1) ion channel] and their possible involvement should be proved or disproved when testing the permeability of Cx hemichannels or Panx channels in a particular cell type.

Net changes in membrane permeability due to hemichannels have been most frequently studied through the use of inhibitors or molecular biology approaches that induce or abolish the expression of Cxs or Panxs. With these experimental approaches it has been proposed that hemichannels (Panx1 and/or Cx26, Cx32, and Cx43) allow the release of precursor or signaling molecules [e.g., including NAD<sup>+</sup>, ATP, adenosine, inositol trisphosphate (IP<sub>3</sub>), and glutamate; Bevans et al., 1998; Stout et al., 2002; Ye et al., 2003; Anderson et al., 2004; Bao et al., 2004a; Locovei et al., 2006; Gossman and Zhao, 2008; Kang et al., 2008; Song et al., 2011], uptake of second messengers [e.g., cyclic ADP-ribose (cADPR), nicotinic acid adenine dinucleotide phosphate (NAADP), nitric oxide (NO), and Ca<sup>2+</sup>; Heidemann et al., 2005; Sánchez et al., 2009, 2010; Schalper et al., 2010; Song et al., 2011; De Bock et al., 2012; Figueroa et al., 2013] and uptake of various metabolites (e.g., glucose, glutathione, and ascorbate; Bruzzone et al., 2001; Ahmad and Evans, 2002; Rana and Dringen, 2007; Retamal et al., 2007a; see **Table 1** for Cx43 hemichannels and Panx1 channels). In addition, it has been demonstrated that Cx hemichannels are permeable to synthetic molecules [e.g., Lucifer yellow, ethidium, calcein, propidium, 5(6)-carboxyfluorescein, and 2-(4-amidinophenyl)-1H-indole-6-carboxamide (DAPI); for review, see Sáez et al., 2010]. The fact that Cx26 and Cx32 hemichannels reconstituted in lipid membranes are permeable to Ca<sup>2+</sup> and cyclic nucleotides, respectively (Harris, 2007; Schalper et al., 2010; Fiori et al., 2012), indicates that no additional binding partners or associated molecules are required for hemichannels to function as conduits for small molecules or ions across the cell membrane. Since the membrane permeability change due to transient hemichannel opening may allow release of enough molecules to reach effective concentrations in a confined extracellular space, astroglial hemichannels have been proposed as membrane pathways for paracrine/autocrine cell signaling with physiological and pathological implications for glial and neuronal cells (Orellana et al., 2011c; Stehberg et al., 2012).

Membrane permeability changes *via* Cx hemichannels are in part explained by variations in the number of hemichannels available at the cell surface. With regard to this, an increase in the number of surface Cx43 or Cx45 hemichannels explains the increase in membrane permeability induced by fibroblast growth

**Table 1 | Overview of substances passing through glial Cx hemichannels and Panx channels and compounds that block these membrane pathways.**

Models	Techniques	Permeant metabolic or signaling molecules	Hemichannel blocking condition used	Reference
Astrocyte cultures	Dye uptake	2-NBDG (uptake)	<b>Cx43</b> , lanthanum ( $\text{La}^{3+}$ ), Gap27	Retamal et al. (2007a)
Astrocyte cultures	Colorimetric Tietze method	Glutathione (release)	Divalent, alcohols, flufenamic acid, carbenoxolone	Rana and Dringen (2007)
Astrocyte cultures	HPLC analysis	Glutamate, aspartate (release)	Divalent, alcohols, flufenamic acid, carbenoxolone	Ye et al. (2003)
Acute hippocampal slices, C6 transfected cells	Bioluminescence ATP imaging	ATP (release)	<b>Cx43</b> , non-transfected C6 cells	Cotrina et al. (1998); Kang et al. (2008)
Astrocyte cultures	Luciferin/luciferase assay	ATP (release)	<b>Panx1</b> , Panx1 knock out mouse	Suadicani et al. (2012)
Microglia cultures treated with amyloid $\beta$	Luciferin/luciferase bioluminescence and enzyme-linked fluorimetric assays	ATP, glutamate (release)	<b>Panx1 and Cx43</b> , $^{10}\text{Panx1}$ , probenecid	Orellana et al. (2011b)
Microglia cultures treated with TNF- $\alpha$	Colorimetric assay	Glutamate (release)	<b>Cx32</b> , Gap24, carbenoxolone	Takeuchi et al. (2006)

This table summarizes most if not all data available on signaling molecules passing through Cx or Panx channels (in bold, column 4) and conditions or blockers of the Cx hemichannels or Panx channels used in each particular study. Citations refer to the initial demonstration of the channel permeation property. The model, method of detection of the permeant compound, and reference where these findings were described are also included. 2-NBDG [2-(N-(7-nitrobenz-2-oxa-1,3-diazol-4-yl)amino)-deoxyglucose] is a fluorescent glucose analog.

factor-1 (FGF-1) in cells that express these proteins (Schalper et al., 2008b). However, in other conditions such as exposure to extracellular solution without divalent cations (Schalper et al., 2008a) or tanyocytes treated with extracellular glucose (Orellana et al., 2012a), the increase in membrane permeability is explained by opening of hemichannels *via* a gating mechanism. In both cases there is a net increase in membrane permeability mediated by hemichannels, possibly without changes in intrinsic permeability properties of hemichannels themselves. Nonetheless, changes in membrane permeability could also result from alterations in permeability features of hemichannels. For instance, protein kinase C (PKC)-mediated phosphorylation of the six subunits of Cx43 hemichannels reconstituted in lipid membranes reduces the pore permeability allowing permeation of the small hydrophilic solute ethylene glycol (Mr 62) but not sucrose (Mr 342; Bao et al., 2007). Changes in other hemichannel permeability properties, such as affinity or charge selectivity induced by covalent modification including phosphorylation by other protein kinases or nitrosylation, cannot be ruled out yet.

The permeability properties depend on the size, shape, and net charge of each permeant ion or molecule while the concentration gradient across the cell membrane acts as the driving force. Since the study of permeability characteristics of a membrane transporter should be done with a rapid time scale (within a few seconds to a minute) it is important to have a library of permeant molecules that allow real time determination of their disappearance or appearance. Transport via Cx43 hemichannels

has been shown to be cooperative and saturable with parameters (e.g.,  $V_{\max}$ ,  $K_m$ , and Hill coefficient) depending on the permeant cationic species (Orellana et al., 2011a). These findings imply that opening of hemichannels does not necessarily lead to loss of important intracellular molecules because of competition effects with other, less important molecules or ions and this interpretation might be valid to transport in both directions across the cell membrane. Of note, the permeability properties of hemichannels to anionic molecules have not been reported yet. To the best of our knowledge, the permeability properties of Panx1 channels remain equally unknown. It is also not known whether channels formed by different Cxs or Panxs show different permeability properties such as size exclusion and charge selectivity. In general, quantitative kinetic properties of permeation of Cx hemichannels and Panx channels remain largely unexplored. **Table 1** summarizes current evidence on the permeability of Cx43, Cx32 hemichannels, and Panx1 channels in brain glial cells.

## REGULATION

Hemichannels are regulated by diverse conditions of the extracellular and intracellular microenvironments. They include  $\text{Ca}^{2+}$  concentration outside and inside the cell, monovalent cation concentration, pH, mechanical stress, extracellular ligands, protein kinases, protein phosphatases, as well as oxidant and reducing agents. Here, the most recent studies not included in previous reviews (Sáez et al., 2010; Wang et al., 2013), will be presented.

### Hemichannel opening and modulation by $\text{Ca}^{2+}$

Unapposed Cx hemichannels of cells in culture are preferentially closed but can be opened by several trigger conditions (reviewed in Sáez et al., 2005, 2010). These include, transmembrane voltage with activation threshold of  $-30$  mV for Cx30 and  $+50$  mV for Cx43 in the presence of normal extracellular  $\text{Ca}^{2+}$  (Valiunas and Weingart, 2000; Wang et al., 2012), mechanical forces/strain (Bao et al., 2004b; Luckprom et al., 2011), a decrease of extracellular  $\text{Ca}^{2+}$  (Li et al., 1996; Stout et al., 2002; Ye et al., 2003; Ramachandran et al., 2007; Torres et al., 2012), an increase of intracellular free  $\text{Ca}^{2+}$  (De Vuyst et al., 2006, 2009; Wang et al., 2012), alterations in phosphorylation status (Bao et al., 2004c) and redox status (Retaim et al., 2007b), and ischemia-mimicking conditions (John et al., 1999; Contreras et al., 2002; Wang et al., 2013).

**Role of extracellular  $\text{Ca}^{2+}$ .** A decrease of extracellular divalent cation concentration was one of the first conditions reported to stimulate Cx43 hemichannel opening, as introduced above. Work in a hepatoma cell line expressing Cx43 demonstrated that a decrease of the extracellular  $\text{Ca}^{2+}$  concentration triggered the uptake of Lucifer yellow, a hemichannel-permeable fluorescent dye (Li et al., 1996). Similar observations were obtained in astrocytes, where hemichannel opening was demonstrated to trigger the release of glutamate and aspartate (Ye et al., 2003). Lowering extracellular  $\text{Mg}^{2+}$  appeared to promote low  $\text{Ca}^{2+}$ -triggered hemichannel opening but  $\text{Ca}^{2+}$  appeared to be the dominant factor. It is thought that normal physiological extracellular  $\text{Ca}^{2+}$  concentrations ( $\sim 1.8$  mM) keep non-junctional Cx hemichannels closed in the plasma membrane, until they become incorporated into gap junction channels where they open by a process called “loop gating” as a consequence of extracellular loop interactions. In general, the half-maximal effective concentration for  $\text{Ca}^{2+}$ -related opening of Cx43 hemichannels is in the order of  $100\ \mu\text{M}$  extracellular  $\text{Ca}^{2+}$ . The proposed mechanism of millimolar  $\text{Ca}^{2+}$  closure of Cx hemichannels involves an interaction of extracellular  $\text{Ca}^{2+}$  with a  $\text{Ca}^{2+}$  binding site that consists of a ring of aspartate residues at the extracellular vestibule of the hemichannel pore thereby closing the channel (Gómez-Hernández et al., 2003). Such a mechanism has been best documented for Cx32 but appears to be also plausible for the astroglial Cxs, Cx30 and Cx43. Recently, Torres et al. (2012) have elegantly exploited the extracellular  $\text{Ca}^{2+}$ -sensitivity of astroglial hemichannels to trigger their opening by photo-activating a  $\text{Ca}^{2+}$  buffer (thereby increasing its  $\text{Ca}^{2+}$  affinity) added to the interstitial fluid of a hippocampal acute slice preparation (discussed further below under Section “Impact of Hemichannel-Mediated Gliotransmission on Synaptic Activity and Behavior”).

**Role of intracellular  $\text{Ca}^{2+}$ .** Besides extracellular  $\text{Ca}^{2+}$ , intracellular cytoplasmic  $\text{Ca}^{2+}$  also influences hemichannel function. In fact, it was found that Cx hemichannel opening triggered by a decrease of extracellular  $\text{Ca}^{2+}$  could be inhibited by ester-loading the cells with the  $\text{Ca}^{2+}$  buffer 1,2-bis(o-aminophenoxy)ethane-N,N,N',N'-tetra-acetic acid (BAPTA), added to dampen intracellular  $\text{Ca}^{2+}$  changes (De Vuyst et al., 2006). Further investigations demonstrated that Cx32 hemichannels are activated by moderate (below  $500\ \text{nM}$ ) changes in intracellular  $\text{Ca}^{2+}$  and inhibited

by  $\text{Ca}^{2+}$  changes above  $500\ \text{nM}$ . Subsequent work showed that Cx43 hemichannels are also characterized by such a biphasic, bell-shaped, response to changes in intracellular  $\text{Ca}^{2+}$  concentration, in ATP release hemichannel studies as well as in dye uptake studies in glioma cells and other cell types (De Vuyst et al., 2009; De Bock et al., 2012). Recently, single channel studies of Cx43 hemichannels robustly confirmed these observations (Wang et al., 2012). Cx hemichannels are  $\text{Ca}^{2+}$  permeable (Sánchez et al., 2009, 2010; Schalper et al., 2010; Fiori et al., 2012) and the biphasic dependency on intracellular  $\text{Ca}^{2+}$  thus confers a positive feedback below  $500\ \text{nM}$  intracellular  $\text{Ca}^{2+}$  concentration ( $\text{Ca}^{2+}$ -induced  $\text{Ca}^{2+}$  entry via Cx43 hemichannels) and negative feedback at higher concentrations. Interestingly,  $\text{IP}_3$  receptor channels present in the endoplasmic reticulum (ER) are  $\text{Ca}^{2+}$  release channels that have a similar bell-shaped  $\text{Ca}^{2+}$  dependency (Bezprozvanny et al., 1991). Positive and negative  $\text{Ca}^{2+}$  feedback at  $\text{IP}_3$  receptor channels forms the basis of  $\text{Ca}^{2+}$  oscillations, thus, it was hypothesized that  $\text{Ca}^{2+}$  feedback at Cx hemichannels could also play a role in  $\text{Ca}^{2+}$  oscillations (De Bock et al., 2012). Experimental work with various peptides targeting Cx hemichannels indeed demonstrated that inhibiting hemichannel opening, or preventing their closure in response to high intracellular  $\text{Ca}^{2+}$ , blocked  $\text{Ca}^{2+}$  oscillations triggered by bradykinin. Thus, Cx hemichannels constitute a putative gliotransmitter release pathway. Also, they may contribute to  $\text{Ca}^{2+}$  oscillations in astrocytes and thereby potentially lead to gliotransmitter release via other  $\text{Ca}^{2+}$ -dependent pathways (Oliet and Mothet, 2006; Zorec et al., 2012). In brain endothelial cells, it was found that Cx hemichannel blocking peptides prevented the opening of the blood–brain barrier, triggered by bradykinin, by inhibiting  $\text{Ca}^{2+}$  oscillations in the endothelial cells (De Bock et al., 2011). Below, we discuss in more detail some peptide-based hemichannel inhibitors.

### Influence of monovalent cations

Elevations in extracellular  $\text{K}^+$  shift the activation potential of Panx1 hemichannels to a more physiological range. Panx1 hemichannels expressed in astrocytes might serve as  $\text{K}^+$  sensors for changes in the extracellular milieu such as those occurring under pathological conditions (Suadicani et al., 2012). This type of regulation might also occur under physiological conditions with high neuronal activity. Thus, elevations in extracellular  $\text{K}^+$  of the magnitude occurring during periods of high neuronal activity have been proposed to affect the intercellular signaling among astrocytes (Scemes and Spray, 2012). Accordingly, the gliotransmitter release in the hippocampus in response to high neuronal activity is sensitive to P2 receptor and Panx1 channel blockers (Heinrich et al., 2012). Cx30 gap junction channels have recently been demonstrated to be regulated by the concentration of external  $\text{K}^+$  (Roux et al., 2011); whether astroglial Cx hemichannels are influenced by the extracellular  $\text{K}^+$  concentration is currently not known.

### Influence of pH

Under pathological conditions, the intracellular and extracellular pH may display abrupt changes. Related to this issue and in the presence of extracellular divalent cations, Cx43 hemichannels are opened by alkaline pH applied at the extracellular side and

preferentially closed at physiologic pH (Schalper et al., 2010). The activity of Cx45 hemichannels recorded at positive membrane potentials and in the absence of extracellular  $\text{Ca}^{2+}$  is drastically reduced by acidification (Valiunas, 2002). In addition, the pH sensitivity might be potentiated by protonated aminosulfonates (Bevans and Harris, 1999), such as taurine that could be in millimolar concentration in the cytoplasm of several cell types including astrocytes (Olson, 1999). This effect is Cx specific; Cx26 but not Cx32 hemichannels are closed by aminosulfonates at constant pH (Bevans and Harris, 1999). At the ultrastructural level (high-resolution atomic force microscopy), Cx26 hemichannels are closed at pH < 6.5 [4-(2-hydroxyethyl)-1-piperazineethanesulfonic acid (HEPES) buffer] and opened reversibly by increasing the pH to 7.6 (Yu et al., 2007). Moreover, molecular studies have revealed that Cx26 hemichannel closure induced by taurine requires the interaction between the cytoplasmic loop and the C-terminal (CT; Locke et al., 2011).

### Influence of mechanical forces

Mechanical stress is another condition that might be relevant under pathological situations. For example, after brain trauma the extracellular medium becomes hypertonic due to the release of intracellular solutes to the extracellular microenvironment (Somjen, 2002). In astrocytes, hypertonicity induces glutamate release through Cx43 hemichannels (Jiang et al., 2011). This response could be mediated by integrin  $\alpha 5\beta 1$  (Batra et al., 2012), a RhoA GTPase and the contractile system (Ponsaerts et al., 2010). This sensitivity is likely to result from the interaction between negatively charged amino acid residues of the CT end (Asp278 and Asp279) and a domain of the intracellular loop (D'Hondt et al., 2013). Activation of Panx1 channels by mechanical stress is not present in all cell types (Bao et al., 2004a; Reyes et al., 2009), suggesting that it should be tested in glial cells in order to validate its possible relevance in these cells.

### Influence of extracellular factors and signals

The functional state of glial Cx hemichannels and Panx1 channels is actively regulated by extracellular signals. In primary cultures of mouse astrocytes, stomatin inhibits Panx1-mediated whole cell currents by interacting with its CT (Zhan et al., 2012). In contrast, pro-inflammatory agents such as the  $\beta$ -amyloid peptide increase the surface expression and activity of Cx43 hemichannels and Panx1 channels in microglia and Cx43 hemichannels in astrocytes (Orellana et al., 2011c). Moreover, in brain astrocytes, epidermal growth factor (EGF) and FGF-2 inhibit Cx hemichannel activity *via* the mitogen-activated protein kinase cascade, and the effect of the growth factors is reversed by interleukin-1 $\beta$  (IL-1 $\beta$ ; Morita et al., 2007). In contrast, pro-inflammatory cytokines [tumor necrosis factor alpha (TNF- $\alpha$ ) and IL-1 $\beta$ ] released by LPS-activated microglia increase the activity of astroglial Cx43 hemichannels via p38 kinase (Retamal et al., 2007b; Orellana et al., 2011c) and this response is inhibited by activation of CB1 receptors by synthetic cannabinoid agonists (Froger et al., 2009). The orchestrated involvement of Cx hemichannels and Panx1 channels has also been found in other experimental preparations. In spinal cord astrocytes, FGF-1 leads to vesicular ATP release followed by sequential activation of Panx1 and Cx43 hemichannels (Garré

et al., 2010). Moreover, up-regulation of astroglial Panx1 channels and Cx43 hemichannels has been found in brain abscess (Karpuk et al., 2011).

Cx43 hemichannels expressed by tanycytes, glial cells present in the hypothalamus, open in seconds after exposure to physiological concentrations of extracellular glucose. This response is mediated by the sequential activation of glucosensing proteins (Orellana et al., 2012a), a response that is absent in cortical astrocytes (Orellana et al., 2010). However, high glucose levels enhance the increase in astroglial Cx43 hemichannel activity induced by hypoxia-reoxygenation (Orellana et al., 2010).

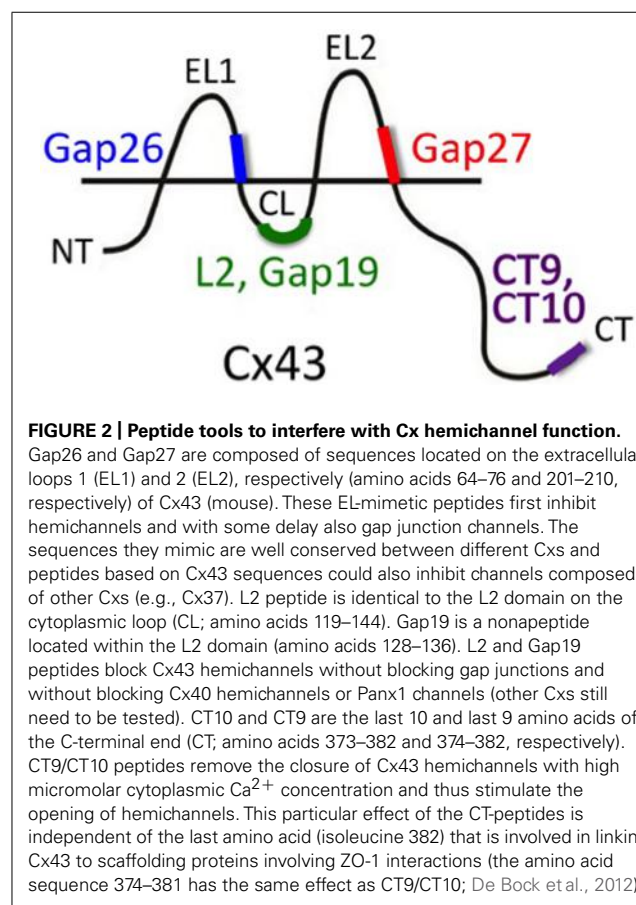
As a result of cell interaction with extracellular signals or conditions that affect the energy supply, intracellular metabolic pathways involving levels of free  $\text{Ca}^{2+}$  concentration, activity of protein kinases and phosphatases, as well as levels or activity of intracellular redox molecules, are affected. Therefore, drastic reduction in ATP levels are expected to favor the dephosphorylated state of Cx43 hemichannels and thus, they could present an increased activity (Bao et al., 2007). Moreover, the lack of energy leads to a rise in intracellular free  $\text{Ca}^{2+}$  that favors the generation of reactive oxygen and nitrogen species including NO. The latter induce rapid nitrosylation of Cx43 and opening of hemichannels (Retamal et al., 2007b; Figueroa et al., 2013). This mechanism might partially explain the increase in Cx43 hemichannel activity observed in astrocytes under ischemia-like conditions since free radical scavengers, dithiothreitol, a sulfhydryl (SH) reducing reagent, and high intracellular levels of reduced glutathione revert the hemichannel activity to levels found in normal cells (Contreras et al., 2002; Retamal et al., 2007b; Orellana et al., 2010). Finally, extracellular ATP mediates the ischemic damage to oligodendrocytes and is partially explained by the activation of Panx1 channels (Domercq et al., 2010). In contrast to Cx43 hemichannels, S-nitrosylation of Panx1 channels reduces their activity (Lohman et al., 2012), suggesting that their opening might be relevant only under conditions where NO is overcome by –SH reducing agents such as reduced glutathione.

## HEMICHANNEL BLOCKERS – MIMETIC PEPTIDES AND OTHERS

Specifically targeting unapposed hemichannels is difficult because they are composed of the same Cx building blocks as gap junction channels. As a consequence, most gap junction blockers also inhibit hemichannels (see Giaume and Theis, 2010). Moreover, many Cx hemichannel/gap junction channel blockers also block Panx channels. Gap junction blockers include glycyrrhetic acid and its derivative carbenoxolone, long-chain alcohols like heptanol or octanol, halogenated general volatile anesthetics like halothane, fatty acids like arachidonic acid and oleic acid, fatty acid amides like oleamide and anandamide, and fenamates like flufenamic acid, niflumic acid, or meclofenamic acid (reviewed in Bodendiek and Raman, 2010). Most of these substances have been used in the past to block hemichannels but the results obtained can only be unequivocally interpreted in terms of hemichannels when the contribution of gap junction channels is negligible or absent. Substances like the trivalent ions gadolinium ( $\text{Gd}^{3+}$ ) and lanthanum ( $\text{La}^{3+}$ ) block hemichannels without inhibiting gap junction channels or Panx1 channels, but these ions also inhibit

other channels including maxi-anion channels (Liu et al., 2006) and  $\text{Ca}^{2+}$  channels (Mlinar and Enyeart, 1993). A possible way to differentiate between Cx hemichannels and Panx channels is the use of long-chain alcohols that block Cx hemichannels but have only a very small effect of Panx channels. In contrast, low concentration (5–10  $\mu\text{M}$ ) of carbenoxolone blocks Panx1 channels and only has a minor inhibitory effect on Cx hemichannels (Schalper et al., 2008a). However, all these compounds are not specific and in addition to their inhibitory effects on Cx and Panx channels (including gap junctions channels and hemichannels) they also affect other neuronal and glial membrane properties which limits their use (see Giaume and Theis, 2010).

A more specific targeting of Cx channels is to be expected, at least in principle, from mimetic peptides of Cx proteins. Peptides identical to certain sequences on the Cx protein have been extensively used to interfere with the Cx channel function (Figure 2). The first Cx mimetic peptides that were introduced in the 1990s were identical to specific domains on the extracellular loops (first or second extracellular loop) of the Cx protein. The sequences mimicked were located in domains thought to be involved in the docking of two hemichannels during formation of a full gap junction channel (Warner et al., 1995). Exogenous addition of peptides mimicking parts of these domains were hypothesized to interact with yet unknown extracellular loop domains, thereby preventing extracellular loop interactions of apposed hemichannels during docking and thus hindering gap junction channel formation.



These domains, known as Gap26 and Gap27, are present on the first and second extracellular loops, respectively. Accordingly, Gap26 and Gap27 peptides were indeed found to inhibit gap junctional coupling (Evans and Boitano, 2001). Interestingly, subsequent work demonstrated that Gap26 and Gap27 peptides also inhibited unapposed hemichannels with which these peptides are supposed to interact (Braet et al., 2003; Evans et al., 2006, 2012; Desplantez et al., 2012; Wang et al., 2012). Currently, clear evidence that these peptides indeed interact with the extracellular loops is only available for Gap26 (Liu et al., 2006). Nevertheless, both Gap26 and Gap27 rapidly inhibit hemichannels within minutes, followed by a somewhat delayed inhibition of gap junction channels, often in the range of hours, with some exceptions (Matchkov et al., 2006). The exact mechanism of hemichannel block is currently not known. It is known that Gap26/27 influence voltage-dependent gating (Wang et al., 2012) but this does not explain their inhibitory action on hemichannels opened by triggers other than voltage. It has been suggested that these peptides inhibit hemichannels by just blocking the pore because of steric hindrance effects (Wang et al., 2007). However, this has been carefully checked and it was found that this only occurs at very high (1 mM and above) concentrations (Wang et al., 2012). Although Gap26/27 peptides proved to be interesting tools to inhibit Cx hemichannels, their delayed inhibition of gap junction channels remains a serious drawback. Moreover, Gap26/27 peptides also show rather limited specificity toward different Cx types. Indeed, the extracellular loop domains mimic sequences that show pronounced homology between different Cx proteins. Thus, Gap27 directed against Cx43 in astrocytes is also known to inhibit channels or hemichannels composed of Cx37, a vascular Cx present in brain blood vessels (Martin et al., 2005).

Besides peptides, antibodies have also been used to target the free extracellular loops of unapposed Cx hemichannels resulting in their inhibition. These tools offer additional advantage because they allow both functional blocking of the hemichannels and visualizing their distribution (Hofer and Dermietzel, 1998; Clair et al., 2008; Riquelme et al., 2013). However, currently single channel electrophysiological data showing hemichannel block by an antibody directed against an extracellular epitope is only demonstrated for Cx43 hemichannel activity induced in  $\beta$ -amyloid-treated astrocytes (Orellana et al., 2011c). Additionally, the specificity toward effects on other Cxs or Panxs still needs to be determined.

To improve specificity toward different Cxs, peptides have been devised that should target sequences on the intracellular domains of the Cx protein. The intracellular sequences are poorly conserved and very different between different Cxs. The L2 peptide is identical to a sequence on the cytoplasmic loop of Cx43. This peptide is known to prevent the closure of gap junction channels by binding to the CT tail, thereby preventing interaction of the CT tail with the cytoplasmic loop of Cx43 where the L2 domain is located (Seki et al., 2004; Hirst-Jensen et al., 2007 and references therein). Conceptually, interaction between the CT tail and the L2 domain is thought to block the gap junction channel pore upon exposure to acidification according to a particle-receptor model, and exogenous addition of L2 peptide prevents this interaction and its associated channel closure. Unexpectedly, it was found

that the L2 peptide inhibited Cx43 hemichannels, based on ATP release studies, indicating that this peptide has distinct effects on unapposed hemichannels and those incorporated into gap junctions (Ponsaerts et al., 2010). Further work with Gap19, a mimetic nonapeptide located within the Cx43 L2 domain, demonstrated a similar action; it inhibited single channel hemichannel currents and ATP release via Cx43 hemichannels while it did not influence gap junctional coupling after 30 min and stimulated coupling after 24 h (Wang et al., 2013). Moreover, the effect appeared to be specific for Cx43 as Gap19 had no effect on Cx40 hemichannels or Panx1 channels. While the effects of L2 and Gap19 are understood at a molecular operational scale, the full details of why preventing interactions between the CT tail and the cytoplasmic loop have such different effects on hemichannels as compared to gap junction channels still needs further clarification. However, distinct effects on hemichannels and gap junction channels have been reported for other Cx channel influencing molecules or conditions; for example, basic FGF (bFGF) and cytokines like TNF- $\alpha$  or IL-1 $\beta$  have all been demonstrated to promote Cx43 hemichannel function while inhibiting gap junctions (De Vuyst et al., 2007; Retamal et al., 2007a). Given the specific actions of L2 and Gap19 peptides at the level of both Cx types and channel types (hemichannels *versus* gap junction channels), these peptides offer promising possibilities to explore the role of astroglial Cx43 hemichannels in the complex environment of intact neural tissues, *ex vivo* or *in vivo*. Recent work has, for example, demonstrated that injection of L2 peptide in the rat amygdala strongly suppresses fear memory (Stehberg et al., 2012; discussed further below under Section “Impact of Hemichannel-Mediated Gliotransmission on Synaptic Activity and Behavior”). Equally interesting with respect to identifying the role and functions of Cx43 hemichannels is the G138R mutation of Cx43 in which a Gly at position 138 is replaced by an Arg. This is one of the several mutants found in the inherited human disease oculodentodigital dysplasia (ODDD). Importantly, G138R mutant Cx43 is characterized by a loss-of-function of gap junctional coupling and a gain-of-function of hemichannels (Dobrowolski et al., 2007, 2008). Thus, this particular mutant Cx43 can be used to stimulate Cx43 hemichannel function as a complementary experimental approach to hemichannel inhibition. Recently, Torres et al. (2012) have exploited such an approach to investigate the role of hemichannels in glial–neuronal communication.

## ROLES OF GLIAL HEMICHANNELS IN HEALTH AND DISEASE

### ASTROGLIAL Ca<sup>2+</sup> WAVES

Initially, gap junction channels were demonstrated to constitute the pathway allowing the propagation of intercellular Ca<sup>2+</sup> signaling between astrocytes, termed as Ca<sup>2+</sup> waves (Finkbeiner, 1992; Venance et al., 1995). Then, after the discovery of an external component that also contributes to this interglial signaling process (Hassinger et al., 1996), the involvement of Cx43 hemichannels and ATP release was identified (Cotrina et al., 1998; Stout et al., 2002). There is a consensus on the interpretation of these two sets of *in vitro* studies and it is admitted that both Cx channel functions are contributing. Indeed, they likely participate in various proportions to Ca<sup>2+</sup> waves depending on the brain structure, the mode of stimulation to trigger the waves, the age and the *in vitro*

conditions (Scemes and Giaume, 2006; Leybaert and Sanderson, 2012). In addition, several of these points could also account for the alternative proposal claiming that in astrocytes the external component is not supported by Cx43 hemichannels but by Panx1 channels (Suadicani et al., 2006; Scemes et al., 2007). This point of controversy remains to be clarified in the future although it is likely that both might participate in various proportions under different conditions.

More recently, several reports have confirmed that Ca<sup>2+</sup> waves in astrocytes are present *in vivo* in the normal brain (Hoogland et al., 2009; Kuga et al., 2011; Mathiesen et al., 2013) as well as in pathological situations (Kuchibhotla et al., 2009; Mathiesen et al., 2013). As expected, the occurrence, amplitude and extent of *in vivo* Ca<sup>2+</sup> waves are much more limited compared to the initial *in vitro* observations. However, as Ca<sup>2+</sup> signaling is considered as the mode of cellular excitability in astrocytes, such waves certainly play a role in the spatial and temporal features of neuroglial interactions. As a consequence, this means that in many cases dynamic neuroglial interactions are not limited to the sole tri-partite synapse but also occur at a more integrated level involving larger cerebral areas (Giaume et al., 2010). This situation is also likely true at the gliovascular interface where there is a high level of Cx expression between astroglial perivascular endfeet (Yamamoto et al., 1990; Simard et al., 2003; Rouach et al., 2008) and where Ca<sup>2+</sup> waves propagate from one initial endfoot to its neighbors (Mulligan and MacVicar, 2004). Such features might optimize the contribution of astrocytes to the control of the cerebral blood flow. However, while a role of Cx43 gap junction channels/hemichannels in pial arteriole dilation has been demonstrated *in vivo* for the glia limitans in response to sciatic stimulation (Xu and Pellegrino, 2007), a similar mechanism remains to be investigated for perivascular astrocytes within the brain parenchyma.

### HEMICHANNELS AS Ca<sup>2+</sup> CHANNELS

As indicated above, glial cells express several Cxs and out of these at least four of them (Cx26, Cx30, Cx32, and Cx43) have been demonstrated to form functional hemichannels (Li et al., 1996; Rhee et al., 1996; Valiunas and Weingart, 2000; Ripp et al., 2004), and at least Cx26, Cx32, and Cx43 serve as a membrane pathway for cell (Sánchez et al., 2009, 2010; Schalper et al., 2010) or liposome (Schalper et al., 2010; Fiori et al., 2012) Ca<sup>2+</sup> inflow. Of course, brief opening of Cx hemichannels could serve to transiently increase the intracellular Ca<sup>2+</sup> concentration that could affect a broad variety of physiological cell functions. For example, Cx43 hemichannels contribute to maintain higher intracellular levels of free Ca<sup>2+</sup> in cells treated with FGF-1 that proliferate and remain healthy (Schalper et al., 2008b). However, sustained hemichannel opening could promote deleterious results, including cell death (Decrock et al., 2009, 2011), but the bell-shaped action of intracellular Ca<sup>2+</sup> might prevent this ending process. Panx1 has also been detected in glial cells, as mentioned above (Iglesias et al., 2009; Domercq et al., 2010; Orellana et al., 2012b). This glycoprotein has been shown to form channels in the ER permeable to Ca<sup>2+</sup> (Vanden Abeele et al., 2006; D’Hondt et al., 2011) but the permeability to Ca<sup>2+</sup> of Panx1 channels present in the cell surface remains elusive. Moreover, direct demonstration of either

Cx- or Panx-based channels as a  $\text{Ca}^{2+}$  membrane pathway in any glial cell type remains to be demonstrated.

### ALTERNATIVE PATHWAY FOR GLUCOSE ENTRY IN INFLAMMATORY ASTROCYTES

Through the so-called astrocyte–neuron lactate shuttle, astrocytes participate in an activity-dependent manner to the uptake of glucose from the blood supply and the delivery of lactate to neurons (Pellerin and Magistretti, 2012). In normal conditions, glucose and lactate transporters are the membrane elements that support this astroglial contribution to brain metabolism. While glucose is well known to be essential for correct brain function, its homeostasis is altered by inflammatory conditions (Allaman et al., 2011). *In vitro*, an inflammatory situation for astrocytes can be mimicked either by co-culturing them with microglia selectively activated by the endotoxin LPS or by directly treating them with pro-inflammatory cytokines, such as TNF- $\alpha$  and IL-1 $\beta$ . Interestingly, in both cases these treatments induce an opposite regulation of Cx43 channels at least in cultured astrocytes: a decrease in gap junctional communication and an activation of hemichannels (Retamal et al., 2007a). In these conditions Cx43 hemichannels were shown to allow the influx of 2-(*N*-(7-nitrobenz-2-oxa-1,3-diazol-4-yl)amino)-2-deoxyglucose (2-NBDG), a glucose fluorescent analog, demonstrating that reactive or inflamed astrocytes can take up more glucose via Cx43 hemichannels when their metabolic coupling through gap junction channels is reduced (Rouach et al., 2008). Such opening of Cx43 hemichannels may represent an alternative metabolic pathway for glucose entry in astrocytes during pathological conditions associated with an inflammation status (Sofroniew and Vinters, 2010). Interestingly, this observation identifies a pathway that could contribute to the increase of glucose uptake found in several uncoupling situations (Tabernero et al., 2006); this was correlated with the up-regulation of GLUT-1 (glucose transporter 1) expression and to the induction of the expression of GLUT-3, an isoform that is not normally expressed in astrocytes, as well for type I and type II hexokinases, respectively (Sánchez-Alvarez et al., 2004). However, the respective contribution of hemichannels and glucose transporters in inflammatory conditions remains to be established. Because the permeability of the blood–brain barrier is increased during the inflammatory response (Schnell et al., 1999), more glucose coming from the circulation could become available to the brain. Thus, in addition to transporters, the entry of glucose through Cx43 hemichannels could contribute to an increase of lactate formation by astrocytes that are adapted for anaerobic metabolism. Finally, the opposite regulation of Cx43 channels (Retamal et al., 2007a) may lead to a failure in intercellular glucose trafficking (Rouach et al., 2008) that could be compensated for by the increase in glucose influx through Cx43 hemichannels in individual astrocytes. Moreover, although not demonstrated yet, Cx43 hemichannels could also support lactate efflux to feed neurons since Cx43 gap junction channels in astrocytes are permeable to lactate (Tabernero et al., 1996; Rouach et al., 2008). As a whole, Cx43 hemichannel activation should certainly contribute to modify the metabolic status of reactive astrocytes, a situation that should be taken into account when considering the role of astroglia in brain inflammation.

### IMPACT OF HEMICHANNEL-MEDIATED GLIOTRANSMISSION ON SYNAPTIC ACTIVITY AND BEHAVIOR

By analogy with the concept of a neurotransmitter, the term “gliotransmitter” has been proposed to name active molecules that are released by astrocytes and regulate neuronal activity as well as synaptic strength and plasticity (Haydon and Carmignoto, 2006). There are mainly three candidates that are proposed to play this role: glutamate, ATP, and D-serine. All of them can be released by a  $\text{Ca}^{2+}$ -dependent vesicular release mechanism in astrocytes (Zorec et al., 2012). However, at least glutamate and ATP have been demonstrated to permeate Cx43 hemichannels in astrocytes (Ye et al., 2003; Kang et al., 2008; Orellana et al., 2011b; Iglesias and Spray, 2012) as well as Panx1 channels in microglia (Orellana et al., 2011c), thus Cx43 and Panx1 channels could also play a role in gliotransmission. Recently, the activation of Cx43 hemichannels in astrocytes was shown to impact synaptic activity and plasticity (Stehberg et al., 2012; Torres et al., 2012). The first evidence comes from hippocampal acute slices in which a decrease in extracellular  $\text{Ca}^{2+}$  concentration is generated by the local photolysis of a photolabile  $\text{Ca}^{2+}$  buffer. This opens Cx43 hemichannels in astrocytes through which ATP is released and activates P2Y<sub>1</sub> purinergic receptors on a subset of inhibitory interneurons, initiating the generation of spikes by interneurons that in turn enhances synaptic inhibition at glutamatergic synapses (Torres et al., 2012). A similar neuroglial loop of interaction acting as a negative feedback mechanism is expected to occur during excessive glutamatergic activity that is associated with a decrease in extracellular  $\text{Ca}^{2+}$  concentration (Rusakov and Fine, 2003). The second set of evidence comes from *in vivo* experiments in which Cx43 hemichannels were inhibited (Stehberg et al., 2012). In this study, the rat basolateral amygdala was microinfused with the TAT-L2 peptide that selectively inhibits Cx43 hemichannels assumed to be only present in astrocytes. Such *in vivo* blockade of Cx43 hemichannels during memory consolidation induces amnesia for auditory fear conditioning, as assessed 24 h after training, without affecting short-term memory, locomotion, or shock reactivity. Moreover, the amnesic effect is transitory, specific for memory consolidation. Learning capacity recovers after co-infusion of the Cx43 hemichannel blocker and a mixture of gliotransmitters including glutamate and ATP. These observations suggest that gliotransmission mediated by Cx43 hemichannels is necessary for fear memory consolidation at the basolateral amygdala. Thus, the study of Stehberg et al. (2012) represents the first *in vivo* demonstration of a physiological role for astroglial Cx43 hemichannels in brain cognitive function. Finally, an *in vivo* contribution of Panx1 channels to cognition has recently been addressed by using a Panx1 knock out mouse (Prochnow et al., 2012). This constitutive knock out mouse was found to have increased excitability and potently enhanced early and persistent long-term potentiation (LTP) responses in the CA1 hippocampal region with additionally impaired spatial memory and object recognition memory. However, while the expression of Panx1 is well documented in hippocampal neurons (MacVicar and Thompson, 2010), its detection at the membrane of astrocytes is still debated (Iglesias et al., 2009; but see Orellana et al., 2010, 2011c). Consequently, it is premature to state that these Panx1-dependent changes in hippocampal models of learning and memory have an astroglial origin.

## NEURONAL DEATH AND BRAIN PATHOLOGIES

While there are now a number of reports indicating that the expression of glial Cxs changes in many brain pathologies and injuries (Giaume et al., 2010), this remains to be investigated in detail for Panxs. On this basis, the question of Cx channels contributing to neuronal death and brain diseases has been debated for many years. Indeed, opposite perspectives regarding the roles of glial Cxs in neuronal death have been discussed and reviewed (see Kirchhoff et al., 2001; Rouach et al., 2002; Perez Velazquez et al., 2003; Nakase and Naus, 2004; Farahani et al., 2005; Giaume et al., 2007; Orellana et al., 2009). In general, this duality was attributed to differences in (i) the experimental models (*in vitro*, *ex vivo*, and *in vivo*) or the protocols used to induce neuronal death, (ii) the mode (pharmacology *versus* transgenic animals) of Cx channel inhibition selected, (iii) the type of neuronal death or pathology investigated, and (iv) the time points considered. However, retrospectively the opposite roles attributed to Cx channels could be simply due to the fact that for a long time this question was solely taking into account the gap junctional function of Cxs. Indeed, in most cases, interpretation of the data was not considering the hemichannel and channel functions of Cxs and Panxs, respectively. Nevertheless, the development of compounds and transgenic animals that discriminate between Cx gap junction channels, Cx hemichannels and Panx channels (see above) has allowed identification of their respective contribution in various *in vitro* and *ex vivo* models of brain pathologies (see Kielian, 2008; Orellana et al., 2009; Bennett et al., 2012). Although hemichannels have been reported to be involved in several brain pathologies or injuries (reviewed in Bennett et al., 2012) as well as infection (Karpuk et al., 2011; Xiong et al., 2012), we will illustrate this situation by two recent examples that demonstrate the impact of glial Cx hemichannel and Panx channel activation in cells on neuronal death.

Modifications in the pattern of Cx and Panx expression in glia are associated with phenotypic changes observed during neuroinflammation and the “reactive gliosis” that is a common feature of most brain diseases (see Sofroniew and Vinters, 2010). Indeed, activated microglia and reactive astrocytes exhibit changes in their respective pattern of expression for Panx1 and Cx43 as well as in their hemichannel function leading to neuronal damage and death (Bennett et al., 2012; Orellana et al., 2012b). When an inflammatory context is mimicked *in vitro* by using LPS treatment, Cx43 hemichannel activity is triggered in astrocytes through the production of TNF- $\alpha$  and IL-1 $\beta$  by activated microglia. These events are not observed when astrocytes are cultured from Cx43 knock out mice (Retamal et al., 2007a). Furthermore, in neuron–astrocyte co-cultures the *N*-methyl-D-aspartate (NMDA)-induced neuronal excitotoxicity is reinforced by TNF- $\alpha$  + IL-1 $\beta$  treatment, while such a potentiating effect is not observed in cultures of neurons alone treated with the two cytokines (Froger et al., 2010). This observation suggests that the well-known protective role of astrocytes against excitotoxicity (Chen and Swanson, 2003) is impaired under pro-inflammatory conditions when astrogli Cx43 hemichannels are activated. Neuron–astrocyte co-cultures, made with astrocytes from Cx43 knock out and neurons from wild-type mice, revealed that the NMDA excitotoxicity is not reinforced by the pro-inflammatory treatment applied on these co-cultures made with Cx43-deficient astrocytes (Froger et al.,

2010). This result suggests that astrogli Cx43 is involved in the potentiated neurotoxicity induced by pro-inflammatory treatments. Interestingly, application (<30 min) of mimetic peptides (Gap26, Gap27) that inhibit Cx43 hemichannels and have no effect on Cx43 gap junctional communication (Retamal et al., 2007a), prevents the potentiated neurotoxicity response induced by pro-inflammatory cytokines (Froger et al., 2010; Orellana et al., 2012b).

Connexin hemichannels might also play a role in the pathological context of neurodegenerative diseases. Indeed, it is becoming increasingly clear that glial cells are critical players in the progressive neurodegeneration of Alzheimer’s disease (Kraft et al., 2013). Among others, the amyloid cascade represents one of the key pathways involved in the pathogenesis of the disease (see Pimplikar, 2009). Using separate primary cultures and co-cultures of microglia, astrocytes, and neurons it was shown that treatment with the  $\beta$ -amyloid peptide (A $\beta$ ) first activates microglia, resulting in the opening of Cx43 hemichannels and Panx1 channels in these cells. Such channel activations allow the release of glutamate and ATP that impair neuronal survival. A $\beta$ -activated microglia also produces TNF- $\alpha$  and IL-1 $\beta$  that, as indicated above, induce Cx43 astrogli hemichannel activation that again results in the release of glutamate and ATP (Orellana et al., 2011c). *In fine* these gliotransmitters originating from glial cells trigger neuronal damage and induce their death. Thus, such a cascade of Cx glial hemichannel and Panx channel activation could partially account for the progression of the neurodegenerative disease. These *in vitro* and *ex vivo* observations could be related to the changes in Cx43 expression observed in reactive astrocytes that contact amyloid deposit in a murine model of Alzheimer’s disease (Mei et al., 2010) and in brain from Alzheimer’s patients (Nagy et al., 1996; Koulakoff et al., 2012).

## CONCLUDING REMARKS

During the last decade our view and understanding of the structure (Maeda and Tsukihara, 2011), mutations (Pfenniger et al., 2011), properties (Rackauskas et al., 2010), and biological roles (Kar et al., 2012) of Cx channels has been incredibly enlarged, and to some extent this is also true for Panx channels (MacVicar and Thompson, 2010; Penuela et al., 2013). Interestingly, in glial cells this feature is exemplary because in addition to their well-documented molecular support for their two channel functions, non-channel functions have been also identified for Cxs, including cell adhesion mechanisms involved in radial migration of cortical neurons (Elias et al., 2007; Cina et al., 2009), modulation of P2Y purinergic receptors signaling (Scemes, 2008), regulation of cytoskeletal dynamics (Olk et al., 2010) and control of gene expression (Iacobas et al., 2004). Such a view could even be further enlarged by the recent report of another new class of membrane protein called calcium homeostasis modulator CALHM1 that shares structural similarities with Cx, Panx, and innexin channels and functional properties similar to hemichannels, such as ATP release in taste transduction (Siebert et al., 2013; Taruno et al., 2013).

In the present review, we have focused on a Cx/Panx-based channel function which 10 years ago was only sparsely considered in the central nervous system and in neuroglial interactions. Since then, the identification of external and intracellular signals that trigger the activation of hemichannels, the understanding of their

biophysics and their regulation have provided a better understanding of the roles that glial Cxs and Panxs play in healthy and diseased brains. Indeed, as reported above, there is now strong evidence to state that Cx and Panx channels in glia have an impact on neuronal activity and survival. However, there are at least two aims that remain to be achieved in order to determine whether and how the contribution of glial Cxs and/or Panxs is causal or secondary in normal and pathological situations. One is to distinguish what is due to gap junction channels *versus* hemichannels, the other is to discriminate between Cx hemichannels and Panx channels. To achieve these goals it is essential to have available pharmacological and genetic tools with glial cell type, Cx type, and Panx type specificities (see Giaume and Theis, 2010). Through a simple pharmacological approach this is unlikely to be achieved since Cx and Panx channels are sensitive to the same agents so far described. However, strategies using short-term treatment with mimetic peptides (Evans et al., 2012) or antibodies targeting extracellular domains (Riquelme et al., 2013) could be developed for all the glial Cxs/Panxs and their specificity demonstrated. In contrast, due to the cytoplasmic location of their two channel ends, gap junction channels are likely less easy to target by a pharmacological strategy. Another more accurate approach consists in the development of transgenic mice with appropriate mutations that prevent channel pairing without affecting hemichannel activity or that block one but not the other channel function. Alternatively, small interfering RNA (siRNA) and transgenic/viral techniques have been used with some success (see Giaume and Theis, 2010). But here again, the expression of multiple Cxs in glial cells makes the task difficult with genetic and molecular approaches. A recent report by Nedergaard's group of an enhanced synaptic plasticity (LTP) due to the engraftment of human glial progenitors into

immunodeficient mice (Han et al., 2013) gives weight to achieve such difficult challenges. Indeed, upon maturation in these grafted mice, human astrocytes were shown to be coupled to host astrocytes, suggesting a contribution of Cx channels in neuroglial interactions during synaptic plasticity. In line with such contribution, double Cx43/Cx30 knock out is associated with reduced LTP (Pannasch et al., 2011). Also, the observation of an up-regulation of astroglial Cxs in reactive astrocytes contacting amyloid plaques in a transgenic murine model of Alzheimer's disease has been validated in human patient brain samples (Nagy et al., 1996; Koulakoff et al., 2012), giving another example of the value in searching for strategies that block Cx channels.

## ACKNOWLEDGMENTS

This review arose from discussions made possible by a Colloquium Abroad grant from the Peter Wall Institute for Advanced Studies, University of British Columbia, in partnership with the Collège de France and the Fondation Hugo du Collège de France, Paris, France, as well as funds from the Vice President Research & International, University of British Columbia. This study includes reference to research that was supported by Grants from ECOS-CONICYT (to Christian Giaume and Juan C. Sáez), The Caisse de Retraite et de Prévoyance des Clercs et Employés de Notaires and the Ligue Européenne Contre la Maladie d'Alzheimer (to Christian Giaume), the Fund for Scientific Research Flanders (to Luc Leybaert) and Belgian Science Policy (Interuniversity Attraction Poles to Luc Leybaert), Fondecyt project 1120214 (to Juan C. Sáez), 1111033 (to Juan C. Sáez), Chilean Science Millennium Institute (P09-022-F; to Juan C. Sáez), the Canadian Institutes for Health Research (to Christian C. Naus), and the Heart and Stroke Foundation of Canada (Christian C. Naus).

## REFERENCES

- Ahmad, S., and Evans, W. H. (2002). Post-translational integration and oligomerization of connexin 26 in plasma membranes and evidence of formation of membrane pores: implications for the assembly of gap junctions. *Biochem. J.* 365, 693–699. doi: 10.1042/BJ20011572
- Allaman, I., Belanger, M., and Magistretti, P. J. (2011). Astrocyte-neuron metabolic relationships: for better and for worse. *Trends Neurosci.* 34, 76–87. doi: 10.1016/j.tins.2010.12.001
- Altevogt, B. M., Kleopa, K. A., Postma, F. R., Scherer, S. S., and Paul, D. L. (2002). Connexin29 is uniquely distributed within myelinating glial cells of the central and peripheral nervous systems. *J. Neurosci.* 22, 6458–6470.
- Alvarez-Maibecin, V., García-Hernández, F., Williams, J. T., and Van Bockstaele, E. J. (2000). Functional coupling between neurons and glia. *J. Neurosci.* 20, 4091–4098.
- Anderson, C. M., Bergher, J. P., and Swanson, R. A. (2004). ATP-induced ATP release from astrocytes. *J. Neurochem.* 88, 246–256. doi: 10.1111/j.1471-4159.2004.02204.x
- Andrew, R. D., MacVicar, B. A., Dudek, F. E., and Hatton, G. I. (1981). Dye transfer through gap junctions between neuroendocrine cells of rat hypothalamus. *Science* 211, 1187–1189. doi: 10.1126/science.7466393
- Anselmi, F., Hernandez, V. H., Crispino, G., Seydel, A., Ortolano, S., Roper, S. D., et al. (2008). ATP release through connexin hemichannels and gap junction transfer of second messengers propagate  $\text{Ca}^{2+}$  signals across the inner ear. *Proc. Natl. Acad. Sci. U.S.A.* 105, 18770–18775. doi: 10.1073/pnas.0800793105
- Arcuino, G., Lin, J. H., Takano, T., Liu, C., Jiang, L., Gao, Q., et al. (2002). Intercellular calcium signaling mediated by point-source burst release of ATP. *Proc. Natl. Acad. Sci. U.S.A.* 99, 9840–9845. doi: 10.1073/pnas.152588599
- Bao, L., Locovei, S., and Dahl, G. (2004a). Pannexin membrane channels are mechanosensitive conduits for ATP. *FEBS Lett.* 572, 65–68. doi: 10.1016/j.febslet.2004.07.009
- Bao, L., Sachs, F., and Dahl, G. (2004b). Connexins are mechanosensitive. *Am. J. Physiol. Cell Physiol.* 287, C1389–C1395. doi: 10.1152/ajpcell.00220.2004
- Bao, X., Reuss, L., and Altenberg, G. A. (2004c). Regulation of purified and reconstituted connexin 43 hemichannels by protein kinase C-mediated phosphorylation of Serine 368. *J. Biol. Chem.* 279, 20058–20066. doi: 10.1074/jbc.M311137200
- Bao, X., Lee, S. C., Reuss, L., and Altenberg, G. A. (2007). Change in permeant size selectivity by phosphorylation of connexin 43 gap-junctional hemichannels by PKC. *Proc. Natl. Acad. Sci. U.S.A.* 104, 4919–4924. doi: 10.1073/pnas.0603154104
- Baranova, A., Ivanov, D., Petrush, N., Pestova, A., Skoblov, M., Kelman, I., et al. (2004). The mammalian pannexin family is homologous to the invertebrate innexin gap junction proteins. *Genomics* 83, 706–716. doi: 10.1016/j.ygeno.2003.09.025
- Bargiello, T. A., Tang, Q., Oh, S., and Kwon, T. (2012). Voltage-dependent conformational changes in connexin channels. *Biochim. Biophys. Acta* 1818, 1807–1822. doi: 10.1016/j.bbamem.2011.09.019
- Batra, N., Burra, S., Siller-Jackson, A. J., Gu, S., Xia, X., Weber, G. F., et al. (2012). Mechanical stress-activated integrin alpha5beta1 induces opening of connexin 43 hemichannels. *Proc. Natl. Acad. Sci. U.S.A.* 109, 3359–3364. doi: 10.1073/pnas.1115967109
- Belousov, A. B., and Fontes, J. D. (2013). Neuronal gap junctions: making and breaking connections during development and injury. *Trends Neurosci.* 36, 227–236. doi: 10.1016/j.tins.2012.11.001
- Bennett, M. V., Contreras, J. E., Bukauskas, F. F., and Sáez, J. C. (2003). New roles for astrocytes: gap junction hemichannels have something to communicate. *Trends Neurosci.* 26, 610–617. doi: 10.1016/j.tins.2003.09.008
- Bennett, M. V., Garré, J. M., Orellana, J. A., Bukauskas, F. F., Nedergaard, M., and Sáez, J. C. (2012). Connexin and pannexin hemichannels in inflammatory responses of glia and

- neurons. *Brain Res.* 1487, 3–15. doi: 10.1016/j.brainres.2012.08.042
- Bevans, C. G., and Harris, A. L. (1999). Regulation of connexin channels by pH. Direct action of the protonated form of taurine and other aminosulfonates. *J. Biol. Chem.* 274, 3711–3719. doi: 10.1074/jbc.274.6.3711
- Bevans, C. G., Kordel, M., Rhee, S. K., and Harris, A. L. (1998). Isoform composition of connexin channels determines selectivity among second messengers and uncharged molecules. *J. Biol. Chem.* 273, 2808–2816. doi: 10.1074/jbc.273.5.2808
- Bezprozvanny, I., Watras, J., and Ehrlich, B. E. (1991). Bell-shaped calcium-response curves of Ins(1,4,5)P<sub>3</sub>- and calcium-gated channels from endoplasmic reticulum of cerebellum. *Nature* 351, 751–754. doi: 10.1038/351751a0
- Bodendiek, S. B., and Raman, G. (2010). Connexin modulators and their potential targets under the magnifying glass. *Curr. Med. Chem.* 17, 4191–4230. doi: 10.2174/092986710793348563
- Braet, K., Vandamme, W., Martin, P. E., Evans, W. H., and Leybaert, L. (2003). Photoliberating inositol-1,4,5-trisphosphate triggers ATP release that is blocked by the connexin mimetic peptide gap 26. *Cell Calcium* 33, 37–48. doi: 10.1016/S0143-4160(02)00180-X
- Bruzzone, R., Barbe, M. T., Jakob, N. J., and Monyer, H. (2005). Pharmacological properties of homomeric and heteromeric pannexin hemichannels expressed in *Xenopus* oocytes. *J. Neurochem.* 92, 1033–1043. doi: 10.1111/j.1471-4159.2004.02947.x
- Bruzzone, R., Hormuzdi, S. G., Barbe, M. T., Herb, A., and Monyer, H. (2003). Pannexins, a family of gap junction proteins expressed in brain. *Proc. Natl. Acad. Sci. U.S.A.* 100, 13644–13649. doi: 10.1073/pnas.2233464100
- Bruzzone, S., Guida, L., Zocchi, E., Franco, L., and De Flora, A. (2001). Connexin 43 hemi channels mediate Ca<sup>2+</sup>-regulated transmembrane NAD<sup>+</sup> fluxes in intact cells. *FASEB J.* 15, 10–12.
- Chen, Y., and Swanson, R. A. (2003). Astrocytes and brain injury. *J. Cereb. Blood Flow Metab.* 23, 137–149. doi: 10.1097/00004647-200302000-00001
- Cina, C., Maass, K., Theis, M., Willecke, K., Bechberger, J. F., and Naus, C. C. (2009). Involvement of the cytoplasmic C-terminal domain of connexin43 in neuronal migration. *J. Neurosci.* 29, 2009–2021. doi: 10.1523/JNEUROSCI.5025-08.2009
- Clair, C., Combettes, L., Pierre, F., Sansonetti, P., and Tran Van Nhieu, G. (2008). Extracellular-loop peptide antibodies reveal a predominant hemichannel organization of connexins in polarized intestinal cells. *Exp. Cell Res.* 314, 1250–1265. doi: 10.1016/j.yexcr.2007.12.021
- Contreras, J. E., Sáez, J. C., Bukauskas, F. F., and Bennett, M. V. (2003). Gating and regulation of connexin 43 (Cx43) hemichannels. *Proc. Natl. Acad. Sci. U.S.A.* 100, 11388–11393. doi: 10.1073/pnas.1434298100
- Contreras, J. E., Sánchez, H. A., Eugenín, E. A., Speidel, D., Theis, M., Willecke, K., et al. (2002). Metabolic inhibition induces opening of unapposed connexin 43 gap junction hemichannels and reduces gap junctional communication in cortical astrocytes in culture. *Proc. Natl. Acad. Sci. U.S.A.* 99, 495–500. doi: 10.1073/pnas.012589799
- Contreras, J. E., Sánchez, H. A., Vélez, L. P., Bukauskas, F. F., Bennett, M. V., and Sáez, J. C. (2004). Role of connexin-based gap junction channels and hemichannels in ischemia-induced cell death in nervous tissue. *Brain Res. Brain Res. Rev.* 47, 290–303. doi: 10.1016/j.brainresrev.2004.08.002
- Cotrina, M. L., Lin, J. H., Alves-Rodrigues, A., Liu, S., Li, J., Azmi-Ghadimi, H., et al. (1998). Connexins regulate calcium signaling by controlling ATP release. *Proc. Natl. Acad. Sci. U.S.A.* 95, 15735–15740. doi: 10.1073/pnas.95.26.15735
- De Bock, M., Culot, M., Wang, N., Bol, M., Decrock, E., De Vuyst, E., et al. (2011). Connexin channels provide a target to manipulate brain endothelial calcium dynamics and blood-brain barrier permeability. *J. Cereb. Blood Flow Metab.* 31, 1942–1957. doi: 10.1038/jcbfm.2011.86
- De Bock, M., Wang, N., Bol, M., Decrock, E., Ponsaerts, R., Bultyck, G., et al. (2012). Connexin 43 hemichannels contribute to cytoplasmic Ca<sup>2+</sup> oscillations by providing a bimodal Ca<sup>2+</sup>-dependent Ca<sup>2+</sup> entry pathway. *J. Biol. Chem.* 287, 12250–12266. doi: 10.1074/jbc.M111.299610
- Decrock, E., De Vuyst, E., Vinken, M., Van Moorhem, M., Vranckx, K., Wang, N., et al. (2009). Connexin 43 hemichannels contribute to the propagation of apoptotic cell death in a rat C6 glioma cell model. *Cell Death Differ.* 16, 151–163. doi: 10.1038/cdd.2008.138
- Decrock, E., Vinken, M., Bol, M., D'Herde, K., Rogiers, V., Vandenabeele, P., et al. (2011). Calcium and connexin-based intercellular communication, a deadly catch? *Cell Calcium* 50, 310–321. doi: 10.1016/j.ceca.2011.05.007
- D'Hondt, C., Iyyathurai, J., Wang, N., Gourdie, R. G., Himpens, B., Leybaert, L., et al. (2013). Negatively charged residues (Asp378 and Asp379) in the last ten amino acids of the C-terminal tail of Cx43 hemichannels are essential for loop/tail interactions. *Biochem. Biophys. Res. Commun.* 432, 707–712. doi: 10.1016/j.bbrc.2013.01.066
- D'Hondt, C., Ponsaerts, R., De Smedt, H., Vinken, M., De Vuyst, E., De Bock, M., et al. (2011). Pannexin channels in ATP release and beyond: an unexpected rendezvous at the endoplasmic reticulum. *Cell. Signal.* 23, 305–316. doi: 10.1016/j.cellsig.2010.07.018
- Desplantez, T., Verma, V., Leybaert, L., Evans, W. H., and Weingart, R. (2012). Gap26, a connexin mimetic peptide, inhibits currents carried by connexin43 hemichannels and gap junction channels. *Pharmacol. Res.* 65, 546–552. doi: 10.1016/j.phrs.2012.02.002
- DeVries, S. H., and Schwartz, E. A. (1992). Hemi-gap-junction channels in solitary horizontal cells of the catfish retina. *J. Physiol.* 445, 201–230.
- De Vuyst, E., Decrock, E., Cabooter, L., Dubyak, G. R., Naus, C. C., Evans, W. H., et al. (2006). Intracellular calcium changes trigger connexin 32 hemichannel opening. *EMBO J.* 25, 34–44. doi: 10.1038/sj.emboj.7600908
- De Vuyst, E., Decrock, E., De Bock, M., Yamasaki, H., Naus, C. C., Evans, W. H., et al. (2007). Connexin hemichannels and gap junction channels are differentially influenced by lipopolysaccharide and basic fibroblast growth factor. *Mol. Biol. Cell* 18, 34–46. doi: 10.1091/mbc.E06-03-0182
- De Vuyst, E., Wang, N., Decrock, E., De Bock, M., Vinken, M., Van Moorhem, M., et al. (2009). Ca(2+) regulation of connexin 43 hemichannels in C6 glioma and glial cells. *Cell Calcium* 46, 176–187. doi: 10.1016/j.ceca.2009.07.002
- Dobrenis, K., Chang, H. Y., Pina-Benabou, M. H., Woodroffe, A., Lee, S. C., Rozental, R., et al. (2005). Human and mouse microglia express connexin36, and functional gap junctions are formed between rodent microglia and neurons. *J. Neurosci. Res.* 82, 306–315. doi: 10.1002/jnr.20650
- Dobrowolski, R., Sasse, P., Schrickel, J. W., Watkins, M., Kim, J. S., Rackauskas, M., et al. (2008). The conditional connexin43G138R mouse mutant represents a new model of hereditary oculodentodigital dysplasia in humans. *Hum. Mol. Genet.* 17, 539–554. doi: 10.1093/hmg/ddm329
- Dobrowolski, R., Sommershof, A., and Willecke, K. (2007). Some oculodentodigital dysplasia-associated Cx43 mutations cause increased hemichannel activity in addition to deficient gap junction channels. *J. Membr. Biol.* 219, 9–17. doi: 10.1007/s00232-007-9055-7
- Domercq, M., Perez-Samartín, A., Aparicio, D., Alberdi, E., Pampliega, O., and Matute, C. (2010). P2X7 receptors mediate ischemic damage to oligodendrocytes. *Glia* 58, 730–740. doi: 10.1002/glia.20958
- Elias, L. A., Wang, D. D., and Kriegstein, A. R. (2007). Gap junction adhesion is necessary for radial migration in the neocortex. *Nature* 448, 901–907. doi: 10.1038/nature06063
- Eugenín, E. A., Eckardt, D., Theis, M., Willecke, K., Bennett, M. V., and Sáez, J. C. (2001). Microglia at brain stab wounds express connexin 43 and in vitro form functional gap junctions after treatment with interferon-gamma and tumor necrosis factor-alpha. *Proc. Natl. Acad. Sci. U.S.A.* 98, 4190–4195. doi: 10.1073/pnas.051634298
- Evans, W. H., and Boitano, S. (2001). Connexin mimetic peptides: specific inhibitors of gap-junctional intercellular communication. *Biochem. Soc. Trans.* 29, 606–612. doi: 10.1042/BST0290606
- Evans, W. H., Bultyck, G., and Leybaert, L. (2012). Manipulating connexin communication channels: use of peptidomimetics and the translational outputs. *J. Membr. Biol.* 245, 437–449. doi: 10.1007/s00232-012-9488-5
- Evans, W. H., De Vuyst, E., and Leybaert, L. (2006). The gap junction cellular internet: connexin hemichannels enter the signalling limelight. *Biochem. J.* 397, 1–14. doi: 10.1042/BJ20060175
- Farahani, R., Pina-Benabou, M. H., Kyrozi, A., Siddiq, A., Barradas, P. C., Chiu, F. C., et al. (2005). Alterations in metabolism and gap junction expression may determine the role of astrocytes as “good samaritans” or executioners. *Glia* 50, 351–361. doi: 10.1002/glia.20213
- Figueroa, X. F., Lillo, M. A., Gaete, P. S., Riquelme, M., and Sáez, J. C. (2013). Diffusion of nitric oxide across cell membranes of the vascular

- wall requires specific connexin-based channels. *Neuropharmacology*. doi: 10.1016/j.neuropharm.2013.02.022 [Epub ahead of print].
- Finkbeiner, S. (1992). Calcium waves in astrocytes—filling in the gaps. *Neuron* 8, 1101–1108. doi: 10.1016/0896-6273(92)90131-V
- Fiori, M. C., Figueroa, V., Zoghbi, M. E., Sáez, J. C., Reuss, L., and Altenberg, G. A. (2012). Permeation of calcium through purified connexin 26 hemichannels. *J. Biol. Chem.* 287, 40826–40834. doi: 10.1074/jbc.M112.383281
- Fróes, M. M., Correia, A. H., Garcia-Abreu, J., Spray, D. C., Campos de Carvalho, A. C., and Neto, M. V. (1999). Gap-junctional coupling between neurons and astrocytes in primary central nervous system cultures. *Proc. Natl. Acad. Sci. U.S.A.* 96, 7541–7546. doi: 10.1073/pnas.96.13.7541
- Froger, N., Orellana, J. A., Calvo, C. F., Amigou, E., Kozoriz, M. G., Naus, C. C., et al. (2010). Inhibition of cytokine-induced connexin43 hemichannel activity in astrocytes is neuroprotective. *Mol. Cell. Neurosci.* 45, 37–46. doi: 10.1016/j.mcn.2010.05.007
- Froger, N., Orellana, J. A., Cohen-Salmon, M., Ezan, P., Amigou, E., Sáez, J. C., et al. (2009). Cannabinoids prevent the opposite regulation of astroglial connexin43 hemichannels and gap junction channels induced by pro-inflammatory treatments. *J. Neurochem.* 111, 1383–1397.
- Fushiki, S., Perez Velazquez, J. L., Zhang, L., Bechberger, J. F., Carlen, P. L., and Naus, C. C. (2003). Changes in neuronal migration in neocortex of connexin43 null mutant mice. *J. Neuropathol. Exp. Neurol.* 62, 304–314.
- Garg, S., Md Syed, M., and Kielian, T. (2005). *Staphylococcus aureus*-derived peptidoglycan induces Cx43 expression and functional gap junction intercellular communication in microglia. *J. Neurochem.* 95, 475–483. doi: 10.1111/j.1471-4159.2005.03384.x
- Garré, J. M., Retamal, M. A., Cassina, P., Barbeito, L., Bukauskas, F. F., Sáez, J. C., et al. (2010). FGF-1 induces ATP release from spinal astrocytes in culture and opens pannexin and connexin hemichannels. *Proc. Natl. Acad. Sci. U.S.A.* 107, 22659–22664. doi: 10.1073/pnas.1013793107
- Giaume, C., Fromaget, C., el Aoumari, A., Cordier, J., Glowinski, J., and Gros, D. (1991). Gap junctions in cultured astrocytes: single-channel currents and characterization of channel-forming protein. *Neuron* 6, 133–143. doi: 10.1016/0896-6273(91)90128-M
- Giaume, C., Kirchhoff, F., Matute, C., Reichenbach, A., and Verkhratsky, A. (2007). Glia: the fulcrum of brain diseases. *Cell Death Differ.* 14, 1324–1335. doi: 10.1038/sj.cdd.4402144
- Giaume, C., Koulakoff, A., Roux, L., Holcman, D., and Rouach, N. (2010). Astroglial networks: a step further in neuroglial and gliovascular interactions. *Nat. Rev. Neurosci.* 11, 87–99. doi: 10.1038/nrn2757
- Giaume, C., Orellana, J. A., Abudara, V., and Sáez, J. C. (2012). Connexin-based channels in astrocytes: how to study their properties. *Methods Mol. Biol.* 814, 283–303. doi: 10.1007/978-1-61779-452-0\_19
- Giaume, C., and Theis, M. (2010). Pharmacological and genetic approaches to study connexin-mediated channels in glial cells of the central nervous system. *Brain Res. Rev.* 63, 160–176. doi: 10.1016/j.brainresrev.2009.11.005
- Gómez-Hernández, J. M., de Miguel, M., Larrosa, B., Gonzalez, D., and Barrio, L. C. (2003). Molecular basis of calcium regulation in connexin-32 hemichannels. *Proc. Natl. Acad. Sci. U.S.A.* 100, 16030–16035. doi: 10.1073/pnas.2530348100
- González, D., Gomez-Hernandez, J. M., and Barrio, L. C. (2006). Species specificity of mammalian connexin-26 to form open voltage-gated hemichannels. *FASEB J.* 20, 2329–2338. doi: 10.1096/fj.06-5828com
- Goodenough, D. A., and Paul, D. L. (2003). Beyond the gap: functions of unpaired connexon channels. *Nat. Rev. Mol. Cell Biol.* 4, 285–294. doi: 10.1038/nrm1072
- Gossman, D. G., and Zhao, H. B. (2008). Hemichannel-mediated inositol 1,4,5-trisphosphate (IP3) release in the cochlea: a novel mechanism of IP3 intercellular signaling. *Cell Commun. Adhes.* 15, 305–315. doi: 10.1080/15419060802357217
- Han, X., Chen, M., Wang, F., Wondrem, M., Wang, S., Shanz, S., et al. (2013). Forebrain engraftment by human glial progenitor cells enhances synaptic plasticity and learning in adult mice. *Cell Stem Cell* 12, 342–353. doi: 10.1016/j.stem.2012.12.015
- Harris, A. L. (2007). Connexin channel permeability to cytoplasmic molecules. *Prog. Biophys. Mol. Biol.* 94, 120–143. doi: 10.1016/j.pbiomolbio.2007.03.011
- Hassinger, T. D., Guthrie, P. B., Atkinson, P. B., Bennett, M. V., and Kater, S. B. (1996). An extracellular signaling component in propagation of astrocytic calcium waves. *Proc. Natl. Acad. Sci. U.S.A.* 93, 13268–13273. doi: 10.1073/pnas.93.23.13268
- Haydon, P. G., and Carmignoto, G. (2006). Astrocyte control of synaptic transmission and neurovascular coupling. *Physiol. Rev.* 86, 1009–1031. doi: 10.1152/physrev.00049.2005
- Heidemann, A. C., Schipke, C. G., and Kettenmann, H. (2005). Extracellular application of nicotinic acid adenine dinucleotide phosphate induces  $\text{Ca}^{2+}$  signaling in astrocytes *in situ*. *J. Biol. Chem.* 280, 35630–35640. doi: 10.1074/jbc.M507338200
- Heinrich, A., Ando, R. D., Turi, G., Rozsa, B., and Sperlagh, B. (2012).  $\text{K}^+$  depolarization evokes ATP, adenosine and glutamate release from glia in rat hippocampus: a microelectrode biosensor study. *Br. J. Pharmacol.* 167, 1003–1020. doi: 10.1111/j.1476-5381.2012.01932.x
- Hirst-Jensen, B. J., Sahoo, P., Kieken, F., Delmar, M., and Sorgen, P. L. (2007). Characterization of the pH-dependent interaction between the gap junction protein connexin43 carboxyl terminus and cytoplasmic loop domains. *J. Biol. Chem.* 282, 5801–5813. doi: 10.1074/jbc.M605233200
- Hofer, A., and Dermietzel, R. (1998). Visualization and functional blocking of gap junction hemichannels (connexons) with antibodies against external loop domains in astrocytes. *Glia* 24, 141–154. doi: 10.1002/(SICI)1098-1136(199809)24:1
- Hoogland, T. M., Kuhn, B., Gobel, W., Huang, W., Nakai, J., Helmchen, F., et al. (2009). Radially expanding transglial calcium waves in the intact cerebellum. *Proc. Natl. Acad. Sci. U.S.A.* 106, 3496–3501. doi: 10.1073/pnas.0809269106
- Iacobas, D. A., Scemes, E., and Spray, D. C. (2004). Gene expression alterations in connexin null mice extend beyond the gap junction. *Neurochem. Int.* 45, 243–250. doi: 10.1016/j.neuint.2003.12.008
- Iglesias, R., Dahl, G., Qiu, F., Spray, D. C., and Scemes, E. (2009). Pannexin 1: the molecular substrate of astrocyte “hemichannels”. *J. Neurosci.* 29, 7092–7097. doi: 10.1523/JNEUROSCI.6062-08.2009
- Iglesias, R. M., and Spray, D. C. (2012). Pannexin1-mediated ATP release provides signal transmission between Neuro2A cells. *Neurochem. Res.* 37, 1355–1363. doi: 10.1007/s11064-012-0720-6
- Jiang, S., Yuan, H., Duan, L., Cao, R., Gao, B., Xiong, Y. F., et al. (2011). Glutamate release through connexin 43 by cultured astrocytes in a stimulated hypertonicity model. *Brain Res.* 1392, 8–15. doi: 10.1016/j.brainres.2011.03.056
- John, S. A., Kondo, R., Wang, S. Y., Goldhaber, J. I., and Weiss, J. N. (1999). Connexin-43 hemichannels opened by metabolic inhibition. *J. Biol. Chem.* 274, 236–240. doi: 10.1074/jbc.274.1.236
- Kang, J., Kang, N., Lovatt, D., Torres, A., Zhao, Z., Lin, J., et al. (2008). Connexin 43 hemichannels are permeable to ATP. *J. Neurosci.* 28, 4702–4711. doi: 10.1523/JNEUROSCI.5048-07.2008
- Kar, R., Batra, N., Riquelme, M. A., and Jiang, J. X. (2012). Biological role of connexin intercellular channels and hemichannels. *Arch. Biochem. Biophys.* 524, 2–15. doi: 10.1016/j.abb.2012.03.008
- Karpuk, N., Burkovetskaya, M., Fritz, T., Angle, A., and Kielian, T. (2011). Neuroinflammation leads to region-dependent alterations in astrocyte gap junction communication and hemichannel activity. *J. Neurosci.* 31, 414–425. doi: 10.1523/JNEUROSCI.5247-10.2011
- Katakowski, M., Buller, B., Wang, X., Rogers, T., and Chopp, M. (2010). Functional microRNA is transferred between glioma cells. *Cancer Res.* 70, 8259–8263. doi: 10.1158/0008-5472.CAN-10-0604
- Kielian, T. (2008). Glial connexins and gap junctions in CNS inflammation and disease. *J. Neurochem.* 106, 1000–1016. doi: 10.1111/j.1471-4159.2008.05405.x
- Kienitz, M. C., Bender, K., Dermietzel, R., Pott, L., and Zoidl, G. (2011). Pannexin 1 constitutes the large conductance cation channel of cardiac myocytes. *J. Biol. Chem.* 286, 290–298. doi: 10.1074/jbc.M110.163477
- Kirchhoff, F., Dringen, R., and Giaume, C. (2001). Pathways of neuron-astrocyte interactions and their possible role in neuroprotection. *Eur. Arch. Psychiatry Clin. Neurosci.* 251, 159–169. doi: 10.1007/s004060170036
- Koulakoff, A., Mei, X., Orellana, J. A., Sáez, J. C., and Giaume, C. (2012). Glial connexin expression and function in the context of Alzheimer’s disease. *Biochim. Biophys. Acta* 1818, 2048–2057. doi: 10.1016/j.bbamem.2011.10.001
- Kozoric, M., and Naus, C. C. (2013). “Gap junction-mediated neuroprotection,” in *Gap Junctions in the Brain: Physiological and Pathological Roles*, ed. E. Dere (London: Academic Press), 231–246. doi: 10.1016/B978-0-12-415901-3.00014-1
- Kraft, A. W., Hu, X., Yoon, H., Yan, P., Xiao, Q., Wang, Y., et al. (2013). “Gap junction-mediated neuroprotection,” in *Gap Junctions in the Brain: Physiological and Pathological Roles*, ed. E. Dere (London: Academic Press), 231–246. doi: 10.1016/B978-0-12-415901-3.00014-1

- (2013). Attenuating astrocyte activation accelerates plaque pathogenesis in APP/PS1 mice. *FASEB J.* 27, 187–198. doi: 10.1096/fj.12-208660
- Kuchibhotla, K. V., Lattarulo, C. R., Hyman, B. T., and Bacskai, B. J. (2009). Synchronous hyperactivity and intercellular calcium waves in astrocytes in Alzheimer mice. *Science* 323, 1211–1215. doi: 10.1126/science.1169096
- Kuga, N., Sasaki, T., Takahara, Y., Matsuki, N., and Ikegaya, Y. (2011). Large-scale calcium waves traveling through astrocytic networks in vivo. *J. Neurosci.* 31, 2607–2614. doi: 10.1523/JNEUROSCI.5319-10.2011
- Kwon, T., Tang, Q., and Bargiello, T. A. (2013). Voltage-dependent gating of the Cx32\*43E1 hemichannel: conformational changes at the channel entrances. *J. Gen. Physiol.* 141, 243–259. doi: 10.1085/jgp.201210839
- Lai, C. P., Bechberger, J. F., Thompson, R. J., MacVicar, B. A., Bruzzone, R., and Naus, C. C. (2007). Tumor-suppressive effects of pannexin 1 in C6 glioma cells. *Cancer Res.* 67, 1545–1554. doi: 10.1158/0008-5472.CAN-06-1396
- Leybaert, L., and Sanderson, M. J. (2012). Intercellular Ca(2+) waves: mechanisms and function. *Physiol. Rev.* 92, 1359–1392. doi: 10.1152/physrev.00029.2011
- Li, H., Liu, T. F., Lazrak, A., Peracchia, C., Goldberg, G. S., Lampe, P. D., et al. (1996). Properties and regulation of gap junctional hemichannels in the plasma membranes of cultured cells. *J. Cell Biol.* 134, 1019–1030. doi: 10.1083/jcb.134.4.1019
- Liu, F., Arce, F. T., Ramachandran, S., and Lal, R. (2006). Nanomechanics of hemichannel conformations: connexin flexibility underlying channel opening and closing. *J. Biol. Chem.* 281, 23207–23217. doi: 10.1074/jbc.M605048200
- Liu, X., Sun, L., Torii, M., and Rakic, P. (2012). Connexin 43 controls the multipolar phase of neuronal migration to the cerebral cortex. *Proc. Natl. Acad. Sci. U.S.A.* 109, 8280–8285. doi: 10.1073/pnas.1205880109
- Locke, D., Kielen, F., Tao, L., Sorgen, P. L., and Harris, A. L. (2011). Mechanism for modulation of gating of connexin26-containing channels by taurine. *J. Gen. Physiol.* 138, 321–339. doi: 10.1085/jgp.201110634
- Locovei, S., Wang, J., and Dahl, G. (2006). Activation of pannexin 1 channels by ATP through P2Y receptors and by cytoplasmic calcium. *FEBS Lett.* 580, 239–244. doi: 10.1016/j.febslet.2005.12.004
- Lohman, A. W., Weaver, J. L., Billaud, M., Sandilos, J. K., Griffiths, R., Straub, A. C., et al. (2012). S-nitrosylation inhibits pannexin 1 channel function. *J. Biol. Chem.* 287, 39602–39612. doi: 10.1074/jbc.M112.397976
- Luckprom, P., Kanjanamekanant, K., and Pavasant, P. (2011). Role of connexin43 hemichannels in mechanical stress-induced ATP release in human periodontal ligament cells. *J. Periodontal Res.* 46, 607–615. doi: 10.1111/j.1600-0765.2011.01379.x
- Ma, W., Compan, V., Zheng, W., Martin, E., North, R. A., Verkhratsky, A., et al. (2012). Pannexin 1 forms an anion-selective channel. *Pflügers Arch.* 463, 585–592. doi: 10.1007/s00424-012-1077-z
- MacVicar, B. A., and Thompson, R. J. (2010). Non-junction functions of pannexin-1 channels. *Trends Neurosci.* 33, 93–102. doi: 10.1016/j.tins.2009.11.007
- Maeda, S., and Tsukihara, T. (2011). Structure of the gap junction channel and its implications for its biological functions. *Cell. Mol. Life Sci.* 68, 1115–1129. doi: 10.1007/s00018-010-0551-z
- Maezawa, I., and Jin, L. W. (2010). Rett syndrome microglia damage dendrites and synapses by the elevated release of glutamate. *J. Neurosci.* 30, 5346–5356. doi: 10.1523/JNEUROSCI.5966-09.2010
- Martin, P. E., Wall, C., and Griffith, T. M. (2005). Effects of connexin-mimetic peptides on gap junction functionality and connexin expression in cultured vascular cells. *Br. J. Pharmacol.* 144, 617–627. doi: 10.1038/sj.bjp.0706102
- Matchkov, V. V., Rahman, A., Bakker, L. M., Griffith, T. M., Nilsson, H., and Aalkjaer, C. (2006). Analysis of effects of connexin-mimetic peptides in rat mesenteric small arteries. *Am. J. Physiol. Heart Circ. Physiol.* 291, H357–H367. doi: 10.1152/ajpheart.00681.2005
- Mathiesen, C., Brazhe, A., Thomsen, K., and Lauritsen, M. (2013). Spontaneous calcium waves in Bergman glia increase with age and hypoxia and may reduce tissue oxygen. *J. Cereb. Blood Flow Metab.* 33, 161–169. doi: 10.1038/jcbfm.2012.175
- Mei, X., Ezan, P., Giaume, C., and Koulakoff, A. (2010). Astroglial connexin immunoreactivity is specifically altered at beta-amyloid plaques in beta-amyloid precursor protein/presenilin1 mice. *Neuroscience* 171, 92–105. doi: 10.1016/j.neuroscience.2010.08.001
- Mlinar, B., and Enyeart, J. J. (1993). Block of current through T-type calcium channels by trivalent metal cations and nickel in neural rat and human cells. *J. Physiol.* 469, 639–652.
- Morita, M., Saruta, C., Kozuka, N., Okubo, Y., Itakura, M., Takahashi, M., et al. (2007). Dual regulation of astrocyte gap junction hemichannels by growth factors and a pro-inflammatory cytokine via the mitogen-activated protein kinase cascade. *Glia* 55, 508–515. doi: 10.1002/glia.20471
- Mulligan, S. J., and MacVicar, B. A. (2004). Calcium transients in astrocyte endfeet cause cerebrovascular constrictions. *Nature* 431, 195–199. doi: 10.1038/nature02827
- Nagy, J. I., Li, W., Hertzberg, E. L., and Marotta, C. A. (1996). Elevated connexin43 immunoreactivity at sites of amyloid plaques in Alzheimer's disease. *Brain Res.* 717, 173–178. doi: 10.1016/0006-8993(95)01526-4
- Nakase, T., and Naus, C. C. (2004). Gap junctions and neurological disorders of the central nervous system. *Biochim. Biophys. Acta* 1662, 149–158. doi: 10.1016/j.bbamem.2004.01.009
- Oh, S., Verselis, V. K., and Bargiello, T. A. (2008). Charges dispersed over the permeation pathway determine the charge selectivity and conductance of a Cx32 chimeric hemichannel. *J. Physiol.* 586, 2445–2461. doi: 10.1113/jphysiol.2008.150805
- Oliet, S. H., and Mothet, J. P. (2006). Molecular determinants of D-serine-mediated gliotransmission: from release to function. *Glia* 54, 726–737. doi: 10.1002/glia.20356
- Olk, S., Turchinovich, A., Grzendowski, M., Stühler, K., Meyer, H. E., Zoidl, G., et al. (2010). Proteomic analysis of astroglial connexin43 silencing uncovers a cytoskeletal platform involved in process formation and migration. *Glia* 58, 494–505. doi: 10.1002/glia.20942
- Olson, J. E. (1999). Osmolyte contents of cultured astrocytes grown in hypoosmotic medium. *Biochim. Biophys. Acta* 1453, 175–179. doi: 10.1016/S0925-4439(98)00090-8
- Orellana, J. A., Díaz, E., Schalper, K. A., Vargas, A. A., Bennett, M. V., and Sáez, J. C. (2011a). Cation permeation through connexin 43 hemichannels is cooperative, competitive and saturable with parameters depending on the permeant species. *Biochem. Biophys. Res. Commun.* 409, 603–609. doi: 10.1016/j.bbrc.2011.05.031
- Orellana, J. A., Froger, N., Ezan, P., Jiang, J. X., Bennett, M. V., Naus, C. C., et al. (2011b). ATP and glutamate released via astroglial connexin 43 hemichannels mediate neuronal death through activation of pannexin 1 hemichannels. *J. Neurochem.* 118, 826–840. doi: 10.1111/j.1471-4159.2011.07210.x
- Orellana, J. A., Shoji, K. F., Abudara, V., Ezan, P., Amigou, E., Sáez, P. J., et al. (2011c). Amyloid beta-induced death in neurons involves glial and neuronal hemichannels. *J. Neurosci.* 31, 4962–4977. doi: 10.1523/JNEUROSCI.6417-10.2011
- Orellana, J. A., Hernández, D. E., Ezan, P., Velarde, V., Bennett, M. V., Giaume, C., et al. (2010). Hypoxia in high glucose followed by reoxygenation in normal glucose reduces the viability of cortical astrocytes through increased permeability of connexin 43 hemichannels. *Glia* 58, 329–343. doi: 10.1002/glia.20926
- Orellana, J. A., Sáez, P. J., Cortes-Campos, C., Elizondo, R. J., Shoji, K. F., Contreras-Duarte, S., et al. (2012a). Glucose increases intracellular free  $\text{Ca}^{2+}$  in tanycytes via ATP released through connexin 43 hemichannels. *Glia* 60, 53–68. doi: 10.1002/glia.21246
- Orellana, J. A., von Bernhardi, R., Giaume, C., and Sáez, J. C. (2012b). Glial hemichannels and their involvement in aging and neurodegenerative diseases. *Rev. Neurosci.* 23, 163–177. doi: 10.1515/revneuro-2011-0065
- Orellana, J. A., Sáez, P. J., Shoji, K. F., Schalper, K. A., Palacios-Prado, N., Velarde, V., et al. (2009). Modulation of brain hemichannels and gap junction channels by pro-inflammatory agents and their possible role in neurodegeneration. *Antioxid. Redox Signal.* 11, 369–399. doi: 10.1089/ars.2008.2130
- Panchin, Y., Kelmanson, I., Matz, M., Lukyanov, K., Usman, N., and Lukyanov, S. (2000). A ubiquitous family of putative gap junction molecules. *Curr. Biol.* 10, R473–R474. doi: 10.1016/S0960-9822(00)00576-5
- Pannasch, U., Vargová, L., Reingruber, J., Ezan, P., Holzman, D., Giaume, C., et al. (2011). Astroglial networks scale synaptic activity and plasticity. *Proc. Natl. Acad. Sci. U.S.A.* 108, 8467–8472. doi: 10.1073/pnas.1016650108
- Paul, D. L., Ebihara, L., Takemoto, L. J., Swenson, K. I., and Goodenough, D. A. (1991). Connexin46, a novel lens gap junction protein, induces voltage-gated currents in nonjunctional plasma membrane of *Xenopus* oocytes. *J. Cell Biol.* 115, 1077–1089. doi: 10.1083/jcb.115.4.1077

- Pellerin, L., and Magistretti, P. J. (2012). Sweet sixteen for ANLS. *J. Cereb. Blood Flow Metab.* 32, 1152–1166. doi: 10.1038/jcbfm.2011.149
- Penuela, S., Gehi, R., and Laird, D. W. (2013). The biochemistry and function of pannexin channels. *Biochim. Biophys. Acta* 1828, 15–22. doi: 10.1016/j.bbamem.2012.01.017
- Perez Velazquez, J. L., Frantseva, M. V., and Naus, C. C. (2003). Gap junctions and neuronal injury: protectants or executioners? *Neuroscientist* 9, 5–9. doi: 10.1177/1073858402239586
- Pfenniger, A., Wohlwend, A., and Kwak, B. R. (2011). Mutations in connexin genes and disease. *Eur. J. Clin. Invest.* 41, 103–116. doi: 10.1111/j.1365-2362.2010.02378.x
- Pimplikar, S. W. (2009). Reassessing the amyloid cascade hypothesis of Alzheimer's disease. *Int. J. Biochem. Cell Biol.* 41, 1261–1268. doi: 10.1016/j.biocel.2008.12.015
- Ponsaerts, R., De Vuyst, E., Retamal, M., D'Hondt, C., Vermeire, D., Wang, N., et al. (2010). Intramolecular loop/tail interactions are essential for connexin 43-hemichannel activity. *FASEB J.* 24, 4378–4395. doi: 10.1096/fj.09-153007
- Prochnow, N., Abdulazim, A., Kurtenbach, S., Wildforster, V., Dvoriantchikova, G., Hanske, J., et al. (2012). Pannexin1 stabilizes synaptic plasticity and is needed for learning. *PLoS ONE* 7:e51767. doi: 10.1371/journal.pone.0051767
- Rackauskas, M., Neverauskas, V., and Skeberdis, V. A. (2010). Diversity and properties of connexin gap junction channels. *Medicina (Kaunas)* 46, 1–12.
- Ramachandran, S., Xie, L. H., John, S. A., Subramaniam, S., and Lal, R. (2007). A novel role for connexin hemichannel in oxidative stress and smoking-induced cell injury. *PLoS ONE* 2:e712. doi: 10.1371/journal.pone.0000712
- Rana, S., and Dringen, R. (2007). Gap junction hemichannel-mediated release of glutathione from cultured rat astrocytes. *Neurosci. Lett.* 415, 45–48. doi: 10.1016/j.neulet.2006.12.043
- Retamal, M. A., Froger, N., Palacios-Prado, N., Ezan, P., Sáez, P. J., Sáez, J. C., et al. (2007a). Cx43 hemichannels and gap junction channels in astrocytes are regulated oppositely by proinflammatory cytokines released from activated microglia. *J. Neurosci.* 27, 13781–13792. doi: 10.1523/JNEUROSCI.2042-07.2007
- Retamal, M. A., Schalper, K. A., Shoji, K. F., Bennett, M. V., and Sáez, J. C. (2007b). Opening of connexin 43 hemichannels is increased by lowering intracellular redox potential. *Proc. Natl. Acad. Sci. U.S.A.* 104, 8322–8327. doi: 10.1073/pnas.0702456104
- Reyes, J. P., Hernandez-Carballo, C. Y., Pérez-Flores, G., Pérez-Cornejo, P., and Arreola, J. (2009). Lack of coupling between membrane stretching and pannexin-1 hemichannels. *Biochem. Biophys. Res. Commun.* 380, 50–53. doi: 10.1016/j.bbrc.2009.01.021
- Rhee, S. K., Bevans, C. G., and Harris, A. L. (1996). Channel-forming activity of immunoaffinity-purified connexin32 in single phospholipid membranes. *Biochemistry* 35, 9212–9223. doi: 10.1021/bi960295m
- Ripps, H., Qian, H., and Zakevicius, J. (2004). Properties of connexin26 hemichannels expressed in *Xenopus* oocytes. *Cell. Mol. Neurobiol.* 24, 647–665. doi: 10.1023/B:CEMN.0000036403.43484.3d
- Riquelme, M. A., Kar, R., Gu, S., and Jiang, J. X. (2013). Antibodies targeting extracellular domain of connexins for studies of hemichannels. *Neuropharmacology*. doi: 10.1016/j.neuropharm.2013.02.021 [Epub ahead of print]
- Rouach, N., Avignone, E., Meme, W., Koulakoff, A., Venance, L., Blomstrand, F., et al. (2002). Gap junctions and connexin expression in the normal and pathological central nervous system. *Biol. Cell* 94, 457–475. doi: 10.1016/S0248-4900(02)00016-3
- Rouach, N., Koulakoff, A., Abudara, V., Willecke, K., and Giaume, C. (2008). Astroglial metabolic networks sustain hippocampal synaptic transmission. *Science* 322, 1551–1555. doi: 10.1126/science.1164022
- Roux, L., Benchenane, K., Rothstein, J. D., Bonvento, G., and Giaume, C. (2011). Plasticity of astroglial networks in olfactory glomeruli. *Proc. Natl. Acad. Sci. U.S.A.* 108, 18442–18446. doi: 10.1073/pnas.1107386108
- Rusakov, D. A., and Fine, A. (2003). Extracellular  $\text{Ca}^{2+}$  depletion contributes to fast activity-dependent modulation of synaptic transmission in the brain. *Neuron* 37, 287–297. doi: 10.1016/S0896-6273(03)00025-4
- Sáez, J. C., Retamal, M. A., Basilio, D., Bukauskas, F. F., and Bennett, M. V. (2005). Connexin-based gap junction hemichannels: gating mechanisms. *Biochim. Biophys. Acta* 1711, 215–224. doi: 10.1016/j.bbamem.2005.01.014
- Sáez, J. C., Schalper, K. A., Retamal, M. A., Orellana, J. A., Shoji, K. F., and Bennett, M. V. (2010). Cell membrane permeabilization via connexin hemichannels in living and dying cells. *Exp. Cell Res.* 316, 2377–2389. doi: 10.1016/j.yexcr.2010.05.026
- Sánchez, H. A., Mese, G., Srinivas, M., White, T. W., and Verselis, V. K. (2010). Differentially altered  $\text{Ca}^{2+}$  regulation and  $\text{Ca}^{2+}$  permeability in Cx26 hemichannels formed by the A40V and G45E mutations that cause keratitis ichthyosis deafness syndrome. *J. Gen. Physiol.* 136, 47–62. doi: 10.1085/jgp.201010433
- Sánchez, H. A., Orellana, J. A., Verselis, V. K., and Sáez, J. C. (2009). Metabolic inhibition increases activity of connexin-32 hemichannels permeable to  $\text{Ca}^{2+}$  in transfected HeLa cells. *Am. J. Physiol. Cell Physiol.* 297, C665–C678. doi: 10.1152/ajpcell.00200.2009
- Sánchez-Alvarez, R., Tabernero, A., and Medina, J. M. (2004). Endothelin-1 stimulates the translocation and upregulation of both glucose transporter and hexokinase in astrocytes: relationship with gap junctional communication. *J. Neurochem.* 89, 703–714. doi: 10.1046/j.1471-4159.2004.02398.x
- Scemes, E. (2008). Modulation of astrocyte P2Y1 receptors by the carboxyl terminal domain of the gap junction protein Cx43. *Glia* 56, 145–153. doi: 10.1002/glia.20598
- Scemes, E. (2012). Nature of plasmalemmal functional “hemichannels.” *Biochim. Biophys. Acta* 1818, 1880–1883. doi: 10.1016/j.bbamem.2011.06.005
- Scemes, E., and Giaume, C. (2006). Astrocyte calcium waves: what they are and what they do. *Glia* 54, 716–725. doi: 10.1002/glia.20374
- Scemes, E., and Spray, D. C. (2012). Extracellular K and astrocyte signaling via connexin and pannexin channels. *Neurochem. Res.* 37, 2310–2316. doi: 10.1007/s11064-012-0759-4
- Scemes, E., Suadicani, S. O., Dahl, G., and Spray, D. C. (2007). Connexin and pannexin mediated cell-cell communication. *Neuron Glia Biol.* 3, 199–208. doi: 10.1017/S1740925X08000069
- Schalper, K. A., Orellana, J. A., Berthoud, V. M., and Sáez, J. C. (2009). Dysfunctions of the diffusional membrane pathways mediated by hemichannels in inherited and acquired human diseases. *Curr. Vasc. Pharmacol.* 7, 486–505. doi: 10.2174/157016109789043937
- Schalper, K. A., Palacios-Prado, N., Orellana, J. A., and Sáez, J. C. (2008a). Currently used methods for identification and characterization of hemichannels. *Cell* Commun. Adhes. 15, 207–218. doi: 10.1080/15419060802014198
- Schalper, K. A., Palacios-Prado, N., Retamal, M. A., Shoji, K. F., Martínez, A. D., and Sáez, J. C. (2008b). Connexin hemichannel composition determines the FGF-1-induced membrane permeability and free  $[\text{Ca}^{2+}]_i$  responses. *Mol. Biol. Cell* 19, 3501–3513. doi: 10.1091/mbc.E07-12-1240
- Schalper, K. A., Sanchez, H. A., Lee, S. C., Altenberg, G. A., Nathanson, M. H., and Sáez, J. C. (2010). Connexin 43 hemichannels mediate the  $\text{Ca}^{2+}$  influx induced by extracellular alkalinization. *Am. J. Physiol. Cell Physiol.* 299, C1504–C1515. doi: 10.1152/ajpcell.00015.2010
- Schnell, L., Fearn, S., Klassen, H., Schwab, M. E., and Perry, V. H. (1999). Acute inflammatory responses to mechanical lesions in the CNS: differences between brain and spinal cord. *Eur. J. Neurosci.* 11, 3648–3658. doi: 10.1046/j.1460-9568.1999.00792.x
- Seki, A., Duffy, H. S., Coombs, W., Spray, D. C., Taffet, S. M., and Delmar, M. (2004). Modifications in the biophysical properties of connexin43 channels by a peptide of the cytoplasmic loop region. *Circ. Res.* 95, e22–e28. doi: 10.1161/01.RES.0000140737.62245.c5
- Sieber, A. P., Ma, Z., Grevet, J. D., Demuro, A., Parker, I., and Foskett, J. K. (2013). Structural and functional similarities of calcium homeostasis modulator 1 (CALHM1) ion channel with connexins, pannexins, and innexins. *J. Biol. Chem.* 288, 6140–6153. doi: 10.1074/jbc.M112.409789
- Silverman, W. R., de Rivero Vaccari, J. P., Locovei, S., Qiu, F., Carlsson, S. K., Scemes, E., et al. (2009). The pannexin 1 channel activates the inflammasome in neurons and astrocytes. *J. Biol. Chem.* 284, 18143–18151. doi: 10.1074/jbc.M109.004804
- Simard, M., Arcuino, G., Takano, T., Liu, Q. S., and Nedergaard, M. (2003). Signaling at the gliovascular interface. *J. Neurosci.* 23, 9254–9262.
- Sofroniew, M. V., and Vinters, H. V. (2010). Astrocytes: biology and pathology. *Acta Neuropathol.* 119, 7–35. doi: 10.1007/s00401-009-0619-8
- Söhl, G., Maxeiner, S., and Willecke, K. (2005). Expression and functions of neuronal gap junctions. *Nat. Rev. Neurosci.* 6, 191–200. doi: 10.1038/nrn1627
- Sohl, G., and Willecke, K. (2004). Gap junctions and the connexin protein family. *Cardiovasc. Res.* 62, 228–232. doi: 10.1016/j.cardiores.2003.11.013

- Somjen, G. G. (2002). Ion regulation in the brain: implications for pathophysiology. *Neuroscientist* 8, 254–267. doi: 10.1177/107385402008003011
- Song, E. K., Rah, S. Y., Lee, Y. R., Yoo, C. H., Kim, Y. R., Yeom, J. H., et al. (2011). Connexin-43 hemichannels mediate cyclic ADP-ribose generation and its  $\text{Ca}^{2+}$ -mobilizing activity by NAD $^+$ /cyclic ADP-ribose transport. *J. Biol. Chem.* 286, 44480–44490. doi: 10.1074/jbc.M111.307645
- Stehberg, J., Moraga-Amaro, R., Salazar, C., Becerra, A., Echeverría, C., Orelana, J. A., et al. (2012). Release of gliotransmitters through astroglial connexin 43 hemichannels is necessary for fear memory consolidation in the basolateral amygdala. *FASEB J.* 26, 3649–3657. doi: 10.1096/fj.11-198416
- Stout, C. E., Costantini, J. L., Naus, C. C., and Charles, A. C. (2002). Intercellular calcium signaling in astrocytes via ATP release through connexin hemichannels. *J. Biol. Chem.* 277, 10482–10488. doi: 10.1074/jbc.M109902200
- Suadicani, S. O., Brosnan, C. F., and Scemes, E. (2006). P2X7 receptors mediate ATP release and amplification of astrocytic intercellular  $\text{Ca}^{2+}$  signaling. *J. Neurosci.* 26, 1378–1385. doi: 10.1523/JNEUROSCI.3902-05.2006
- Suadicani, S. O., Flores, C. E., Urban-Maldonado, M., Beelitz, M., and Scemes, E. (2004). Gap junction channels coordinate the propagation of intercellular  $\text{Ca}^{2+}$  signals generated by P2Y receptor activation. *Glia* 48, 217–229. doi: 10.1002/glia.20071
- Suadicani, S. O., Iglesias, R., Wang, J., Dahl, G., Spray, D. C., and Scemes, E. (2012). ATP signaling is deficient in cultured Pannexin1-null mouse astrocytes. *Glia* 60, 1106–1116. doi: 10.1002/glia.22338
- Swayne, L. A., Sorbara, C. D., and Bennett, S. A. (2010). Pannexin 2 is expressed by postnatal hippocampal neural progenitors and modulates neuronal commitment. *J. Biol. Chem.* 285, 24977–24986. doi: 10.1074/jbc.M110.130054
- Tabernero, A., Giaume, C., and Medina, J. M. (1996). Endothelin-1 regulates glucose utilization in cultured astrocytes by controlling intercellular communication through gap junctions. *Glia* 16, 187–195. doi: 10.1002/(SICI)1098-1136(199603)16:3
- Tabernero, A., Medina, J. M., and Giaume, C. (2006). Glucose metabolism and proliferation in glia: role of astrocytic gap junctions. *J. Neurochem.* 99, 1049–1061. doi: 10.1111/j.1471-4159.2006.04088.x
- Takeuchi, H., Jin, S., Wang, J., Zhang, G., Kawanokuchi, J., Kuno, R., et al. (2006). Tumor necrosis factor-alpha induces neurotoxicity via glutamate release from hemichannels of activated microglia in an autocrine manner. *J. Biol. Chem.* 281, 21362–21368. doi: 10.1074/jbc.M600504200
- Taruno, A., Vingtdeux, V., Ohmoto, M., Ma, Z., Dvoryanchikov, G., Li, A., et al. (2013). CALHM1 ion channel mediates purinergic neurotransmission of sweet, bitter and umami tastes. *Nature* 495, 223–226. doi: 10.1038/nature11906
- Theis, M., Söhl, G., Eiberger, J., and Willecke, K. (2005). Emerging complexities in identity and function of glial connexins. *Trends Neurosci.* 28, 188–195. doi: 10.1016/j.tins.2005.02.006
- Thompson, R. J., and Macvicar, B. A. (2008). Connexin and pannexin hemichannels of neurons and astrocytes. *Channels (Austin)* 2, 81–86. doi: 10.4161/chan.2.2.6003
- Torres, A., Wang, F., Xu, Q., Fujita, T., Dobrowski, R., Willecke, K., et al. (2012). Extracellular  $\text{Ca}^{2+}$  acts as a mediator of communication from neurons to glia. *Sci. Signal.* 5, ra8. doi: 10.1126/scisignal.2002160
- Valiunas, V. (2002). Biophysical properties of connexin-45 gap junction hemichannels studied in vertebrate cells. *J. Gen. Physiol.* 119, 147–164. doi: 10.1085/jgp.119.2.147
- Valiunas, V., and Weingart, R. (2000). Electrical properties of gap junction hemichannels identified in transfected HeLa cells. *Pflügers Arch.* 440, 366–379. doi: 10.1007/s004240000294
- Vanden Abeele, F., Bidaux, G., Gordienko, D., Beck, B., Panchin, Y. V., Baranova, A. V., et al. (2006). Functional implications of calcium permeability of the channel formed by pannexin 1. *J. Cell Biol.* 174, 535–546. doi: 10.1083/jcb.200601115
- Venance, L., Piomelli, D., Glowinski, J., and Giaume, C. (1995). Inhibition by anandamide of gap junctions and intercellular calcium signalling in striatal astrocytes. *Nature* 376, 590–594. doi: 10.1038/376590a0
- Vinken, M., Decrock, E., Leybaert, L., Bultynck, G., Himpens, B., Vanhaecke, T., et al. (2012). Non-channel functions of connexins in cell growth and cell death. *Biochim. Biophys. Acta* 1818, 2002–2008. doi: 10.1016/j.bbamem.2011.06.011
- Vogt, A., Hormuzdi, S. G., and Monyer, H. (2005). Pannexin1 and Pannexin2 expression in the developing and mature rat brain. *Brain Res.* Mol. Brain Res. 141, 113–120. doi: 10.1016/j.molbrainres.2005.08.002
- Wang, J., Ma, M., Locovei, S., Keane, R. W., and Dahl, G. (2007). Modulation of membrane channel currents by gap junction protein mimetic peptides: size matters. *Am. J. Physiol. Cell Physiol.* 293, C1112–C1119. doi: 10.1152/ajpcell.00097.2007
- Wang, N., De Bock, M., Antoons, G., Gadicherla, A. K., Bol, M., Decrock, E., et al. (2012). Connexin mimetic peptides inhibit Cx43 hemichannel opening triggered by voltage and intracellular  $\text{Ca}^{2+}$  elevation. *Basic Res. Cardiol.* 107, 304. doi: 10.1007/s00395-012-0304-2
- Wang, N., De Vuyst, E., Ponsaerts, R., Boengler, K., Palacios-Prado, N., Wauman, J., et al. (2013). Selective inhibition of Cx43 hemichannels by Gap19 and its impact on myocardial ischemia/reperfusion injury. *Basic Res. Cardiol.* 108, 309. doi: 10.1007/s00395-012-0309-x
- Warner, A., Clements, D. K., Parikh, S., Evans, W. H., and DeHaan, R. L. (1995). Specific motifs in the external loops of connexin proteins can determine gap junction formation between chick heart myocytes. *J. Physiol.* 488 (Pt 3), 721–728.
- Wasseff, S. K., and Scherer, S. S. (2011). Cx32 and Cx47 mediate oligodendrocyte:astrocyte and oligodendrocyte:oligodendrocyte gap junction coupling. *Neurobiol. Dis.* 42, 506–513. doi: 10.1016/j.nbd.2011.03.003
- Wiencken-Barger, A. E., Djukic, B., Casper, K. B., and McCarthy, K. D. (2007). A role for Connexin43 during neurodevelopment. *Glia* 55, 675–686. doi: 10.1002/glia.20484
- Willecke, K., Eiberger, J., Degen, J., Eckardt, D., Romualdi, A., Guldenagel, M., et al. (2002). Structural and functional diversity of connexin genes in the mouse and human genome. *Biol. Chem.* 383, 725–737. doi: 10.1515/BC.2002.076
- Xiong, J., Burkovetskaya, M., Karpuk, N., and Kielian, T. (2012). IL-1RI (interleukin-1 receptor type I) signalling is essential for host defence and hemichannel activity during acute central nervous system bacterial infection. *ASN Neuro* 4, pii: e00085. doi: 10.1042/AN20120008
- Xu, H. L., and Pelligrino, D. A. (2007). ATP release and hydrolysis contribute to rat pial arteriolar dilatation elicited by neuronal activation. *Exp. Physiol.* 92, 647–651. doi: 10.1113/expphysiol.2006.036863
- Yamamoto, T., Ochalski, A., Hertzberg, E. L., and Nagy, J. I. (1990). On the organization of astrocytic gap junctions in rat brain as suggested by LM and EM immunohistochemistry of connexin43 expression. *J. Comp. Neurol.* 302, 853–883. doi: 10.1002/cne.903020414
- Ye, Z. C., Wyeth, M. S., Baltan-Tekkok, S., and Ransom, B. R. (2003). Functional hemichannels in astrocytes: a novel mechanism of glutamate release. *J. Neurosci.* 23, 3588–3596.
- Yu, J., Bippes, C. A., Hand, G. M., Muller, D. J., and Sosinsky, G. E. (2007). Aminosulfonate modulated pH-induced conformational changes in connexin26 hemichannels. *J. Biol. Chem.* 282, 8895–8904. doi: 10.1074/jbc.M609317200
- Zappala, A., Li Volti, G., Serapide, M. F., Pellitteri, R., Falchi, M., et al. (2007). Expression of pannexin2 protein in healthy and ischemized brain of adult rats. *Neuroscience* 148, 653–667. doi: 10.1016/j.neuroscience.2007.06.028
- Zhan, H., Moore, C. S., Chen, B., Zhou, X., Ma, X. M., Ijichi, K., et al. (2012). Stomatin inhibits pannexin-1-mediated whole-cell currents by interacting with its carboxyl terminal. *PLoS ONE* 7:e39489. doi: 10.1371/journal.pone.0039489
- Zorec, R., Araque, A., Carmignoto, G., Haydon, P. G., Verkhratsky, A., and Parpura, V. (2012). Astroglial excitability and gliotransmission: an appraisal of  $\text{Ca}^{2+}$  as a signalling route. *ASN Neuro* 4, pii: e00080. doi: 10.1042/AN20110061

**Conflict of Interest Statement:** The authors declare that the research was conducted in the absence of any commercial or financial relationships that could be construed as a potential conflict of interest.

**Received:** 23 April 2013; **paper pending published:** 21 May 2013; **accepted:** 21 June 2013; **published online:** 17 July 2013. **Citation:** Giaume, C., Leybaert, L., Naus, CC and Sáez JC (2013) Connexin and pannexin hemichannels in brain glial cells: properties, pharmacology, and roles. *Front. Pharmacol.* 4:88. doi: 10.3389/fphar.2013.00088

This article was submitted to Frontiers in Pharmacology of Ion Channels and Channelopathies, a specialty of Frontiers in Pharmacology.

Copyright © 2013 Giaume, Leybaert, Naus and Sáez. This is an open-access article distributed under the terms of the Creative Commons Attribution License, which permits use, distribution and reproduction in other forums, provided the original authors and source are credited and subject to any copyright notices concerning any third-party graphics etc.



# A comparative antibody analysis of Pannexin1 expression in four rat brain regions reveals varying subcellular localizations

**Angela C. Cone<sup>1</sup>, Cinzia Ambrosi<sup>1</sup>, Eliana Scemes<sup>2</sup>, Maryann E. Martone<sup>1,3</sup> and Gina E. Sosinsky<sup>1,3\*</sup>**

<sup>1</sup> National Center for Microscopy and Imaging Research, Center for Research in Biological Systems, University of California, San Diego, La Jolla, CA, USA

<sup>2</sup> Dominick P Purpura Department of Neuroscience, Albert Einstein College of Medicine, Pelham Parkway Albert Einstein College of Medicine, Bronx, NY, USA

<sup>3</sup> Department of Neurosciences, University of California, San Diego, La Jolla, CA, USA

**Edited by:**

Aida Salameh, Heart Centre  
University of Leipzig, Germany

**Reviewed by:**

Brant Isakson, University of Virginia,  
USA

Katja Blanke, Heart Center Leipzig,  
Germany

Christian Naus, University of British  
Columbia, Canada

**\*Correspondence:**

Gina E. Sosinsky, National Center for  
Microscopy and Imaging Research,  
University of California, San Diego,  
School of Medicine, BSB 1070, 9500  
Gilman Drive, MC 0608, La Jolla, CA  
92093-0608, USA.

e-mail: gsosinsky@ucsd.edu

Pannexin1 (Panx1) channels release cytosolic ATP in response to signaling pathways. Panx1 is highly expressed in the central nervous system. We used four antibodies with different Panx1 anti-peptide epitopes to analyze four regions of rat brain. These antibodies labeled the same bands in Western blots and had highly similar patterns of immunofluorescence in tissue culture cells expressing Panx1, but Western blots of brain lysates from Panx1 knockout and control mice showed different banding patterns. Localizations of Panx1 in brain slices were generated using automated wide field mosaic confocal microscopy for imaging large regions of interest while retaining maximum resolution for examining cell populations and compartments. We compared Panx1 expression over the cerebellum, hippocampus with adjacent cortex, thalamus, and olfactory bulb. While Panx1 localizes to the same neuronal cell types, subcellular localizations differ. Two antibodies with epitopes against the intracellular loop and one against the carboxy terminus preferentially labeled cell bodies, while an antibody raised against an N-terminal peptide highlighted neuronal processes more than cell bodies. These labeling patterns may be a reflection of different cellular and subcellular localizations of full-length and/or modified Panx1 channels where each antibody is highlighting unique or differentially accessible Panx1 populations. However, we cannot rule out that one or more of these antibodies have specificity issues. All data associated with experiments from these four antibodies are presented in a manner that allows them to be compared and our claims thoroughly evaluated, rather than eliminating results that were questionable. Each antibody is given a unique identifier through the NIF Antibody Registry that can be used to track usage of individual antibodies across papers and all image and metadata are made available in the public repository, the Cell Centered Database, for on-line viewing, and download.

**Keywords:** purinergic receptors, pannexin channels, ATP signaling, large field mosaic fluorescent imaging, paracrine signaling, connexin, knockout mouse

## INTRODUCTION

One mechanism of paracrine cell–cell communication occurs by ATP release and signal transduction through purinergic receptors (Burnstock, 2011). In the nervous system, ATP signaling stimulates neurotransmission, neuromodulation, and secretion as well as playing a role in cell proliferation, differentiation, and inflammation (Fields and Stevens, 2000). Membrane bound purinergic receptors are found on the plasma membrane of neurons and non-neuronal cells such as astrocytes and microglia (Fields and Stevens, 2000). Several studies have shown an association of the purinergic receptors with pannexin1 (Panx1), a connexin-like protein, which when stimulated acts as an ATP release channel (Locovei et al., 2006b; Nishida et al., 2008; Silverman et al., 2009; Kim and Kang, 2011; Poornima et al., 2011; Vessey et al., 2011).

**Abbreviations:** CNS, central nervous system; Panx1, pannexin1.

*In situ* hybridization imaging demonstrated high expression levels of Panx1 mRNA in the central nervous system (Ray et al., 2005; Vogt et al., 2005).

Panx1 has been proposed to fulfill a function in adaptive/inflammation responses following specific stimuli (Sosinsky et al., 2011). Panx1 channels have been shown to release ATP during gustatory channel response in taste bud cells (Romanov et al., 2007), the activation of the immune response in macrophages (Pelegrin and Surprenant, 2006), T lymphocytes (Schenk et al., 2008), and neurons (Silverman et al., 2009), pressure overload-induced fibrosis in the heart (Nishida et al., 2008) and NMDA receptor epileptiform electrical activity in the hippocampus (Thompson et al., 2008). This signaling pathway involves an “ATP-induced ATP release” mechanism whereby ATP stimulation of ionotropic P2X or metabotropic P2Y receptors signals intracellular components that favor opening of Panx1 channels (pannexons). ATP is then released from cells. Higher concentration

of extracellular ATP released from the cell then acts to close the open pannexon in a negative feed-back loop (Qiu and Dahl, 2009). Linked to paracrine (calcium) wave signaling, this “ATP-induced ATP release” allows for a small, localized number of cells to be stimulated and respond to stresses such as metabolic inhibition, mechanical stress and invading pathogens (Dubyak, 2009). Panx1 is part of the cryopyrin and neuronal inflammasome (Kanneganti et al., 2007; Silverman et al., 2009). The inflammasome is responsible for activation of inflammatory processes and induces pyroptosis, a process of programmed cell death distinct from apoptosis. In particular, Panx1 has been found to co-immunoprecipitate with components of the neuronal inflammasome suggesting that the central nervous system (CNS) inflammasome is pre-formed (Silverman et al., 2009). A recent study showed that Panx1 channels in the hippocampus contributed to seizures by releasing ATP when induced by kainic acid and that deletion of Panx1 or the Panx1 channel blocker reduced the amount of ATP that is released and improves the behavioral manifestation of seizures (Santiago et al., 2011).

Immunolabeling studies have shown that Panx1 is widely expressed in cells throughout the body such as CNS neurons, lens epithelial cells, retinal sensory cells, astrocytes, erythrocytes, cardiac myocytes, and macrophages (Dvoriantchikova et al., 2006a; Dvoriantchikova et al., 2006b; Locovei et al., 2006a; Zappala et al., 2006; Zoidl et al., 2007; Karpuk et al., 2011; Kienitz et al., 2011). However, its cellular and subcellular protein distributions in brain regions have not been thoroughly characterized across wide expanses of this complex organ and there have been some conflicting results among different antibodies (Ray et al., 2006; Zappala et al., 2006; Zoidl et al., 2007). In this study, we apply wide field mosaic imaging to examine Panx1 expression in the rat brain across four distinct regions that include cerebellum, hippocampus, and cortex, olfactory bulb, and thalamus while still retaining high spatial resolution. We compared the labeling patterns of four different Panx1 antibodies in rat brain tissue in addition to model cell culture systems using Western blot analysis, and immunocytochemistry. Three of these antibodies are polyclonal antibodies (one raised in rabbit and two in chicken) while the fourth is a mouse monoclonal antibody. Two of these antibodies, one from Diatheva and the other developed and validated in Gerhard Dahl's laboratory, have been used in several publications (described in more detail in the Results section) while two were developed and validated by our laboratory. The three polyclonal antibodies show fairly similar neuronal labeling patterns across the four brain regions while the Mo503 monoclonal antibody also labeled the same neurons, but with different subcellular localizations. The four antibodies recognize four different epitopes across the protein (**Figure 1**). In tissue culture cells, we found that both the immunofluorescence and Western blot labeling were highly similar, however there are significant differences in Western blots of tissue among these antibodies.

Because Western blots are frequently treated as “gold standard” controls, especially when used in combination with KO mouse models, there is the widely held opinion that Western blot bands ultimately determine specificity. A recent publication exemplifies this debate by showing that (1) numerous antibodies pass all tests of specificity except the final test in KO mouse tissue,

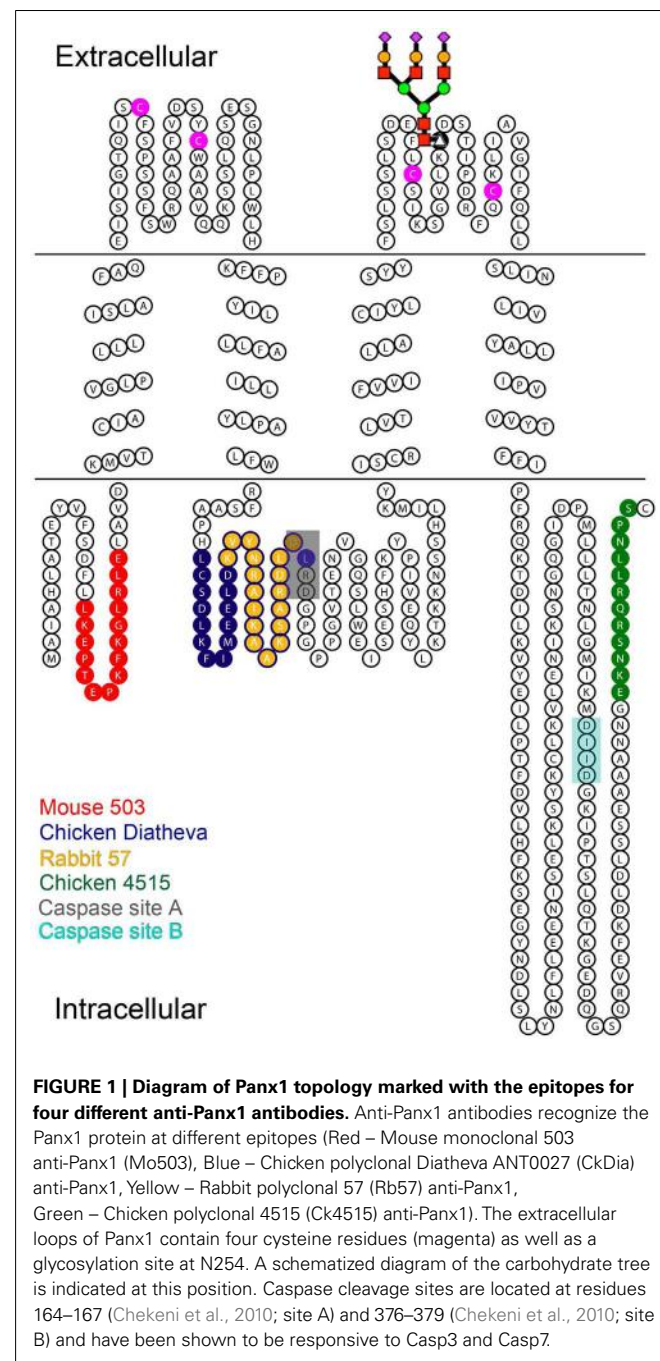


**FIGURE 1 | Diagram of Panx1 topology marked with the epitopes for four different anti-Panx1 antibodies.** Anti-Panx1 antibodies recognize the Panx1 protein at different epitopes (Red – Mouse monoclonal 503 anti-Panx1 (Mo503), Blue – Chicken polyclonal Diatheva ANT0027 (CkDia) anti-Panx1, Yellow – Rabbit polyclonal 57 (Rb57) anti-Panx1, Green – Chicken polyclonal 4515 (Ck4515) anti-Panx1). The extracellular loops of Panx1 contain four cysteine residues (magenta) as well as a glycosylation site at N254. A schematized diagram of the carbohydrate tree is indicated at this position. Caspase cleavage sites are located at residues 164–167 (Chekeni et al., 2010; site A) and 376–379 (Chekeni et al., 2010; site B) and have been shown to be responsive to Casp3 and Casp7.

(2) some antibodies pass all tests of specificity by Western blot, but not when using brain tissue, and (3) numerous antibodies pass all rigorous tests of specificity by Western blot, but fail when used for immunohistochemistry (Herkenham et al., 2011), causing the authors to re-assess the results in previous publications that used those antibodies. In the case of pannexins, immunolabeling results have been unclear and controversial. For example, in the study of Panx1 knockout mice by Bargiolas et al. (2011) where *in situ* hybridization images of Panx1 KO brain tissue were devoid of staining for Panx1 transcripts, the authors state that only one antibody (Penuela et al., 2007) out of six tested showed

specificity for Panx1 in Western blot of their knockout animals. The Diatheva and Dahl antibodies were two of the five the authors claim to be non-specific. It has always been the case that specificity of antibodies, particularly when used on intact tissues, is hard if not impossible to prove. By these criteria, the results obtained in Western blots in the present study should cause us to discard our findings. However, it should be pointed out that the extra bands we see on Westerns of tissue lysates may represent cellular constituents present at the more complex tissue level that are unfolded on SDS gels. These unfolded proteins may expose amino acid sequences similar to the epitopes used to generate antibodies that are not accessible in intact tissue with folded proteins and not present in simpler cultured cells. This may be especially true since most antibodies these days are generated by short peptides and not folded proteins. We previously showed that connexin antibodies generated against the same C-terminal peptide are highly conformation dependent (Sosinsky et al., 2007).

Here, we advocate for a more balanced approach where we compare all data (Western blots and images from several antibodies) to each other to look for conserved and variable features. We believe that consistency among imaging and cell culture controls with recombinant proteins are also important for antibody validation. Tests of these antibodies on tissue lysates from two different Panx1 KO mice demonstrate that they recognize Panx1 bands, however additional bands are labeled in the KO for some of the antibodies and these vary between KO animals. Thus, it is still unclear whether differences seen between the four antibodies are due to different epitopes being recognized, non-specificity, or the presence of some residual Panx1 protein in KO tissues. Nevertheless, scientific papers continue to be published with these antibodies and/or these KO mouse models, so we discuss strategies for publishing this kind of data by recommending several standards.

## MATERIALS AND METHODS

### ANTIBODY INFORMATION

For immunofluorescence experiments, we used either goat anti-Myc (Abcam, Catalog# ab19234, Cambridge, MA, USA) or mouse anti-Myc (Abcam, Catalog# ab32, Cambridge, MA, USA) for co-labeling with either mouse monoclonal anti-Panx1 or rabbit polyclonal anti-Panx1 antibodies, respectively. Both antibodies were used at a 1:250 dilution. GFAP, an astrocytic marker, was labeled using a Guinea pig anti-GFAP (Advanced ImmunoChemical Inc., Long Beach, CA, USA) at a 1:800 dilution.

The four Panx1 antibodies used in this study were (1) a commercial chicken anti-Panx1 (Diatheva ANT0027, denoted as *CkDia*, Diatheva, Fano, Italy; NIF antibody registry number: AB\_10013320), (2) chicken anti-Panx1 (obtained from Gerhard Dahl, University of Miami and denoted as *Ck4515*; NIF antibody registry number: AB\_10013321), (3) rabbit anti-Panx1 (denoted as *Rb57*; NIF antibody registry number: AB\_10013322), and (4) mouse anti-Panx1 (denoted as *Mo503*; NIF antibody registry number: AB\_10013323). All antibodies were affinity purified using standard procedures.

- (1) *CkDia*: chicken polyclonal antibody *CkDia* generated against a peptide containing amino acids corresponding to 135–165 of

the cytoplasmic loop of the mouse Pannexin1. This antibody was previously characterized in mouse brain by Zappala et al. (2006).

- (2) *Ck4515*: chicken polyclonal anti-human Panx1 antibody (#4515, a gift from Dr. Gerhard Dahl at the University of Miami Medical School) raised against a peptide containing the most C-terminal amino acid residues (EKNSRQRLLNPS) in the human Panx1 sequence (Locovei et al., 2006a) and shows cross-reactivity between rat, mouse, and human Panx1 (Boassa et al., 2007).
- (3) *Rb57*: rabbit polyclonal antibody *Rb57* generated for our laboratory by Abgent, Inc. (San Diego, CA, USA) against a peptide containing amino acids 148–164 (KVYNRAIKAKSARDLD) of the first intracellular loop. This sequence is invariant among mouse, rat, and human sequences.
- (4) *Mo503*: monoclonal antibody *Mo503* generated by Abgent, Inc. (San Diego, CA, USA) for our laboratory against a peptide containing amino acids 17–31 (LKEPTEPKFKGLRLE) of the N-terminus of Panx1 and denoted as *Mo503*. This sequence is invariant among mouse, rat, and human sequences.

The characterization of the Laird laboratory antibody, denoted *RbCT-395*, is described in Penuela et al. (2007). Its epitope is at residues 395–409 (QRVEFKDLDLSSEAA) of mouse Panx1 and is just upstream of the end of the C-terminus.

### CELL CULTURE AND IMMUNOCYTOCHEMISTRY

HeLa cells (ATCC Catalog #CCL-2, Manassas, VA, USA) were cultured in Cellgro DMEM (Mediatech, Inc., Manassas, VA, USA) medium supplemented with 10% FBS in a 37°C incubator with 10% CO<sub>2</sub>. Transient transfections were carried out using 2 mL of Lipofectamine reagent (Invitrogen, Carlsbad, CA, USA) and 0.5 mg of DNA encoding Panx1-myc fusion protein in a pRK5 plasmid (Bruzzone et al., 2003). This transfection mixture was added into each cell culture well containing 2 mL of medium and allowed to incubate with cells for 2–4 h. The transfection medium was removed and replaced with regular growth medium. Transfected cells were allowed to continue growing for 24–48 h after transfection then fixed and prepared for fluorescent imaging. Coverslips with transfected HeLa cells were fixed in 4% paraformaldehyde for 20 min at room temperature (*CkDia* and *Ck4515*) or fixed with ice cold 100% methanol for 10 min then rinsed into PBS to rehydrate (*Rb57* and *Mo503*). The different fixation methods were used because while the *CkDia*, *Ck4515*, and *Mo503* nicely label Panx1 in tissue culture cells and brain tissue using 2–4% paraformaldehyde, in these dual labeling experiments, the goat anti-Myc antibodies gave significant background with paraformaldehyde fixation. For these experiments, anti-Panx1 antibodies were used at 1:250 dilutions with an overnight incubation at 4°C, and all secondary antibodies were used at 1:100 for 1–2 h at room temperature. The cells were briefly permeabilized with 0.1% Triton X100, then blocked with 1% BSA, 3% normal donkey serum, 50 mM glycine, and cold water fish gelatin in PBS. A summary of conditions for each of these antibodies is shown in **Table 1**. For fluorescence visualization, FITC and Cy5 conjugated donkey secondary antibodies were used (Jackson ImmunoResearch Laboratories, Inc.,

**Table 1 | Summary of labeling information for the four Panx1 antibodies used in this analysis.**

Panx1 antibody	Source	Catalog #	Antibody ID#	Cell fixation	Tissue fixation	Antigen retrieval
CkDia	Diatheva	ANT0027	AB_10013320	2% PFA or MeOH	4% PFA	No
Ck4515	Laboratory of G. Dahl		AB_10013321	2% PFA or MeOH	4% PFA	No
Rb57	This lab		AB_10013322	MeOH	4% PFA	Yes
Mo503	This lab		AB_10013323	2% PFA or MeOH	4% PFA	No

Various conditions were utilized to achieve performance with each antibody in the applications presented in this body of work. PFA, paraformaldehyde; MeOH, cold methanol. Use this table to quickly reference these differences in specimen preparation with the unique NIF antibody ID (Neuroscience Information Framework Antibody Identifier [http://antibodyregistry.org/antibody17/antibodyform.html?gui\\_type=advanced](http://antibodyregistry.org/antibody17/antibodyform.html?gui_type=advanced)).

West Grove, PA, USA). Confocal images stacks were obtained using an Olympus Fluoview 1000 microscope (Olympus USA, PA, USA).

#### PREPARATION OF RAT BRAIN TISSUE AND IMMUNOHISTOCHEMISTRY

All experiments involving vertebrate animals conform to the National Institutes of Health *Guide for the Care and Use of Laboratory Animals* and were approved by the Institutional Animal Care and Use Committee of the University of California San Diego. The animal welfare assurance number is A3033-01. Rats were fully anesthetized and Ringer's solution containing xylocaine and heparin was perfused transcardially for 3 min followed by 4% paraformaldehyde for 10 min. Here, we show images obtained from an 8-week-old female Sprague-Dawley, however, mosaic images from other rat brains we examined had the same Panx1 patterns. The brain was removed and post-fixed in 4% paraformaldehyde overnight at 4°C. Sagittal sections were cut on a Leica vibratome at a thickness of 75 microns and stored at -20°C in cryoprotectant solution (30% glycerol, 30% ethylene glycol in PBS) until processed.

Before immunolabeling, each sagittal section was severed into the four regions to be imaged (cerebellum, thalamus, olfactory bulb, and hippocampus) to facilitate optimal flatness when mounting on slides for subsequent wide scale imaging. Tissue sections to be labeled with the Rb57 anti-Panx1 antibody underwent antigen retrieval using heat and 10 mM citric acid pH 6.5 for 10 min (100°C water bath in microwave oven; von Wasielewski et al., 1994). Free-floating tissue sections were blocked with 3% normal donkey serum, 1% bovine serum albumin, 1% cold water fish gelatin, 0.1% Triton X100, and 50 mM glycine in PBS for 1 h at room temperature. Guinea pig anti-GFAP and anti-Panx1 primary antibodies were applied overnight at 4°C. FITC and Cy5 or FITC and Rhodamine RedX conjugated donkey secondary antibodies (Jackson ImmunoResearch Laboratories, Inc., West Grove, PA, USA) were applied for 2.5 h at room temperature. The Mo503 primary antibody was detected using a Rhodamine RedX conjugated donkey anti-mouse secondary antibody having minimal cross-reaction to rat in order to avoid detection of endogenous rat immunoglobulin in the tissue (Jackson ImmunoResearch Laboratories, Inc., Catalog# 715-295-151). The immunolabeled tissue samples were incubated with 0.5 μM DAPI nuclear stain (Invitrogen, Carlsbad, CA, USA) for 20 min at room temperature and carefully mounted as flat as possible using gelvatol as the mounting medium.

#### WESTERN BLOTS

Lysates were prepared from MDCK cells stably over-expressing Panx1 in addition to endogenous Panx1 as previously described (Boassa et al., 2007; Ambrosi et al., 2010). Normal rodent brain lysates were obtained from G-Biosciences (Maryland Heights, MO; GenLysate Protein lysates of normal rat brain NLR-02, and normal mouse brain NLM-02). Normal rodent brain lysates were also obtained from Enzo Life Sciences, Inc. (Farmingdale, NY, USA). These included mouse brain lysates, Immunoblotting Standard SW-104, and rat brain lysates, Immunoblotting Standard SW-103. Proteins in the lysates were separated by SDS-PAGE on a 4–20% pre-cast gel (Invitrogen, Carlsbad, CA, USA). Proteins were transferred to PVDF membrane (Millipore, Billerica, MA, USA), using NuPAGE transfer buffer (Invitrogen). Bands on Western blots were identified using the four anti-Panx1 antibodies with HRP-conjugated secondary antibodies (Calbiochem); the chemiluminescence reaction was visualized using SuperSignal West Pico ECL (Thermo Scientific, Waltham, MA, USA) and Kodak Gel Logic 2200 gel visualizer (Carestream Health, Inc., Rochester, NY, USA) or X-ray film. The Mo503 and Rb57 antibodies were used at a 1:5000 dilution in blocking solution (1X PBS-T with 5% milk). The Ck4515 and CkDia antibodies were diluted 1:2000 in a blocking solution made with 2% milk and 0.5 M NaCl in 1X PBS-T. This stringent condition significantly reduced the background of these two antibodies.

Lysates from matched Panx1 wild type and KO tissues were generated from animals from Genentech (Qu et al., 2011) and KOMP (Qiu et al., 2011; Santiago et al., 2011). Methods for the preparation of tissues lysates and Western blots for the KOMP KO are described in (Santiago et al., 2011). General methods for preparation of tissue lysates from the Genentech animals were prepared using methods as described in Penuela et al. (2007).

#### WIDE SCALE FLUORESCENT IMAGING

Overlapping 3D image stacks were acquired with an Olympus Fluoview 1000 laser scanning confocal microscope equipped with a 40×, NA 1.3, oil-immersion objective lens, and a special *x*, *y*, *z* montaging stage. A multi-area time-lapse was performed using the Olympus ASW1.7 software to define the boundaries of the tissue area for the acquisition volume. The individual tiles of the montage were acquired as *z* stacks of 4–6 sections (~0.5–0.7 mm/section) using sequential line scanning and then a maximum intensity projection of each stack is computed to make the individual tiles. The tiles were stitched together post-data acquisition using National

Center for Microscopy and Imaging Research (NCMIR) developed ImageJ plugins to project, flat field, normalize, align, and combine into a mosaic (Chow et al., 2006; Kenyon et al., 2010). Software is available for download<sup>1</sup>. The resulting reconstructed mosaic image was downloaded and opened in Photoshop (Adobe Systems Inc., San Jose, CA, USA) to rotate, crop, and adjust color balance of the image.

### IMAGE DEPOSITION INTO THE CELL CENTERED DATABASE

Mosaic images were acquired using an automated imaging workflow system developed at NCMIR to upload imaging data with its associated metadata directly from the microscopes in our facility and register them as microscopy products within the CCDB (Bouwer et al., 2011). This complex system for data collection, storage, and manipulation funnels large numbers of valuable datasets directly into the CCDB (Martone et al., 2008). Eighteen datasets resulting from this publication have been released to the public through the CCDB. Our large scale mosaics can be browsed or downloaded through the Cell Centered Database (CCDB; Martone et al., 2002, 2008) at <http://ccdb.ucsd.edu> by selecting project ID P20002. Because these data sets are quite large and rich in information, each of these reconstructed mosaic images (usually 1–4 GB in size) is viewable at full resolution and annotatable without downloading using the Web Image Browser (WIB<sup>2</sup>), a visualization program based on GIS technology similar to that used for Google maps, but specialized for microscopy imaging data. Through the WIB, users can turn on and off channels and adjust contrast of large microscopic imaging data sets.

## RESULTS

This work focuses on the characterization of four different anti-Panx1 antibodies in selected areas of the rat brain and compares cellular localizations. In our study, we ask the question: “What are the similarities and differences in tissue labeling patterns between four antibodies generated against different parts of the same molecule?” The diagram in **Figure 1** shows the topology of the Panx1 monomer and the epitopes of the four anti-Panx1 antibodies examined. Common features provide clues as to how Panx1 is localized to cellular sub-types, while dissimilar labeling may provide information about possible differences between neurons or microenvironments in one area of the brain versus another. It is difficult to point to which antibody is specific or non-specific as the Rb57 antibody produces the most bands in a Western blot, however the overall pattern of labeled cells in brain tissue matches that of the Ck4515 and CkDia with the exception of cells lining the vessels that are not labeled by Ck4515. As noted previously, epitopes are highly conformation dependent and accessibilities may be different in tissues where proteins are folded as opposed to Western blots where proteins are unfolded. Incubation of the peptide used for generating Rb57 antibody eliminated immunofluorescence staining in canine cardiac tissue (Dolmatova et al., 2012). Differences in the labeling patterns may also indicate non-specific interactions of the antibody that can occur due to recognition of similar short amino acid sequences. For Panx1, this has been especially problematic

(Bargiolas et al., 2011) indicating unanticipated complexity when comparing simple tissue culture systems with intact tissue. Two of these antibodies have already been characterized in publications (CkDia and Ck4515), while the other two were developed by us using a contracted company and validated within our own laboratory. The specificity of the Ck4515 anti-Panx1 antibody was characterized in a previous publication by Western blot and immunofluorescence staining in oocytes, erythrocytes and heart capillaries (Locovei et al., 2006a). While not explicitly stated in Locovei et al. (2006a), the Ck4515 antibody was validated for specificity in exogenously expressing oocytes using peptide competition experiments and incubation with preimmune serum (Gerhard Dahl, personal communication). This antibody was reported to show no immunofluorescence in staining of Panx1 KO mouse tissue (Zoidl et al., 2007) and has been used with several tissues (Ransford et al., 2009; Silverman et al., 2009; Dolmatova et al., 2012). The specificity of CkDia antibody was originally characterized in mouse brain and in transfected cells by Zappala et al. (2006) who demonstrated a single band on Western blot that was absent in parental HeLa cell lysate and eliminated by preabsorbing the antibody with the immunizing antigen. CkDia has been used in several publications (Romanov et al., 2007; Tang et al., 2008; Zhang et al., 2008; Huang et al., 2011).

However, none of these antibodies has been compared to each other using the same specimens and controls. As part of these controls, we present Western blot data on Panx1 KO mice tissues. It should be noted that while Panx1 labeling with recombinant Panx1 in cultured cells gave consistent results, the Western blots from KO animals were not entirely clean or consistent between tissues and/or KO mice.

### PANX1 LABELING IN CULTURED CELLS

Each of these four antibodies was first tested using transfected Panx1-myc HeLa cells, a system where there is no endogenous Panx1, to ensure that the antibody labeled exogenously expressed tagged Panx1 (e.g., myc, Flag, His etc.), and showed almost complete overlap with an antibody for the epitope tag. For immunofluorescence experiments, HeLa cells transiently transfected with Panx1-myc demonstrated the specificity of each of the four anti-Panx1 antibodies based on the overlap of Panx1 with commercial and well-characterized myc antibodies (**Figure 2**). A negative control omitting primary antibodies from the initial incubation showed no labeling (unpublished results). In addition, no staining corresponding to the glycosylated or unglycosylated Panx1 bands were obtained in Western blots of parental HeLa cell lysates for these four antibodies (data not shown; Zappala et al., 2006). These four anti-Panx1 antibodies performed similarly in labeling cultured cells. **Figure 2** shows that in non-expressing cells there is typically little or no fluorescence. Co-localization of the labeling pattern between Panx1 protein (grayscale, column1) and the myc tag (grayscale, column2) resulted in yellow in the merged RGB image (column 3) that showed expression at the cell membrane as well as in intracellular populations, as has been previously published (Boassa et al., 2007; Penuela et al., 2007; Boassa et al., 2008; Penuela et al., 2009). The CkDia Panx1 antibody displayed some low-level background fluorescence in non-transfected cells when compared to the myc labeling, that is not present with the other

<sup>1</sup><https://confluence.crbs.ucsd.edu/display/ncmir/Mosaic+Plugins+for+ImageJ>

<sup>2</sup><http://openccdb.org/software/index.shtml>

three antibodies. These antibodies were also tested for immunofluorescence with transfected HEK 293T cells, and MDCK cells over-expressing Panx1 and showed the same overlapping labeling patterns (unpublished results).

We used over-expressing Panx1 MDCK cells containing both endogenous Panx1 and exogenous untagged Panx1 for our Western blot analysis (**Figure 2 right hand column**). These cells provided a very strong signal for detecting Panx1 in Western blots and have two strong bands ~48 and ~52 kDa in size that are labeled by all four antibodies. It has been previously established that Panx1 in SDS-PAGE/Western Blots runs as three bands that are correlated with their glycosylation status (Boassa et al., 2007; Penuela et al., 2007). The Western blot in **Figure 3** far left panel shows that the lower band in **Figure 2** was resolved into two bands using a different lysate of the same cell line. This pattern of three bands was evident with each of the four antibodies tested (unpublished results). We have previously named these three bands as GLY0 (non-glycosylated, bottom band), GLY1 (partially glycosylated, middle band), and GLY2 (fully glycosylated, upper band). Our previous analyses (Boassa et al., 2007, 2008) and that of others (Penuela et al., 2007) demonstrated that the fully glycosylated GLY2 Panx1 species localized to the plasma membrane while the GLY0 and GLY1 Panx1 species are found in intracellular compartments. It should be noted that parental MDCK cells containing only endogenous Panx1 show a similar profile, but the GLY0, GLY1, and GLY2 bands have weaker intensities consistent with less expression (Penuela et al., 2007). These Panx1 protein bands were used to compare for molecular weights with endogenous Panx1 found in brain tissue (**Figure 3**).

#### WESTERN BLOT LABELING OF BRAIN TISSUE

While model cultured cells represent excellent homogeneous and easily manipulated systems for understanding expression and trafficking, we focused our study on expression patterns of Panx1 in the more complex organization of brain tissue, a heterogeneous organ containing several cell types intermingled and interacting within spatial domains. We originally tested Western blots of commercially available rat and mouse brain lysates with all four antibodies (data not shown). We analyzed the rodent brain lysates after SDS-PAGE and Western blotting and the Panx1 banding patterns comparing rat to mouse brain were similar. Although each of the four antibodies gave highly similar banding patterns in tissue culture cells, there were variations in the banding patterns in Westerns of the same rat and mouse brain lysates using these four Panx1 antibodies. We also performed Western blots of rat cerebellum lysates, however the banding pattern for each antibody looked the same as the total rat brain lysates.

As additional controls for validating our antibodies using Western blots, we analyzed banding patterns between wild type and KO mice generated independently by two different labs (Qu et al., 2011; Santiago et al., 2011). Contrary to what has been reported by Bargiotas et al. (2011), we see a reduction or elimination of bands in the 36–55 kDa region of expected Panx1 bands (see bracketed region indicated in the far left Western) of the KO tissue with all antibodies. However, we also saw bands in the ~20 kDa range that also were eliminated or decreased. Residual weak bands in the KO

lanes may be a result of incomplete knock-down of the Panx1 protein in these two knockout models. Every antibody tested, even CT-395 (which Bargiotas et al. stated was the one successful antibody to show knockout of Panx1), showed additional bands that are not eliminated or reduced in a KO tissue. As an example, the Mo503 antibody showed a much more dramatic reduction in spleen (**Figure 3B**) than in brain KO tissues (**Figure 3C**). Additionally, the 64 kDa bands in the spleen lysate of the Genentech KO mouse were not present in the brain lysates of the KOMP KO mouse. Particularly, while the CT-395 antibody Western blot in **Figure 3** does not show Panx1 bands in the knockout lane in this figure, longer exposures of the Western blot show Panx1 bands in the expected 36–55 kDa region (data not shown). Thus, we not only saw differences between different antibodies, but also differences between KO models and even KO tissues from the same animals. It is important to note that a quantitative real time polymerase chain reaction (qRT-PCR) analysis of Panx1 transcripts in several tissues demonstrated that Panx1 knockout animals generated by KOMP using the knockout first strategy (Testa et al., 2004) are hypomorphs rather than true knockouts (Hanstein et al., submitted).

#### PANX1 LABELING IN FOUR BRAIN REGIONS

We focused on cerebellum, hippocampus, olfactory bulb, and thalamus, four areas of the rat brain that have all been reported to have high Panx1 expression using *in situ* hybridization in either mouse or brain tissue (Ray et al., 2005; Vogt et al., 2005; Weickert et al., 2005; Lein et al., 2007). Wide scale immunofluorescence mosaic images allowed us to image large morphological domains while still retaining labeling information at the cellular resolution scale. Immunolabeled sagittal rat brain slices corresponding approximately to a lateral position of 1.40–2.10 mm of the Paxinos and Watson (1998) rat brain atlas were imaged in four large regions (**Figures 4–9**). In addition, the hippocampus and olfactory bulb images contain areas of nearby neocortex. In **Figures 4, 6, 7, and 9**, we show only one montage using the CkDia antibody but also show full resolution views from within montages of brain regions labeled with each of the four antibodies. The Panx1 labeling is always shown in green. Each tissue slice was also labeled with anti-GFAP antibodies to distinguish astrocytes (red) while cell nuclei were stained with DAPI (blue).

Because image data is rich in information and each montage at full resolution is typically over 2 GB, we chose to make all montages publicly available, rather than show down-sampled mosaics, except as an example for each area. Each of these mosaics at full resolution has been deposited in the CCDB under project ID P20002 and can be viewed using the Web Image Browser (WIB) or downloaded onto a reader's computer via the CCDB portal<sup>3</sup>. **Table 2** contains URLs linking to each of these large data sets for viewing using the WIB.

#### Cerebellum

Examples of the cerebellar cell types labeled by the anti-Panx1 antibodies are shown in **Figures 4 and 5**. These include Purkinje

<sup>3</sup><http://ccdb.ucsd.edu>

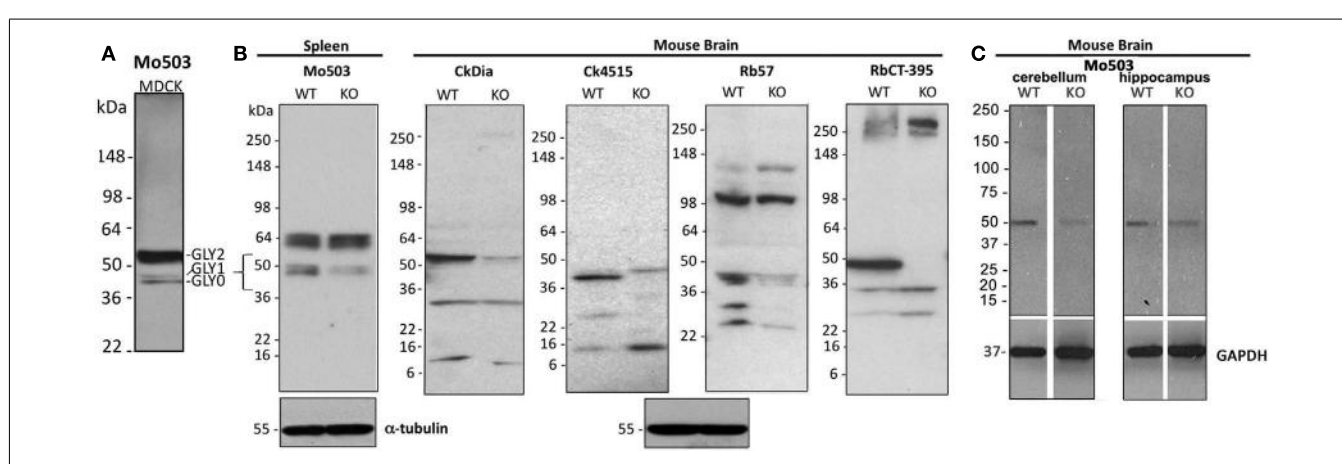
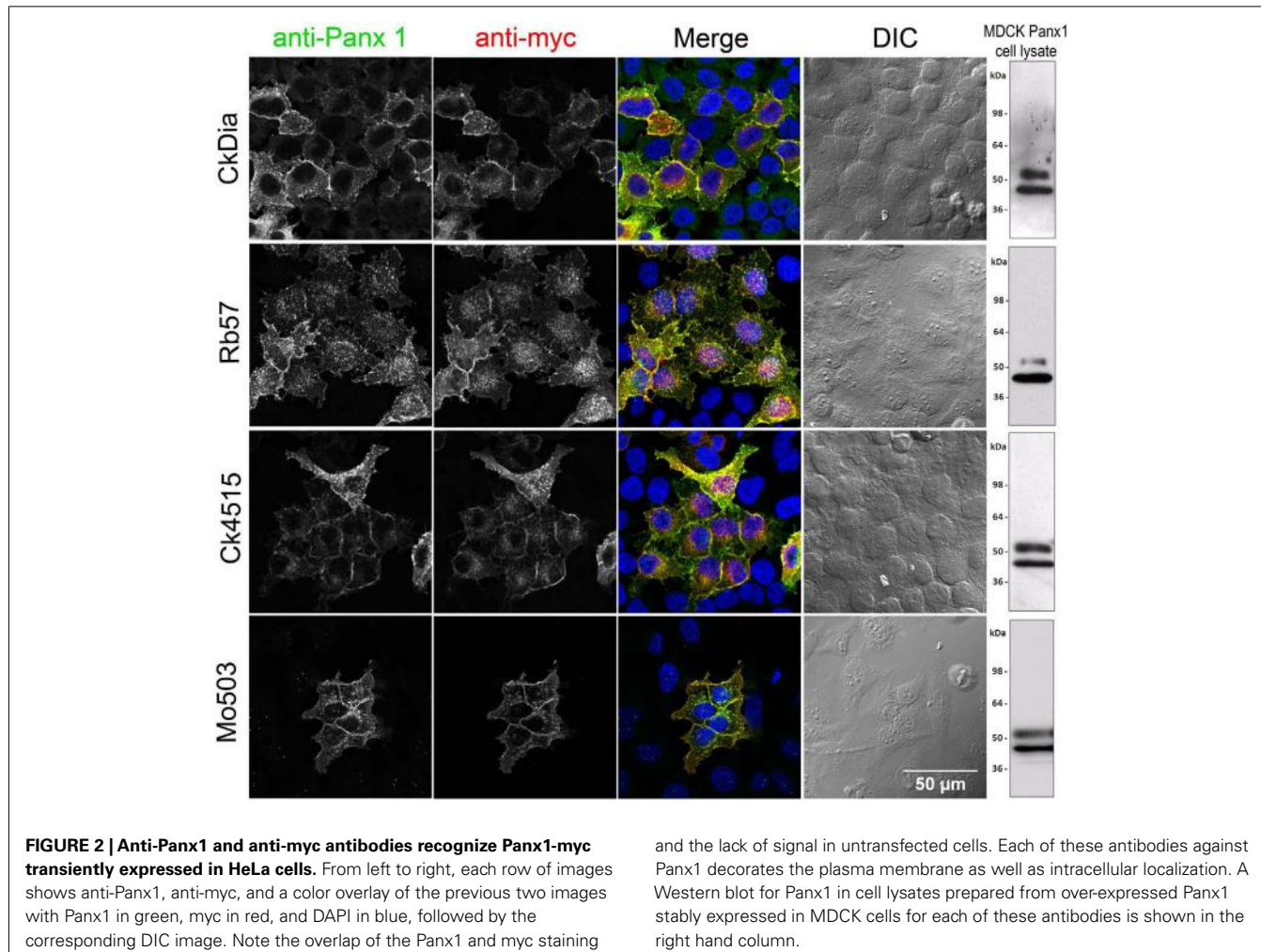


**FIGURE 2 | Anti-Panx1 and anti-myc antibodies recognize Panx1-myc transiently expressed in HeLa cells.** From left to right, each row of images shows anti-Panx1, anti-myc, and a color overlay of the previous two images with Panx1 in green, myc in red, and DAPI in blue, followed by the corresponding DIC image. Note the overlap of the Panx1 and myc staining and the lack of signal in untransfected cells. Each of these antibodies against Panx1 decorates the plasma membrane as well as intracellular localization. A Western blot for Panx1 in cell lysates prepared from over-expressed Panx1 stably expressed in MDCK cells for each of these antibodies is shown in the right hand column.

show decreases in the KO tissue. The Western blot at the far right uses the CT-395 antibody developed by the Laird laboratory and serves as a control for matching against our antibodies.  $\alpha$ -tubulin blots are shown as a loading control. (C) Cerebellum and hippocampus tissue lysates from a KOMP generated Panx1 KO show decreased intensity from wild type in Western blots. Here, Western blotting against GAPDH was used as a loading control.

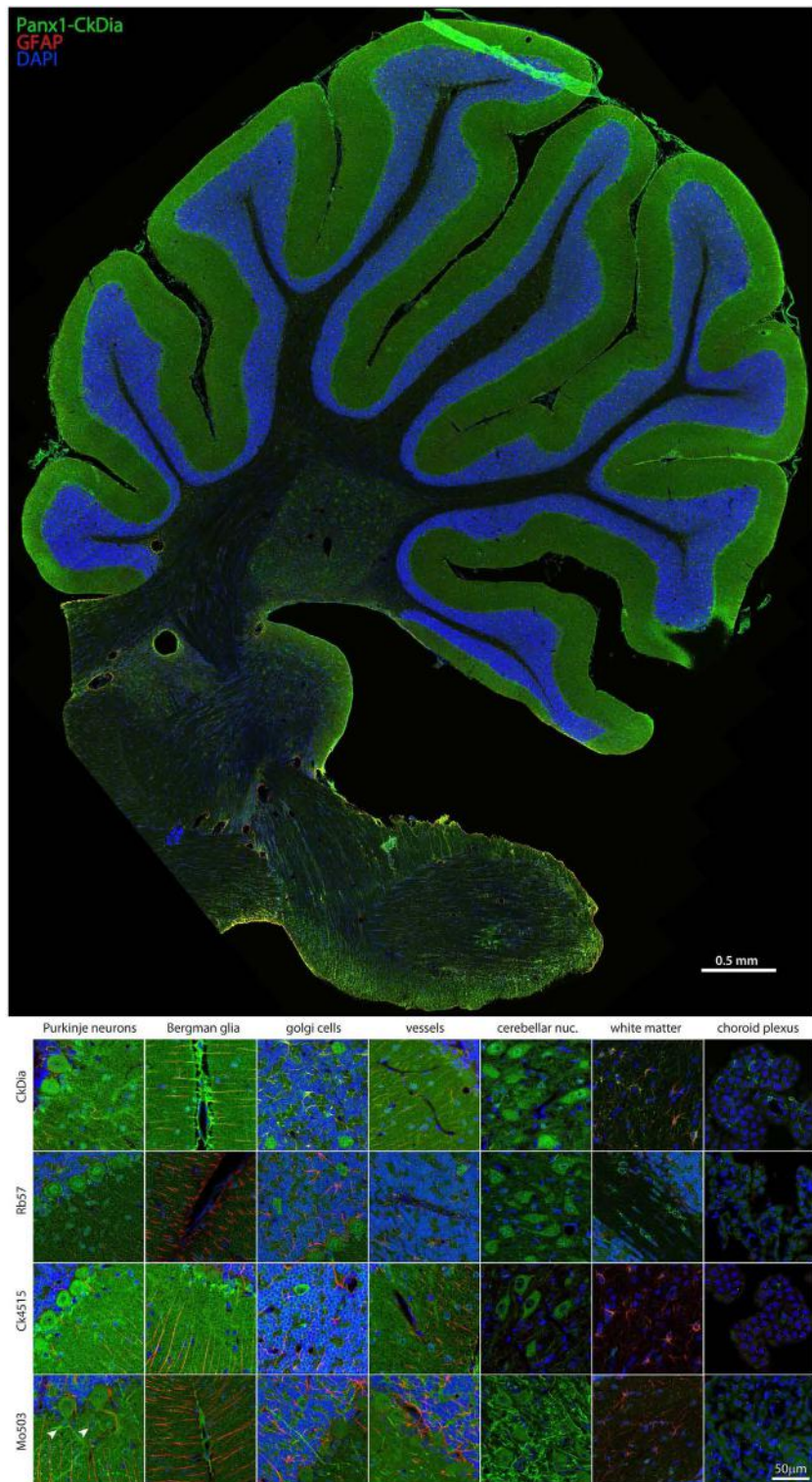


**FIGURE 4 | Large scale mosaic imaging of rat brain cerebellum.** Top: this representative cerebellum montage is labeled with CkDia anti-Panx1 antibody (green), GFAP (red), and DAPI (blue, nuclei). This mosaic image is made up of 587 tiles. Each tile is a maximum intensity projection of a stack of five

Z-sections that were stitched together to reconstruct this single, high-resolution 2D image. Bottom: full resolution views of cerebellar regions and cell types labeled by the four anti-Panx1 antibodies. Arrowheads in the Mo503 left hand image = stellate cells.

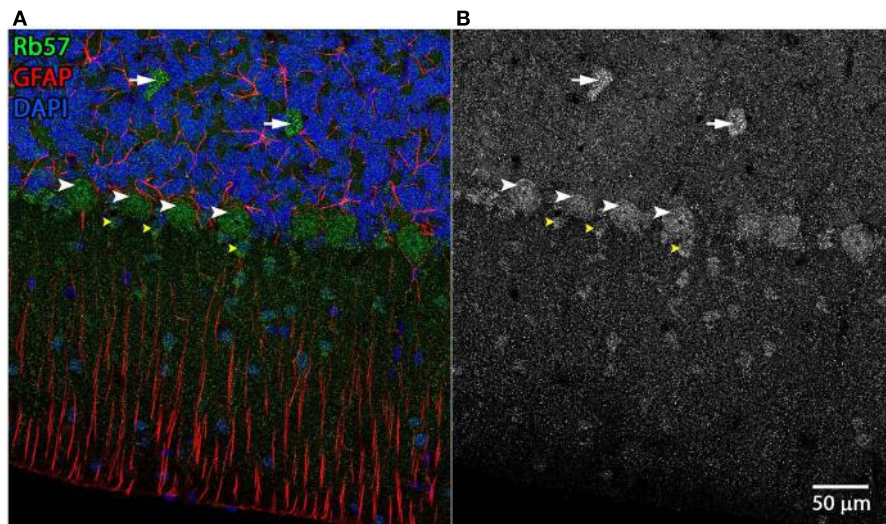


**FIGURE 5 | Cerebellar cell types labeled by Rb57 anti-Panx1 antibody.** Labeling of rat cerebellum tissue with the Rb57 anti-Panx1 antibody reveals expression in Purkinje neurons (white arrowheads), Golgi cells within the granular layer (white arrows),

Bergmann glia within the molecular layer of the cerebellum (yellow arrowheads), and additional cell bodies in the molecular layer that may be stellate cells. **(A)** Merged image **(B)** Panx1 channel shown in grayscale.

neurons, Golgi neurons, Bergman glia, and their parent cells, the Golgi epithelial cells, as well as cells within the deep cerebellar nuclei, all of which have been previously reported to contain significant amounts of Panx1 in mouse brain (Ray et al., 2006; Zappala et al., 2006). In comparing the staining patterns of these four antibodies (**Figure 4**, bottom), some patterns of differential antibody labeling across cerebellum tissue became apparent. For example, we found that the Mo503 antibody labels stellate cells or basket cells of the molecular layer (**Figure 4**, white arrowheads). The Rb57 antibody labeled cell bodies within the white matter while the CkDia antibody labels astrocytes within the white matter (**Figure 4**, bottom column 6). The three polyclonal antibodies labeled the Bergman glia; however no glial staining was observed with the Mo503 anti-Panx1 antibody (**Figure 4**, bottom, column 2). In Purkinje neurons, the labeling of all four antibodies was localized to the cell bodies, however, some staining of the axonal processes were visible, especially with the Mo503 antibody. The choroid plexus subcellular distribution was more speckled although some hints of apparent plasma membrane staining can be seen using the CkDia antibody. In the higher magnification view shown in **Figure 5**, labeling of rat cerebellum tissue with the Rb57 anti-Panx1 antibody revealed expression in Purkinje neurons (white arrowheads), Bergmann glia within the molecular layer of the cerebellum (yellow arrowheads), as well as Golgi neurons within the granular layer (white arrows). In general, all three polyclonal antibodies labeled Panx1 in astrocytes in the cerebellum. This overlap was more obvious when viewing the image through the WIB and the red GFAP channel was turned off.

### Hippocampus

Examples of hippocampal cell types (and neocortex lying superficial to the hippocampus) labeled by the anti-Panx1 antibodies are shown in **Figures 6** and **7**. These images contain

pyramidal neurons and astrocytes that have been previously reported to express Panx1 at the protein level in mouse brain (Zappala et al., 2006; Zappala et al., 2007; Karpuk et al., 2011). Vessel labeling by CkDia and Rb57 antibodies was difficult to distinguish from astrocyte end feet that are wrapped around the vessels and highly labeled in this brain region. Interestingly, even in instances where all four antibodies label the same cell type in consensus, like in the pyramidal neurons of the hippocampus (**Figure 6**), there were still differences at the subcellular level. In this case, the three polyclonal anti-Panx1 antibodies label the cell body and adjacent portion of the apical dendrite, while the Mo503 anti-Panx1 labeling is restricted to the dendrites of these cells (**Figure 7**). In many cell types the Mo503 preferentially labels dendrites or other cellular extensions and weakly labels cell bodies such as in the hippocampal pyramidal neurons and pyramidal cells of the neocortex region, while the polyclonal antibodies often highlight the cell bodies (**Figures 4** and **6–9**). Astrocytes in this region were labeled with the three polyclonal antibodies, but not by the monoclonal Mo503 antibody.

### Olfactory Bulb

The anti-Panx1 antibodies shown in **Figure 8** labeled several olfactory bulb cell types. These include the mitral cells, cells within the glomeruli of the main olfactory bulb (MOB) and cells within the exterior plexiform layer of the accessory olfactory bulb (AOB), and cells of the adjacent neocortex. In the examples of blood vessels from this region the Rb57 antibody sporadically labels cells lining the vessels, presumptively endothelial cells (**Figure 8**, bottom, column 3). Panx1 immunostaining has been previously reported in stria blood vessels in the cochlea (Wang et al., 2009) and in the endothelial cells of cardiac capillaries (Locovei et al., 2006a) using the Ck4515 antibody and

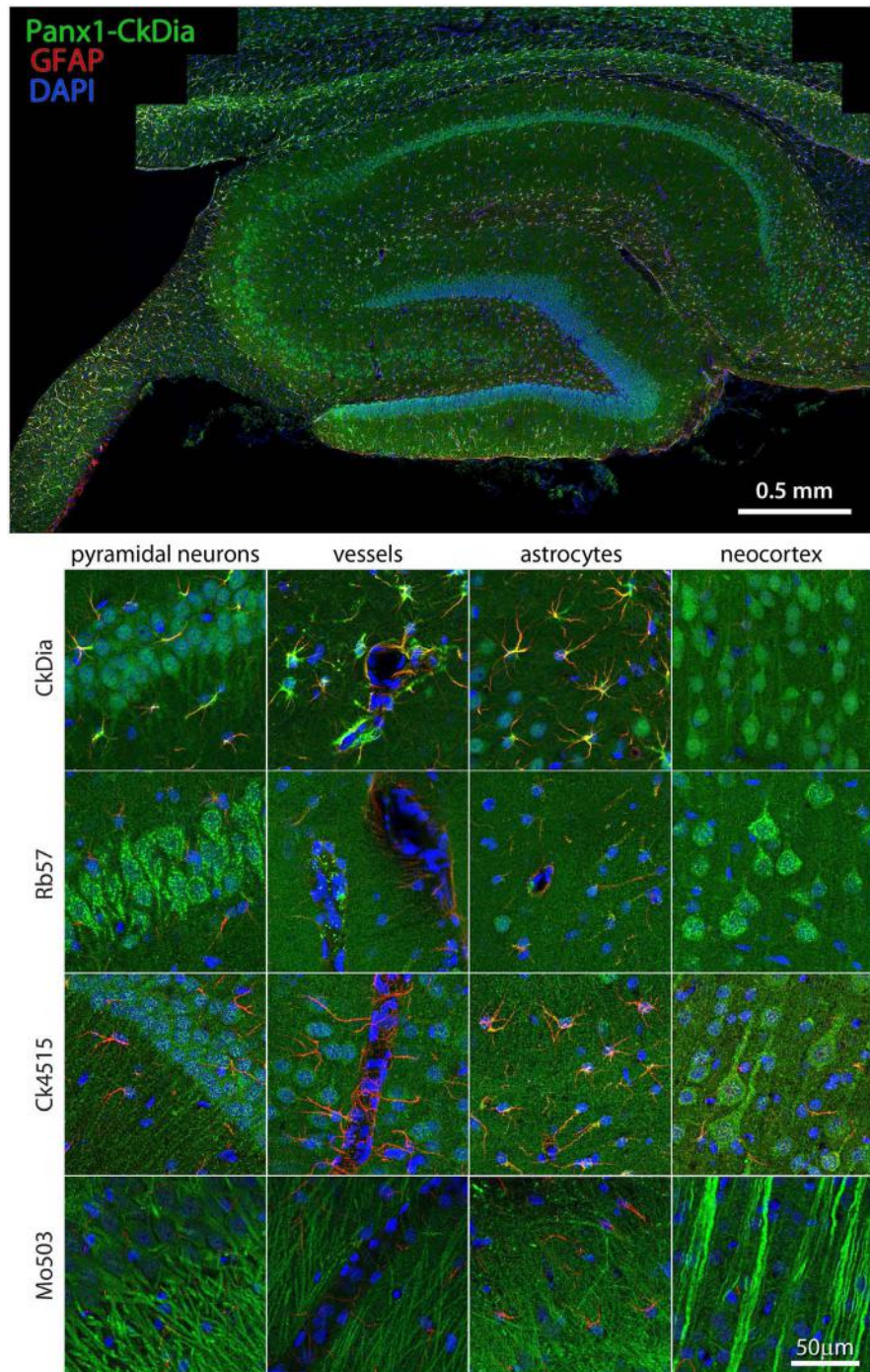


**FIGURE 6 | Large scale mosaic imaging of hippocampus and neocortex lying adjacent to the hippocampus.** Top: This representative hippocampus montage is labeled with CkDia anti-Panx1 antibody (green), GFAP (red), and counterstained nuclei with DAPI (blue). This mosaic image is

made up of 167 tiles. Each tile is a maximum intensity projection of a stack of four Z-sections that were stitched together to reconstruct this single, high-resolution 2D image. Bottom: full resolution views of hippocampal regions and cell types labeled by the four anti-Panx1 antibodies.

in endothelial cells of lens capillaries (Dvoriantchikova et al., 2006b) using a different rabbit polyclonal antibody. Two red blood cells that are quite rare with this type of specimen preparation can be seen clearly in this instance within the blood

vessel (white arrows), confirming robust Panx1 expression in erythrocytes (Locovei et al., 2006a). Again, as shown in the mitral cells, exterior plexiform layer, and neocortex, the polyclonal antibodies highlighted the neuronal cell bodies much more

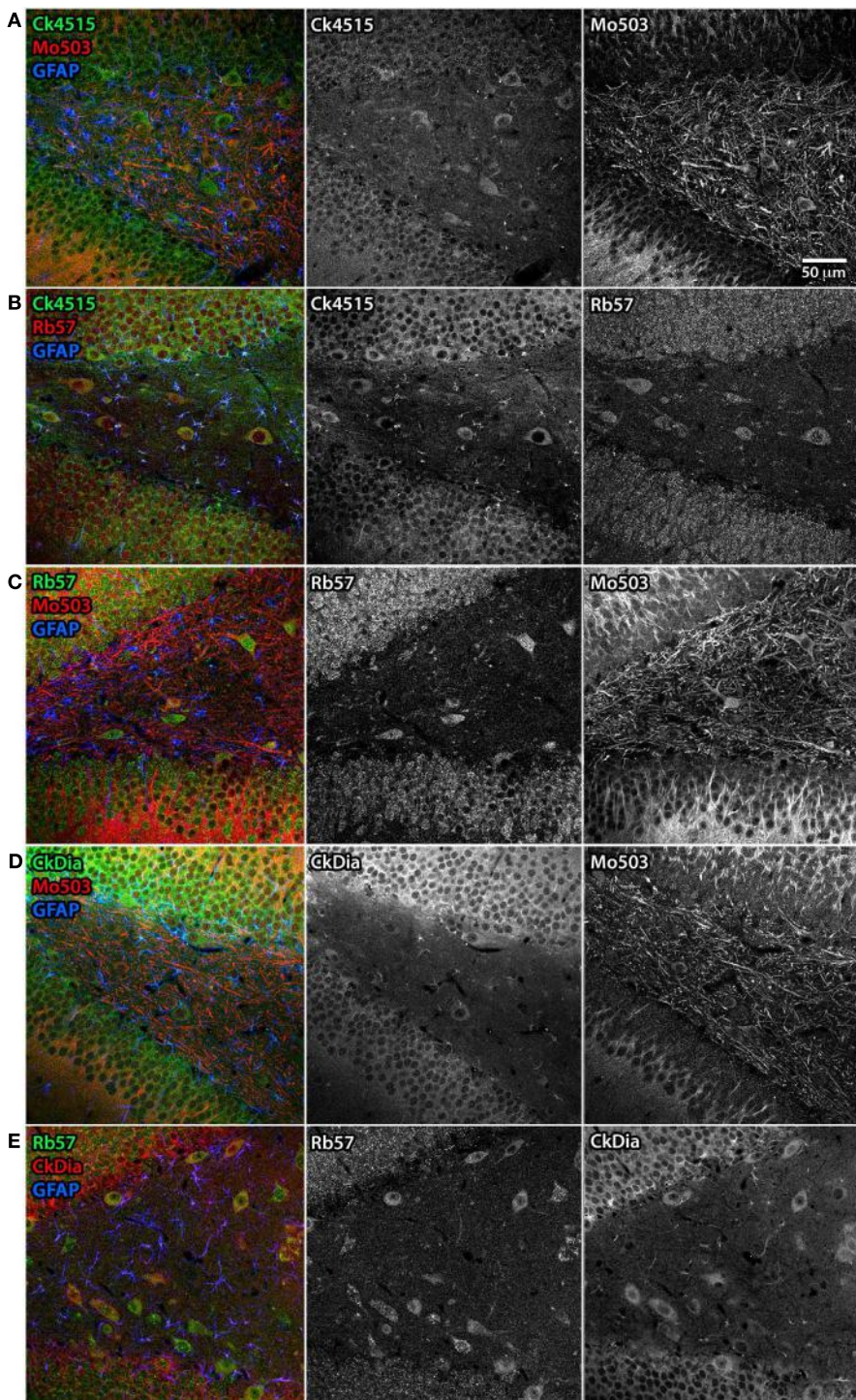


**FIGURE 7 | Differential subcellular labeling of Panx1 in the dentate gyrus of the rat hippocampus with combinations of four anti-Panx1 antibodies.** Although the neurons of the hippocampus are a consensus cell type labeled by all four of the Panx1 antibodies, there are differences in the apparent subcellular localization of the protein population recognized by each antibody. In these five panels, each antibody is shown in black and white (middle and right hand images) and as a composite color image in the left hand images. In all composite images, astrocytes are labeled with anti-GFAP (blue). **(A)** Co-labeling with Ck4515 and Mo503. **(B)** Co-labeling

with Ck4515 and Rb57. **(C)** Co-labeling with Rb57 and Mo503. **(D)** Co-labeling with CkDia and Mo503. **(E)** Co-labeling with Rb57 and CkDia. Tissue slices labeled with Rb57 (**B,C,E**) underwent antigen retrieval prior to immunolabeling. Co-labeling tissue with the polyclonal antibodies reveals that these primarily highlight the cell body and the adjacent portion of the dendrite however the Mo503 antibody (red) decorates the long dendrites of these cells with less noticeable staining at the cell bodies. However, there is a substantial degree of overlap in staining between all the antibodies.

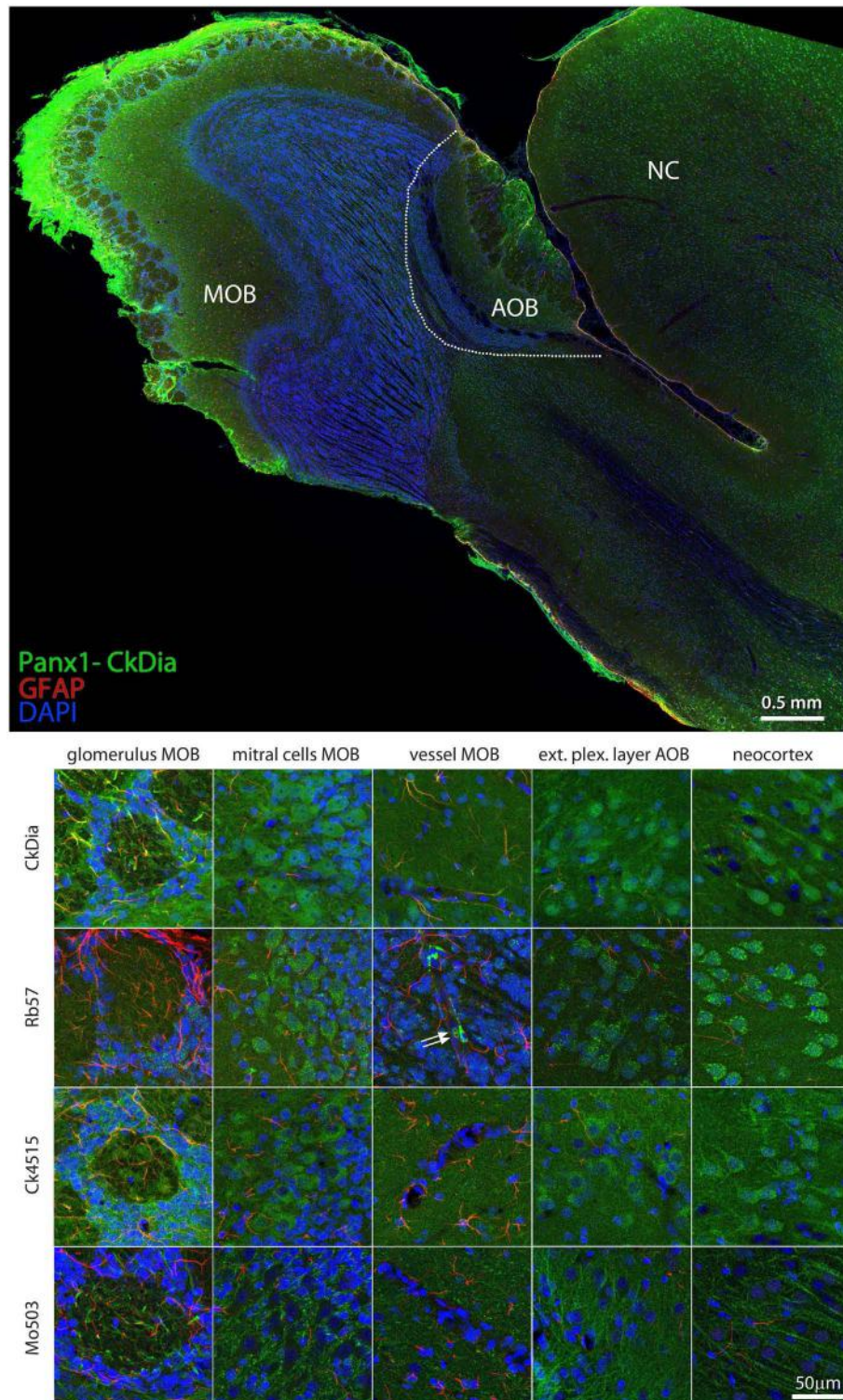
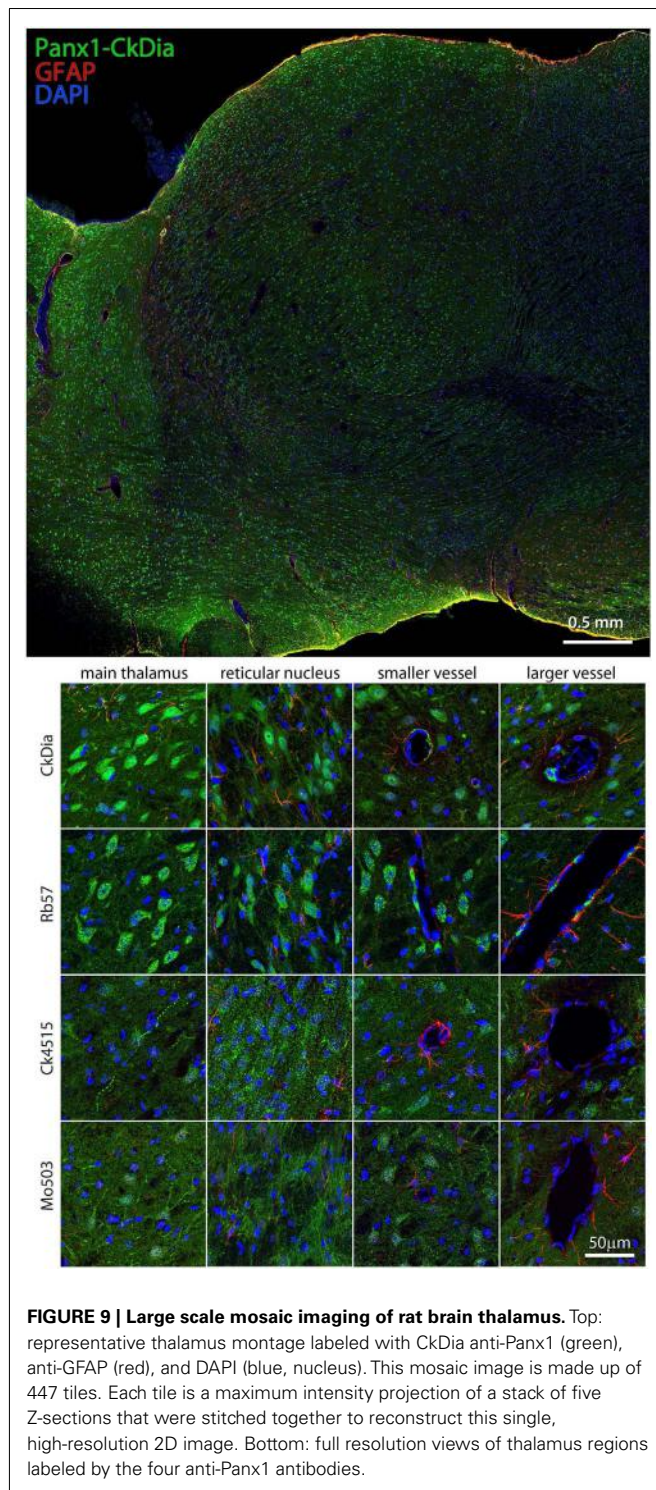


**FIGURE 8 | Large scale mosaic imaging of rat brain olfactory bulb and neocortex lying adjacent to the olfactory bulb.** Top: representative montage labeled with CkDia anti-Panx1 antibody (green), anti-GFAP (red), and DAPI (blue, nuclei). This mosaic image is made up of 649 tiles. Each tile is a maximum intensity projection of a stack of five

Z-sections that were stitched together to reconstruct this single, high-resolution 2D image. Bottom: full resolution views of olfactory bulb regions and cell types labeled by the four anti-Panx1 Abs. White arrows = red blood cells; MOB, main olfactory bulb; AOB, accessory olfactory bulb; NC, neocortex.



than the Mo503 antibody that preferentially stained the neuronal processes.

### Thalamus

Previous *in situ* hybridization studies showed staining with Panx1 mRNA probes in the mouse thalamus and in particular, reticular thalamic neurons (Ray et al., 2005). We found in this tissue, Panx1

localized mostly to neuronal cell bodies, although the Mo503 and Ck4515 do delineate neuronal processes. As with the other brain regions, the Rb57 and CkDia antibodies recognize sporadic cells lining blood vessels, presumably endothelial cells, while the other two do not (Figure 9). Interestingly, this brain region had the least labeling of Panx1 in astrocytes. It has been shown previously that astrocytes cultured from specific brain regions show differential expression patterns of adrenergic receptors (Ernsberger et al., 1990) and the differing astrocytic labeling we see in the various brain regions could be attributed to this phenomenon.

### DISCUSSION

Panx1 is the most studied and best characterized isoform of the pannexin protein family. It has been demonstrated to form large conductance channels in neurons, glial cells, and erythrocytes (Locovei et al., 2006a; Thompson et al., 2008; Iglesias et al., 2009). The opening of Panx1 channels has been induced by various experimental conditions, including activation of purinergic receptors, stretch, high intracellular calcium, and membrane depolarization (Bao et al., 2004; Locovei et al., 2006b; Pelegrin and Surprenant, 2006). Panx1 is insensitive to variations in extracellular calcium concentrations over a wide range (Bruzzone et al., 2005) and opens at negative resting potential in response to mechanical stress and at micromolar increase of intracellular calcium (Bao et al., 2004; Locovei et al., 2006a). In conjunction with the sensitivity of Panx1 to extracellular ATP through purinergic receptors of the P2Y and P2X type (Locovei et al., 2007), it has been postulated that a prime function of Panx1 channels are as ATP release conduits mediating extracellular propagation of  $\text{Ca}^{2+}$  waves (Locovei et al., 2006a,b). Astrocytes propagate  $\text{Ca}^{2+}$  waves (Cornell-Bell et al., 1990; Arcuino et al., 2002) and have been suggested to be an important mechanism in neuronal – glial signal transmission (Nedergaard et al., 2003; Newman, 2003; Volterra and Steinbauer, 2004).

It has been proposed that Panx1 channels are involved in pathways activated upon a strong stimulus, such as inflammation (Kanneganti et al., 2007; Silverman et al., 2009), ischemia (Thompson et al., 2006), or myocardial infarction (Dolmatova et al., 2012). In keeping with the hypothesis that Panx1 channels open only upon a stimulus, Panx1 channels are constitutively closed (Bao et al., 2004; Bruzzone et al., 2005). Panx1 channels (pannexons) lack sensitivity to extracellular  $\text{Ca}^{2+}$ , an important property, as Panx1 channels will not be open under physiological ionic conditions. In neurons and possibly astrocytes, Panx1 may contribute to novel forms of synaptic and non-synaptic communication and  $\text{Ca}^{2+}$  wave propagation (MacVicar and Thompson, 2010). In mammalian skin, Panx1 plays a key role in keratinocyte differentiation. Furthermore, in the cardiac, nervous, and immune systems, Panx1 activation is implicated in ischemic, excitotoxic, and ATP-dependent cell death such that Panx1 coupling with purinergic receptors triggers an inflammasome mediated response (Kanneganti et al., 2007; Pelegrin et al., 2008; Silverman et al., 2009). Reactive astrocytes immediately bordering an abscess exhibited open Panx1 channels during the acute inflammatory period, which dissipated as the infection evolved (Karpuk et al., 2011). Additionally, P<sub>2</sub>X<sub>7</sub> receptor activation induces Panx1 channel opening in astrocytes (Scemes et al., 2007; Iglesias et al., 2009; Suadicani et al., 2012). Panx1

**Table 2 | List of URLs linking to display of full resolution large-scale mosaic images using four different anti-Panx1 antibodies of four regions within the rat brain studies here.**

Brain region	Panx1 Ab	CCDB MP ID	URL
Cerebellum	CkDia	56630	<a href="http://purl.oclc.org/NET/56630_CkDia_Cer">http://purl.oclc.org/NET/56630_CkDia_Cer</a>
Cerebellum (Alternate)	CkDia	57185	<a href="http://purl.oclc.org/NET/57185_CkDia_Cer">http://purl.oclc.org/NET/57185_CkDia_Cer</a>
Thalamus	CkDia	48338	<a href="http://purl.oclc.org/NET/48338_CkDia_Thal">http://purl.oclc.org/NET/48338_CkDia_Thal</a>
Thalamus (Alternate)	CkDia	46648	<a href="http://purl.oclc.org/NET/46648_CkDia_Thal">http://purl.oclc.org/NET/46648_CkDia_Thal</a>
Hippocampus	CkDia	48367	<a href="http://purl.oclc.org/NET/48367_CkDia_Hip">http://purl.oclc.org/NET/48367_CkDia_Hip</a>
Olfactory bulb	CkDia	58640	<a href="http://purl.oclc.org/NET/58640_CkDia_Olf">http://purl.oclc.org/NET/58640_CkDia_Olf</a>
Cerebellum	Ck4515	44959	<a href="http://purl.oclc.org/NET/44959_Ck4515_Cer">http://purl.oclc.org/NET/44959_Ck4515_Cer</a>
Thalamus	Ck4515	48920	<a href="http://purl.oclc.org/NET/48920_Ck4515_Thal">http://purl.oclc.org/NET/48920_Ck4515_Thal</a>
Hippocampus	Ck4515	48902	<a href="http://purl.oclc.org/NET/48902_Ck4515_Hip">http://purl.oclc.org/NET/48902_Ck4515_Hip</a>
Olfactory bulb	Ck4515	48664	<a href="http://purl.oclc.org/NET/48664_Ck4515_Olf">http://purl.oclc.org/NET/48664_Ck4515_Olf</a>
Cerebellum	Mo503	45305	<a href="http://purl.oclc.org/NET/45305_Mo503_Cer">http://purl.oclc.org/NET/45305_Mo503_Cer</a>
Thalamus	Mo503	58721	<a href="http://purl.oclc.org/NET/58721_Mo503_Thal">http://purl.oclc.org/NET/58721_Mo503_Thal</a>
Hippocampus	Mo503	58445	<a href="http://purl.oclc.org/NET/58445_Mo503_Hip">http://purl.oclc.org/NET/58445_Mo503_Hip</a>
Olfactory bulb	Mo503	58675	<a href="http://purl.oclc.org/NET/58675_Mo503_Olf">http://purl.oclc.org/NET/58675_Mo503_Olf</a>
Cerebellum	Rb57	45276	<a href="http://purl.oclc.org/NET/45276_Rb57_Cer">http://purl.oclc.org/NET/45276_Rb57_Cer</a>
Thalamus	Rb57	59247	<a href="http://purl.oclc.org/NET/59247_Rb57_Thal">http://purl.oclc.org/NET/59247_Rb57_Thal</a>
Hippocampus	Rb57	56258	<a href="http://purl.oclc.org/NET/56258_Rb57_Hip">http://purl.oclc.org/NET/56258_Rb57_Hip</a>
Olfactory bulb	Rb57	58377	<a href="http://purl.oclc.org/NET/58377_Rb57_Olf">http://purl.oclc.org/NET/58377_Rb57_Olf</a>

Eighteen full resolution montage images are viewable using the WIB tool by clicking on these URLs. Two high quality montages for which individual images are not shown in the galleries in **Figures 4–9** are also available for viewing and downloading and are denoted by “Alternate” under the brain region category. CkDia, Chicken Diatheva ANT0027 polyclonal antibody; Ck4515, Chicken 4515 polyclonal antibody (Dahl laboratory); Rb57, Rabbit 57 polyclonal antibody (Sosinsky lab); Mouse monoclonal 503 polyclonal antibody (Sosinsky lab). Each brain region is displayed with anterior facing left, and the reconstructed images have been cropped and color balance adjusted using Photoshop. All images (raw and processed) as well as associated metadata can be downloaded through the CCDB using the listed microscopy product identification number (MPID).

channel activity has been implicated recently in inflammasome formation in cultured neurons and astrocytes (Silverman et al., 2009). The latter data suggest a crucial role for Panx1 in several cell death pathways in the nervous system (Bargiolas et al., 2009; MacVicar and Thompson, 2010), although a recent Panx1 KO mouse showed no morphological changes in brain slices by histological analysis or changes in IL-1 $\beta$  from macrophages (Bargiolas et al., 2011). The authors stated in the on-line supporting information that five out of six commonly used anti-Panx1 antibodies tested on KO mouse tissue in Western blots were “non-specific,” however no original data detailing protein specificity from these Western blots or immunofluorescence imaging was provided. It is possible that in actuality some tissues of that particular KO mouse still contain Panx1 protein or again, Western blots are not the only diagnostic to be trusted for Panxs.

### GENERATING A PANX1 ANTIBODY TOOL-KIT

The four antibodies used in this study performed well in cell culture by labeling exogenous protein with an independent tag and showed a consistent and similar banding pattern on Western blots. In generating or testing antibodies against anti-Panx1 peptides, we used several standard criteria for a “good” antibody. One quality for a good Panx1 antibody generated was the ability to recognize recombinant protein containing an appended independent tag when expressed in tissue culture cells such that an antibody against the tag overlapped with the Panx1 staining. As important, was that the Panx1 labeling patterns in exogenously expressing

cultured cells would be similar to those found in endogenously expressing Panx1 cells. In our case, endogenously expressing Panx1 cell staining was very similar to transfected cells (Boassa et al., 2007). Another criterion was that in model systems, antibodies would recognize recombinant protein and endogenous protein on Western blots in a manner consistent with their expected molecular size and/or post-translational modifications. As a negative control, elimination of the primary antibody would abolish signal on Western blots of tissue culture cells and/or on tissue. For recombinant Panx1 in cells, Western blots of parental cell lines provide a critical negative control. We showed using Panx1 KO mice as a negative control (**Figures 3B,C**) that these four antibodies recognize Panx1 at its expected sizes as well as some sizes that are not yet explainable. There are some non-specific bands on some of the Western blots that do not disappear in the knock out tissue lysates consistently, as they are only present in some tissue samples. It is worth noting that Qiu et al. (2011) and Santiago et al. (2011) used the Ck4515 antibody to validate lack of expression in a Panx1 KO. Notably, two recent publications (Burns et al., 2012; Lohman et al., 2012) used immunoblotting, immunohistochemistry, and RT-PCR methods to cross-validate expression patterns in cerebral vasculature. However, it is important to remember that RT-PCR methods assay for mRNA expression, which can be different from protein expression. For example, Lohman et al. (2012) demonstrated that HEK293 cells, a cell line that has been documented in several studies as being negative for Panx1 expression, has residual Panx1 mRNA but no protein

expression as assayed by Western blots and immunohistochemical imaging.

This work focused on imaging Panx1 expression in select areas of the rat brain and compared their cellular localizations. Although Panx1 antibodies have been criticized for lack of specificity, this comparative labeling study takes into account the differences between antibody epitopes and labeling requirements and utilizes their unique qualities. Uncertainty in the antibodies currently available (both privately and commercially) is due to various reasons. It is hard to find a single antibody that can perform well by recognizing the Panx1 protein under all Western blot and immuno-microscopy conditions, which has been shown for other protein targets as well especially in brain tissue (Herkenham et al., 2011). Another reason for uncertainty about Panx1 antibodies has been the failure to fully characterize, at the protein level, the original report of a Panx1 KO mouse that was generated several years ago (Anselmi et al., 2008). Now additional Panx1 KO mouse lines have been generated by various techniques and so far they all perform differently under these rigorous tests by Western blot. Because of this discrepancy and the difficulty in brain tissue preservation, there are few published cellular level images of Panx1 protein expression in brain and all have limited fields of view (Ray et al., 2006; Zappala et al., 2006; Zoidl et al., 2007; Karpuk et al., 2011). We performed these experiments in rat brain because no non-specific cross-reaction would occur due to labeling the same species that the antibodies were generated against (a mouse against mouse reaction).

### COMPARISON OF PROTEIN LABELING TO *IN SITU* HYBRIDIZATION STUDIES

The ability to combine gross structural imaging with high-resolution microscopy on a large scale significantly advances our ability to detect and analyze multiple brain regions. The trade-off between resolution and field of view leads to targeted investigations limited to regions of the brain that are determined to be heavily labeled and well studied while ignoring areas that may be smaller or more subtly labeled. *In situ* hybridization provided a first estimate of where pannexins are located (Baranova et al., 2004; Vogt et al., 2005; Weickert et al., 2005). *In situ* hybridization provides a first approach to assembling a protein expression map in tissues because it is easier and faster to generate riboprobes than antibodies. However, proteins in the nervous system can be very far removed from where the genes are expressed; thus, *in situ* hybridization investigations give only a limited view of expression patterns. Correlation between the two types of staining can be difficult, because antibodies do not always label the protein in the cell body, leading to difficulties in ascertaining the identity of labeled axons and dendrites.

For the most part, our antibody labeling across brain domains are similar to those obtained with *in situ* hybridization. Strong staining has been observed in the cerebellum, hippocampus, olfactory bulb, and thalamus (Ray et al., 2005; Vogt et al., 2005). In the cerebellum (Vogt et al., 2005), found that all layers showed signal but it was highest in Purkinje cells, Golgi cells, and deep cerebellar nuclear cells. In the olfactory bulb, we found that the strongest signal was in the mitral cell layer and AOB. Vogt et al. (2005) showed that some labeling occurred in the granule cell layer of the olfactory

bulb. The hippocampus contained high Panx1 expression in the dentate gyrus and all CA regions, pyramidal cells, stratum oriens, radiatum, and lacunosum-moleculare. (Vogt et al., 2005) found that co-labeling with GFAP and NeuN antibodies with riboprobes highlighted that neurons were labeled but astrocytes were not. In particular, Vogt et al. (2005) found that GABAergic interneurons and pyramidal neurons showed significant Panx1 staining. In our study, we found that, while there were consistencies between the four antibody labels, the subcellular distribution could vary as shown in the pyramidal neurons of the hippocampus. We observed Panx1 staining in astrocytes using all of the polyclonal antibodies including CkDia, although initial characterization of this antibody by Zappala et al. (2006) did not include descriptions of astrocytic staining. It should be noted that Panx1 expression in astrocytes was recently demonstrated *in vivo* both functionally and by immunohistochemistry (Karpuk et al., 2011; Santiago et al., 2011) and in Western blot analysis of cultured astrocytes (Huang et al., 2007; Iglesias et al., 2009; Silverman et al., 2009; Suadicani et al., 2012). High Panx1 RNA expression was documented from staining of the thalamic reticular nucleus (Ray et al., 2005), while we find protein labeling of sporadic cells in this region with each antibody that was used for staining.

### CONSISTENT AND VARIABLE FEATURES BETWEEN THE FOUR ANTIBODY LABELING PATTERNS

A major goal of this study was to determine subcellular patterns of expression across the different brain regions and search for consistent patterns between the four antibodies. Each of these antibodies has a unique epitope with only two (CkDia and Rb57) of them overlapping. As such, these two antibodies had similar domain and subcellular labeling patterns, in that they tended to highlight the neuronal cell bodies as well as astrocytes, and endothelial cells in most of the brain regions we imaged. Some images are suggestive of plasma membrane staining, particularly with the Mo503 antibody. However, electron microscopy of these slices will be necessary to unequivocally determine this, since it is sometimes difficult to determine proteins or protein complexes that lie just underneath or within the plasma membrane. The Ck4515 antibody, a very commonly used antibody within the pannexin field, has an expression pattern that is closer to the CkDia and Rb57 labeling patterns than the Mo503 labeling. Our results in hippocampus with the Ck4515 antibody were similar to those of Santiago et al. (2011) who used an antibody generated against the same peptide as Ck4515 and showed labeling in neurons, astrocytes, and perivascular astrocytic endfeet in hippocampal area CA1. That study also showed no non-specific labeling in KO mouse tissue.

### MODIFICATIONS TO PANX1 GENE EXPRESSION THAT COULD IMPACT EXPRESSION PATTERNS

Other considerations in understanding Panx1 labeling include post-translational modifications or differentially translated Panx1 that could complicate various banding patterns that were unanticipated from tissue culture control experiments. Using the same tissue lysate, the Western blot protein patterns varied depending on the antibody and presented a more complex situation than tissue culture cells. Our Western blots of the same rat and mouse brain lysates varied from two to eight major bands depending

on the probing antibody. In other published studies, bands were shown at ~43, ~52, and ~96 kDa in Western blots of mouse and rat brain lysates (Wang et al., 2009) while five bands corresponding in approximate size to exogenously expressed Panx1 protein were recently shown in rat brain lysate by Western blot (Kienitz et al., 2011).

Several factors may influence the number of bands seen on Western blots. Glycosylation results in having multiple bands although the number can range depending on the tissue and cell type (Boassa et al., 2007; Penuela et al., 2007). Furthermore, these glycosylated species were shown to give rise to spatial separation of the fully glycosylated GLY2 in the plasma membrane and the GLY0 and GLY1 isotypes in intracellular compartments such as the ER. Recently, Panx1 has been shown to have two potential caspase cleavage sites of which one site was cleaved by caspases 3 and 7 (Chekeni et al., 2010). Either of these two sites, cleaved separately or in combination in brain tissue, would cause differential recognition of the resulting protein by these four antibodies (Table 3, see sites in Figure 1). Panx1 has also recently been shown to be expressed as three additional splice variants in the pituitary gland (Li et al., 2011) that would also give rise to differential recognition of Panx1 species of 48 kDa by all antibodies for the full-length (“Panx1a” splice variant), 40 kDa for Ck4515, and Mo503 antibodies for the “Panx1c” splice variant or 35 kDa recognized by CkDia, Rb57, and Mo503 for the “Panx1d” splice variant. In addition, it is important to note that glycosylation of several of these Panx1 species will affect the experimentally measured monomer size if the Panx1 species retains the N254 glycosylation site. Lastly, while inhibitors of proteolytic enzymes are typically included in lysate protocols and prevent gross damage, proteolytic cleavage may still occur during the dissection and homogenization process.

The complex labeling patterns we see may be a reflection of different cellular and subcellular localizations, where each antibody is highlighting unique subpopulations of accessible Panx1 epitopes of this dynamically expressed and processed protein. For example, in many cell types the Mo503 antibody preferentially labels dendrites and not cell bodies, while the other antibodies often highlight the cell bodies. The mouse antibody is unique in that it was generated against part of the N-terminus. Our tissue labeling results are consistent with tissue culture systems where Panx1 is localized to both the plasma membrane and intracellular membrane compartments. It is important to note that some tissue culture cells such as bEnd3 vascular endothelial cells show

only intracellular immunofluorescence that correlated with the appearance of only the GLY0 band on Western blots (Boassa et al., 2007). At the present time, we believe a more in-depth analysis of Panx1 gene and protein modifications will be necessary to fully interpret the bands we see on our Western blots.

## NEUROINFORMATICS RESOURCES AND TOOLS FOR DECIPHERING PANX1 PROTEIN EXPRESSION

Although we cannot conclusively establish localization of pannexin protein because of the variability between antibodies, tissues, and assay systems, we believe that this paper illustrates several best practices that should be employed in all immunolabeling studies to make it easier to compare findings and to ensure that problematic information is not suppressed during the publication process, but rather exposed so that the community has accurate information (MacArthur, 2012). As a first step, we provided all identifying information for each antibody (vendor, catalog#, clone ID, and Antibody Registry URI). The Antibody Registry is a web resource that issues a stable, traceable, permanent identifier for an antibody created by commercial vendors or individual labs so that a researcher can easily find the antibody used in a scientific paper and trace that antibody back to the creator. Often, manufacturers have more than one antibody to the same protein, and it is important that the catalog number be included for all reagents. However, commercial vendor IDs may not be stable over time, as vendors go out of business or sell their product lines. For this reason, the Neuroscience Information Framework (NIF<sup>4</sup>), a project designed to make it easier to identify resources of relevance to neuroscience (Gardner et al., 2008), created the Antibody Registry<sup>5</sup>. The Antibody Registry currently contains >900,000 antibodies, largely from commercial sources. Each is given its own unique accession number, much like a gene sequence in GenBank that can be used to uniquely identify an antibody. Currently, there are 16 commercially available Panx1 antibodies listed on the Antibody Registry. There are many more that were privately generated and used in publications such Bargiolas et al. (2011); Huang et al. (2007). Again, we include the identifiers for our four antibodies in the materials and methods of the paper, so that text mining algorithms and authors can identify the usage of these antibodies without ambiguity. If such identifiers were routinely used, researchers could pull out all papers that use a particular reagent. More importantly, if problems like specificity come to light, notifications can be placed on those papers whose results may need to be re-analyzed or re-interpreted.

A second best practice is to publish all the data from a paper rather than selecting only the best exemplars. In our case, we show all Western blots for all antibodies and provide access to the full resolution brain maps via the CCDB. We believe that for novel proteins or those for which it is difficult to develop good probes, the type of survey study we publish here provides a public platform and forum, for evaluating the specificity of the reagents and ensuring that problems with these reagents are widely disseminated rather than suppressed. Often times, such knowledge is known by experts in the field, but it may take years for this knowledge to

**Table 3 | Differential recognition of predicted fragments resulting from caspase cleavage of Panx1.**

	Ck4515	CkDia	Rb57	Mo503
Full-length Panx1	48*	48*	48*	48*
Caspase site A cleavage	30*	18	18	18
Caspase site B cleavage	6	42*	42*	42*
Double caspase cleavage at both sites	6	18	18	18

These antibodies are predicted to recognize differently sized fragments (expressed in kDa) of the Panx1 protein after caspase cleavage (see Figure 1 for schematic). \* = fragment containing the N-glycosylation site.

<sup>4</sup><http://neuinfo.org>

<sup>5</sup><http://antibodyregistry.org>

percolate to the wider community (MacArthur, 2012), leading to continued use of faulty reagents during this time.

Finally, ensuring that papers are published in open access journals or deposited within Pub Med Central or made available through a pre-print service is critical, to ensure that search engines can gain access to the Materials and Methods section of the paper.

Thus, with this study we attempt to promote explorations that move beyond the question of why peptide specific antibodies do and do not label in brain tissue and instead examine how they work differently, the complexity of the biological system and how to interpret further imaging experiments. Our imaging strategy provides a novel approach such that we release the datasets (montages, associated metadata, and “raw” images) in the CCDB in their full size, resolution and complexity rather than presenting only down-sampled and/or redacted images that one typically finds in publications. By doing so, this unrestricted available data rich resource promotes further data mining and explorations by the public. Other resources like the Allen Brain Atlas and GEN-SAT may be useful for interpreting our datasets. The Allen Brain Atlas, a publicly available image database for *in situ* hybridization images of mouse brain and associated tools for information extraction and visualization (Lein et al., 2007), is very useful as a first step for correlating with gene expression hotspots. The Gene Expression Nervous System Atlas (GENSAT) project uses bacterial artificial chromosome (BAC) vectors in combination with transgenic mouse to EGFP tag proteins in the CNS for light microscopy (Gong et al., 2003). While, transgenic Panx1-EGFP is not yet available in this on-line digital atlas and there is the risk that recombinant Panx1-EGFP may not traffic the same as wild type protein, the GENSAT database can be used to correlate with other proteins in the database for overlap in expression patterns. The 18 montages from this study significantly increase the number and expanse of published images of Panx1 labeling in brain. However, no comprehensive protein expression atlas yet exists for the rodent brain, equivalent in breadth to the Allen Brain Atlas. As we see here, antibody labeling is highly variable and dependent on specimen preparation protocols, even with antibodies to the same protein. Our study points out the importance of thorough characterization and unambiguous identification of the antibody reagents used to report findings. Currently, identification of antibody reagents from published studies is very difficult, as most

authors do not provide enough detailed information (e.g., catalog number) to identify the exact antibody used (Bandrowski et al., submitted). The Neurosciences Informatics Framework (NIF<sup>6</sup>) has created a large antibody registry where antibodies receive a uniform resource identifier (URI) that can be used to reference these reagents in papers (see Table 1<sup>7</sup>). We encourage the use of these numbers in their papers.

In summary, because this situation occurs more frequently than is documented, we recommend the following protocol: (1) Entire data sets should be made available on-line, (2) Reagents need to be specified, (3) In order to clarify who else uses these reagents, each antibody should have a unique URI, like those utilized by NIF. Reproducibility of reagents and protocols are critical. A recent editorial in Nature highlighted significant reproducibility issues in clinical drug trials because of insufficient or selective reporting (Begley and Ellis, 2012). Here we embrace the difficulties by publishing in a form that is fully vetted, showing all the data. By being able to manipulate the levels via the WIB, researchers can form their own opinion of the data. We encourage readers to leave comments via the Frontiers website.

## ACKNOWLEDGMENTS

We thank Dr. Daniela Boassa for her efforts in the early part of this project, discussions and the antibody development and validation. We are particularly grateful to Drs. Dale Laird and Silvia Penuela for the gift of the CT-395 antibody and lysates that were prepared using Panx1 KO mice provided to them by Dr. Vishva Dixit at Genentech. We thank Dr. Dixit in aiding this work. We thank Dr. Gerhard Dahl for the gift of the Ck4515 antibody and his steadfast encouragement for this project. This work was started under NSF grant MCB-0543934 and completed with support from NIH grant GM072881 (GS). Angela Cone was supported by NIH NRSA postdoctoral fellowship GM092457. NIH support for NS052245 to Dr. E. Scemes is acknowledged. Additional NIH funds for the CCDB (DA016602 awarded to Maryann E. Martone), Open CCDB (GM082949 awarded to Maryann E. Martone and Mark Ellisman), and NCMIR (RR004050 awarded to Mark Ellisman) are recognized for their funding of this project.

<sup>6</sup><http://neuroinfo.org>

<sup>7</sup>[http://antibodyregistry.org/antibody17/antibodyform.html?gui\\_type=advanced](http://antibodyregistry.org/antibody17/antibodyform.html?gui_type=advanced)

## REFERENCES

- Ambrosi, C., Gassmann, O., Pranskevich, J. N., Boassa, D., Smock, A., Wang, J., et al. (2010). Pannexin1 and Pannexin2 channels show quaternary similarities to connexons and different oligomerization numbers from each other. *J. Biol. Chem.* 285, 24420–24431.
- Anselmi, F., Hernandez, V. H., Crispino, G., Seydel, A., Ortolano, S., Roper, S. D., et al. (2008). ATP release through connexin hemichannels and gap junction transfer of second messengers propagate Ca<sup>2+</sup> signals across the inner ear. *Proc. Natl. Acad. Sci. U.S.A.* 105, 18770–18775.
- Arcuino, G., Lin, J. H., Takano, T., Liu, C., Jiang, L., Gao, Q., et al. (2002). Intercellular calcium signaling mediated by point-source burst release of ATP. *Proc. Natl. Acad. Sci. U.S.A.* 99, 9840–9845.
- Bao, L., Locovei, S., and Dahl, G. (2004). Pannexin membrane channels are mechanoinsensitive conduits for ATP. *FEBS Lett.* 572, 65–68.
- Baranova, A., Ivanov, D., Petrush, N., Pestova, A., Skoblov, M., Kelmanson, I., et al. (2004). The mammalian pannexin family is homologous to the invertebrate innexin gap junction proteins. *Genomics* 83, 706–716.
- Bargiotas, P., Krenz, A., Hormuzdi, S. G., Ridder, D. A., Herb, A., Barakat, W., et al. (2011). Pannexins in ischemia-induced neurodegeneration. *Proc. Natl. Acad. Sci. U.S.A.* 108, 20772–20777.
- Bargiotas, P., Monyer, H., and Schwaninger, M. (2009). Hemichannels in cerebral ischemia. *Curr. Mol. Med.* 9, 186–194.
- Begley, C. G., and Ellis, L. M. (2012). Drug development: raise standards for preclinical cancer research. *Nature* 483, 531–533.
- Boassa, D., Ambrosi, C., Qiu, F., Dahl, G., Gaietta, G., and Sosinsky, G. (2007). Pannexin1 channels contain a glycosylation site that targets the hexamer to the plasma membrane. *J. Biol. Chem.* 282, 31733–31743.
- Boassa, D., Qiu, F., Dahl, G., and Sosinsky, G. (2008). Trafficking dynamics of glycosylated pannexin 1 proteins. *Cell Commun. Adhes.* 15, 119–132.
- Bouwer, J., Astakov, V., Wong, W., Molina, T., Rowley, V., Lamont, S., et al. (2011). Petabyte data management and automated data workflow in neuroscience: delivering data from the instruments to the researcher’s fingertips. *Microsc. Microanal.* 17, 276–277.

- Bruzzone, R., Barbe, M. T., Jakob, N. J., and Monyer, H. (2005). Pharmacological properties of homomeric and heteromeric pannexin hemichannels expressed in *Xenopus* oocytes. *J. Neurochem.* 92, 1033–1043.
- Bruzzone, R., Hormuzdi, S. G., Barbe, M. T., Herb, A., and Monyer, H. (2003). Pannexins, a family of gap junction proteins expressed in brain. *Proc. Natl. Acad. Sci. U.S.A.* 100, 13644–13649.
- Burns, A. R., Phillips, S. C., and Sokoya, E. M. (2012). Pannexin protein expression in the rat middle cerebral artery. *J. Vasc. Res.* 49, 101–110.
- Burnstock, G. (2011). Introductory overview of purinergic signalling. *Front. Biosci. (Elite Ed.)* 3, 896–900.
- Chekeni, F. B., Elliott, M. R., Sandilos, J. K., Walk, S. F., Kinchen, J. M., Lazarowski, E. R., et al. (2010). Pannexin 1 channels mediate ‘find-me’ signal release and membrane permeability during apoptosis. *Nature* 467, 863–867.
- Chow, S. K., Hakozaki, H., Price, D. L., MacLean, N. A., Deerinck, T. J., Bouwer, J. C., et al. (2006). Automated microscopy system for mosaic acquisition and processing. *J. Microsc.* 222, 76–84.
- Cornell-Bell, A. H., Finkbeiner, S. M., Cooper, M. S., and Smith, S. J. (1990). Glutamate induces calcium waves in cultured astrocytes: long-range glial signaling. *Science* 247, 470–473.
- Dolmatova, E., Spagnol, G., Boassa, D., Baum, J. R., Keith, K., Ambrosi, C., et al. (2012). Cardiomyocyte ATP release through pannexin 1 aids in early fibroblast activation. *Am. J. Physiol. Heart Circ. Physiol.* 303, H1208–H1218.
- Dubyak, G. R. (2009). Both sides now: multiple interactions of ATP with pannexin-1 hemichannels. Focus on “A permeant regulating its permeation pore: inhibition of pannexin 1 channels by ATP.” *Am. J. Physiol. Cell Physiol.* 296, C235–C241.
- Dvortanchikova, G., Ivanov, D., Panchin, Y., and Shestopalov, V. I. (2006a). Expression of pannexin family of proteins in the retina. *FEBS Lett.* 580, 2178–2182.
- Dvortanchikova, G., Ivanov, D., Pestova, A., and Shestopalov, V. (2006b). Molecular characterization of pannexins in the lens. *Mol. Vis.* 12, 1417–1426.
- Ernsberger, P., Iacovitti, L., and Reis, D. J. (1990). Astrocytes cultured from specific brain regions differ in their expression of adrenergic binding sites. *Brain Res.* 517, 202–208.
- Fields, R. D., and Stevens, B. (2000). ATP: an extracellular signaling molecule between neurons and glia. *Trends Neurosci.* 23, 625–633.
- Gardner, D., Akil, H., Ascoli, G. A., Bowden, D. M., Bug, W., Donohue, D. E., et al. (2008). The neuroscience information framework: a data and knowledge environment for neuroscience. *Neuroinformatics* 6, 149–160.
- Gong, S., Zheng, C., Doughty, M. L., Losos, K., Didkovsky, N., Schambra, U. B., et al. (2003). A gene expression atlas of the central nervous system based on bacterial artificial chromosomes. *Nature* 425, 917–925.
- Herkenham, M., Rathore, P., Brown, P., and Listwak, S. J. (2011). Cautionary notes on the use of NF-kappaB p65 and p50 antibodies for CNS studies. *J. Neuroinflammation* 8, 141.
- Huang, Y., Grinspan, J. B., Abrams, C. K., and Scherer, S. S. (2007). Pannexin 1 is expressed by neurons and glia but does not form functional gap junctions. *Glia* 55, 46–56.
- Huang, Y. A., Stone, L. M., Pereira, E., Yang, R., Kinnamon, J. C., Dvoryanchikov, G., et al. (2011). Knocking out P2X receptors reduces transmitter secretion in taste buds. *J. Neurosci.* 31, 13654–13661.
- Iglesias, R., Dahl, G., Qiu, F., Spray, D. C., and Scemes, E. (2009). Pannexin 1: the molecular substrate of astrocyte “hemichannels.” *J. Neurosci.* 29, 7092–7097.
- Kanneganti, T. D., Lamkanfi, M., Kim, Y. G., Chen, G., Park, J. H., Franchi, L., et al. (2007). Pannexin-1-mediated recognition of bacterial molecules activates the cryopyrin inflammasome independent of Toll-like receptor signaling. *Immunity* 26, 433–443.
- Karpuk, N., Burkovetskaya, M., Fritz, T., Angle, A., and Kielian, T. (2011). Neuroinflammation leads to region-dependent alterations in astrocyte gap junction communication and hemichannel activity. *J. Neurosci.* 31, 414–425.
- Kenyon, K. A., Bushong, E. A., Mauer, A. S., Strehler, E. E., Weinberg, R. J., and Burette, A. C. (2010). Cellular and subcellular localization of the neuron-specific plasma membrane calcium ATPase PMCA1a in the rat brain. *J. Comp. Neurol.* 518, 3169–3183.
- Kienitz, M. C., Bender, K., Dermietzel, R., Pott, L., and Zoidl, G. (2011). Pannexin 1 constitutes the large conductance cation channel of cardiac myocytes. *J. Biol. Chem.* 286, 290–298.
- Kim, J. E., and Kang, T. C. (2011). The P<sub>2</sub>X<sub>7</sub> receptor-pannexin-1 complex decreases muscarinic acetylcholine receptor-mediated seizure susceptibility in mice. *J. Clin. Invest.* 121, 2037–2047.
- Lein, E. S., Hawrylycz, M. J., Ao, N., Ayres, M., Bensinger, A., Bernard, A., et al. (2007). Genome-wide atlas of gene expression in the adult mouse brain. *Nature* 445, 168–176.
- Li, S., Tomic, M., and Stojilkovic, S. S. (2011). Characterization of novel Pannexin 1 isoforms from rat pituitary cells and their association with ATP-gated P2X channels. *Gen. Comp. Endocrinol.* 174, 202–210.
- Locovei, S., Bao, L., and Dahl, G. (2006a). Pannexin 1 in erythrocytes: function without a gap. *Proc. Natl. Acad. Sci. U.S.A.* 103, 7655–7659.
- Locovei, S., Wang, J., and Dahl, G. (2006b). Activation of pannexin 1 channels by ATP through P2Y receptors and by cytoplasmic calcium. *FEBS Lett.* 580, 239–244.
- Locovei, S., Scemes, E., Qiu, F., Spray, D. C., and Dahl, G. (2007). Pannexin 1 is part of the pore forming unit of the P<sub>2</sub>X<sub>7</sub> receptor death complex. *FEBS Lett.* 581, 483–488.
- Lohman, A. W., Billaud, M., Straub, A. C., Johnstone, S. R., Best, A. K., Lee, M., et al. (2012). Expression of pannexin isoforms in the systemic murine arterial network. *J. Vasc. Res.* 49, 405–416.
- MacArthur, D. (2012). Methods: face up to false positives. *Nature* 487, 427–428.
- MacVicar, B. A., and Thompson, R. J. (2010). Non-junction functions of pannexin-1 channels. *Trends Neurosci.* 33, 93–102.
- Martone, M., Gupta, A., Wong, M., Qian, X., Sosinsky, G., Ludascher, B., et al. (2002). A cell-centered database for electron tomographic data. *J. Struct. Biol.* 138, 145.
- Martone, M. E., Tran, J., Wong, W. W., Sargis, J., Fong, L., Larson, S., et al. (2008). The cell centered database project: an update on building community resources for managing and sharing 3D imaging data. *J. Struct. Biol.* 161, 220–231.
- Nedergaard, M., Ransom, B., and Goldman, S. A. (2003). New roles for astrocytes: redefining the functional architecture of the brain. *Trends Neurosci.* 26, 523–530.
- Newman, E. A. (2003). New roles for astrocytes: regulation of synaptic transmission. *Trends Neurosci.* 26, 536–542.
- Nishida, M., Sato, Y., Uemura, A., Narita, Y., Tozaki-Saitoh, H., Nakaya, M., et al. (2008). P<sub>2</sub>Y<sub>6</sub> receptor-Galpha12/13 signalling in cardiomyocytes triggers pressure overload-induced cardiac fibrosis. *EMBO J.* 27, 3104–3115.
- Paxinos, G., and Watson, W. (1998). *The Rat Brain in Stereotaxic Coordinates*. San Diego: Academic Press.
- Pelegrin, P., Barroso-Gutierrez, C., and Surprenant, A. (2008). P<sub>2</sub>X<sub>7</sub> receptor differentially couples to distinct release pathways for IL-1beta in mouse macrophage. *J. Immunol.* 180, 7147–7157.
- Pelegrin, P., and Surprenant, A. (2006). Pannexin-1 mediates large pore formation and interleukin-1beta release by the ATP-gated P<sub>2</sub>X<sub>7</sub> receptor. *EMBO J.* 25, 5071–5082.
- Penuela, S., Bhalla, R., Gong, X. Q., Cowan, K. N., Celetti, S. J., Cowan, B. J., et al. (2007). Pannexin 1 and pannexin 3 are glycoproteins that exhibit many distinct characteristics from the connexin family of gap junction proteins. *J. Cell. Sci.* 120, 3772–3783.
- Penuela, S., Bhalla, R., Nag, K., and Laird, D. W. (2009). Glycosylation regulates pannexin intermixing and cellular localization. *Mol. Biol. Cell* 20, 4313–4323.
- Poornima, V., Madhupriya, M., Kootar, S., Sujatha, G., Kumar, A., and Bera, A. K. (2011). P<sub>2</sub>X<sub>7</sub> Receptor-pannexin 1 hemichannel association: effect of extracellular calcium on membrane permeabilization. *J. Mol. Neurosci.* 46, 585–594.
- Qiu, F., and Dahl, G. (2009). A permeant regulating its permeation pore: inhibition of pannexin 1 channels by ATP. *Am. J. Physiol. Cell Physiol.* 296, C250–C255.
- Qiu, F., Wang, J., Spray, D. C., Scemes, E., and Dahl, G. (2011). Two non-vesicular ATP release pathways in the mouse erythrocyte membrane. *FEBS Lett.* 585, 3430–3435.
- Qu, Y., Misaghi, S., Newton, K., Gilmour, L. L., Louie, S., Cupp, J. E., et al. (2011). Pannexin-1 is required for ATP release during apoptosis but not for inflammasome activation. *J. Immunol.* 186, 6553–6561.
- Ransford, G. A., Fregien, N., Qiu, F., Dahl, G., Conner, G. E., and Salathe, M. (2009). Pannexin 1 contributes to ATP release in airway epithelia. *Am. J. Respir. Cell Mol. Biol.* 41, 525–534.
- Ray, A., Zoidl, G., Wahle, P., and Dermietzel, R. (2006). Pannexin expression in the cerebellum. *Cerebellum* 5, 189–192.
- Ray, A., Zoidl, G., Weickert, S., Wahle, P., and Dermietzel, R. (2005). Site-specific and developmental expression of pannexin1 in the mouse nervous system. *Eur. J. Neurosci.* 21, 3277–3290.

- Romanov, R. A., Rogachevskaja, O. A., Bystrova, M. F., Jiang, P., Margolskee, R. F., and Kolesnikov, S. S. (2007). Afferent neurotransmission mediated by hemichannels in mammalian taste cells. *EMBO J.* 26, 657–667.
- Santiago, M. F., Veliskova, J., Patel, N. K., Lutz, S. E., Caille, D., Charollais, A., et al. (2011). Targeting pannexin1 improves seizure outcome. *PLoS ONE* 6:e25178. doi:10.1371/journal.pone.0025178
- Scemes, E., Suadicani, S. O., Dahl, G., and Spray, D. C. (2007). Connexin and pannexin mediated cell-cell communication. *Neuron Glia Biol.* 3, 199–208.
- Schenk, U., Westendorf, A. M., Radaelli, E., Casati, A., Ferro, M., Fumagalli, M., et al. (2008). Purinergic control of T cell activation by ATP released through pannexin-1 hemichannels. *Sci. Signal.* 1, ra6.
- Silverman, W. R., De Rivero Vaccari, J. P., Locovei, S., Qiu, F., Carlsson, S. K., Scemes, E., et al. (2009). The pannexin 1 channel activates the inflamasome in neurons and astrocytes. *J. Biol. Chem.* 284, 18143–18151.
- Sosinsky, G. E., Boassa, D., Dermietzel, R., Duffy, H. S., Laird, D. W., Macvicar, B., et al. (2011). Pannexin channels are not gap junction hemichannels. *Channels (Austin)* 5, 193–197.
- Sosinsky, G. E., Solan, J. L., Gaietta, G. M., Ngan, L., Lee, G. J., MacKey, M. R., et al. (2007). The C-terminus of connexin43 adopts different conformations in the Golgi and gap junction as detected with structure-specific antibodies. *Biochem. J.* 408, 375–385.
- Suadicani, S. O., Iglesias, R., Wang, J., Dahl, G., Spray, D. C., and Scemes, E. (2012). ATP signaling is deficient in cultured Pannexin1-null mouse astrocytes. *Glia* 60, 1106–1116.
- Tang, W., Ahmad, S., Shestopalov, V. I., and Lin, X. (2008). Pannexins are new molecular candidates for assembling gap junctions in the cochlea. *Neuroreport* 19, 1253–1257.
- Testa, G., Schaft, J., Van Der Hoeven, F., Glaser, S., Anastassiadis, K., Zhang, Y., et al. (2004). A reliable lacZ expression reporter cassette for multipurpose, knockout-first alleles. *Genesis* 38, 151–158.
- Thompson, R. J., Jackson, M. F., Olah, M. E., Rungra, R. L., Hines, D. J., Beazley, M. A., et al. (2008). Activation of pannexin-1 hemichannels augments aberrant bursting in the hippocampus. *Science* 322, 1555–1559.
- Thompson, R. J., Zhou, N., and MacVicar, B. A. (2006). Ischemia opens neuronal gap junction hemichannels. *Science* 312, 924–927.
- Vessey, D. A., Li, L., and Kelley, M. (2011). P<sub>2</sub>X<sub>7</sub> receptor agonists pre- and postcondition the heart against ischemia-reperfusion injury by opening pannexin-1/P<sub>2</sub>X<sub>7</sub> channels. *Am. J. Physiol. Heart Circ. Physiol.* 301, H881–H887.
- Vogt, A., Hormuzdi, S. G., and Monyer, H. (2005). Pannexin1 and Pannexin2 expression in the developing and mature rat brain. *Brain Res. Mol. Brain Res.* 141, 113–120.
- Volterra, A., and Steinhauser, C. (2004). Glial modulation of synaptic transmission in the hippocampus. *Glia* 47, 249–257.
- von Wasielewski, R., Werner, M., Nolte, M., Wilkens, L., and Georgii, A. (1994). Effects of antigen retrieval by microwave heating in formalin-fixed tissue sections on a broad panel of antibodies. *Histochemistry* 102, 165–172.
- Wang, X. H., Streeter, M., Liu, Y. P., and Zhao, H. B. (2009). Identification and characterization of pannexin expression in the mammalian cochlea. *J. Comp. Neurol.* 512, 336–346.
- Weickert, S., Ray, A., Zoidl, G., and Dermietzel, R. (2005). Expression of neural connexins and pannexin1 in the hippocampus and inferior olive: a quantitative approach. *Brain Res. Mol. Brain Res.* 133, 102–109.
- Zappala, A., Cicero, D., Serapide, M. F., Paz, C., Catania, M. V., Falchi, M., et al. (2006). Expression of pannexin1 in the CNS of adult mouse: cellular localization and effect of 4-aminopyridine-induced seizures. *Neuroscience* 141, 167–178.
- Zappala, A., Li Volti, G., Serapide, M. F., Pellitteri, R., Falchi, M., La Delia, F., et al. (2007). Expression of pannexin2 protein in healthy and ischemized brain of adult rats. *Neuroscience* 148, 653–667.
- Zhang, L., Deng, T., Sun, Y., Liu, K., Yang, Y., and Zheng, X. (2008). Role for nitric oxide in permeability of hippocampal neuronal hemichannels during oxygen glucose deprivation. *J. Neurosci. Res.* 86, 2281–2291.
- Zoidl, G., Petrasch-Parwez, E., Ray, A., Meier, C., Bunse, S., Habbes, H. W., et al. (2007). Localization of the pannexin1 protein at postsynaptic sites in the cerebral cortex and hippocampus. *Neuroscience* 146, 9–16.
- Conflict of Interest Statement:** The authors declare that the research was conducted in the absence of any commercial or financial relationships that could be construed as a potential conflict of interest.
- Received: 19 October 2012; paper pending published: 05 November 2012; accepted: 09 January 2013; published online: 06 February 2013.*
- Citation: Cone AC, Ambrosi C, Scemes E, Martone ME and Sosinsky GE (2013) A comparative antibody analysis of Pannexin1 expression in four rat brain regions reveals varying subcellular localizations. *Front. Pharmacol.* 4:6. doi: 10.3389/fphar.2013.00006*
- This article was submitted to Frontiers in Pharmacology of Ion Channels and Channelopathies, a specialty of Frontiers in Pharmacology.*
- Copyright © 2013 Cone, Ambrosi, Scemes, Martone and Sosinsky. This is an open-access article distributed under the terms of the Creative Commons Attribution License, which permits use, distribution and reproduction in other forums, provided the original authors and source are credited and subject to any copyright notices concerning any third-party graphics etc.*



# Regulation of gap junctions by nitric oxide influences the generation of arrhythmias resulting from acute ischemia and reperfusion *in vivo*

Ágnes Végh\*, Márton Gönczi, Gottfried Miskolczi and Mária Kovács

Department of Pharmacology and Pharmacotherapy, University of Szeged, Szeged, Hungary

**Edited by:**

Aida Salameh, Heart Centre  
University of Leipzig, Germany

**Reviewed by:**

Stephane Hatem, University of Pierre  
and Marie Curie, France  
Cor De Wit, Universität zu Lübeck,  
Germany

**\*Correspondence:**

Ágnes Végh, Department of  
Pharmacology and Pharmacotherapy,  
University of Szeged, Dóm tér 12,  
6720 Szeged, Hungary  
e-mail: vegh.agnes@med.u-szeged.hu

Myocardial ischemia resulting from sudden occlusion of a coronary artery is one of the major causes in the appearance of severe, often life-threatening ventricular arrhythmias. Although the underlying mechanisms of these acute arrhythmias are many and varied, there is no doubt that uncoupling of gap junctions (GJs) play an important role especially in arrhythmias that are generated during phase Ib, and often terminate in sudden cardiac death. In the past decades considerable efforts have been made to explore mechanisms which regulate the function of GJs, and to find new approaches for protection against arrhythmias through the modulation of GJs. These investigations led to the development of GJ openers and inhibitors. The pharmacological modulation of GJs, however, resulted in conflicting results. It is still not clear whether opening or closing of GJs would be advantageous for the ischemic myocardium. Both maneuvers can result in protection, depending on the models, endpoints and the time of opening and closing of GJs. Furthermore, although there is substantial evidence that preconditioning decreases or delays the uncoupling of GJs, the precise mechanisms by which this attains have not yet been elucidated. In our own studies in anesthetized dogs preconditioning suppressed the ischemia and reperfusion-induced ventricular arrhythmias, and this protection was associated with the preservation of GJ function, manifested in less marked changes in electrical impedance, as well as in the maintenance of GJ permeability and phosphorylation of connexin43. Since we have substantial previous evidence that nitric oxide (NO) is an important trigger and mediator of the preconditioning-induced antiarrhythmic protection, we hypothesized that NO, among its several effects, may lead to this protection by influencing cardiac GJs. The hypotheses and theories relating to the pharmacological modulation of GJs will be discussed with particular attention to the role of NO.

**Keywords:** ischemia/reperfusion, arrhythmias, gap junction, nitric oxide

## INTRODUCTION

Traveling on the London underground you may frequently hear “Mind the gap! Mind the gap!” This warning call is also valid for the heart when the genesis of arrhythmias is considered. Gaps not only separate but also connect cells by forming special channels, termed gap junctions (GJs), which allow fast electrical and metabolic cross-talk between the neighboring cells. In myocardial tissue, these GJ channels are accumulated in clusters located in the intercalated disks, and they represent low resistance pathways between the adjacent cells, allowing fast spread of impulse from the one cell to the other (electrical coupling). These channels can also transfer small molecules (less than 1,000 Da) resulting in tight metabolic intercellular communication (metabolic coupling). Since, the shape of the ventricular cardiomyocytes is elongated and the GJs are preferably located in the longitudinal end of the cell, under normal conditions, the action potential is propagated in longitudinal direction (Spach et al., 1981; Rudy and Quan, 1987; Peters and Wit, 1998; Rohr, 2004). This uniform anisotropy that mainly results from the structural

arrangement (longitudinal vs. transversal) and electrical properties of GJs (low resistance), makes possible that the heart behaves as an electrical syncytium. However, under pathologic conditions, such as the acute myocardial ischemia, as the consequence of the rapid metabolic changes (Shaw and Rudy, 1997), these GJs are uncoupled, resulting in the closure of the low resistance pathways and changes in impulse propagation. In homogeneity (non-uniform anisotropy) develops within the cardiac tissue as regards the electrical conduction, which leads ultimately to arrhythmia generation (Spear et al., 1992; De Groot and Coronel, 2004).

The present paper will focus on the role of GJs in the generation of ventricular arrhythmias due to acute myocardial ischemia. We will discuss how the pharmacological modulation of GJs would influence these ischemia-induced early ventricular arrhythmias, and put forth a hypothesis, based mainly on our own studies in anesthetized dogs, that nitric oxide (NO), an important endogenous modulator of heart function, may also regulate cardiac GJs. We provide evidence that the effect of NO on GJs might have a

role in the cardioprotective (antiarrhythmic) effect of preconditioning and NO donors.

## THE ROLE OF GAP JUNCTIONS IN THE ACUTE ISCHEMIA-INDUCED VENTRICULAR ARRHYTHMIAS

There seems to be consensus in respect that arrhythmias occurring soon (within 3 min) after the onset of the coronary artery occlusion result from those ionic and electrophysiological changes which are due to the rapid switch of myocardial metabolism from aerobic to anaerobic mode (Janse et al., 1986). These metabolic changes (loss of ATP, fall in intracellular pH, accumulation of lactate, etc.) are apparent within seconds or minutes after the onset of ischemia and directly affect the function of ion channels and exchangers, resulting in considerable alterations in impulse generation and conduction (Cascio, 2001). Without going into details, conditions develop during this early phase of ischemia favor reentry, which is thought to be the main mechanism underlying the phase Ia arrhythmias (Kléber, 1983; Janse et al., 1986).

Although processes underlying generation of phase Ib arrhythmias are less well understood, there is no doubt that uncoupling of GJs play an important role. As is mentioned above in the uniformly anisotropic heart the transfer of an impulse is largely dependent upon the resistance of GJs, which is lower in longitudinal than transversal direction (Hoyt et al., 1989; Saffitz et al., 1995). This provides longitudinal preference over transversal conduction (Spach et al., 1981; Peters and Wit, 1998) and a safety for normal cell-to-cell impulse propagation (Spach and Heidlage, 1995). However, under ischemic conditions, particularly with the progression of ischemia, the further loss of ATP and intracellular K<sup>+</sup>, the accumulation of harmful metabolites and ions, the release of catecholamines, etc., would result in a milieu in which the uncoupling of GJs increases (White et al., 1990; Dhein, 1998). This leads to non-uniform changes in tissue resistance and inhomogeneous impulse conduction (Wojtczak, 1979; Kléber et al., 1987; Cascio et al., 2005) which initiate and maintain reentry during phase Ib (Spach et al., 1988). On the other hand, the increased resistance resulting from interruption of cell-to-cell coupling decreases the injury current, although at moderate levels of uncoupling this current would still be sufficient to induce delayed after-depolarization and trigger focal activity (Janse and van Capelle, 1982). Another consequence of the “metabolic overload” in the ischemic myocardium which largely accounts for the uncoupling of GJs is the reduced phosphorylation of connexin43 (Cx43), which is the primary structural protein of GJs in the ventricle (Söhl and Willecke, 2004). The ischemia-induced dephosphorylation of Cx43 results in conformational changes in connexin and leads to the closure of GJs and translocation of Cx43 from the membrane to the cytosol (Beardslee et al., 2000). This ischemia-induced Cx43 dephosphorylation and the subsequent closure of GJs occurs within 30 min (Beardslee et al., 2000; Schulz et al., 2003), making possible to use the measurement of Cx43 phosphorylation as a tool for the assessment of GJ function even during such a relatively short period of ischemia.

Functionally, GJ channels can be in open and closed state, although the conductance of a single channel may vary between several states – from closed, residual to the several levels of conducting (open) states – which are regulated by phosphorylation

of the C-terminal of the connexin (Kwak and Jongsma, 1996). The assessment of GJ function particularly under *in vivo* conditions is rather difficult. Most of the currently used methods provide only indirect evidence on the coupling status of GJs. Measurement of GJ permeability using small molecular weight dyes (Ruiz-Meana et al., 2001) or the determination of connexin phosphorylation (Ando et al., 2005) allows evaluation of coupling only at a certain time point. Although measuring conduction velocity by activation mapping techniques (Rohr et al., 1998; Henriquez et al., 2001), or tissue impedance (resistivity and phase angle) changes by the use of a four-pin electrode method (Kléber et al., 1987; Cinca et al., 1997; Padilla et al., 2003) make possible continuous recording, these methods represent also only indirect assessment of GJ function. These methodological problems have been discussed in details previously (Garcia-Dorado et al., 2004; Végh and Papp, 2011). Nevertheless, despite these difficulties the combination of the available methods and techniques allow us to estimate the function of GJs and their role in arrhythmogenesis under various physiological and pathophysiological conditions.

## THE ROLE OF GAP JUNCTIONS IN ARRHYTHMOGENESIS AND IN THE ANTIARRHYTHMIC EFFECT OF PRECONDITIONING

There were two studies (Smith et al., 1995; Cinca et al., 1997), both performed in anesthetized pigs, which provided the first *in vivo* evidence that GJs play an important role in the generation of the ischemia-induced ventricular arrhythmias. The first study pointed out a relationship between changes in tissue impedance and the occurrence of arrhythmias, showing that the appearance of phase Ib arrhythmias during a 60-min coronary artery occlusion was preceded by a steep increase in tissue resistivity around the 15 min of ischemia (Smith et al., 1995). The second study (Cinca et al., 1997) reported that ischemic preconditioning delays uncoupling of GJs and shifts the onset of the Ib phase arrhythmias to a later period of the ischemia. Our own studies in dogs (Papp et al., 2007) showed somewhat similar results, but the rise in tissue resistivity prior to the occurrence of the phase Ib arrhythmias was not as marked as either in pigs (Smith et al., 1995) or isolated heart preparation (Kléber et al., 1987). Furthermore, preconditioning in dogs not only delayed but significantly decreased the tissue impedance changes (Papp et al., 2007) and, as that we have pointed out previously (Végh et al., 1992a), preconditioning resulted in an absolute reduction in the number and severity of arrhythmias without shifting them to a later period of the occlusion. Preconditioning also preserved GJ permeability and phosphorylation of Cx43 determined both at 25 and 60 min of ischemia, suggesting that preconditioning in this species not only delays but indeed reduces the closure of GJs (Papp et al., 2007). There might be many explanations of these dissimilarities, among which the difference in the preexisting collateral system between dogs and pigs seems to play a major role. This has been thoroughly discussed previously (Végh and Papp, 2011).

Although the mechanisms by which preconditioning influences GJ coupling has not yet been elucidated, it seems reasonable to hypothesize that mediators and signaling pathways, which are thought to play role in this form of cardioprotection, may target

and modify GJs, perhaps at the level of connexins. This hypothesis is supported by the fact that GJ channels exist and can switch between various conductance states, which depend on the phosphorylation status of connexins (Kwak et al., 1995; Kwak and Jongsma, 1996). The phosphorylation of the C-terminal of connexins, which determines whether GJs are in open or closed state, involves kinases or kinase-mediated signaling pathways which are activated in response to a preconditioning stimulus. Thus, several kinases, such as protein kinase A (PKA), the various isoforms of PKC, PKG, as well as mitogen-activated protein (MAP) and tyrosine kinases (TK), etc., which have been identified as parts of the preconditioning-induced signaling cascade (Downey et al., 2008), were also shown to target connexins (Dhein, 2004; Salameh and Dhein, 2005). For example, the preconditioning-induced reduction in myocardial damage was associated with a PKC-activated enhanced Cx43 phosphorylation in the rabbit isolated hearts (Miura et al., 2004).

Since the different kinases and kinase isoforms may phosphorylate connexins differently, the resulting responses regarding the regulation of GJ coupling would also be different. Indeed, there are many, sometimes conflicting results reported in both normal and diseased hearts as concerns the activation of a certain kinase pathway and changes in GJ function (Salameh and Dhein, 2005; Dhein et al., 2011). These differences seem to largely depend on the preparations, models and species used, as well as on the experimental conditions applied. Since the regulatory role of the various kinase and signaling pathways on GJs have been excellently discussed previously (e.g., Dhein, 1998; Salameh and Dhein, 2005), it is not purposed to discuss these further. *Nota bene* the exploration of mechanisms which affect GJ function led to the idea that the generation of arrhythmias might be influenced through the modulation of GJs (Dhein et al., 2010).

## PHARMACOLOGICAL MODIFICATION OF GAP JUNCTIONAL COUPLING AND ARRHYTHMIAS

During the past two decades, a number of drugs have been described and developed which facilitate or inhibit the coupling of GJs (reviewed by Dhein, 2004; Dhein et al., 2010). These were used, in part, as tools for obtaining information on the physiological and pathophysiological roles of GJs, in part, as drugs purposing to develop novel antiarrhythmic therapy (Dhein and Tudyka, 1995; Dhein, 2004; Salameh and Dhein, 2005). However, the pharmacological modification of GJ coupling raises also many questions, in particular, when the acute ischemia-induced ventricular arrhythmias are considered. It is still not clear whether opening or closing of GJs during ischemia would be advantageous for arrhythmia suppression. As we, and others (De Groot et al., 2001; De Groot and Coronel, 2004; Végh and Papp, 2011) have suggested both maneuvers can result in protection. There is no doubt that keeping GJs open during ischemia and thereby maintaining conduction velocity (De Groot and Coronel, 2004) would result in an antiarrhythmic effect. This has been proved by several *in vitro* and *in vivo* studies using synthetic antiarrhythmic peptides, such as AAP10 and rotigaptide (Dhein et al., 1994; Müller et al., 1997; Grover and Dhein, 2001; Xing et al., 2003, 2005; Végh and Papp, 2011). However, more controversial results were obtained with the use of uncouplers, indicating the complexity of the regulation

of GJs in both normal and diseased hearts (Garcia-Dorado et al., 1997; Salameh and Dhein, 2005). These differences may be related to the uncoupler used, the model and endpoint examined, as well as the time of administration of the uncoupler to close GJs (Végh and Papp, 2011).

We have experimental evidence that in dogs both the GJ opener rotigaptide and the uncoupler carbenoxolone given prior to and during coronary artery occlusion protected against the ischemia-induced severe ventricular arrhythmias (Végh and Papp, 2011). The fact that the uncoupler carbenoxolone induced an antiarrhythmic effect was indeed surprising, since one would have expected that closing of GJs during ischemia result in enhanced gap junctional uncoupling and arrhythmias. The results of tissue resistivity measurements showed that immediately after the onset of the coronary artery occlusion the decline in phase angle (a measure of increased membrane capacitance due to closure of GJs; Padilla et al., 2003) was more marked in the carbenoxolone treated dogs than in the controls (Papp et al., 2008; Végh and Papp, 2011). Although these early impedance changes are thought not to be attributed to closure of GJs (Kléber et al., 1987), it cannot rule out the possibility that there might be cells within the ischemic area which are severely injured and uncoupled even soon after the onset of the coronary artery occlusion (Wolk et al., 1999; Daleau et al., 2001; Vetterlein et al., 2006). Furthermore, in dogs infused with carbenoxolone the steep increase in resistivity and decline in phase angle that occur usually around the 15 min of the occlusion were also absent. In these dogs the two characteristic arrhythmia phases disappeared, and although ectopic activity could be observed over the entire occlusion period, the total number of ectopic beats was significantly less than in the controls (Végh and Papp, 2011). We proposed that this finding could perhaps be associated with the phenomenon termed “paradoxical restoration of conduction” (Rohr et al., 1997). This suggests that in the border zone, the viable cells are electrically depressed through electrotonic interactions from their neighboring ischemic cells resulting in slowing of conduction (De Groot and Coronel, 2004). However, with the facilitation of uncoupling, such as may occur during ischemia in the presence of an uncoupler, this electrotonic interaction decreases, resulting in an improvement in conduction and, subsequently, a reduction in arrhythmia severity (De Groot and Coronel, 2004). Whatever the precise mechanism is, it seems that carbenoxolone given prior to and during ischemia attenuates impedance changes during the “critical” phase of ischemia and reduces phase Ib arrhythmias, and this effect is similar to that seen with the GJ opener rotigaptide and with preconditioning (Papp et al., 2008; Végh and Papp, 2011).

Interestingly, carbenoxolone almost completely abolished the antiarrhythmic effect of ischemic preconditioning. When it was given prior to and during the preconditioning procedure (two 5-min occlusion and reperfusion insults) both the impedance changes and the ectopic activity were markedly increased during the short ischemic periods compared to the preconditioned dogs without carbenoxolone administration (Papp et al., 2007). In these carbenoxolone treated preconditioned dogs the tissue impedance changes during the prolonged occlusion were as marked as in the non-preconditioned controls, and the severity of arrhythmias, particularly during phase Ib, was also substantially increased.

Furthermore, preservation of the phosphorylated form of Cx43 afforded by preconditioning was abolished with the administration of carbenoxolone. Our conclusion was that closing of GJs prior to preconditioning perhaps inhibits the transfer of endogenous substances that are released by the short preconditioning ischemia and reperfusion insults thus inhibiting the activation of signaling pathways leading to cardioprotection (Papp et al., 2007).

As has been mentioned above, many endogenous substances are thought to regulate GJs function by activating various protein kinases (Dhein, 1998; Salameh and Dhein, 2005). Our previous research focused on the exploration of mechanisms involved in the antiarrhythmic effect of ischemic preconditioning, provided substantial evidence that NO is one of the key mediators which plays essential trigger and mediator role in the preconditioning-induced cardioprotection (Végh et al., 1992c). Thus it seemed reasonable to hypothesize that the antiarrhythmic effect of preconditioning and of NO donors (György et al., 2000) may, in part, be accomplished through the modulation of GJ channels.

## EVIDENCE FOR THE ROLE OF NITRIC OXIDE IN THE REGULATION OF CARDIAC GAP JUNCTIONS

The evidence that NO may modulate GJ function comes mainly from studies in non-cardiac tissues (Roh et al., 2002; Patel et al., 2006), especially from those which are dealing with vessel physiology where NO is one of the most important physiological mediators (Kameritsch et al., 2003; Rodenwaldt et al., 2007). These studies showed that NO is able to modify GJ permeability (Bolanos and Medina, 1996; Kameritsch et al., 2003) and the expression of connexin isoforms (Roh et al., 2002; Hoffmann et al., 2003; Yao et al., 2005). This latter would be especially important under chronic conditions where the regulatory role of NO on the expression of connexins has to be considered in terms of the development of chronic heart diseases (Poelzing and Rosembaum, 2004; Akar et al., 2007; Kontogeorgis et al., 2008; Kim et al., 2010; Radosinska et al., 2011). Changes in Cx43 expression play also an important role in the delayed phase of cardioprotection induced by rapid cardiac pacing 24 h prior to ischemia in dogs (Gönczi et al., 2012). In case of the acute and shorter periods of ischemic challenge (such as a 30- to 60-min ischemia) and its arrhythmia consequences, the alterations of GJ conductance, resulting from changes in connexin phosphorylation, seem to be the more likely mechanism through which NO may modify GJ function. However, the signaling pathways, which regulate the level and phosphorylation status of Cx43 and thus modulate the GJ channel properties, are even less well understood in the myocardium than in the other non-cardiac tissues. For example, it has been proposed that stimulation of both  $\alpha_1$  and  $\beta$  adrenoceptors, although through the activation of different pathways and protein kinases (PKC and PKA, respectively), leads to connexin phosphorylation and to the opening of GJs (Saez et al., 1997; Weng et al., 2002). In contrast, the activation of the guanylyl cyclase-cGMP pathway and the subsequent stimulation of PKG would result in closing of these channels (Dhein, 1998). A more recent study, however, showed that in H9c2 cells, isolated from the rat myocardium, the hypoxia-induced loss in total Cx43 protein content was restored by acetylcholine and also by the administration of the NO donor S-nitroso-N-acetylpenicillamine (SNAP; Zhang et al., 2006). Since the protective effect of

acetylcholine was inhibited by L-NAME, it was suggested that acetylcholine prevents the hypoxia-induced decrease of Cx43 and improves GJ coupling via a NO-mediated pathway.

In our own studies, using sodium nitroprusside (SNP) as an NO donor and administered in intracoronary infusion 20 min prior to and throughout a 60-min occlusion period of the left anterior descending (LAD) coronary artery in anesthetized dogs, we have found that SNP almost completely abolished the severe ventricular ectopic activity and attenuated the increase in tissue resistivity but it did not substantially influence the decrease in phase angle that resulted from occlusion (Gönczi et al., 2009). In the presence of SNP infusion, there was indeed a more marked reduction in phase angle during the first 10-min period of occlusion; and this effect was very similar to that seen with the administration of carbenoxolone (Papp et al., 2008; Végh and Papp, 2011). Furthermore, SNP, like carbenoxolone, abrogated the steep decline in phase angle that occurred in the controls just prior to the appearance of the phase Ib arrhythmias; i.e., the impedance changes remained virtually constant during this critical period of ischemia (i.e., between 15 and 20 min). Despite similarities of impedance changes of SNP and carbenoxolone, these *in vivo* impedance measurements do not provide an answer to the question, as to whether NO, derived from SNP, opens or closes GJs, and whether opening or closing of GJs leads to the antiarrhythmic effect of SNP. However, the fact, that in the presence of SNP the rapid impedance changes that precede the occurrence of phase Ib arrhythmias were markedly attenuated (and in parallel the ectopic activity was virtually disappeared), suggests a preserved GJ function during ischemia and confirms that of our previous supposition that the rate of uncoupling prior to phase Ib is of particular importance in the generation of arrhythmias (Papp et al., 2007; Végh and Papp, 2011). A further evidence that NO may preserve GJ function derived from the *in vitro* measurements. These showed that compared to the controls, SNP maintained GJ permeability and Cx43 phosphorylation even after 60 min of ischemia. In the presence of SNP, the membrane fraction of Cx43 remained largely in phosphorylated form and the metabolic coupling of the adjacent cells was significantly improved. Thus it seems from these results that NO, derived from NO donors, protects the heart against the ischemia-induced early ventricular arrhythmias, and that this effect, at least in part, can be attributed to the effect of NO, or of the NO-stimulated pathways on GJs, as their function is largely preserved in the presence of SNP (Gönczi et al., 2009).

More recent experimental data resulting from the administration of sodium nitrite support this hypothesis. Under experimental conditions sodium nitrite is used as an exogenous nitrite source to prove the importance and the potential therapeutic benefit of nitrite anion. Inorganic nitrites and nitrates, which are natural oxidative metabolites of NO, have been considered for a long time as inert molecules playing not a compelling role in NO physiology. However, over the last decade emerging evidence suggests that inorganic nitrites and nitrates may serve as important reservoirs for NO (reviewed, e.g., Lundberg and Govoni, 2004; Lefer, 2009), since these metabolites, particularly under hypoxic and anoxic conditions, can readily be reduced back to NO (Zweier et al., 1995; Bryan, 2006). This mechanism may provide an increased NO availability under ischemic conditions independently from NO

synthase (NOS) activity which is otherwise reduced in the absence of oxygen (Zweier et al., 1995). A number of studies in various experimental animal models have proved that nitrite anion has an important biological function and might represent an effective means to attenuate ischemia and reperfusion injury (e.g., Webb et al., 2004; Duranski et al., 2005; Shiva et al., 2007).

Thus in our anesthetized dog model, we infused sodium nitrite intravenously in a dose of  $0.2 \mu\text{g kg}^{-1} \text{ min}^{-1}$ , starting the infusion 10 min prior to and maintained throughout the entire 25 min occlusion of the LAD coronary artery, and changes in tissue impedance in parallel with arrhythmia distribution were assessed (Gönczi et al., 2010). We found that in the presence of sodium nitrite infusion the total number of ventricular premature beats during the occlusion was markedly reduced ( $472 \pm 105$  vs.  $147 \pm 77$ ;  $P < 0.05$ ) and the impedance changes were substantially less pronounced than in the controls (Gönczi et al., 2010). This is illustrated in **Figure 1** which clearly shows that in dogs infused with sodium nitrite, the steep increase in resistivity and the decline in phase angle that usually occur around the 14–15 min of ischemia in the control animals were abrogated and the number of ectopic beats during phase Ib was markedly suppressed. In these experiments we also used a mapping electrode, which collects signals from 31 unipolar electrode points of the epicardial surface of the ischemic area in order to evaluate changes in the epicardial ST-segment and in total activation time (TAT) by creating ST and activation maps. The results show that compared with control dogs, in dogs infused with sodium nitrite both the ischemia-induced increases in epicardial ST-segment and TAT were considerable reduced (**Figure 2**). In this study, at the end of the 25 min occlusion period, myocardial tissue samples were taken from the hearts for the assessment of metabolic coupling and Cx43 phosphorylation, as has been described previously (Gönczi et al., 2009). **Figure 3A** shows that the administration of sodium nitrite preserved the phosphorylated form of Cx43 within the ischemic LAD area compared with the control hearts in which the occlusion of the LAD resulted in marked dephosphorylation of Cx43. GJ permeability, determined by double dye loading (Ruiz-Meana et al., 2001; Papp et al., 2007), was also maintained even after the 25 min of ischemia in hearts infused with sodium nitrite (**Figure 3B**).

The results support our previous proposal (Végh and Papp, 2011) that in arrhythmia point of view the modification of GJ function, for example, by preventing the ischemia-induced dephosphorylation of Cx43, would particularly be important during that “critical” phase of ischemia when the rate of uncoupling of GJs rapidly increases, and when other factors, implicated in arrhythmogenesis, are also present. Furthermore, we suggest that NO might be one of the endogenous substances which would regulate GJs not only in vascular tissues (reviewed recently by Loot-Wilson et al., 2012) but also in cardiac myocytes. There is emerging evidence for a cross-talk between NO signaling and connexins in the vasculature which is essential for normal vascular function (Looft-Wilson et al., 2012). Although a strong proof is lacking for such an NO-mediated modulation of GJ proteins in cardiac myocytes, we assume that there might be similar interactions between NO and GJs also within the myocardium, since NO derives either from the “classical” NO donors or inorganic nitrates, or generated during a preconditioning stimulus

influenced the electrical and metabolic properties of GJs and resulted in simultaneous alterations in arrhythmia generation. We have proposed previously the most likely scenario for the antiarrhythmic effect afforded by preconditioning is that the preconditioning stimulus triggers the generation and the release of NO from the vascular endothelial cells and also from cardiac myocytes (Parratt and Végh, 1996; Végh and Parratt, 1996). NO by diffusing to cardiac myocytes stimulates soluble guanylyl cyclase and increases cGMP within the myocardium since the inhibition of soluble guanylyl cyclase completely abolished the antiarrhythmic protection (Végh et al., 1992b). cGMP could modify arrhythmogenesis by a number of ways involving the inhibition of calcium entry through L-type calcium channels (Sun et al., 2007), modification of the cGMP/cAMP balance by influencing cGMP-dependent phosphodiesterase and/or the direct depression of cardiac myocytes, resulting in reduced oxygen demand during prolonged ischemia (Parratt and Végh, 1996; Végh and Parratt, 1996). There is evidence that in vascular endothelium both the endogenously produced (Straub et al., 2011) and the exogenously administered (Hoffmann et al., 2003; Rodenwaldt et al., 2007) NO can acutely increase GJ coupling by a cGMP-dependent mechanism. cGMP through the inhibition of the cGMP-dependent phosphodiesterase prevents the degradation of cAMP and stimulates the cAMP-PKA pathway (Francis et al., 2010). This has been shown to enhance the coupling of GJs (Hoffmann et al., 2003). The stimulation of the soluble guanylyl cyclase-cGMP pathway by NO and the subsequent activation of protein kinase G (Patel et al., 2006) might be another signaling mechanism which can lead to connexin phosphorylation and modification of GJ coupling (Lampe and Lau, 2004).

More recent studies suggests that NO can modify GJ function independent from the activation of the NO-induced cGMP-PKG pathway. Such a mechanism is S-nitrosylation during which NO reversibly binds to the thiol groups of cysteine residue of proteins resulting in S-nitrosothiols (SNO). S-nitrosylation not only allows the storage and transport of NO (Dejam et al., 2004; Lima et al., 2010) but modulates the activity of several cardiac functions, including cardiac ion channels (Gonzalez et al., 2009), mitochondrial respiration (Sun et al., 2006, 2007), formation of reactive oxygen species (Sun et al., 2006), or gap junctional connexins (Straub et al., 2011). For example, in the myoendothelial junction, where the vascular endothelial and smooth muscle cells are connected NO has been found to enhance the opening of this special form of GJs through S-nitrosylation of Cx43 (Straub et al., 2011). It is reasonable to assume that S-nitrosylation of Cx43 would be a possible alternative mechanism by which NO regulates the function of GJs also in cardiac myocytes, especially under conditions of increased NO availability. This may occur, for example, after preconditioning (Kiss et al., 2010), the administration of NO donors (György et al., 2000; Gönczi et al., 2009), including sodium nitrite. There is evidence that S-nitrosylation plays an important role in cardioprotection afforded by preconditioning (Sun et al., 2007; Murphy and Steenbergen, 2008). As to whether S-nitrosylation of Cx43, indeed, plays a role in the modulation of GJ function by NO and, if so, how much this mechanism accounts for the antiarrhythmic effect is still not known and warrants further examinations.

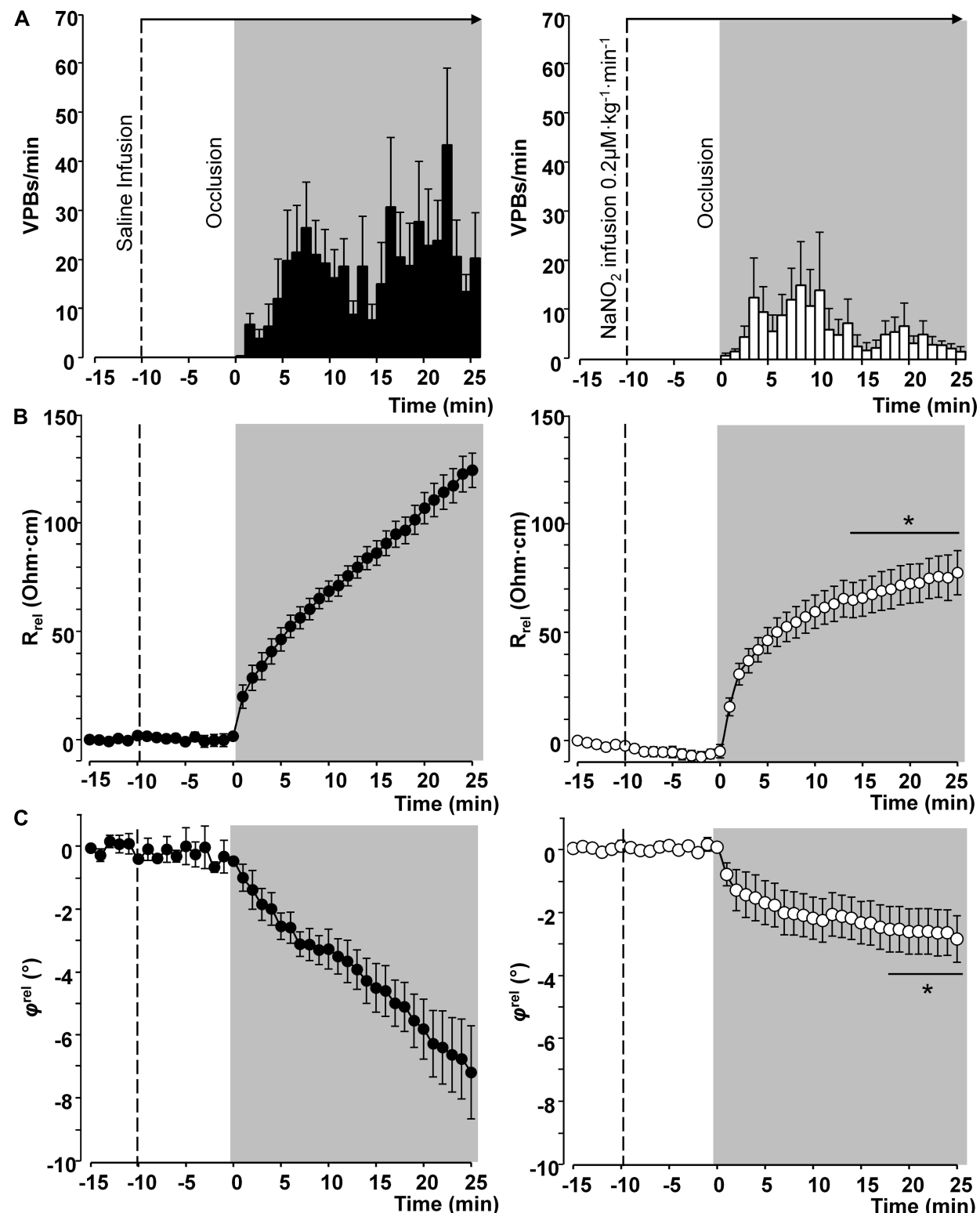


**FIGURE 1 |** Distribution of ventricular premature beats (VPBs) and relative changes in tissue impedance (resistivity and phase angle) at one minute intervals during a 25-min coronary artery occlusion in control dogs and in dogs infused with sodium nitrite. Compared with the controls, the infusion of sodium nitrite markedly reduced the number of

VPBs (**A**) and attenuated the rise in tissue resistivity (**B**) and the decline in phase angle (**C**), particularly during the critical period of ischemia (between 15 and 25 min) when the change of phase angle remained virtually constant. Values are means  $\pm$  SEM obtained from nine dogs in each group.  $*P < 0.05$  compared with the controls.

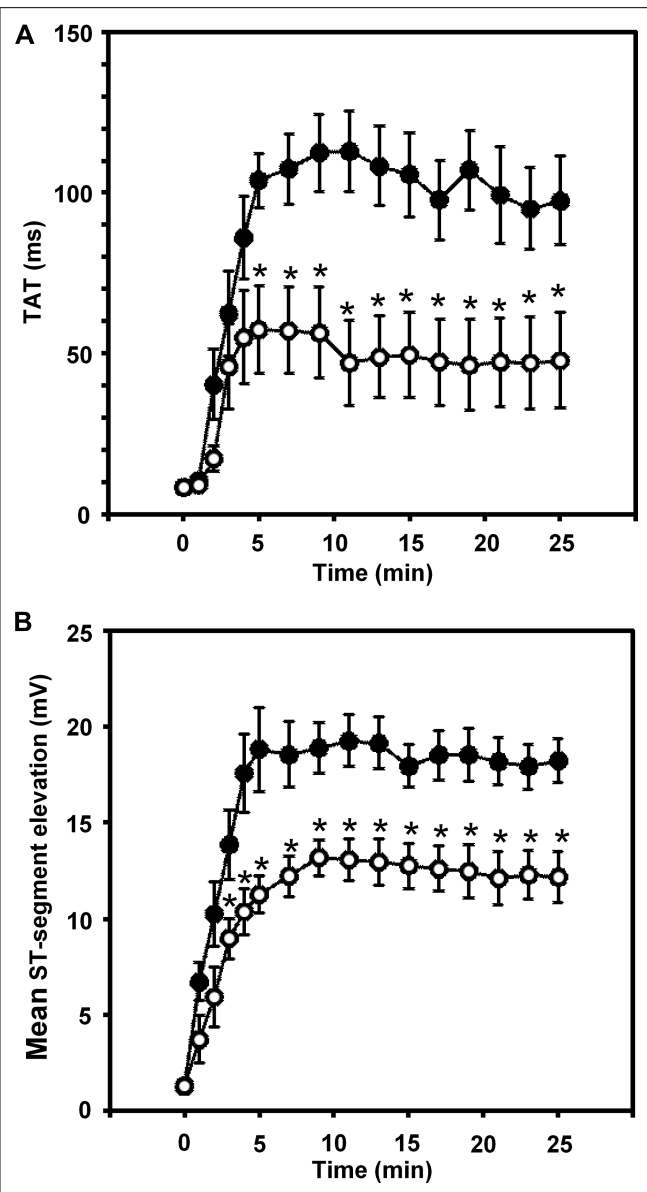


**FIGURE 2 |** Changes in the total activation time (TAT) (A) and in the epicardial ST-segment (B) during a 25-min occlusion of the anterior descending branch of the left coronary artery. In control dogs, both indices of ischemia severity were markedly increased, especially during the initial 5 min of the occlusion. These changes were significantly reduced in the presence of the intravenous infusion of sodium nitrite. Values are means  $\pm$  SEM. \*P < 0.05 compared with the controls.

## SUMMARY

We hypothesized that NO derives from either endogenous (induced by preconditioning) or exogenous sources (administration of NO donors) is able to modulate GJ function, and that this effect of NO, in part, plays a role in the protection against the severe ventricular arrhythmias that results from an acute ischemia and reperfusion insult in anesthetized dogs. To support this hypothesis in the present article we summarized our results obtained from previous and more recent studies which aimed to examine

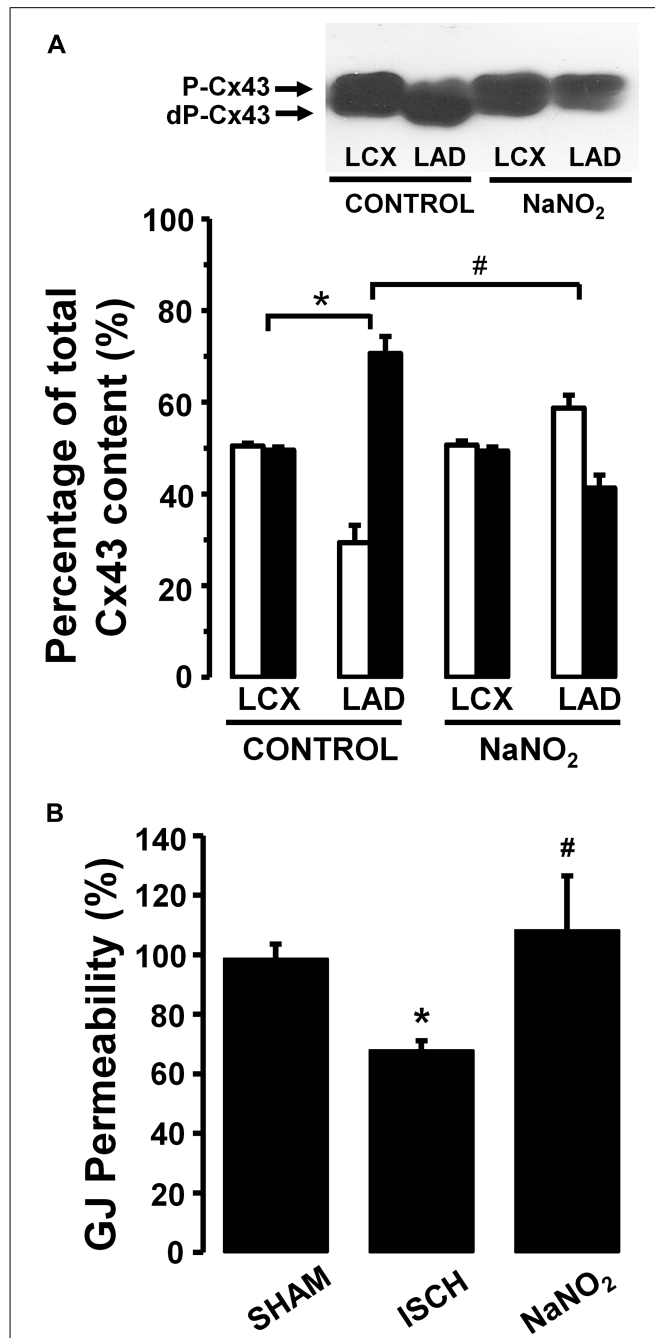


**FIGURE 3 | (A)** A representative Western blot and changes in the phosphorylated (P-Cx43; open columns) and dephosphorylated Cx43 (dP-Cx43; filled columns) isoforms as a percentage of the total sarcolemmal Cx43 content, following a 25-min LAD occlusion. The phospho/dephospho ratio within the normal area is around 51/49  $\pm$  1%. This shifted to 29/71  $\pm$  4% in hearts of the control dogs when subjected to a 25-min occlusion. Infusion of sodium nitrite prevented this shift and preserved the phosphorylated form of this protein both within the normal non-ischemic (52/48  $\pm$  1%) and the ischemic myocardial region (59/41  $\pm$  3%). **(B)** Changes in gap junction permeability in sham-control (SHAM) and ischemic control (ISCH) hearts, as well as in hearts infused with sodium nitrite (NaNO<sub>2</sub>). Sodium nitrite prevented the ischemia-induced reduction in gap junction permeability. Values are means  $\pm$  SEM. #P < 0.05 compared with the ischemic control samples. \*P < 0.05 compared with non-ischemic samples.

the regulatory role of NO on cardiac GJs in relation to arrhythmogenesis (Gönczi et al., 2009, Gönczi et al., 2010). The results give a strong support for this hypothesis, since in the presence of increased NO availability the function of GJs seems to be well preserved, as have been shown by both the *in vivo* and *in vitro* measurements. These measures, albeit provide only indirect evidence, clearly indicate that a maintained NO availability during a prolonged ischemic insult, resulting from either a preconditioning stimulus or the administration of drugs that liberate NO, inhibits the ischemia-induced tissue impedance changes and dephosphorylation of Cx43, and maintains the metabolic coupling between cells. These effects of NO are especially pronounced during that critical period of ischemia when factors and mechanisms, involved in the generation of the phase Ib arrhythmias are present and fully activated. As a result of the preserved GJ function, the Ib phase of arrhythmias are markedly suppressed. Although the precise mechanisms by which NO attains this GJ modulating

effect is still not fully understood, we discussed hypotheses and theories which propose a role for NO in the regulation of GJs. These involve NO-mediated signaling cascades including protein kinases which might have a role in connexin phosphorylation, the classical NO-soluble guanylyl cyclase-cGMP pathway with the subsequent PKG activation and the cGMP-independent mechanism of NO through which NO is able to bind and modify proteins via S-nitrosylation. As to whether all these mechanisms are acting together or there is one particular mechanism which preferentially acts under certain circumstances is unknown and requires further investigations.

## ACKNOWLEDGMENTS

These works were supported over the years by the Hungarian Scientific Research Foundation (OTKA; project numbers 75281 and 105252). We appreciate the skilful technical assistance of Erika Bakó and Irén Biczók).

## REFERENCES

- Akar, F. G., Nass, R. D., Hahn, S., Cingolani, E., Shah, M., Hesketh, G. G., et al. (2007). Dynamic changes in conduction velocity and gap junction properties during development of pacing-induced heart failure. *Am. J. Physiol. Heart Circ. Physiol.* 293, H1223–H1230. doi: 10.1152/ajpheart.00079.2007
- Ando, M., Katare, R. G., Kakimura, Y., Zhang, D., Yamasaki, F., Muramoto, K., et al. (2005). Efferent vagal nerve stimulation protects heart against ischemia-induced arrhythmias by preserving connexin43 protein. *Circulation* 112, 164–170. doi: 10.1161/CIRCULATIONAHA.104.525493
- Beardslee, M. A., Lerner, D. L., Tardos, P. N., Lang, J. G., Beyer, E. C., Yamada, K. A., et al. (2000). Dephosphorylation and intracellular redistribution of ventricular connexin43 during electrical uncoupling induced by ischemia. *Circ. Res.* 87, 656–662. doi: 10.1161/01.RES.87.8.656
- Bolanos, J. P., and Medina, J. M. (1996). Induction of nitric oxide synthase inhibits gap junction permeability in cultured rat astrocytes. *J. Neurochem.* 66, 2091–2099. doi: 10.1046/j.1471-4159.1996.66052091.x
- Bryan, N. S. (2006). Nitrite in nitric oxide biology: cause or consequence? A systems-based review. *Free Radic. Biol. Med.* 41, 691–701. doi: 10.1016/j.freeradbiomed.2006.05.019
- Cascio, W. E. (2001). Myocardial ischemia: what factors determine arrhythmogenesis? *J. Cardiovasc. Electrophysiol.* 12, 726–729. doi: 10.1046/j.1540-8167.2001.00726.x
- Cascio, W. E., Yang, H., Muller-Borer, B. J., and Johnson, T. A. (2005). Ischemia-induced arrhythmia: the role of connexins, gap junctions, and attendant changes in impulse propagation. *J. Electrocardiol.* 38, 55–59. doi: 10.1016/j.jelectrocard.2005.06.019
- Cinca, J., Warren, M., Careno, A., Trejo-Sanchez, M., Armadans, L., Gomez, P., et al. (1997). Changes in myocardial electrical impedance induced by coronary artery occlusion in pigs with and without preconditioning. *Circulation* 96, 3079–3086. doi: 10.1161/01.CIR.96.9.3079
- Daleau, P., Boudriau, S., Michaud, M., Jolicœur, C., and Kingma, J. G. (2001). Preconditioning in the absence or presence of sustained ischemia modulates myocardial Cx43 protein levels and gap junction distribution. *Can. J. Physiol. Pharmacol.* 79, 371–378. doi: 10.1139/y01-004
- De Groot, J. R., and Coronel, R. (2004). Acute ischemia-induced gap junctional uncoupling and arrhythmogenesis. *Cardiovasc. Res.* 62, 323–334. doi: 10.1016/j.cardiores.2004.01.033
- De Groot, J. R., Wilms-Schopman, F. J. G., Ophof, T., Remme, C. A., and Coronel, R. (2001). Late ventricular arrhythmias during acute regional ischemia in the isolated blood perfused pig heart. Role of electrical cellular coupling. *Cardiovasc. Res.* 50, 362–372. doi: 10.1016/S0008-6363(01)00222-X
- Dejam, A., Hunter, C. J., Schechter, A. N., and Gladwin, M. T. (2004). Emerging role of nitrite in human biology. *Blood Cells Mol. Dis.* 32, 423–429. doi: 10.1016/j.bcmd.2004.02.002
- Dhein, S. (1998). Gap junction channels in the cardiovascular system: pharmacological and physiological modulation. *Trends Pharmacol. Sci.* 19, 229–241. doi: 10.1016/S0165-6147(98)01192-4
- Dhein, S. (2004). Pharmacology of gap junctions in the cardiovascular system. *Cardiovasc. Res.* 62, 287–298. doi: 10.1016/j.cardiores.2004.01.019
- Dhein, S., Hagen, A., Jozwiak, J., Dietze, A., Garbade, J., Barten, M., et al. (2010). Improving cardiac gap junction communication as a new antiarrhythmic mechanism: the action of antiarrhythmic peptides. *Naunyn Schmiedebergs Arch. Pharmacol.* 381, 221–234. doi: 10.1007/s00210-009-0473-1
- Dhein, S., Jozwiak, J., Hagen, A., Seidel, T., Dietze, A., Salameh, A., et al. (2011). “The role of gap junctions in impulse propagation in the heart: new aspects of arrhythmogenesis and new antiarrhythmic agents targeting gap junctions,” in *Heart Rate and Rhythm. Molecular Basis, Pharmacological Modulation and Clinical Applications*, eds O. N. Tripathi, U. Ravens, and M. C. Sanguineti (Berlin: Springer-Verlag), 503–524.
- Dhein, S., Manicone, N., Müller, A., Gerwin, R., Ziskoven, U., Irankhahi, A., et al. (1994). A new synthetic antiarrhythmic peptide reduces dispersion of epicardial activation recovery intervals and diminishes alterations of epicardial activation patterns induced by regional ischemia. *Naunyn Schmiedebergs Arch. Pharmacol.* 350, 174–184. doi: 10.1007/BF00241093
- Dhein, S., and Tudyka, T. (1995). The therapeutic potential of antiarrhythmic peptides. Cellular coupling as a new antiarrhythmic target. *Drugs* 49, 851–855. doi: 10.2165/00003495-199549060-00001
- Downey, J. M., Krieg, T., and Cohen, M. V. (2008). Mapping preconditioning's signaling pathways: an engineering approach. *Ann. N. Y. Acad. Sci.* 1123, 187–196. doi: 10.1196/annals.1420.022
- Duranski, M. R., Greer, J. J., Dejam, A., Jaganmohan, S., Hogg, N., Langston, W., et al. (2005). Cytoprotective effects of nitrite during *in vivo* ischemia-reperfusion of the heart and liver. *J. Clin. Invest.* 115, 1232–1240. doi: 10.1172/JCI22493
- Francis, S. H., Busch, J. L., and Corbin, J. D. (2010). cGMP-dependent protein kinases and cGMP phosphodiesterases in nitric oxide and cGMP action. *Pharmacol. Rev.* 62, 525–563. doi: 10.1124/pr.110.002907
- Garcia-Dorado, D., Inserte, J., Ruiz-Meana, M., Gonzalez, M., Solares, J., Julia, M., et al. (1997). Gap junction uncoupler heptanol prevents cell-to-cell progression of hypercontracture and limits necrosis during myocardial reperfusion. *Circulation* 96, 3579–3586. doi: 10.1161/01.CIR.96.10.3579
- Garcia-Dorado, D., Rodriguez-Sinovas, A., and Ruiz-Meana, M. (2004). Gap junction-mediated spread of cell injury and death during myocardial ischaemia-reperfusion. *Cardiovasc. Res.* 61, 386–401. doi: 10.1016/j.cardiores.2003.11.039
- Gönczi, M., Kiss, A., and Végh, Á. (2010). The antiarrhythmic protection resulting from sodium nitrite ( $\text{NaNO}_2$ ) administration involves modulation of gap junctions. *J. Mol. Cell. Cardiol.* 48, S102 (P-2-26-2) (abstract).
- Gönczi, M., Kovács, M., Seprényi, G., and Végh, Á. (2012). The involvement of gap junctions in the delayed phase of the protection induced by cardiac pacing in dogs. *Clin. Sci.* 123, 39–51. doi: 10.1042/CS20110501
- Gönczi, M., Papp, R., Kovács, M., Seprényi, G., and Végh, Á. (2009). Modulation of gap junctions by nitric

- oxide contributes to the antiarrhythmic effect of sodium nitroprusside. *Br. J. Pharmacol.* 156, 786–793. doi: 10.1111/j.1476-5381.2008.00089.x
- Gonzalez, D. R., Treuer, A., Sun, Q. A., Stamler, J. S., and Hare, J. M. (2009). S-nitrosylation of cardiac ion channels. *J. Cardiovasc. Pharmacol.* 54, 188–195. doi: 10.1097/FJC.0b013e3181b72c9f
- Grover, R., and Dhein, S. (2001). Structure-activity relationship of novel peptides related to the antiarrhythmic peptide AAP10 which reduce the dispersion of epicardial action potential duration. *Peptides* 22, 1011–1021. doi: 10.1016/S0196-9781(01)00419-3
- György, K., Végh, Á., Rastegar, M. A., Papp, J. G., and Parratt, J. R. (2000). Isosorbide-2-mononitrate reduces the consequences of myocardial ischaemia, including arrhythmia severity: implications for preconditioning. *Cardiovasc. Drugs Ther.* 14, 481–488. doi: 10.1023/A:1007832921391
- Henriquez, A. P., Vogel, R., Muller-Borer, B. J., Henriquez, C. S., Weingart, R., and Cascio, W. E. (2001). Influence of dynamic gap junction resistance on impulse propagation in ventricular myocardium: a computer stimulation study. *Biophys. J.* 81, 2112–2121. doi: 10.1016/S0006-3495(01)75859-6
- Hoffmann, A., Gloe, T., Pohl, U., and Zahler, S. (2003). Nitric oxide enhances de novo formation of endothelial gap junctions. *Cardiovasc. Res.* 60, 421–430. doi: 10.1016/j.cardiores.2003.04.001
- Hoyt, R. H., Cohen, M. L., and Saffitz, J. E. (1989). Distribution and three-dimensional structure of intercellular junctions in canine myocardium. *Circ. Res.* 64, 563–574. doi: 10.1161/01.RES.64.3.563
- Janse, M. J., Kléber, A. G., Capucci, A., Coronel, R., and Wilms-Schopman, F. (1986). Electrophysiological basis for arrhythmias caused by acute ischemia. *J. Mol. Cell. Cardiol.* 18, 339–355. doi: 10.1016/S0022-2828(86)80987-7
- Janse, M. J., and van Capelle, F. J. L. (1982). Electrotonic interactions across an inexcitable region as a cause of ectopic activity in acute regional myocardial ischemia. A study in intact porcine and canine hearts and computer models. *Circ. Res.* 50, 527–537. doi: 10.1161/01.RES.50.4.527
- Kameritsch, P., Hoffmann, A., and Pohl, U. (2003). Opposing effects of nitric oxide on different connexins expressed in the vascular system. *Cell. Commun. Adhes.* 10, 305–309.
- Kim, S. K., Pak, H. N., Park, J. H., Fang, Y. F., Kim, G. I., Park, Y. D., et al. (2010). Cardiac cell therapy with mesenchymal stem cell induces cardiac nerve sprouting, angiogenesis, and reduced connexin43-positive gap junctions, but concomitant electrical pacing increases connexin43-positive gap junctions in canine heart. *Cardiol. Young* 20, 308–317. doi: 10.1017/S1047951110000132
- Kiss, A., Juhász, L., Seprényi, G., Kupai, K., Kaszaki, J., and Végh, Á. (2010). The role of nitric oxide, superoxide and peroxynitrite in the anti-arrhythmic effects of preconditioning and peroxynitrite infusion in anaesthetized dogs. *Br. J. Pharmacol.* 160, 1263–1272. doi: 10.1111/j.1476-5381.2010.00774.x
- Kléber, A. G. (1983). Resting membrane potential, extracellular potassium activity, and intracellular sodium activity during acute global ischemia in isolated perfused guinea pig hearts. *Circ. Res.* 52, 442–450. doi: 10.1161/01.RES.52.4.442
- Kléber, A. G., Rieger, C. B., and Janse, M. J. (1987). Electrical uncoupling and increase in extracellular resistance after induction of ischemia in isolated, arterially perfused rabbit papillary muscle. *Circ. Res.* 61, 271–279. doi: 10.1161/01.RES.61.2.271
- Kontogeorgis, A., Kaba, R. A., Kang, E., Feig, J. E., Gupta, P. P., Ponzio, M., et al. (2008). Short-term pacing in the mouse alters cardiac expression of connexin43. *BMC Physiol.* 8:8. doi: 10.1186/1472-6793-8-8
- Kwak, B. R., Hermanns, M. M. P., De Jonge, H. R., Lohmann, S. M., Jongsma, H. J., and Chanson, M. (1995). Differential regulation of distinct types of gap junction channels by similar phosphorylating conditions. *Mol. Biol. Cell* 6, 1707–1709.
- Kwak, B. R., and Jongsma, H. J. (1996). Regulation of cardiac gap junction channel permeability and conductance by several phosphorylation conditions. *Mol. Cell. Biochem.* 157, 93–99. doi: 10.1007/BF00227885
- Lampe, P. D., and Lau, A. F. (2004). The effects of connexin phosphorylation on gap junctional communication. *Int. J. Biochem. Cell Biol.* 36, 1171–1183. doi: 10.1016/S1357-2725(03)00264-4
- Lefer, D. J. (2009). Emerging role of nitrite in myocardial protection. *Arch. Pharm. Res.* 32, 1127–1138. doi: 10.1007/s12272-009-1804-y
- Lima, B., Forrester, M. T., Hess, D. T., and Stamler, J. S. (2010). S-nitrosylation in cardiovascular signaling. *Circ. Res.* 106, 633–646. doi: 10.1161/CIRCRESAHA.109.207381
- Looft-Wilson, R. C., Billaud, M., Johnstone, S. R., Straub, A. C., and Isakson, B. E. (2012). Interaction between nitric oxide signaling and gap junctions: effects on vascular function. *Biochim. Biophys. Acta* 1818, 1895–1902. doi: 10.1016/j.bbapm.2011.07.031
- Lundberg, J. O., and Govoni, M. (2004). Inorganic nitrite is a possible source for systemic generation of nitric oxide. *Free Radic. Biol. Med.* 37, 395–400. doi: 10.1016/j.freeradbiomed.2004.04.027
- Miura, T., Ohnuma, Y., Kuno, A., Tanno, M., Ichikawa, Y., Nakamura, Y., et al. (2004). Protective role of gap junctions in preconditioning against myocardial infarction. *Am. J. Physiol. Heart Circ. Physiol.* 286, H214–H221. doi: 10.1152/ajpheart.00441.2003
- Müller, A., Gottwald, M., Tudyka, T., Linke, W., Klaus, W., and Dhein, S. (1997). Increase in gap junction conductance by an antiarrhythmic peptide. *Eur. J. Pharmacol.* 327, 65–72. doi: 10.1016/S0014-2999(97)89679-3
- Murphy, E., and Steenbergen, C. (2008). Mechanisms underlying acute protection from cardiac ischemia-reperfusion injury. *Physiol. Rev.* 88, 581–609. doi: 10.1152/physrev.00024.2007
- Padilla, F., Garcia-Dorado, D., Rodriguez-Sinovas, A., Ruiz-Meana, M., Inserte, J., and Soler-Soler, J. (2003). Protection afforded by ischemic preconditioning is not mediated by effects on cell-to-cell electrical coupling during myocardial ischemia-reperfusion. *Am. J. Physiol.* 285, H1909–H1916. doi: 10.1152/ajpheart.00438.2003
- Papp, R., Gönczi, M., Kovács, M., Seprényi, G., and Végh, Á. (2007). Gap junctional uncoupling plays a trigger role in the antiarrhythmic effect of ischaemic preconditioning. *Cardiovasc. Res.* 74, 396–405. doi: 10.1016/j.cardiores.2007.02.021
- Papp, R., Gönczi, M., and Végh, Á. (2008). Role of gap junctions in arrhythmias induced by acute myocardial ischaemia. *Cardiol. Hung.* 38, 116–122.
- Parratt, J. R., and Végh, Á. (1996). Endothelial cells, nitric oxide and ischaemic preconditioning. *Basic Res. Cardiol.* 91, 27–30. doi: 10.1007/BF00788857
- Patel, L. S., Mitchell, C. K., Dubinsky, W. P., and O'Brien, J. O. (2006). Regulation of gap junction coupling through the neuronal connexin Cx35 by nitric oxide and cGMP. *Cell Commun. Adhes.* 13, 41–54. doi: 10.1080/1541906060631474
- Peters, N. S., and Wit, A. L. (1998). Myocardial architecture and ventricular arrhythmogenesis. *Circulation* 97, 1746–1754. doi: 10.1161/01.CIR.97.17.1746
- Poelzing, S., and Rosembaum, D. S. (2004). Altered connexin43 expression produces arrhythmia substrate in heart failure. *Am. J. Physiol. Heart Circ. Physiol.* 287, H1762–H1770. doi: 10.1152/ajpheart.00346.2004
- Radosinska, J., Bacova, B., Bertanova, I., Navarova, J., Zhukovska, A., Shysh, A., et al. (2011). Myocardial NOS activity and connexin43 expression in untreated and omega-3 fatty acids-treated spontaneously hypertensive and hereditary hypertriglyceridemic rats. *Mol. Cell. Biochem.* 347, 163–173. doi: 10.1007/s11010-010-0625-0
- Rodenwaldt, B., Pohl, U., and Wit, C. (2007). Endogenous and exogenous NO attenuates conduction of vasoconstrictions along arterioles in the microcirculation. *Am. J. Physiol. Heart Circ. Physiol.* 292, H2341–H2348. doi: 10.1152/ajpheart.01061.2006
- Roh, C. R., Heo, J. H., Yang, S. H., and Bae, D. S. (2002). Regulation of connexin 43 by nitric oxide in primary uterine myocytes from term pregnant women. *Am. J. Obstet. Gynecol.* 187, 434–440. doi: 10.1067/mob.2002.123600
- Rohr, S. (2004). Role of gap junctions in propagation of the cardiac action potential. *Cardiovasc. Res.* 62, 309–312. doi: 10.1016/j.cardiores.2003.11.035
- Rohr, S., Kucera, J. P., Fast, V. G., and Kléber, A. G. (1997). Paradoxical improvement of impulse conduction in cardiac tissue by partial cellular uncoupling. *Science* 275, 841–844. doi: 10.1126/science.275.5301.841
- Rohr, S., Kucera, J. P., and Kléber, A. G. (1998). Slow conduction in cardiac tissue. I. Effects of a reduction of excitability versus a reduction of electrical coupling on microconduction. *Circ. Res.* 83, 781–794. doi: 10.1161/01.RES.83.8.781
- Rudy, Y., and Quan, W. L. (1987). A model study of the effects of the discrete cellular structure on electrical propagation in cardiac tissue. *Circ. Res.* 61, 815–823. doi: 10.1161/01.RES.61.6.815
- Ruiz-Meana, M., Garcia-Dorado, D., Lane, S., Pina, P., Inserte, J., Mirabet, M., et al. (2001). Persistence of gap junction communication during myocardial ischaemia. *Am. J. Physiol. Heart Circ. Physiol.* 280, H2563–H2571.

- Saez, J. C., Naim, A. C., Czernik, A. J., Fishman, G. I., Spray, D. C., and Hertzberg, E. L. (1997). Phosphorylation of connexin43 and the regulation of neonatal rat cardiac myocyte gap junctions. *J. Mol. Cell. Cardiol.* 29, 2131–2145. doi: 10.1006/jmcc.1997.0447
- Saffitz, J. E., Davis, L. M., Darrow, B. J., Kanter, H. L., Laing, J. G., and Beyer, E. C. (1995). The molecular basis of anisotropy: role of gap junctions. *J. Cardiovasc. Electrophysiol.* 6, 498–510. doi: 10.1111/j.1540-8167.1995.tb00423.x
- Salameh, A., and Dhein, S. (2005). Pharmacology of gap junctions. New pharmacological targets for treatment of arrhythmia, seizure and cancer? *Biochim. Biophys. Acta* 1719, 36–58. doi: 10.1016/j.bbamem.2005.09.007
- Schulz, R., Gres, P., Skyschally, A., Duschin, A., Belosjorow, S., Konietzka, I., et al. (2003). Ischemic preconditioning preserves connexin43 phosphorylation during sustained ischemia in pig hearts *in vivo*. *FASEB J.* 17, 1355–1357. doi: 10.1096/fj.02-0975fje
- Shaw, R. M., and Rudy, Y. (1997). Ionic mechanisms of propagation in cardiac tissue. Roles of sodium and L-type calcium currents during reduced excitability and decreased gap junction coupling. *Circ. Res.* 81, 727–741. doi: 10.1161/01.RES.81.5.727
- Shiva, S., Sack, M. N., Greer, J. J., Duranski, M., Ringwood, L. A., Burwell, L., et al. (2007). Nitrite augments tolerance to ischemia/reperfusion injury via the modulation of mitochondrial electron transfer. *J. Exp. Med.* 204, 2089–2012. doi: 10.1084/jem.20070198
- Smith, W. T., Fleet, W. F., Johnson, T. A., Engle, C. L., and Cascio, W. E. (1995). The 1b phase of ventricular arrhythmias in ischemic *in situ* porcine heart is related to changes in cell-to-cell electrical coupling. *Circulation* 92, 3051–3060. doi: 10.1161/01.CIR.92.10.3051
- Söhl, G., and Willecke, K. (2004). Gap junctions and the connexin protein family. *Cardiovasc. Res.* 62, 228–232. doi: 10.1016/j.cardiores.2003.11.013
- Spach, M. S., Dolbert, P. C., and Heidlage, J. F. (1988). Influence of the passive anisotropic properties on directional differences in propagation following modification of the sodium conductance in human atrial muscle. A model of reentry based anisotropic discontinuous propagation. *Circ. Res.* 62, 811–832. doi: 10.1161/01.RES.62.4.811
- Spach, M. S., and Heidlage, J. F. (1995). The stochastic nature of cardiac propagation at a microscopic level. Electrical description of myocardial architecture and its application to conduction. *Circ. Res.* 76, 366–380. doi: 10.1161/01.RES.76.3.366
- Spach, M. S., Miller, W. T., Geselowitz, D. B., Barr, R. C., Kootsey, J. M., and Johnson, E. A. (1981). The discontinuous nature of propagation in normal canine cardiac muscle. Evidence for recurrent discontinuities of intracellular resistance that affect the membrane currents. *Circ. Res.* 48, 39–54. doi: 10.1161/01.RES.48.1.39
- Spear, J. F., Kleval, R. S., and Moore, E. N. (1992). The role of myocardial anisotropy in arrhythmogenesis associated with myocardial ischemia and infarction. *J. Cardiovasc. Electrophysiol.* 3, 579–588.
- Straub, A. C., Billaud, M., Johnstone, S. R., Best, A. K., Yemen, S., Dwyer, S. T., et al. (2011). Compartmentalized connexin 43 S-nitrosylation/denitrosylation regulates heterocellular communication in the vessel wall. *Arterioscler. Thromb. Vasc. Biol.* 31, 399–407. doi: 10.1161/ATVBAHA.110.215939
- Sun, J., Morgan, M., Shen, R. F., Steenbergen, C., and Murphy, E. (2007). Preconditioning results in S-nitrosylation of proteins involved in regulation of mitochondrial energetics and calcium transport. *Circ. Res.* 101, 1155–1163. doi: 10.1161/CIRCRESAHA.107.155879
- Sun, J., Steenbergen, C., and Murphy, E. (2006). S-nitrosylation: NO-related redox signaling to protect against oxidative stress. *Antioxid. Redox Signal.* 8, 1693–1705. doi: 10.1089/ars.2006.1693
- Végh, Á., Komori, S., Szekeres, L., and Parratt, J. R. (1992a). Antiarrhythmic effects of preconditioning in anaesthetized dogs and rats. *Cardiovasc. Res.* 26, 487–495. doi: 10.1093/cvr/26.5.487
- Végh, Á., Papp, J. G., Szekeres, L., and Parratt, J. R. (1992b). The local intra-coronary administration of methylene blue prevents the pronounced antiarrhythmic effect of ischaemic preconditioning. *Br. J. Pharmacol.* 107, 910–911. doi: 10.1111/j.1476-5381.1992.tb13384.x
- Végh, Á., Szekeres, L., and Parratt, J. R. (1992c). Preconditioning of the ischaemic myocardium; involvement of the l-arginine – nitric oxide pathway. *Br. J. Pharmacol.* 107, 648–652. doi: 10.1111/j.1476-5381.1992.tb14501.x
- Végh, Á., and Papp, R. (2011). “Possible mechanisms of the acute ischemia-induced ventricular arrhythmias: the involvement of gap junctions,” in *Heart Rate and Rhythm. Molecular Basis, Pharmacological Modulation and Clinical Applications*, eds O. N. Tripathi, U. Ravens, and M. C. Sanguineti (Berlin: Springer-Verlag), 525–543.
- Végh, Á., and Parratt, J. R. (1996). “Ischaemic preconditioning markedly reduces the severity of ischaemia and reperfusion-induced arrhythmias; role of endogenous myocardial protective substances,” in *Myocardial Preconditioning*, eds C. L. Wainwright and J. R. Parratt (Berlin: Springer), 35–60.
- Vetterlein, F., Mühlfeld, C., Cetegen, C., Volkmann, R., Schrader, C., and Hellige, G. (2006). Redistribution of connexin43 in regional acute ischemic myocardium: influence of ischemic preconditioning. *Am. J. Physiol.* 291, H813–H819. doi: 10.1152/ajpheart.0177.2005
- Webb, A., Bond, R., McLean, P., Uppal, R., Benjamin, N., and Ahluwalia, A. (2004). Reduction of nitrite to nitric oxide during ischemia protects against myocardial ischemia-reperfusion damage. *Proc. Natl. Acad. Sci. U.S.A.* 101, 13683–13688. doi: 10.1073/pnas.0402927101
- Weng, S., Lauven, T., Schaefer, L., Polontchouk, R., Grover, S., and Dhein, S. (2002). Pharmacological modulation of gap junction coupling by an antiarrhythmic via protein kinase C activation. *FASEB J.* 16, 1114–1116.
- White, R. L., Doeller, J. E., Verselis, V. K., and Wittenberg, B. A. (1990). Gap junctional conductance between pairs of ventricular myocytes is modulated synergistically by  $H^+$  and  $Ca^{++}$ . *J. Gen. Physiol.* 95, 1061–1075. doi: 10.1085/jgp.95.6.1061
- Wojtczak, J. (1979). Contractures and increase in internal longitudinal resistance of cow ventricular muscle induced by hypoxia. *Circ. Res.* 44, 88–95. doi: 10.1161/01.RES.44.1.88
- Wolk, R., Cobbe, S. M., Hicks, M. N., and Kane, K. A. (1999). Functional, structural and dynamic basis of electrical heterogeneity in healthy and diseased cardiac muscle: implications for arrhythmogenesis and anti-arrhythmic drug therapy. *Pharmacol. Ther.* 84, 207–231. doi: 10.1016/S0163-7258(99)00033-9
- Xing, D., Kjolby, A. L., Nielsen, M. S., Petersen, J. S., Harlow, K. W., Holstein-Rathlou, N. H., et al. (2003). ZP123 increases gap junctional conductance and prevents re-entrant ventricular tachycardia during myocardial ischemia in open chest dogs. *J. Cardiovasc. Electrophysiol.* 14, 510–520. doi: 10.1046/j.1540-8167.2003.02329.x
- Xing, D., Kjolby, A. L., Petersen, J. S., and Martins, J. B. (2005). Pharmacological stimulation of cardiac gap junction coupling does not affect ischaemia-induced focal ventricular tachycardia or triggered activity in dogs. *Am. J. Physiol. Heart Circ. Physiol.* 288, H511–H516. doi: 10.1152/ajpheart.00720.2004
- Yao, J., Hiramatsu, N., Zhu, Y., Morioka, T., Takeda, M., Oite, T., et al. (2005). Nitric oxide-mediated regulation of connexin43 expression and gap junctional intercellular communication in mesangial cells. *J. Am. Soc. Nephrol.* 16, 58–67. doi: 10.1681/ASN.2004060453
- Zhang, Y., Kikinuma, Y., Ando, H., Katare, R. G., Yamasaki, F., Sugiyura, T., et al. (2006). Acetylcholine inhibits the hypoxia-induced reduction of connexin43 protein in rat cardiomyocytes. *J. Pharmacol. Sci.* 101, 214–222. doi: 10.1254/jphs.FP0051023
- Zweier, J. L., Wang, P., Samoilov, A., and Kuppusamy, P. (1995). Enzyme-independent formation of nitric oxide in biologic tissues. *Nat. Med.* 1, 804–809. doi: 10.1038/nm0895-804

**Conflict of Interest Statement:** The authors declare that the research was conducted in the absence of any commercial or financial relationships that could be construed as a potential conflict of interest.

**Received:** 14 February 2013; **paper pending published:** 08 April 2013; **accepted:** 29 May 2013; **published online:** 14 June 2013.

**Citation:** Végh Á, Gönczi M, Miskolczi G and Kovács M (2013) Regulation of gap junctions by nitric oxide influences the generation of arrhythmias resulting from acute ischemia and reperfusion *in vivo*. *Front. Pharmacol.* 4:76. doi: 10.3389/fphar.2013.00076

This article was submitted to Frontiers in Pharmacology of Ion Channels and Channelopathies, a specialty of Frontiers in Pharmacology.

Copyright © 2013 Végh, Gönczi, Miskolczi and Kovács. This is an open-access article distributed under the terms of the Creative Commons Attribution License, which permits use, distribution and reproduction in other forums, provided the original authors and source are credited and subject to any copyright notices concerning any third-party graphics etc.



# Inverse relationship between tumor proliferation markers and connexin expression in a malignant cardiac tumor originating from mesenchymal stem cell engineered tissue in a rat *in vivo* model

Cathleen Spath<sup>1†</sup>, Franziska Schlegel<sup>1†</sup>, Sergey Leontyev<sup>2</sup>, Friedrich-Wilhelm Mohr<sup>2</sup> and Stefan Dhein<sup>2\*</sup>

<sup>1</sup> Translational Centre for Regenerative Medicine, Leipzig, Germany

<sup>2</sup> Clinic for Cardiac Surgery, Heart Centre Leipzig, Leipzig, Germany

**Edited by:**

Aida Salameh, Heart Centre  
University of Leipzig, Germany

**Reviewed by:**

Aida Salameh, Heart Centre  
University of Leipzig, Germany  
Masahito Oyamada, Fuji Women's  
University, Japan  
Narcis Tribulova, Slovak Academy of  
Sciences, Slovakia.

**\*Correspondence:**

Stefan Dhein, Heart Centre Leipzig,  
Clinic for Cardiac Surgery, University  
of Leipzig, Strümpellstr. 39, D-04289  
Leipzig, Germany.

e-mail: dhes@medizin.uni-leipzig.de

<sup>†</sup>Cathleen Spath and Franziska  
Schlegel have contributed equally to  
this work.

**Background:** Recently, we demonstrated the beneficial effects of engineered heart tissues for the treatment of dilated cardiomyopathy in rats. For further development of this technique we started to produce engineered tissue (ET) from mesenchymal stem cells. Interestingly, we observed a malignant tumor invading the heart with an inverse relationship between proliferation markers and connexin expression.

**Methods:** Commercial CD54+/CD90+/CD34-/CD45- bone marrow derived mesenchymal rat stem cells (cBM-MSC), characterized were used for production of mesenchymal stem-cell-ET (MSC-ET) by suspending them in a collagen I, matrigel-mixture and cultivating for 14 days with electrical stimulation. Three MSC-ET were implanted around the beating heart of adult rats for days. Another three MSC-ET were produced from freshly isolated rat bone marrow derived stem cells (sBM-MSC).

**Results:** Three weeks after implantation of the MSC-ETs the hearts were surgically excised. While in 5/6 cases the ET was clearly distinguishable and was found as a ring containing mostly connective tissue around the heart, in 1/6 the heart was completely surrounded by a huge, undifferentiated, pleomorphic tumor originating from the cMSC-ET (cBM-MSC), classified as a high grade malignant sarcoma. Quantitatively we found a clear inverse relationship between cardiac connexin expression (Cx43, Cx40, or Cx45) and increased Ki-67 expression (Cx43:  $p < 0.0001$ , Cx45:  $p < 0.03$ , Cx40:  $p < 0.014$ ). At the tumor-heart border there were significantly more Ki-67 positive cells ( $p = 0.001$ ), and only 2% Cx45 and Ki-67-expressing cells, while the other connexins were nearly completely absent ( $p < 0.0001$ ).

**Conclusion and Hypothesis:** These observations strongly suggest the hypothesis, that invasive tumor growth is accompanied by reduction in connexins. This implicates that gap junction communication between tumor and normal tissue is reduced or absent, which could mean that growth and differentiation signals can not be exchanged.

**Keywords:** connexins, gap junctions, sarcoma, proliferation, tumour, Cx43, Cx40, Cx45

## INTRODUCTION

There is a long standing debate about factors that may be involved in the invasive growth of tumors. Among these gap junctions have been discussed since Werner Loewenstein proposed that gap junction intercellular communication (GJIC) might play a role in tumorigenesis and that reduced communication may account for loss of growth inhibition (Loewenstein and Kanno, 1966; Loewenstein, 1980). Since that time a number of papers has shown that in primary tumors or tumor cell lines connexins can be downregulated or even be absent, that oncogenes or cancerogenic drugs often inhibit gap junction channel function or reduce connexin expression (Loewenstein and Kanno, 1966; Trosko et al., 1990; Lampe, 1994; Laird et al., 1999; Mesnil et al., 2005; Salameh and Dhein, 2005; Cronier et al., 2009). However, on the other hand, some researchers found a role of gap junctions promoting invasion, cell

extravasation, and migration of tumor cells (Naoi et al., 2007; Saito-Katsuragi et al., 2007; Ezumi et al., 2008), while others do not support this view (Yano et al., 2006; Sato et al., 2008). This lead to the interpretation that connexins might be “differentially regulated during the dissemination of specific tumor types” (Naus and Laird, 2010), and that down-regulation of connexin in early tumors might be linked to invasion, but in later states elevation in connexins can occur facilitating extravasation and formation of secondary tumors (Naus and Laird, 2010). Regarding tumor cells, GJIC may exist among normal or (pre-)cancerous cells (homologous GJIC) or between normal and (pre)cancerous cells (heterologous GJIC), (Yamasaki et al., 1995), or may be absent. Thus, an open question is, whether there are gap junctions at the border between a tumor and the neighboring tissue. Another issue of debate is the role of connexins in stem cells (Trosko et al., 2004). In recent

years, mesenchymal stem cells (MSC) gained huge interest in regenerative medicine and tissue engineering. To their exceptional advantages belongs their multipotent differentiation capacity to cell lineages, including myocytes, osteocytes, chondrocytes, tenocytes, and adipocytes (Pittenger et al., 1999). Additionally, MSC can be derived from different tissues, like bone marrow (BM), adipose tissue, and umbilical cord (Zuk et al., 2001; Romanov et al., 2003). Until today, MSC, mostly BM-MSC, have been successfully transplanted in animal models as well as in human patients suffering from for instance myocardial infarction, dilated cardiomyopathy, stroke, neuroimmunological, and neurodegenerative diseases (Horwitz et al., 1999; Bang et al., 2005; Nagaya et al., 2005; Karussis et al., 2008; Tang et al., 2009; Chin et al., 2010). Furthermore MSC have kept entering tumor research. Several *in vivo* and *in vitro* studies have shown the ability of MSC to inhibit tumor growth in different malignancies (Maestroni et al., 1999; Ohlsson et al., 2003; Nakamura et al., 2004; Khakoo et al., 2006; Tian et al., 2010). In contrast, various scientific groups observed, that MSC could promote metastasis (Karnoub et al., 2007) and enhance tumor growth (Gunn et al., 2006; Zhu et al., 2006; Spaeth et al., 2009), which is assumed to be attributable to for instance immunosuppression (Djouad et al., 2003) or drug resistance (Kurtova et al., 2009). Moreover several types of MSC may transform to malignant cells *in vitro* and *in vivo* (Rubio et al., 2005; Miura et al., 2006; Zhou et al., 2006; Tolar et al., 2007). Due to these contradictory observations, Wong (2011) discussed in her paper the question, whether MSC are “angels or demons.”

A kicking point about the role of a cell within a given tissue is the question, whether this cell can communicate with its neighboring cells, which may regulate growth and differentiation of the cell *via* gap junctional intercellular communication (Loewenstein, 1980; Trosko et al., 1990). In that context, an even older standing debate than the scientific efforts in mesenchymal stem cells is the questions about the role of connexins in tumor growth and communicating with its surrounding. Gap Junction channels are made from two hemichannels (connexons) contributed by either of the neighboring cells. A connexon consists of 6 connexins, 4-transmembrane spanning proteins, with an intracellular N- and C-terminal. Twenty-one connexin isoforms are presently known, which – besides other properties – differ in their molecular weight, their gating properties, and their tissue distribution (Evans and Martin, 2002; Söhl and Willecke, 2004).

Another open question in current regenerative medicine, in particular cardiovascular approaches to BM-MSC therapy by BM-MSC injection, is whether adult BM-MSC can form malignant tumors or not, and whether in such a case these cells may communicate with normal tissue. In favor of this idea Valiunas et al. (2004) showed in commercially available human MSC that these cells can express Cx43, Cx40, and Cx45, and found punctuate Cx43 and Cx40 staining in regions of close cell–cell contact, while Cx45 was mostly found cytoplasmically. In addition, they showed that these cells formed functional gap junction channels within their population and with transfected HeLa cells.

In an investigation, which originally was aimed to investigate the possible use of BM-MSC for cardiac tissue replacement therapy by using these cells to form engineered heart tissue instead of neonatal rat cardiomyocytes, which have been previously used

(Zimmermann et al., 2006; Leontyev et al., 2013) we observed tumor formation in mesenchymal stem-cell-engineered tissue (MSC-ET) after transplantation *in vivo*, and found characteristic gap junction protein distributions.

The primary idea behind our study was to replace cardiomyocytes in engineered heart tissue (Leontyev et al., 2013) by mesenchymal stem cells. To our surprise we observed a malignant tumor originating from the ET. This tumor showed an interesting reverse relationship between proliferation and expression of the cardiac connexins Cx43, Cx40, and Cx45. Thus, those areas where the tumor invaded the heart, were negative for cardiac connexins but positive for Ki-67. In contrast – areas in the middle of the tumor were negative for the proliferation marker Ki-67 but positive for connexins. Thus, this tumor exhibits both Cx-positive and -negative areas.

## MATERIALS AND METHODS

### USED MSC LINES

We used two types of BM-MSC: (a) isolated by ourselves (sBM-MSC; see below) and (b) a commercial rat BM-MSC (cBM-MSC) from Gibco (S1601-100; Gibco, Darmstadt, Germany).

### BM-MSC ISOLATION

For the isolation of sBM-MSC we used male Sprague Dawley rats weighing about 250–350 g. The rats were anesthetized with: fentanyl (0.005 mg/kg), midazolamhydrochloride (2 mg/kg), medetomidinehydrochloride (0.15 mg/kg), and ketamine (75 mg/kg). Afterward the rats were killed by excising the heart. The femora and tibias were dissected aseptically and washed with PBS. The bone epiphyses were cut off and each remaining diaphysis was placed in one pipette tip, which then was put in a Falcon tube. In order to get the bone marrow out of the cavities we centrifuged the bones (200 × g, 5 min, 21°C) (Dobson et al., 1999). The cell pellets were purified from tissue remnants by a 100 µm<sup>2</sup>-filter and seeded on 75 mm<sup>2</sup>-flasks (one pellet per flask).

### MSC CULTURE

Both cell lines were cultured at 5% CO<sub>2</sub> and 37°C in Dulbecco modified Eagle medium-low glucose supplemented with 10% fetal bovine serum and 2.5% Streptomycin/Penicillin. The first medium change was performed after 3 days to remove the non-adherent cells (Strawn et al., 2004). Afterward the medium was removed every 3–4 days. When the MSC reached 80% confluence, they were trypsinized and plated at a density between 2 and 6 × 10<sup>3</sup>/cm<sup>2</sup>.

### CHARACTERIZATION OF MSC: FLOW CYTOMETRY AND ADIPOGENIC DIFFERENTIATION

For characterization we performed flow cytometry and adipogenic differentiation for three cultures of sBM-MSC (passage 3). For cBM-MSC (passage 6) we could validate the manufacturer’s descriptions (CD29+, CD44+, CD90+, CD106+ (>70%), CD11b-, CD34-, CD45- (<5%) and adipogenic-, chondrogenic-, and osteogenic-differentiation).

Using flow cytometry analysis (LSR II, Becton Dickinson, Heidelberg, Germany) we analyzed expression of two MSC-markers: CD54 and CD90 and two negative-markers: CD34 and CD45 (Pittenger et al., 1999; Wan et al., 2008; Hong et al., 2009). Briefly, cells

were incubated with FITC-mouse monoclonal antibodies against rat – CD34 (Santa Cruz; sc-7324), CD45 (BD; 550616), CD54 (BD; 554969), and CD90 Thy1/Thy1.1 (BD; 554894). For the control served isotype-identical antibodies: Mouse IgG1 κ (BD; 550616) and Mouse IgG2a κ (BD; 553456). Labeled cells were detected on a LSR II (Becton Dickinson, Heidelberg, Germany) by collecting 10.000 events using FACSDiva software (Becton Dickinson, Heidelberg, Germany).

To proof evidence of multipotency of MSC we induced adipogenic differentiation by the STEMPRO®Adipogenesis Differentiation Kit (Gibco, Darmstadt, Germany). After 3 weeks, lipid vacuoles within cells were detected by Oil-Red-O-staining in both cell lines (Pittenger et al., 1999).

#### **ENGINEERED TISSUE PRODUCTION FROM MSC (MSC-ET PRODUCTION)**

For creating a MSC-ET,  $2.5 \times 10^6$  cultured MSC/ml, either (a) sBM-MSC or (b) cBM-MSC, were mixed with matrigel, collagen I, and serum containing media and were formed to rings by casting into a circular structure as described (Leontyev et al., 2013). Briefly, for preparing ET rings,  $5 \times 10^6$  cells suspended in a total volume of  $910 \mu\text{l}$  M199 with 20% fetal calf serum and penicillin/streptomycin were mixed  $200 \mu\text{l}$  matrigel (Becton Dickinson, Heidelberg, Germany),  $500 \mu\text{l}$  collagen I (5.5 mg/ml; Sigma, Taufkirchen, Germany),  $70 \mu\text{l}$  0.1 M NaOH (4%) and 320 double concentrated M199 medium containing 20% horse serum and 4% fetal calf serum, the pH was adjusted to 7.4 with HEPES (Zimmermann et al., 2006). The cell mixture was cast into a circular ring-like structure of 10 mm diameter and 2 mm wall thickness and allowed to solidify for 1 h. Thereafter, M199 media was added carefully. After 24 h medium was changed. ET rings were then allowed to grow in M199 media (supplemented with 10% horse serum, 1% fetal calf serum, 2% chick embryo extract). After 5 days of consolidation time MSC-ETs were electrically stimulated (1 Hz, 1 mV, and 0.1 mA) for further 6 days. In total the MSC-ETs were cultivated for 2 weeks. We obtained six mesenchymal stem cell Engineered Tissues (sMSC-ET) from sBM-MSC (passage 3) and seven cMSC-ETs from cBM-MSC (passage 6).

#### **CHRONIC MSC-ET IMPLANTATION IN THE RAT**

Subsequently three of six sMSC-ETs and three of seven cMSC-ETs were implanted around the beating heart of adult female Sprague Dawley rats, which were obtained from University of Leipzig (the remaining BM-ETs were used for pre-implantation histology, see below). The ring-like MSC-ETs were implanted around the whole heart, i.e., around the free wall of the left and right ventricles in a circular manner below the valve plane. Rats were housed in controlled facility with 12:12 h light/dark cycle with standard laboratory diet.

In animals undergoing surgery: rats were anesthetized by combined intramuscular application of fentanyl (0.005 mg/kg), midazolam (2 mg/kg); medetomidin (0.15 mg/kg) and after intubation isoflurane (1.5%), which was continued as inhalation anesthesia (0.8–1% isoflurane). The thorax was opened by sternotomy. The MSC-ET was directly implanted from the culture disk to the animal. MSC-ET rings were placed on the beating heart in the middle of the left and right ventricle and actively fixed with four to five (8/0 Prolene, Ethicon) single-knot sutures.

All animals received immunosuppression for 30 days (day 80–110) with cyclosporin (5 mg/kg/day), methylprednisolone (5 mg/kg/day), and azathioprine (2 mg/kg/day). After 1 month the rat hearts were surgically excised and preserved for histological analysis of the MSC-ETs *in vivo*.

#### **HISTOLOGY**

Cultivated *in vitro* MSC-ETs and rat hearts with the transplanted MSC-ETs were fixed in 4% buffered formaldehyde solution and embedded in paraffin for cutting 4  $\mu\text{m}$  thick sections, and processed for standard Hematoxylin Eosin staining, and Azan-novum, Elastica van Gieson and immunohistological staining. For evaluating the amount of collagen fibers of the MSC-ET we used the Azan-novum staining. Therefore the object slides were incubated for 7 min in 0.1% Kernechtrubin solution, which stained nuclei red. Subsequently collagen tissue was stained blue by 5 min in aniline blue-Orange G. Existence of elastic fibers could be shown by Elastica-van-Gieson-staining. Paraffin slides were put in resorcin-fuchsin for 15 min and elastic fibers turned into a dark purple. Nucleoli were stained brown by incubating for 5 min in Weigert's Hematoxylin.

#### **IMMUNOHISTOCHEMISTRY**

After a 10 min rinsing step in TBS, 4  $\mu\text{m}$  paraffin sections were immersed in 0.01 M sodium citrate buffer (pH 6.0) and cooked in a microwave for 30 min at 600 W. The endogenous peroxidase activity was inhibited by incubating for 10 min in a solution consisting of 60% methanol, 40% TBS, and 0.3% hydrogen peroxide. Microscopic slides were blocked with 2% BSA for 1 h and afterward they were incubated with 1:100 diluted rabbit polyclonal anti-von Willebrand Factor (Ab6994, Abcam, Cambridge, UK) overnight at 4°C. Subsequently, the samples were incubated with a secondary anti-rabbit peroxidase-conjugated antibody (1:200) for 1 h at room temperature. Von Willebrand Factor positive vessels were visualized by staining them red with the chromogen AEC for 20 min at room temperature and nuclei were counterstained by Mayer's hematoxylin.

For Cx40, Cx43, Cx45, CD90, CD20, CD3, CD45, and ki-67 we used a polyclonal Cx40 antibody (AB1726, Millipore, Schwalbach, Germany), a polyclonal rabbit anti-rat Cx43 antibody (C6219, Sigma, Taufkirchen, Germany), a rabbit anti-Cx45 antibody (AB1742, Chemicon, Temecula, CA, USA), a mouse monoclonal CD90 antibody (ab225, Abcam, Cambridge, UK), a goat polyclonal anti-CD20 antibody (Sc-7735, Santa Cruz, CA, USA), a mouse monoclonal anti-CD45 antibody (Sc-53047, Santa Cruz, CA, USA), a goat polyclonal anti-CD3-ε antibody (Sc-1127, Santa Cruz, CA, USA), and a goat antibody against ki-67 (Sc7846, SantaCruz, CA, USA). The immunofluorescence protocols varied with regard to permeabilization and blocking. For each staining protocol exposure times and antibody dilutions were tested and optimized separately prior to the final experiments. The specificity of immunostaining for Cx40, Cx43, Cx45 was tested prior to these experiments using transfected HeLa cells as described (Hagen et al., 2009).

For Cx40 staining, the paraffin-fixed sections were permeabilized for 15 min in a TBS solution with 0.1% Trypsin and 0.1% CaCl<sub>2</sub> (pH 7.8). For Cx43 labeling slides were put in sodium

citrate buffer (pH 6.0) and cooked in a microwave for 30 min at 600 W. The Cx45 and CD90 slides were permeabilized for 30 min in 1% Triton in PBS and blocked for further 60 min in 2% BSA in PBS. Cx40 and Cx43 slides were blocked for 60 min in 2% BSA in TBS. Afterward the slides were incubated with anti-Cx40 (1:100), anti-Cx43 (1:2000), anti-Cx45 (1:100), anti-CD90 (1:100), or anti-ki-67 (1:100) overnight at 4°C. Next, the slides were incubated with the appropriate Alexa Flour 488 or Alexa Flour 555 conjugated secondary antibodies (1:250) (Sigma, Taufkirchen, Germany) at room temperature for 1 h. Background autofluorescence was inhibited immersing for 1 min in 0.1% Chicago Blue in TBS. Nuclei were stained for 1 min with DAPI in TBS.

For histomorphometric investigations single slides were taken and the total field area for 10 randomly selected fields was examined. The heart sections were analyzed by blinded observers by using microscopy Zeiss AxioPlan2 Microscope (Jena, Germany) equipped with a digital microscope camera (AxioCam MRC5 Zeiss, Jena, Germany). Exposure times and intensity for taking immunofluorescence pictures were adjusted for the series of pictures. The digital images were analyzed using AxioVision 4.6 (Zeiss, Jena, Germany).

## STATISTICS

All data are given as MEANS  $\pm$  SEM of  $n$  experiments. The data were statistically analyzed by ANOVA, and if ANOVA indicated

**Table 1 | characteristics of the two groups of bone marrow derived stem cells used in this study.**

%	sBM-MSC	cBM-MSC
CD90	94 $\pm$ 3	99 $\pm$ 1
CD54	72 $\pm$ 4	96 $\pm$ 1
CD34	0 $\pm$ 0	0 $\pm$ 0
CD45	13 $\pm$ 2	0 $\pm$ 0
Adipocyte formation rate	10 $\pm$ 1	22 $\pm$ 0.3

The percentage of cells which was positive for a certain antigen (FACS analysis; mesenchymal marker: CD90, CD54; hematopoietic markers: CD34, CD45) is given as well as the percentage of MSC which could be transformed to adipocytes. All values are given as means  $\pm$  SEM.

**Table 2 | Characteristics of the engineered tissues (ET) made from the two groups of bone marrow derived stem cells used in this study.**

%	<i>In vitro</i> ET		<i>In vivo</i> ET	
	sMSC-ET	cMSC-ET	sMSC-ET	cMSC-ET
Troponin <sup>+</sup> cells	0.3 $\pm$ 0.1	0.3 $\pm$ 0.2	0.5 $\pm$ 0.2	0.1 $\pm$ 0.05
Cx43 <sup>+</sup> cells	38 $\pm$ 2	74 $\pm$ 4#	57 $\pm$ 9*	50 $\pm$ 11*
CD90 <sup>+</sup> cells	38 $\pm$ 14	77 $\pm$ 5#	16 $\pm$ 4*	16 $\pm$ 7*
Vessels/mm <sup>2</sup>	4 $\pm$ 1	20 $\pm$ 8#	49 $\pm$ 9*	39 $\pm$ 2*#
Collagen	70 $\pm$ 2	64 $\pm$ 2	37 $\pm$ 3*	28 $\pm$ 9*
Elastic fibers	0	0	1.8 $\pm$ 0.2*	0.9 $\pm$ 0.15*

The percentage of cells which was positive for a certain antigen (CD90, Cx43, troponin I) is given as well as the number of vessels/mm<sup>2</sup> and the percentage of the area which was covered by collagen or elastic fibers. All values are given as means  $\pm$  SEM. Significance (*in vivo* vs. *in vitro*) are indicated by an asterisk, significance between sBM-ET and cBM-ET is marked by # ( $p < 0.05$ ).

significance, by *post hoc* Tukey HSD or by a Chi-square test as appropriate on a level of significance of 0.05 using SYSTAT software (SYSTAT 11.0; Jandel Scientific, Erkrath, Germany).

## RESULTS

### FACS ANALYSIS AND ADIPOGENIC DIFFERENTIATION OF ADULT MESENCHYMAL STEM CELLS PRIOR TO TISSUE ENGINEERING AND TRANSPLANTATION

Bone marrow derived mesenchymal stem cells (passage 3) exhibited an expression of the mesenchymal surface markers CD90 and CD54, and to a lower extent for the hematopoietic marker CD45, while they were negative for the second hematopoietic marker CD34. In comparison the commercial cBM-MSC (passage 6) also were positive for CD90 and CD54, but were negative for both CD34 and CD45 (**Table 1**).

Both types of BM-MSC showed the ability of adipogenic differentiation, which was somewhat higher in cBM-MSC. After 3 weeks of incubation with adipogenic supplementation,  $10 \pm 0.93\%$  of the sBM-MSC and  $21.69 \pm 0.31\%$  of the cBM-MSC developed Oil-Red-O-positive lipid droplets (**Table 1**). Non-treated control cultures did not show spontaneous adipogenic formations after 3 weeks of cultivation (not shown).

### FORMATION OF MSC-ETS *IN VITRO* AND *IN VIVO*

The MSC-ETs (sMSC-ETs; cMSC-ETs) did not exhibit any contractions. Histological analysis of *in vitro* MSC-ET after 14 days of culture showed that both types of MSC-ET had a high amount of collagen, no elastic fibers, only very few vessels, almost no myocytes (defined as troponin I expressing cells), but considerable numbers of Cx43 or CD90 positive cells (see **Table 2**; **Figure 1**). Under *in vitro* conditions the MSC-ETs did not exhibit specific Cx45 but showed slight Cx40 staining (**Figures 1C,D**). After 30 days of implantation, the collagen content and the percentage of cells positive for the mesenchymal marker CD90 was reduced, while the number of vessels was increased, and a new formation of elastic fibers could be observed (**Table 2**).

Surprisingly, in one of the three cMSC-ET-transplanted rats the heart was completely surrounded by a sarcoma originating from the cMSC-ET, which nearly filled the whole thorax. This was not observed with sMSC-ETs. This tumor showed highly interesting features regarding the distribution and expression of gap junction

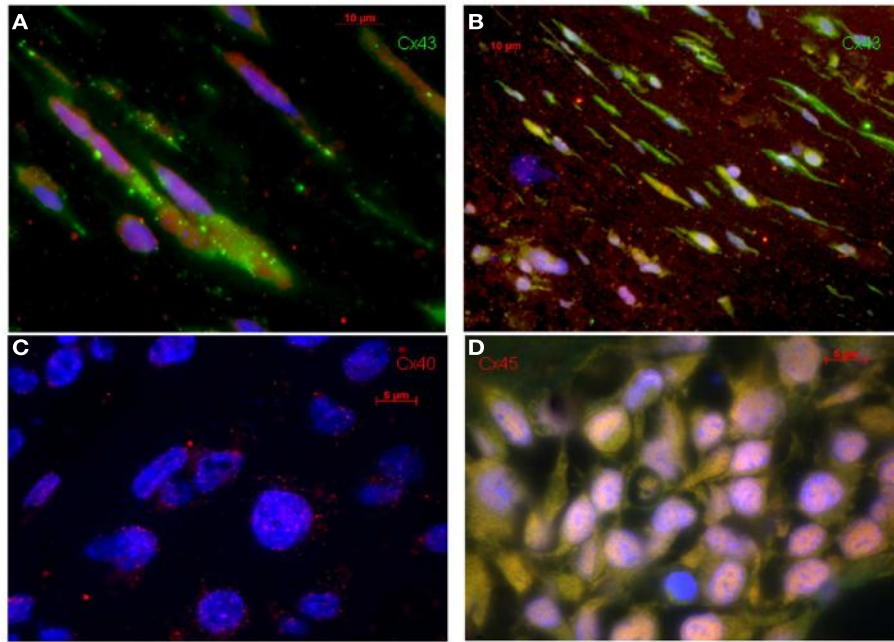


**FIGURE 1 | Original immunohistological images from *in vitro* MSC-ETs. (A)** sMSC-ET and **(B)** cMSC-ET. Red: troponin I, green: Cx43, blue: DAPI. In both types no cross striation for troponin I can be seen. There are numerous cells expressing Cx43. However, Cx43

is mostly located intracellularly and is distributed irregularly. **(C,D)** Show Cx40 and Cx45 staining in cMSC-ET. Note the slight punctate Cx40 staining [red; **(C)**] and the absence of a specific (red) Cx45 staining **(D)**.

proteins showing no intercellular gap junction protein expression at the border between heart and tumor, while the tumor expressed connexins in its inner center (but see below). Such tumor formation was not observed in any of the other rats.

#### MORPHOLOGY AND MACROSCOPIC ANATOMY OF THE SARCOMA

The measured diameter of the solid tumor was from minimum 3.28 mm to maximum 12.39 mm. In comparison, the heart exhibited a size of 9.03 mm (diameter measured at the widest transverse section) and 13.48 mm (at the longitudinal section). The solid neoplasm was well bounded and of tubercular shape. The intersection was white-greely colored and it showed various lesions as indicated by bleedings and necrosis, which reminded to the typical description of a sarcoma (Fletcher, 1992). Figures 2A,B show the macroscopic aspect of this tumor.

#### PATHOLOGY

Regarding the growth and location of the tumor, it became obvious that the tumor was originating from the cMSC-ET. The ET had been implanted around the rat heart and the growth direction of the neoplasm was from the ET to the heart with several infiltrations of the cardiac tissue.

The picture of the HE-staining (Figure 2C) was characterized by closely, side by side laying cells and sparsely surrounding collagen. The cells exhibited atypical nuclei and atypical cytoplasm. The pleomorphic cells showed different sizes and their shape was from clumsily oval through to round and only a few spindle shaped. Some nuclei were equipped with nucleoli, but an eminent majority of them were oversized and had a vesicular appearance, which

resulted in hypochromatic staining. The type of growth differed between undirected and storiform and a few septums made of collagen tissue caused a knotty division. Many inflammatory infiltrates, predominantly consisting of lymphocytes, were found at the transition between the neoplasm and the heart, in particular, at spots, where the tumor had infiltrated the cardiac tissue. Atypical, polynuclear giant cells were not detected, as would be expected for a malignant giant cell tumor of soft tissues (Guccione and Enzinger, 1972; Angervall et al., 1981). By HE-staining we did not find any differentiation characteristics such as lipoblasts or osteoid formation, together with a high nucleus/plasma ratio, which implied, that the tumor is probably an undifferentiated pleomorphic sarcoma. A lymphoma could be excluded by the finding that the tumor cells were negative for CD3, CD20, and CD45.

#### GRADING

Following the hypothesis of this tumor being a sarcoma, there are two acknowledged grading systems for soft tissue sarcomas. We used the FNCLCC-system (Fédération Nationale des Centre de Lutte contre le cancer), because it correlates better with the clinical prognosis than the NCI-System (National Cancer Institute) (Guillou et al., 1997). The FNCLCC-system is based on three parameters: tumor differentiation, mitotic activity and necrosis, whereas the grading depends crucial on the histological type. According to the FNCLCC-system the tumor in this case exhibited an undifferentiated pattern, which couldn't clearly dedicated to one special type (=score 3). Moreover, we found 41 mitoses in 10 high-power fields ( $1 \text{ HPF} = 0.1734 \text{ mm}^2$ ), which also gives a score value of 3. Less than 50% of the tumor tissue consisted

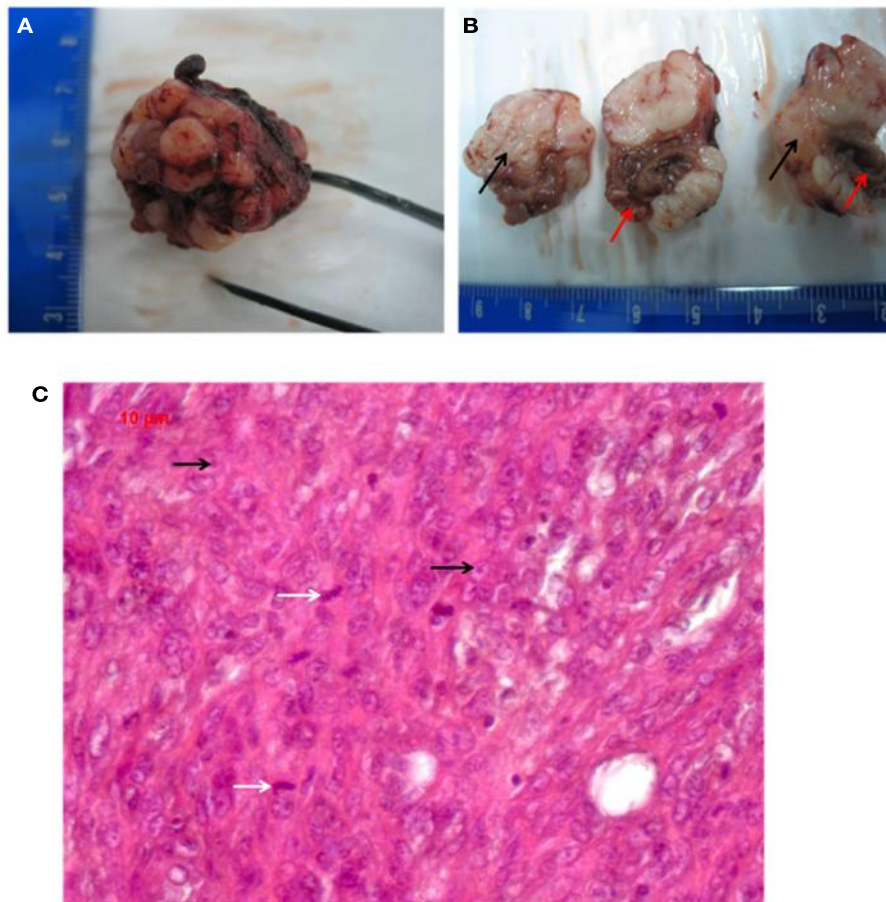


**FIGURE 2 | (A,B)** Macroscopic pathology of the tumor (red arrows point to the heart, black arrows indicate the grayish tumor mass). **(C)** Shows the HE histology (white arrows indicate mitosis; black arrows point to nucleoli).

of necrotic areas (=score 1), so that the total score was 7 (=7/8) corresponding to a high grade malignant sarcoma (Guillou et al., 1997; Deyrup and Weiss, 2006).

#### DISTRIBUTION OF THE CONNEXINS 40, 43, AND 45 IN THE SARCOMA AND THE HEART TISSUE

Immunohistochemical investigations revealed that the tumor cells in the middle of the tumor were positive for all three cardiac connexins, i.e., connexin 40, 43, and 45. By comparing the fluorescence signals of the three connexins, we recognized that most cells stained positive for Cx43, while a smaller percentage expressed Cx45 and Cx40. All of the three connexins were uniformly located in the cytoplasm of the sarcoma cells, while the plasma membrane was almost free of an immunopositive connexin signal and there was no accentuation of the connexins near the nucleus. In particular, there were no selective accumulations of the fluorescence between adjacent cells at the cell–cell-borders, which implies that functional gap junctions are less probable (Figure 3). In contrast, in the heart we found the typical localization of connexins at the plasma membrane with accentuation at the cell–cell contacts in particular at the cellular poles (Figures 3B,D,F).

Regarding the connixin expression, the sarcoma cells in the present tumor can be divided into two areas: the first is the sarcoma itself and the second is the transition zone between cardiac tissue and sarcoma including the infiltrative growing sarcoma cells (Figure 3B). The vast majority of sarcoma cells in the middle and outer area of the tumor are positive for the three connexins (Figures 3A,C,E), while in close vicinity of the transition zone the sarcoma cells lost their positive connexin signal (Cx43, Cx40, Cx45), which indicated that the tumor cells at the border do not express any of the cardiac connexins (Figures 3B,D,F). In the heart Cx43 is most prominently expressed.

With regard to the question whether connexin expression and tumor growth may be interrelated we also investigated the expression of Ki-67, a marker of cell proliferation. In the middle of the tumor only  $37 \pm 2\%$  of the cells were Ki-67 positive, while at the tumor-heart border significantly ( $p = 0.0007$ ) more cells were Ki-67 positive, i.e.,  $51 \pm 7\%$  Ki-67<sup>+</sup> cells. This was accompanied by a significant reduction in positivity for all cardiac connexins ( $p < 0.001$ ) from  $30 \pm 6$  to  $2 \pm 2\%$  of the cells expressing any of the three connexins ( $p < 0.001$ ). It became obvious, that cells which were positive for Ki-67 mostly were negative for Cx43,

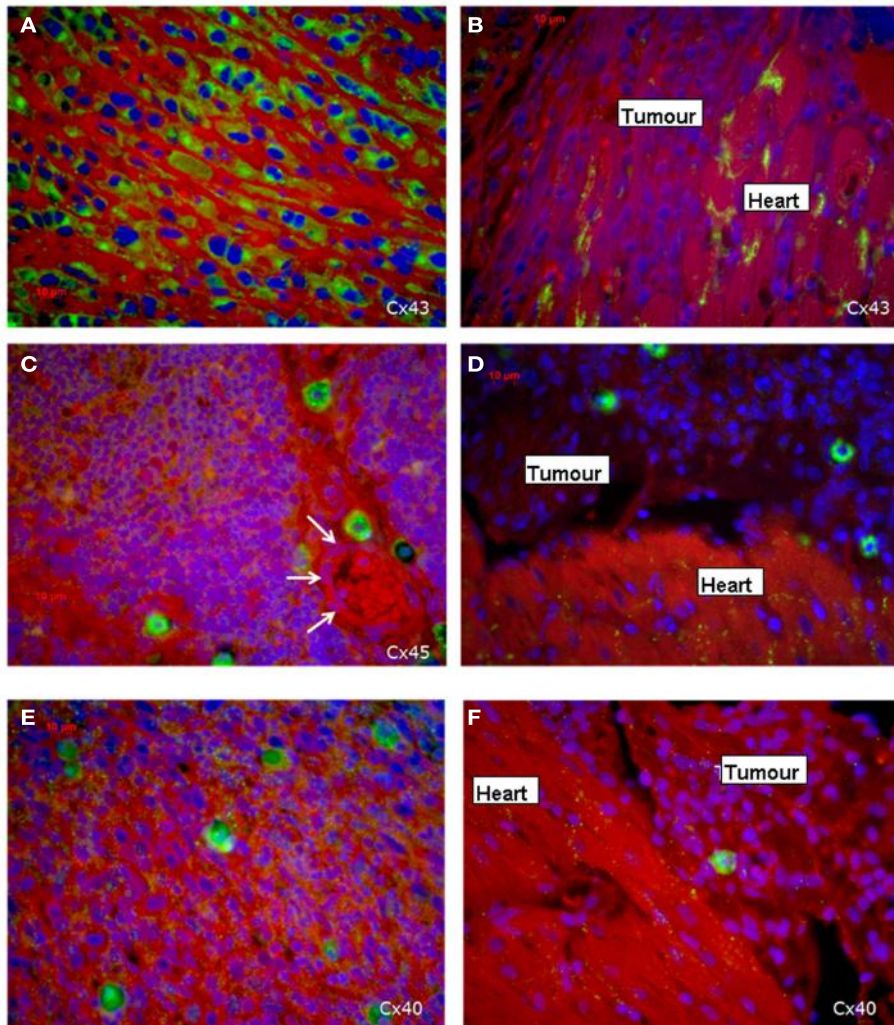


**FIGURE 3 | Expression of the three cardiac connexins Cx43 (A,B), Cx45 (C,D), and Cx40 (E,F) (connexins are stained green). (A,C,E)** Show the expression within the middle of the tumor, while **(B,D,F)** demonstrate the

loss of connixin expression in the invading zone of the tumor close to the heart and a regular distribution of connexins in the heart itself. The white arrows indicate a vessel.

Cx40, or Cx45 (Figure 4). In particular, at the tumor-heart border, where the tumor infiltrated the heart, there were nearly no cells which showed immunopositivity for connixin (Figure 5). Quantitatively, in the middle of the tumor we found a clear statistical relationship between expression of Ki-67 and the lack connixin expression (Chi-square test: Cx43:  $p < 0.0001$ ; Cx45:  $p < 0.03$ , Cx40:  $p < 0.014$ ) where those cells expressing Ki-67 co-expressed significantly more rarely connixin (Figure 6A). At the tumor-heart border all cells expressing Ki-67 were negative for Cx43 and Cx40, and only 2% co-expressed Ki-67 and Cx45 (Figure 6B).

## DISCUSSION

As a main finding we observed an inverse relationship between the expression of connexins, i.e., Cx43, Cx40, or Cx45, and of cell proliferation marker Ki-67 (which is not present in G0 phase). Moreover, in those parts of the tumor which invaded the heart, i.e., in the growth zone with highest Ki-67 expression, connixin

expression was nearly absent. These data are in favor of the hypothesis that tumors cells are not communicating with their surrounding normal tissue when they grow invasively. In the present case the tumor did not express any of the typical cardiac connexins at the tumor-heart border where infiltrative growth was found. That could mean, that these tumor cells can not get growth-inhibitory signals from the normal cells *via* GJIC, thus, enabling invasive growth. This is similar to Mesnil et al. (1994) who found in a coculture of tumorigenic and non-tumorigenic rat liver epithelial cell lines that Cx43 was abundantly expressed in non-tumorigenic cells and was absent in tumorigenic cells. The zone lacking Cx43 indicated the boundary between tumorigenic and non-tumorigenic cells, similar to our tumor-heart border (Mesnil et al., 1994). The finding, that the sarcoma cells showed connexins rather predominantly intracytoplasmic than in the cytoplasmic membrane suggests that these connexins may not represent functional intercellular channels. A similar expression

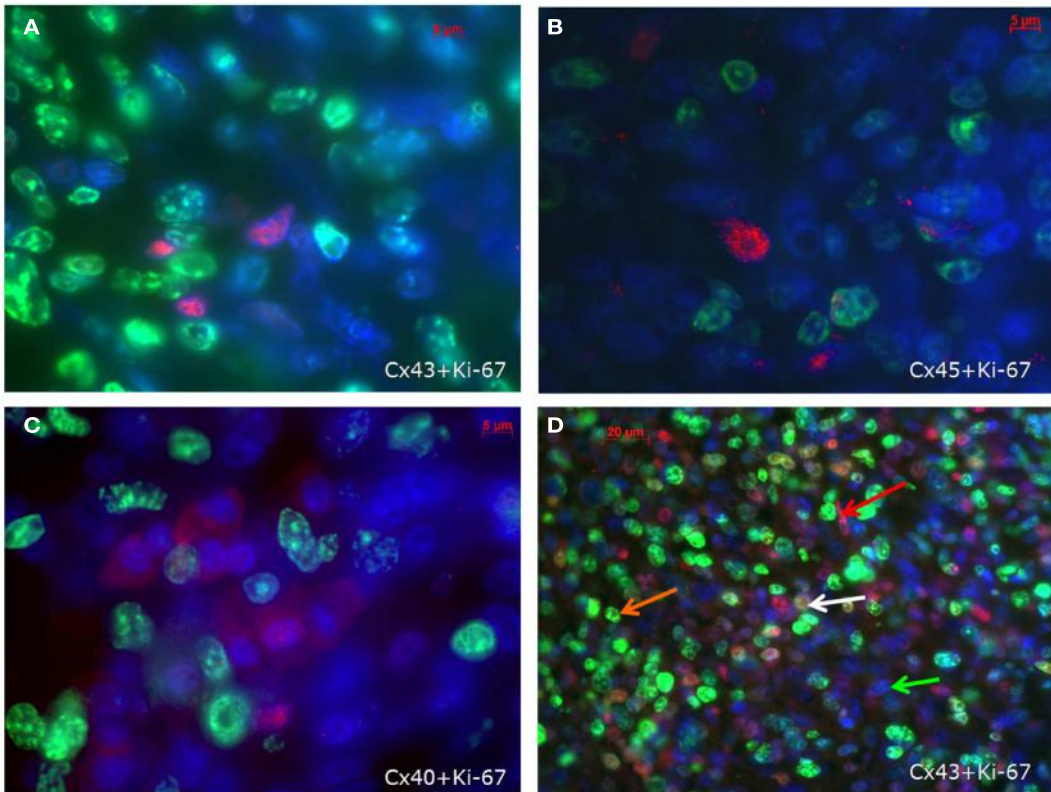


**FIGURE 4 | Co-staining of Ki-67 (green) and Cx43 (A), Cx45 (B) and Cx40 (C) (connexins are stained red) in the inner part of the tumour.** In (D) an overview is shown at a lower magnification.

Besides cells negative for both antigens (green arrow), cells are either positive for Ki-67 (orange arrow) or for Cx43 (red arrow). Only few cells co-express Cx43 and Ki-67 (white arrow).

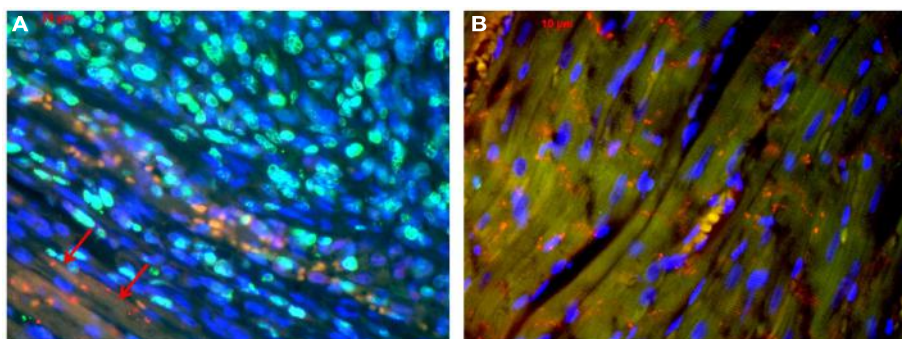


**FIGURE 5 | Tumor-heart border [(A); red arrows mark the transition to the heart] and non-infiltrated normal heart tissue (B).** Co-staining of Ki-67 (green), Cx43 (red), and nuclei (blue).

pattern has been shown for Cx32 and Cx43 in colorectal adenoma and even augmented in carcinoma (Kanczuga-Koda et al., 2010). By this aberrant localization, despite the expression of connexins in the tumor, the absence of detectable connexin signals in the membrane of the sarcoma cells probably means that they will not form functional gap junctions. This may lead to insufficient homologous GJIC within the tumor (Yamasaki et al., 1995). Similarly, Kalimi et al. (1992) reported of a reduction

of homologous GJIC in v-raf- and v-raf/v-myc-transformed rat liver epithelial cells and a loss of heterologous GJIC in v-raf/v-myc-transformed cells by using scrape loading-dye transfer and fluorescence-recovery-after-photobleaching (FRAP) assays.

The role of GJIC in tumors is not entirely clear: on the one hand there are several tumors which do not express any connexin, e.g., HeLa cells (King et al., 2000a), and while many tumor-promoting agents down regulate GJIC (Salameh and Dhein, 2005),

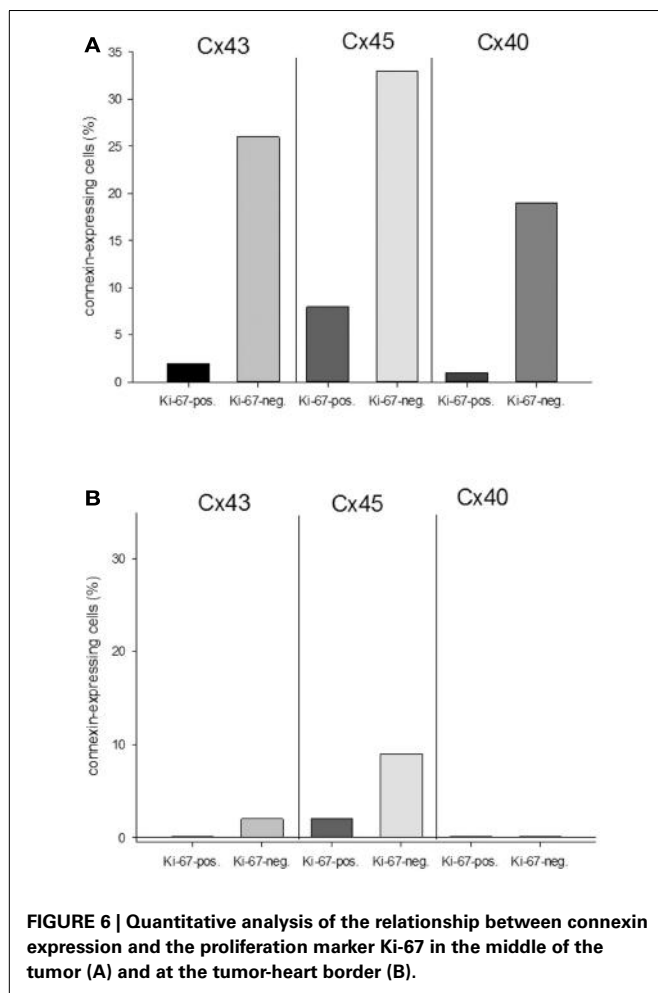


**FIGURE 6 | Quantitative analysis of the relationship between connexin expression and the proliferation marker Ki-67 in the middle of the tumor (A) and at the tumor-heart border (B).**

and while tumor oncogenes like *ras*, *src*, *raf*, and *mos* have been shown to downregulate GJIC (Trosko et al., 2004). On the other hand there are also reports that suggest that connexins expressed in tumor cells may support the process of extravasation, invasion, and metastasis (Lin et al., 2002; Elzarrad et al., 2008). Regarding our study, in the tumor cells in our observation connexins are expressed. However, these connexins are obviously located predominantly if not solely intracellularly, so that they probably do not form functional channels. However, there was an interesting difference between the middle of the tumor and its invading border: while in the middle cells expressed connexins, they did not or almost not at the border.

The lack of membranous connexins would support the idea that the tumor cells do not communicate with the neighboring cells and, thus, can not receive growth inhibition signals from them. They are blind for the neighbor cells since they do not express the same connexins. Consequently, they do not see them and thus proliferate without inhibition. Although attractive, this view is probably too unilateral. Other signals may come from secreted growth inhibitors from other cells or from the microenvironment (Trosko et al., 1993; Barcellos-Hoff and Brooks, 2001). Regarding the role of connexins, we have to discriminate channel-related functions from channel-independent functions.

Thus, although not membrane-bound, connexin proteins are not functionless but can exert regulatory functions on growth and differentiation: it was shown that the carboxy terminal of Cx43 can associate with  $\beta$ -catenin. Thereby, Cx43 can regulate the cytosolic concentration of  $\beta$ -catenin. A reduction in Cx43, or phosphorylation at S262 by FGF-2, can increase the free cytosolic  $\beta$ -catenin which then in turn can translocate to the nucleus where it can activate TCF/LEF transcription factors and genes related to proliferation (like cyclin D, c-myc, c-jun) (Ai et al., 2000; Holnthoner et al., 2002; Doble and Woodgett, 2003). Furthermore the  $\beta$ -catenin-pool is regulated by wnt-Frizzled-receptor-signaling which reduces GSK3 activity. GSK3 constitutively phosphorylates  $\beta$ -catenin and thereby marks it for proteasomal degradation (Holnthoner et al., 2002; Doble and Woodgett, 2003).

Besides  $\beta$ -catenin, the secreted cysteine-rich and heparin binding protein CCN3 can interact with the carboxy terminal of Cx43 thereby inhibiting cellular proliferation (Fu et al., 2004; Gellhaus et al., 2004).

Among the abundant proteins which can interact with connexin43, zonula-occludens protein-1 (ZO-1), a scaffolding protein, is among the best investigated. The binding of ZO-1 to connexin43 also fixes its binding partner ZONAB (ZO-1 associated nucleic acid binding protein) together with CDK4 at the membrane and prevents from its translocation to the nucleus. If ZONAB is released it can together with CDK4 contribute to G1/S-transition (Giepmans and Moolenaar, 1998; Sourisseau et al., 2006). However, the binding of ZO-1 to connexin seems to be at least mostly related to membrane-bound connexin.

Taken together, besides acting as intercellular communication channel there is growing evidence that Cx43 can serve as an anti-proliferative nexus platform or binding “hub” for proteins which regulate growth. By docking to Cx43, the free concentration of these proteins is controlled. Depending on Cx43 concentration or phosphorylation status the other proteins may be released from the “hub” and translocate to the nucleus, where they can induce gene transcription linked to proliferation. Accordingly, a close relationship between Cx43 and important growth controlling genes was shown by Jacobas et al. (2005a,b).

This view is supported by our data showing that the increase in intracellular connexin is negatively related to the proliferation marker Ki-67.

Interestingly, the tumor data suggest that some factor in the middle of the tumor seemed to inhibit the synthesized connexins from being transported to the membrane. From the present data it remains unclear whether the connexin found intracellularly was monomeric or whether it was already oligomerized to connexons. Thus, it remains speculative to conclude on which level of the gap junction formation the process was arrested. However, it is tempting to speculate that an agent which would overcome this arrest may restore GJIC and thereby growth control.

Another issue worth some discussion is the stem cell. The observed sarcoma seemed to originate from the stem-cell-derived ET, which would mean that BM-MSC of a low passage (in that case sixth passage) were able to transform to a malignant tumor. While some investigators found functional connexins in MSC (Valiunas et al., 2004), other researchers reported that stem cells typically have no functional gap junctional intercellular communication

and, thus, their growth control is assumed to be realized *via* secreted factors or other extracellular signals from their surrounding (Trosko et al., 2004). Accordingly, although the cells in our ET expressed connexins, these were predominantly located intracellularly. To become a tumor cell, it is necessary that a cell is immortalized and that it starts proliferation. Stem cells are considered to be immortal cells, which are under a non-gap-junction growth control, and according to the theory from Trosko et al. (2004) the carcinogenic process in this case would mean that this naturally immortal stem cell is prevented from mortalization or terminal differentiation. We can only speculate which factors in the present observation may have contributed, and besides scaffold factors it may be factors from the matrigel material or other factors yet unknown.

However, these observations finally may suggest that connexins like Cx43 might be interesting pharmacological anti-tumor targets. Drugs would need to re-establish the transfer of connexins to the membrane and their integration so that functional channels can be formed in those cells which express connexins intracellularly. Other drugs could act by re-expressing connexins and re-establishing GJIC. However, to achieve growth control this approach would require that the connexins re-expressed or re-integrated in the tumor are compatible with those of the surrounding normal tissue. This will not be possible in every case and may be problematic in particular for metastasis, since connexins may have a supportive role in the process of invasion/metastasis (Ito et al., 2000; Lin et al., 2002; Elzarrad et al., 2008). However, in a tumor as in the observed case, the proliferative invasive parts did not express connexins and re-establishing gap junctional intercellular communication could bear the chance to achieve growth control in these cells. There are some reports which show the principle feasibility of this approach (Zhang et al., 1998; King et al., 2000b; Momiyama et al., 2003).

## LIMITATIONS

As a limitation, it must be taken into account that we only tested for the three cardiac connexins, and not all 21 isoforms. However, since we were interested in the question whether the tumor may form gap junctions with the heart, these would have to contain the cardiac isoforms. Moreover, it would be interesting but was technically not possible to know if these tumor cells were definitively lacking any functional intercellular gap junction communication.

## REFERENCES

- Ai, Z., Fischer, A., Spray, D. C., Brown, A. M., and Fishman, G. I. (2000). Wnt-1 regulation of connexin43 in cardiac myocytes. *J. Clin. Invest.* 105, 161–171.
- Angervall, L., Hagmar, B., Kindblom, L. G., and Merck, C. (1981). Malignant giant cell tumor of soft tissues: a clinicopathologic, cytologic, ultrastructural, angiographic, and microangiographic study. *Cancer* 47, 736–747.
- Bang, O. Y., Lee, J. S., Lee, P. H., and Lee, G. (2005). Autologous mesenchymal stem cell transplantation in stroke patients. *Ann. Neurol.* 57, 874–882.
- Barcellos-Hoff, M. H., and Brooks, A. L. (2001). Extracellular signaling through the microenvironment: a hypothesis relating carcinogenesis, bystander effects, and genomic instability. *Radiat. Res.* 156, 618–627.
- Chin, S. P., Poey, A. C., Wong, C. Y., Chang, S. K., Teh, W., Mohr, T. J., et al. (2010). Cryopreserved mesenchymal stromal cell treatment is safe and feasible for severe dilated ischemic cardiomyopathy. *Cyotherapy* 12, 31–37.
- Cronier, L., Crespin, S., Strale, P. O., Defamie, N., and Mesnil, M. (2009). Gap junctions and cancer: new functions for an old story. *Antioxid. Redox Signal.* 11, 323–338.
- Dei Tos, A. P. (2006). Classification of pleomorphic sarcomas: where are we now? *Histopathology* 48, 51–62.
- Deyrup, A. T., and Weiss, S. W. (2006). Grading of soft tissue sarcomas: the challenge of providing precise information in an imprecise world. *Histopathology* 48, 42–50.
- Djouad, F., Plence, P., Bony, C., Tropel, P., Apparailly, F., Sany, J., et al. (2003). Immunosuppressive effect of mesenchymal stem cells favors tumor growth in allogeneic animals. *Blood* 102, 3837–3844.
- Doble, B. W., and Woodgett, J. R. (2003). GSK-3: tricks of the trade for a multi-tasking kinase. *J. Cell Sci.* 116, 1175–1186.
- Dobson, K. R., Reading, L., Haberey, M., Marine, X., and Scutt, A. (1999). Centrifugal isolation of bone marrow from bone: an improved method for the recovery and quantitation of bone marrow osteoprogenitor cells from rat tibiae and femurae. *Calcif. Tissue Int.* 65, 411–413.
- Elzarrad, M. K., Haroon, A., Wilkecke, K., Dobrowolski, R., Gillespie,

Because of the use of a conventional fluorescence microscopy the optical section thickness could be variable. However, we used 4  $\mu\text{m}$  thin sections.

Regarding the grading of the tumor and its entity, the previously described macroscopy of the tumor and the fact that the EHT consisted of 100% mesenchymal stem cells, led us to the assumption that it had to be a sarcoma originating from the MSC. The following histological examinations underlined this and suggested a pleomorphic sarcoma. However, since we did not investigate this by the use of detailed further immunohistochemistry, we cannot exclude the possibility, that it could also be a dedifferentiated high grade pleomorphic sarcoma (i.e., pleomorphic leiomyosarcoma, pleomorphic rhabdomyosarcoma) (Dei Tos, 2006). Moreover, it remains unclear whether the malignant transformation might be inborn to these cells or whether it might be caused/initiated by the treatment of these cells during the process of ET formation. However, this might be of less importance for the observation of lack of communication proteins at the tumor-heart border, which is the focus of the Present study.

## CONCLUSION

Taken together, we conclude that a pleomorphic sarcoma in the rat does not express connexins at the locations of invasive growth, and that proliferative activity and connexin expression are negatively correlated. Moreover, our data show that this type of tumor does not express tissue-specific connexins at the tumor tissue border. In consequence, we would underline the theory of Kalimi et al. (1992) that probably such a tumor does not get growth limitation signals from the surrounding normal tissue, which might lead to unlimited infiltrating growth. Regarding pharmacological perspectives a review of the current literature (see above) shows that re-establishing of GJIC may help to bring the cells under growth control again, but on the other hand it may also facilitate the metastatic process by enhancing the adhesivity of tumor cells to, e.g., vascular endothelium.

## ACKNOWLEDGMENTS

Supported by BMBF/TRM Leipzig promotional reference 0313909, grant given to Stefan Dhein and Franziska Schlegel, and by a grant given to Stefan Dhein by ProCordis, Leipzig, Germany.

- Elzarrad, M. K., Haroon, A., Willecke, K., Dobrowolski, R., Gillespie, M. N., and Al-Mehdi, A. B. (2008). Connexin-43 upregulation in micrometastases and tumor vasculature and its role in tumor cell attachment to pulmonary endothelium. *BMC Med.* 6:20. doi:10.1186/1741-7015-6-20
- Evans, W. H., and Martin, P. (2002). Gap junctions: structure and function. *Mol. Membr. Biol.* 19, 121–136.
- Ezumi, K., Yamamoto, H., Murata, K., Higashiyama, M., Damidinsuren, B., Nakamura, Y., et al. (2008). Aberrant expression of connexin 26 is associated with lung metastasis of colorectal cancer. *Clin. Cancer Res.* 14, 677–684.
- Fletcher, C. D. (1992). Pleomorphic malignant fibrous histiocytoma: fact or fiction? A critical reappraisal based on 159 tumors diagnosed as pleomorphic sarcoma. *Am. J. Surg. Pathol.* 16, 213–228.
- Fu, C. T., Bechberger, J. F., Ozog, M. A., Perbal, B., and Naus, C. C. (2004). CCN3 (NOV) interacts with connexin43 in C6 glioma cells: possible mechanism of connexin-mediated growth suppression. *J. Biol. Chem.* 279, 36943–36950.
- Gellhaus, A., Dong, X., Propson, S., Maass, K., Klein-Hitpass, L., Kibschull, M., et al. (2004). Connexin43 interacts with NOV: a possible mechanism for negative regulation of cell growth in choriocarcinoma cells. *J. Biol. Chem.* 279, 36931–36942.
- Giempans, B. N., and Moolenaar, W. H. (1998). The gap junction protein connexin43 interacts with the second PDZ domain of the zona occludens-1 protein. *Curr. Biol.* 8, 931–934.
- Guccione, J. G., and Enzinger, F. M. (1972). Malignant giant cell tumor of soft parts. An analysis of 32 cases. *Cancer* 29, 1518–1529.
- Guillou, L., Coindre, J. M., Bonichon, F., Nguyen, B. B., Terrier, P., Collin, F., et al. (1997). Comparative study of the National Cancer Institute and French Federation of Cancer Centers Sarcoma Group grading systems in a population of 410 adult patients with soft tissue sarcoma. *J. Clin. Oncol.* 15, 350–362.
- Gunn, W. G., Conley, A., Deininger, L., Olson, S. D., Prokopp, D. J., and Gregory, C. A. (2006). A crosstalk between myeloma cells and marrow stromal cells stimulates production of DKK1 and interleukin-6: a potential role in the development of lytic bone disease and tumor progression in multiple myeloma. *Stem Cells* 24, 986–991.
- Hagen, A., Dietze, A., and Dhein, S. (2009). Human cardiac gap junction coupling: effects of antiarrhythmic peptide AAP10. *Cardiovasc. Res.* 83, 405–415.
- Holnthoner, W., Pillinger, M., Groger, M., Wolff, K., Ashton, A. W., Albanese, C., et al. (2002). Fibroblast growth factor-2 induces Lef/Tcf-dependent transcription in human endothelial cells. *J. Biol. Chem.* 277, 45847–45853.
- Hong, D., Chen, H. X., Xue, Y., Li, D. M., Wan, X. C., Ge, R., et al. (2009). Osteoblastogenic effects of dexamethasone through upregulation of TAZ expression in rat mesenchymal stem cells. *J. Steroid Biochem. Mol. Biol.* 116, 86–92.
- Horwitz, E. M., Prokopp, D. J., Fitzpatrick, L. A., Koo, W. W., Gordon, P. L., Neel, M., et al. (1999). Transplantability and therapeutic effects of bone marrow-derived mesenchymal cells in children with osteogenesis imperfecta. *Nat. Med.* 5, 309–313.
- Iacobas, D. A., Iacobas, S., Li, W. E., Zoidl, G., Dermietzel, R., and Spray, D. C. (2005a). Genes controlling multiple functional pathways are transcriptionally regulated in connexin43 null mouse heart. *Physiol. Genomics* 20, 211–223.
- Iacobas, D. A., Iacobas, S., and Spray, D. C. (2005b). “Use of cDNA arrays to explore gene expression in genetically manipulated mice and cell lines,” in *Practical Methods in Cardiovascular Research*, eds S. Dhein, F. W. Mohr, and M. Delmar (Berlin: Springer), 907–915.
- Ito, A., Katoh, F., Kataoka, T. R., Okada, M., Tsubota, N., Asada, H., et al. (2000). A role for heterologous gap junctions between melanoma and endothelial cells in metastasis. *J. Clin. Invest.* 105, 1189–1197.
- Kalimi, G. H., Hampton, L. L., Trosko, J. E., Thorgeirsson, S. S., and Huggett, A. C. (1992). Homologous and heterologous gap-junctional intercellular communication in v-raf-, v-myc-, and v-raf/v-myc-transduced rat liver epithelial cell lines. *Mol. Carcinog.* 5, 301–310.
- Kanczuga-Koda, L., Koda, M., Sulkowski, S., Wincewicz, A., Zalewski, B., and Sulkowska, M. (2010). Gradual loss of functional gap junction within progression of colorectal cancer – a shift from membranous CX32 and CX43 expression to cytoplasmic pattern during colorectal carcinogenesis. *In vivo* 24, 101–107.
- Karnoub, A. E., Dash, A. B., Vo, A. P., Sullivan, A., Brooks, M. W., Bell, G. W., et al. (2007). Mesenchymal stem cells within tumor stroma promote breast cancer metastasis. *Nature* 449, 557–563.
- Karussis, D., Kassis, I., Kurkalli, B. G., and Slavin, S. (2008). Immunomodulation and neuroprotection with mesenchymal bone marrow stem cells (MSCs): a proposed treatment for multiple sclerosis and other neuroimmunological/neurodegenerative diseases. *J. Neurol. Sci.* 265, 131–135.
- Khakoo, A. Y., Pati, S., Anderson, S. A., Reid, W., Elshal, M. F., Rovira, I. I., et al. (2006). Human mesenchymal stem cells exert potent anti-tumorigenic effects in a model of Kaposi's sarcoma. *J. Exp. Med.* 203, 1235–1247.
- King, T. J., Fukushima, L. H., Donlon, T. A., Hieber, A. D., Shimabukuro, K. A., and Bertram, J. S. (2000a). Correlation between growth control, neoplastic potential and endogenous connexin43 expression in HeLa cell lines: implications for tumor progression. *Carcinogenesis* 21, 311–315.
- King, T. J., Fukushima, L. H., Hieber, A. D., Shimabukuro, K. A., Sakr, W. A., and Bertram, J. S. (2000b). Reduced levels of connexin43 in cervical dysplasia: inducible expression in a cervical carcinoma cell line decreases neoplastic potential with implications for tumor progression. *Carcinogenesis* 21, 1097–1109.
- Kurtova, A. V., Balakrishnan, K., Chen, R., Ding, W., Schnabl, S., Quiroga, M. P., et al. (2009). Diverse marrow stromal cells protect CLL cells from spontaneous and drug-induced apoptosis: development of a reliable and reproducible system to assess stromal cell adhesion-mediated drug resistance. *Blood* 114, 4441–4450.
- Laird, D. W., Fistouris, P., Batist, G., Alpert, L., Huynh, H. T., Carytinos, G. D., et al. (1999). Deficiency of connexin43 gap junctions is an independent marker for breast tumors. *Cancer Res.* 59, 4104–4110.
- Lampe, P. D. (1994). Analyzing phorbol ester effects on gap junctional communication: a dramatic inhibition of assembly. *J. Cell Biol.* 127, 1895–1905.
- Leontyev, S., Schlegel, F., Spath, C., Schmidel, R., Nichtitz, M., Boldt, A., et al. (2013). Transplantation of engineered heart tissue (EHT) as biological cardiac assist device for treatment of dilated cardiomyopathy. *Eur. J. Heart Fail.* 15, 23–35.
- Lin, J. H., Takano, T., Cotrina, M. L., Arcuino, G., Kang, J., Liu, S., et al. (2002). Connexin43 enhances the adhesivity and mediates the invasion of malignant glioma cells. *J. Neurosci.* 22, 4302–4311.
- Loewenstein, W. R. (1980). Junctional cell-to-cell communication and growth control. *Ann. N. Y. Acad. Sci.* 339, 39–45.
- Loewenstein, W. R., and Kanno, Y. (1966). Intercellular communication and the control of tissue growth: lack of communication between cancer cells. *Nature* 209, 1248–1249.
- Maestroni, G. J., Hertens, E., and Galli, P. (1999). Factor(s) from non-macrophage bone marrow stromal cells inhibit Lewis lung carcinoma and B16 melanoma growth in mice. *Cell. Mol. Life Sci.* 55, 663–667.
- Mesnil, M., Asamoto, M., Piccoli, C., and Yamasaki, H. (1994). Possible molecular mechanism of loss of homologous and heterologous gap junctional intercellular communication in rat liver epithelial cell lines. *Cell Adhes. Commun.* 2, 377–384.
- Mesnil, M., Crespin, S., Avanzo, J. L., and Zaidan-Dagli, M. L. (2005). Defective gap junctional intercellular communication in the carcinogenic process. *Biochim. Biophys. Acta* 1719, 125–145.
- Miura, M., Miura, Y., Padilla-Nash, H. M., Molinolo, A. A., Fu, B., Patel, V., et al. (2006). Accumulated chromosomal instability in murine bone marrow mesenchymal stem cells leads to malignant transformation. *Stem Cells* 24, 1095–1103.
- Momiyama, M., Omori, Y., Ishizaki, Y., Nishikawa, Y., Tokairin, T., Ogawa, J., et al. (2003). Connexin26-mediated gap junctional communication reverses the malignant phenotype of MCF-7 breast cancer cells. *Cancer Sci.* 94, 501–507.
- Nagaya, N., Kangawa, K., Itoh, T., Iwase, T., Murakami, S., Miyahara, Y., et al. (2005). Transplantation of mesenchymal stem cells improves cardiac function in a rat model of dilated cardiomyopathy. *Circulation* 112, 1128–1135.
- Nakamura, K., Ito, Y., Kawano, Y., Kurozumi, K., Kobune, M., Tsuda, H., et al. (2004). Antitumor effect of genetically engineered mesenchymal stem cells in a rat glioma model. *Gene Ther.* 11, 1155–1164.
- Naoi, Y., Miyoshi, Y., Taguchi, T., Kim, S. J., Arai, T., Tamaki, Y., et al. (2007). Connexin26 expression is associated with lymphatic vessel invasion and

- poor prognosis in human breast cancer. *Breast Cancer Res. Treat.* 106, 11–17.
- Naus, C. C., and Laird, D. W. (2010). Implications and challenges of connexin connections to cancer. *Nat. Rev. Cancer* 10, 435–441.
- Ohlsson, L. B., Varas, L., Kjellman, C., Edvardsen, K., and Lindvall, M. (2003). Mesenchymal progenitor cell-mediated inhibition of tumor growth in vivo and in vitro in gelatin matrix. *Exp. Mol. Pathol.* 75, 248–255.
- Pittenger, M. F., Mackay, A. M., Beck, S. C., Jaiswal, R. K., Douglas, R., Mosca, J. D., et al. (1999). Multilineage potential of adult human mesenchymal stem cells. *Science* 284, 143–147.
- Romanov, Y. A., Svintsitskaya, V. A., and Smirnov, V. N. (2003). Searching for alternative sources of postnatal human mesenchymal stem cells: candidate MSC-like cells from umbilical cord. *Stem Cells* 21, 105–110.
- Rubio, D., Garcia-Castro, J., Martin, M. C., de la Fuente, R., Cigudosa, J. C., Lloyd, A. C., et al. (2005). Spontaneous human adult stem cell transformation. *Cancer Res.* 65, 3035–3039.
- Saito-Katsuragi, M., Asada, H., Niizeki, H., Katoh, F., Masuzawa, M., Tsutsumi, M., et al. (2007). Role for connexin 26 in metastasis of human malignant melanoma: communication between melanoma and endothelial cells via connexin 26. *Cancer* 110, 1162–1172.
- Salameh, A., and Dhein, S. (2005). Pharmacology of gap junctions. New pharmacological targets for treatment of arrhythmia, seizure and cancer? *Biochim. Biophys. Acta* 1719, 36–58.
- Sato, H., Hagiwara, H., Senba, H., Fukumoto, K., Nagashima, Y., Yamasaki, H., et al. (2008). The inhibitory effect of connexin 32 gene on metastasis in renal cell carcinoma. *Mol. Carcinog.* 47, 403–409.
- Söhl, G., and Willecke, K. (2004). Gap junctions and the connexin protein family. *Cardiovasc. Res.* 62, 228–232.
- Sourisseau, T., Georgiadis, A., Tsapara, A., Ali, R. R., Pestell, R., Matter, K., et al. (2006). Regulation of PCNA and cyclin D1 expression and epithelial morphogenesis by the ZO-1-regulated transcription factor ZONAB/DbpA. *Mol. Cell. Biol.* 26, 2387–2398.
- Spaeth, E. L., Dembinski, J. L., Sasser, A. K., Watson, K., Klopp, A., Hall, B., et al. (2009). Mesenchymal stem cell transition to tumor-associated fibroblasts contributes to fibrovascular network expansion and tumor progression. *PLoS ONE* 4:e4992. doi:10.1371/journal.pone.0004992
- Strawn, W. B., Richmond, R. S., Ann Tallant, E., Gallagher, P. E., and Ferrario, C. M. (2004). Renin-angiotensin system expression in rat bone marrow hematopoietic and stromal cells. *Br. J. Haematol.* 126, 120–126.
- Tang, J., Wang, J., Yang, J., Kong, X., Zheng, F., Guo, L., et al. (2009). Mesenchymal stem cells over-expressing SDF-1 promote angiogenesis and improve heart function in experimental myocardial infarction in rats. *Eur. J. Cardiothorac. Surg.* 36, 644–650.
- Tian, K., Yang, S., Ren, Q., Han, Z., Lu, S., Ma, F., et al. (2010). p38 MAPK contributes to the growth inhibition of leukemic tumor cells mediated by human umbilical cord mesenchymal stem cells. *Cell. Physiol. Biochem.* 26, 799–808.
- Tolar, J., Nauta, A. J., Osborn, M. J., Panoskaltsis Mortari, A., McElmurry, R. T., Bell, S., et al. (2007). Sarcoma derived from cultured mesenchymal stem cells. *Stem Cells* 25, 371–379.
- Trosko, J. E., Chang, C. C., Madhukar, B. V., and Dupont, E. (1993). “Oncogenesis, tumor suppressor genes, and intercellular communication in the ‘oncogeny as partially blocked ontogeny’ hypothesis,” in *New Frontiers in Cancer Causation*, ed. O. H. Iversen (Washington: Taylor & Francis), 181–197.
- Zhu, W., Xu, W., Jiang, R., Qian, H., Chen, M., Hu, J., et al. (2006). Mesenchymal stem cells derived from bone marrow favor tumor cell growth in vivo. *Exp. Mol. Pathol.* 80, 267–274.
- Zimmermann, W. H., Melnychenko, I., Wasmeier, G., Didie, M., Naito, H., Nixdorff, U., et al. (2006). Engineered heart tissue grafts improve systolic and diastolic function in infarcted rat hearts. *Nat. Med.* 12, 452–458.
- Zuk, P. A., Zhu, M., Mizuno, H., Huang, J., Futrell, J. W., Katz, A. J., et al. (2001). Multilineage cells from human adipose tissue: implications for cell-based therapies. *Tissue Eng.* 7, 211–228.
- Conflict of Interest Statement:** The authors declare that the research was conducted in the absence of any commercial or financial relationships that could be construed as a potential conflict of interest.
- Received:** 13 February 2013; **paper pending published:** 27 February 2013; **accepted:** 25 March 2013; **published online:** 17 April 2013.
- Citation:** Spath C, Schlegel F, Leontyev S, Mohr F-W and Dhein S (2013) Inverse relationship between tumor proliferation markers and connexin expression in a malignant cardiac tumor originating from mesenchymal stem cell engineered tissue in a rat in vivo model. *Front. Pharmacol.* 4:42. doi:10.3389/fphar.2013.00042
- This article was submitted to Frontiers in Pharmacology of Ion Channels and Channelopathies, a specialty of Frontiers in Pharmacology.
- Copyright © 2013 Spath, Schlegel, Leontyev, Mohr and Dhein. This is an open-access article distributed under the terms of the Creative Commons Attribution License, which permits use, distribution and reproduction in other forums, provided the original authors and source are credited and subject to any copyright notices concerning any third-party graphics etc.



# Role of connexins in human congenital heart disease: the chicken and egg problem

Aida Salameh\*, Katja Blanke and Ingo Daehnert

Clinic for Pediatric Cardiology, Heart Centre, University of Leipzig, Leipzig, Germany

**Edited by:**

Stefan Dhein, University of Leipzig, Germany

**Reviewed by:**

Aleksandra Sindic, University of Zagreb, Croatia

Jose Francisco Ek-Vitorin, University of Arizona, USA

Donglin Bai, University of Western Ontario, Canada

**\*Correspondence:**

Aida Salameh, Clinic for Pediatric Cardiology, Heart Centre, University of Leipzig, Struempellstr. 39, 04289 Leipzig, Germany

e-mail: aida.salameh@med.uni-leipzig.de

Inborn cardiac diseases are among the most frequent congenital anomalies and are the main cause of death in infants within the first year of age in industrialized countries when not adequately treated. They can be divided into simple and complex cardiac malformations. The former ones, for instance atrial and ventricular septal defects, valvular or subvalvular stenosis or insufficiency account for up to 80% of cardiac abnormalities. The latter ones, for example transposition of the great vessels, Tetralogy of Fallot or Shone's anomaly often do not involve only the heart, but also the great vessels and although occurring less frequently, these severe cardiac malformations will become symptomatic within the first months of age and have a high risk of mortality if the patients remain untreated. In the last decade, there is increasing evidence that cardiac gap junction proteins, the connexins (Cx), might have an impact on cardiac anomalies. In the heart, mainly three of them (Cx40, Cx43, and Cx45) are differentially expressed with regard to temporal organogenesis and to their spatial distribution in the heart. These proteins, forming gap junction channels, are most important for a normal electrical conduction and coordinated synchronous heart muscle contraction and also for the normal embryonic development of the heart. Animal and also some human studies revealed that at least in some cardiac malformations alterations in certain gap junction proteins are present but until today no particular gap junction mutation could be assigned to a specific cardiac anomaly. As gap junctions have often been supposed to transmit growth and differentiation signals from cell to cell it is reasonable to assume that they are somehow involved in misdirected growth present in many inborn heart diseases playing a primary or contributory role. This review addresses the potential role of gap junctions in the development of inborn heart anomalies like the conotruncal heart defects.

**Keywords:** connexin, gap junction, cardiac malformations, cardiac morphogenesis, mutation

## INTRODUCTION

Congenital heart defects belong to the most frequent inborn anomalies with a prevalence of about 10 out of 1000 live births (Schwedler et al., 2011). The pathology ranges from moderate defects like atrial septal defects (ASDs) or ventricular septal defects (VSDs), patent ductus arteriosus or pulmonary valve stenosis up to severe and complex heart diseases like Morbus Fallot, hypoplastic right or left heart syndrome, transposition of the great arteries (TGA), Ebstein's malformation or Truncus arteriosus communis (TAC). Depending on the severity of the heart disease clinical course varies from spontaneous recovery up to the necessity for multiple surgical interventions and a life-long medical treatment. Nowadays, as pediatric surgery achieved a high level of standard most of the children have a good prognosis with respect to life expectancy and most of them may reach adulthood.

Interestingly, inborn cardiac diseases tend to occur with increased frequency in familial clusters with a significantly elevated risk for cardiac malformations in first degree relatives, siblings or twins. Regarding the latter ones: the prevalence of an inborn heart disease, if either of the twins is affected, is considerably higher for a monozygotic twin sibling compared to a dizygotic twin sibling (Mitchell et al., 1971; Wang et al., 2012). Additionally, if in a monozygotic twinship both twins exhibit any congenital heart

defect, then with over 90% incidence both will have the same heart malformation (Seides et al., 1979).

However, up to present the precise cause for the development of an inborn heart disease remains unknown. There are several reports about the influence of exogenous noxa, chromosomal aberration, and genetic and environmental factors, but even for inborn cardiac defects which occur together with well-defined gene variants, for instance the Holt–Oram syndrome or Noonan syndrome (the so-called Mendelian syndromes) or are associated with chromosomal anomalies (for instance Trisomie 18 or 21), the penetrance of the cardiac defect does not reach 100%, and also the type of cardiac defect (i.e., ASD or VSD, pulmonary valve stenosis, etc.) is not identical within a specific syndrome (van der Bom et al., 2011). Thus, it seems obvious that inborn cardiac diseases have a multifactorial genesis and the etiology of most cases remains uncertain (Nora, 1968; Blue et al., 2012).

In the last decade, increasing evidence appeared that cardiac gap junction proteins, the connexins (Cx), might have an impact on cardiac anomalies. In the heart, mainly three of them (Cx40, Cx43 and Cx45) are differentially expressed with regard to temporal organogenesis and spatial distribution. The connexins are named after their molecular weight and the species in which they

occur, i.e., the human Cx43 (hCx43) has a molecular weight of approximately 43 kDa (Eiberger et al., 2001).

Connexin proteins form gap junction channels, which can be considered as pore-like channels permeable for cations, anions, and small molecules with low molecular weights (Simpson et al., 1977). A complete dodecameric gap junction channel is composed of two hemichannels (connexons) contributed by two adjacent cells and one hemichannel consists of six protein subunits. The connexins are transmembrane proteins with four transmembrane domains (M1–M4), two extracellular loops (E1, E2), one intracellular loop, and the N- and C-terminus at the cytoplasmic side of the cell (Unwin and Zampighi, 1980). The C-terminus, which is the most variant part of a connexin differs in length and amino acid sequence and also contains various consensus sequences for a number of protein kinases. For the Cx43 protein it is known that protein kinase A and C (PKA and PKC), mitogen-activated protein kinase, cyclin kinase 1, and some more precisely regulate Cx43 turnover as well as gap junctional communication (Lampe, 1994; Kwak et al., 1995; TenBroek et al., 2001; Polontchouk et al., 2002; Lampe and Lau, 2004). Its protein structure with its phosphorylation sites is presented in **Figure 1** (according to Giepmans, 2004). Besides Cx43 phosphorylation sites have also been identified within the C-terminal tail of Cx40 and Cx45 which alter their channel permeability and electrophysiological properties (Lampe and Lau, 2004).

It is known that some cardiac connexins, particularly Cx43, have considerable short half-lives of about 2–3 h (Darrow et al., 1995; Beardslee et al., 1998). Such a short half-life suggests that the permanent adaptation of the communication structure (i.e., the gap junctions) to environmental conditions might be of pronounced importance for cardiac cells and also might point towards a large functional relevance of connexins in ensuring cardiac development and function. As an example, it was shown that Cx43 changed its localization quickly after starting cyclic mechanical stretch (within 24 h) from a circumferential distribution to an accentuation at the cell poles; similarly polar accentuation was lost after discontinuation of stretch (Salameh et al., 2010). This shows how cells adapt their communication structure (given by the geometric distribution of Cx43) to an external factor (cyclic mechanical stretch) with a time span of 8–12 times the half-life time of Cx43, which is a reasonable period to assume a complete turnover of the protein.

In the human *adult* heart, the spatial distribution of the three connexins (Cx40, Cx43, and Cx45) is not uniform, as they are localized in specialized compartments: atrial myocytes express both Cx40 and Cx43 at similar levels whereas Cx45 is much lower in the atria. In the ventricles, the dominant connexin is Cx43 and in the sinus node and the conduction system of the heart both Cx40 and Cx45 are found (Davis et al., 1995). This non-uniform distribution is the basis for a regular impulse formation, a normal electrical conduction and coordinated synchronous heart muscle contraction. Furthermore, in order to allow regular rhythmic activation of the heart the connexins are typically assembled to gap junction channels at the intercalated disks which are located at the cell poles (Peters et al., 1994; van Rijen et al., 2006). This facilitates conduction of the action potential from cell to cell along the cell axis (Dhein et al., 2011). However, connexins also exist at

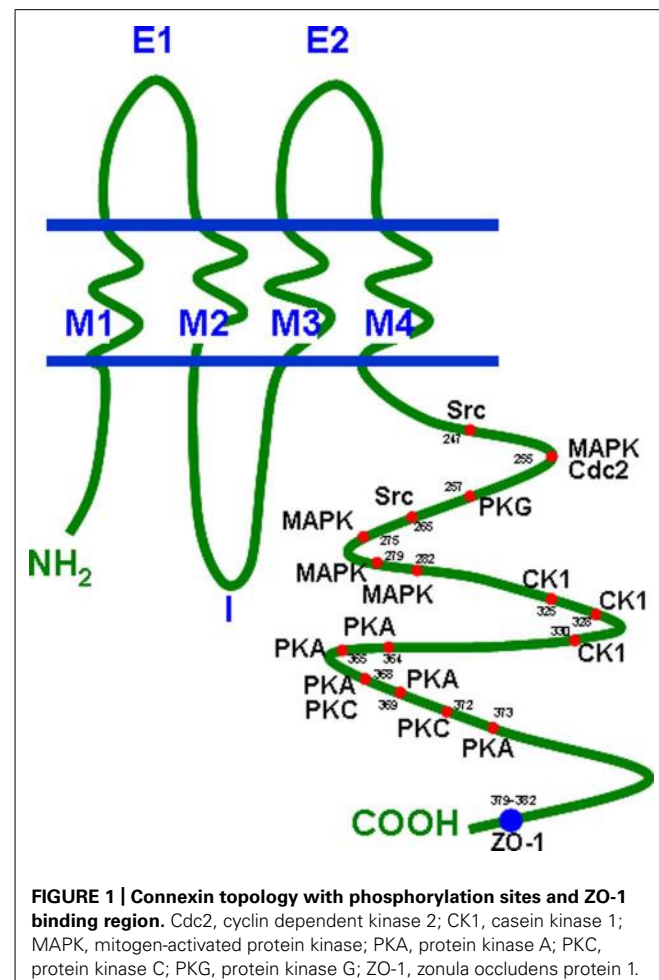


**FIGURE 1 | Connexin topology with phosphorylation sites and ZO-1 binding region.** Cdc2, cyclin dependent kinase 2; CK1, casein kinase 1; MAPK, mitogen-activated protein kinase; PKA, protein kinase A; PKC, protein kinase C; PKG, protein kinase G; ZO-1, zonula occludens protein 1.

the lateral border of the cells but at lower abundance. This results in a fast conduction along the fiber axis and a slower conduction transverse to the axis (Dhein et al., 2011).

Besides their functions in the adult heart, the connexins are also most important for the normal embryonic heart development.

Studies in mice revealed that Cx40 is initially expressed in the atrial compartments and later in both ventricles, whereas its expression is turned up earlier in the left ventricle. In contrast to Cx43, Cx40 is not expressed within the muscular structures of the interventricular septum. However, Cx40 is expressed in the His-Bundle and the bundle branches. Cx43 is seen in both ventricles and the interventricular septum in early development and later on also in the atrial compartments. In the conduction system Cx43 is not represented (Delorme et al., 1997; Alcolea et al., 1999). Cx45 is in early cardiogenesis the only connexin expressed in all cardiac compartments and its loss resulted in conduction block and cushion defects with lethal outcome at embryonic day 10 (Kumai et al., 2000; Nishii et al., 2001). During further morphogenesis it is progressively down-regulated and absent in the adult mouse ventricle. The expression pattern of connexins during development of the human heart is less well examined, but the connexin labeling pattern in human fetal heart resembles that of the mouse heart, with the exception that in the atria of human

fetal hearts Cx43 is only expressed at very low levels whilst in the mouse heart it is abundant (Kaba et al., 2001; Coppen et al., 2003). Thus, although comprehensive analyses are still missing, at least to some extent connexin expression pattern in the mouse heart parallels that of human fetal hearts.

Furthermore, to stress the importance that not only the correct temporal expression of a connexin is essential for normal heart growth but also the level of connexin expression, studies in mice revealed that both homozygous Cx43 knock-out and Cx43 over-expression may result in outflow tract obstruction and conotruncal cardiac malformations (Reaume et al., 1995; Ewart et al., 1997). This, demonstrates the importance of an exact regulation of Cx43-expression for normal heart growth. What is most interesting is that in a mouse model a point mutation in the Cx43 gene led to a reduction in Cx43 expression, a reduction in gap junction coupling and a disruption of gap junction plaque assembly. These changes were accompanied by cardiac defects like patent foramen ovale, enhanced fibrosis, worsening of right and left ventricular function, and also conduction anomalies. Extracardiac changes resembled the syndrome of oculodentodigital dysplasia (ODDD; Flenniken et al., 2005). This inborn syndrome is also seen in man and up to today over 60 mutations in the Cx43 gene have been described associated with this syndrome. Unlike the situation in mice, human cardiac malformations are not very common in ODDD. In man, only in few cases of ODDD conduction anomalies (atrioventricular block, right bundle branch block) and the appearance of VSDs and pulmonary stenosis have been described (Paznekas et al., 2003, 2009).

Moreover, a study with Cx40 knock-out mice demonstrated the importance of this connexin in generation of the mature apex to base activation of the heart (Sankova et al., 2012). Additionally, Kirchhoff et al. (2000) reported on various mice knock-out models with either Cx40 and/or Cx43 homozygous or heterozygous ablation with the occurrence of conduction anomalies and cardiac malformations (ASDs or VSDs, myocardial hypertrophy). In their study, the authors also found out that Cx43 haploinsufficiency even impaired the morphological phenotype of Cx40 deficiency. This was confirmed by another study of Simon et al. (2004) who detected malformed ventricles with an abnormal orientation in Cx40 and Cx43 double knock-out mice.

Conotruncal malformations, including TAC (birth prevalence 0.011%), double outlet right/left ventricle (birth prevalence 0.016%), Tetralogy of Fallot (TOF; birth prevalence 0.042%), and TGA (birth prevalence 0.032%; van der Bom et al., 2012), typically show malformations of the cardiac outflow tract. The critical time frame for the origination of conotruncal heart defects seems to be the fifth week of human embryonic development. At this specific moment in time the common outflow tract of the right and left heart, the Truncus arteriosus, is divided by a spiral shaped septum which ensures the correct association of the great arteries to the corresponding ventricles. Depending on the nature of malformation of the aorticopulmonary septum the afore mentioned cardiac defects may occur: a complete absence of the septum results in the development of TAC (common arterial trunk), lack of septal spiralization leads to TGA and anterior malalignment of the septum together with incomplete closure to double outlet right/left ventricle or TOF.

Hence, it is conceivable that the genesis of these cardiac defects might have the same etiopathologic origin and since the connexins play an important role in cardiac development it might be possible that certain alterations in temporal or spatial distribution of the main cardiac connexins may be at least co-responsible for conotruncal malformations. On the other side, it may also be imagined that conotruncal malformations themselves may secondarily lead to alterations in connexin expression and distribution.

Nearly 20 years ago, Britz-Cunningham et al. (1995) analyzed Cx43 mutations in patients with cardiac malformations and defects of laterality and they found missense mutations in parts of the Cx43 gene encoding for consensus phosphorylation sites within the Cx43 C-terminus. The authors could demonstrate that these mutations altered Cx43 phosphorylation by PKA or PKC, both protein kinases known to be important for Cx43–intercellular communication.

With these very interesting and new observations the authors started a world-wide discussion on whether or not Cx43 mutations are responsible or at least partly responsible for the development of cardiac malformations.

Therefore, the aim of this review is to discuss today's knowledge of connexin alterations in human conotruncal heart defects and the possible impact of connexins on the development of the same.

## TRUNCUS ARTERIOSUS COMMUNIS

Truncus arteriosus communis can be classified into three different types depending on the outflow of the pulmonary artery: type 1 (rare): pulmonary trunk originates from the lateral wall of the TAC and branches into one left and one right pulmonary artery; type 2 (common type): two pulmonary arteries with proximate origins separately branch off from the posterolateral aspect the common arterial trunk; type 3 (rare): both pulmonary arteries originate separately from the left and right lateral side of the common trunk. The symptoms of this heart defect include right heart hypertrophy, pulmonary overflow with consecutive pulmonary hypertension, Eisenmenger's syndrome, and heart failure (**Figure 2** gives the normal cardiac anatomy, in **Figure 3**, TAC type 3 is depicted).

The clinical picture of TAC is often associated with the DiGeorge syndrome (2q11 microdeletion, conotruncal heart malformations, thymic and parathyroid hypoplasia, cleft palate, and facial dysmorphisms). This inborn malady is evoked by disturbances in the migration of the cardiac neural crest cells. Kirby et al. (1983) have demonstrated in their seminal study done in chick embryos that ablation of a certain portion of the neural crest cells resulted in conotruncal heart defects including common arterial trunk. More recently, Huang et al. (1998a,b) could show in mice embryos that alterations in Cx43 gene dosage also resulted in conotruncal heart defects with pathologic morphology of the right ventricle, thinning of the myocardium and narrowing of the right ventricular outflow tract (RVOT). Moreover, they could demonstrate that gap junctional communication was increased in neural crest cells of Cx43 overexpressing mice and decreased in those of Cx43 knock-out mice. This phenomenon was accompanied by corresponding migration changes in the cardiac neural crest cells and by a perturbation of cardiomyocyte proliferation. Thus, the authors concluded that intercellular communication in

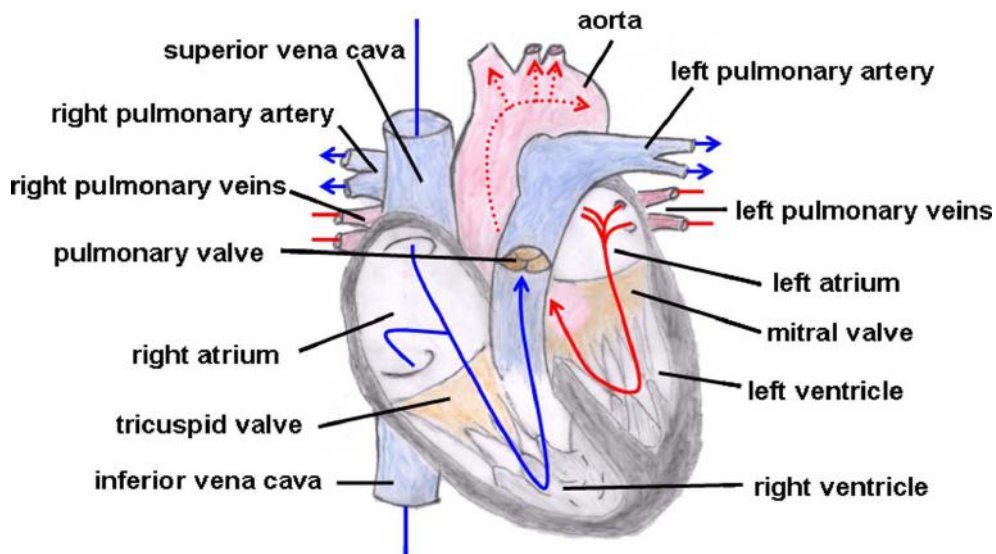


**FIGURE 2 | Normal cardiac anatomy.** The blue arrows give the flow of oxygen-poor blood from both caval veins via the right atrium and the right ventricle to the left and right pulmonary artery. The red arrows give the flow of oxygen-rich blood from the pulmonary veins via the left atrium and the left ventricle to the aorta.

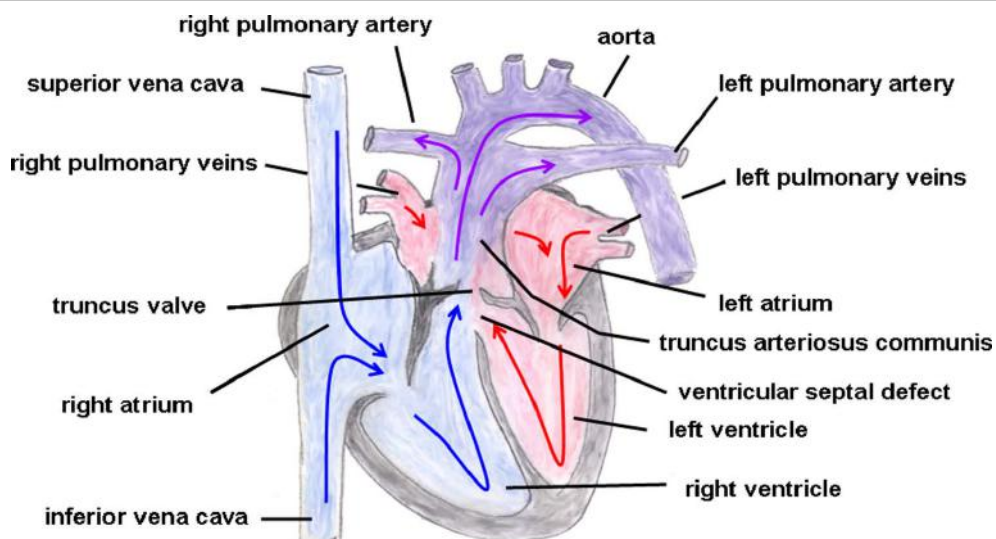


**FIGURE 3 | Truncus arteriosus communis.** Both great arteries (i.e., pulmonary artery and aorta) emerge together from a solitary arterial trunk. The blue arrows give the flow of oxygen-poor blood from both caval veins via the right atrium and the right ventricle and via the

truncus valve to the Truncus arteriosus communis. The red arrows give the flow of oxygen-rich blood from the pulmonary veins via the left atrium and the left ventricle to the Truncus arteriosus communis.

cardiac neural crest cells might be important for the myocardialization of the ventricular outflow tract, i.e., the regular shaping of the outflow septum. The impact of Cx43 on the development of the aorticopulmonary septum was underlined by a study of Waller et al. (2000) who also found that gain or loss of Cx43 function results in outflow tract anomalies and preferentially in persistent arterial trunk. In addition, induction of mutagenesis with N-ethyl-N-nitrosourea in mice revealed that in the Cx43 gene

a G to A substitution which generated a premature stop codon was sufficient to cause conotruncal malformation and coronary aneurysms (Yu et al., 2004). In addition to this result, Yu et al. (2004) also reported on a point mutation within another protein, the semaphorin, which resulted in common arterial trunk and interrupted aortic arch. Since the semaphorin family is supposed to give environmental cues for the migration of neural crest cells (Brown et al., 2001) it seems clear that perturbation of neural

crest cell migration might hinder the correct formation of the arterial trunk. This viewpoint is also supported by the excellent review of Hutson and Kirby (2003), who pointed out that aortic arch formation and outflow tract septation deeply depend on a correct deployment of cardiac neural crest cells. However, Cx43 is obviously not the only responsible factor for cardiac neural crest migration: there are several other protein families including growth factors [i.e., fibroblast growth factor, bone morphogenetic protein (BMP) or Wnt signaling pathway] as well as transcription factors (i.e., AP2, Sox9, FoxD) or adhesion molecules like N-cadherin being responsible for cardiac neural crest development. These factors and pathways are outlined in the comprehensive review of Kirby and Hutson (2010). Therefore, it can be concluded from the aforesaid that disturbances in Cx43-expression are very important factors in the pathogenesis of TAC but not the sole ones.

There are no experimental studies existing on the potential influence of Cx40 or Cx45 on the development of persistent arterial trunk.

### TRANSPOSITION OF THE GREAT ARTERIES

The hallmark of this cardiac malformation is the ventriculoarterial discordance in such a way that the aorta arises from the morphological right ventricle and the pulmonary artery from the morphological left ventricle with both main vessels remaining parallel to each other (i.e., they do not cross over, which would be the normal condition; Martins and Castela, 2008; **Figure 4**). Moreover, atypical origins of the coronary arteries and VSDs or ASDs are not uncommon. Depending on whether the aorta is located on the right or left side of the pulmonary artery this cardiac malformation is sub-classified into d(exter)- or l(aevus)-transposition,

respectively. Additionally, a distinction can be made between complete transpositions, i.e., concordant atrioventricular and discordant ventriculoarterial connections (the atria are connected to their corresponding ventricles but the great arteries emerge from the “wrong” ventricle) and congenitally corrected transpositions with atrioventricular and ventriculoarterial discordance [the right atrium (influx of venous blood) is connected to the left ventricle from which the pulmonary artery originates and the left atrium (influx of arterial blood) is coupled to the right ventricle from which the aorta emerges]. In the first condition, both circuits (systemic and pulmonary circulation) run in parallel resulting in a severe hypoxic status in which the survival depends on the adequate mixing between the two circulations be it via a VSD or ASD or a patent ductus arteriosus Botalli, whereas in the second condition (systemic and pulmonary circulation run in series) patients could remain asymptomatic over a longer period of time.

The exact etiology of this cardiac defect still remains undetected. However, some risk factors like maternal diabetes mellitus (Lisowski et al., 2010), herbicides (Loffredo et al., 2001), maternal use of antiepileptic medication (Thomas et al., 2008) have been identified as well as some cases associated with the DiGeorge syndrome (Laitenberger et al., 2008). Although neural crest cell migration plays a significant role in the pathogenesis of conotruncal heart defects, surprisingly, TGA could not be detected experimentally after neural crest ablation (Kirby, 2002). Interestingly enough, Costell et al. (2002) presented a mouse model of perlecan (heparan sulfate proteoglycan 2) null mutation exhibiting the cardiac phenotype of complete TGA, and the authors concluded from their study that perlecan has a role in the organization and differentiation of the outflow tract mesenchyme. Additionally, the highly mutagenic agent *N*-ethyl-*N*-nitrosourea

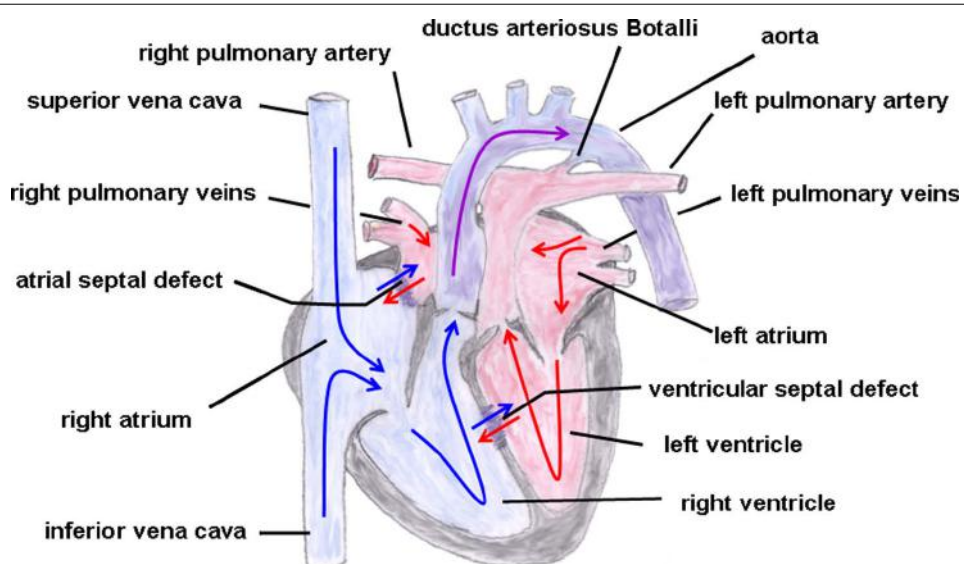


**FIGURE 4 | Transposition of the great arteries.** The ventriculoarterial discordance with the pulmonary artery connected to the left and the aorta connected to the right ventricle is shown. Also depicted is an atrial and ventricular septal defect and a patent ductus arteriosus Botalli. The blue

arrows give the flow of oxygen-poor blood from both caval veins via the right atrium and the right ventricle to the aorta. The red arrows give the flow of oxygen-rich blood from the pulmonary veins via the left atrium and the left ventricle to the pulmonary artery.

also had the ability to induce TGA in mice, but more commonly TAC and outflow tract anomalies together with coronary aneurysms were seen (Yu et al., 2004). Whether this Cx43 point mutation described in the study of Yu et al. (2004), which was found together with outflow tract anomalies, might also account for the heart defect “transposition of the great arteries” still remains to be elucidated. However, it was shown in a very recent study on human myocardial anomalies including TGA that N-cadherin and Cx43 expression and distribution was not altered in both left and right ventricle as compared to normal hearts (Mahtab et al., 2012). Although in this study the number of cases is considerably small (only three hearts were examined) the authors could clearly show that Cx43 together with N-cadherin accrued at the intercalated disks with a normal pattern. To date, there are no studies available describing pathological alterations of Cx40, Cx43, or Cx45 having a causal relationship in the development of TGA. However, in a study of Haefliger et al. (2000) done in mice the influence of another connexin, the Cx37, on this cardiac defect was examined. This connexin isoform, expressed in larger quantities in endothelial cells in a number of vessels and only very sparsely in cardiomyocytes, seems to play a not unimportant role in conotruncal development. Mice treated with all-trans retinoic acid during early embryonic life exhibited complete transposition of aorta and pulmonary arteries. Ventricles of these mice showed an abnormal high expression of Cx37, but whether the expression level of Cx37 is really a co-factor for the heart defect TGA is not finally clarified, as it seems so that the Cx37 over-expression was not directly linked to that cardiac malformation (Haefliger et al., 2000). Nevertheless, it should be taken into account that Cx37 typically is expressed in vascular endothelium and thus the described malformations may also be influenced by changes in angiogenesis or vascular function. However, this is unclear at present.

## DOUBLE OUTLET RIGHT VENTRICLE

The characteristic of this heart defect is the origination of both great arteries (aorta and pulmonary artery) from the right ventricle (shown in **Figure 5**). This malformation occurs in variable forms depending on the degree of malposition of the great arteries, the location of the concomitant VSD and the occurrence of RVOT obstruction. Thus, a distinction can be made between a VSD-type double outlet right ventricle (DORV; VSD with sub-aortic location), Fallot-type DORV (VSD with sub-aortic location and pulmonary stenosis) and TGA-type DORV (VSD with sub-pulmonary location, Taussig–Bing syndrome; Artrip et al., 2006). Therefore, depending on the exact morphology of the DORV, the clinical manifestation is different: DORV physiology might resemble a large unrestrictive VSD, a TOF or a TGA. This heterogeneity also implies different operative approaches and the timing of surgical repair. Associated cardiac malformations include a juxtaposition of atrial appendages, obstruction of the aortic arch, mitral atresia, or atrioventricular septal defects. Moreover, extracardiac manifestations can be found, such as heterotaxia, esophageal atresia, exomphalos, and chromosomal anomalies like the trisomy 18 (Tennstedt et al., 1999). An involvement of the neural crest zone in the development of DORV has been described, but as outlined in the comprehensive review of Obler et al. (2008) disturbances in

neural crest cell migration might not be the unique reason for the formation of a DORV.

About 10 years ago, Gu et al. (2003) published a study about Cx40 homozygous null mice, showing that if Cx40 is completely knocked-out cardiac malformations like DORV or TOF occurred. However, given the fact that only 30% of the Cx40<sup>-/-</sup> mice exhibited cardiac malformations the authors suggested that down-regulation of Cx40 in the neural crest zone might play an indirect role in the development of the described heart defects. Moreover, a very recent study in mice revealed that if Hand2 (a transcription factor involved in the morphogenesis of limbs), which is expressed in cardiac neural crest cells and also in the right ventricle and outflow tract, is deleted outflow tract anomalies, i.e., DORV and VSD occurred (Holler et al., 2010). The authors also found that Cx40, which is expressed in neural crest cells of wild-type mice, was significantly reduced in the Hand2 knock-out mice and they concluded from their experiments that Hand2 directly binds to the Cx40 promoter, thereby enhancing Cx40 expression, and that intercellular communication is a critical part for a proper outflow tract development.

A human study focusing on possible mutations of Cx43 in the development of cardiac defects was done on cardiac material of aborted fetuses, and the authors reported on eight Cx43 mutations which they found in a heart with DORV (Chen et al., 2005). These mutations were in the C-terminus near the transmembrane region and one mutation (the Pro283Leu missense mutation) was thought to limit Cx43 degradation. As the amount of Cx43 is important for the development of the conotruncus the authors concluded that this point mutation might be involved in the occurrence of DORV.

## TETRALOGY OF FALLOT

In the year 1888, the French physician Étienne-Louis Arthur Fallot described a congenital heart defect with four cardiac malformations: (1) right ventricular hypertrophy, (2) pulmonary stenosis (valvular or infundibular), (3) VSD with (4) overriding of the aortic root (**Figure 6**). This congenital heart anomaly is the most frequent inborn cyanotic heart disease. Nowadays, in infants with Morbus Fallot primary repair is done in early childhood, mostly below the age of 1 year, and the prognosis of these patients is excellent with most of them reaching adulthood (Shinebourne et al., 2006; Christian et al., 2009). Associated with Morbus Fallot anomalies of the coronary arteries, ASDs, a right aortic arch and also extracardiac anomalies like gastrointestinal or facial anomalies might exist (Piran et al., 2011). TOF typically occurs sporadically, but also familiar recurrences have been described. The etiology is multifactorial, but maternal diabetes mellitus, maternal intake of retinoic acid, and phenylketonuria have been reported as risk factors (Bailliard and Anderson, 2009). Moreover, an association with chromosomal anomalies which include trisomy 13, 18, and 21 exist. Especially the coincidence of Morbus Fallot together with 22q11.2 microdeletion is not infrequent. Maeda et al. (2000) reported in a study that of 212 Japanese patients 28 patients (13%) had 22q11.2 microdeletion and that all of these 28 patients had at least one extracardiac abnormality. Thus, the authors concluded that, at least in syndromic Morbus Fallot, 22q11.2 microdeletion is quite common (Maeda et al., 2000), although its pathogenetic role

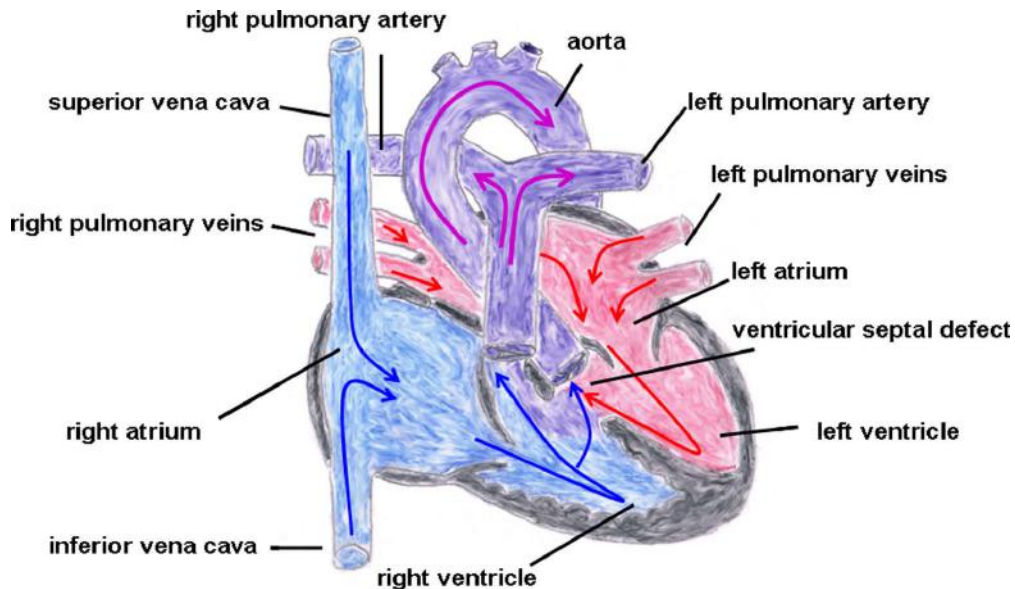


**FIGURE 5 | Double outlet right ventricle (VSD-type).** Origination of both great arteries (aorta and pulmonary artery) from the right ventricle with a concomitant ventricular septal defect. The blue arrows give the flow of oxygen-poor blood from both caval veins via the right atrium

and the right ventricle to the pulmonary artery and aorta. The red arrows give the flow of oxygen-rich blood from the pulmonary veins via the left atrium, the left ventricle to the aorta.

is still unclear. Moreover, some studies involving non-syndromic TOF described dominant mutations in genes encoding for various transcription factors, like GATA4, Nkx2.5, or ZFMP2/FOG2 (Goldmundt et al., 2001; Nemer et al., 2006; De Luca et al., 2011).

Given the accepted fact that regular Cx43 expression is important for neural crest development (Waldo et al., 1999) the question arises if mutations in the Cx43 gene might also be responsible for the occurrence of Morbus Fallot. A very early publication on this subject was done by Reaume et al. (1995), who created a Cx43 knock-out mouse and could demonstrate that these mice had outflow tract anomalies and died soon after birth. However, the full picture of Morbus Fallot was not seen, suggesting that additional factors might be required. Few years later Sullivan et al. (1998) presented a study in which they used a dominant negative strategy to reduce gap junctional coupling within the cardiac neural crest cells. They could also demonstrate that outflow tract obstruction, right ventricular hypertrophy, and abnormal bulging of the right ventricle occurred, but the full syndrome of Morbus Fallot was not observed.

One recent study seemed to confirm the findings of Britz-Cunningham et al. (1995) on mutations in the C-terminus tail of Cx43 in patients with inborn cardiac defects (Wang et al., 2010). In the analysis of Wang et al. (2010) over 400 Chinese children were included. Most of these children had VSDs or ASDs or Morbus Fallot, and three heterozygous missense mutations in the C-terminus were found in all these patients with congenital heart defects, whereas no mutations were detectable in the normal control subjects. As the C-terminus includes important phosphorylation sites (Figure 1) the authors concluded that the mutations could have an impact on the structure of Cx43 and on normal channel function. In contrast, 1 year later another very

interesting study came to a radically opposed conclusion: in this study, 300 patients with conotruncal heart defects including Fallot's Tetralogy were investigated and the authors discovered two silent mutations in the Cx43 gene in eight patients, but no mutations were found which would alter Cx43 amino acid sequence (Huang et al., 2011). Moreover, this working group constructed a mouse model with homozygous or heterozygous mutations of serine residues known to be targeted by PKC or CK1 (casein kinase 1), both enzymes being important for channel conductance and the assembly of Cx43 gap junction channels. Surprisingly, in the hearts of these mice, which were viable with a normal life-span, no changes in Cx43 distribution or expression, and no congenital heart defects, were detected. The authors concluded that Cx43 does not contribute to a large extent to the development of heart malformations. Thus, the question of whether or not mutation in Cx43 gene is involved in the origination of Morbus Fallot remains unsolved.

Another study group analyzed Cx43 expression and distribution in patients with Morbus Fallot and they found that in these patients Cx43, which is normally confined to the poles of the cardiomyocytes, was distributed around the entire circumference of the cells. Moreover, total Cx43 staining, analyzed by a fluorescence activated cell sorting (FACS)-approach, was significantly lower in the patient group having Morbus Fallot compared to the control group (patients with VSDs; Kołcz et al., 2002, 2005). The authors concluded from their studies that these connexin alterations might be responsible for cardiac arrhythmias, seen frequently in patients with Morbus Fallot and that changes in Cx43 localization might contribute to a dysfunction of the right ventricle. However, it should be noted that histological analyses were not carried out on the intact heart tissue but on single cardiomyocytes cultured in

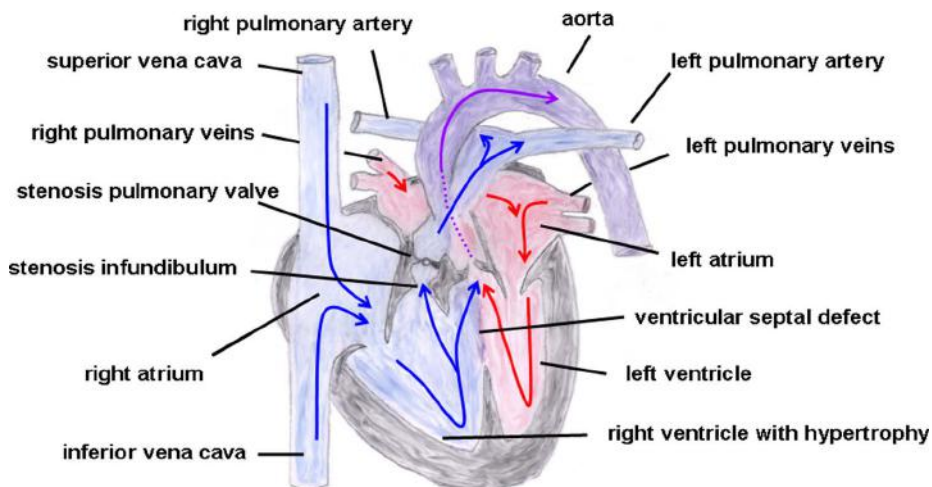


**FIGURE 6 |** **Tetralogy of Fallot.** Depicted are the four cardiac malformations described by Fallot: (1) right ventricular hypertrophy, (2) pulmonary stenosis (valvular and infundibular), (3) ventricular septal defect with (4) overriding of the aortic root. The blue arrows give the flow of oxygen-poor blood from both

caval veins via the right atrium and the right ventricle to the pulmonary artery and via the ventricular septal defect to the aorta (right-left shunt). The red arrows give the flow of oxygen-rich blood from the pulmonary veins via the left atrium and the left ventricle to the aorta.

Petri dishes. Since Cx43 has a very short half-time it is not unlikely that the described Cx43 re-distribution is more due to the culture conditions than to the heart defect or a more complex response of somehow altered cardiomyocytes to the culture conditions. In the end, the precise role of Cx43 in the development of Morbus Fallot cannot be assessed.

Given the information that the other important connexin, Cx40, is also involved in cardiac morphogenesis, several working groups have analyzed this connexin in relation to the occurrence of TOF. These studies done in man revealed that Morbus Fallot was associated with above-average frequency with copy number variants in the Cx40 gene (Greenway et al., 2009; Soemedi et al., 2012). Moreover, it was shown by Greenway et al. (2009) that in TOF patients Cx40 expression in RVOT, which is malformed in Fallot's Tetralogy, was enhanced. This finding could indicate that Cx40 might be among the disease genes involved in the occurrence of Morbus Fallot.

Since mutations in the C-terminus of Cx43 have been found in TOF patients, another interesting aspect to consider would be if the C-terminal end of Cx40 might also be mutated in patients with Morbus Fallot. A very interesting study published this year (Guida et al., 2013) characterized over 150 patients with non-syndromic Fallot and found in 1% of their patients a heterozygous nucleotide change in the Cx40 gene leading to altered amino acid sequence. This Pro265Ser variant was not seen in healthy volunteers [amino acid 265 is the binding region for src (sarcoma Rous kinase)]. Further experiments of this working group on the cellular level revealed that this mutant Cx40 led to a reduced gap junctional coupling. In addition, introducing the Pro265Ser mutant of Cx40 into zebrafishes also was associated with malformations of the heart tube.

However, a definite clarification whether connexins are causally involved in the development of Morbus Fallot or whether their change in expression is an epiphenomenon is still pending.

## POSSIBLE MOLECULAR MECHANISMS

The role of connexins in the development of cardiac malformation has emerged over the past decade by introducing the knock-in and knock-out mice and a lot of research has been done in this field. However, still only little is known about the signaling pathways in these mice to unravel how connexin alterations might be linked to the origination of conotruncal heart defects. By contrast, some studies have been published which used an approach from a different perspective. Dupays et al. (2005) described in their study results on Nkx2.5-deficient mice. They found out that in homozygous Nkx2.5 null mice embryos Cx40, Cx43, and Cx45 could not be detected within the myocardium, whereas these connexins were still detectable in other organs. Moreover, although 75% of these embryos had a normal sequence of cardiac activation and conduction along the conduction system, heart rate was very slow. In the other remaining 25% of mutant mice the ventricle was the first chamber being activated thus showing a reverse action of cardiac excitation. The Nkx2.5 null mice embryos also exhibited an insufficient development of the ventricular trabeculae. Besides, heart malformations like ASDs and VSDs have been seen although complex cardiac malformations could not be detected maybe because of premature death occurring in these mice (Terada et al., 2011). However, in man Nkx2.5 mutations are also associated with cardiac malformations like ASDs and VSDs and additionally with other more complex cardiac malformations (Morbus Fallot, pulmonary atresia; Schott et al., 1998; Wang et al., 2011). However, for obvious reasons analysis of connexin expression could not be done in the patients' hearts.

Another transcription factor which has been described in the context of the Holt–Oram syndrome is the T-box transcription factor Tbx5 (Basson et al., 1997). Patients suffering from this inborn syndrome have malformed limbs and cardiac defects like ASD, VSD, and also more severe cardiac malformations. In a mouse model of heterozygous

Tbx5 mutants Bruneau et al. (2001) could demonstrate that a phenotype similar to the Holt–Oram syndrome occurred, and that interestingly Cx40 gene expression was down-regulated in the atria and ventricles of these mice.

GATA4 is another transcription factor known to be associated with cardiac development. Recently, a point mutation of GATA4 was detected within a large cohort of kindred persons, who exhibited ASDs and in some cases also VSDs and abnormalities of the pulmonary valve (Garg et al., 2003). All these family members carried a glycine to serine substitution at position 296 of GATA4, which was accompanied by a diminished binding ability to the DNA consensus sequence and in addition by reduced interaction with Tbx5.

Consistent with all these findings Linhares et al. (2004) showed that in the Cx40 promoter binding sites exist for Tbx5, Nkx2.5, and GATA4. Both nuclear factors Nkx2.5 and GATA4 transactivate the Cx40 promoter thereby regulating Cx40 expression. This was compatible with the finding that in Nkx2.5 knock-out mice Cx40 expression was markedly down-regulated. On the other hand, the nuclear factor Tbx5 seemed to have a more repressive role on the Cx40 promoter, which was in contrast to the finding of Bruneau et al. (2001), who demonstrated the opposite. A possible explanation discussed by Linhares et al. (2004) would be that the promoter sequence used in their study was considerably shorter than that of Bruneau et al. (2001) therefore lacking important necessary elements.

Thus, besides connexin mutations seen in human cardiac malformations also mutations in transcription factors accompanied by altered connexin expression might have an impact on inborn heart defects.

However, a detailed description of how signaling pathways may be linked to cardiac malformations awaits further studies.

Nevertheless, a problem with these mice knock-out studies is that the finally resulting cardiac phenotype is not investigated with regard to the molecular mechanisms linking the knock-out-target to the cardiac development. Moreover, from a cardiological point of view it is remarkable that mutations or knock-out in very different genes very often result in ASDs or VSDs. This might indicate

that between connexins, transcription factors like Nkx2.5, Tbx5, GATA4, etc. and cardiac malformations there might exist one (or more) missing links which still need to be elucidated.

## CONCLUSION

Taken together, until now there is no conclusive evidence that human inborn conotruncal heart defects are caused by mutations or changes in connexins. From the view point of cell biology it is tempting to speculate that a protein so deeply involved in intercellular communication, regulation of growth and differentiation as well as of cell cycle could be involved in the pathogenesis of malformation. However, although Cx43 knock-out mice can present malformation of the RVOT with some similarity to Morbus Fallot, this does not warrant the conclusion that Morbus Fallot results from Cx43 changes. There probably are many regulatory steps and proteins involved in cardiac organogenesis, so that the malfunction of each and any may cause a common phenotype. This leads to our present view that the pathogenesis of conotruncal human inborn heart defects seems multifactorial and that there is at present for the majority of inborn cardiac malformations no evidence for a direct or causal role of connexins. Although, studies in mice revealed that at least in some cases of cardiac defects a pathogenetic involvement of connexins might be evident, this does not exclude that other proteins with an impact on protein trafficking or membrane anchoring may be involved and may lead to secondary changes in connexins either as an epiphenomenon or playing an aggravating role. In addition, the cardiac defect could cause hemodynamic changes which would lead to altered local stretch. Since stretch has an effect on cytoskeleton and on the subcellular distribution of Cx43 (Salameh et al., 2010), this also may lead to secondary changes in connexin expression and localization. Whether such changes have a feedback effect on cellular growth and differentiation is unclear. In summary, a direct unifactorial role of connexins in human inborn conotruncal heart defect seems improbable, but a more complex role or a bystander effect is reasonable.

Not chicken, not egg, but complex bidirectional interactions between connexins and tissue developments and vice-versa.

## REFERENCES

- Alcolea, S., Théveniau-Ruissy, M., Jarry-Guichard, T., Marics, I., Tzouanacou, E., Chauvin, J. P., et al. (1999). Downregulation of connexin 45 gene products during mouse heart development. *Circ. Res.* 84, 1365–1379. doi: 10.1161/01.RES.84.12.1365
- Artrip, J. H., Sauer, H., Campbell, D. N., Mitchell, M. B., Haun, C., Almodovar, M. C., et al. (2006). Biventricular repair in double outlet right ventricle: surgical results based on the STS-EACTS International Nomenclature classification. *Eur. J. Cardiothorac. Surg.* 29, 545–550. doi: 10.1016/j.ejcts.2005.12.038
- Bailliard, F., and Anderson, R. H. (2009). Tetralogy of Fallot. *Orphanet J. Rare Dis.* 4, 2. doi: 10.1186/1750-1172-4-2
- Basson, C. T., Bachinsky, D. R., Lin, R. C., Levi, T., Elkins, J. A., Soult, J., et al. (1997). Mutations in human TBX5 [corrected] cause limb and cardiac malformation in Holt–Oram syndrome. *Nat. Genet.* 15, 30–35. doi: 10.1038/ng0197-30
- Beardslee, M. A., Laing, J. G., Beyer, E. C., and Saffitz, J. E. (1998). Rapid turnover of connexin 43 in the adult rat heart. *Circ. Res.* 83, 629–635. doi: 10.1161/01.RES.83.6.629
- Blue, G. M., Kirk, E. P., Sholler, G. F., Harvey, R. P., and Winlaw, D. S. (2012). Congenital heart disease: current knowledge about causes and inheritance. *Med. J. Aust.* 197, 155–159. doi: 10.5694/mja12.10811
- Britz-Cunningham, S. H., Shah, M. M., Zuppan, C. W., and Fletcher, W. H. (1995). Mutations of the connexin43 gap-junction gene in patients with heart malformations and defects of laterality. *N. Engl. J. Med.* 332, 1323–1329. doi: 10.1056/NEJM199505183322002
- Brown, C. B., Feinter, L., Lu, M. M., Ma, X., Webber, A. L., Jia, L., et al. (2001). PlexinA2 and semaphorin signaling during cardiac neural crest development. *Development* 128, 3071–3080.
- Bruneau, B. G., Nemer, G., Schmitt, J. P., Charron, F., Robitaille, L., Caron, S., et al. (2001). A murine model of Holt–Oram syndrome defines roles of the T-box transcription factor Tbx5 in cardiogenesis and disease. *Cell* 106, 709–721. doi: 10.1016/S0092-8674(01)00493-7
- Chen, P., Xie, L. J., Huang, G. Y., Zhao, X. Q., and Chang, C. (2005). Mutations of connexin43 in fetuses with congenital heart malformations. *Chin. Med. J. (Engl.)* 118, 971–976.
- Christian, A., Webb, G., and Redington, A. N. (2009). Tetralogy of Fallot. *Lancet* 374, 1462–1471. doi: 10.1016/S0140-6736(09)60657-7
- Coppens, S. R., Kaba, R. A., Halliday, D., Dupont, E., Skepper, J. N., Elneil, S., et al. (2003). Comparison of connexin expression patterns in the developing mouse heart and human foetal heart. *Mol. Cell. Biochem.* 242, 121–127. doi: 10.1023/A:1021150014764
- Costell, M., Carmona, R., Gustafsson, E., González-Iriarte, M., Fässler, R., and Muñoz-Chápuli, R. (2002). Hyperplastic conotruncal endocardial cushions and transposition of great arteries in perlecan-null

- mice. *Circ. Res.* 91, 158–164. doi: 10.1161/01.RES.0000026056.81424.DA
- Darrow, B. J., Laing, J. G., Lampe, P. D., Saffitz, J. E., and Beyer, E. C. (1995). Expression of multiple connexins in cultured neonatal rat ventricular myocytes. *Circ. Res.* 76, 381–387. doi: 10.1161/01.RES.76.3.381
- Davis, L. M., Rodefeld, M. E., Green, K., Beyer, E. C., and Saffitz, J. E. (1995). Gap junction protein phenotypes of the human heart and conduction system. *J. Cardiovasc. Electrophysiol.* 6, 813–822. doi: 10.1111/j.1540-8167.1995.tb00357.x
- Delorme, B., Dahl, E., Jarry-Guichard, T., Briand, J. P., Willecke, K., Gros, D., et al. (1997). Expression pattern of connexin gene products at the early developmental stages of the mouse cardiovascular system. *Circ. Res.* 81, 423–437. doi: 10.1161/01.RES.81.3.423
- De Luca, A., Sarkozy, A., Ferese, R., Consoli, F., Lepri, F., Dentici, M. L., et al. (2011). New mutations in ZFPM2/FOG2 gene in tetralogy of Fallot and double outlet right ventricle. *Clin. Genet.* 80, 184–190. doi: 10.1111/j.1399-0004.2010.01523.x
- Dhein, S., Rothe, S., Busch, A., Rojas Gomez, D. M., Boldt, A., Reutemann, A., et al. (2011). Effects of metoprolol therapy on cardiac gap junction remodelling and conduction in human chronic atrial fibrillation. *Br. J. Pharmacol.* 164, 607–616. doi: 10.1111/j.1476-5381.2011.01460.x
- Dupays, L., Jarry-Guichard, T., Mazurais, D., Calmels, T., Izumo, S., Gros, D., et al. (2005). Dysregulation of connexins and inactivation of NFATc1 in the cardiovascular system of Nkx2-5 null mutants. *J. Mol. Cell. Cardiol.* 38, 787–798. doi: 10.1016/j.yjmcc.2005.02.021
- Eiberger, J., Degen, J., Romualdi, A., Deutsch, U., Willecke, K., and Söhl, G. (2001). Connexin genes in the mouse and human genome. *Cell Commun. Adhes.* 8, 163–165. doi: 10.3109/15419060109080717
- Ewart, J. L., Cohen, M. F., Meyer, R. A., Huang, G. Y., Wessels, A., Gourdie, R. G., et al. (1997). Heart and neural tube defects in transgenic mice overexpressing the Cx43 gap junction gene. *Development* 124, 1281–1292.
- Fleniken, A. M., Osborne, L. R., Anderson, N., Ciliberti, N., Fleming, C., Gittens, J. E., et al. (2005). A Gja1 missense mutation in a mouse model of oculodentodigital dysplasia. *Development* 132, 4375–4386. doi: 10.1242/dev.02011
- Garg, V., Kathiriya, I. S., Barnes, R., Schluterman, M. K., King, I. N., Butler, C. A., et al. (2003). GATA4 mutations cause human congenital heart defects and reveal an interaction with TBX5. *Nature* 424, 443–447. doi: 10.1038/nature01827
- Giepmans, B. N. (2004). Gap junctions and connexin-interacting proteins. *Cardiovasc. Res.* 62, 233–245. doi: 10.1016/j.cardiores.2003.12.009
- Goldmuntz, E., Geiger, E., and Benson, D. W. (2001). NFKX2.5 mutations in patients with tetralogy of Fallot. *Circulation* 104, 2565–2568. doi: 10.1161/hc4601.098427
- Greenway, S. C., Pereira, A. C., Lin, J. C., DePalma, S. R., Israel, S. J., Mesquita, S. M., et al. (2009). De novo copy number variants identify new genes and loci in isolated sporadic tetralogy of Fallot. *Nat. Genet.* 41, 931–935. doi: 10.1038/ng.415
- Gu, H., Smith, F. C., Taffet, S. M., and Delmar, M. (2003). High incidence of cardiac malformations in connexin40-deficient mice. *Circ. Res.* 93, 201–206. doi: 10.1161/01.RES.0000084852.65396.70
- Guida, V., Ferese, R., Rocchetti, M., Bonetti, M., Sarkozy, A., Cecchetti, S., et al. (2013). A variant in the carboxyl-terminus of connexin 40 alters GAP junctions and increases risk for tetralogy of Fallot. *Eur. J. Hum. Genet.* 21, 69–75. doi: 10.1038/ejhg.2012.109
- Haefliger, J. A., Polikar, R., Schnyder, G., Burdet, M., Sutter, E., Pexieder, T., et al. (2000). Connexin37 in normal and pathological development of mouse heart and great arteries. *Dev. Dyn.* 218, 331–344. doi: 10.1002/(SICI)1097-0177(200006)218:331–344.3.CO;2-1
- Holler, K. L., Hendershot, T. J., Troy, S. E., Vincentz, J. W., Firulli, A. B., and Howard, M. J. (2010). Targeted deletion of Hand2 in cardiac neural crest-derived cells influences cardiac gene expression and outflow tract development. *Dev. Biol.* 341, 291–304. doi: 10.1016/j.ydbio.2010.02.001
- Huang, G. Y., Cooper, E. S., Waldo, K., Kirby, M. L., Gilula, N. B., and Lo, C. W. (1998a). Gap junction-mediated cell-cell communication modulates mouse neural crest migration. *J. Cell Biol.* 143, 1725–1734. doi: 10.1083/jcb.143.6.1725
- Huang, G. Y., Wessels, A., Smith, B. R., Linask, K. K., Ewart, J. L., and Lo, C. W. (1998b). Alteration in connexin 43 gap junction gene dosage impairs conotruncal heart development. *Dev. Biol.* 198, 32–44. doi: 10.1016/S0012-1606(98)80027-4
- Huang, G. Y., Xie, L. J., Linask, K. L., Zhang, C., Zhao, X. Q., Yang, Y., et al. (2011). Evaluating the role of connexin43 in congenital heart disease: screening for mutations in patients with outflow tract anomalies and the analysis of knock-in mouse models. *J. Cardiovasc. Dis. Res.* 2, 206–212. doi: 10.4103/0975-3583.89804
- Hutson, M. R., and Kirby, M. L. (2003). Neural crest and cardiovascular development: a 20-year perspective. *Birth Defects Res. C Embryo Today* 69, 2–13. doi: 10.1002/bdrc.10002
- Kaba, R. A., Coppen, S. R., Dupont, E., Skepper, J. N., Elneil, S., Haw, M. P., et al. (2001). Comparison of connexin 43, 40 and 45 expression patterns in the developing human and mouse hearts. *Cell Commun. Adhes.* 8, 339–343. doi: 10.3109/15419060109080750
- Kirby, M. L. (2002). Embryogenesis of transposition of the great arteries: a lesson from the heart. *Circ. Res.* 91, 87–89. doi: 10.1161/01.RES.0000028301.40791.4F
- Kirby, M. L., Gale, T. F., and Stewart, D. E. (1983). Neural crest cells contribute to normal aorticopulmonary septation. *Science* 220, 1059–1061. doi: 10.1126/science.6844926
- Kirby, M. L., and Hutson, M. R. (2010). Factors controlling cardiac neural crest cell migration. *Cell Adh. Migr.* 4, 609–621. doi: 10.4161/cam.4.4.13489
- Kirchhoff, S., Kim, J. S., Hagendorff, A., Thönnissen, E., Krüger, O., Lamers, W. H., et al. (2000). Abnormal cardiac conduction and morphogenesis in connexin40 and connexin43 double-deficient mice. *Circ. Res.* 87, 399–405. doi: 10.1161/01.RES.87.5.399
- Kolcz, J., Drukala, J., Bzowska, M., Rajwa, B., Korohoda, W., and Malec, E. (2005). The expression of connexin 43 in children with Tetralogy of Fallot. *Cell. Mol. Biol. Lett.* 10, 287–303.
- Kolcz, J., Rajwa, B., Drukala, J., Dobrucki, J., Korohoda, W., and Malec, E. (2002). Three-dimensional visualization of connexin 43 on the human cardiomyocytes. *Appl. Immunohistochem. Mol. Morphol.* 10, 247–252. doi: 10.1097/00022744-200209000-00011
- Kumai, M., Nishii, K., Nakamura, K., Takeda, N., Suzuki, M., and Shibata, Y. (2000). Loss of connexin45 causes a cushion defect in early cardiogenesis. *Development* 127, 3501–3512.
- Kwak, B. R., Hermans, M. M. P., De Jonge, H. R., Lohmann, S. M., Jongsma, H. J., and Chanson, M. (1995). Differential regulation of distinct types of gap junction channels by similar phosphorylating conditions. *Mol. Biol. Cell* 6, 1707–1719.
- Laitenberger, G., Donner, B., Gebauer, J., and Hoehn, T. (2008). D-transposition of the great arteries in a case of microduplication 22q11.2. *Pediatr. Cardiol.* 29, 1104–1106. doi: 10.1007/s00246-007-9150-7
- Lampe, P. D. (1994). Analyzing phorbol ester effects on gap junctional communication: a dramatic inhibition of assembly. *J. Cell Biol.* 127, 1895–1905. doi: 10.1083/jcb.127.6.1895
- Lampe, P. D., and Lau, A. F. (2004). The effects of connexin phosphorylation on gap junctional communication. *Int. J. Biochem. Cell. Biol.* 36, 1171–1186. doi: 10.1016/S1357-2725(03)00264-4
- Linhares, V. L., Almeida, N. A., Menezes, D. C., Elliott, D. A., Lai, D., Beyer, E. C., et al. (2004). Transcriptional regulation of the murine connexin40 promoter by cardiac factors Nkx2-5, GATA4 and Tbx5. *Cardiovasc. Res.* 64, 402–411. doi: 10.1016/j.cardiores.2004.09.021
- Lisowski, L. A., Verheijen, P. M., Copel, J. A., Kleinman, C. S., Wassink, S., Visser, G. H., et al. (2010). Congenital heart disease in pregnancies complicated by maternal diabetes mellitus. An international clinical collaboration, literature review, and meta-analysis. *Herz* 35, 19–26. doi: 10.1007/s00059-010-3244-3
- Loffredo, C. A., Silbergeld, E. K., Ferencz, C., and Zhang, J. (2001). Association of transposition of the great arteries in infants with maternal exposures to herbicides and rodenticides. *Am. J. Epidemiol.* 153, 529–536. doi: 10.1093/aje/153.6.529
- Maeda, J., Yamagishi, H., Matsuoka, R., Ishihara, J., Tokumura, M., Fukushima, H., et al. (2000). Frequent association of 22q11.2 deletion with tetralogy of Fallot. *Am. J. Med. Genet.* 92, 269–272. doi: 10.1002/(SICI)1096-8628(20000605)92:3<269::AID-AJMG.B>3.0.CO;2-1
- Mahtab, E. A., Gittenberger-de Groot, A. C., Vicente-Steyn, R., Lievenema, H., Rijlaarsdam, M. E., Hazekamp, M. G., et al. (2012). Disturbed myocardial connexin 43 and N-cadherin expressions in hypoplastic left heart syndrome and borderline left ventricle. *J. Thorac. Cardiovasc. Surg.* 144, 1315–1322. doi: 10.1016/j.jtcvs.2012.02.011
- Martins, P., and Castela, E. (2008). Transposition of the great arteries. *Orphanet J. Rare Dis.* 3, 27. doi: 10.1186/1750-1172-3-27
- Mitchell, S. C., Korones, S. B., and Berendes, H. W. (1971). Congenital heart disease in 56,109

- births. Incidence and natural history. *Circulation* 43, 323–332. doi: 10.1161/01.CIR.43.3.323
- Nemer, G., Fadlalah, F., Usta, J., Nemer, M., Dbaibo, G., Obeid, M., et al. (2006). A novel mutation in the GATA4 gene in patients with Tetralogy of Fallot. *Hum. Mutat.* 27, 293–294. doi: 10.1002/humu.9410
- Nishii, K., Kumai, M., and Shiba, Y. (2001). Regulation of the epithelial-mesenchymal transformation through gap junction channels in heart development. *Trends Cardiovasc. Med.* 11, 213–218. doi: 10.1016/S1050-1738(01)00103-7
- Nora, J. J. (1968). Multifactorial inheritance hypothesis for the etiology of congenital heart diseases: the genetic-environmental interaction. *Circulation* 38, 604–617. doi: 10.1161/01.CIR.38.3.604
- Obler, D., Juraszek, A. L., Smoot, L. B., and Natowicz, M. R. (2008). Double outlet right ventricle: etiologies and associations. *J. Med. Genet.* 45, 481–497. doi: 10.1136/jmg.2008.057984
- Paznekas, W. A., Boyadjiev, S. A., Shapiro, R. E., Daniels, O., Wollnik, B., Keegan, C. E., et al. (2003). Connexin 43 (GJA1) mutations cause the pleiotropic phenotype of oculodentodigital dysplasia. *Am. J. Hum. Genet.* 72, 408–418. doi: 10.1086/346090
- Paznekas, W. A., Karczeski, B., Vermeer, S., Lowry, R. B., Delatycki, M., Laurence, F., et al. (2009). GJA1 mutations, variants, and connexin 43 dysfunction as it relates to the oculodentodigital dysplasia phenotype. *Hum. Mutat.* 30, 724–733. doi: 10.1002/humu.20958
- Peters, N. S., Severs, N. J., Rothery, S. M., Lincoln, C., Yacoub, M. H., and Green, C. R. (1994). Spatiotemporal relation between gap junctions and fascia adherens junctions during postnatal development of human ventricular myocardium. *Circulation* 90, 713–725. doi: 10.1161/01.CIR.90.2.713
- Piran, S., Bassett, A. S., Grewal, J., Swaby, J. A., Morel, C., Oechslin, E. N., et al. (2011). Patterns of cardiac and extracardiac anomalies in adults with tetralogy of Fallot. *Am. Heart J.* 161, 131–137. doi: 10.1016/j.ahj.2010.09.015
- Polontchouk, L., Ebelt, B., Jackels, M., and Dhein, S. (2002). Chronic effects of endothelin 1 and angiotensin II on gap junctions and intercellular communication in cardiac cells. *FASEB J.* 16, 87–89.
- Reaume, A. G., de Sousa, P. A., Kulakrani, S., Langille, B. L., Zhu, D., Davies, T. C., et al. (1995). Cardiac malformation in neonatal mice lacking connexin 43. *Science* 267, 1831–1834. doi: 10.1126/science.7892609
- Salameh, A., Wustmann, A., Karl, S., Blanke, K., Apel, D., Rojas-Gomez, D., et al. (2010). Cyclic mechanical stretch induces cardiomyocyte orientation and polarization of the gap junction protein connexin43. *Circ. Res.* 106, 1592–1602. doi: 10.1161/CIRCRESAHA.109.214429
- Sankova, B., Benes, J. Jr., Krejci, E., Dupays, L., Theveniau-Ruissy, M., Miquerol, L., et al. (2012). The effect of connexin40 deficiency on ventricular conduction system function during development. *Cardiovasc. Res.* 95, 469–479. doi: 10.1093/cvr/cvs210
- Schott, J. J., Benson, D. W., Basison, C. T., Pease, W., Silberbach, G. M., Moak, J. P., et al. (1998). Congenital heart disease caused by mutations in the transcription factor NKX2-5. *Science* 281, 108–111. doi: 10.1126/science.281.5373.108
- Schwedler, G., Lindinger, A., Lange, P. E., Sax, U., Olchvary, J., Peters, B., et al. (2011). Frequency and spectrum of congenital heart defects among live births in Germany: a study of the Competence Network for Congenital Heart Defects. *Clin. Res. Cardiol.* 100, 1111–1117. doi: 10.1007/s00392-011-0355-7
- Seides, S. F., Shemin, R. J., and Morrow, A. G. (1979). Congenital cardiac abnormalities in monozygotic twins. Report and review of the literature. *Br. Heart J.* 42, 742–745. doi: 10.1136/heart.42.6.742
- Shinebourne, E. A., Babu-Narayan, S. V., and Carvalho, J. S. (2006). Tetralogy of Fallot: from fetus to adult. *Heart* 92, 1353–1359. doi: 10.1136/heart.2005.061143
- Simon, A. M., McWhorter, A. R., Dones, J. A., Jackson, C. L., and Chen, H. (2004). Heart and head defects in mice lacking pairs of connexins. *Dev. Biol.* 265, 369–383. doi: 10.1016/j.ydbio.2003.09.036
- Simpson, I., Rose, B., and Loewenstein, W. R. (1977). Size limit of molecules permeating the junctional membrane channels. *Science* 195, 294–296. doi: 10.1126/science.831276
- Soemedi, R., Topf, A., Wilson, I. J., Darlay, R., Rahman, T., Glen, E., et al. (2012). Phenotype-specific effect of chromosome 1q21.1 rearrangements and GJA5 duplications in 2436 congenital heart disease patients and 6760 controls. *Hum. Mol. Genet.* 21, 1513–1520. doi: 10.1093/hmg/ddr589
- Sullivan, R., Huang, G. Y., Meyer, R. A., Wessels, A., Linask, K. K., and Lo, C. W. (1998). Heart malformations in transgenic mice exhibiting dominant negative inhibition of gap junctional communication in neural crest cells. *Dev. Biol.* 204, 224–234. doi: 10.1006/dbio.1998.9089
- TenBroek, E. M., Lampe, P. D., Solan, J. L., Reynhout, J. K., and Johnson, R. G. (2001). Ser364 of connexin43 and the upregulation of gap junction assembly by cAMP. *J. Cell Biol.* 155, 1307–1318. doi: 10.1083/jcb.200102017
- Tennstedt, C., Chaoui, R., Korner, H., and Dietel, M. (1999). Spectrum of congenital heart defects and extracardiac malformations associated with chromosomal abnormalities: results of a seven year necropsy study. *Heart* 82, 34–39.
- Terada, R., Warren, S., Lu, J. T., Chien, K. R., Wessels, A., and Kasahara, H. (2011). Ablation of Nkx2-5 at mid-embryonic stage results in premature lethality and cardiac malformation. *Cardiovasc. Res.* 91, 289–299. doi: 10.1093/cvr/cvr037
- Thomas, S. V., Ajaykumar, B., Sindhu, K., Francis, E., Namboodiri, N., Sivasankaran, S., et al. (2008). Cardiac malformations are increased in infants of mothers with epilepsy. *Pediatr. Cardiol.* 29, 604–608. doi: 10.1007/s00246-007-9161-4
- Unwin, P. N. T., and Zampighi, G. (1980). Structure of the junction between communicating cells. *Nature* 283, 545–549. doi: 10.1038/283545a0
- van der Bom, T., Bouma, B. J., Meijboom, F. J., Zwinderman, A. H., and Mulder, B. J. (2012). The prevalence of adult congenital heart disease, results from a systematic review and evidence based calculation. *Am. Heart J.* 164, 568–575. doi: 10.1016/j.ahj.2012.07.023
- van der Bom, T., Zomer, A. C., Zwinderman, A. H., Meijboom, F. J., Bouma, B. J., and Mulder, B. J. (2011). The changing epidemiology of congenital heart disease. *Nat. Rev. Cardiol.* 8, 50–60. doi: 10.1038/nr cardio.2010.166
- van Rijen, H. V., van Veen, T. A. B., Gros, D., Wilders, R., and de Bakker, J. M. T. (2006). “Connexin and cardiac arrhythmias,” in *Cardiovascular Gap Junctions*, ed. S. Dhein (Basel: Karger Verlag), 150–160.
- Waldo, K. L., Lo, C. W., and Kirby, M. L. (1999). Connexin 43 expression reflects neural crest patterns during cardiovascular development. *Dev. Biol.* 208, 307–323. doi: 10.1006/dbio.1999.9219
- Waller, B. R. III, McQuinn, T., Phelps, A. L., Markwald, R. R., Lo, C. W., Thompson, R. P., et al. (2000). Conotruncal anomalies in the trisomy 16 mouse: an immunohistochemical analysis with emphasis on the involvement of the neural crest. *Anat. Rec.* 260, 279–293. doi: 10.1002/1097-0185(20001101)260
- Wang, B., Wen, Q., Xie, X., Liu, S., Liu, M., Tao, Y., et al. (2010). Mutation analysis of connexin43 gene in Chinese patients with congenital heart defects. *Int. J. Cardiol.* 145, 487–489. doi: 10.1016/j.ijcard.2009.06.026
- Wang, J., Xin, Y. F., Liu, X. Y., Liu, Z. M., Wang, X. Z., and Yang, Y. Q. (2011). A novel NKKX2-5 mutation in familial ventricular septal defect. *Int. J. Mol. Med.* 27, 369–375. doi: 10.3892/ijmm.2010.585
- Wang, X., Wang, J., Zhao, P., Guo, Y., Wu, L., Sun, J., et al. (2012). Familial congenital heart disease: data collection and preliminary analysis. *Cardiol. Young* 23, 394–399. doi: 10.1017/S1047951112001035
- Yu, Q., Shen, Y., Chatterjee, B., Siegfried, B. H., Leatherbury, L., Rosenthal, J., et al. (2004). ENU induced mutations causing congenital cardiovascular anomalies. *Development* 131, 6211–6223. doi: 10.1242/dev.01543

**Conflict of Interest Statement:** The authors declare that the research was conducted in the absence of any commercial or financial relationships that could be construed as a potential conflict of interest.

*Received: 13 February 2013; accepted: 15 May 2013; published online: 03 June 2013.*

*Citation: Salameh A, Blanke K and Daehnert I (2013) Role of connexins in human congenital heart disease: the chicken and egg problem. Front. Pharmacol. 4:70. doi: 10.3389/fphar.2013.00070 This article was submitted to Frontiers in Pharmacology, a specialty of Frontiers in Pharmacology.*

*Copyright © 2013 Salameh, Blanke and Daehnert. This is an open-access article distributed under the terms of the Creative Commons Attribution License, which permits use, distribution and reproduction in other forums, provided the original authors and source are credited and subject to any copyright notices concerning any third-party graphics etc.*



# Connexin mutants and cataracts

**Eric C. Beyer<sup>1</sup>\*, Lisa Ebihara<sup>2</sup> and Viviana M. Berthoud<sup>1</sup>**

<sup>1</sup> Department of Pediatrics, University of Chicago, Chicago, IL, USA

<sup>2</sup> Department of Physiology and Biophysics, Rosalind Franklin Health Sciences University, North Chicago, IL, USA

**Edited by:**

Stefan Dhein, Universitätsklinik Leipzig Herzzentrum Leipzig GmbH, Germany

**Reviewed by:**

Luc Leybaert, Ghent University, Belgium

Richard Warth, University of Regensburg, Germany

**\*Correspondence:**

Eric C. Beyer, Department of Pediatrics, University of Chicago, 900 East 57th Street, KCB 5152, Chicago, IL 60637, USA.

e-mail: ecbeyer@uchicago.edu

The lens is a multicellular, but avascular tissue that must stay transparent to allow normal transmission of light and focusing of it on the retina. Damage to lens cells and/or proteins can cause cataracts, opacities that disrupt these processes. The normal survival of the lens is facilitated by an extensive network of gap junctions formed predominantly of connexin46 and connexin50. Mutations of the genes that encode these connexins (*GJA3* and *GJA8*) have been identified and linked to inheritance of cataracts in human families and mouse lines. *In vitro* expression studies of several of these mutants have shown that they exhibit abnormalities that may lead to disease. Many of the mutants reduce or modify intercellular communication due to channel alterations (including loss of function or altered gating) or due to impaired cellular trafficking which reduces the number of gap junction channels within the plasma membrane. However, the abnormalities detected in studies of other mutants suggest that they cause cataracts through other mechanisms including gain of hemichannel function (leading to cell injury and death) and formation of cytoplasmic accumulations (that may act as light scattering particles). These observations and the anticipated results of ongoing studies should elucidate the mechanisms of cataract development due to mutations of lens connexins and abnormalities of other lens proteins. They may also contribute to our understanding of the mechanisms of disease due to connexin mutations in other tissues.

**Keywords:** connexin46, connexin50, cataract, lens, gap junction

## THE LENS AND CATARACTS

The lens is a transparent organ whose main function is to transmit light and focus it on the retina. It sits suspended between two clear fluids (the aqueous humor and the vitreous) and has no direct blood supply (Figure 1A). The lens is comprised of two cell types: epithelial cells that form a single layer along the anterior surface and fiber cells that form the bulk of the organ (Figure 1B). At the lens equator, epithelial cells differentiate into fiber cells, a process that involves cell elongation and loss of nuclei and organelles. This differentiation process occurs throughout the lifespan of the organism. Lens fiber cells contain very high concentrations of small soluble proteins called crystallins. These proteins act as chaperones and increase the refractive index (but do not interfere with transparency). Mature fiber cells have limited metabolic activities, are non-dividing, and must survive for the lifespan of the organism. Most of the metabolic, synthetic, and active transport machinery in the lens is localized to surface (nucleated) cells (Mathias and Rae, 2004).

A cataract is a cloudiness or opacity in the lens. It may cause a decrease in vision and may eventually lead to blindness. This disease has substantial public health consequences, because cataracts are the leading cause of blindness worldwide (Resnikoff et al., 2004). Even in those countries where cataractous lenses are surgically removed and replaced with prosthetic intraocular lenses, this eye pathology has a major financial impact. Therefore, many efforts have been devoted to determine the factors that lead to cataract formation and to develop treatments to prevent their

formation. Cataracts can be subdivided according to their anatomical location within the lens (e.g., cortical, nuclear, sub-capsular), their appearance (e.g., total, pulverulent), and most commonly by a combination of these two parameters (e.g., nuclear pulverulent). They can also be subdivided according to their etiology (e.g., congenital, disease-related, or age-related). The specific biochemical and structural changes associated with cataract formation are diverse, but a common biochemical change is the presence of high molecular weight insoluble protein aggregates (Moreau and King, 2012).

Because the lens does not have a direct blood supply, the nutrients for the organ all derive from the fluids in which it is suspended. Specifically, the aqueous humor (which is dynamically produced from the plasma and subsequently resorbed) provides the main source for inorganic and organic ions, carbohydrates, glutathione, amino acids, and oxygen. The aqueous humor is also the repository for metabolites and carbon dioxide produced by lens cells. Ions and nutrients reach cells in the interior through an internal "circulation" in which flow of ions and water drives the movement of solutes throughout the organ. A model of this circulation has been developed based on surface currents recorded from lenses (Robinson and Patterson, 1982; Parmelee, 1986; Mathias et al., 1997) and measurements of hydrostatic pressures at different depths within the lens (Gao et al., 2011). In this model, current carried by ions (and associated water and solutes) enters the lens along the extracellular spaces at the anterior and posterior poles, it crosses fiber cell membranes in the lens interior, and it flows back to the surface

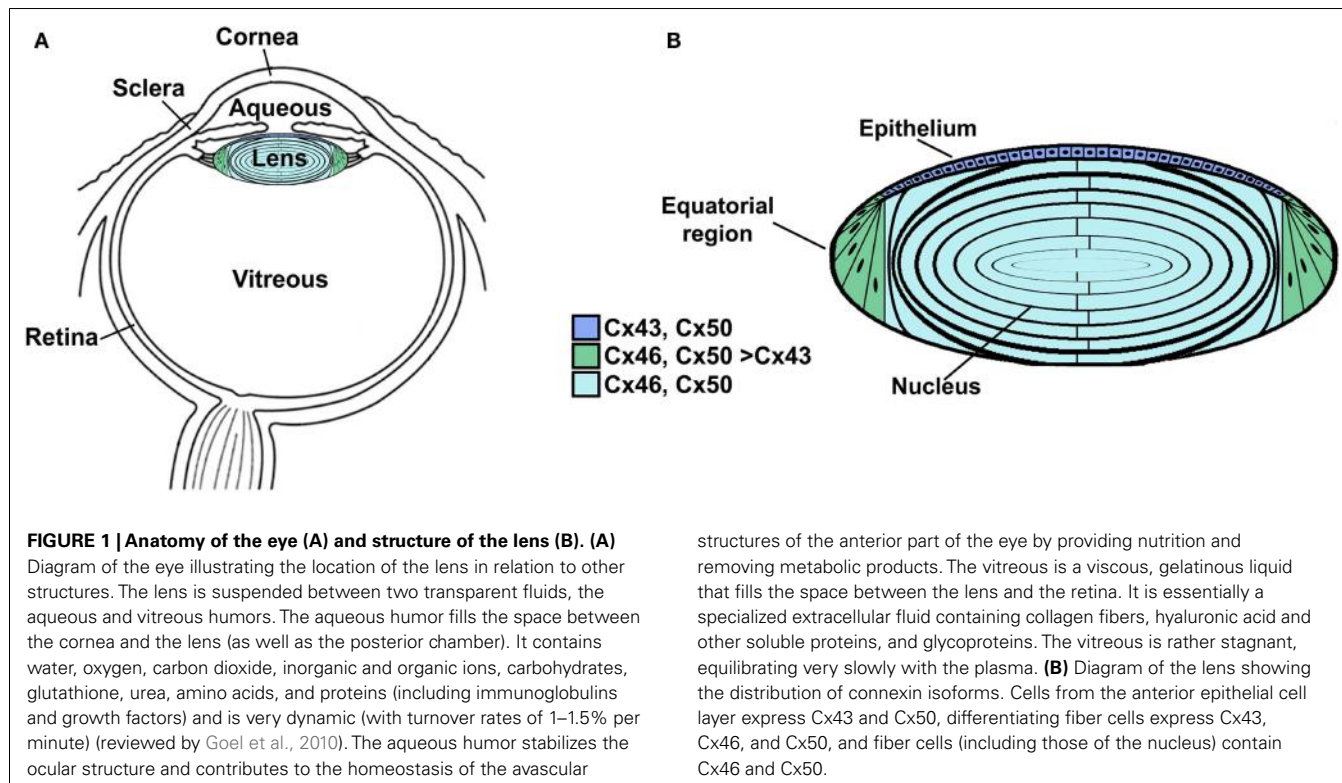


**FIGURE 1 | Anatomy of the eye (A) and structure of the lens (B).** (A)

Diagram of the eye illustrating the location of the lens in relation to other structures. The lens is suspended between two transparent fluids, the aqueous and vitreous humors. The aqueous humor fills the space between the cornea and the lens (as well as the posterior chamber). It contains water, oxygen, carbon dioxide, inorganic and organic ions, carbohydrates, glutathione, urea, amino acids, and proteins (including immunoglobulins and growth factors) and is very dynamic (with turnover rates of 1–1.5% per minute) (reviewed by Goel et al., 2010). The aqueous humor stabilizes the ocular structure and contributes to the homeostasis of the avascular

structures of the anterior part of the eye by providing nutrition and removing metabolic products. The vitreous is a viscous, gelatinous liquid that fills the space between the lens and the retina. It is essentially a specialized extracellular fluid containing collagen fibers, hyaluronic acid and other soluble proteins, and glycoproteins. The vitreous is rather stagnant, equilibrating very slowly with the plasma. (B) Diagram of the lens showing the distribution of connexin isoforms. Cells from the anterior epithelial cell layer express Cx43 and Cx50, differentiating fiber cells express Cx43, Cx46, and Cx50, and fiber cells (including those of the nucleus) contain Cx46 and Cx50.

at the equator (through a cell-to-cell pathway) (Mathias et al., 2007, 2010). The hydrostatic pressure gradient also drives water flow toward the exterior (Gao et al., 2011). The lens circulatory system provides a pathway for internal fiber cells to obtain essential nutrients, remove potentially toxic metabolites, and maintain resting potentials (Goodenough, 1979; Piatigorsky, 1980). Thus, fiber cell survival and the maintenance of transparency depend on the function of epithelial cells and on communication between lens cells (Goodenough, 1992).

### LENS GAP JUNCTIONS AND CONNEXINS

Intercellular communication among the cells of the lens is facilitated by an extensive network of gap junctions. Gap junctions are membrane specializations that contain clusters of intercellular channels that are permeable to ions and small solutes ( $\leq 1$  kDa). Lens fiber cells share ions and small metabolites through gap junction channels, and consequently behave as a functional syncytium (Goodenough et al., 1980; Mathias and Rae, 1989). Epithelial and fiber cells contain morphologically and physiologically distinct gap junctions (Rae and Kuszak, 1983; Miller and Goodenough, 1986).

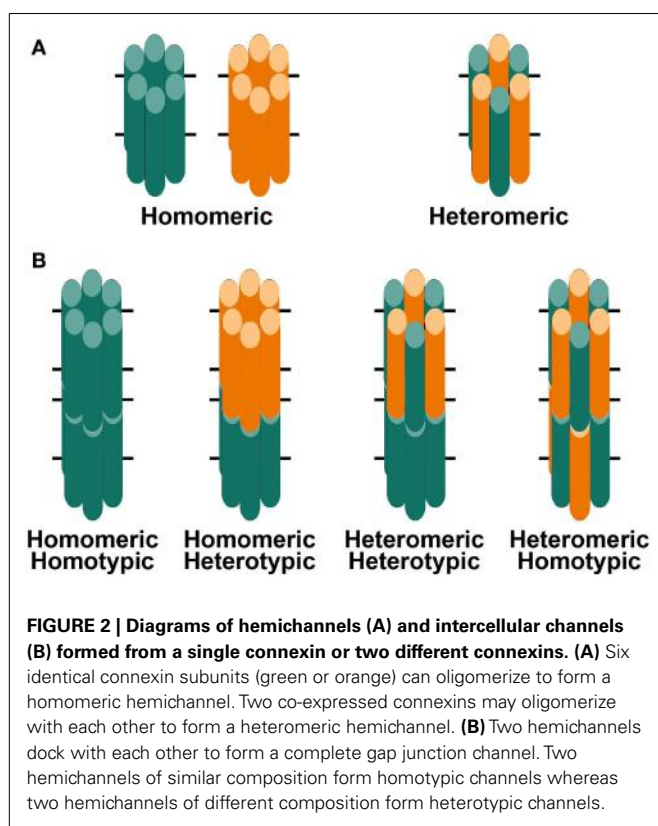
Gap junction channels are oligomeric assemblies of members of a family of related proteins called connexins (Cx) (Beyer and Berthoud, 2009). Connexins contain four transmembrane domains connected by two extracellular loops and one cytoplasmic loop. The amino and carboxyl termini of the polypeptide are in the cytoplasm. Six connexins oligomerize to form a connexin hemichannel which traffics to the plasma membrane of one cell where it can dock with another hemichannel from an adjacent cell to form a complete gap junction channel (Figure 2). Channels formed by diverse connexins differ in physiological properties

including unitary conductance, permeability, gating, and regulation by different protein kinase-dependent pathways (reviewed in Harris, 2001, 2007; Saez et al., 2003). Thus, the regulation of intercellular communication and the permeation of different molecules in different regions of the lens are determined by the repertoire of connexins expressed.

Three connexins have been identified in the lens with somewhat overlapping expression patterns (Figure 1B). Cx43 is expressed in lens epithelial cells (Musil et al., 1990), but its expression is turned off as epithelial cells in the equatorial region differentiate into fiber cells. Cx50 is also expressed in epithelial cells (TenBroek et al., 1994; Dahm et al., 1999; Rong et al., 2002). Cx46 and Cx50 become abundantly expressed in the differentiating cells and are the two most abundant connexins in lens fiber cells (Paul et al., 1991; White et al., 1992). Cx46 and Cx50 co-localize at gap junction plaques and can form mixed hexamers (Paul et al., 1991; Jiang and Goodenough, 1996). (Heteromeric mixing is illustrated schematically in Figure 2).

Transcripts for a fourth connexin, Cx23, have been detected in the zebrafish embryo lens (Irvine et al., 2008) and in the mouse lens (Puk et al., 2008). Cx23 has been implicated in fiber cell differentiation, because fiber cells in mice expressing a missense mutation of Cx23 did not appear to elongate properly (Puk et al., 2008). Lens cells from other mammalian species may also express Cx23, since it has been identified as an expressed sequence in mRNA from whole eyes or lenses<sup>1</sup>. However, Cx23 transcript

<sup>1</sup>Accession numbers for *Oryctogalulus cuniculus* EST from eye: EB384661.1, EB384662.1; *Bos taurus* EST from lens: EG705869.1; *Macaca mulatta* EST from lens: EG703836.



was not detected in RNA isolated from human lenses (Sonntag et al., 2009). Moreover, while Cx23 protein has been detected in proteomic studies of mouse lens membrane proteins (Bassnett et al., 2009), it was not detected in human samples (Wang et al., 2013). Therefore, Cx23 is not included in **Figure 1B** nor considered further in this review.

## MOUSE STUDIES IMPLICATE CONNEXINS IN CATARACTOGENESIS

The importance of gap junction-mediated lens intercellular communication for the maintenance of lens transparency has been substantiated by a number of genetic studies in mice. Targeted deletion of either Cx46 or Cx50 results in the development of cataracts in homozygous (but not heterozygous) null mice (Gong et al., 1997; White et al., 1998). The Cx50-null mice have a milder cataract than the Cx46-null mice (Gerido et al., 2003), but Cx50-null mice exhibit microphthalmia and smaller lenses (Gong et al., 1997; White et al., 1998; Rong et al., 2002). The onset of the cataract phenotype in Cx50 knock-out mice occurs within the first postnatal week (White et al., 1998; Rong et al., 2002) whereas the cataracts in Cx46-null mice are visible by the third week of age (Gong et al., 1997). The solubility of some crystallins is decreased in both Cx50- and Cx46-null mice. Double knock-out mice lacking both the Cx46 and Cx50 genes show dense lens opacities that are far more extensive than those observed in either the Cx46 or Cx50 single null mice (Xia et al., 2006).

Transgenic mice over-expressing Cx50 also develop severe cataracts (Chung et al., 2007). This finding suggests that any

significant alteration of connexin levels in these cells (either absence or a major increase) may lead to cataract formation.

The role of Cx43 in normal lens function is uncertain. Lenses of prenatal or newborn Cx43-null mice appear normal and transparent (White et al., 2001) and Berthoud and Beyer, unpublished observations), but Gao and Spray (1998) have observed ultrastructural abnormalities in these lenses. The long-term effects of the loss of Cx43 in the lens cannot be determined in these mice, because global deletion of Cx43 results in neonatal lethality (Reaume et al., 1995). However, the lenses of animals with a conditional deletion of Cx43 are transparent and develop normally through at least 6 months of age, even though intercellular transfer of neurobiotin and Lucifer yellow among epithelial cells is decreased (DeRosa et al., 2009).

The cataract trait in several mutant mouse strains has been mapped to the lens connexin loci. The *No2* mouse carries a missense mutation within the coding region of Cx50 resulting in a change of amino acid residue 47 from aspartate to alanine (Cx50D47A) and develops congenital cataracts (Favor, 1983; Steele et al., 1998); these cataracts are less severe in heterozygous than in homozygous animals. Mice carrying a Cx50 mutation at amino acid residue 64 (changing from valine to alanine, Cx50V64A) exhibit dominantly inherited cataracts (Graw et al., 2001). Another mouse with cataracts, *lop10*, carries a missense mutation at amino acid residue 22 of Cx50 (Cx50G22R) (Chang et al., 2002). Both cataracts and microphthalmia have been observed in mice with the semi-dominant mutation, Cx50R205G (Xia et al., 2012).

## CONNEXIN MUTATIONS AND CONGENITAL CATARACTS IN HUMANS

Mutations in lens connexins have been associated with human disease. Missense and frame shift mutations of the Cx46 and Cx50 genes have been identified in members of families with inherited cataracts of various different phenotypes. These mutants and their associated cataract phenotypes are summarized in **Table 1** (Cx46) and **Table 2** (Cx50). Other than the few exceptions noted in the tables, nearly all of the cataracts are inherited as autosomal dominant traits. The positions of these mutations in relation to the membrane topology of these connexins are shown in **Figure 3**.

Mutations in Cx43 have been associated with oculodentodigital dysplasia, a disease which is only rarely accompanied by cataracts. Therefore, Cx43 mutations are not considered in this review.

Our laboratories have been interested in determining the biochemical, cell biological and physiological abnormalities in the behaviors of these human mutants. We have expressed different cataract-associated connexin mutants using *in vitro* expression systems, by transfection of communication- and connexin-deficient mammalian cells and by microinjection of *in vitro* transcribed connexin cRNAs into *Xenopus* oocytes. We have identified several different abnormalities (as illustrated by different examples in **Table 3**). In this paper, we will review some of these findings and consider their implications for understanding cataract pathogenesis. The data summarized will primarily derive from the human connexin mutant experiments performed in our laboratories.

Typically, we have performed functional and cellular screening tests in parallel. These initial studies are designed to test whether a mutant construct induces a level of intercellular conductance

**Table 1 | Human Cx46 mutants linked to cataract formation.**

Position and alteration	Disease phenotype		Reference
	Cataract appearance	Other features	
G2D	Nuclear pulverulent and posterior polar		Yao et al. (2011)
D3Y	Zonular pulverulent		Addison et al. (2006)
L11S	"Ant-egg"		Hansen et al. (2006)
T19M	Posterior polar		Santhiya et al. (2010)
V28M	Variable		Devi et al. (2005)
F32L	Nuclear pulverulent		Jiang et al. (2003)
R33L	Finely granular embryonal		Guleria et al. (2007a)
V44M			Zhou et al. (2010), Bennett and Shiels (2011)
W45S	Nuclear		Ma et al. (2005)
D47N	Nuclear		Yang et al. (2011)
P59L	Nuclear punctate		Bennett et al. (2004)
N63S	Zonular pulverulent		MacKay et al. (1999)
R76G	Total		Devi et al. (2005)
R76H	Lamellar nuclear opacity with surrounding pulverulent nuclear opacities; lamellar with moderate opacity of the fetal nucleus and Y-shaped condensations in the anterior suture	Dominant inheritance with incomplete penetrance	Burdon et al. (2004), Hansen et al. (2009)
T87M	"Pearl box"		Guleria et al. (2007b)
G143R	Coppock-like		Zhang et al. (2012a)
P187L	Homogeneous zonular pulverulent		Rees et al. (2000)
P187S	Nuclear pulverulent		Ding et al. (2011)
N188I	Nuclear coralliform		Zhang et al. (2012b)
N188T	Nuclear pulverulent		Li et al. (2004)
F206I	Embryonal nuclear		Wang and Zhu (2012)
fs380	Zonular pulverulent		MacKay et al. (1999)

When the descriptions of the cataract phenotype differed in different reports, both are listed, but separated by a semi-colon. All cataracts were inherited as dominant traits.

above that seen in untransfected cells or water-injected *Xenopus* oocytes and whether the construct leads to the formation of gap junction plaques. Plaque formation is identified as immunoreactive connexin that localizes along appositional membranes with a punctate distribution (examples are shown for wild type Cx46 and Cx50 in Figures 4 and 5).

### CONNEXIN MUTANTS WITH ABNORMALITIES OF CELLULAR BIOSYNTHESIS OR DEGRADATION

The most frequently observed phenotype is a cataract-associated connexin mutant that does not induce a significant intercellular conductance and forms very few or no gap junction plaques. Examples include Cx50R23T, Cx50D47N, Cx50P88S, Cx50P88Q, and Cx46fs380 (Berthoud et al., 2003; Minogue et al., 2005; Arora et al., 2006, 2008; Thomas et al., 2008) (Table 3 and Figures 4 and 5). Among these mutants, Cx50R23T rarely forms small plaques (Thomas et al., 2008), while Cx46fs380 never forms them (Minogue et al., 2005). These differences likely reflect variations in the severity of the trafficking defects and the specific mechanisms involved.

For many of the mutants that do not form plaques, immunoreactive connexin localizes within the cytoplasm. Co-localization

studies using antibodies directed against compartments of the protein biosynthetic/secretory pathway have shown that the mutant connexins are contained within the ER, ERGIC, and/or Golgi apparatus (e.g., Cx50D47N and Cx46fs380) (Minogue et al., 2005; Arora et al., 2008). The connexin within these subcellular compartments likely represents mutant protein that has been retained within the export pathway due to misfolding and/or incomplete/improper oligomerization. The interpretation that some of the mutant connexins (e.g., Cx50D47N, Cx50P88Q, Cx50P88S) are misfolded is supported by the presence of gap junction plaques at the plasma membrane after incubation of expressing cells under conditions that should promote protein folding (reduced temperatures or chemical chaperone treatment) (Berthoud et al., 2003; Arora et al., 2006, 2008).

The cytoplasmic retention of a cataract-linked mutant has been explored in detail for Cx46fs380. This mutant contains a frame shift that causes a change in reading frame such that the connexin contains an abnormal C-terminal sequence. We have shown that a two amino acid motif (FF) within the abnormal polypeptide is responsible for its localization within the ERGIC and Golgi (Minogue et al., 2005). This motif has been identified as a trafficking signal in other proteins.

**Table 2 | Human Cx50 mutants linked to cataract formation.**

Position and alteration	Disease phenotype		Reference
	Cataract appearance	Other features	
R23T	Nuclear		Willoughby et al. (2003)
I31T	Fetal and embryonic nuclear		Wang et al. (2009)
T39R	Complete	Microcornea and iris hypoplasia	Sun et al. (2011)
V44E	Total	Microcornea and variably associated with myopia	Devi and Vijayalakshmi (2006)
W45S	Jellyfish-like		Vanita et al. (2008b)
G46R	Complete	Microcornea	Sun et al. (2011)
G46V	Total		Minogue et al. (2009)
D47N	Nuclear pulverulent		Arora et al. (2008), Wang et al. (2011)
D47Y			Lin et al. (2008)
E48K	"Zonular nuclear" pulverulent		Berry et al. (1999)
V64G	Nuclear		Ma et al. (2005)
S73F	Dense and "star-shaped," various locations in the nucleus or the poles		Hansen et al. (2009)
V79L	"Full moon" with Y-sutural opacities		Vanita et al. (2006)
P88Q	Lamellar pulverulent; balloon-like with Y-sutural opacities		Arora et al. (2006), Vanita et al. (2008a)
P88S	Zonular pulverulent		Shiels et al. (1998)
P189L	Star-shaped nuclear opacity with a whitish central core	Microcornea	Hansen et al. (2007)
R198Q		Microcornea and variably associated with myopia	Devi and Vijayalakshmi (2006)
R198W		Microcornea without microphthalmia	Hu et al. (2010)
fs203	Total	Recessive inheritance. Associated with nystagmus and amblyopia	Ponnam et al. (2007)
I247M	Zonular pulverulent	May be a polymorphism rather than a disease-causing mutation	Polyakov et al. (2001), Graw et al. (2009)
c776InsG	Triangular cataract	Recessive inheritance	Schmidt et al. (2008)
S258F	Nuclear		Gao et al. (2010)
S259Y			Hansen et al. (2009)
S276F	Pulverulent nuclear		Yan et al. (2008)
L281C	Lamellar/zonular		Kumar et al. (2011)

When the descriptions of the cataract phenotype differed in different reports, both are listed, but separated by a semi-colon. All cataracts were inherited as dominant traits, except as noted.

Cx50P88S is an interesting mutant that does not form gap junction plaques when expressed by itself. It has a cytoplasmic localization, but little of the protein is localized within compartments of the biosynthetic/secretory pathway. Rather, this mutant forms cytoplasmic inclusions (1–5/cell) of 0.6–2.7  $\mu\text{m}$  in diameter (Berthoud et al., 2003). Similar inclusions are observed after transfection of several different cell lines. The Cx50P88S accumulations are very long lived (as compared to the turnover of the wild type protein in these expression systems) and correspond to closely apposed circular or semicircular membrane stacks that likely originate from the rough endoplasmic reticulum (Berthoud et al., 2003; Lichtenstein et al., 2009). Some of the Cx50P88S inclusions co-localize with components of the autophagic degradation pathway, and their turnover is altered by interventions that affect

autophagy. Thus, the persistence of the Cx50P88S accumulations likely results from insufficient degradation capacity of constitutive autophagy (Lichtenstein et al., 2011). We have also studied another cataract-associated mutant of this connexin at the same position, Cx50P88Q. Although this mutant forms some cytoplasmic inclusions like Cx50P88S, the glutamine substitution seems to have less severe consequences than the serine substitution, since many cells expressing Cx50P88Q contain immunoreactive connexin that co-localizes with markers for the ER or Golgi (Arora et al., 2006).

Additional kinds of cellular and biochemical abnormalities may be predicted for some of the identified cataract-associated mutants. For example, phosphorylation events have been implicated in regulation of many aspects of the connexin life cycle and

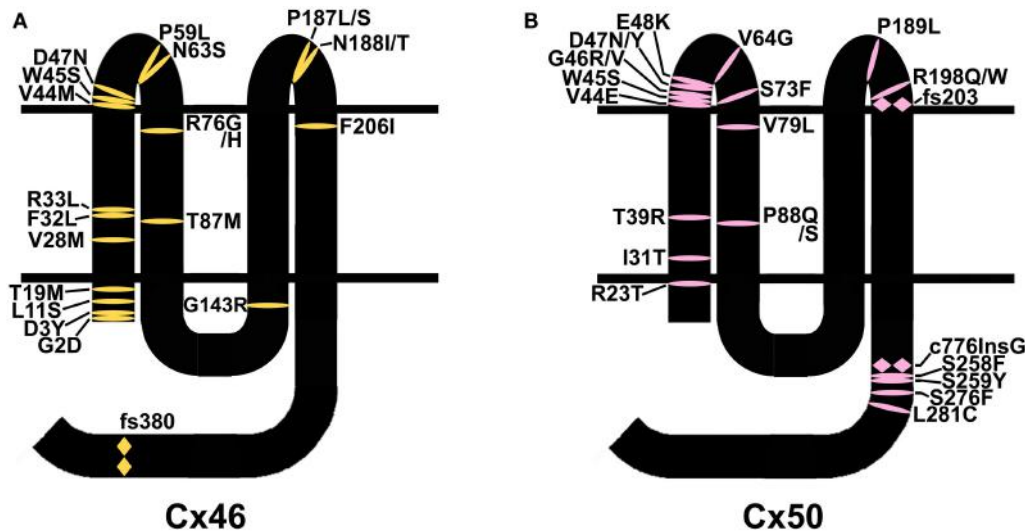


**FIGURE 3 | Diagram illustrating the topology of the human lens connexins, Cx46 (A) and Cx50 (B) and the locations of missense (I) and frame shift (fs) mutations identified in members of families**

with **inherited cataracts**. While included in **Table 2**, Cx50I247M has not been included in the Cx50 diagram, since it may actually be a polymorphism.

physiology (reviewed by Solan and Lampe, 2005; Moreno and Lau, 2007). Two Cx50 mutants, Cx50S258F and Cx50S259Y, alter amino acids that are phosphorylated in the wild type protein as shown in a proteomic study of human lens membrane proteins (Wang et al., 2013); however, the cellular and physiological behaviors of these mutants have not yet been studied. In the *Lop10* mouse, expression of the Cx50 mutant reduces the abundance of phosphorylated forms of Cx46, and the Cx46 alterations may contribute to the cataracts in these animals (Chang et al., 2002). The carboxyl termini of both Cx46 and Cx50 are sensitive to cleavage by calpains (Kistler and Bullivant, 1987; Lin et al., 1997; Jacobs et al., 2004). When expressed in heterologous systems, the resulting truncated Cx50 forms channels with reduced function (DeRosa et al., 2006) and sensitivity to intracellular pH (Lin et al., 1998; Xu et al., 2002). It is likely that some of the mutants within the C-terminal region of the connexin may interfere with this cleavage.

These studies allow prediction of some consequences of mutant connexin expression in the lens. All of the mutants with this general phenotype (loss of function due to a severe reduction in the number or complete absence of gap junctions) should reduce intercellular communication between lens fiber cells, regardless of their different mechanisms of retention/accumulation. In the lens, interactions of these mutants with other lens fiber cell proteins (including wild type connexins) might alter their trafficking or function as well. The mutants that are retained within the ER might cause ER stress and might lead to stimulation of the unfolded protein response. A study of the Cx50G22R and Cx50S50P mutant mice concluded that the unfolded protein response might be a contributing factor to the cataracts in these animals (Alapure et al., 2012). The stable cytoplasmic inclusions formed by some mutants (e.g., Cx50P88S) may cause light scattering and act as nucleation particles for accumulation/aggregation of other proteins.

## CONNEXIN MUTANTS WITH ABNORMALITIES OF CHANNEL BEHAVIOR

The gap junction conductance between a pair of cells depends on the number of channels, their open probabilities, and their single channel conductances. The trafficking mutants discussed above are complete (or near complete) loss of function mutants, because they effectively have reduced the number of intercellular channels.

There are other mutants that form non-functional channels (e.g., Cx50W45S, Cx46D3Y, and Cx46L11S) which make abundant gap junction plaques, but have no gap junction channel activity when expressed by themselves (Tong et al., 2011, 2013) (**Table 3** and **Figure 3**). These mutants effectively have an open probability of zero (or no unitary conductance).

Because mutant lens connexins can oligomerize with wild type Cx46 and/or Cx50 to form gap junction channels, several of the cataract-associated mutant lens connexins have been studied for their ability to alter the function of co-expressed wild type lens connexins. Some of these mutants (e.g., Cx46N63S, Cx46fs380) do not inhibit the function of either Cx46 or Cx50 (Pal et al., 2000). Other mutants (e.g., Cx50P88S, Cx50P88Q, Cx50W45S, Cx50E48K, Cx46D3Y, Cx46L11S), decrease the junctional conductance supported by their wild type counterparts (Pal et al., 1999; Arora et al., 2006; Banks et al., 2009; Tong et al., 2011, 2013). In the case of Cx50P88S, a single mutant subunit is sufficient to inhibit function of a full gap junction channel (Pal et al., 1999). Some lens connexin mutants that inhibit their homologous wild type counterparts do not act as strong dominant negative inhibitors of the other lens fiber cell connexin. For example, Cx46D3Y and Cx46L11S inhibit wild type Cx46, but they do not block wild type Cx50 (Tong et al., 2013). In addition, the function of certain lens connexin mutants such as Cx46D3Y is partially rescued by heterotypically pairing cells expressing the mutant connexin with cells expressing wild type lens connexins (Tong et al., 2013). HeLa

**Table 3 | Examples of cataract-associated lens connexin mutants with different cellular or physiological abnormalities.**

Mutant	Intercellular channel function	Plaque formation	ER/Golgi localization (without plaques)	Accumulation at other cellular sites	Hemichannel function	Effects on co-expressed wild type connexin	
						Cx50	Cx46
Cx50D47N	None	Absent	Yes	No	None	No effect	No effect
Cx46fs380	None	Absent	Yes	No	None	No effect	Inhibition
Cx50R23T	None	Very rare	Yes	No	Weak inhibition	Inhibition	
Cx50P88Q	None	Absent	Yes	Yes	Inhibition		
Cx50P88S	None	Absent	No	No	Inhibition		
Cx50V45S	None	Normal	No	No	No effect		
Cx46N63S	None					No effect	
Cx46D3Y	None	Normal	No	No	Reduced and altered sensitivity to divalent cations	Hemichannels with altered properties	Hemichannels with altered properties
Cx46L11S	None	Normal	No	No	Reduced	Hemichannels with altered properties	Hemichannels with altered properties
Cx50G46V	Normal	Normal	No	No	Increased	Increased hemichannel function	Increased hemichannel function

Properties of mutants were all determined for each connexin when expressed by itself, except for the co-expression results. Blanks represent parameters that have not been tested.

cells expressing an EGFP fusion protein of Cx46D3Y have been reported to show increased intercellular transfer of Lucifer yellow or ethidium as compared to cells expressing wild type Cx46-EGFP (Schlingmann et al., 2012).

The direct link between loss of connexin function and cataracts is an active area of research. The studies of Matthias and colleagues (reviewed in Mathias et al., 2010) have established that loss of function of either Cx46 or Cx50 (as observed in “knock-out” mice) reduces coupling conductance between lens fiber cells. Reductions of intercellular communication would be anticipated to decrease the circulation of gap junction permeant molecules (including water, ions, and metabolites) between lens cells. Indeed, Gao et al. (2011) observed that reductions in gap junction channels in genetically manipulated mice resulted in a proportional decrease in the gradient of intracellular hydrostatic pressure from the center to the periphery of the lens. One hypothesis links connexin function, calcium levels and proteolysis of crystallins to cataracts based on studies of the Cx46-null mice. These animals have nuclear cataracts associated with generation of a cleaved form of  $\gamma$ -crystallin and significant amounts of NaOH-insoluble  $\alpha$ -,  $\beta$ -, and  $\gamma$ -crystallins in the lens nucleus (Gong et al., 1997). Cx46-null mice also have elevated levels of calcium in their lens nuclear regions (Baruch et al., 2001; Gao et al., 2004) and increased activation of calcium-dependent protease activity, likely due to the calpain3 isozyme, Lp82 (Baruch et al., 2001). Moreover, cataract formation is delayed in Cx46-null mice that are also deficient in the gene (*Capn3*) encoding this protease (Tang et al., 2007). However, the mechanism linking Cx46 function to cataracts in humans may be somewhat different, since *CAPN3* mRNA expression has only been identified in skeletal muscle in people (Fougerousse et al., 1998).

Connexin mutants could also affect parameters such as voltage gating, sensitivity to intracellular pH or channel permeability that would lead to altered function, but not necessarily complete loss of function. As summarized in **Table 4**, Cx46 and Cx50 exhibit some differences in many of these physiological properties. Studies of mouse connexins have identified mutants (like Cx50S50P) that alter the voltage-dependent gating properties of co-expressed Cx46 or Cx50 (DeRosa et al., 2007). Interestingly, mouse Cx50S50P is also a potent inhibitor of co-expressed Cx43, suggesting that intercellular communication may be interrupted in lens epithelial cells where these two connexins are co-expressed (DeRosa et al., 2009). Another mouse mutant, Cx50R205G, blocks the gap junction channel function of co-expressed wild type Cx50, but only affects the gating of Cx46 channels (Xia et al., 2012).

## CONNEXIN FUNCTIONS BEYOND INTERCELLULAR COMMUNICATION

In addition to forming intercellular channels, connexins can also form functional hemichannels that induce large, relatively non-selective conductances in single plasma membranes. These conductances are caused by permeation through “undocked” single connexons. This phenomenon has been best demonstrated in primary cultures of various cells and in expression systems. One of the most dramatic examples is the large permeabilities induced by expression of Cx46 in single *Xenopus* oocytes that can be gated by modulation of extracellular concentrations of divalent cations

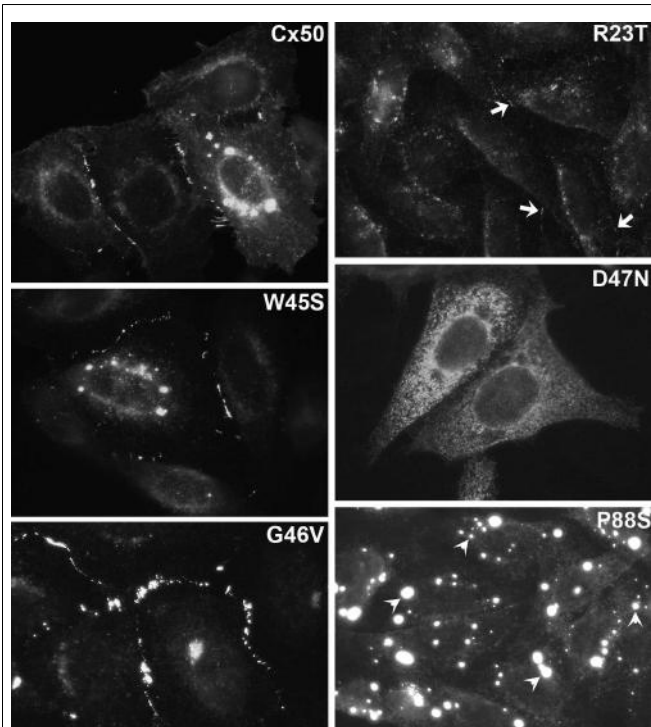


**FIGURE 4 | Immunofluorescent localization of wild type Cx50 and of different cataract-associated Cx50 mutants (R23T, W45S, D47N, G46V, and P88S) after their expression by transfection of HeLa cells.** Similar to wild type Cx50, W45S and G46V show abundant localization in a punctate distribution along appositional membranes corresponding to gap junction plaques. The abundance of plaques is very reduced for R23T, but small spots at appositional membranes are occasionally observed. D47N and P88S show no localization consistent with gap junction plaque formation. D47N is found in a reticular, cytoplasmic distribution. P88S localizes in intensely fluorescent cytoplasmic inclusions. Reproduced and adapted from Berthoud et al. (2003), Arora et al. (2008), Thomas et al. (2008), and Tong et al. (2011).

including calcium (Paul et al., 1991). Because Cx46 hemichannels are mechanosensitive, it has been proposed that their opening plays a physiological role during lens accommodation (Bao et al., 2004). Opening of such hemichannels has been demonstrated in isolated mouse lens fiber cells (Ebihara et al., 2010). The ability of some mutant lens connexins to form functional hemichannels has been assessed. Unlike wild type Cx46, many of the cataract-associated Cx46 mutants do not form functional hemichannels (e.g., Cx46L11S, Cx46fs380). Others exhibit a reduced ability to form them (e.g., Cx46D3Y, Cx46N63S) (Pal et al., 2000; Tong et al., 2013). Thus, entry of sodium and calcium into lens cells expressing these mutants would be impaired if Cx46 hemichannels serve as conduits for these ions in the normal lens.

Cataract-associated mutants may also form hemichannels with altered properties (like gating or charge selectivity) as compared with the wild type connexin. For example, Cx46N63S forms hemichannels with increased sensitivity to the extracellular concentration of magnesium ions (Ebihara et al., 2003). Cx46D3Y forms hemichannels that have altered charge selectivity and voltage gating (Tong et al., 2013).

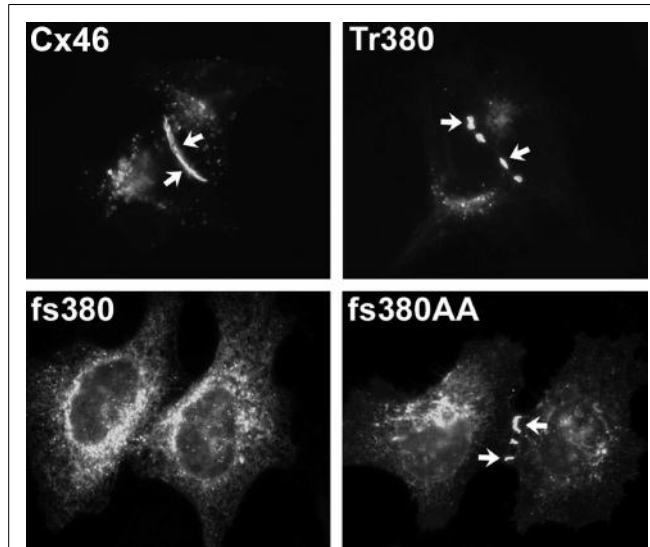


**FIGURE 5 | Immunofluorescent localization of wild type Cx46, the cataract-associated mutant Cx46fs380 (fs380), Cx46 truncated after amino acid 379 (Tr380) and Cx46fs380 with the FF motif replaced by AA (fs380AA) in transfected HeLa cells.** Wild type Cx46 localizes in an intense, linear distribution along appositional membranes as expected for large gap junctions, but such staining is absent for Cx46fs380 which is only found in a cytoplasmic distribution. The cytoplasmic retention must be due to the abnormal sequence in the carboxyl terminus of Cx46fs380, since its removal by truncation (Tr380) restores gap junction formation. Similarly, gap junction formation is restored when the FF motif in Cx46fs380 is replaced with two alanines (fs380AA). Reproduced and adapted from Minogue et al. (2005).

A very striking alteration of hemichannel properties is exemplified by Cx50G46V, a mutant found in a patient with total cataract (Minogue et al., 2009). This mutant forms gap junction plaques and supports intercellular communication normally. However, unlike wild type Cx50, Cx50G46V has a greatly increased ability to form functional hemichannels (Minogue et al., 2009; Tong et al., 2011). Expression of this mutant increases the proportion of apoptotic cells and causes cell death (Minogue et al., 2009) (Figure 6), suggesting that opening of the hemichannels would also cause severe cell damage *in vivo*. This cytotoxicity appears dominant, since co-expression of Cx50G46V with wild type Cx46 or Cx50 also decreases cell (oocyte) viability (Tong et al., 2011). Connexin mutants with enhanced hemichannel activity may cause fiber cell death through a complex sequence of events including loss of membrane potential, disruption of transmembrane ion gradients, and entry of calcium ions, leading to activation of intracellular proteases and decreased metabolic activity.

Connexins may also be involved in functions not directly associated with their channel forming ability. Cx50 is required for normal growth of the lens. As mentioned above, mice that are null for Cx50 (but not those null for Cx46) have smaller lenses (Gong et al., 1997; White et al., 1998). The decreased lens size appears to result from reduced proliferation of lens epithelial cells, especially during the first few days of postnatal life (Sellitto et al., 2004). It has been speculated that this proliferative deficiency is due to a connexin function other than intercellular exchange of

**Table 4 | Physiological properties of wild type Cx50 and Cx46.**

Property	Cx50	Cx46	Reference
Unitary gap junctional channel conductance	~220 pS	~150 pS	Srinivas et al. (1999), Hopperstad et al. (2000)
Ionic selectivity	Cations > anions	Cations > anions	Srinivas et al. (1999), Trexler et al. (2000)
Dye permeability	DAPI, NB >> LY	DAPI >> LY	Srinivas et al. (1999), Trexler et al. (2000), Thomas et al. (2008)
Sensitivity to transjunctional voltage	++	+	Ebihara and Steiner (1993), White et al. (1994), Srinivas et al. (1999), Hopperstad et al. (2000)
Sensitivity to intracellular pH	+	+	Eckert (2002), Xu et al. (2002)
Sensitivity to activated MAPK	++	-	Shakespeare et al. (2009)
Ability to form functional hemichannels	+	+++	Paul et al. (1991), Ebihara and Steiner (1993), Beahm and Hall (2002)

Except for the final row, the properties refer to those of intercellular channels formed of each connexin as determined from studies in expression systems.

pS, picoSiemens; DAPI, 4',6-diamidino-2-phenylindole; NB, Neurobiotin; LY, Lucifer yellow; MAPK, Mitogen-activated protein kinase.

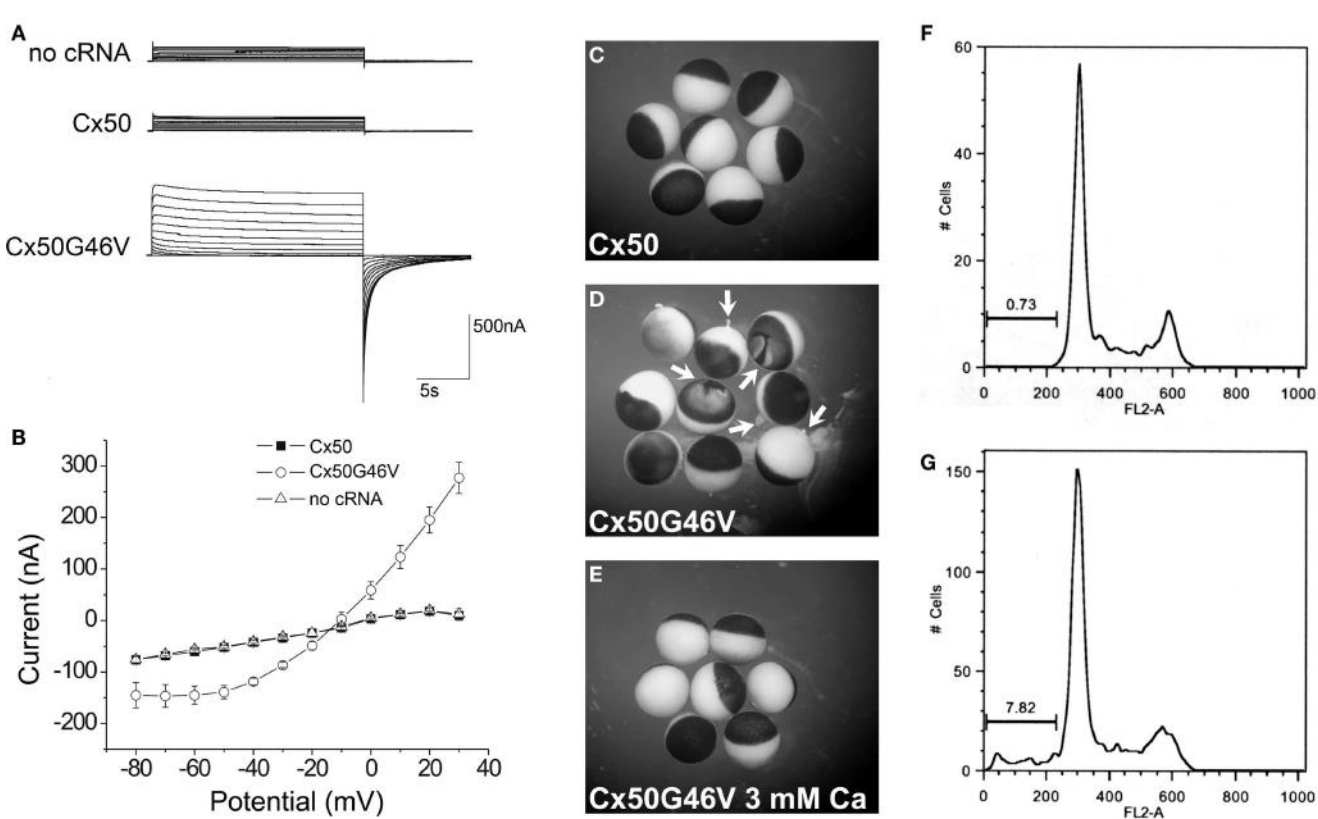


**FIGURE 6 | The Cx50G46V mutant induces large hemichannel currents, cytotoxicity, and apoptosis. (A)** Hemichannel currents elicited in response to a series of voltage pulses in control *Xenopus* oocytes (no cRNA) or oocytes injected with cRNA encoding wild type Cx50 or Cx50G46V. The mutant induces much larger currents than wild type Cx50 or control oocytes. **(B)** Steady-state current-voltage relationships in control (no cRNA), wild type Cx50, and Cx50G46V cRNA-injected oocytes. The mutant induces large outward currents that activate on depolarization. **(C–E)** *Xenopus* oocytes were injected with similar amounts of Cx50 (**C**) or Cx50G46V cRNA (**D,E**) and incubated in modified Barth's solution containing 1 mM Ca<sup>2+</sup> (**C,D**) or 3 mM Ca<sup>2+</sup> (**E**) overnight at 18°C. Oocytes injected with Cx50G46V cRNA showed obvious discoloration, membrane disruption, and leakage of yolk

(arrows in **D**) when incubated in modified Barth's solution containing 1 mM Ca<sup>2+</sup> (**D**) while oocytes injected with Cx50 cRNA showed no apparent detrimental changes when studied under identical conditions (**C**). The rate of cell death of the Cx50G46V cRNA-injected oocytes was significantly reduced by increasing the external calcium concentration from 1 to 3 mM (**E**). **(F,G)**. Graphs show the results of cell cycle analysis of propidium iodide-stained HeLa cells induced to express wild type Cx50 (**F**) or Cx50G46V (**G**). This analysis revealed a substantial population of cells in the sub-G1 fraction, a marker for apoptosis, in cells expressing Cx50G46V but not in cells expressing Cx50 implying that expression of this mutant increased the proportion of apoptotic cells. Reproduced and adapted from Minogue et al. (2009).

ions and small molecules, since introduction of Cx46 into the Cx50 locus does not restore normal lens growth to Cx50-null mice (Martinez-Wittingham et al., 2004). Over-expression of Cx50 also leads to a decrease in lens size (Chung et al., 2007); thus, the proper level of Cx50 expression is required for normal lens development and growth.

The growth and differentiation promoting properties of Cx50 (and the roles of different portions of the molecule) have been further analyzed. Expression of the chicken Cx50 ortholog (including non-functional mutants) or a chicken Cx46 chimera containing the Cx50 carboxyl terminus promotes differentiation of chicken lens cells in culture (Gu et al., 2003; Banks et al., 2007). The mechanism for this “non-channel”-induced effect of Cx50 has not been clarified, but it has been suggested that it involves interactions of its carboxyl terminus with other cellular proteins to modulate intracellular signaling critical for lens cell differentiation. The major intrinsic protein, aquaporin0, is among the lens proteins that can interact with lens connexins (Yu and Jiang, 2004; Yu et al., 2005).

It is plausible that some human Cx50 mutants affect protein interactions or differentiation promoting properties involved in the normal development of the lens and other eye structures. In some of the families with inherited cataracts, affected individuals have small lenses. Moreover, in some pedigrees, the cataracts are associated with additional abnormalities including microcornea, iris hypoplasia, and myopia (see **Tables 1** and **2**).

## CONCLUSIONS AND PERSPECTIVES

In conclusion, there are many different derangements in the cellular/biochemical behavior and function of the Cx46 and Cx50 mutants that have been linked to cataract formation.

As discussed, the most common abnormality caused by a mutation is improper trafficking and reduced gap junction plaque formation. Such mutations occur at positions throughout the connexin polypeptide, likely because deleterious substitutions of many different residues may cause misfolding (e.g., Cx50D47N). Many identified mutations involve substitutions of amino acids near the amino terminus or within the first transmembrane domain (**Figure 3**). Since these regions contribute to the channel pore, mutants within them (if targeted properly to the plasma membrane) would be expected to cause functional alterations (e.g., Cx46L11S). The extracellular loops are the other regions with a large number of mutations. Since the structure of these domains is critical for docking between hemichannels and for gating of hemichannels, it would be expected that mutants in this region would affect function if the mutant connexin is appropriately targeted to the plasma membrane (e.g., Cx50G46V).

Elucidating the abnormalities produced by many of these mutations will help to understand the pathogenesis of cataracts and of other diseases caused by mutations in other members of the connexin family. Indeed, reduced formation of gap junctions

leading to loss of function is also one of the most commonly observed abnormalities of disease-associated Cx26, Cx32, and Cx43 mutants (reviewed by Laird, 2010; Abrams and Scherer, 2012; Scott et al., 2012; Xu and Nicholson, 2012).

The cataracts associated with Cx46 and Cx50 mutants are predominantly inherited as autosomal dominant traits. This is similar to the inheritance pattern of oculodentodigital dysplasia caused by Cx43 mutants, but differs from Cx32 and most Cx26 mutants which cause disease in a recessive fashion. In some cases, the mutant connexin acts as a “dominant-negative” inhibitor of the function of the co-expressed wild type protein (like Cx50P88S) (Pal et al., 1999). But, other lens connexin mutants show little or no inhibition of the function of the wild type counterparts when studied in expression systems (**Table 3**). The absence of cataracts in mice that are heterozygous-null for Cx46 or Cx50 (Gong et al., 1997; White et al., 1998) implies that haplod deficiency of these connexins in mice is not sufficient to cause disease. Thus, there must be additional abnormalities conferred by the mutations that lead to lens opacities. Some of these other abnormalities such as formation of cytoplasmic inclusions or gain of hemichannel function have been considered in this review.

It is noteworthy that there are significant differences in the anatomical locations or appearances of the cataracts caused by different lens connexin mutations and among individuals within a single pedigree or in different pedigrees with the same mutation (**Tables 1** and **2**). Some of the phenotypic dissimilarities between different mutants likely reflect the variety of altered cellular/biochemical mechanisms, since mutants may disrupt different protein–protein interactions and affect different processes. The phenotypic differences among people with the same mutant allele imply that there are other genes that contribute to the phenotype. This conclusion is supported by the strain-dependent differences in severity of the cataracts in Cx46- and Cx50-null mice (Gong et al., 1999; Gerido et al., 2003). The differential severities of the cataracts in Cx46-null mice may partially result from differences in expression of HSP27/25 and ERp29 between strains (Hoehnwarter et al., 2008).

Finally, we can anticipate further progress in the elucidation of the mechanisms involved in cataract formation based on the characterization of additional mutants in expression systems and through the study of corresponding mutants using animal models. Eventually, these studies will contribute to the development of therapeutic approaches to prevent the formation or progression of cataracts due to connexin mutations, and perhaps those due to other genetic or non-genetic causes.

## ACKNOWLEDGMENTS

This work was supported by National Institute of Health grants RO1 EY08368 (to Eric C. Beyer) and RO1 EY10589 (to Lisa Ebihara).

## REFERENCES

- Abrams, C. K., and Scherer, S. S. (2012). Gap junctions in inherited human disorders of the central nervous system. *Biochim. Biophys. Acta* 1818, 2030–2047.
- Addison, P. K., Berry, V., Holden, K. R., Espinal, D., Rivera, B., Su, H., et al. (2006). A novel mutation in the connexin 46 gene (GJA3) causes autosomal dominant zonular pulverulent cataract in a Hispanic family. *Mol. Vis.* 12, 791–795.
- Alapure, B. V., Stull, J. K., Firtina, Z., and Duncan, M. K. (2012). The unfolded protein response is activated in connexin 50 mutant mouse lenses. *Exp. Eye Res.* 102, 28–37.
- Arora, A., Minogue, P. J., Liu, X., Reddy, M. A., Ainsworth, J. R., Bhattacharya, S. S., et al. (2006). A novel GJA8 mutation is associated with autosomal dominant lamellar pulverulent cataract: further evidence with congenital nuclear pulverulent cataracts. *J. Med. Genet.* 45, 155–160.
- Arora, A., Minogue, P. J., Liu, X., Addison, P. K., Russel-Eggitt, I., Webster, A. R., et al. (2008). A novel connexin50 mutation associated with congenital nuclear pulverulent cataracts. *J. Med. Genet.* 45, 155–160.

- for gap junction dysfunction in human cataract. *J. Med. Genet.* 43, e2.
- Banks, E. A., Toloue, M. M., Shi, Q., Zhou, Z. J., Liu, J., Nicholson, B. J., et al. (2009). Connexin mutation that causes dominant congenital cataracts inhibits gap junctions, but not hemichannels, in a dominant negative manner. *J. Cell Sci.* 122, 378–388.
- Banks, E. A., Yu, X. S., Shi, Q., and Jiang, J. X. (2007). Promotion of lens epithelial-fiber differentiation by the C-terminus of connexin 45.6 a role independent of gap junction communication. *J. Cell Sci.* 120, 3602–3612.
- Bao, L., Sachs, F., and Dahl, G. (2004). Connexins are mechanosensitive. *Am. J. Physiol. Cell. Physiol.* 287, C1389–C1395.
- Baruch, A., Greenbaum, D., Levy, E. T., Nielsen, P. A., Gilula, N. B., Kumar, N. M., et al. (2001). Defining a link between gap junction communication, proteolysis, and cataract formation. *J. Biol. Chem.* 276, 28999–29006.
- Bassnett, S., Wilmarth, P. A., and David, L. L. (2009). The membrane proteome of the mouse lens fiber cell. *Mol. Vis.* 15, 2448–2463.
- Beahm, D. L., and Hall, J. E. (2002). Hemichannel and junctional properties of connexin 50. *Biophys. J.* 82, 2016–2031.
- Bennett, T. M., MacKay, D. S., Knopf, H. L., and Shiels, A. (2004). A novel missense mutation in the gene for gap-junction protein  $\alpha 3$  (*GJA3*) associated with autosomal dominant “nuclear punctate” cataracts linked to chromosome 13q. *Mol. Vis.* 10, 376–382.
- Bennett, T. M., and Shiels, A. (2011). A recurrent missense mutation in *GJA3* associated with autosomal dominant cataract linked to chromosome 13q. *Mol. Vis.* 17, 2255–2262.
- Berry, V., MacKay, D., Khaliq, S., Francis, P. J., Hameed, A., Anwar, K., et al. (1999). Connexin 50 mutation in a family with congenital “zonular nuclear” pulverulent cataract of Pakistani origin. *Hum. Genet.* 105, 168–170.
- Berthoud, V. M., Minogue, P. J., Guo, J., Williamson, E. K., Xu, X., Ebihara, L., et al. (2003). Loss of function and impaired degradation of a cataract-associated mutant connexin50. *Eur. J. Cell Biol.* 82, 209–221.
- Beyer, E. C., and Berthoud, V. M. (2009). “The family of connexin genes,” in *Connexins: A Guide*, eds A. Harris, and D. Locke (New York: Humana Press), 3–26.
- Burdon, K. P., Wirth, M. G., Mackey, D. A., Russell-Egitt, I. M., Craig, J. E., Elder, J. E., et al. (2004). A novel mutation in the Connexin 46 gene causes autosomal dominant congenital cataract with incomplete penetrance. *J. Med. Genet.* 41, e106.
- Chang, B., Wang, X., Hawes, N. L., Ojakian, R., Davison, M. T., Lo, W. K., et al. (2002). A *Gja8* (Cx50) point mutation causes an alteration of  $\alpha 3$  connexin (Cx46) in semi-dominant cataracts of *Lop 10* mice. *Hum. Mol. Genet.* 11, 507–513.
- Chung, J., Berthoud, V. M., Novak, L., Zoltoski, R., Heilbrunn, B., Minogue, P. J., et al. (2007). Transgenic overexpression of connexin50 induces cataracts. *Exp. Eye Res.* 84, 513–528.
- Dahm, R., Van Marle, J., Prescott, A. R., and Quinlan, R. A. (1999). Gap junctions containing alpha8-connexin (MP70) in the adult mammalian lens epithelium suggests a re-evaluation of its role in the lens. *Exp. Eye Res.* 69, 45–56.
- DeRosa, A. M., Mese, G., Li, L., Sellitto, C., Brink, P. R., Gong, X., et al. (2009). The cataract causing Cx50-S50P mutant inhibits Cx43 and intercellular communication in the lens epithelium. *Exp. Cell Res.* 315, 1063–1075.
- DeRosa, A. M., Mui, R., Srinivas, M., and White, T. W. (2006). Functional characterization of a naturally occurring Cx50 truncation. *Invest. Ophthalmol. Vis. Sci.* 47, 4474–4481.
- DeRosa, A. M., Xia, C. H., Gong, X., and White, T. W. (2007). The cataract-inducing S50P mutation in Cx50 dominantly alters the channel gating of wild-type lens connexins. *J. Cell Sci.* 120, 4107–4116.
- Devi, R. R., Reena, C., and Vijayalakshmi, P. (2005). Novel mutations in *GJA3* associated with autosomal dominant congenital cataract in the Indian population. *Mol. Vis.* 11, 846–852.
- Devi, R. R., and Vijayalakshmi, P. (2006). Novel mutations in *GJA8* associated with autosomal dominant congenital cataract and microcornea. *Mol. Vis.* 12, 190–195.
- Ding, X., Wang, B., Luo, Y., Hu, S., Zhou, G., Zhou, Z., et al. (2011). A novel mutation in the connexin 46 (*GJA3*) gene associated with congenital cataract in a Chinese pedigree. *Mol. Vis.* 17, 1343–1349.
- Ebihara, L., Liu, X., and Pal, J. D. (2003). Effect of external magnesium and calcium on human connexin46 hemichannels. *Biophys. J.* 84, 277–286.
- Ebihara, L., and Steiner, E. (1993). Properties of a nonjunctional current expressed from a rat connexin46 cDNA in *Xenopus* oocytes. *J. Gen. Physiol.* 102, 59–74.
- Ebihara, L., Tong, J. J., Vertel, B., White, T. W., and Chen, T. L. (2010). Properties of connexin 46 hemichannels in dissociated lens fiber cells. *Invest. Ophthalmol. Vis. Sci.* 52, 882–889.
- Eckert, R. (2002). pH gating of lens fibre connexins. *Pflugers Arch.* 443, 843–851.
- Favor, J. (1983). A comparison of the dominant cataract and recessive specific-locus mutation rates induced by treatment of male mice with ethylnitrosourea. *Mutat. Res.* 110, 367–382.
- Fougnerousse, F., Durand, M., Suel, L., Pourquie, O., Delezoide, A. L., Romero, N. B., et al. (1998). Expression of genes (CAPN3, SGCA, SGCB, and TTN) involved in progressive muscular dystrophies during early human development. *Genomics* 48, 145–156.
- Gao, J., Sun, X., Martinez-Wittingham, F. J., Gong, X., White, T. W., and Mathias, R. T. (2004). Connections between connexins, calcium, and cataracts in the lens. *J. Gen. Physiol.* 124, 289–300.
- Gao, J., Sun, X., Moore, L. C., White, T. W., Brink, P. R., and Mathias, R. T. (2011). Lens intracellular hydrostatic pressure is generated by the circulation of sodium and modulated by gap junction coupling. *J. Gen. Physiol.* 137, 507–520.
- Gao, X., Cheng, J., Lu, C., Li, X., Li, F., Liu, C., et al. (2010). A novel mutation in the connexin 50 gene (*GJA8*) associated with autosomal dominant congenital nuclear cataract in a Chinese family. *Curr. Eye Res.* 35, 597–604.
- Gao, Y., and Spray, D. C. (1998). Structural changes in lenses of mice lacking the gap junction protein connexin43. *Invest. Ophthalmol. Vis. Sci.* 39, 1198–1209.
- Gerido, D. A., Sellitto, C., Li, L., and White, T. W. (2003). Genetic background influences cataractogenesis, but not lens growth deficiency, in Cx50-knockout mice. *Invest. Ophthalmol. Vis. Sci.* 44, 2669–2674.
- Goel, M., Picciani, R. G., Lee, R. K., and Bhattacharya, S. K. (2010). Aqueous humor dynamics: a review. *Open. Ophthalmol. J.* 4, 52–59.
- Gong, X., Agopian, K., Kumar, N. M., and Gilula, N. B. (1999). Genetic factors influence cataract formation in  $\alpha 3$  connexin knockout mice. *Dev. Genet.* 24, 27–32.
- Gong, X., li, E., Klier, G., Huang, Q., Wu, Y., Lei, H., et al. (1997). Disruption of  $\alpha 3$  connexin gene leads to proteolysis and cataractogenesis in mice. *Cell* 91, 833–843.
- Goodenough, D. A. (1979). Lens gap junctions: a structural hypothesis for nonregulated low-resistance intercellular pathways. *Invest. Ophthalmol. Vis. Sci.* 18, 1104–1122.
- Goodenough, D. A. (1992). The crystalline lens. A system networked by gap junctional intercellular communication. *Semin. Cell Biol.* 3, 49–58.
- Goodenough, D. A., Dick, J., and Lyons, J. E. (1980). Lens metabolic cooperation: a study of mouse lens transport and permeability visualized with freeze-substitution autoradiography and electron microscopy. *J. Cell Biol.* 86, 576–589.
- Graw, J., Loster, J., Soewarto, D., Fuchs, H., Meyer, B., Reis, A., et al. (2001). Characterization of a mutation in the lens-specific MP70 encoding gene of the mouse leading to a dominant cataract. *Exp. Eye Res.* 73, 867–876.
- Graw, J., Schmidt, W., Minogue, P. J., Rodriguez, J., Tong, J. J., Klopp, N., et al. (2009). The *Gja8* allele encoding CX50I247M is a rare polymorphism, not a cataract-causing mutation. *Mol. Vis.* 15, 1881–1885.
- Gu, S., Yu, X. S., Yin, X., and Jiang, J. X. (2003). Stimulation of lens cell differentiation by gap junction protein connexin 45.6. *Invest. Ophthalmol. Vis. Sci.* 44, 2103–2111.
- Guleria, K., Sperling, K., Singh, D., Varon, R., Singh, J. R., and Vanita, V. (2007a). A novel mutation in the connexin 46 (*GJA3*) gene associated with autosomal dominant congenital cataract in an Indian family. *Mol. Vis.* 13, 1657–1665.
- Guleria, K., Vanita, V., Singh, D., and Singh, J. R. (2007b). A novel “pearl box” cataract associated with a mutation in the connexin 46 (*GJA3*) gene. *Mol. Vis.* 13, 797–803.
- Hansen, L., Mikkelsen, A., Nurnberg, P., Nurnberg, G., Anjum, I., Eiberg, H., et al. (2009). Comprehensive mutational screening in a cohort of Danish families with hereditary congenital cataract. *Invest. Ophthalmol. Vis. Sci* 50, 3291–3303.
- Hansen, L., Yao, W., Eiberg, H., Funding, M., Riise, R., Kjaer, K.

- W., et al. (2006). The congenital "ant-egg" cataract phenotype is caused by a missense mutation in connexin46. *Mol. Vis.* 12, 1033–1039.
- Hansen, L., Yao, W., Eiberg, H., Kjaer, K. W., Baggesen, K., Hejtmancik, J. F., et al. (2007). Genetic heterogeneity in microcornea-cataract: five novel mutations in CRYAA, CRYGD, and GJA8. *Invest. Ophthalmol. Vis. Sci.* 48, 3937–3944.
- Harris, A. L. (2001). Emerging issues of connexin channels: biophysics fills the gap. *Q. Rev. Biophys.* 34, 325–472.
- Harris, A. L. (2007). Connexin channel permeability to cytoplasmic molecules. *Prog. Biophys. Mol. Biol.* 94, 120–143.
- Hoehnwarter, W., Tang, Y., Ackermann, R., Pleissner, K. P., Schmid, M., Stein, R., et al. (2008). Identification of proteins that modify cataract of mouse eye lens. *Proteomics* 8, 5011–5024.
- Hopperstad, M. G., Srinivas, M., and Spray, D. C. (2000). Properties of gap junction channels formed by Cx46 alone and in combination with Cx50. *Biophys. J.* 79, 1954–1966.
- Hu, S., Wang, B., Zhou, Z., Zhou, G., Wang, J., Ma, X., et al. (2010). A novel mutation in GJA8 causing congenital cataract-microcornea syndrome in a Chinese pedigree. *Mol. Vis.* 16, 1585–1592.
- Iovine, M. K., Gumpert, A. M., Falk, M. M., and Mendelson, T. C. (2008). Cx23, a connexin with only four extracellular-loop cysteines, forms functional gap junction channels and hemichannels. *FEBS Lett.* 582, 165–170.
- Jacobs, M. D., Soeller, C., Sisley, A. M., Cannell, M. B., and Donaldson, P. J. (2004). Gap junction processing and redistribution revealed by quantitative optical measurements of connexin46 epitopes in the lens. *Invest. Ophthalmol. Vis. Sci.* 45, 191–199.
- Jiang, H., Jin, Y., Bu, L., Zhang, W., Liu, J., Cui, B., et al. (2003). A novel mutation in GJA3 (connexin46) for autosomal dominant congenital nuclear pulverulent cataract. *Mol. Vis.* 9, 579–583.
- Jiang, J. X., and Goodenough, D. A. (1996). Heteromeric connexons in lens gap junction channels. *Proc. Natl. Acad. Sci. U.S.A.* 93, 1287–1291.
- Kistler, J., and Bullivant, S. (1987). Protein processing in lens intercellular junctions: cleavage of MP70 to MP38. *Invest. Ophthalmol. Vis. Sci.* 28, 1687–1692.
- Kumar, M., Agarwal, T., Khokhar, S., Kumar, M., Kaur, P., Roy, T. S., et al. (2011). Mutation screening and genotype phenotype correlation of  $\alpha$ -crystallin,  $\gamma$ -crystallin and GJA8 gene in congenital cataract. *Mol. Vis.* 17, 693–707.
- Laird, D. W. (2010). The gap junction proteome and its relationship to disease. *Trends Cell Biol.* 20, 92–101.
- Li, Y., Wang, J., Dong, B., and Man, H. (2004). A novel connexin46 (GJA3) mutation in autosomal dominant congenital nuclear pulverulent cataract. *Mol. Vis.* 10, 668–671.
- Lichtenstein, A., Gaietta, G. M., Deerink, T. J., Crum, J., Sosinsky, G. E., Beyer, E. C., et al. (2009). The cytoplasmic accumulations of the cataract-associated mutant, Connexin50P88S, are long-lived and form in the endoplasmic reticulum. *Exp. Eye Res.* 88, 600–609.
- Lichtenstein, A., Minogue, P. J., Beyer, E. C., and Berthoud, V. M. (2011). Autophagy: a pathway that contributes to connexin degradation. *J. Cell Sci.* 124, 910–920.
- Lin, J. S., Eckert, R., Kistler, J., and Donaldson, P. (1998). Spatial differences in gap junction gating in the lens are a consequence of connexin cleavage. *Eur. J. Cell Biol.* 76, 246–250.
- Lin, J. S., Fitzgerald, S., Dong, Y., Knight, C., Donaldson, P., and Kistler, J. (1997). Processing of the gap junction protein connexin50 in the ocular lens is accomplished by calpain. *Eur. J. Cell Biol.* 73, 141–149.
- Lin, Y., Liu, N. N., Lei, C. T., Fan, Y. C., Liu, X. Q., Yang, Y., et al. (2008). [A novel GJA8 mutation in a Chinese family with autosomal dominant congenital cataract]. *Zhonghua Yi Xue Za Zhi.* 25, 59–62.
- Ma, Z., Zheng, J., Yang, F., Ji, J., Li, X., Tang, X., et al. (2005). Two novel mutations of connexin genes in Chinese families with autosomal dominant congenital nuclear cataract. *Br. J. Ophthalmol.* 89, 1535–1537.
- MacKay, D., Ionides, A., Kibar, Z., Rouleau, G., Berry, V., Moore, A., et al. (1999). Connexin46 mutations in autosomal dominant congenital cataract. *Am. J. Hum. Genet.* 64, 1357–1364.
- Martinez-Wittingham, F. J., Sellitto, C., White, T. W., Mathias, R. T., Paul, D., and Goodenough, D. A. (2004). Lens gap junctional coupling is modulated by connexin identity and the locus of gene expression. *Invest. Ophthalmol. Vis. Sci.* 45, 3629–3637.
- Mathias, R. T., Kistler, J., and Donaldson, P. (2007). The lens circulation. *J. Membr. Biol.* 216, 1–16.
- Mathias, R. T., and Rae, J. L. (1989). "Cell to cell communication in lens," in *Cell Interaction and Gap Junction*, eds N. Sperelakis, and W. C. Cole (Boca Raton, FL: CRC Press, Inc.), 29–50.
- Mathias, R. T., and Rae, J. L. (2004). The lens: local transport and global transparency. *Exp. Eye Res.* 78, 689–698.
- Mathias, R. T., Rae, J. L., and Baldo, G. J. (1997). Physiological properties of the normal lens. *Physiol. Rev.* 77, 21–50.
- Mathias, R. T., White, T. W., and Gong, X. (2010). Lens gap junctions in growth, differentiation, and homeostasis. *Physiol. Rev.* 90, 179–206.
- Miller, T. M., and Goodenough, D. A. (1986). Evidence for two physiologically distinct gap junctions expressed by the chick lens epithelial cell. *J. Cell Biol.* 102, 194–199.
- Minogue, P. J., Liu, X., Ebihara, L., Beyer, E. C., and Berthoud, V. M. (2005). An aberrant sequence in a connexin46 mutant underlies congenital cataracts. *J. Biol. Chem.* 280, 40788–40795.
- Minogue, P. J., Tong, J. J., Arora, A., Russell-Eggett, I., Hunt, D. M., Moore, A. T., et al. (2009). A mutant connexin50 with enhanced hemichannel function leads to cell death. *Invest. Ophthalmol. Vis. Sci.* 50, 5837–5845.
- Moreau, K. L., and King, J. A. (2012). Protein misfolding and aggregation in cataract disease and prospects for prevention. *Tr. Molec. Med.* 18, 273–282.
- Moreno, A. P., and Lau, A. F. (2007). Gap junction channel gating modulated through protein phosphorylation. *Prog. Biophys. Mol. Biol.* 94, 107–119.
- Musil, L. S., Beyer, E. C., and Goodenough, D. A. (1990). Expression of the gap junction protein connexin43 in embryonic chick lens: molecular cloning, ultrastructural localization, and post-translational phosphorylation. *J. Membr. Biol.* 116, 163–175.
- Pal, J. D., Berthoud, V. M., Beyer, E. C., MacKay, D., Shiels, A., and Ebihara, L. (1999). Molecular mechanism underlying a Cx50-linked congenital cataract. *Am. J. Physiol. Cell. Physiol.* 276, C1443–C1446.
- Pal, J. D., Liu, X., MacKay, D., Shiels, A., Berthoud, V. M., Beyer, E. C., et al. (2000). Connexin46 mutations linked to congenital cataract show loss of gap junction channel function. *Am. J. Physiol. Cell. Physiol.* 279, C596–C602.
- Parmelee, J. T. (1986). Measurement of steady currents around the frog lens. *Exp. Eye Res.* 42, 433–441.
- Paul, D. L., Ebihara, L., Takemoto, L. J., Swenson, K. I., and Goodeough, D. A. (1991). Connexin46, a novel lens gap junction protein, induces voltage-gated currents in nonjunctional plasma membrane of Xenopus oocytes. *J. Cell Biol.* 115, 1077–1089.
- Piatigorsky, J. (1980). Intracellular ions, protein metabolism, and cataract formation. *Curr. Top. Eye Res.* 3, 1–39.
- Polyakov, A. V., Shagina, I. A., Khlebnikova, O. V., and Evgrafov, O. V. (2001). Mutation in the connexin 50 gene (GJA8) in a Russian family with zonular pulverulent cataract. *Clin. Genet.* 60, 476–478.
- Ponnambal, S. P., Ramesha, K., Tejwani, S., Ramamurthy, B., and Kannabiran, C. (2007). Mutation of the gap junction protein alpha 8 (GJA8) gene causes autosomal recessive cataract. *J. Med. Genet.* 44, e85.
- Puk, O., Loster, J., Dalke, C., Soewarto, D., Fuchs, H., Budde, B., et al. (2008). Mutation in a novel connexin-like gene (Gif1) in the mouse affects early lens development and causes a variable small-eye phenotype. *Invest. Ophthalmol. Vis. Sci.* 49, 1525–1532.
- Rae, J. L., and Kuszak, J. R. (1983). The electrical coupling of epithelium and fibers in the frog lens. *Exp. Eye Res.* 36, 317.
- Reaume, A. G., Desousa, P. A., Kulakarni, S., Langille, B. L., Zhu, D. G., Davies, T. C., et al. (1995). Cardiac malformation in neonatal mice lacking connexin43. *Science* 267, 1831–1834.
- Rees, M. I., Watts, P., Fenton, I., Clarke, A., Snell, R. G., Owen, M. J., et al. (2000). Further evidence of autosomal dominant congenital zonular pulverulent cataracts linked to 13q11 (CZP3) and a novel mutation in connexin 46 (GJA3). *Hum. Genet.* 106, 206–209.

- Resnikoff, S., Pascolini, D., Etya'ale, D., Kocur, I., Pararajasegaram, R., Pokharel, G. P., et al. (2004). Global data on visual impairment in the year 2002. *Bull. World Health Organ.* 82, 844–851.
- Robinson, K. R., and Patterson, J. W. (1982). Localization of steady currents in the lens. *Curr. Eye Res.* 2, 843–847.
- Rong, P., Wang, X., Niesman, I., Wu, Y., Benedetti, L. E., Dunia, I., et al. (2002). Disruption of *Gja8* ( $\alpha 8$  connexin) in mice leads to microphthalmia associated with retardation of lens growth and lens fiber maturation. *Development* 129, 167–174.
- Saez, J. C., Berthoud, V. M., Branes, M. C., Martinez, A. D., and Beyer, E. C. (2003). Plasma membrane channels formed by connexins: their regulation and functions. *Physiol. Rev.* 83, 1359–1400.
- Santhiya, S. T., Kumar, G. S., Sudhakar, P., Gupta, N., Klopp, N., Illig, T., et al. (2010). Molecular analysis of cataract families in India: new mutations in the *CRYBB2* and *GJA3* genes and rare polymorphisms. *Mol. Vis.* 16, 1837–1847.
- Schlingmann, B., Schadzek, P., Busko, S., Heisterkamp, A., and Ngezahayo, A. (2012). Cataract-associated D3Y mutation of human connexin46 (hCx46) increases the dye coupling of gap junction channels and suppresses the voltage sensitivity of hemichannels. *J. Bioenerg. Biomembr.* 44, 607–614.
- Schmidt, W., Klopp, N., Illig, T., and Graw, J. (2008). A novel *GJA8* mutation causing a recessive triangular cataract. *Mol. Vis.* 14, 851–856.
- Scott, C. A., Tattersall, D., O'Toole, E. A., and Kelsell, D. P. (2012). Connexins in epidermal homeostasis and skin disease. *Biochim. Biophys. Acta* 1818, 1952–1961.
- Sellitto, C., Li, L., and White, T. W. (2004). Connexin50 is essential for normal postnatal lens cell proliferation. *Invest. Ophthalmol. Vis. Sci.* 45, 3196–3202.
- Shakespeare, T. I., Sellitto, C., Li, L., Rubinos, C., Gong, X., Srinivas, M., et al. (2009). Interaction between Connexin50 and mitogen-activated protein kinase signaling in lens homeostasis. *Mol. Biol. Cell* 20, 2582–2592.
- Shiels, A., MacKay, D., Ionides, A., Berry, V., Moore, A., and Bhattacharya, S. (1998). A missense mutation in the human connexin50 gene (*GJA8*) underlies autosomal dominant "zonular pulverulent" cataract, on chromosome 1q. *Am. J. Hum. Genet.* 62, 526–532.
- Solan, J. L., and Lampe, P. D. (2005). Connexin phosphorylation as a regulatory event linked to gap junction channel assembly. *Biochim. Biophys. Acta* 1711, 154–163.
- Sonntag, S., Sohl, G., Dobrowolski, R., Zhang, J., Theis, M., Winterhager, E., et al. (2009). Mouse lens connexin23 (Gje1) does not form functional gap junction channels but causes enhanced ATP release from HeLa cells. *Eur. J. Cell Biol.* 88, 65–77.
- Srinivas, M., Costa, M., Gao, Y., Fort, A., Fishman, G. I., and Spray, D. C. (1999). Voltage dependence of macroscopic and unitary currents of gap junction channels formed by mouse connexin50 expressed in rat neuroblastoma cells. *J. Physiol. (Lond.)* 517(Pt 3), 673–689.
- Sun, W., Xiao, X., Li, S., Guo, X., and Zhang, Q. (2011). Mutational screening of six genes in Chinese patients with congenital cataract and microcornea. *Mol. Vis.* 17, 1508–1513.
- Steele, E. C. J., Lyon, M. F., Favor, J., Guillot, P. V., Boyd, Y., and Church, R. L. (1998). A mutation in the connexin 50 (Cx50) gene is a candidate for the No2 mouse cataract. *Curr. Eye Res.* 17, 883–889.
- Tang, Y., Liu, X., Zoltoski, R. K., Novak, L. A., Herrera, R. A., Richard, I., et al. (2007). Age-related cataracts in  $\alpha 3$ Cx46-knockout mice are dependent on a calpain 3 isoform. *Invest. Ophthalmol. Vis. Sci.* 48, 2685–2694.
- TenBroek, E. M., Johnson, R., and Louis, C. F. (1994). Cell-to-cell communication in a differentiating ovine lens culture system. *Invest. Ophthalmol. Vis. Sci.* 35, 215–228.
- Thomas, B. C., Minogue, P. J., Valiunas, V., Kanaporis, G., Brink, P. R., Berthoud, V. M., et al. (2008). Cataracts are caused by alterations of a critical N-terminal positive charge in connexin50. *Invest. Ophthalmol. Vis. Sci.* 49, 2549–2556.
- Tong, J. J., Minogue, P. J., Guo, W., Chen, T. L., Beyer, E. C., Berthoud, V. M., et al. (2011). Different consequences of cataract-associated mutations at adjacent positions in the first extracellular boundary of connexin50. *Am. J. Physiol. Cell. Physiol.* 300, C1055–C1064.
- Tong, J. J., Sohn, B. C., Lam, A., Walters, D. E., Vertel, B. M., and Ebihara, L. (2013). Properties of two cataract associated mutations located in the N-terminus of Connexin 46. *Am. J. Physiol Cell Physiol.* doi:10.1152/ajpcell.00344.2012
- Trexler, E. B., Bukauskas, F. F., Kronengold, J., Bargiello, T. A., and Verselis, V. K. (2000). The first extracellular loop domain is a major determinant of charge selectivity in connexin46 channels. *Biophys. J.* 79, 3036–3051.
- Vanita, V., Hennies, H. C., Singh, D., Nurnberg, P., Sperling, K., and Singh, J. R. (2006). A novel mutation in *GJA8* associated with autosomal dominant congenital cataract in a family of Indian origin. *Mol. Vis.* 12, 1217–1222.
- Vanita, V., Singh, J. R., Singh, D., Varon, R., and Sperling, K. (2008a). A mutation in *GJA8* (p.P88Q) is associated with "balloon-like" cataract with Y-sutural opacities in a family of Indian origin. *Mol. Vis.* 14, 1171–1175.
- Vanita, V., Singh, J. R., Singh, D., Varon, R., and Sperling, K. (2008b). A novel mutation in *GJA8* associated with jellyfish-like cataract in a family of Indian origin. *Mol. Vis.* 14, 323–326.
- Wang, K., Wang, B., Wang, J., Zhou, S., Yun, B., Suo, P., et al. (2009). A novel *GJA8* mutation (p.I31T) causing autosomal dominant congenital cataract in a Chinese family. *Mol. Vis.* 15, 2813–2820.
- Wang, K. J., and Zhu, S. Q. (2012). A novel p.F206I mutation in Cx46 associated with autosomal dominant congenital cataract. *Mol. Vis.* 18, 968–973.
- Wang, L., Luo, Y., Wen, W., Zhang, S., and Lu, Y. (2011). Another evidence for a D47N mutation in *GJA8* associated with autosomal dominant congenital cataract. *Mol. Vis.* 17, 2380–2385.
- Wang, Z., Han, J., David, L. L., and Schey, K. L. (2013). Proteomics and phosphoproteomics analysis of human lens fiber cell membranes. *Invest. Ophthalmol. Vis. Sci.* 54, 1135–1143.
- White, T. W., Bruzzone, R., Wolfram, S., Paul, D. L., and Goodenough, D. A. (1994). Selective interactions among the multiple connexin proteins expressed in the vertebrate lens: the second extracellular domain is a determinant of compatibility between connexins. *J. Cell Biol.* 125, 879–892.
- White, T. W., Goodenough, D. A., and Paul, D. L. (1998). Targeted ablation of connexin50 in mice results in microphthalmia and zonular pulverulent cataracts. *J. Cell Biol.* 143, 815–825.
- White, T. W., Sellitto, C., Paul, D. L., and Goodenough, D. A. (2001). Prenatal lens development in connexin43 and connexin50 double knockout mice. *Invest. Ophthalmol. Vis. Sci.* 42, 2916–2923.
- Willoughby, C. E., Arab, S., Gandhi, R., Zeinali, S., Arab, S., Luk, D., et al. (2003). A novel *GJA8* mutation in an Iranian family with progressive autosomal dominant congenital nuclear cataract. *J. Med. Genet.* 40, e124.
- Xia, C. H., Chang, B., DeRosa, A. M., Cheng, C., White, T. W., and Gong, X. (2012). Cataracts and microphthalmia caused by a *gja8* mutation in extracellular loop 2. *PLoS ONE*. 7:e52894. doi:10.1371/journal.pone.0052894
- Xia, C. H., Cheng, C., Huang, Q., Cheung, D., Li, L., Dunia, I., et al. (2006). Absence of  $\alpha 3$  (Cx46) and  $\alpha 8$  (Cx50) connexins leads to cataracts by affecting lens inner fiber cells. *Exp. Eye Res.* 83, 688–696.
- Xu, J., and Nicholson, B. J. (2012). The role of connexins in ear and skin physiology – functional insights from disease-associated mutations. *Biochim. Biophys. Acta* 1828, 167–178.
- Xu, X., Berthoud, V. M., Beyer, E. C., and Ebihara, L. (2002). Functional role of the carboxyl terminal domain of human connexin 50 in gap junctional channels. *J. Membr. Biol.* 186, 101–112.
- Yan, M., Xiong, C., Ye, S. Q., Chen, Y., Ke, M., Zheng, F., et al. (2008). A novel connexin 50 (*GJA8*) mutation in a Chinese family with a dominant congenital pulverulent nuclear cataract. *Mol. Vis.* 14, 418–424.
- Yang, G., Xing, B., Liu, G., Lu, X., Jia, X., Lu, X., et al. (2011). A novel mutation in the *GJA3* (connexin46) gene is associated with autosomal dominant congenital nuclear cataract

- in a Chinese family. *Mol. Vis.* 17, 1070–1073.
- Yao, K., Wang, W., Zhu, Y., Jin, C., Shentu, X., Jiang, J., et al. (2011). A novel *GJA3* mutation associated with congenital nuclear pulverulent and posterior polar cataract in a Chinese family. *Hum. Mutat.* 32, 1367–1370.
- Yu, X. S., and Jiang, J. X. (2004). Interaction of major intrinsic protein (aquaporin-0) with fiber connexins in lens development. *J. Cell Sci.* 117, 871–880.
- Yu, X. S., Yin, X., Lafer, E. M., and Jiang, J. X. (2005). Developmental regulation of the direct interaction between the intracellular loop of connexin 45.6 and the C terminus of major intrinsic protein (aquaporin-0). *J. Biol. Chem.* 280, 22081–22090.
- Zhang, L., Qu, X., Su, S., Guan, L., and Liu, P. (2012a). A novel mutation in *GJA3* associated with congenital Coppock-like cataract in a large Chinese family. *Mol. Vis.* 18, 2114–2118.
- Zhang, X., Wang, L., Wang, J., Dong, B., and Li, Y. (2012b). Coralliform cataract caused by a novel connexin46 (*GJA3*) mutation in a Chinese family. *Mol. Vis.* 18, 203–210.
- Zhou, Z., Hu, S., Wang, B., Zhou, N., Zhou, S., Ma, X., et al. (2010). Mutation analysis of congenital cataract in a Chinese family identified a novel missense mutation in the connexin 46 gene (*GJA3*). *Mol. Vis.* 16, 713–719.

**Conflict of Interest Statement:** The authors declare that the research was conducted in the absence of any commercial or financial relationships that could be construed as a potential conflict of interest.

*Received: 15 February 2013; accepted: 26 March 2013; published online: 15 April 2013.*

*Citation: Beyer EC, Ebihara L and Berthoud VM (2013) Connexin mutants and cataracts. *Front. Pharmacol.* 4:43. doi: 10.3389/fphar.2013.00043*

*This article was submitted to Frontiers in Pharmacology of Ion Channels and Channelopathies, a specialty of Frontiers in Pharmacology.*

*Copyright © 2013 Beyer, Ebihara and Berthoud. This is an open-access article distributed under the terms of the Creative Commons Attribution License, which permits use, distribution and reproduction in other forums, provided the original authors and source are credited and subject to any copyright notices concerning any third-party graphics etc.*



# Role of connexins in infantile hemangiomas

**Katja Blanke\*, Ingo Dähnert and Aida Salameh**

Department of Pediatric Cardiology, Heart Center Leipzig, University of Leipzig, Germany

**Edited by:**

Stefan Dhein, Universitätsklinik  
Leipzig Herzzentrum Leipzig GmbH,  
Germany

**Reviewed by:**

Hiroshi Hibino, Niigata University,  
Japan

Felicitas Bosen, Rheinische  
Friedrich-Wilhelms-Universität Bonn,  
Germany

**\*Correspondence:**

Katja Blanke, Department of Pediatric  
Cardiology, Heart Center Leipzig,  
University of Leipzig, Strümpellstraße  
39, 04289 Leipzig, Germany.  
e-mail: katjablanke@web.de

The circulatory system is one of the first systems that develops during embryogenesis. Angiogenesis describes the formation of blood vessels as a part of the circulatory system and is essential for organ growth in embryogenesis as well as repair in adulthood. A dysregulation of vessel growth contributes to the pathogenesis of many disorders. Thus, an imbalance between pro- and antiangiogenic factors could be observed in infantile hemangioma (IH). IH is the most common benign tumor during infancy, which appears during the first month of life. These vascular tumors are characterized by rapid proliferation and subsequently slower involution. Most IHs regress spontaneously, but in some cases they cause disfigurement and systemic complications, which requires immediate treatment. Recently, a therapeutic effect of propranolol on IH has been demonstrated. Hence, this non-selective  $\beta$ -blocker became the first-line therapy for IH. Over the last years, our understanding of the underlying mechanisms of IH has been improved and possible mechanisms of action of propranolol in IH have postulated. Previous studies revealed that gap junction proteins, the connexins (Cx), might also play a role in the pathogenesis of IH. Therefore, affecting gap junctional intercellular communication is suggested as a novel therapeutic target of propranolol in IH. In this review we summarize the current knowledge of the molecular processes, leading to IH and provide new insights of how Cxs might be involved in the development of these vascular tumors.

**Keywords:** blood vessel, angiogenesis, connexins, infantile hemangioma,  $\beta$ -adrenoceptor, propranolol

The circulatory system is one of the first systems that develops during embryogenesis. For the development of other organs a sufficient supply with oxygen and nutrients is required, which is mediated through blood vessels as a part of the circulatory system. The formation of blood vessels plays a major role in growth and development of organs in the embryo as well as wound healing and organ regeneration in adulthood (Carmeliet, 2005). The establishment of the circulatory system is a two step process. During vasculogenesis endothelial precursor cells form a primitive vascular network. This primitive network expands during angiogenesis by sprouting and growth of pre-existing vessels, thereby forming new blood vessels. As a result a highly organized vascular network is formed, consisting of arteries, veins, and capillaries (Eichmann et al., 2005). In view of the crucial role of angiogenesis in life, it is not surprising that this process underlies accurate regulatory mechanisms, requiring a finely tuned balance between pro- and antiangiogenic factors (Conway et al., 2001). An imbalance of these mediators and thus, a dysregulation of vessel growth are associated with the pathogenesis of many disorders, especially tumorigenesis (Carmeliet and Jain, 2000; Carmeliet, 2003). Folkman (1971) proposed for the first time the critical role of angiogenesis in tumor growth and metastasis. While angiogenesis is essential for the formation of new blood vessels in the embryogenesis, most blood vessels remain quiescent in adulthood. However, in tumorigenesis there is a shift in favor of proangiogenic factors, which induce angiogenesis and as a result the formation of new blood vessels. The underlying mechanisms of how angiogenesis promotes tumor progression and metastasis are not completely understood. In the past, more and more research focused on the influence of

gap junctional coupling during tumorigenesis (Naus et al., 1991; Jamieson et al., 1998; Yamasaki et al., 1999; Saunders et al., 2001; Zhang et al., 2003).

Intercellular communication within the vasculature is essential for vessel formation and the maintenance of normal vascular function. In the vascular system a direct cell-to-cell communication is ensured by transmembrane channels, known as gap junctions. Gap junction channels, linking the cytoplasm of neighboring cells, allow an electrical coupling as well as a metabolic coupling via exchange of metabolites, ions, and other messenger molecules up to a molecular mass of 1 kDa. A gap junction channel consists of two hemichannels (connexons), whereby each neighboring cell contributes one hemichannel. Each connexon is composed of six gap junction proteins, called connexins (Cx) (Dhein et al., 2002). In mammals, at least 21 connexin isoforms have been characterized (Söhl and Willecke, 2004). All Cxs are comprised of four transmembrane-spanning domains, two extracellular domains, and a cytoplasmatic amino- and carboxy-terminal region. In the vascular wall four Cxs have been found: Cx37, Cx40, Cx43, and Cx45 (Hill et al., 2001; Isakson et al., 2006, 2008). In most cases, Cx45 is expressed only by smooth muscle cells (Krüger et al., 2000; Li and Simard, 2001; Rummery et al., 2002). In contrast, Cx37, Cx40, and Cx43 have been detected in both, smooth muscle and endothelial cells, while Cx37 and Cx40 are predominantly expressed by endothelial cells and Cx43 is the major connexin isoform in smooth muscle cells (Little et al., 1995; Gabriels and Paul, 1998; van Kempen and Jongasma, 1999; Severs et al., 2001; Haeffliger et al., 2004). As Cxs are expressed by endothelial cells as well as smooth muscle cells heterocellular coupling may occur between

endothelial cells and smooth muscle cells (myoendothelial junctions). In addition, homocellular coupling between endothelial cells or smooth muscle cells, respectively, does also occur (De Wit, 2004). There is increasing evidence, suggesting a role of vascular gap junctions in the conduction of vasomotor response, the regulation of vascular cell proliferation and migration as well as vascular cell growth, differentiation, and development (Coutinho et al., 2003; Liao et al., 2007; Chadjichristos et al., 2008). However, numerous diseases with vascular abnormalities exhibit an alteration in expression and/or distribution of these Cxs (Laird, 2006; Brisset et al., 2009; Figueroa and Duling, 2009; Johnstone et al., 2009). Previous *in vitro* and *in vivo* studies indicated an influence of gap junctions in tumorigenesis, usually demonstrating a decrease in connexin expression in several neoplastic cells (Czyz, 2008). In addition to vascular abnormalities, mutations in a number of genes, encoding different Cxs, are associated with various further disorders (Kar et al., 2012). For example, mutations in the Cx26 gene (*GJB2*) cause genetic deafness (Martínez et al., 2009). Moreover, mutations in the Cx32 gene (*GJB1*) are involved in the pathogenesis of X-linked Charcot–Marie–Tooth neuropathy (Scherer and Kleopa, 2012), while mutations in the gene encoding Cx43 (*GJA1*) result in oculodentodigital dysplasia (Paznekas et al., 2009). Cxs are also known to play an important role in the heart and previous studies showed several cardiac malformations caused by mutations in the cardiac Cx43 and Cx40 gene (*GJA1* and *GJA5*, respectively) (Delmar and Makita, 2012).

Vascular anomalies are classified into two categories based on their clinico-pathophysiologic behavior and endothelial cell characteristics: vascular malformations and hemangiomas (Mullican and Glowacki, 1982). While vascular malformations describe structural abnormalities in vessels with normal endothelial turnover, hemangiomas represent vascular tumors, arising as a result of rapid growth of endothelial cells (Bruckner and Frieden, 2003). The most common benign vascular tumor during infancy is the infantile hemangioma (IH).

In this review we summarize the current knowledge of the pathogenesis of IHs and suggest a role of Cxs in the development of these vascular tumors.

Most hemangiomas are not present at birth, but appear during the first month of life with an incidence of 5–10% of all infants, and up to 30% of premature babies, especially those with a birth weight less than 1500 g (Drolet et al., 1999, 2008; Greenberger and Bischoff, 2011). Additionally, there is a higher risk in female than in male infants and it is often seen in Caucasian children (Hemangioma Investigator Group et al., 2007). There are several types of hemangioma. The capillary hemangioma is the most common form of hemangioma, characterized by a closely packed aggregation of small capillaries, separated by thin, connective tissue (Mentzel et al., 1994). The capillaries are normal in size and diameter, but high in number. Another type of hemangioma is the cavernous hemangioma, composed of enlarged, dilated blood vessels with blood-filled cavities between them. A compound hemangioma exists when there is a mix of the capillary and cavernous form. IHs may occur throughout the body, including skin, muscle, bone, and internal organs. Mostly, they are found on the skin of the head and neck area (60%). They can also emerge anywhere else on the skin surface

(superficial hemangiomas) like the trunk (25%), limbs (15%) as well as under the skin (deep hemangiomas), and rarely in organs like liver, intestine, lung, or brain (Finn et al., 1983). At first, IHs usually appear as small scratch or bruise red bump, which is why they are also called “strawberry marks”. Depending on the depth of tissue involvement, the hemangiomas display a bright red (outer layers of the skin), crimson, purple, bluish, or normal skin (deep under the skin surface) color. There also exist mixed hemangiomas, combining clinical features of superficial and deep hemangiomas (Chang et al., 2008). The size of IHs may also vary, ranging from a few millimeters to several centimeters in diameter (Drolet et al., 1999). In addition to size there are differences in the shape of hemangiomas. Most tumors are circumscribed and exhibit a round or oval shape, but in some cases they may follow the shape of the affected region. Although, the majority of IHs are solitary and localized, some hemangiomas may be diffuse and segmental, covering a broad range of the cutaneous surface. Hemangiomas, which cannot clearly be classified as localized or segmental hemangiomas, often referred as intermediate hemangiomas (Chiller et al., 2002). The IH displays a characteristic life cycle, consisting of an early proliferation phase and subsequently involution. A few weeks from birth the tumor starts to grow rapidly. The duration of the proliferation phase varies between different hemangioma subtypes, while superficial hemangiomas grow earlier in infancy and faster than deep hemangiomas. However, most growth occurs during the first 4–6 month of life (Hochman et al., 2011). After the proliferation phase, which may last up to 12 month, the tumor undergoes involution and regression. This can take as long as 5–10 years (Phung et al., 2005). In this period the involved skin is blanching and the tumor is shrinking and softening. In 90% of cases IHs regress spontaneously over the years and no specific treatment is required (Margileth and Museles, 1965; Neri et al., 2012). However, hemangiomas may cause disfigurement due to scar tissue or atrophic, wrinkled, telangiectatic skin (Wirth and Lowitt, 1998). In some cases, IHs lead to serious complications, affecting breathing, vision, eating, or hearing, some become life-threatening and require immediate treatment. The management of hemangiomas is non-uniform due to their heterogeneity and depends on several factors like the location and size of the tumor, the depth of the affected region, the age of the patient as well as the occurring complications (Maguiness and Frieden, 2012). Therefore, the treatment of IHs almost follows on a case-by-case basis. Besides surgical management like excision of the hemangioma or laser treatment, children often received a medical therapy (Adams, 2001). Since 1960s corticosteroids have been the standard treatment for IH (Cohen and Wang, 1972). Some infants with life-threatening hemangiomas failed to respond to corticosteroids. In that case the administration of interferon-alpha seemed to be successful in treating of hemangiomas (Ricketts et al., 1994; Chang et al., 1997; Tamayo et al., 1997; Azzopardi and Wright, 2012). Both, corticosteroid and interferon-alpha management are associated with a number of side effects and therefore, the interest in alternate therapies has increased recently (Barlow et al., 1998; Boon et al., 1999). In the last years, advances in the treatment of IHs have occurred. As part of this, a new therapeutic strategy has been added, using propranolol. The therapeutic effect of propranolol was first described by

Léauté-Labrèze et al. (2008). They treated a child, suffering from a capillary hemangioma, with steroids. Nevertheless, the hemangioma still grew and simultaneously an obstructive hypertrophic cardiomyopathy developed. Therefore, they administered propranolol and observed an involution of the hemangioma. Numerous other studies followed, confirming this inhibitory effect of propranolol on the growth of hemangiomas and thus, this non-selective  $\beta$ -blocker became the first-line therapy for IH (Holmes et al., 2011; Starkey and Shahidullah, 2011). Until today, the effect of propranolol on IH is not completely understood, but with improving knowledge of the pathogenesis of IH several possible mechanisms of action of the  $\beta$ -blocker arised (Storch and Hoeger, 2010). It is believed that propranolol leads to (1) suppression of angiogenesis (2) vasoconstriction of the capillaries, and (3) induction of apoptosis.

Propranolol is a non-selective  $\beta$ -blocker, inhibiting  $\beta_1$ - and  $\beta_2$ -adrenoceptors, and has no partial agonistic effect. In the vasculature  $\beta_2$ -adrenoceptor is the most abundant  $\beta$ -adrenoceptor, which is expressed by a number of cell types, including endothelial cells (Guimarães and Moura, 2001; Iaccarino et al., 2005).  $\beta$ -adrenoceptors are a class of G<sub>s</sub>-protein-coupled receptors. Binding of catecholamines on the receptors results in stimulation of the sympathetic nervous system, which plays a major role in regulation of the vascular system. Once the  $\beta$ -adrenoceptors are activated by catecholamines, a series of signaling pathways are initiated. This includes the stimulation of the adenylyl cyclase, which converts adenosine triphosphate (ATP) into cyclic adenosine monophosphate (cAMP). The second messenger cAMP in turn activates the cAMP-dependent protein kinase A (PKA), which phosphorylates numerous intracellular target proteins, involved in the control of cell proliferation, differentiation, and migration. A recent study revealed the important role of  $\beta$ -adrenoceptor stimulation in endothelial cells as a major contributor to the initiation of IH (Mayer et al., 2012). During the characteristic proliferating phase the hemangioma is composed of a highly packed mass of rapidly dividing endothelial cells with increased mitotic rates. Furthermore, pericytes around endothelial cells, and several cell types like mast cells, and myeloid cells in the interstitium of the tumor have been identified. At the involuted phase tumor growth has stopped and an increase in the number of mast cells has been observed. On cellular level these two phases can be separated by specific markers. In the proliferating hemangioma there is an increase in the expression of proangiogenic factors like vascular endothelial growth factor (VEGF) as well as basic fibroblast growth factor (bFGF), platelet-derived growth factor (PDGF), type IV collagenase, insulin-like growth factor 2 (IGF-2), proliferating cell nuclear antigen (PCNA), the integrins  $\alpha 5\beta 3$  as well as  $\alpha 5\beta 1$ , hypoxia-inducible factor (HIF)-1 $\alpha$ , and the matrix metalloproteinases (MMP)-2 and MMP-9 (Takahashi et al., 1994; Chang et al., 1999; Ritter et al., 2002; Kleinman et al., 2007; Zhong et al., 2009). In contrast, the involution phase is characterized by a reduced expression of VEGF, bFGF, and IGF-2 as well as an increased expression of the tissue inhibitor of metalloproteinases (TIMP)-1 (Takahashi et al., 1994; Chang et al., 1999; Przewratil et al., 2009, 2010; Zhong et al., 2009). Furthermore, there is an increase in apoptosis, inducing the regression of hemangiomas (Razon et al., 1998).

Vascular endothelial growth factor is a major regulator of vasculogenesis and angiogenesis and was first described as a vascular permeability factor released by tumor cells (Senger et al., 1983). With regard to IH, VEGF seems to play a key role in the pathogenesis of this vascular tumor. VEGF accelerates tumor growth via different mechanisms, comprising stimulation of proliferation as well as migration, increased vascular permeability, and inhibition of apoptosis (Harris et al., 2002). It is described that catecholamine-mediated  $\beta$ -adrenoceptor stimulation induces a release and enhanced expression of VEGF in numerous cell types like cancerous cells (Greenberger and Bischoff, 2011; Ji et al., 2013). Furthermore, it has been shown that this is under the control of the cAMP/PKA pathway, activating Src tyrosine kinases and consequently, the extracellular signal-regulated kinase (ERK)/mitogen-activated protein kinase (MAPK) signaling cascade, which in fact results in an enhanced VEGF expression (Eliceiri et al., 1999; Pagès et al., 2000). VEGF exerts its effect, especially via a paracrine pathway, by binding to its tyrosine kinase receptor, mostly expressed on endothelial cells. There are several lines of evidence, suggesting a predominant role of the binding of VEGF-A to VEGFR-2 to stimulate angiogenesis (Kieran et al., 2012). The ligand–receptor-interaction again triggers a cascade of signals, including the ERK/MAPK signaling pathway, which results in the phosphorylation of nuclear transcriptional factors and induction of the expression of several genes, responsible for the proliferation of vascular endothelial cells (D'Angelo et al., 1997; Storch and Hoeger, 2010). Therefore, the proangiogenic phenotype is sustained. In a similar fashion, the expression of bFGF is modulated by  $\beta$ -adrenoceptor. Thus, a blockade of the  $\beta$ -adrenoceptor-mediated up-regulation of VEGF and bFGF and hence, an inhibition of angiogenesis by propranolol seem to be important in the management of IH (Ji et al., 2013). Beside  $\beta$ -adrenoceptor stimulation, VEGF expression is also increased by hypoxia, a powerful inducer of vasculogenesis and angiogenesis (Sakurai and Kudo, 2011). Like many other tumors IH develops a hypoxic microenvironment, which becomes obvious by increased expression and stabilization of HIF-1 $\alpha$  during the proliferation phase of the tumor. Moreover, previous studies demonstrated a link between  $\beta$ -adrenoceptors and HIF-1 $\alpha$  in several cancer cells, indicating an up-regulation of HIF-1 $\alpha$  by catecholamine-mediated  $\beta$ -adrenoceptor stimulation also under normoxic conditions (Chim et al., 2012). Recently, it has been shown that the Src tyrosine kinases are involved in the hypoxia-induced VEGF expression by transactivating the epidermal growth factor receptor (EGFR) tyrosine kinase, which in turn stimulates the Akt and ERK1/2 pathways (Hu et al., 2010). These data suggest a role for propranolol in IH via suppression of the HIF-1 $\alpha$ -mediated VEGF expression. Collectively, one possible mechanism of action of propranolol on IH might be the reduction of the expression of proangiogenic factors like VEGF and consequently, inhibition of angiogenesis. In relation to its antiangiogenic effect in IH, propranolol could also act via inhibition of the expression of MMPs, the most prominent proteinase family associated with tumorigenesis. The involvement of MMPs in IH is supported by the finding of elevated concentrations of MMP-2 and MMP-9 in the proliferation phase.

Furthermore, it is well described that catecholamine-mediated stimulation of  $\beta$ -adrenoceptors leads to an increased expression of MMP-2 and MMP-9 (Storch and Hoeger, 2010). Based on the role of MMP-2 and MMP-9 in the migration of endothelial cells and tubulogenesis, a reduction of the expression of these proteinases by propranolol also indicates an antiangiogenic effect of the  $\beta$ -blocker. This is in accordance with the growth arrest and shrinking of the tumor after treatment with propranolol.

Another hypothesized effect of propranolol in IH is the induction of vasoconstriction. In this regard, VEGF again seems to be crucial. VEGF is able to increase vascular permeability and mediates vasodilatation, both coupled to the formation of nitric oxide (NO), and therefore contributes to tumor growth. In their study Parenti et al. (1998) revealed the intracellular pathway of the VEGF/NO-induced proliferation of endothelial cells. They demonstrated an increase in cytosolic calcium [apparently by activation of phospholipase C  $\gamma$  (PLC  $\gamma$ )] upon VEGF stimulation, activating the calcium/calmodulin-dependent endothelial nitric oxide synthase (iNOS), which causes the production and release of NO. NO in turn stimulates the guanylyl cyclase/cyclic guanosine monophosphate (cGMP)/protein kinase G (PKG) cascade, resulting in vasodilatation of endothelial cells. Furthermore, cGMP activates the ERK/MAPK signaling pathway, leading to cell proliferation. Catecholamines are also able to mediate vasodilatation by stimulation of  $\beta_2$ -adrenoceptors (Storch and Hoeger, 2010). Accordingly, another possible mechanism of how propranolol affects IH is the prevention of relaxation of capillary endothelial cells, consequently leading to vasoconstriction. The link between  $\beta$ -adrenoceptors, VEGF expression, and NO formation points out that there is a complex interaction of multiple signaling cascades, causing vasodilatation. The vasoconstrictive effect of propranolol on hemangiomas is emphasized by the blanching and softening of the tumor after propranolol application.

The third mechanism of action of propranolol in IH represents the induction of apoptosis. Previous studies demonstrated a role of  $\beta$ -adrenoceptor signaling in cell survival, implicating the  $\beta$ -adrenoceptor-induced transactivation of EGFR via the Src tyrosine kinase as a critical step. This transactivation stimulates a number of antiapoptotic signaling cascades, including the MAPK cascade, the phosphatidylinositol 3-kinase (PI3K)/Akt pathway as well as the nuclear factor  $\kappa$ B (NF $\kappa$ B) cascade (Zhang et al., 2009). As a result, cell proliferation is stimulated, expression of antiapoptotic proteins is induced, and the caspase cascade is inhibited. Hence, propranolol could induce apoptosis by preventing the  $\beta$ -adrenoceptor-mediated cell survival.

Among the above mentioned mechanisms, the success of propranolol therapy in IH might also be attributable in affecting intercellular communication. In the past, it has been described that a reduction in intercellular communication is associated with increased susceptibility of cells to neoplastic transformation (Geletu et al., 2012). As gap junction channels conduct growth-regulating signals from cell-to-cell, an impaired gap junctional coupling results in uncontrolled cell growth and therefore, leading to tumor promotion. Furthermore, studies, investigating the involvement of gap junction intercellular communication (GJIC) in carcinogenesis, confirmed a major role of connexin expression

and localization in the control of cell growth (Yamasaki et al., 1999). Many reports show a down-regulation of connexin expression in numerous neoplastic cell lines and primary tumors (Czyz, 2008). Interestingly, a previous study revealed a role of Cxs in the pathogenesis of hemangiomas (Simon and McWhorter, 2002). They found that mice, lacking both Cx37 and Cx40 die perinatally with abnormalities in the vascular system. These vascular anomalies include hemorrhages in skin, testis, intestine, stomach, and lung, accompanied by dilated blood vessels and congestion in the affected tissue. Furthermore, they observed abnormal vascular channels, coalescing into a cavernous blood pool. These vascular abnormalities were only detected when both Cx37 and Cx40 are absent. In contrast, mice lacking either Cx37 or Cx40 are viable and do not exhibit such severe vascular phenotypes. Thus, the authors suggested an overlapping function of both Cxs in the development and maintenance of the vasculature in mouse. In a follow-up study the authors could confirm the dependency of Cx37 and Cx40 on each other in the vascular endothelium, demonstrating that specific ablation of either endothelial Cx37 or Cx40 results not only in an elimination of the target connexin, but also in a substantial decrease of the non-ablated connexin (Simon and McWhorter, 2003). Moreover, they revealed a reduced interendothelial dye-transfer in aorta of mice, lacking Cx37 or Cx40, respectively. The effect of Cx40 ablation on dye-transfer was more pronounced than ablation of Cx37 and was age-dependent. Elimination of both Cxs in embryonic aortas completely abolished dye-transfer in these mice. Thus, expression of Cx37 and Cx40 could be crucial for effective endothelial coupling by forming heteromeric gap-junction channels, which in turn are required for normal development and functional maintenance of the mouse vascular endothelium. This is in accordance with other reports, indicating a coexpression of Cx37 and Cx40 in endothelial cells (Yeh et al., 1998; Ko et al., 1999; Simon and McWhorter, 2002). Other studies also demonstrated the important role of Cx37 and Cx40 in the vascular system, implicating a decrease in intercellular communication and consequently, an impairment of angiogenesis after knock-down of these Cxs (Gärtner et al., 2012). A lot of research has been carried out to elucidate the underlying mechanisms of the regulation of connexin expression, most of them focused on Cx43. The  $\beta$ -adrenoceptor-mediated signaling pathway has been identified as a major modulator of the Cx43 expression. It has been postulated that  $\beta$ -adrenoceptor stimulation leads to a PKA-dependent activation of the three MAPK p38, c-Jun N-terminal kinase (JNK), and ERK1/2, resulting in a translocation of transcriptional factors like activator protein 1 (AP1) and cAMP response element-binding protein (CREB) into the nucleus, which finally bind to the Cx43 promoter and thus, inducing connexin expression (Salameh et al., 2009). Furthermore,  $\beta$ -adrenoceptor stimulation induces elevated concentration of intracellular calcium, which in turn activates the calcineurin pathway. The protein phosphatase calcineurin dephosphorylates the transcriptional factor nuclear factor of activated T cells (NFAT), which also translocates into the nucleus and induce the expression of Cx43 (Salameh et al., 2009). Although, less data are available of the regulation of Cx37 and Cx40, these observations indicate an involvement of  $\beta$ -adrenoceptor signaling in the

regulation of their expression. For example, this is supported by the study of Dupays et al. (2003), detecting multiple binding sites for AP 1 in the Cx40 gene and hence, suggesting an important role of this transcription factor also in the expression of Cx40. In this regard, a further mechanism of action of propranolol in IH might affect connexin expression. Surprisingly, a recent study demonstrated an increased Cx43 protein expression in rat cardiomyocytes after metoprolol application (Salameh et al., 2010). Since these findings do not fit into the classical scheme of action of the  $\beta_1$ -selective adrenoceptor blocker, it is postulated that metoprolol exerts this Cx43-elevating effect *via* a  $\beta_1$ -adrenoceptor independent mechanism, possibly by inhibition of Cx43 degradation. This so-called ancillary effect of  $\beta$ -blockers is well known and could also be observed for propranolol. Marano et al. (2002) revealed an antihypertrophic effect of propranolol, presumably due to its membrane-stabilizing effect and independently from its  $\beta$ -adrenergic blocking activity. Hence, propranolol may increase connexin expression independent of  $\beta$ -adrenoceptor blockade. Beside the connexin expression, GJIC is regulated by posttranslational modifications of Cxs, especially phosphorylation, ensuring a correct assembly and establishment of a complete functional gap junction channel. The carboxy-terminal region of Cxs contains consensus sequences, which can be phosphorylated by several protein kinases. Depending on the protein kinase, phosphorylating the connexin, and the phosphorylated amino residue (serine, threonine, or tyrosine) of the connexin, an increase or decrease in GJIC may occur (Dhein et al., 2002). Previous data indicated that Src tyrosine kinase is able to phosphorylate Cx43 on tyrosine residue (tyr) 247 and tyr265, resulting in reduced GJIC. In addition, Src initiates multiple signaling cascades, activating a number of protein kinases, which in turn phosphorylate Cx43 (Pahuja et al., 2007). On the one hand, Src activates the Ras/Raf/MEK/MAPK pathway. MAPK are serine/threonine-selective protein kinases, which can also phosphorylate Cx43 on serine residues and block GJIC (Warn-Cramer et al., 1996). On the other hand, Src stimulates PLC, leading to an increase in cytosolic calcium levels and activation of the calcium-dependent protein kinase C (PKC). Additionally, Src may phosphorylates PKC and thus, directly activates this protein kinase. PKC, a serine/threonine protein kinase, is again able to phosphorylate Cx43 on serine residues, which mostly correlates with a reduction in GJIC (Pahuja et al., 2007). As described above, Src-mediated signaling cascades play a pivotal role in the pathogenesis of IH *via* inducing the expression of angiogenic factors, causing vasodilatation, and inhibiting of apoptosis. Up to now, the suggested explanations for the therapeutic effect of propranolol, leading to regression of IH, focused on the prevention of these events. However, it is also conceivable that the blockade of the Src-mediated pathways by propranolol suppress connexin phosphorylation, leading to enhanced GJIC. Recently, a study of Johnstone et al. (2012) revealed a MAPK-mediated phosphorylation of Cx43 at the specific serine residues of its C-terminus, promoting vascular smooth muscle cell (VSMC) proliferation, independently of GJIC. It has been shown that in response to PDGF Cx43 become phosphorylated by MAPK, followed by an interaction of the phosphorylated Cx43 with the cell cycle regulator cyclin E and its associated kinase cyclin-dependent

kinase (CDK)-2 at the cell membrane. Subsequently, the complex of phosphorylated Cx43, cyclin E and CDK-2 internalizes and activates downstream targets of cyclin E and CDK-2, like retinoblastoma (Rb) protein, which in turn stimulates VSMC proliferation. They could also observed that this MAPK-mediated Cx43 phosphorylation is crucial in regulation of neointima formation *in vivo*. Due to the fact that PDGF is elevated in the proliferation phase of IH, the PDGF-induced proliferation of VSMC through mechanisms, involving MAPK-mediated Cx43 phosphorylation and complex formation of phosphorylated Cx43 with cyclin E and CDK-2, could also play an important role in the pathogenesis of IH. As described above,  $\beta$ -adrenoceptor stimulation results in activation of MAPK, thereby enhancing the phosphorylation of Cx43, which could be suppressed by propranolol (Salameh et al., 2009). Furthermore, Ji et al. (2013) demonstrated that  $\beta$ -adrenoceptor antagonists interact with cell cycle regulators, for example phospho-Rb, and thus, inhibit cell proliferation. Therefore, it could be suggested that propranolol prevent the  $\beta$ -adrenoceptor-mediated activation of the MAPK cascade and thus, the phosphorylation of Cx43. Hence, no interaction of Cx43 with cell cycle regulators occur and promotion of cell proliferation is avoided, which finally could lead to regression of the IH.

Until today, the role of Cxs in IH is not fully understood and further experiments are required to clarify the involvement of Cxs in the development of IH. As described by Gärtner et al. (2012) knock-down of Cx37, Cx40, and Cx43, respectively, *via* siRNA interference in 3D Matrigel culture of human umbilical vein endothelial cells (HUVEC) resulted in an impairment of capillary network formation. It would be interesting to determine the capillary formation in an angiogenesis assay of endothelial cells of mice, lacking both Cx37 and Cx40, which showed hemorrhages in different organs (Simon and McWorter, 2002). Based on the findings of Simon and McWorter (2003) that elimination of Cx37 and Cx40 lead to a complete loss of endothelial dye-transfer in embryonic aortas of mice, Patch clamp analysis could provide further insights into the functionality of gap junction channels in the aortic wall of these mice by investigation of the electrical gap junctional coupling. In addition, expression and activity of key regulators of the connexin expression, for example Src kinase, MAPK, transcription factors, as well as downstream targets of Cxs, involved in cell cycle regulation and cell proliferation, should be studied in hemangioma tissue of these mice. Among animal models, an important starting point to reveal a role of Cxs in IH might be to determine the expression and localization of these gap junction proteins in biopsies of infants with IH. In a next step, the above mentioned molecular pathways, possibly involved in IH, could be examined in human hemangioma tissue.

In summary, there are some explanations for the therapeutic effect of propranolol on IH, including the reduction of the expression of angiogenic factors, stimulation of vasoconstriction, and triggering of apoptosis. Although, the underlying mechanisms are not completely understood, there is evidence of a pivotal role of  $\beta$ -adrenoceptor stimulation, leading to the activation of a number of signaling pathways. Furthermore, these pathways are also involved in the regulation of Cxs. In this regard, another mechanism of

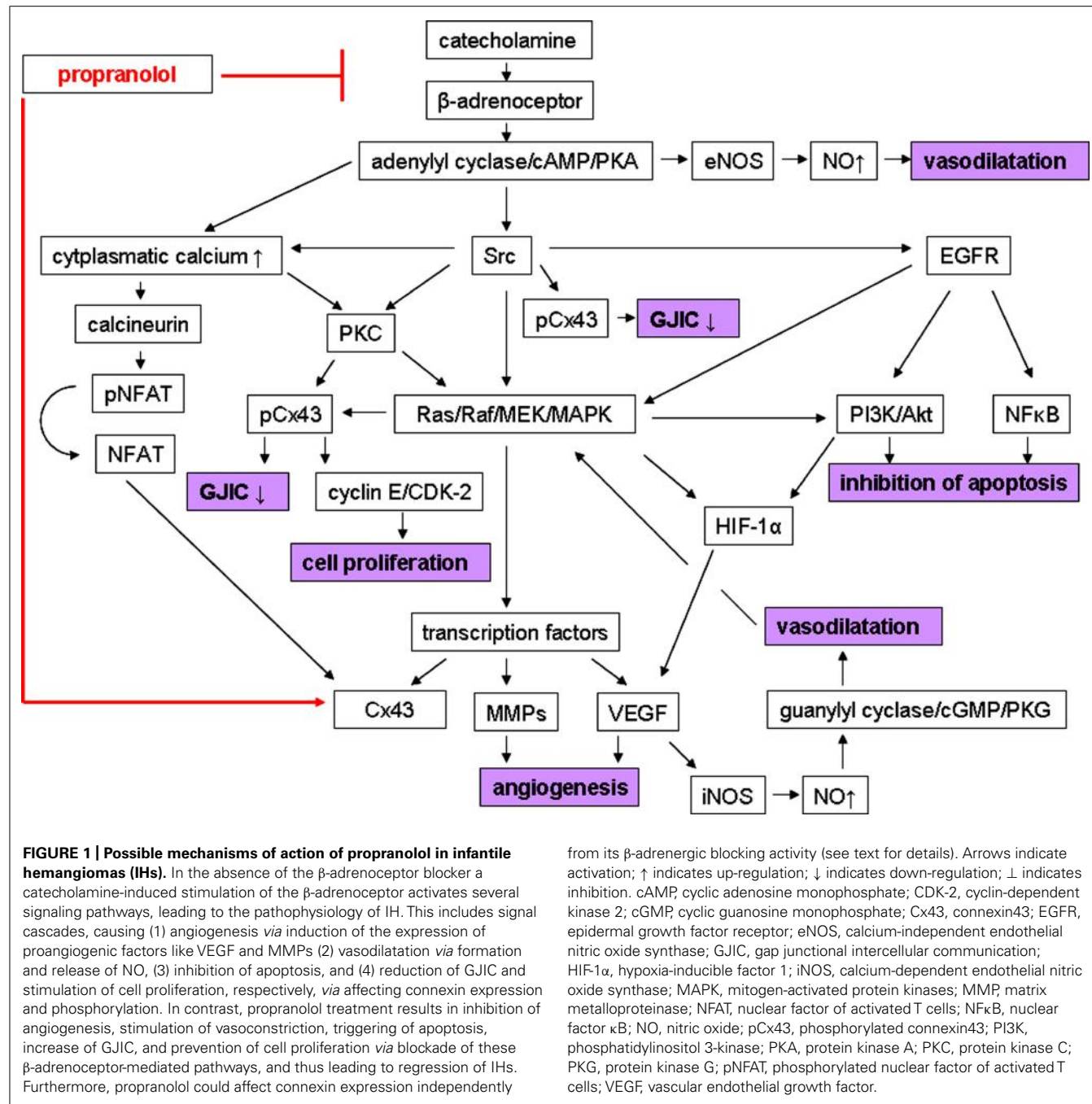


**FIGURE 1 | Possible mechanisms of action of propranolol in infantile hemangiomas (IHs).** In the absence of the β-adrenoceptor blocker a catecholamine-induced stimulation of the β-adrenoceptor activates several signaling pathways, leading to the pathophysiology of IH. This includes signal cascades, causing (1) angiogenesis *via* induction of the expression of proangiogenic factors like VEGF and MMPs (2) vasodilatation *via* formation and release of NO, (3) inhibition of apoptosis, and (4) reduction of GJIC and stimulation of cell proliferation, respectively, *via* affecting connexin expression and phosphorylation. In contrast, propranolol treatment results in inhibition of angiogenesis, stimulation of vasoconstriction, triggering of apoptosis, increase of GJIC, and prevention of cell proliferation *via* blockade of these β-adrenoceptor-mediated pathways, and thus leading to regression of IHs. Furthermore, propranolol could affect connexin expression independently

from its β-adrenergic blocking activity (see text for details). Arrows indicate activation; ↑ indicates up-regulation; ↓ indicates down-regulation; ⊥ indicates inhibition. cAMP, cyclic adenosine monophosphate; CDK-2, cyclin-dependent kinase 2; cGMP, cyclic guanosine monophosphate; Cx43, connexin43; EGFR, epidermal growth factor receptor; eNOS, calcium-independent endothelial nitric oxide synthase; GJIC, gap junctional intercellular communication; HIF-1α, hypoxia-inducible factor 1; iNOS, calcium-dependent endothelial nitric oxide synthase; MAPK, mitogen-activated protein kinases; MMP, matrix metalloproteinase; NFAT, nuclear factor of activated T cells; NFκB, nuclear factor κB; NO, nitric oxide; pCx43, phosphorylated connexin43; PI3K, phosphatidylinositol 3-kinase; PKA, protein kinase A; PKC, protein kinase C; PKG, protein kinase G; pNFAT, phosphorylated nuclear factor of activated T cells; VEGF, vascular endothelial growth factor.

action of propranolol has been postulated *via* enhancement of GJIC and inhibition of cell proliferation by affecting connexin expression and phosphorylation. All these possible mechanisms of action of propranolol in IH are illustrated in Figure 1.

## CONCLUSION

Over the last years, knowledge of the molecular mechanisms of IH has improved, clarifying that several signaling cascades are involved in the progression of these vascular tumors and that there is a cross-talk between them. Since propranolol has been

identified as a new therapeutic option in treating IH, various studies focused on the underlying mechanisms of how propranolol affects hemangiomas. Until today, propranolol has become the first-line therapy in IH and some possible mechanisms of action of propranolol in IH have been postulated, implicating Cxs as a novel therapeutic target of propranolol in IH. The challenge for the future will be to elucidate the cellular and molecular basis and pathways of IH in greater detail to completely understand the mechanism of action of propranolol and finally, to optimize therapy for infants with IH.

## REFERENCES

- Adams, D. M. (2001). The nonsurgical management of vascular lesions. *Facial Plast. Surg. Clin. North Am.* 9, 601–608.
- Azzopardi, S., and Wright, T. C. (2012). Novel strategies for managing infantile hemangiomas: a review. *Ann. Plast. Surg.* 68, 226–228.
- Barlow, C. F., Priebe, C. J., Mulliken, J. B., Barnes, P. D., MacDonald, D., Folkman, J., et al. (1998). Spastic diplegia as a complication of interferon Alfa-2a treatment of hemangiomas of infancy. *J. Pediatr.* 132, 527–530.
- Boon, L. M., MacDonald, D. M., and Mulliken, J. B. (1999). Complications of systemic corticosteroid therapy for problematic hemangioma. *Plast. Reconstr. Surg.* 104, 1616–1623.
- Brisset, A. C., Isakson, B. E., and Kwak, B. R. (2009). Connexins in vascular physiology and pathology. *Antioxid. Redox Signal.* 11, 267–282.
- Bruckner, A. L., and Frieden, I. J. (2003). Hemangiomas of infancy. *J. Am. Acad. Dermatol.* 48, 477–493.
- Carmeliet, P. (2003). Angiogenesis in health and disease. *Nat. Med.* 9, 653–660.
- Carmeliet, P. (2005). Angiogenesis in life, disease and medicine. *Nature* 438, 932–936.
- Carmeliet, P., and Jain, R. K. (2000). Angiogenesis in cancer and other diseases. *Nature* 407, 249–257.
- Chadjichristos, C. E., Morel, S., Derouette, J. P., Sutter, E., Roth, I., Brisset, A. C., et al. (2008). Targeting connexin 43 prevents platelet-derived growth factor-BB-induced phenotypic change in porcine coronary artery smooth muscle cells. *Circ. Res.* 102, 653–660.
- Chang, E., Boyd, A., Nelson, C. C., Crowley, D., Law, T., Keough, K. M., et al. (1997). Successful treatment of infantile hemangiomas with interferon-alpha-2b. *J. Pediatr. Hematol. Oncol.* 19, 237–244.
- Chang, J., Most, D., Bresnick, S., Mehrara, B., Steinbrech, D. S., Reinisch, J., et al. (1999). Proliferative hemangiomas: analysis of cytokine gene expression and angiogenesis. *Plast. Reconstr. Surg.* 103, 1–9.
- Chang, L. C., Haggstrom, A. N., Drolet, B. A., Baselga, E., Chamlin, S. L., Garzon, M. C., et al. (2008). Growth characteristics of infantile hemangiomas: implications for management. *Pediatrics* 122, 360–367.
- Chiller, K. G., Passaro, D., and Frieden, I. J. (2002). Hemangiomas of infancy: clinical characteristics, morphologic subtypes, and their relationship to race, ethnicity, and sex. *Arch. Dermatol.* 138, 1567–1576.
- Chim, H., Armijo, B. S., Miller, E., Gliniak, C., Serret, M. A., and Gosain, A. K. (2012). Propranolol induces regression of hemangioma cells through HIF-1 $\alpha$ -mediated inhibition of VEGF-A. *Ann. Surg.* 256, 146–156.
- Cohen, S. R., and Wang, C. I. (1972). Steroid treatment of hemangioma of the head and neck in children. *Ann. Otol. Rhinol. Laryngol.* 81, 584–590.
- Conway, E. M., Collen, D., and Carmeliet, P. (2001). Molecular mechanisms of blood vessel growth. *Cardiovasc. Res.* 49, 507–521.
- Coutinho, P., Qiu, C., Frank, S., Tammer, K., and Becker, D. (2003). Dynamic changes in connexin expression correlate with key events in the wound healing process. *Cell Biol. Int.* 27, 525–541.
- Czyz, J. (2008). The stage-specific function of gap junctions during tumourigenesis. *Cell. Mol. Biol. Lett.* 13, 92–102.
- D'Angelo, G., Lee, H., and Weiner, R. I. (1997). cAMP-dependent protein kinase inhibits the mitogenic action of vascular endothelial growth factor and fibroblast growth factor in capillary endothelial cells by blocking Raf activation. *J. Cell. Biochem.* 67, 353–366.
- Delmar, M., and Makita, N. (2012). Cardiac connexins, mutations and arrhythmias. *Curr. Opin. Cardiol.* 27, 236–241.
- De Wit, C. (2004). Connexins pave the way for vascular communication. *News Physiol. Sci.* 19, 148–153.
- Dhein, S., Polontchouk, L., Salameh, A., and Haefliger, J. A. (2002). Pharmacological modulation and differential regulation of the cardiac gap junction proteins connexin 43 and connexin 40. *Biol. Cell* 94, 409–422.
- Drolet, B. A., Esterly, N. B., and Frieden, I. J. (1999). Hemangiomas in children. *N. Engl. J. Med.* 341, 173–181.
- Drolet, B. A., Swanson, E. A., Frieden, I. J., and Hemangioma Investigator Group. (2008). Infantile hemangiomas: an emerging health issue linked to an increased rate of low birth weight infants. *J. Pediatr.* 153, 712–715.
- Dupays, L., Mazurais, D., Rücker-Martin, C., Calmels, T., Bernot, D., Cronier, L., et al. (2003). Genomic organization and alternative transcripts of the human Connexin40 gene. *Gene* 305, 79–90.
- Eichmann, A., Yuan, L., Moyon, D., Lenoble, F., Pardanaud, L., and Breant, C. (2005). Vascular development from precursor cells to branched arterial and venous networks. *Int. J. Dev. Biol.* 49, 259–267.
- Eliceiri, B. P., Paul, R., Schwartzberg, P. L., Hood, J. D., Leng, J., and Cheresh, D. A. (1999). Selective requirement for Src kinases during VEGF-induced angiogenesis and vascular permeability. *Mol. Cell* 4, 915–924.
- Figueroa, X. F., and Duling, B. R. (2009). Gap junctions in the control of vascular function. *Antioxid. Redox Signal.* 11, 251–266.
- Finn, M. C., Glowacki, J., and Mulliken, J. B. (1983). Congenital vascular lesions: clinical application of a new classification. *J. Pediatr. Surg.* 18, 894–900.
- Folkman, J. (1971). Tumor angiogenesis: therapeutic implications. *N. Engl. J. Med.* 285, 1182–1186.
- Gabriels, J. E., and Paul, D. L. (1998). Connexin43 is highly localized to sites of disturbed flow in rat aortic endothelium but connexin37 and connexin40 are more uniformly distributed. *Circ. Res.* 83, 636–643.
- Gärtner, C., Ziegelhöffer, B., Kostelka, M., Stepan, H., Mohr, F. W., and Dhein, S. (2012). Knock-down of endothelial connexins impairs angiogenesis. *Pharmacol. Res.* 65, 347–357.
- Geletu, M., Trotman-Grant, A., and Raptis, L. (2012). Mind the gap; regulation of gap junctional, intercellular communication by the SRC oncogene product and its effectors. *Anticancer Res.* 32, 4245–4250.
- Greenberger, S., and Bischoff, J. (2011). Infantile hemangioma—mechanism(s) of drug action on a vascular tumor. *Cold Spring Harb. Perspect. Med.* 1, a006460.
- Guimarães, S., and Moura, D. (2001). Vascular adrenoceptors: an update. *Pharmacol. Rev.* 53, 319–356.
- Haefliger, J. A., Nicod, P., and Meda, P. (2004). Contribution of connexins to the function of the vascular wall. *Cardiovasc. Res.* 62, 345–356.
- Harris, S. R., Schoeffner, D. J., Yoshiji, H., and Thorgeirsson, U. P. (2002). Tumor growth enhancing effects of vascular endothelial growth factor are associated with increased nitric oxide synthase activity and inhibition of apoptosis in human breast carcinoma xenografts. *Cancer Lett.* 179, 95–101.
- Hemangioma Investigator Group, Haggstrom, A. N., Drolet, B. A., Baselga, E., Chamlin, S. L., Garzon, M. C., et al. (2007). Prospective study of infantile hemangiomas: demographic, prenatal, and perinatal characteristics. *J. Pediatr.* 150, 291–294.
- Hill, C. E., Phillipps, J. K., and Sandow, S. L. (2001). Heterogeneous control of blood flow amongst different vascular beds. *Med. Res. Rev.* 21, 1–60.
- Hochman, M., Adams, D. M., and Reeves, T. D. (2011). Current knowledge and management of vascular anomalies: infantile hemangiomas. *Arch. Facial Plast. Surg.* 13, 145–151.
- Holmes, W. J., Mishra, A., Gorst, C., and Liew, S. H. (2011). Propranolol as first-line treatment for rapidly proliferating infantile haemangiomas. *J. Plast. Reconstr. Aesthet. Surg.* 64, 445–451.
- Hu, H. T., Ma, Q. Y., Zhang, D., Shen, S. G., Han, L., Ma, Y. D., et al. (2010). HIF-1 $\alpha$  links beta-adrenoceptor agonists and pancreatic cancer cells under normoxic condition. *Acta Pharmacol. Sin.* 31, 102–110.
- Iaccarino, G., Ciccarelli, M., Sorrento, D., Galasso, G., Campanile, A., Santulli, G., et al. (2005). Ischemic neoangiogenesis enhanced by beta2-adrenergic receptor overexpression: a novel role for the endothelial adrenergic system. *Circ. Res.* 97, 1182–1189.
- Isakson, B. E., Best, A. K., and Duling, B. R. (2008). Incidence of protein on actin bridges between endothelium and smooth muscle in arterioles demonstrates heterogeneous connexin expression and phosphorylation. *Am. J. Physiol. Heart Circ. Physiol.* 294, H2898–H2904.
- Isakson, B. E., Damon, D. N., Day, K. H., Liao, Y., and Duling, B. R. (2006). Connexin40 and connexin43 in mouse aortic endothelium: evidence for coordinated regulation. *Am. J. Physiol. Heart Circ. Physiol.* 290, H1199–H1205.
- Jamieson, S., Going, J. J., D'Arcy, R., and George, W. D. (1998). Expression of gap junction proteins connexin 26 and connexin 43 in normal human breast and in breast tumours. *J. Pathol.* 184, 37–43.
- Ji, Y., Chen, S., Li, K., Xiao, X., Zheng, S., and Xu, T. (2013). The role of beta-adrenergic receptor signaling in the proliferation of hemangioma-derived endothelial cells. *Cell Div.* 8, 1.
- Johnstone, S., Isakson, B., and Locke, D. (2009). Biological and biophysical properties of vascular connexin channels. *Int. Rev. Cell Mol. Biol.* 278, 69–118.
- Johnstone, S. R., Kroncke, B. M., Straub, A. C., Best, A. K., Dunn, C. A., Mitchell, L. A., et al. (2012). MAPK phosphorylation of connexin 43 promotes binding of cyclin E and smooth muscle cell proliferation. *Circ. Res.* 111, 201–211.
- Kar, R., Batra, N., Riquelme, M. A., and Jiang, J. X. (2012). Biological role of

- connexin intercellular channels and hemichannels. *Arch. Biochem. Biophys.* 524, 2–15.
- Kieran, M. W., Kalluri, R., and Cho, Y. J. (2012). The VEGF pathway in cancer and disease: responses, resistance, and the path forward. *Cold Spring Harb. Perspect. Med.* 2, a006593.
- Kleinman, M. E., Greives, M. R., Churgin, S. S., Blechman, K. M., Chang, E. I., Ceradini, D. J., et al. (2007). Hypoxia-induced mediators of stem/progenitor cell trafficking are increased in children with hemangioma. *Arterioscler. Thromb. Vasc. Biol.* 27, 2664–2670.
- Ko, Y. S., Yeh, H. I., Rothery, S., Dupont, E., Coppen, S. R., and Severs, N. J. (1999). Connexin make-up of endothelial gap junctions in the rat pulmonary artery as revealed by immunofluorescence and triple-label immunogold electron microscopy. *J. Histochem. Cytochem.* 47, 683–692.
- Krüger, O., Plum, A., Kim, J. S., Winterhager, E., Maxeiner, S., Halasz, G., et al. (2000). Defective vascular development in connexin 45-deficient mice. *Development* 127, 4179–4193.
- Laird, D. W. (2006). Life cycle of connexins in health and disease. *Biochem. J.* 394, 527–543.
- Léauté-Labrèze, C., Dumas de la Roque, E., Hubiche, T., Boralevi, F., Thambo, J. B., and Taïeb, A. (2008). Propranolol for severe hemangiomas of infancy. *N. Engl. J. Med.* 358, 2649–2651.
- Li, X., and Simard, J. M. (2001). Connexin45 gap junction channels in rat cerebral vascular smooth muscle cells. *Am. J. Physiol. Heart Circ. Physiol.* 281, H1890–H1898.
- Liao, Y., Regan, C. P., Manabe, I., Owens, G. K., Day, K. H., Damon, D. N., et al. (2007). Smooth muscle-targeted knockout of connexin43 enhances neointimal formation in response to vascular injury. *Arterioscler. Thromb. Vasc. Biol.* 27, 1037–1042.
- Little, T. L., Beyer, E. C., and Duling, B. R. (1995). Connexin 43 and connexin 40 gap junctional proteins are present in arteriolar smooth-muscle and endothelium in vivo. *Am. J. Physiol.* 268, H729–H739.
- Maguiness, S. M., and Frieden, I. J. (2012). Management of difficult infantile hemangiomas. *Arch. Dis. Child.* 97, 266–271.
- Marano, G., Palazzi, S., Fadda, A., Vergari, A., and Ferrari, A. U. (2002). Attenuation of aortic banding-induced cardiac hypertrophy by propranolol is independent of beta-adrenoceptor blockade. *J. Hypertens.* 20, 763–769.
- Margileth, A. M., and Museles, M. (1965). Cutaneous hemangiomas in children: diagnosis and conservative management. *JAMA* 194, 523–526.
- Martínez, A. D., Acuña, R., Figueroa, V., Maripillan, J., and Nicholson, B. (2009). Gap-junction channels dysfunction in deafness and hearing loss. *Antioxid. Redox Signal.* 11, 309–322.
- Mayer, M., Minichmayr, A., Klement, F., Hroncek, K., Wertaschnigg, D., Arzt, W., et al. (2012). Tocotrienol with the  $\beta$ -2-sympathomimetic hexoprenaline increases occurrence of infantile haemangioma in preterm infants. *Arch. Dis. Child. Fetal Neonatal Ed.* 98, F2–F4.
- Mentzel, T., Calonje, E., and Fletcher, C. D. (1994). Vascular tumors of the skin and soft tissue: overview of newly characterized entities and variants. *Pathologe* 15, 259–270.
- Mulliken, J. B., and Glowacki, J. (1982). Hemangiomas and vascular malformations in infants and children: a classification based on endothelial characteristics. *Plast. Reconstr. Surg.* 69, 412–422.
- Naus, C. C., Bechberger, J. F., Caveney, S., and Wilson, J. X. (1991). Expression of gap junction genes in astrocytes and C6 glioma cells. *Neurosci. Lett.* 126, 33–36.
- Neri, I., Balestri, R., and Patrizi, A. (2012). Hemangiomas: new insight and medical treatment. *Dermatol. Ther.* 25, 322–334.
- Pagès, G., Milanini, J., Richard, D. E., Berra, E., Gothié, E., Viñals, F., et al. (2000). Signaling angiogenesis via p42/p44 MAP kinase cascade. *Ann. N. Y. Acad. Sci.* 902, 187–200.
- Pahujaa, M., Anikin, M., and Goldberg, G. S. (2007). Phosphorylation of connexin43 induced by Src: regulation of gap junctional communication between transformed cells. *Exp. Cell Res.* 313, 4083–4090.
- Parenti, A., Morbidelli, L., Cui, X. L., Douglas, J. G., Hood, J. D., Granger, H. J., et al. (1998). Nitric oxide is an upstream signal of vascular endothelial growth factor-induced extracellular signal-regulated kinase1/2 activation in postcapillary endothelium. *J. Biol. Chem.* 273, 4220–4226.
- Paznekas, W. A., Karczeski, B., Vermeer, S., Lowry, R. B., Delatycki, M., Laurence, F., et al. (2009). GJA1 mutations, variants, and connexin 43 dysfunction as it relates to the oculodentodigital dysplasia phenotype. *Hum. Mutat.* 30, 724–733.
- Phung, T. L., Hochman, M., and Mihm, M. C. (2005). Current knowledge of the pathogenesis of infantile hemangiomas. *Arch. Facial Plast. Surg.* 7, 319–321.
- Przewratil, P., Sitkiewicz, A., and Andrzejewska, E. (2010). Local serum levels of vascular endothelial growth factor in infantile hemangioma: intriguing mechanism of endothelial growth. *Cytokine* 49, 141–147.
- Przewratil, P., Sitkiewicz, A., Wyka, K., and Andrzejewska, E. (2009). Serum levels of vascular endothelial growth factor and basic fibroblastic growth factor in children with hemangiomas and vascular malformations – preliminary report. *Pediatr. Dermatol.* 26, 399–404.
- Razon, M. J., Kräling, B. M., Mulliken, J. B., and Bischoff, J. (1998). Increased apoptosis coincides with onset of involution in infantile hemangioma. *Microcirculation* 5, 189–195.
- Ricketts, R. R., Hatley, R. M., Corden, B. J., Sabio, H., and Howell, C. G. (1994). Interferon-alpha-2a for the treatment of complex hemangiomas of infancy and childhood. *Ann. Surg.* 219, 605–612.
- Ritter, M. R., Dorrell, M. I., Edmonds, J., Friedlander, S. F., and Friedlander, M. (2002). Insulin-like growth factor 2 and potential regulators of hemangioma growth and involution identified by large-scale expression analysis. *Proc. Natl. Acad. Sci. U.S.A.* 99, 7455–7460.
- Rummery, N. M., Hickey, H., McGurk, G., and Hill, C. E. (2002). Connexin37 is the major connexin expressed in the media of caudal artery. *Arterioscler. Thromb. Vasc. Biol.* 22, 1427–1432.
- Sakurai, T., and Kudo, M. (2011). Signaling pathways governing tumor angiogenesis. *Oncology* 81(Suppl. 1), 24–29.
- Salameh, A., Blanke, K., Dhein, S., and Janousek, J. (2010). Cardiac gap junction channels are upregulated by metoprolol: an unexpected effect of beta-blockers. *Pharmacology* 85, 203–210.
- Salameh, A., Krautblatter, S., Karl, S., Blanke, K., Gomez, D. R., Dhein, S., et al. (2009). The signal transduction cascade regulating the expression of the gap junction protein connexin43 by beta-adrenoceptors. *Br. J. Pharmacol.* 158, 198–208.
- Saunders, M. M., Seraj, M. J., Li, Z., Zhou, Z., Winter, C. R., Welch, D. R., et al. (2001). Breast cancer metastatic potential correlates with a breakdown in homospecific and heterospecific gap junctional intercellular communication. *Cancer Res.* 61, 1765–1767.
- Scherer, S. S., and Kleopa, K. A. (2012). X-linked Charcot-Marie-Tooth disease. *J. Peripher. Nerv. Syst.* 17(Suppl. 3), 9–13.
- Seenger, D. R., Galli, S. J., Dvorak, A. M., Perruzzi, C. A., Harvey, V. S., and Dvorak, H. F. (1983). Tumor cells secrete a vascular permeability factor that promotes accumulation of ascites fluid. *Science* 219, 983–985.
- Severs, N. J., Rothery, S., Dupont, E., Coppen, S. R., Yeh, H. I., Ko, Y. S., et al. (2001). Immunocytochemical analysis of connexin expression in the healthy and diseased cardiovascular system. *Microsc. Res. Tech.* 52, 301–322.
- Simon, A. M., and McWhorter, A. R. (2002). Vascular abnormalities in mice lacking the endothelial gap junction proteins connexin37 and connexin40. *Dev. Biol.* 251, 206–220.
- Simon, A. M., and McWhorter, A. R. (2003). Decreased intercellular dye-transfer and downregulation of non-ablated connexins in aortic endothelium deficient in connexin37 or connexin40. *J. Cell Sci.* 116, 2223–2236.
- Söhl, G., and Willecke, K. (2004). Gap junctions and the connexin protein family. *Cardiovasc. Res.* 62, 228–232.
- Starkey, E., and Shahidullah, H. (2011). Propranolol for infantile hemangiomas: a review. *Arch. Dis. Child.* 96, 890–893.
- Storch, C. H., and Hoeger, P. H. (2010). Propranolol for infantile hemangiomas: insights into the molecular mechanisms of action. *Br. J. Dermatol.* 163, 269–274.
- Takahashi, K., Mulliken, J. B., Kozakewich, H. P., Rogers, R. A., Folkman, J., and Ezekowitz, R. A. (1994). Cellular markers that distinguish the phases of hemangioma during infancy and childhood. *J. Clin. Invest.* 93, 2357–2364.
- Tamayo, L., Ortiz, D. M., Orozco-Covarrubias, L., Durán-McKinster, C., Mora, M. A., Avila, E., et al. (1997). Therapeutic efficacy of interferon alfa-2b in infants with life-threatening giant hemangiomas. *Arch. Dermatol.* 133, 1567–1571.
- van Kempen, M. J., and Jongasma, H. J. (1999). Distribution of connexin37, connexin40 and connexin43 in the aorta and coronary artery of several mammals. *Histochem. Cell Biol.* 112, 479–486.
- Warn-Cramer, B. J., Lampe, P. D., Kurata, W. E., Kanemitsu, M. Y., Loo, L. W., Eckhart, W., et al. (1996). Characterization of the mitogen-activated protein kinase phosphorylation sites on the connexin-43 gap junction protein. *J. Biol. Chem.* 271, 3779–3786.

- Wirth, F. A., and Lowitt, M. H. (1998). Diagnosis and treatment of cutaneous vascular lesions. *Am. Fam. Physician* 57, 765–773.
- Yamasaki, H., Krutovskikh, V., Mesnil, M., Tanaka, T., Zaidan-Dagli, M. L., and Omori, Y. (1999). Role of connexin (gap junction) genes in cell growth control and carcinogenesis. *C. R. Acad. Sci. III* 322, 151–159.
- Yeh, H. I., Rothery, S., Dupont, E., Coppen, S. R., and Severs, N. J. (1998). Individual gap junction plaques contain multiple connexins in arterial endothelium. *Circ. Res.* 83, 1248–1263.
- Zhang, D., Ma, Q., Shen, S., and Hu, H. (2009). Inhibition of pancreatic cancer cell proliferation by propranolol occurs through apoptosis induction: the study of beta-adrenoceptor antagonist's anticancer effect in pancreatic cancer cell. *Pancreas* 38, 94–100.
- Zhang, W., DeMatta, J. A., Song, H., and Couldwell, W. T. (2003). Communication between malignant glioma cells and vascular endothelial cells through gap junctions. *J. Neurosurg.* 98, 846–853.
- Zhong, S., Yang, G., Xia, C., Duanlian, Z., and Shan, S. (2009). Expression of matrix metalloproteinase and its tissue inhibitor in haemangioma. *J. Huazhong Univ. Sci. Technolog. Med. Sci.* 29, 614–619.

**Conflict of Interest Statement:** The authors declare that the research was conducted in the absence of any commercial or financial relationships that could be construed as a potential conflict of interest.

*Received: 19 February 2013; accepted: 25 March 2013; published online: 16 April 2013.*

*Citation: Blanke K, Dähnert I and Salameh A (2013) Role of connexins in infantile hemangiomas. *Front. Pharmacol.* 4:41. doi: 10.3389/fphar.2013.00041*

*This article was submitted to Frontiers in Pharmacology of Ion Channels and Channelopathies, a specialty of Frontiers in Pharmacology.*

*Copyright © 2013 Blanke, Dähnert and Salameh. This is an open-access article distributed under the terms of the Creative Commons Attribution License, which permits use, distribution and reproduction in other forums, provided the original authors and source are credited and subject to any copyright notices concerning any third-party graphics etc.*



# Neurological manifestations of oculodentodigital dysplasia: a Cx43 channelopathy of the central nervous system?

Marijke De Bock<sup>†</sup>, Marianne Kerrebrouck<sup>†</sup>, Nan Wang and Luc Leybaert\*

Physiology Group, Department of Basic Medical Sciences, Ghent University, Ghent, Belgium

**Edited by:**

Aida Salameh, Heart Centre  
University of Leipzig, Germany

**Reviewed by:**

Heike Wulff, University of California,  
Davis, USA

Charles K. Abrams, SUNY  
Downstate, USA

**\*Correspondence:**

Luc Leybaert, Physiology Group,  
Department of Basic Medical  
Sciences, Faculty of Medicine and  
Health Sciences, Ghent University,  
De Pintelaan 185, Building B  
(Rm 310), 9000 Ghent, Belgium  
e-mail: luc.leybaert@ugent.be

<sup>†</sup>These authors have contributed  
equally to this work.

The coordination of tissue function is mediated by gap junctions (GJs) that enable direct cell-cell transfer of metabolic and electric signals. GJs are formed by connexins of which Cx43 is most widespread in the human body. In the brain, Cx43 GJs are mostly found in astroglia where they coordinate the propagation of  $\text{Ca}^{2+}$  waves, spatial  $\text{K}^+$  buffering, and distribution of glucose. Beyond its role in direct intercellular communication, Cx43 also forms unapposed, non-junctional hemichannels in the plasma membrane of glial cells. These allow the passage of several neuro- and gliotransmitters that may, combined with downstream paracrine signaling, complement direct GJ communication among glial cells and sustain glial-neuronal signaling. Mutations in the *GJA1* gene encoding Cx43 have been identified in a rare, mostly autosomal dominant syndrome called oculodentodigital dysplasia (ODDD). ODDD patients display a pleiotropic phenotype reflected by eye, hand, teeth, and foot abnormalities, as well as craniofacial and bone malformations. Remarkably, neurological symptoms such as dysarthria, neurogenic bladder (manifested as urinary incontinence), spasticity or muscle weakness, ataxia, and epilepsy are other prominent features observed in ODDD patients. Over 10 mutations detected in patients diagnosed with neurological disorders are associated with altered functionality of Cx43 GJs/hemichannels, but the link between ODDD-related abnormal channel activities and neurologic phenotype is still elusive. Here, we present an overview on the nature of the mutants conveying structural and functional changes of Cx43 channels and discuss available evidence for aberrant Cx43 GJ and hemichannel function. In a final step, we examine the possibilities of how channel dysfunction may lead to some of the neurological manifestations of ODDD.

**Keywords:** oculodentodigital dysplasia, Cx43, gap junction, hemichannel, astrocyte

## INTRODUCTION: ODDD MUTATIONS, CLINICAL MANIFESTATIONS AND REVIEW FOCUS

Oculodentodigital syndrome or oculodentodigital dysplasia (ODDD, OMIM #164200) is a mostly autosomal dominant disease caused by mutations in the *GJA1* gene which is located on chromosome 6 (q21-q23.2). ODDD is a rare disease (prevalence < 1/1,000,000<sup>1</sup>) and symptoms have been mostly described in Caucasian families; it is uncertain though whether this is a matter of clustering or of inconsistent screening in other populations. In the affected families, male and female patients are found in equal numbers while in sporadic forms of ODDD, females seem to be more susceptible (reviewed in Paznekas et al., 2009; Avshalumova et al., 2013).

*GJA1* encodes for one of the most abundant connexin (Cx) proteins, Cx43. Cxs are a family of transmembrane proteins with molecular weights (MW) varying from 26 to 60 kilodaltons (kDa) on which the current nomenclature is based (Cx43 has a MW of ~43 kDa). In vertebrates, Cxs are the building blocks of gap junction (GJ) channels, intercellular channels that connect the cytoplasm of two neighboring cells. A GJ channel

consists of two hemichannels (HCs), each composed of six Cx proteins and delivered by each of the coupled cells. Cx43 is ubiquitously present in the human body in a large array of tissues and cells (reviewed in Laird, 2006). As a result, ODDD patients exhibit a pleiotropic phenotype with manifestations in a large variety of organ systems. Externally, mostly eyes, teeth, hands and feet are affected. Typical craniofacial dysmorphisms include a thin nose with hypoplastic *alae nasi*, small anteverted nares and prominent *columnella*. Some patients additionally have dysplastic ears. Ophthalmological anomalies include microphthalmia, microcornea, iris abnormalities, cataracts, glaucoma and optical neuropathy. Malformations of the extremities are another hallmark of ODDD and include syndactyly of fingers and toes. Additionally, camptodactyly (fixed flexion deformity of fingers and toes) and clinodactyly (lateral curvature of the fingers) are frequently observed. In the oral region, mandibular overgrowth, cleft lip, and cleft palate may be present. Abnormalities in primary and permanent teeth such as microdontia, partial anodontia, enamel hypoplasia, caries, and early tooth loss are observed in most patients. Brittle nails and hair abnormalities sometimes appear and skin diseases like palmoplantar keratoderma and sub-clinical wound healing defects are possible as well (Paznekas et al.,

<sup>1</sup><http://www.orpha.net>

2003; Gong et al., 2006; Thibodeau et al., 2010; Churko et al., 2011; Amano et al., 2012).

In addition to this large variety of physically observable features, the disease is also characterized by cardiac and neurological malfunctioning. The cardiac phenotype is observed in 3% of the ODDD patients and includes endocardial cushion defects, atrial or ventricular septum defects, recurrent ventricular tachycardia, atrioventricular block, and idiopathic atrial fibrillation (Paznekas et al., 2003, 2009). Cardiac arrhythmia caused by a Cx43 mutation (E42K) has been associated with “sudden infant death syndrome” (Van Norstrand et al., 2012), making it plausible that some of the ODDD mutations result in a cardiac phenotype. Neurological symptoms are not universally seen, but about 30% of the patient population has been diagnosed with neurological problems that include conductive hearing loss, dysarthria (speech articulation problems), neurogenic bladder (voiding problems), ataxia (gait disturbance), muscle weakness, spasticity, and seizures. MRI imaging studies have brought up diffuse bilateral abnormalities in the subcortical cerebral white matter, possibly indicating a slow progressive leukodystrophy. Mental retardation may occur but is rare (Paznekas et al., 2003, 2009; Amador et al., 2008; Joss et al., 2008; Furuta et al., 2012). Of note, in most families, the appearance of neurological symptoms is unpredictable, but in 4 families genotyped for having the L90V, L113P, K134N, or G138R mutant, all ODDD patients exhibit neurological traits (Paznekas et al., 2009). Cardiac and neurological manifestations in ODDD have only started to emerge in the past decade and the list of “new” ODDD features still seems to expand continuously. Brice and co-workers have for instance recently described a case of lymphedema in ODDD (Brice et al., 2013). Given the low prevalence, the high pleiotropy and the still growing list of previously unnoticed ODDD features, currently, there are no clear data available about the life expectancy of the patients.

In this review, we focus on the neurological manifestations of ODDD and explore how Cx43 mutations and consequent channel aberrations may link to some of these manifestations (**Table 1**). We start with an overview of connexins and its channels (section Connexin Channels: Gap Junctions and Hemichannels), provide an in depth analysis of the consequence of ODDD mutations on channel function (section ODDD-Linked Mutations and Cx43 Channel Function) and end by examining how channel dysfunction may lead to alterations in neural tissue functioning (section Neurological Phenotype in ODDD—Link to Aberrant Cx43 Channels). Several excellent reviews have highlighted each of these aspects (Kielian, 2008; Laird, 2008, 2010; Chew et al., 2010; Orellana et al., 2011; Abrams and Scherer, 2012; Eugenin et al., 2012); here we aimed to correlate channel dysfunction with neurological manifestations and explore possible relations in the framework of currently available knowledge.

## CONNEXIN CHANNELS: GAP JUNCTIONS AND HEMICHANNELS

Cxs form two kinds of functional channels: GJs and HCs. GJs mediate the direct diffusion of ions and molecules with MWs up to 1.5 kDa, including inositol 1,4,5 trisphosphate (IP<sub>3</sub>), cyclic nucleotides, and energy molecules such as ATP (reviewed in Alexander and Goldberg, 2003), thereby contributing to the

coordination of cell function in several organs and tissues. GJ channels are for instance implicated in the propagation of intercellular Ca<sup>2+</sup> waves (ICWs) (reviewed by Leybaert and Sanderson, 2012), metabolic and electric coupling in astrocytes and cardiomyocytes (Rouach et al., 2008; Meme et al., 2009; Desplantez et al., 2012), exchange of bone modulating molecules (reviewed in Batra et al., 2012) and synchronization of smooth muscle cell contraction in the bladder and uterus (Miyoshi et al., 1996; Neuhaus et al., 2002). Moreover, GJs may also spread cell death signals to neighboring cells, thereby contributing to tissue/organ damage in pathology (Decrock et al., 2012). HCs can be present both as GJ precursors in the plasma membrane (PM) or as non-junctional channels, not incorporated into GJs. For a long time, it was thought that HCs remain closed until they form a GJ channel, since uncontrolled HC opening would lead to membrane depolarization and depletion of essential molecules from the cytoplasm, ultimately leading to cell dysfunction and possibly cell death. The first evidence of functional HCs, derived from *in vitro* work whereby Cx46 was expressed in *Xenopus laevis* oocytes, confirmed that HC opening resulted in uptake of Lucifer yellow, but also in depolarization and cell death (Paul et al., 1991). Research over the past decades has identified numerous scenarios in which HCs are activated (see section ODDD-Linked Mutations and Cx43 Channel Function). HCs have been shown to be involved in different forms of paracrine signaling through the release of ATP (Kang et al., 2008), glutamate (Ye et al., 2003), glutathione (Rana and Dringen, 2007), NAD<sup>+</sup> (Goodenough and Paul, 2003), and prostaglandins (Jiang and Cherian, 2003; Orellana et al., 2011). HC-mediated ATP release functions as a paracrine signal in the propagation of ICWs (Leybaert and Sanderson, 2012) and evidence is accruing that HCs may additionally contribute to “center-surround” antagonism in the retina (Kamermans et al., 2001; Goodenough and Paul, 2003), osteogenesis (reviewed in Civitelli, 2008; Batra et al., 2012), regulation of vascular permeability (De Bock et al., 2011), central chemoreception (Huckstepp et al., 2010), atherosclerotic plaque formation (Wong et al., 2006), induction of astrogliosis (O’Carroll et al., 2008), ischemia-related cell death (Danesh-Meyer et al., 2008, 2012; Davidson et al., 2012; Wang et al., 2013a,b and reviewed in Contreras et al., 2004; Bargiolas et al., 2009) as well as in the propagation of apoptotic signals (Decrock et al., 2009). The role of HCs has been heavily debated since the discovery of pannexin channels, transmembrane channels that have similar tissue distribution and properties as HCs but are not likely to form GJ channels (Spray et al., 2006; Iglesias et al., 2009; Scemes, 2012). Much of the published data on the possible role of both HCs and pannexin channels is based on indirect measures that might be prone to misinterpretation and these issues are considered in detail in another review in this Frontiers Research Topic (Giaume et al., 2013).

## CONNEXIN LIFE CYCLE AND CHANNEL ASSEMBLY

Because of the relatively short Cx half-life (1–6 h), there is a continuous synthesis and breakdown of the protein, enabling fast adaptation of GJ intercellular communication (GJIC) to the physiological needs of the tissue (reviewed in Herve et al., 2007;

**Table 1 | Overview of ODDD-linked mutations in different Cx43 domains, their effect on Cx channel properties and the associated neurologic phenotypes.**

NH2	Proposed role in:		
	<ul style="list-style-type: none"> <li>• fast gating</li> <li>• stabilization of open conformation</li> </ul>		
	Influence on GJs	Influence on HCs	Neurologic phenotype
G2V	Normal number of GJ plaques No GJIC DN effect	n.a.	n.a.
G2fs	n.a.	n.a.	Psychomotor regression Seizures Hypomyelination Atrophy
D3N	Normal number of GJ plaques No GJIC DN effect	n.a.	Neurogenic bladder UMN dysfunction
L7V	Normal number of GJ plaques No GJIC DN effect	n.a.	n.a.
L11P	↓ Presence in PM ↓ Number of GJ plaques No GJIC DN effect	n.a.	No neurological findings
L11F	n.a.	n.a.	Sensorineural deafness
Y17S	↓ Presence in PM ↓ Number of GJ plaques No GJIC DN effect	no HC activity	UMN dysfunction MRI white matter changes urinary incontinence
S18P	↓ Presence in PM ↓ Number of GJ plaques No GJIC DN effect	n.a.	No neurological findings
TM1	Proposed role in:		
	<ul style="list-style-type: none"> <li>• Pore lining</li> <li>• Loop gating</li> </ul>		
	Influence on GJs	Influence on HCs	Neurologic phenotype
G21R	↓ Number of GJ plaques No GJIC DN effect	no HC activity	UMN dysfunction
G22E	Normal GJ plaques	n.a.	MRI white matter changes
K23T	Normal GJ plaques	n.a.	UMN dysfunction MRI white matter changes Tremor
V24A	n.a.	n.a.	Sensorineural hearing loss
W25C	n.a.	n.a.	Motor deficits Sensory deficits (peripheral) Lesions in brain and brainstem

(Continued)

**Table 1 | Continued**

I31M	↓ Presence in PM ↓ Number of GJ plaques ↓ Phosphorylation No GJIC	↑ HC activity	n.a.
R33X	No presence in PM DN effect	n.a.	UMN dysfunction MRI white matter changes MRI gray matter changes Speech delay
A40V	↓ Number of GJ plaques No GJIC	no HC activity	Gait difficulties Urinary urgency
E42K	Normal (number of) GJ plaques No GJIC	n.a.	n.a.
<b>EL1/2</b>	<b>Proposed role in:</b> <ul style="list-style-type: none"><li>• Stabilization protein structure</li><li>• HC docking</li><li>• Loop gating</li><li>• Permselectivity?*</li><li>• Heterotypic compatibility</li></ul>		
	<b>Influence on GJs</b>	<b>Influence on HCs</b>	<b>Neurologic phenotype</b>
Q49K	Normal presence in PM No GJIC DN effect	n.a.	No neurologic findings
Q49P	n.a.	n.a.	Urinary incontinence
F52dup	Intracellular retention No GJIC No DN effect	no HC activity	No neurologic findings
R76S	Normal presence in PM No GJIC	n.a.	MRI white matter changes Epilepsy
R76H	Normal presence in PM Normal GJ plaques ↓ GJIC <sup>#</sup> No DN effect	n.a.	n.a.
H194P	↓ Presence in PM No GJIC	normal HC activity	No neurological findings
R202H	Intracellular retention ↓ Number of GJ plaques No GJIC No DN effect (except on dye coupling)	n.a.	No neurological findings
<b>TM2</b>	<b>Proposed role in:</b> <ul style="list-style-type: none"><li>• Chemical gating (<math>pH_i</math>)</li><li>• Permselectivity?*</li></ul>		
	<b>Influence on GJs</b>	<b>Influence on HCs</b>	<b>Neurologic phenotype</b>
V85M	n.a.	n.a.	Spastic paraplegia <sup>†</sup>
L90V	↓ Number of GJ plaques ↓ GJIC DN effect	no HC activity	Urinary incontinence Spastic paraplegia Epilepsy MRI white matter changes

(Continued)

**Table 1 | Continued**

H95R	n.a.	n.a.	Urinary incontinence MRI white matter changes Spasticity
V96A	n.a.	n.a.	MRI white matter changes
<b>CL</b>	<b>Proposed role in:</b> <ul style="list-style-type: none"> <li>• Fast gating</li> <li>• Chemical gating (<math>pH_i</math> and <math>[Ca^{2+}]_i</math>)</li> </ul>		
	<b>Influence on GJs</b>	<b>Influence on HCs</b>	<b>Neurologic phenotype</b>
K102N	Normal GJ plaques	n.a.	MRI white matter changes Urinary incontinence
L106P	n.a.	n.a.	Urinary incontinence Spasticity
L113P	n.a.	n.a.	Spastic paraparesis UMN dysfunction MRI white matter changes
I130T	↑ Presence in PM ↓ Number of GJ plaques ↓ GJIC ↓ Phosphorylation No DN effect	no HC activity	Spastic paresis Epilepsy Brain atrophy/hypoplasia Urinary incontinence MRI white matter changes
K134E	↓ Number of GJ plaques ↓ GJIC	no HC activity	UMN dysfunction MRI white matter changes
K134N	↓ Number of GJ plaques ↓ GJIC	n.a.	UMN dysfunction
G138R	↑ Presence in PM Normal GJ plaques No GJIC DN effect	↑ HC activity	Spastic bladder paraparesis? Tremor UMN dysfunction Urinary incontinence MRI white matter changes
G143S	↑ Presence in PM Normal GJ plaques No GJIC DN effect	↑ HC activity	n.a.
<b>TM3</b>	<b>Proposed role in:</b> <ul style="list-style-type: none"> <li>• Cx isoform compatibility in heteromeric channels</li> </ul>		
	<b>Influence on GJs</b>	<b>Influence on HCs</b>	<b>Neurologic phenotype</b>
T154A	Normal GJ plaques ↓ GJIC DN effect	n.a.	MRI white matter changes Psychomotor delay Gait difficulties UMN dysfunction Urinary incontinence
T154N	n.a.	n.a.	Tremor Spastic paraparesis

(Continued)

**Table 1 | Continued**

TM4			
	Influence on GJs	Influence on HCs	Neurologic phenotype
V216L	↓ Amount of GJ plaques ↓ GJIC ↓ Phosphorylation DN effect	n.a.	Spasticity UMN dysfunction MRI white matter changes Neurogenic bladder/Urinary incontinence Hyperreflexia
S220Y	n.a.	n.a.	Developmental and language disorder
CT	<b>Proposed role in:</b> <ul style="list-style-type: none"> <li>• Fast gating</li> <li>• Chemical gating</li> <li>• Interacts with cytoskeletal binding partners and scaffolding proteins</li> <li>• Main target for post-translation modifications</li> </ul>		
	Influence on GJs	Influence on HCs	Neurologic phenotype
fs230	No presence in the PM DN effect	n.a.	No neurological findings
fs260	No presence in the PM DN effect	n.a.	No neurological findings
c.932delC	No presence in the PM DN effect	n.a.	n.a.

For references see text. Neurological traits are from Paznekas et al. (2003) and Abrams and Scherer (2012) and references therein, unless indicated.

\*The role of the EL domains in the determination of Cx channel permselectivity has been suggested based on observations in Cx46 channels. TM2 is implicated in regulating permselectivity of Cx26 channels. Thus far, nothing is known on the role of these domains in regulating permselectivity of Cx43 channels.

#Only for certain exogenous markers. With other markers, GJIC is similar to WT Cx43.

‡Quintáns et al., 2013

DN, dominant negative effect; n.a., data not available; PM, plasma membrane; UMN, upper motor neuron.

Mutants in italic font are inherited in an autosomal recessive manner.

Rackauskas et al., 2010). This is for instance illustrated in the myometrium, where steroid hormones control the expression level of Cxs before and after parturition (Risek et al., 1990). Like most transmembrane proteins, Cxs are co-translationally integrated into the rough endoplasmic reticulum (ER) membrane where they adopt their native transmembrane configuration (Falk, 2000; Vanslyke et al., 2009). Hydropathy plots reveal that all Cx proteins share a common topology: four transmembrane alpha-helices (TM1-4) are connected through two extracellular loops (EL1-2). In each loop, three cysteine residues form intramolecular disulphide bonds that are required for appropriate folding of the protein (Dahl et al., 1992; Foote et al., 1998). The Cx protein further contains three intracellular domains: a cytoplasmic loop (CL), an amino-terminal domain (NT), and the carboxyl-terminal region (CT). The best conserved protein regions are the ELs and the TM domains, whereas the CT- and CL-regions show marked divergence (reviewed in Nicholson, 2003; Saez et al., 2003; Wei et al., 2004). The subsequent oligomerization of Cx proteins into HCs starts in the ER, progressing to the trans-Golgi network (Falk, 2000; Vanslyke et al., 2009). During this process, newly synthesized HCs remain closed in order to protect and maintain the integrity of the

lumens of the intracellular compartments (Moreno, 2005; Laird, 2006).

After leaving the ER, Cxs first pass the ER-Golgi intermediate compartment and then transit through the cis- and trans-Golgi network before being shuttled to the PM. Pleomorphic vesicles and tubular extensions departing from the Golgi apparatus contribute to the delivery of HCs to the PM (Gaietta et al., 2002; Laird, 2006). It is not entirely clear to what extent post-translational modifications are required for Cx transport to the PM. Some data suggest that Cx43 is transiently phosphorylated early in the secretory pathway, but the vast majority of phosphorylation is thought to occur at the cell surface (Lampe et al., 2000; Solan and Lampe, 2007 and reviewed in Lampe and Lau, 2004), where it plays a complex role in Cx channel gating (see further). Notably, once inserted into the cell membrane, HCs undergo specific adhesions and dock with HCs of neighboring cells to form GJs. Hundreds to thousands of GJ channels cluster in plaques at the cell-cell interface with newly formed GJs located at the border of the plaque and older channels located centrally. These central channels are targeted for internalization and degradation of GJ channels (reviewed in Goodenough and Paul, 2003; Laird, 2006).

Internalization is mediated through large double-membrane bound vesicles that contain a complete GJ channel. These vesicles are called “annular junctions” or “connexosomes” (Gaietta et al., 2002; Laird, 2006) and also contain Cx-binding proteins and molecules that function as chaperones for internalization and intracellular degradation through the proteasomal or lysosomal pathway (Qin et al., 2003; Thevenin et al., 2013). Cxs have been shown to be a substrate for ubiquitination that is known to guide proteins to proteasomes. Connexosomes are identified in the majority of cell types, but are for instance difficult to find in hepatocytes. It therefore remains possible that Cxs are additionally internalized and degraded through the endosomal cascade. Furthermore, internalization of Cx43 has been suggested to occur via a clathrin-mediated, caveolae-dependent process. Clearly, more studies are required to investigate all possible pathways of internalization/degradation. The proteasomal pathway may be responsible for ER-associated degradation, while lysosomes degrade Cxs that are recycled to the PM through endosomes (Laird, 2006).

## ODDD-LINKED MUTATIONS AND Cx43 CHANNEL FUNCTION

### Cx43 MUTATIONS AND CHANNEL GATING

Collectively, there are over 62, mostly missense, mutations found throughout the expanse of the Cx43 protein that are associated with ODDD. All Cx domains have specific functions, be it in Cx trafficking, Cx assembly or channel gating. In contrast to “benign” polymorphisms that have no discernible effect on Cx43 channel function, a minority of mutants promote channel opening/function; however, most mutants carry loss-of-function mutations and may involve those leading to inappropriate membrane sorting, those leading to improper folding, interfering with the HC docking process, and those giving rise to altered permeability or gating. The latter implies a fast and reversible shift in the channel’s conductive properties which can be due to conformational changes or which can be mediated by Cx-linked adaptor molecules and proteins (Bukauskas et al., 2000; Cottrell et al., 2003; Herve et al., 2007; Moreno and Lau, 2007).

Cx channels—both GJs and HCs—are sensitive to changes in voltage, intracellular pH and  $[Ca^{2+}]_i$ , allowing swift adaptations (faster than those brought about by assembly/disassembly) of GJIC and paracrine signaling to comply to the specific needs of the tissue. In terms of voltage-dependent channel gating, GJs are influenced mainly by the transjunctional voltage ( $V_j$ ) which defines the difference in voltage measured between two coupled cells. In contrast, HCs are highly sensitive to  $V_m$ : they remain preferentially “silent” at inside negative potentials but are activated upon depolarization by a gating mechanism that resembles gating transitions associated with the docking of extracellular loop domains; therefore this gating is also referred to as loop gating (or slow gating) (Trexler et al., 1996; Bukauskas and Verselis, 2004; Gonzalez et al., 2006; Verselis et al., 2009). Loop gating represents transitions between the fully open and closed states whereas fast ( $<1\text{ ms}$ ) HC gating involves transitions to long-lasting substates. Chemical gating, achieved by changes in the intra- or extracellular environment, much resembles gating transitions observed with slow voltage gating; therefore, it has been proposed that both phenomena are mediated by the same mechanisms.

Cx43 mutations are found in all protein domains, each of which has been associated with specific functions in terms of channel oligomerization, trafficking, gating and permeability. Importantly, many of the known mutations causing ODDD occur in residues that are highly conserved throughout the animal kingdom (Paznekas et al., 2003), hinting toward their importance in channel regulation. Below, we discuss the different Cx43 mutations that have been characterized in terms of trafficking, channel assembly and channel function. Unfortunately though, for most mutant channels there is not yet a clear structural-functional correlation that would allow a better understanding of what is going wrong with the channels. The effects of the Cx43 mutations are often not predictable from their location in the primary structure and mutations located at different domains may cause similar channel dysfunction phenotypes, ultimately leading to the ODDD phenotype.

### N-TERMINAL Cx43 MUTATIONS

Deletion of the first N-terminal amino acids (AAs 2–7) disables Cx43 trafficking and most of the Cx43 protein is retained in the intracellular compartment. Overall, the Y17S mutation has similar effects (Shao et al., 2012), although a few plaque-like structures remained observable at the PM (Shibayama et al., 2005; Lai et al., 2006). Nevertheless, given the problematic trafficking of this mutant, neither HC activity nor GJIC was detected (Lai et al., 2006). Unfortunately, fairly little is known on the role of the Cx43 N-terminal domain in terms of oligomerization or trafficking. Most of the other N-terminal missense mutations, including G2V, D3N, L7V, L11P, and S18P, do allow a normal Cx life cycle, but result in non-functional GJs, as evidenced by the lack of dye transfer and the absence of electrical coupling (Shibayama et al., 2005; Churko et al., 2011; Shao et al., 2012). In these mutant channels, the closed state is thus relatively more stable than the open one. Importantly, these mutant proteins exert a dominant negative effect on WT Cx43 in terms of coupling, indicating that the patients are likely experiencing more than 50% loss of normal Cx43 function, despite having one functional allele (Shao et al., 2012).

A hydrophobic core built around W4 has been put forward as a structural determinant of the Cx43 N-terminal domain, governing interactions with the TM1 domain. Replacement of G2 with a valine residue was suggested to introduce additional hydrophobic interactions, not present in the WT channel that would abolish NT-TM1 interactions (Shao et al., 2012). Based on electron crystallography of Cx26 channels and electrophysiological studies performed in Cx46 channels, interactions between the NT and the TM1 domains are suggested to keep the channel in the open conformation (Maeda et al., 2009; Kronengold et al., 2012). Preventing NT-TM1 interactions may thus be one mechanism by which the mutants result in non-functional GJ channels.

### Cx43 MUTATIONS IN THE TRANSMEMBRANE DOMAINS

The crystal structure of a C-terminally truncated Cx43 channel at 7.5 Å resolution indicates the presence of 24 transmembrane  $\alpha$ -helices within each hemichannel, grouped in two concentric rings around the central pore (Unger et al., 1997, 1999); however,

there has been controversy regarding the identities of the principal pore-lining segments. The substituted cysteine accessibility method (SCAM) that enables the identification of pore lining residues, has pointed out that TM3 might delineate the inner pore of Cx32 GJs (Skerrett et al., 2002); however, currently, most evidence points to the amphipathic TM1 as the major pore-lining domain in channels composed of Cx46 (Zhou et al., 1997; Kronengold et al., 2003a,b), Cx50 (Verselis et al., 2009) Cx32 (Oh et al., 1997; Tang et al., 2009) and Cx26 (Sanchez et al., 2010). The crystal structure of a Cx26 channel at 3.5 Å resolution confirms that TM1, but also TM2, are part of the inner lumen wall, whereas TM3 and TM4 face the hydrophobic environment (Maeda et al., 2009).

In TM1, mutants G21R, G22E, K23T, I31M, R33X, A40V, and E42K have all been identified in ODDD patients. Of these G21R, G22E, K23T, and E42K [the latter causing sudden infant death syndrome (Van Norstrand et al., 2012)], encounter normal trafficking to the PM and insertion into GJ plaques; yet cells are not electrically coupled (data on channel function of G22E and K23T mutant channels are still lacking) (Roscoe et al., 2005; Shibayama et al., 2005; Abrams and Scherer, 2012; Van Norstrand et al., 2012; Huang et al., 2013). When the Cx43-G21R mutant is co-expressed with endogenous WT Cx43, it negatively influences dye coupling (Shibayama et al., 2005). Both I31M and A40V mutants exhibit disturbed membrane insertion with just a fraction of the channels present in GJ plaques; these were, however, not sufficient to sustain GJIC (Shibayama et al., 2005; Dobrowolski et al., 2007). With respect to HC activity, G21R and A40V do not form functional HCs but I31M mutant channels release more ATP compared to the Cx43 WT. The half-life of the I31M mutant was not prolonged pointing to altered gating mechanisms or a shift in permselectivity (Lai et al., 2006; Dobrowolski et al., 2007). Additionally, Cx43-I31M presents with reduced phosphorylation that is, up to a certain degree, required for proper GJIC (Dobrowolski et al., 2007). This is quite surprising as Cx43 has thus far not been shown to be phosphorylated in transmembrane domains (reviewed in Johnstone et al., 2012; Marquez-Rosado et al., 2012). In addition, isoleucine residues are not generally direct targets for phosphorylation. Thus, it is more likely that a phosphorylation in TM1 is associated with conformational changes that somehow mask candidate phosphorylation sites in other protein domains.

Known mutations located in TM2 (L90V), TM3 (T154A), or TM4 (V216L) all form channels that are present as punctae in the PM, but the coupling capacity of each mutant channel is reduced. All mutants furthermore exert dominant negative effects on WT Cx43 when in a heteromeric or heterotypic conformation (McLachlan et al., 2005; Shibayama et al., 2005; Beahm et al., 2006; Churko et al., 2011). The H95R mutant (TM2) has additionally been described in an ODDD patient, but unfortunately, the manuscript provided no functional data (Honkaniemi et al., 2005). Earlier data indicate that this residue is involved in pH sensitivity of Cx43 channels (Ek et al., 1994): introducing a negative or positive charge at position 95 yields GJ channels that exhibit reduced or increased sensitivity to intracellular acidification, respectively. Finally, residues located in TM2 have

been proposed to play a role in determining permselectivity. Permeation of the Ca<sup>2+</sup> mobilizing messenger IP<sub>3</sub> for instance, is abolished in GJ channels composed of the mutant Cx26-V84L which is associated with hereditary deafness. The mutant protein has, however, no effect on unitary conductance and permeability to Lucifer yellow, which remain indistinguishable from WT Cx26 (Beltramello et al., 2005). This suggests that subtle structural modifications in the channel pore may selectively hinder the passage of biologically relevant molecules, possibly by altering certain interactions between the permeant and the channel pore. As this valine is highly conserved (V85 in Cx43) it may well be involved in determining IP<sub>3</sub> transfer through Cx43 channels. ODDD patients carrying a V85M mutant were recently identified (Fenwick et al., 2008; Quintáns et al., 2013), but again, the implications of this mutant on channel trafficking/gating/permselectivity were not studied.

### Cx43 MUTATIONS IN THE EXTRACELLULAR LOOPS

The extracellular loops are characterized by conserved, cysteine-rich patterns (CX<sub>6</sub>CX<sub>3</sub>C in EL1 and CX<sub>4/5</sub>CX<sub>5</sub>C in EL2), and intramolecular disulphide bridges in and between the ELs stabilize the protein's tertiary structure (Dahl et al., 1992; Bruzzone et al., 1996; Foote et al., 1998). In Cx43 these involve C54, C61 and C65 in EL1 and C187, C192 and C198 in EL2. Mutations of each of these cysteines could result in distorted loops resulting in improper protein folding and retention in intracellular compartments. Although mutations of conserved cysteines have not been associated with ODDD, two mutations that lie in direct proximity to conserved cysteine residues (F52dup and Cx43-R202H) cannot be traced back to the PM (Shibayama et al., 2005; Lai et al., 2006). Other mutants (Q49K, R76S/H, H194P) are inserted into the lipid bilayer (Sokolova et al., 2002; McLachlan et al., 2005; Shibayama et al., 2005; Dobrowolski et al., 2007; Abrams and Scherer, 2012; Huang et al., 2013); yet, electrical coupling is abolished (Sokolova et al., 2002; McLachlan et al., 2005). Based on a model proposed by Foote et al. in which the interdigitation of apposed ELs is required for docking and thus GJ formation (Foote et al., 1998), even those mutants that are present in the PM, may not form GJs due to distorted loops. This is further supported by the fact that HC activity of Cys-less Cx43 mutant channels appears normal both *in vitro* and *in vivo* (Bao et al., 2004; Tong et al., 2007). Also for ODDD-linked mutants like H194P in which the insertion of a proline induces a kink in the EL2 domain, HC activity is normal (Dobrowolski et al., 2007). In addition, those mutant proteins that cannot traffic to the PM in a homomeric configuration, can do so when assembled in a heteromeric channel with WT Cx43 (Shibayama et al., 2005; Lai et al., 2006). Interestingly, main and subconductance states of these WT:R202H and WT:F52dup channels were not different from homomeric WT channels (Shibayama et al., 2005). The single channel conductance of Cx43-R76H channels was substantially reduced compared to WT Cx43 channels (Huang et al., 2013). Slow voltage gating of Cx channels generally involves the coordinated response of all Cx monomers in the channel (Bukauskas and Verselis, 2004; Kwon et al., 2012). This might explain why a remaining electrical coupling is observed in heteromeric WT:R202H channels. At the same time, however, the

mutant proteins may narrow the pore as compared to homo-meric WT channels, preventing the diffusion of larger molecules like Lucifer yellow while leaving its electrical conduction intact (Shibayama et al., 2005).

### Cx43 MUTATIONS LOCATED IN THE CYTOPLASMIC LOOP

It is now firmly established that the CL domain is of utmost importance for Cx channel gating. It has for instance been shown to contain the preferred interaction site for calmodulin (CaM; region 136–158) and as such, to mediate the closure of GJ channels in response to increasing  $[Ca^{2+}]_i$  (Zhou et al., 2007; Myllykoski et al., 2009). Indeed,  $Ca^{2+}$ -induced closure of GJs is likely to be mediated by intracellular effector proteins since the uncoupled state may persist long after  $[Ca^{2+}]_i$  has been restored (Cotrina et al., 1998; Lurtz and Louis, 2003, 2007). Even more important, it is now widely accepted that the L2 region (second half of the CL; amino acids 119–144) serves as a receptor domain for the CT and that this CT-CL interaction, also known as the ball-and-chain mechanism, is implicated in both voltage gating and chemical gating of GJs by intracellular pH changes (Ek et al., 1994; Ek-Vitorin et al., 1996; Bukauskas et al., 2000; Anumonwo et al., 2001; Moreno et al., 2002; Shibayama et al., 2006). A CT-CL interaction is also important for the regulation of Cx43 HCs by extracellular  $Ca^{2+}$ , since a conformational change induced by an increase of extracellular  $Ca^{2+}$  masks the CT from antibody binding, which is most likely to be the result of its association with the “receptor”-domain (Liu et al., 2006). The modulation of HCs in response to changes in  $[Ca^{2+}]_i$  has only been outlined over the last decade, demonstrating that HCs are differently influenced by  $[Ca^{2+}]_i$  as compared to GJs. While GJs generally close with a  $[Ca^{2+}]_i$  elevation, HCs display a bimodal response: a moderate increase in  $[Ca^{2+}]_i$  up to 500 nM strongly promotes HC opening while this effect disappears with  $[Ca^{2+}]_i > 500$  nM. Further increases in  $[Ca^{2+}]_i$  to the micromolar level tend to close the HCs (Shintani-Ishida et al., 2007; De Vuyst et al., 2009; Wang et al., 2012a). Mechanistically,  $Ca^{2+}$ -activation of Cx43 HCs is mediated by CaM-dependent signaling (De Vuyst et al., 2009) and necessitates a CT-CL interaction (Ponsaerts et al., 2010). Most notably, the necessity of CT-CL interaction to trigger opening of Cx43 HCs stands in stark contrast to the fact that such interaction results in closure of GJs (reviewed in Iyyathurai et al., 2013). Addition of a CT-mimicking peptide prevented HC closure at high  $[Ca^{2+}]_i$  and restored HC activity of CT truncated Cx43 (Ponsaerts et al., 2010), while not affecting HC activation by modest ( $< 500$  nM)  $[Ca^{2+}]_i$ .

Several ODDD-associated mutations have been identified in the CL domain, most of which are located in the L2 region. Cx43-I130T HCs are transported to the PM and assemble into GJ plaques. Moreover, mutant levels in the PM exceed those of WT Cx43 which might indicate a reduced degree of protein degradation. Despite of this, the mutant exhibits reduced dye and electrical coupling and HC activity is disrupted (Shibayama et al., 2005; Lai et al., 2006; Kalcheva et al., 2007). K134E/N mutants show a reduced degree of plaque formation and electrical coupling and a decrease in unitary conductance (Shibayama et al., 2005). Both I130 and K134, forming ionic bonds with C-terminal aspartate residues, are suggested to be involved in CT-CL

interactions (Seki et al., 2004; Hirst-Jensen et al., 2007). As discussed higher, CT-CL interactions are necessary for HC opening while they result in closure of GJs. However, I130T and K134E mutant channels are closed in both the GJ and HC configuration, indicating that mechanisms different from altered CT-CL interactions may contribute to the closure of GJs.

Two CL mutations located further downstream in the L2 region (G138R and G143S), result in GJ channels that fail to sustain electrical or dye coupling and have a dominant negative effect on WT or endogenous (NRK—normal rat kidney—cells) Cx43. Interestingly, HC activity, measured by dye uptake and ATP release, is increased in both mutants (Roscoe et al., 2005; Dobrowolski et al., 2007, 2008). It is possible that the differential effects of these mutants on GJs and HCs mutants result from reinforced CT-CL interactions, caused by stronger electrostatic interactions between the CL equipped with an additional positively charged arginine residue (G138R), with negatively charged residues in the CT (Gong et al., 2007). Likewise, a shift from a non-polar glycine to a polar serine residue (G143S) may account for a higher number of hydrogen bonds that lock the CT to the CL. Further work is needed to substantiate these possibilities.

### C-TERMINAL Cx43 MUTATIONS

As highlighted above, the CT functions as a gating particle that alters its state in response to changes in the extra-or intracellular environment. The CT domain is additionally the primary target for post-translational modifications like S-nitrosylation (Retamal et al., 2006) and phosphorylation (reviewed by Johnstone et al., 2012). The majority of phosphorylation events occur on serine residues although tyrosine phosphorylation is abundant as well (Lampe and Lau, 2004; Solan and Lampe, 2007). Phosphorylation of Cx proteins seems to be intricately involved in Cx trafficking to the PM. Additionally, both under basal and stimulated conditions, Cx channel activity appears to be regulated by ongoing phosphorylation-dephosphorylation events. Substitution of C-terminal serines (S325, S328, S330) by alanines has indicated that phosphorylation of these serines is required for a fully open state of Cx43 GJs while phosphorylation of other residues (S255, S279, S282, S368, Y247, and Y265) favors channel closure (Ek-Vitorin and Burt, 2013). However, much of the details on how Cx phosphorylation can determine trafficking, turnover and the activity state of HCs and GJs still remains to be resolved (Johnstone et al., 2012). One detailed example of Cx channel regulation by phosphorylation is phosphorylation of the Cx43 CT tail by pH-dependent kinases which might introduce negative charges at this site, potentiating CT-CL interaction (Yahuaca et al., 2000).

Although the CT is the primary interaction domain of Cx-associated partner proteins like *zonula occludens* 1, tubulin, microtubules, and caveolins that may regulate protein trafficking and function (Giepmans et al., 2001; Langlois et al., 2008; Saidi Brikci-Nigassa et al., 2012); work with CT-truncated Cx43 mutants has repetitively shown that CT-truncated proteins are present at the PM of mammalian cells (Unger et al., 1999; Moreno et al., 2002; Kang et al., 2006; Maass et al., 2007). Oppositely, most of the ODDD-linked CT mutations are not inserted in the PM: the frame shift mutations fs230 and fs260 result in preliminary truncated Cx43 and present with reduced ability to form

plaques while having a dominant negative effect on WT Cxs with respect to trafficking (Lai et al., 2006; Gong et al., 2007; Churko et al., 2011). In the atrial tissue of a patient with idiopathic atrial fibrillation, a frame shift mutation caused by a single nucleotide deletion (c.932delC) was identified. The mutation renders a Cx43 protein exhibiting aberrant CT amino acids starting from position 346 followed by a premature stop codon, leading to prompt truncation. The protein remains intracellular and exerts a dominant negative effect on wild type Cx43 (as well as Cx40) in the atrial tissue (Thibodeau et al., 2010). Importantly, all previously reported work with CT-truncated mutants was indeed based on exogenous expression systems and the c.932delC mutant was similarly observed at the PM when exogenously expressed in HeLa cells where it even sustained dye coupling, though to a smaller extent than WT Cx43 (Hong et al., 2010). Another major difference between exogenous CT-truncated mutants and the ODDD mutants is that in the former the CT is absent while with frame shifts and single nucleotide deletion mutants, a CT is still (partly) present, albeit with a wrong amino acid sequence which could give a different outcome on trafficking.

## NEUROLOGICAL PHENOTYPE IN ODDD - LINK TO ABERRANT Cx43 CHANNELS

Apart from the physical appearances linked to ODDD, several of the above described mutations have been associated with seizures, spasticity, gait difficulties, tremor and incontinence. These symptoms are for the bigger part clinical manifestations of underlying neuronal damage in the central nervous system (CNS). Patients may also suffer from hearing loss and decreased visual acuity or blindness; however, the latter two phenotypes are infrequent and only observed in a small fraction of the patients presenting with neurological traits. Magnetic resonance imaging (MRI) and computed tomography (CT) scans of patients' brains revealed abnormalities in both white and gray matter (Loddenkemper et al., 2002; Amador et al., 2008; Joss et al., 2008; Paznekas et al., 2009; Alao et al., 2010; Abrams and Scherer, 2012). One patient was reported to exhibit central or sensorineural hearing loss which is associated with damaged cranial nerve VIII (cochlear part) that transmits signals from the cochlea to the inner ear. Loss of visual acuity (decreased sharp vision) or blindness result from atrophy of the optic nerve that relays visual information from the retina (via the thalamus) to the visual cortex. Similar loss of visual acuity follows optical nerve neuritis observed in the demyelinating disease multiple sclerosis (Florio and Maniscalco, 2011). Spasticity is a muscle control disorder characterized by stiff, uncontrollable muscles with hyperreactivity toward exogenous stimulation, and is generally associated with hyperactive, persisting reflexes (hyperreflexia). Tremor is characterized by involuntary rhythmic muscle contractions. According to the alpha/gamma-coactivation theory, muscle contraction is controlled by both alpha and gamma motor neurons. The alpha component delivers a feed forward command resulting in force delivery by activating extrafusal muscle fibers. The gamma motor component controls the length of muscle spindles (intrafusal muscle fibers), thereby delivering input to a servo-controlled neuronal circuit that receives feedback on the length status from the sensory output of muscle spindles. Spasticity may develop

as a result of aberrantly increased gamma motor neuron activity, resulting in increased tension in the muscle spindles that become oversensitive to external stimulation. Increased gamma motor drive may occur as a consequence of decreased central (cerebral and cerebellar) inhibitory input on spinal gamma motor neurons (reviewed in Sheean and McGuire, 2009). Ataxia is a cerebellar phenomenon that manifests as a lack of voluntary muscle coordination, typically observed as disturbances in the gait pattern. Interestingly, one patient carrying the W25C (TM1) mutation presented with all characteristic craniofacial features and extremity anomalies, as well as with spastic tetraparesis, hyperreflexia and sensory disturbances (numbness in feet), indicating widespread sensori-motor neurological deficits (Furuta et al., 2012). In two siblings characterized for having an R33X mutation, myelination deficits were described (Joss et al., 2008). The other major neurological deficit, namely seizure activity, results from a repetitive and synchronized, excessive neuronal activity in the CNS. Epilepsy has long been viewed as a channelopathy and involves epileptogenic (genesis of the disease) and ictogenic (genesis of an epileptic ictus or seizure) components. Currently, our understanding of epileptogenesis is very incomplete, at least at a mechanistic level. Ictogenesis is related to an imbalance between glutamatergic excitation and (mostly) GABAergic inhibition, and has been associated with dysfunctional channels, mostly voltage-gated  $\text{Na}^+$ ,  $\text{K}^+$ ,  $\text{Cl}^-$ , and  $\text{Ca}^{2+}$  channels that determine neuronal action potential firing. Moreover, the extracellular concentration of  $\text{Na}^+$ ,  $\text{K}^+$ ,  $\text{Cl}^-$ , and  $\text{Ca}^{2+}$  may influence the glial cells and thereby exert control over neuronal activity. It is hypothesized that dysfunctional  $\text{Na}^+$ ,  $\text{K}^+$ ,  $\text{Cl}^-$ , or  $\text{Ca}^{2+}$  channels alter the threshold for neuronal depolarization and action potential firing, thereby shifting the balance between excitation and inhibition. At the microscopic level, epileptic brain regions are characterized by injured neurons, gliosis, axonal sprouting, and the formation of new, aberrant, synaptic connections (reviewed in D'Ambrosio, 2004; Dichter, 2009; Reid et al., 2009).

Cx43 is abundant in astrocytes and can additionally be found in activated microglia, developing neurons, and endothelial cells (Orellana et al., 2009, 2011; Avila et al., 2011; Wang et al., 2012b) (**Figure 1**). Given its ubiquitous presence, it is not surprising that around 30% of the ODDD patients exhibit neurological symptoms. This number may further increase as neurological investigations of ODDD patients are becoming progressively more detailed.

## ODDD-ASSOCIATED MUTATIONS AND THEIR IMPLICATIONS FOR ASTROCYTE FUNCTIONING IN THE NEUROGLOVASCULAR UNIT

Despite being originally described as "brain glue," established functions of glia nowadays suggest an active role in brain function and information processing (reviewed in Allen and Barres, 2009). Together with neurons, glial cells work in concert with vascular and blood cells to establish the neurovascular unit, which should better be called the neurogliovascular unit (**Figure 1**). The concept of a neurogliovascular unit has been central in exploring improved strategies and approaches to treat stroke patients (reviewed in Berezowski et al., 2012; Kur et al., 2012).

Astrocytes are involved in key aspects of the nervous tissue including preservation of blood-brain barrier (BBB) integrity,

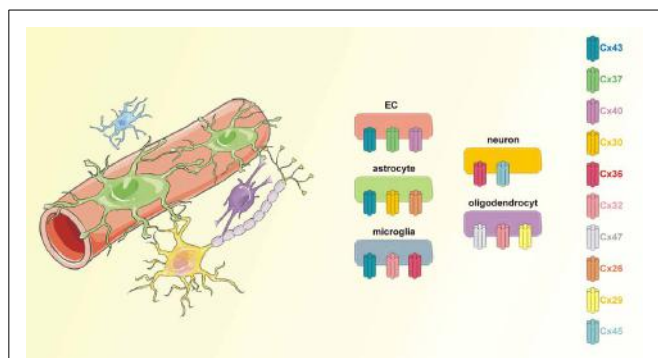


**FIGURE 1 | Connexins in the neurogliovascular unit.** The neurogliovascular unit is a functional unit in which astrocytes are centrally involved. Astrocytic endfeet are tightly associated with endothelial cells that form the BBB while at their other site, astrocytes contact pre- and postsynaptic neuronal membranes. Additionally, astrocytes may contact other glial cells like microglia and oligodendrocytes. Each of the cell types in the neurogliovascular unit is endowed with a set of connexins proteins. Importantly, Cx43 is present in astrocytes as well as in BBB endothelial cells and microglial cells.

modulation of blood supply, maintenance of brain homeostasis, myelination, and neurotransmission. The combined ablation of Cx30 and Cx43, which results in coupling-deficient astrocytes, lowers the threshold for epileptiform events (Theis et al., 2003; Wallraff et al., 2006), alters astrocyte energy metabolism (Rouach et al., 2008), gives rise to swollen astrocytic endfeet (Ezan et al., 2012) and leads to parenchymal vacuolation (Lutz et al., 2012). Astrocyte-targeted deletion of Cx43 severely reduces cell–cell coupling although it is not completely abolished, likely due to compensatory actions of Cx30 (Theis et al., 2003; Wallraff et al., 2006; Unger et al., 2012). Astrocyte-specific Cx43-ablated mice have been shown to exhibit reduced motor performance (Frisch et al., 2003), similar to ODDD patients suffering from cerebellar ataxia; yet, astrocyte-targeted deletion of Cx43 does not affect viability or astrocyte morphology nor does it cause neurodegeneration or astrogliosis (Theis et al., 2003). Conclusions from knock-out studies should be drawn with caution, as recent work in the heart has indicated that transgenic animals with a 5 amino acid deletion of the Cx43 CT have a much stronger cardiac phenotype than those with a complete deletion of the CT (Lubkemeier et al., 2013). In addition, mice missing one copy of the Cx43 allele do not mimic ODDD (Paznekas et al., 2009).

Below we describe how aberrant astrocytic signaling, due to defective Cx43, may contribute to ODDD-linked neurological symptoms.

#### Connexins and astrocytes contribute to blood-brain barrier function

Proper electrical signaling in the CNS requires a strict composition of the microenvironment around synapses and axons. The composition of the brain interstitial fluid is largely maintained by capillary endothelial cells that constitute the blood-brain barrier (BBB) and that survey solute diffusion in and out the brain (a highly comparable barrier is present between the capillaries and nervous tissue in the spinal cord). Astrocytic endfeet nearly

completely enwrap these capillary endothelial cells, inducing and maintaining barrier properties. Cx43 may contribute to astrocyte maintenance of the endothelial barrier, as mice lacking Cx30 and astrogial Cx43 have a weakened BBB that is more vulnerable to hydrostatic vascular pressure and shear stress but that is otherwise intact in the absence of a pathological insult (Ezan et al., 2012; Lutz et al., 2012). It is not known whether this is mediated by the Cx protein itself or by an effect related to GJs or HCs. It is equally unknown whether a putative GJ involvement would be limited to GJs between astrocytic endfeet or between endfeet and endothelial cells. *In vitro* evidence has suggested astrocyte–endothelial communication via GJs (as well as HCs) (reviewed in Braet et al., 2001), but *in vivo* evidence argues against this possibility (Simard et al., 2003).

In a first approximation, it is conceivable that Cx43 mutations that result in a trafficking defect or loss of channel function may give similar manifestations as Cx43 silencing. BBB leakage enables the entry of potentially neurotoxic, circulating compounds that directly affect neuronal survival, but also gives rise to inflammation, edema and hypoxia, which will ultimately result in additional injury to the neural tissue. At the same time, the ionic homeostasis of the brain's interstitial compartment becomes disturbed, particularly the increased K<sup>+</sup> concentration will interfere with action potential propagation and synaptic transmission. Additionally, influx of albumin and other circulating compounds can cause astrogliosis, characterized by the upregulation of GFAP (glial fibrillary acidic protein), astrocyte swelling and proliferation (David et al., 2009; Das et al., 2012), and promote extracellular K<sup>+</sup> accumulation by indirect effects (Ivens et al., 2007; Janigro, 2012), favoring seizure activity by mechanisms described below.

#### Connexins and astrocytes control nutrient supply to the nervous tissue

While astrocytic endfeet contact the BBB endothelium and its associated basement membrane at one side, at the other end, astrocytic processes project toward pre- and postsynaptic neuronal membranes forming the “tripartite synapse” (Allen and Barres, 2009). Here, astrocytes exert homeostatic control over neural network excitability: they provide neurons with energy and substrates for neurotransmission while removing excessive neurotransmitters and K<sup>+</sup> from the extracellular space by spatial buffering and siphoning. As such, neurons are protected from energy deprivation, large depolarisations and hyperexcitation that would eventually lead to neuronal death.

Astrocytes control blood flow and nutrient (oxygen and glucose) supply to those regions where neuronal activity is high by a process termed functional hyperemia or neurovascular coupling that acts at the level of cerebral arterioles and possibly also pericytes (Zonta et al., 2003 and reviewed in Iadecola and Nedergaard, 2007; Attwell et al., 2010; Petzold and Murthy, 2011). Unlike peripheral arterioles where the vasomotor response is propagated along smooth muscle cells, these do not seem to play a role in the regulation of blood flow in the CNS. Indeed, Xu et al. (2008) have shown that selective astrocyte death abolishes vasodilation despite the continued presence of viable smooth muscle cells (Xu et al., 2008). Although less documented, the

vasomodulatory action of astrocytes can also imply a vasoconstriction (Mulligan and MacVicar, 2004; Metea and Newman, 2006; Filosa and Blanco, 2007; Gordon et al., 2008). Candidate astrocyte messengers mediating the vasomotor response include  $K^+$  as well as gliotransmitters (glutamate, ATP, adenosine, and NO) and arachidonic acid metabolites (reviewed in Mulligan and MacVicar, 2004; Koehler et al., 2006; Iadecola and Nedergaard, 2007; Attwell et al., 2010). A Cx43 mimetic peptide that prevents both HC opening and GJIC, has been shown to prevent neurovascular coupling (Xu et al., 2008); however, it remains to be established exactly how Cx channels contribute to neurovascular coupling. Likely, Cx channels mediate the propagation of ICWs between astrocytes, possibly spreading the vasomotor response. Increased blood flow in local parenchymal capillaries requires for example an upstream vasodilation in arterioles and pial vessels, which might be communicated by Cx-based astrocytic ICWs. ICWs rely on both a direct communication of  $Ca^{2+}$  mobilizing messengers mediated by GJs and an paracrine route involving the release of a  $Ca^{2+}$  mobilizing messenger in the extracellular space (Leybaert and Sanderson, 2012). Astrocytic  $Ca^{2+}$  changes play a key role in neurovascular coupling (Takano et al., 2006), with rises in  $[Ca^{2+}]_i$  along the path of the  $Ca^{2+}$  wave enabling the release of vasoactive messengers (Zonta et al., 2003; Mulligan and MacVicar, 2004). Additionally, HCs may provide a release pathway for vasoactive substances, yet this remains to be determined. Defective GJIC or HC responses are expected to disable ICWs and neurovascular coupling, resulting in a relative oxygen and glucose shortage during neuronal activity that may lead to convulsions and, on a longer term, to neuronal cell death. Chronically disturbed neurovascular coupling may lead to neurodegeneration (Zlokovic, 2011; Lasta et al., 2013) and this may be a possible mechanism at the basis of the motor deficiencies observed in ODDD patients.

#### **Connexins and astrocyte modulation of synaptic transmission**

Neuronal action potential firing is always accompanied by an increase of  $K^+$  levels in the extracellular space. Astrocytes buffer these excessive  $K^+$  ions through inward rectifier  $K^+$  channels (Kir4.1) aided by  $Na^+/K^+$  pump activity and passive uptake with water through aquaporin 4 channels. Altered activity of both  $K^+$  channels and  $Na^+$  channels in the astrocyte PM are considered pro-epileptic (D'Ambrosio, 2004). Subsequently,  $K^+$  is redistributed over networks of GJ-connected astrocytes (reviewed in Carlen, 2012; Steinhauser and Seifert, 2012). Like  $K^+$ , glutamate, the brain's major excitatory neurotransmitter, is taken up and diluted in those astrocytic networks during synaptic activity, keeping its levels in the synaptic cleft low and sheltering neurons from excitotoxic injury. Inside the astrocytes, glutamate is converted to glutamine that is shuttled back to presynaptic nerve terminals where it is reconverted to glutamate. Disturbed redistribution of glutamate and  $K^+$  in the astrocytic networks, via GJ loss or abnormal GJ channel gating and permselectivity, may lead to a local accumulation of both substances, paving the way for epileptic seizure activity (reviewed in Pannasch et al., 2011). The swelling of astrocytes may additionally result in a decreased extracellular space volume further increasing ambient concentrations of  $K^+$  and glutamate sensed by neurons. Reduced expression of

Cx43 has been shown to increase expression of glutamate transporters (Unger et al., 2012), likely as a means to compensate the inadequate uptake of glutamate form the extracellular environment; its functional implications are, however, unknown. Also note that the clearance and redistribution of  $K^+$  is partially maintained in the hippocampus when Cx43 and Cx30 expression is silenced in astrocytes (Wallraff et al., 2006), indicating that mechanisms other than those related to astrocytic Cxs contribute to spatial buffering.

More than just exerting homeostatic control over the extracellular compartment, astrocytes are now considered to also more actively contribute to synaptic transmission, by responding to neuronal activity and releasing gliotransmitters. Individual astrocytes can contact up to 140,000 synapses (Bushong et al., 2002) and express a plethora of neurotransmitter receptors that in most cases trigger an increase in  $[Ca^{2+}]_i$ . In response to this, they release gliotransmitters that include glutamate, D-serine, ATP, adenosine, and GABA of which neurones on their turn express receptors (Perea and Araque, 2010; Orellana et al., 2011; Pannasch et al., 2012). HCs composed of Cx43 may well-contribute to gliotransmitter release as a  $[Ca^{2+}]_i$ -controlled diffusive pathway: HCs open with a  $[Ca^{2+}]_i$  increase up to 500 nM and close again at higher concentrations (see Cx43 Mutations Located in the Cytoplasmic Loop). Stehberg and co-workers have tested the hypothesis of gliotransmitter release via HC opening by making use of an inhibitory peptide (L2 peptide) that specifically targets Cx43 HCs without inhibiting Cx43 GJs (Ponsaerts et al., 2010). This work, performed *in vivo*, demonstrated that stereotactic injection of this peptide (coupled to a TAT-translocation motif) in the basolateral amygdala, blocked the consolidation of fear memory while addition of a cocktail of putative gliotransmitters rescued the L2-mediated inhibition of fear memory consolidation (Stehberg et al., 2012). Besides being activated by a moderate  $[Ca^{2+}]_i$  increase, HCs are also activated by a lowering of extracellular  $Ca^{2+}$ . Extracellular  $Ca^{2+}$  can decrease as a result of neuronal activity and Nedergaard and co-workers have recently demonstrated that this may trigger astrocytic HC opening with consequent ATP release (Torres et al., 2012). The latter was demonstrated to activate inhibitory interneurons that put a brake on excitatory firing (Torres et al., 2012). Additionally, adenosine, derived from ATP degradation, has anticonvulsant effects as it inhibits presynaptic neurotransmitter release (Pascual et al., 2005). Overall, HC activation in astrocytes may thus contribute to gliotransmitter release, but with the evidence presently available, this may lead to excitatory as well as inhibitory signaling.

The contribution of Cx channels to ictogenesis has an ambiguous, two-faced aspect: on the one hand GJs have an anticonvulsive effect with respect to their  $K^+$  and glutamate buffering capacity, but on the other hand, GJs may act in a pro-convulsive way as well. In this respect, Cx43 gene ablation or pharmacological block of GJs reduced seizure activity while agents that potentiate cell-cell coupling enhanced neuronal bursting (Kohling et al., 2001; Wallraff et al., 2006; Yoon et al., 2010). Mechanistically, neuron-derived glutamate may trigger a  $[Ca^{2+}]_i$  increase in astrocytes that further stimulates glutamate release from these cells. The  $Ca^{2+}$  signal can propagate to neighboring

astrocytes in the form of an intercellular  $\text{Ca}^{2+}$  wave, modulating groups of remotely located synapses and inducing a hyperexcited  $[\text{Ca}^{2+}]_i$  state over the entire astrocyte network (Giaume, 2010). Additionally, astrocyte GJs provide an intercellular route for the supply of energy substrates like glucose and lactate that are required for neuronal activity (Rouach et al., 2008). Once the astrocytic distribution of these substrates is compromised, energy delivery may become below demand, causing the accumulation of glutamate and  $\text{K}^+$  that may act in a pro-convulsive manner. Finally, both GJs and HCs have been implicated in the spread of apoptosis between astrocytes (Nodin et al., 2005; Eugenin and Berman, 2007; Decrock et al., 2009) which may well-break ground for epileptic seizures (Briellmann et al., 2002; Willoughby et al., 2003; Kang et al., 2006). With respect to HCs, Cx43 mutations giving a gain of HC function (I31M, G143S, and G138R) are, theoretically, expected to result in increased neuronal cell death, caused by excessively elevated neuronal  $[\text{Ca}^{2+}]_i$  (reviewed in Bennett et al., 2012). However, up to date, none of these gain-of-function mutants has been associated with epileptic seizures in ODDD patients (Abrams and Scherer, 2012). On the other hand, some mutants that result in a loss of HC function (L90V and I130T) are also associated with epileptic seizure activity which may result from a decrease in ATP release and consequent inhibitory signaling. At this stage, it is not clear what the net effect of an astrocytic HC contribution would be on excitability and ictogenesis but it emerges that the involvement of HCs in ictogenesis is, like for GJs, a double-edged sword. The use of novel tools such as the Gap19 peptide (Wang et al., 2013a) and the L2 peptide (Ponsaerts et al., 2010; Stehberg et al., 2012) may shed more light on the role of HCs in the healthy or pathological brain. In comparison to non-specific Cx channel blockers and peptides like Gap26/Gap27, L2/Gap19 peptides specifically block HCs composed of Cx43 (but not those composed of Cx40 and Panx1) while not blocking GJs.

When looking over the currently available evidence for ODDD-associated epilepsy, seizures have been reported in patients exhibiting mutants that give both dysfunctional HCs and GJs (**Table 2**); the loss of efficient  $\text{K}^+$  and glutamate buffering and inadequate nutrient supply may thus play a primary role in the appearance of an epileptic phenotype in ODDD, although this requires further research. Epilepsy has thus far not been reported for mutants with a gain of HC function.

**Table 2 | List of ODDD-linked mutations associated with epileptic seizures and their effect on Cx43 HCs and GJs.**

Mutant	PM presence and plaque formation	GJIC	HC function
G2fs	n.a.	n.a.	n.a.
R76S	Normal presence in PM	X	n.a.
L90V	Normal GJ plaques	↓	X
I130T	Increased presence in PM but reduced number of GJ plaques	↓	X

n.a., no data available.

X, absence of detectable GJIC or HC activity.

### Connexins and astrocyte-oligodendrocyte interactions involved in axonal myelination

As a last example of the astrocytic contribution to normal CNS function we highlight the role of astrocytes in axonal myelination. Astrocytes themselves do not produce myelin, but they are connected to oligodendrocytes, the brain's myelinating cells, via Cx43/Cx47 GJs (Orthmann-Murphy et al., 2007). Loss-of-function mutations in the Cx47 gene (*GJA12/GJC2*) lie at the basis of Pelizaeus-Merzbacher-like disease (PMLD1), an early onset, progressive dysmyelinating disorder affecting the CNS, and are also known to cause a distinct form of late onset hereditary spastic paraparesis (SPG44). In both cases, Cx47 mutations prevent the formation of functional Cx47/Cx47 and Cx43/Cx47 GJs causing hypomyelinating leukoencephalopathy (Orthmann-Murphy et al., 2007, 2009). The role of astrocyte-oligodendrocyte GJs is unclear but possibly relates to  $\text{K}^+$  shunting between both cell types. Although astrocytes and oligodendrocytes are also connected through Cx30/Cx32 GJs, these do not seem to compensate for the loss of Cx43/Cx47 coupling, probably as a consequence of differences in conductance, gating, and permeability (Orthmann-Murphy et al., 2007). We expect that spasticity observed with ODDD is similarly related to non-functional Cx43/Cx47 GJs caused by mutations in the *GJA1* gene; however, there are, to our knowledge, no records that address astrocyte-oligodendrocyte coupling with ODDD-linked Cx43 mutants. The observation of a severe downregulation of astrocytic Cx43 in demyelinating lesions of patients suffering from Baló's disease, a disorder characterized by astrocytopathy and demyelination (Masaki et al., 2012), may give credit to the hypothesis that aberrant Cx43 function in astrocytes results in anomalous axonal myelination.

Finally, the retention of processed or unprocessed Cx43 protein can cause glial cell death through a process known as the “unfolded protein response” or through ER stress (reviewed by Roussel et al., 2013). The unfolded protein response and ER stress have been implicated in different neurodegenerative diseases, including those with progressive motor dysfunction (Huntington's disease, amyotrophic lateral sclerosis) as observed in ODDD as well.

### IMPLICATIONS OF ODDD-LINKED MUTATIONS IN CNS CELLS OTHER THAN ASTROCYTES BBB-ECS

The role of Cxs, including Cx43, in BBB endothelial cells is only starting to emerge. Endothelial GJs have been implicated in maintenance of the interendothelial junctional complex (Nagasawa et al., 2006) and more recently, we have shown that  $\text{Ca}^{2+}$  dynamics triggered by low extracellular  $\text{Ca}^{2+}$  or inflammatory substances were sustained by GJs and HCs and contributed to disturbed BBB function and increased permeability (De Bock et al., 2011, 2012, 2013). Additionally, work from others has indicated that Cx43 HCs contribute to endothelial cell loss during pathologic insults (Danesh-Meyer et al., 2012). The effect of a Cx43 loss-of-function has not been studied at the level of the BBB, although one might expect a dysfunctional barrier due to a disorganisation of the junctions. On the other hand, following the observation that HCs contribute to increasing permeability, those

mutants exhibiting increased HC activity are expected to render the BBB leaky to circulating compounds. The implications of such a leaky BBB have been outlined above.

### Neurons

Cx43 is not expressed in adult neurons but it is prominently present in neuroblast cells where its role in embryonic development of the cortex becomes more and more acknowledged. Radial glial cells, the neuronal stem cells of the embryonic cerebral cortex, originate in the ventricular zone and differentiate into neuronal cells as the neocortex forms. These neuronal cells subsequently migrate to their final destination in the cortical plate. Additionally, radial glia give rise to radial fibers that form a guidance scaffold for neuronal migration. Cx43 can be found in the neuronal progenitors (or neuroblasts) as well as in the glial scaffold. Expression of the Cx43-T154A mutant that is able to make adhesions but is unable to form functional GJ channels in the developing cortex did not abolish the migration of new born neurons, but expression of the Cx43-C61S mutant that lacks docking ability (with maintained HC function) did prevent migration of new neurons. These observations suggested that channel activity does not play a role but Cxs are involved as adhesive contact points between the scaffold and the migrating neurones (Elias et al., 2007). More recently, it was shown that conditional Cx43 knock-out in radial glia disrupts neuronal migration, and this could be rescued by expression of full-length Cx43 but not by expression of CT-truncated Cx43 (removal of the last 125 residues) (Cina et al., 2009). These findings indicate that the C-terminal tail, which is known to interact with scaffolding proteins like ZO-1 and cytoskeletal tubulin (Giepmans et al., 2001), crucially links adhesive Cx43 properties to the cytoskeleton. Cx43 additionally co-localizes with proteins specialized in cell adhesion to neighboring cells or to the extracellular matrix (Nagasaki et al., 2006; Li et al., 2010; Sato et al., 2011). Although both studies suggest that the Cx43 channel pore has no function in neuronal migration, other studies have indicated that Cx43 HCs and GJs play a role in the initiation and propagation of  $\text{Ca}^{2+}$  signals in and between neuronal precursor cells respectively. These  $\text{Ca}^{2+}$  signals are likely to play a role in neuronal proliferation. Blocking HCs/GJs reduced neuronal motility, likely by interfering with Rho-GTPase activity, and gave rise to defective neurogenesis (Weissman et al., 2004; Liu et al., 2008, 2010). Cx43 knock-out mice generally do not present with a severely distorted cortex which might be explained by the fact that other Cxs like Cx30 or Cx26 contribute to neuronal migration (Elias et al., 2007), compensating for the loss of Cx43. One mouse strain that lacks Cx43 in embryonic radial glia, termed Shuffler, mimics part of the neuronal phenotype observed in ODDD (gait disturbance and ataxia). The mice exhibit structural abnormalities in the cerebellum, hippocampus and cortex which can explain the neuronal deficits. Importantly, the phenotype of these mice differs from other Cx43 knock-out mice strains in which no neurological phenotype was observed, suggesting that the genetic background is an important determinant of the occurrence of neurological symptoms (Wiencken-Barger et al., 2007). Such effect may apply for humans as well and might account for the rather low prevalence of neurological manifestations in ODDD patients.

### Microglia

Microglial cells are the resident innate immune effector cells of the CNS and are essential in the primary defense against pathologic insults. Resting amoeboid microglia continuously scan the nervous tissue and rapidly respond to inflammatory molecules, pathogens or tissue injury by transforming into ramified cells that exhibit a high rate of proliferation and migration (reviewed in Kettenmann et al., 2011). Their activation involves the release of pro-inflammatory cytokines, free radicals and glutamate (Candelario-Jalil et al., 2007; Sumi et al., 2010; Takeuchi et al., 2011) which are all generally believed to be neurotoxic. Indeed, microglial activation is observed in many neurodegenerative diseases including Alzheimer's disease, Parkinson's disease, Huntington's disease, and amyotrophic lateral sclerosis (Orellana et al., 2009) as well as in epilepsy (reviewed in Mirrione and Tsirka, 2011; Vezzani et al., 2012). In addition to direct neurotoxic effects, cytokines and other molecules released by microglia may inhibit GJIC between astrocytes (Meme et al., 2006) while stimulating HCs (Retamal et al., 2007), or activate BBB endothelial cells (Orellana et al., 2009), further contributing to neurodegeneration and epilepsy via mechanisms described above. However, in certain scenarios, microglia may also contribute to CNS repair through scavenging of reactive oxygen species, the release of neurotrophic factors and the removal of neurotoxic substances (Rouach et al., 2004, reviewed in Mika and Prochnow, 2012; Aguzzi et al., 2013). The role of Cx43 in the CNS' immune cells is uncertain. Whereas some groups find no indication for the presence of microglial Cx43 in the resting or ramified state

**Table 3 | List of ODDD mutations linked to upper motor neuron dysfunction, tremor, gait disturbances, and spasticity, indicating neurodegeneration.**

Mutant	PM presence and plaque formation	GJIC	HC function
D3N	Normal number of plaques	↓	n.a.
Y17S	Reduced presence in PM with reduced number of GJ plaques	X	X
G21R	Reduced number of GJ plaques	X	X
K23T	Normal GJ plaques	n.a.	n.a.
R33X	Not present in PM	X	X
A40V	Reduced number of GJ plaques	X	X
L90V	Normal GJ plaques	↓	X
H95R	n.a.	n.a.	n.a.
L106P	n.a.	n.a.	n.a.
L113P	n.a.	n.a.	n.a.
I130T	Increased presence in PM but reduced number of GJ plaques	↓	X
K134E/N	Reduced number of GJ plaques	↓	X
G138R	Increased presence in PM with normal number of GJ plaques	X	↑
T154A/N	Normal number of GJ plaques	↓	n.a.
V216L	Reduced number of GJ plaques	↓	n.a.

n.a., no data available.

X, absence of detectable GJIC or HC activity.

(Dobrenis et al., 2005; Theodoric et al., 2012), others do report an increase in microglial Cx43 in inflammatory conditions (Eugenin et al., 2001; Garg et al., 2005; Shaikh et al., 2012). HCs have been implicated in glutamate release which could contribute to neuronal/astrocyte cell death and epilepsy (Ye et al., 2003; Takeuchi et al., 2008). In addition, dye coupling between microglial cells has been observed upon exposure to inflammatory conditions (Eugenin et al., 2001; Martinez et al., 2002). The functional implications of this activation-dependent microglial coupling remain unclear. Similar as in peripheral immune cells where Cx43 levels increase during inflammation, GJs could be involved in the cell–cell transfer of immunogens, rendering antigen cross-presentation more efficient (Neijissen et al., 2005). Altogether, altered Cx43 expression/channel function could disturb the proper microglial response to inflammation, failing in the defense against neurodegenerative mediators but contributing to neuronal bursting activity.

## CONCLUSIONS

ODDD manifests as a pleiotropic disease with patients exhibiting both morphological and functional deficiencies caused by mutations in the widespread *GJA1* gene. The *GJA1* gene product Cx43 plays a leading role in CNS physiology and it thus comes with no surprise that neurological symptoms are included in the still expanding list of ODDD features. Analysis of the different mutants demonstrates that they can either alter insertion of Cx43 in the PM, GJ channel formation or HC/GJ channel gating. All CNS cells expressing aberrant Cx43 are potential contributors to nervous tissue dysfunction or damage, with a major involvement of astrocytes as the prime cell type expressing Cx43. In this paper we gave an overview of those mutants associated with nervous tissue dysfunction along with their outcome on Cx43 function. The information currently available on the possible effects of ODDD-linked mutations on Cx43 expression/channel function is impressive, as can be appreciated from **Table 1**. However, there is still a paucity of reports that document and analyze the mechanism by which the mutants give the neurological phenotype in a detailed manner. Thus, it remains difficult to present a clear genotype/phenotype correlation. None of the mutants identified thus far have been characterized for their specific effect on the function of astrocytes or other cells of the neuroglial vascular unit, and therefore, genotype/phenotype linkage still remains in the realm of speculation. ODDD is, with a few exceptions, subject to an autosomal dominant inheritance pattern but unfortunately,

thus far, there is no clear hypothesis that explains this pattern. Having one dysfunctional allele may cause a CNS phenotype in ODDD while in homozygous astrocyte-specific Cx43 knock-out animals no severe alterations are observed (Theis et al., 2003). This observation may plead in favor for a dominant negative effect of mutant Cx43 on co-expressed WT Cx43 protein. Most of the Cx43 mutants exhibit dominant negative effects, but a comparison of dominant negative mutants and neurological phenotypes is unfortunately inconclusive. The dominant negative effect of Cx43 mutants does not guarantee neurological findings (see for instance L11P and S18P) while mutants that do not exert a dominant effect may give a severe neurological phenotype (I130T). Trans-dominant negative effects of the mutants on other co-expressed Cxs are another likely explanation. Such effects have for instance been used to explain the dominant expression pattern of syndromic deafness caused by *GJB2* (Cx26) mutations (reviewed in Laird, 2008). On the other hand, loss-of-function mutations of Cx26 and Cx30 have thus far not been associated with neuropathology (Abrams and Scherer, 2012). In the heart, Cx43-R33X mutants exert trans-dominant effects on Cx37 and Cx40 (Huang et al., 2013), whereas G138R does not (Dobrowolski et al., 2008). Unfortunately, we are not aware of any studies tackling this question with regards to the CNS. The (trans-)dominant effect of Cx43 mutants may additionally be cell type specific as the mouse G60S mutant has dominant negative effects on WT Cx43 in ovarian granulosa cells (Flenniken et al., 2005) but not in astrocytes (Wasseff et al., 2010). Finally, as illustrated in **Table 2**, epilepsy seems to be associated with loss of function ODDD mutants. We carefully checked this for motor deficiencies (**Table 3**) and found that a motor phenotype is always associated with mutants that give a loss or reduction of GJs, while the mutant's effects on HC function are variable. This generates a number of interesting working hypotheses that are open to be tested, hopefully strengthening our understanding of how ODDD mutants lead to channelopathy, CNS cell dysfunction and neurodegeneration.

## ACKNOWLEDGMENTS

This work was supported by the Fund for Scientific Research Flanders (FWO—grant numbers G.0354.07, G.0140.08 and 3G.0134.09 to Luc Leybaert) and the Interuniversity Attraction Poles Program (Belgian Science Policy Projects P6/31 and P7/10 to Luc Leybaert). **Figure 1** was produced using Servier medical art.

## REFERENCES

- Abrams, C. K., and Scherer, S. S. (2012). Gap junctions in inherited human disorders of the central nervous system. *Biochim. Biophys. Acta* 1818, 2030–2047. doi: 10.1016/j.bbamem.2011.08.015
- Aguzzi, A., Barres, B. A., and Bennett, M. L. (2013). Microglia: scapegoat, saboteur, or something else? *Science* 339, 156–161. doi: 10.1126/science.1227901
- Alao, M. J., Bonneau, D., Holder-Espinasse, M., Goizet, C., Manouvrier-Hanu, S., Mezel, A., et al. (2010). Oculo-dento-digital dysplasia: lack of genotype–phenotype correlation for *GJA1* mutations and usefulness of neuro-imaging. *Eur. J. Med. Genet.* 53, 19–22. doi: 10.1016/j.ejmg.2009.08.007
- Alexander, D. B., and Goldberg, G. S. (2003). Transfer of biologically important molecules between cells through gap junction channels. *Curr. Med. Chem.* 10, 2045–2058. doi: 10.2147/0929867033456927
- Allen, N. J., and Barres, B. A. (2009). Neuroscience: glia – more than just brain glue. *Nature* 457, 675–677. doi: 10.1038/457675a
- Amador, C., Mathews, A. M., Del Carmen Montoya, M., Laughridge, M. E., Everman, D. B., and Holden, K. R. (2008). Expanding the neurologic phenotype of oculodentodigital dysplasia in a 4-generation Hispanic family. *J. Child Neurol.* 23, 901–905. doi: 10.1177/0883073808317730
- Amano, K., Ishiguchi, M., Aikawa, T., Kimata, M., Kishi, N., Fujimaki, T., et al. (2012). Cleft lip in oculodentodigital dysplasia suggests novel roles for connexin43. *J. Dent. Res.* 91, 38S–44S. doi: 10.1177/0022034512447952
- Anumonwo, J. M., Taffet, S. M., Gu, H., Chanson, M., Moreno, A. P., and Delmar, M. (2001). The carboxyl terminal domain regulates the unitary conductance and voltage dependence of connexin40 gap junction

- channels. *Circ. Res.* 88, 666–673. doi: 10.1161/hh0701.088833
- Attwell, D., Buchan, A. M., Charpak, S., Lauritzen, M., Macvicar, B. A., and Newman, E. A. (2010). Glial and neuronal control of brain blood flow. *Nature* 468, 232–243. doi: 10.1038/nature09613
- Avila, M. A., Sell, S. L., Hawkins, B. E., Hellmich, H. L., Boone, D. R., Crookshanks, J. M., et al. (2011). Cerebrovascular connexin expression: effects of traumatic brain injury. *J. Neurotrauma* 28, 1803–1811. doi: 10.1089/neu.2011.1900
- Avshalumova, L., Fabrikant, J., and Koriakos, A. (2013). Overview of skin diseases linked to connexin gene mutations. *Int. J. Dermatol.* doi: 10.1111/ijd.12062. [Epub ahead of print].
- Bao, X., Chen, Y., Reuss, L., and Altenberg, G. A. (2004). Functional expression in *Xenopus* oocytes of gap-junctional hemichannels formed by a cysteine-less connexin 43. *J. Biol. Chem.* 279, 9689–9692. doi: 10.1074/jbc.M311438200
- Bargiolas, P., Monyer, H., and Schwaninger, M. (2009). Hemichannels in cerebral ischemia. *Curr. Mol. Med.* 9, 186–194. doi: 10.2174/156652409787581646
- Batra, N., Kar, R., and Jiang, J. X. (2012). Gap junctions and hemichannels in signal transmission, function and development of bone. *Biochim. Biophys. Acta* 1818, 1909–1918. doi: 10.1016/j.bbamem.2011.09.018
- Beahm, D. L., Oshima, A., Gaietta, G. M., Hand, G. M., Smock, A. E., Zucker, S. N., et al. (2006). Mutation of a conserved threonine in the third transmembrane helix of alpha- and beta-connexins creates a dominant-negative closed gap junction channel. *J. Biol. Chem.* 281, 7994–8009. doi: 10.1074/jbc.M506533200
- Beltramello, M., Piazza, V., Bukauskas, F. F., Pozzan, T., and Mammano, F. (2005). Impaired permeability to Ins(1,4,5)P<sub>3</sub> in a mutant connexin underlies recessive hereditary deafness. *Nat. Cell Biol.* 7, 63–69. doi: 10.1038/ncb1205
- Bennett, M. V., Garre, J. M., Orellana, J. A., Bukauskas, F. F., Nedergaard, M., and Saez, J. C. (2012). Connexin and pannexin hemichannels in inflammatory responses of glia and neurons. *Brain Res.* 1487, 3–15. doi: 10.1016/j.brainres.2012.08.042
- Berezowski, V., Fukuda, A. M., Cecchelli, R., and Badaut, J. (2012). Endothelial cells and astrocytes: a concerto en duo in ischemic pathophysiology. *Int. J. Cell Biol.* 2012, 176287. doi: 10.1155/2012/176287
- Braet, K., Paemeleire, K., D'Herde, K., Sanderson, M. J., and Leybaert, L. (2001). Astrocyte-endothelial cell calcium signals conveyed by two signalling pathways. *Eur. J. Neurosci.* 13, 79–91. doi: 10.1046/j.jneuro.2001.01372.x
- Brice, G., Ostergaard, P., Jeffery, S., Gordon, K., Mortimer, P., and Mansour, S. (2013). A novel mutation in GJA1 causing oculodentodigital syndrome and primary lymphoedema in a three generation family. *Clin. Genet.* doi: 10.1111/cge.12158. [Epub ahead of print].
- Briellmann, R. S., Kalnins, R. M., Berkovic, S. F., and Jackson, G. D. (2002). Hippocampal pathology in refractory temporal lobe epilepsy: T2-weighted signal change reflects dentate gliosis. *Neurology* 58, 265–271. doi: 10.1212/WNL.58.2.265
- Bruzzone, R., White, T. W., and Paul, D. L. (1996). Connections with connexins: the molecular basis of direct intercellular signaling. *Eur. J. Biochem.* 238, 1–27. doi: 10.1111/j.1432-1033.1996.0001q.x
- Bukauskas, F. F., Jordan, K., Bukauskene, A., Bennett, M. V., Lampe, P. D., Laird, D. W., et al. (2000). Clustering of connexin 43-enhanced green fluorescent protein gap junction channels and functional coupling in living cells. *Proc. Natl. Acad. Sci. U.S.A.* 97, 2556–2561. doi: 10.1073/pnas.050588497
- Bukauskas, F. F., and Verselis, V. K. (2004). Gap junction channel gating. *Biochim. Biophys. Acta* 1662, 42–60. doi: 10.1016/j.bbamem.2004.01.008
- Bushong, E. A., Martone, M. E., Jones, Y. Z., and Ellisman, M. H. (2002). Protoplasmic astrocytes in CA1 stratum radiatum occupy separate anatomical domains. *J. Neurosci.* 22, 183–192.
- Candelario-Jalil, E., de Oliveira, A. C., Graf, S., Bhatia, H. S., Hull, M., Munoz, E., et al. (2007). Resveratrol potently reduces prostaglandin E2 production and free radical formation in lipopolysaccharide-activated primary rat microglia. *J. Neuroinflammation* 4, 25. doi: 10.1186/1742-2094-4-25
- Carlen, P. L. (2012). Curious and contradictory roles of glial connexins and pannexins in epilepsy. *Brain Res.* 1487, 54–60. doi: 10.1016/j.brainres.2012.06.059
- Chew, S. S., Johnson, C. S., Green, C. R., and Danesh-Meyer, H. V. (2010). Role of connexin43 in central nervous system injury. *Exp. Neurol.* 225, 250–261. doi: 10.1016/j.expneurol.2010.07.014
- Churko, J. M., Shao, Q., Gong, X. Q., Swoboda, K. J., Bai, D., Sampson, J., et al. (2011). Human dermal fibroblasts derived from oculodentodigital dysplasia patients suggest that patients may have wound-healing defects. *Hum. Mutat.* 32, 456–466. doi: 10.1002/humu.21472
- Cina, C., Maass, K., Theis, M., Willecke, K., Bechberger, J. F., and Naus, C. C. (2009). Involvement of the cytoplasmic C-terminal domain of connexin43 in neuronal migration. *J. Neurosci.* 29, 2009–2021. doi: 10.1523/JNEUROSCI.5025-08.2009
- Civitelli, R. (2008). Cell-cell communication in the osteoblast/osteocyte lineage. *Arch. Biochem. Biophys.* 473, 188–192. doi: 10.1016/j.abb.2008.04.005
- Contreras, J. E., Sanchez, H. A., Veliz, L. P., Bukauskas, F. F., Bennett, M. V., and Saez, J. C. (2004). Role of connexin-based gap junction channels and hemichannels in ischemia-induced cell death in nervous tissue. *Brain Res.* 1040, 290–303. doi: 10.1016/j.brainresrev.2004.08.002
- Cotrina, M. L., Kang, J., Lin, J. H., Bueno, E., Hansen, T. W., He, L., et al. (1998). Astrocytic gap junctions remain open during ischemic conditions. *J. Neurosci.* 18, 2520–2537.
- Cottrell, G. T., Lin, R., Warn-Cramer, B. J., Lau, A. F., and Burt, J. M. (2003). Mechanism of v-Src- and mitogen-activated protein kinase-induced reduction of gap junction communication. *Am. J. Physiol. Cell Physiol.* 284, C511–C520. doi: 10.1152/ajpcell.00214.2002
- D'Ambrosio, R. (2004). The role of glial membrane ion channels in seizures and epileptogenesis. *Pharmacol. Ther.* 103, 95–108. doi: 10.1016/j.pharmthera.2004.05.004
- Dahl, G., Werner, R., Levine, E., and Rabadian-Diehl, C. (1992). Mutational analysis of gap junction formation. *Biophys. J.* 62, 172–180. discussion: 180–172. doi: 10.1016/S0006-3495(92)81803-9
- Danesh-Meyer, H. V., Huang, R., Nicholson, L. F., and Green, C. R. (2008). Connexin43 antisense oligodeoxynucleotide treatment down-regulates the inflammatory response in an *in vitro* interphase organotypic culture model of optic nerve ischaemia. *J. Clin. Neurosci.* 15, 1253–1263. doi: 10.1016/j.jocn.2008.08.002
- Danesh-Meyer, H. V., Kerr, N. M., Zhang, J., Eady, E. K., O'Carroll, S. J., Nicholson, L. F., et al. (2012). Connexin43 mimetic peptide reduces vascular leak and retinal ganglion cell death following retinal ischaemia. *Brain* 135, 506–520. doi: 10.1093/brain/awr338
- Das, A., Wallace, G. C. 4th., Holmes, C., McDowell, M. L., Smith, J. A., Marshall, J. D., et al. (2012). Hippocampal tissue of patients with refractory temporal lobe epilepsy is associated with astrocyte activation, inflammation, and altered expression of channels and receptors. *Neuroscience* 220, 237–246. doi: 10.1016/j.neuroscience.2012.06.002
- David, Y., Cacheaux, L. P., Ivens, S., Lapilover, E., Heinemann, U., Kaufer, D., et al. (2009). Astrocytic dysfunction in epileptogenesis: consequence of altered potassium and glutamate homeostasis? *J. Neurosci.* 29, 10588–10599. doi: 10.1523/JNEUROSCI.2323-09.2009
- Davidson, J. O., Green, C. R., Nicholson, L. F., O'Carroll, S. J., Fraser, M., Bennet, L., et al. (2012). Connexin hemichannel blockade improves outcomes in a model of fetal ischemia. *Ann. Neurol.* 71, 121–132. doi: 10.1002/ana.22654
- De Bock, M., Culot, M., Wang, N., Bol, M., Decrock, E., De Vuyst, E., et al. (2011). Connexin channels provide a target to manipulate brain endothelial calcium dynamics and blood-brain barrier permeability. *J. Cereb. Blood Flow Metab.* 31, 1942–1957. doi: 10.1038/jcbfm.2011.86
- De Bock, M., Culot, M., Wang, N., da Costa, A., Decrock, E., Bol, M., et al. (2012). Low extracellular Ca<sup>2+</sup> conditions induce an increase in brain endothelial permeability that involves intercellular Ca<sup>2+</sup> waves. *Brain Res.* 1487, 78–87. doi: 10.1016/j.brainres.2012.06.046
- De Bock, M., Wang, N., Decrock, E., Bol, M., Gadicherla, A., Culot, M., et al. (2013). Endothelial calcium dynamics: connexin channels and blood brain barrier function. *Prog. Neurobiol.* 108, 1–20. doi: 10.1016/j.pneurobio.2013.06.001
- Decrock, E., De Vuyst, E., Vinken, M., Van Moorhem, M., Vranckx, K., Wang, N., et al. (2009). Connexin 43 hemichannels contribute to the propagation of apoptotic cell death in a rat C6 glioma cell model. *Cell Death Differ.* 16, 151–163. doi: 10.1038/cdd.2008.138
- Decrock, E., Krysko, D. V., Vinken, M., Kaczmarek, A., Crispino, G., Bol, M., et al. (2012). Transfer of IP(3) through gap junctions is critical,

- but not sufficient, for the spread of apoptosis. *Cell Death Differ.* 19, 947–957. doi: 10.1038/cdd.2011.176
- Desplantez, T., McCain, M. L., Beauchamp, P., Rigoli, G., Rothenthaler, B., Parker, K. K., et al. (2012). Connexin43 ablation in foetal atrial myocytes decreases electrical coupling, partner connexins, and sodium current. *Cardiovasc. Res.* 94, 58–65. doi: 10.1093/cvr/cvs025
- De Vuyst, E., Wang, N., Decrock, E., De Bock, M., Vinken, M., Van Moerhem, M., et al. (2009). Ca(2+) regulation of connexin 43 hemichannels in C6 glioma and glial cells. *Cell Calcium* 46, 176–187. doi: 10.1016/j.ceca.2009.07.002
- Dichter, M. A. (2009). Emerging concepts in the pathogenesis of epilepsy and epileptogenesis. *Arch. Neurol.* 66, 443–447. doi: 10.1001/archneurol.2009.10
- Dobrenis, K., Chang, H. Y., Pina-Benabou, M. H., Woodroffe, A., Lee, S. C., Rozental, R., et al. (2005). Human and mouse microglia express connexin36, and functional gap junctions are formed between rodent microglia and neurons. *J. Neurosci. Res.* 82, 306–315. doi: 10.1002/jnr.20650
- Dobrowski, R., Sasse, P., Schrickel, J. W., Watkins, M., Kim, J. S., Rackauskas, M., et al. (2008). The conditional connexin43G138R mouse mutant represents a new model of hereditary oculodentodigital dysplasia in humans. *Hum. Mol. Genet.* 17, 539–554. doi: 10.1093/hmg/ddm329
- Dobrowski, R., Sommershof, A., and Willecke, K. (2007). Some oculodentodigital dysplasia-associated Cx43 mutations cause increased hemichannel activity in addition to deficient gap junction channels. *J. Membr. Biol.* 219, 9–17. doi: 10.1007/s00232-007-9055-7
- Ek, J. F., Delmar, M., Perzova, R., and Taffet, S. M. (1994). Role of histidine 95 on pH gating of the cardiac gap junction protein connexin43. *Circ. Res.* 74, 1058–1064. doi: 10.1161/01.RES.74.6.1058
- Ek-Vitorin, J. F., and Burt, J. M. (2013). Structural basis for the selective permeability of channels made of communicating junction proteins. *Biochim. Biophys. Acta* 1828, 51–68. doi: 10.1016/j.bbamem.2012.02.003
- Ek-Vitorin, J. F., Calero, G., Morley, G. E., Coombs, W., Taffet, S. M., and Delmar, M. (1996). PH regulation of connexin43: molecular analysis of the gating particle. *Biophys. J.* 71, 1273–1284. doi: 10.1016/S0006-3495(96)79328-1
- Elias, L. A., Wang, D. D., and Kriegstein, A. R. (2007). Gap junction adhesion is necessary for radial migration in the neocortex. *Nature* 448, 901–907. doi: 10.1038/nature06063
- Eugenin, E. A., Basilio, D., Saez, J. C., Orellana, J. A., Raine, C. S., Bukauskas, F., et al. (2012). The role of gap junction channels during physiologic and pathologic conditions of the human central nervous system. *J. Neuroimmune Pharmacol.* 7, 499–518. doi: 10.1007/s11481-012-9352-5
- Eugenin, E. A., and Berman, J. W. (2007). Gap junctions mediate human immunodeficiency virus-bystander killing in astrocytes. *J. Neurosci.* 27, 12844–12850. doi: 10.1523/JNEUROSCI.4154-07.2007
- Eugenin, E. A., Eckardt, D., Theis, M., Willecke, K., Bennett, M. V., and Saez, J. C. (2001). Microglia at brain stab wounds express connexin 43 and *in vitro* form functional gap junctions after treatment with interferon-gamma and tumor necrosis factor-alpha. *Proc. Natl. Acad. Sci. U.S.A.* 98, 4190–4195. doi: 10.1073/pnas.051634298
- Ezan, P., Andre, P., Cisternino, S., Saubamea, B., Boulay, A. C., Doutremer, S., et al. (2012). Deletion of astroglial connexins weakens the blood-brain barrier. *J. Cereb. Blood Flow Metab.* 32, 1457–1467. doi: 10.1038/jcbfm.2012.45
- Falk, M. M. (2000). Cell-free synthesis for analyzing the membrane integration, oligomerization, and assembly characteristics of gap junction connexins. *Methods* 20, 165–179. doi: 10.1006/meth.1999.0934
- Fenwick, A., Richardson, R. J., Butterworth, J., Barron, M. J., and Dixon, M. J. (2008). Novel mutations in GJA1 cause oculodentodigital syndrome. *J. Dent. Res.* 87, 1021–1026. doi: 10.1177/154405910808701108
- Filosa, J. A., and Blanco, V. M. (2007). Neurovascular coupling in the mammalian brain. *Exp. Physiol.* 92, 641–646. doi: 10.1113/expphysiol.2006.036368
- Flenniken, A. M., Osborne, L. R., Anderson, N., Ciliberti, N., Fleming, C., Gittens, J. E., et al. (2005). A Gja1 missense mutation in a mouse model of oculodentodigital dysplasia. *Development* 132, 4375–4386. doi: 10.1242/dev.02011
- Florio, C., and Maniscalco, G. T. (2011). Improvement of visual acuity in patients with severe visual loss affected by multiple sclerosis treated with natalizumab: a case report. *Neurol. Sci.* 31(Suppl. 3), 325–327. doi: 10.1007/s10072-010-0349-7
- Foote, C. I., Zhou, L., Zhu, X., and Nicholson, B. J. (1998). The pattern of disulfide linkages in the extracellular loop regions of connexin 32 suggests a model for the docking interface of gap junctions. *J. Cell Biol.* 140, 1187–1197. doi: 10.1083/jcb.140.5.1187
- Frisch, C., Theis, M., De Souza Silva, M. A., Dere, E., Sohl, G., Teubner, B., et al. (2003). Mice with astrocyte-directed inactivation of connexin43 exhibit increased exploratory behaviour, impaired motor capacities, and changes in brain acetylcholine levels. *Eur. J. Neurosci.* 18, 2313–2318. doi: 10.1046/j.1460-9568.2003.02971.x
- Furuta, N., Ikeda, M., Hirayama, K., Fujita, Y., Amanuma, M., and Okamoto, K. (2012). A novel GJA1 mutation in oculodentodigital dysplasia with progressive spastic paraparesis and sensory deficits. *Intern. Med.* 51, 93–98. doi: 10.2169/internmedicine.51.5770
- Gaietta, G., Deerinck, T. J., Adams, S. R., Bouwer, J., Tour, O., Laird, D. W., et al. (2002). Multicolor and electron microscopic imaging of connexin trafficking. *Science* 296, 503–507. doi: 10.1126/science.1068793
- Garg, S., Md Syed, M., and Kielland, T. (2005). Staphylococcus aureus-derived peptidoglycan induces Cx43 expression and functional gap junction intercellular communication in microglia. *J. Neurochem.* 95, 475–483. doi: 10.1111/j.1471-4159.2005.03384.x
- Giaume, C. (2010). Astroglial wiring is adding complexity to neuroglial networking. *Front. Neuroenerg.* 2:129. doi: 10.3389/fnene.2010.00129
- Giaume, C., Leybaert, L., Naus, C. C., and Saez, J. C. (2013). Connexin and pannexin hemichannels in brain glial cells: properties, pharmacology, and roles. *Front. Pharmacol.* 4:88. doi: 10.3389/fphar.2013.00088
- Giepmans, B. N., Verlaan, I., and Moolenaar, W. H. (2001). Connexin-43 interactions with ZO-1 and alpha- and beta-tubulin. *Cell Commun. Adhes.* 8, 219–223. doi: 10.3109/15419060109080727
- Gong, X. Q., Shao, Q., Langlois, S., Bai, D., and Laird, D. W. (2007). Differential potency of dominant negative connexin43 mutants in oculodentodigital dysplasia. *J. Biol. Chem.* 282, 19190–19202. doi: 10.1074/jbc.M609653200
- Gong, X. Q., Shao, Q., Lounsbury, C. S., Bai, D., and Laird, D. W. (2006). Functional characterization of a GJA1 frameshift mutation causing oculodentodigital dysplasia and palmoplantar keratoderma. *J. Biol. Chem.* 281, 31801–31811. doi: 10.1074/jbc.M605961200
- Gonzalez, D., Gomez-Hernandez, J. M., and Barrio, L. C. (2006). Species specificity of mammalian connexin-26 to form open voltage-gated hemichannels. *FASEB J.* 20, 2329–2338. doi: 10.1096/fj.06-5828com
- Goodenough, D. A., and Paul, D. L. (2003). Beyond the gap: functions of unpaired connexon channels. *Nat. Rev. Mol. Cell Biol.* 4, 285–294. doi: 10.1038/nrm1072
- Gordon, G. R., Choi, H. B., Rungta, R. L., Ellis-Davies, G. C., and MacVICAR, B. A. (2008). Brain metabolism dictates the polarity of astrocyte control over arterioles. *Nature* 456, 745–749. doi: 10.1038/nature07525
- Herve, J. C., Derangeon, M., Bahbouhi, B., Mesnil, M., and Sarrouilhe, D. (2007). The connexin turnover, an important modulating factor of the level of cell-to-cell junctional communication: comparison with other integral membrane proteins. *J. Membr. Biol.* 217, 21–33. doi: 10.1007/s00232-007-9054-8
- Hirst-Jensen, B. J., Sahoo, P., Kieken, F., Delmar, M., and Sorgen, P. L. (2007). Characterization of the pH-dependent interaction between the gap junction protein connexin43 carboxyl terminus and cytoplasmic loop domains. *J. Biol. Chem.* 282, 5801–5813. doi: 10.1074/jbc.M605233200
- Hong, H. M., Yang, J. J., Shieh, J. C., Lin, M. L., and Li, S. Y. (2010). Novel mutations in the connexin43 (GJA1) and GJA1 pseudogene may contribute to nonsyndromic hearing loss. *Hum. Genet.* 127, 545–551. doi: 10.1007/s00439-010-0791-x
- Honkaniemi, J., Kalkkila, J. P., Koivisto, P., Kahara, V., Latvala, T., and Simola, K. (2005). Letter to the editor: Novel GJA1 mutation in oculodentodigital dysplasia. *Am. J. Med. Genet. A* 139, 48–49.
- Huang, T., Shao, Q., Macdonald, A., Xin, L., Lorentz, R., Bai, D., et al. (2013). Autosomal recessive GJA1 (Cx43) gene mutations cause oculodentodigital dysplasia by distinct mechanisms. *J. Cell Sci.* 126, 2857–2866. doi: 10.1242/jcs.123315
- Huckstepp, R. T., id Bihi, R., Eason, R., Spyer, K. M., Dicke, N., Willecke, K., et al. (2010). Connexin

- hemichannel-mediated CO<sub>2</sub>-dependent release of ATP in the medulla oblongata contributes to central respiratory chemosensitivity. *J. Physiol.* 588, 3901–3920. doi: 10.1113/jphysiol.2010.192088
- Iadecola, C., and Nedergaard, M. (2007). Glial regulation of the cerebral microvasculature. *Nat. Neurosci.* 10, 1369–1376. doi: 10.1038/nn2003
- Iglesias, R., Dahl, G., Qiu, F., Spray, D. C., and Scemes, E. (2009). Pannexin 1: the molecular substrate of astrocyte “hemichannels”. *J. Neurosci.* 29, 7092–7097. doi: 10.1523/JNEUROSCI.6062-08.2009
- Ivens, S., Kaufer, D., Flores, L. P., Bechmann, I., Zumsteg, D., Tomkins, O., et al. (2007). TGF-beta receptor-mediated albumin uptake into astrocytes is involved in neocortical epileptogenesis. *Brain* 130, 535–547. doi: 10.1093/brain/awl317
- Iyathurai, J., D’Hondt, C., Wang, N., De Bock, M., Himpens, B., Retamal, M. A., et al. (2013). Peptides and peptide-derived molecules targeting the intracellular domains of Cx43: gap junctions versus hemichannels. *Neuropharmacology*. doi: 10.1016/j.neuropharm.2013.04.050. [Epub ahead of print].
- Janigro, D. (2012). Are you in or out? Leukocyte, ion, and neurotransmitter permeability across the epileptic blood-brain barrier. *Epilepsia* 53(Suppl. 1), 26–34. doi: 10.1111/j.1528-1167.2012.03472.x
- Jiang, J. X., and Cherian, P. P. (2003). Hemichannels formed by connexin 43 play an important role in the release of prostaglandin E(2) by osteocytes in response to mechanical strain. *Cell Commun. Adhes.* 10, 259–264.
- Johnstone, S. R., Billaud, M., Lohman, A. W., Taddeo, E. P., and Isakson, B. E. (2012). Posttranslational modifications in connexins and pannexins. *J. Membr. Biol.* 245, 319–332. doi: 10.1007/s00232-012-9453-3
- Joss, S. K., Ghazawy, S., Tomkins, S., Ahmed, M., Bradbury, J., and Sheridan, E. (2008). Variable expression of neurological phenotype in autosomal recessive oculodentodigital dysplasia of two sibs and review of the literature. *Eur. J. Pediatr.* 167, 341–345. doi: 10.1007/s00431-007-0468-1
- Kalcheva, N., Qu, J., Sandeep, N., Garcia, L., Zhang, J., Wang, Z., et al. (2007). Gap junction remodelling and cardiac arrhythmogenesis in a murine model of oculodentodigital dysplasia. *Proc. Natl. Acad. Sci. U.S.A.* 104, 20512–20516. doi: 10.1073/pnas.0705472105
- Kamermans, M., Fahrenfort, I., Schultz, K., Janssen-Bienhold, U., Sjoerdsma, T., and Weiler, R. (2001). Hemichannel-mediated inhibition in the outer retina. *Science* 292, 1178–1180. doi: 10.1126/science.1060101
- Kang, J., Kang, N., Lovatt, D., Torres, A., Zhao, Z., Lin, J., et al. (2008). Connexin 43 hemichannels are permeable to ATP. *J. Neurosci.* 28, 4702–4711. doi: 10.1523/JNEUROSCI.5048-07.2008
- Kang, T. C., Kim, D. S., Kwak, S. E., Kim, J. E., Won, M. H., Kim, D. W., et al. (2006). Epileptogenic roles of astroglial death and regeneration in the dentate gyrus of experimental temporal lobe epilepsy. *Glia* 54, 258–271. doi: 10.1002/glia.20380
- Kettenmann, H., Hanisch, U. K., Noda, M., and Verkhratsky, A. (2011). Physiology of microglia. *Physiol. Rev.* 91, 461–553. doi: 10.1152/physrev.00011.2010
- Kielian, T. (2008). Glial connexins and gap junctions in CNS inflammation and disease. *J. Neurochem.* 106, 1000–1016. doi: 10.1111/j.1471-4159.2008.05405.x
- Koehler, R. C., Gebremedhin, D., and Harder, D. R. (2006). Role of astrocytes in cerebrovascular regulation. *J. Appl. Physiol.* 100, 307–317. doi: 10.1152/japplphysiol.00938.2005
- Kohling, R., Gladwell, S. J., Bracci, E., Vreugdenhil, M., and Jefferys, J. G. (2001). Prolonged epileptiform bursting induced by 0-Mg(2+) in rat hippocampal slices depends on gap junctional coupling. *Neuroscience* 105, 579–587. doi: 10.1016/S0306-4522(01)00222-6
- Kronengold, J., Srinivas, M., and Verselis, V. K. (2012). The N-terminal half of the connexin protein contains the core elements of the pore and voltage gates. *J. Membr. Biol.* 245, 453–463. doi: 10.1007/s00232-012-9457-z
- Kronengold, J., Trexler, E. B., Bukauskas, F. F., Bargiello, T. A., and Verselis, V. K. (2003a). Pore-lining residues identified by single channel SCAM studies in Cx46 hemichannels. *Cell Commun. Adhes.* 10, 193–199.
- Kronengold, J., Trexler, E. B., Bukauskas, F. F., Bargiello, T. A., and Verselis, V. K. (2003b). Single-channel SCAM identifies pore-lining residues in the first extracellular loop and first transmembrane domains of Cx46 hemichannels. *J. Gen. Physiol.* 122, 389–405. doi: 10.1085/jgp.200308861
- Kur, J., Newman, E. A., and Chan-Ling, T. (2012). Cellular and physiological mechanisms underlying blood flow regulation in the retina and choroid in health and disease. *Prog. Retin. Eye Res.* 31, 377–406. doi: 10.1016/j.preteyes.2012.04.004
- Kwon, T., Roux, B., Jo, S., Klauda, J. B., Harris, A. L., and Bargiello, T. A. (2012). Molecular dynamics simulations of the Cx26 hemichannel: insights into voltage-dependent loop-gating. *Biophys. J.* 102, 1341–1351. doi: 10.1016/j.bpj.2012.02.009
- Lai, A., Le, D. N., Paznekas, W. A., Gifford, W. D., Jabs, E. W., and Charles, A. C. (2006). Oculodentodigital dysplasia connexin43 mutations result in non-functional connexin hemichannels and gap junctions in C6 glioma cells. *J. Cell Sci.* 119, 532–541. doi: 10.1242/jcs.02770
- Laird, D. W. (2006). Life cycle of connexins in health and disease. *Biochem. J.* 394, 527–543. doi: 10.1042/BJ20051922
- Laird, D. W. (2008). Closing the gap on autosomal dominant connexin-26 and connexin-43 mutants linked to human disease. *J. Biol. Chem.* 283, 2997–3001. doi: 10.1074/jbc.R700041200
- Laird, D. W. (2010). The gap junction proteome and its relationship to disease. *Trends Cell Biol.* 20, 92–101. doi: 10.1016/j.tcb.2009.11.001
- Lampe, P. D., and Lau, A. F. (2004). The effects of connexin phosphorylation on gap junctional communication. *Int. J. Biochem. Cell Biol.* 36, 1171–1186. doi: 10.1016/S1357-2725(03)00264-4
- Lampe, P. D., TenBroek, E. M., Burt, J. M., Kurata, W. E., Johnson, R. G., and Lau, A. F. (2000). Phosphorylation of connexin43 on serine368 by protein kinase C regulates gap junctional communication. *J. Cell Biol.* 149, 1503–1512. doi: 10.1083/jcb.149.7.1503
- Langlois, S., Cowan, K. N., Shao, Q., Cowan, B. J., and Laird, D. W. (2008). Caveolin-1 and -2 interact with connexin43 and regulate gap junctional intercellular communication in keratinocytes. *Mol. Biol. Cell* 19, 912–928. doi: 10.1091/mbc.E07-06-0596
- Lasta, M., Pemp, B., Schmidl, D., Boltz, A., Kaya, S., Palkovits, S., et al. (2013). Neurovascular dysfunction precedes neural dysfunction in the retina of patients with type 1 diabetes. *Invest. Ophthalmol. Vis. Sci.* 54, 842–847. doi: 10.1167/iovs.12-10873
- Leybaert, L., and Sanderson, M. J. (2012). Intercellular Ca<sup>2+</sup> waves: mechanisms and function. *Physiol. Rev.* 92, 1359–1392. doi: 10.1152/physrev.00029.2011
- Li, J., Cheng, L., Wang, L. J., Liu, H. C., Li, L., Wang, X. L., et al. (2010). Cell surface sialic acid inhibits Cx43 gap junction functions in constructed HeLa cancer cells involving in sialylated N-cadherin. *Mol. Cell. Biochem.* 344, 241–251. doi: 10.1007/s11010-010-0548-9
- Liu, F., Arce, F. T., Ramachandran, S., and Lal, R. (2006). Nanomechanics of hemichannel conformations: connexin flexibility underlying channel opening and closing. *J. Biol. Chem.* 281, 23207–23217. doi: 10.1074/jbc.M605048200
- Liu, X., Hashimoto-Torii, K., Torii, M., Ding, C., and Rakic, P. (2010). Gap junctions/hemichannels modulate interkinetic nuclear migration in the forebrain precursors. *J. Neurosci.* 30, 4197–4209. doi: 10.1523/JNEUROSCI.4187-09.2010
- Liu, X., Hashimoto-Torii, K., Torii, M., Haydar, T. F., and Rakic, P. (2008). The role of ATP signaling in the migration of intermediate neuronal progenitors to the neocortical subventricular zone. *Proc. Natl. Acad. Sci. U.S.A.* 105, 11802–11807. doi: 10.1073/pnas.0805180105
- Loddenkemper, T., Grote, K., Evers, S., Oelerich, M., and Stogbauer, F. (2002). Neurological manifestations of the oculodentodigital dysplasia syndrome. *J. Neurol.* 249, 584–595. doi: 10.1007/s004150200068
- Lukemeyer, I., Requardt, R. P., Lin, X., Sasse, P., Andrie, R., Schrickel, J. W., et al. (2013). Deletion of the last five C-terminal amino acid residues of connexin43 leads to lethal ventricular arrhythmias in mice without affecting coupling via gap junction channels. *Basic Res. Cardiol.* 108, 348. doi: 10.1007/s00395-013-0348-y
- Lurtz, M. M., and Louis, C. F. (2003). Calmodulin and protein kinase C regulate gap junctional coupling in lens epithelial cells. *Am. J. Physiol. Cell Physiol.* 285, C1475–C1482. doi: 10.1152/ajpcell.00361.2002
- Lurtz, M. M., and Louis, C. F. (2007). Intracellular calcium regulation of connexin43. *Am. J. Physiol. Cell Physiol.* 293, C1806–C1813. doi: 10.1152/ajpcell.00630.2006
- Lutz, S. E., Raine, C. S., and Brosnan, C. F. (2012). Loss of astrocyte connexins 43 and 30 does not significantly alter susceptibility or severity of acute experimental autoimmune encephalomyelitis in mice. *J. Neuroimmunol.* 245, 8–14. doi: 10.1016/j.jneuroim.2012.01.007

- Maass, K., Shibayama, J., Chase, S. E., Willecke, K., and Delmar, M. (2007). C-terminal truncation of connexin43 changes number, size, and localization of cardiac gap junction plaques. *Circ. Res.* 101, 1283–1291. doi: 10.1161/CIRCRESAHA.107.162818
- Maeda, S., Nakagawa, S., Suga, M., Yamashita, E., Oshima, A., Fujiyoshi, Y., et al. (2009). Structure of the connexin 26 gap junction channel at 3.5 Å resolution. *Nature* 458, 597–602. doi: 10.1038/nature07869
- Marquez-Rosado, L., Solan, J. L., Dunn, C. A., Norris, R. P., and Lampe, P. D. (2012). Connexin43 phosphorylation in brain, cardiac, endothelial and epithelial tissues. *Biochim. Biophys. Acta* 1818, 1985–1992. doi: 10.1016/j.bbamem.2011.07.028
- Martinez, A. D., Eugenin, E. A., Branes, M. C., Bennett, M. V., and Saez, J. C. (2002). Identification of second messengers that induce expression of functional gap junctions in microglia cultured from newborn rats. *Brain Res.* 943, 191–201. doi: 10.1016/S0006-8993(02)02621-5
- Masaki, K., Suzuki, S. O., Matsushita, T., Yonekawa, T., Matsuoka, T., Isobe, N., et al. (2012). Extensive loss of connexins in Balo's disease: evidence for an auto-antibody-independent astrocytopathy via impaired astrocyte-oligodendrocyte/myelin interaction. *Acta Neuropathol.* 123, 887–900. doi: 10.1007/s00401-012-0972-x
- McLachlan, E., Manias, J. L., Gong, X. Q., Lounsbury, C. S., Shao, Q., Bernier, S. M., et al. (2005). Functional characterization of oculodentodigital dysplasia-associated Cx43 mutants. *Cell Commun. Adhes.* 12, 279–292. doi: 10.1080/15419060500514143
- Meme, W., Calvo, C. F., Froger, N., Ezan, P., Amigou, E., Koulakoff, A., et al. (2006). Proinflammatory cytokines released from microglia inhibit gap junctions in astrocytes: potentiation by beta-amyloid. *FASEB J.* 20, 494–496.
- Meme, W., Vandecasteele, M., Giaume, C., and Venance, L. (2009). Electrical coupling between hippocampal astrocytes in rat brain slices. *Neurosci. Res.* 63, 236–243. doi: 10.1016/j.neures.2008.12.008
- Metea, M. R., and Newman, E. A. (2006). Glial cells dilate and constrict blood vessels: a mechanism of neurovascular coupling. *J. Neurosci.* 26, 2862–2870. doi: 10.1523/JNEUROSCI.4048-05.2006
- Mika, T., and Prochnow, N. (2012). Functions of connexins and large pore channels on microglial cells: the gates to environment. *Brain Res.* 1487, 16–24. doi: 10.1016/j.brainres.2012.07.020
- Mirrione, M. M., and Tsirka, S. E. (2011). “A functional role for microglia in epilepsy,” in *Clinical and Genetic Aspects of Epilepsy*, ed Z. Afawi (New York, NY: InTech), 3–22.
- Miyoshi, H., Boyle, M. B., MacKay, L. B., and Garfield, R. E. (1996). Voltage-clamp studies of gap junctions between uterine muscle cells during term and preterm labor. *Biophys. J.* 71, 1324–1334. doi: 10.1016/S0006-3495(96)79332-3
- Moreno, A. P. (2005). Connexin phosphorylation as a regulatory event linked to channel gating. *Biochim. Biophys. Acta* 1711, 164–171. doi: 10.1016/j.bbamem.2005.02.016
- Moreno, A. P., Chanson, M., Elenes, S., Anumonwo, J., Scerri, I., Gu, H., et al. (2002). Role of the carboxyl terminal of connexin43 in transjunctional fast voltage gating. *Circ. Res.* 90, 450–457. doi: 10.1161/hh0402.105667
- Moreno, A. P., and Lau, A. F. (2007). Gap junction channel gating modulated through protein phosphorylation. *Prog. Biophys. Mol. Biol.* 94, 107–119. doi: 10.1016/j.pbiomolbio.2007.03.004
- Mulligan, S. J., and MacVicar, B. A. (2004). Calcium transients in astrocyte endfeet cause cerebrovascular constrictions. *Nature* 431, 195–199. doi: 10.1038/nature02827
- Myllykoski, M., Kuczera, K., and Kursula, P. (2009). Complex formation between calmodulin and a peptide from the intracellular loop of the gap junction protein connexin43: Molecular conformation and energetics of binding. *Biophys. Chem.* 144, 130–135. doi: 10.1016/j.bpc.2009.08.001
- Nagasawa, K., Chiba, H., Fujita, H., Kojima, T., Saito, T., Endo, T., et al. (2006). Possible involvement of gap junctions in the barrier function of tight junctions of brain and lung endothelial cells. *J. Cell. Physiol.* 208, 123–132. doi: 10.1002/jcp.20647
- Neijssen, J., Herberds, C., Drijfhout, J. W., Reits, E., Janssen, L., and Neefjes, J. (2005). Cross-presentation by intercellular peptide transfer through gap junctions. *Nature* 434, 83–88. doi: 10.1038/nature03290
- Neuhaus, J., Weimann, A., Stolzenburg, J. U., Wolburg, H., Horn, L. C., and Dorschner, W. (2002). Smooth muscle cells from human urinary bladder express connexin 43 *in vivo* and *in vitro*. *World J. Urol.* 20, 250–254. doi: 10.1016/j.cib.19410
- Nicholson, B. J. (2003). Gap junctions - from cell to molecule. *J. Cell. Sci.* 116, 4479–4481. doi: 10.1242/jcs.00821
- Nodin, C., Nilsson, M., and Blomstrand, F. (2005). Gap junction blockage limits intercellular spreading of astrocytic apoptosis induced by metabolic depression. *J. Neurochem.* 94, 1111–1123. doi: 10.1111/j.1471-4159.2005.03241.x
- O'Carroll, S. J., Alkadhi, M., Nicholson, L. F., and Green, C. R. (2008). Connexin 43 mimetic peptides reduce swelling, astrogliosis, and neuronal cell death after spinal cord injury. *Cell Commun. Adhes.* 15, 27–42. doi: 10.1080/15419060802014164
- Oh, S., Ri, Y., Bennett, M. V., Trexler, E. B., Verselis, V. K., and Bargiello, T. A. (1997). Changes in permeability caused by connexin 32 mutations underlie X-linked Charcot-Marie-Tooth disease. *Neuron* 19, 927–938. doi: 10.1016/S0896-6273(00)80973-3
- Orellana, J. A., Figueroa, X. F., Sanchez, H. A., Contreras-Duarte, S., Velarde, V., and Saez, J. C. (2011). Hemichannels in the neurovascular unit and white matter under normal and inflamed conditions. *CNS Neurol. Disord. Drug Targets* 10, 404–414. doi: 10.2174/187152711794653869
- Orellana, J. A., Saez, P. J., Shoji, K. F., Schalper, K. A., Palacios-Prado, N., Velarde, V., et al. (2009). Modulation of brain hemichannels and gap junction channels by pro-inflammatory agents and their possible role in neurodegeneration. *Antioxid. Redox Signal.* 11, 369–399. doi: 10.1089/ars.2008.2130
- Orthmann-Murphy, J. L., Freidin, M., Fischer, E., Scherer, S. S., and Abrams, C. K. (2007). Two distinct heterotypic channels mediate gap junction coupling between astrocyte and oligodendrocyte connexins. *J. Neurosci.* 27, 13949–13957. doi: 10.1523/JNEUROSCI.3395-07.2007
- Orthmann-Murphy, J. L., Salsano, E., Abrams, C. K., Buzzi, A., Uziel, G., Freidin, M. M., et al. (2009). Hereditary spastic paraparesis is a novel phenotype for GJA12/GJC2 mutations. *Brain* 132, 426–438. doi: 10.1093/brain/awn328
- Pannasch, U., Derangeon, M., Chever, O., and Rouach, N. (2012). Astroglial gap junctions shape neuronal network activity. *Commun. Integr. Biol.* 5, 248–254. doi: 10.1016/j.cib.2012.07.002
- Pannasch, U., Vargova, L., Reingruber, J., Ezan, P., Holcman, D., Giaume, C., et al. (2011). Astroglial networks scale synaptic activity and plasticity. *Proc. Natl. Acad. Sci. U.S.A.* 108, 8467–8472. doi: 10.1073/pnas.1016650108
- Pascual, O., Casper, K. B., Kubera, C., Zhang, J., Revilla-Sanchez, R., Sul, J. Y., et al. (2005). Astrocytic purinergic signaling coordinates synaptic networks. *Science* 310, 113–116. doi: 10.1126/science.1116916
- Paul, D. L., Ebihara, L., Takemoto, L. J., Swenson, K. I., and Goodenough, D. A. (1991). Connexin46, a novel lens gap junction protein, induces voltage-gated currents in non-junctional plasma membrane of Xenopus oocytes. *J. Cell Biol.* 115, 1077–1089. doi: 10.1083/jcb.115.4.1077
- Paznekas, W. A., Boyadjiev, S. A., Shapiro, R. E., Daniels, O., Wollnik, B., Keegan, C. E., et al. (2003). Connexin 43 (GJA1) mutations cause the pleiotropic phenotype of oculodentodigital dysplasia. *Am. J. Hum. Genet.* 72, 408–418. doi: 10.1086/346090
- Paznekas, W. A., Karczeski, B., Vermeer, S., Lowry, R. B., Delatycki, M., Laurence, F., et al. (2009). GJA1 mutations, variants, and connexin 43 dysfunction as it relates to the oculodentodigital dysplasia phenotype. *Hum. Mutat.* 30, 724–733. doi: 10.1002/humu.20958
- Perea, G., and Araque, A. (2010). GLIA modulates synaptic transmission. *Brain Res. Rev.* 63, 93–102. doi: 10.1016/j.brainresrev.2009.10.005
- Petzold, G. C., and Murthy, V. N. (2011). Role of astrocytes in neurovascular coupling. *Neuron* 71, 782–797. doi: 10.1016/j.neuron.2011.08.009
- Ponsaerts, R., De Vuyst, E., Retamal, M., D'Hondt, C., Vermeire, D., Wang, N., et al. (2010). Intramolecular loop/tail interactions are essential for connexin 43-hemichannel activity. *FASEB J.* 24, 4378–4395. doi: 10.1096/fj.09-153007
- Qin, H., Shao, Q., Igoudra, S. A., Alaoui-Jamali, M. A., and Laird, D. W. (2003). Lysosomal and proteasomal degradation play distinct roles in the life cycle of Cx43 in gap junctional intercellular communication-deficient and -competent breast tumor cells. *J. Biol. Chem.* 278, 30005–30014. doi: 10.1074/jbc.M3000614200
- Quintáns, B., Martínez-Montero, P., Ordóñez-Ugalde, A., Esteban-Pérez, P., and Gómez-González, B. (2012). Astroglial gap junctions regulate synaptic transmission in the hippocampus. *Neuroscience* 208, 103–112. doi: 10.1016/j.neuroscience.2012.07.030

- J., Sanz, I., Escudero, A., et al. (2013). "Oculodentodigital dysplasia: variable neurological phenotype associated with the p.V85M mutation in connexin 43," in *International Conference on Spinocerebellar Degenerations* (Paris), 39
- Rackauskas, M., Neverauskas, V., and Skeberdis, V. A. (2010). Diversity and properties of connexin gap junction channels. *Medicina* 46, 1–12.
- Rana, S., and Dringen, R. (2007). Gap junction hemichannel-mediated release of glutathione from cultured rat astrocytes. *Neurosci. Lett.* 415, 45–48. doi: 10.1016/j.neulet.2006.12.043
- Reid, C. A., Berkovic, S. F., and Petrou, S. (2009). Mechanisms of human inherited epilepsies. *Prog. Neurobiol.* 87, 41–57. doi: 10.1016/j.pneurobio.2008.09.016
- Retamal, M. A., Cortes, C. J., Reuss, L., Bennett, M. V., and Saez, J. C. (2006). S-nitrosylation and permeation through connexin 43 hemichannels in astrocytes: induction by oxidant stress and reversal by reducing agents. *Proc. Natl. Acad. Sci. U.S.A.* 103, 4475–4480. doi: 10.1073/pnas.0511118103
- Retamal, M. A., Frogner, N., Palacios-Prado, N., Ezan, P., Saez, P. J., Saez, J. C., et al. (2007). Cx43 hemichannels and gap junction channels in astrocytes are regulated oppositely by proinflammatory cytokines released from activated microglia. *J. Neurosci.* 27, 13781–13792. doi: 10.1523/JNEUROSCI.2042-07.2007
- Risek, B., Guthrie, S., Kumar, N., and Gilula, N. B. (1990). Modulation of gap junction transcript and protein expression during pregnancy in the rat. *J. Cell Biol.* 110, 269–282. doi: 10.1083/jcb.110.2.269
- Roscoe, W., Veitch, G. I., Gong, X. Q., Pellegrino, E., Bai, D., McLachlan, E., et al. (2005). Oculodentodigital dysplasia-causing connexin43 mutants are non-functional and exhibit dominant effects on wild-type connexin43. *J. Biol. Chem.* 280, 11458–11466. doi: 10.1074/jbc.M409564200
- Rouach, N., Calvo, C. F., Duquennoy, H., Glowinski, J., and Giaume, C. (2004). Hydrogen peroxide increases gap junctional communication and induces astrocyte toxicity: regulation by brain macrophages. *Glia* 45, 28–38. doi: 10.1002/glia.10300
- Rouach, N., Koulakoff, A., Abudara, V., Willecke, K., and Giaume, C. (2008). Astroglial metabolic networks sustain hippocampal synaptic transmission. *Science* 322, 1551–1555. doi: 10.1126/science.1164022
- Roussel, B. D., Kruppa, A. J., Miranda, E., Crowther, D. C., Lomas, D. A., and Marciniak, S. J. (2013). Endoplasmic reticulum dysfunction in neurological disease. *Lancet Neurol.* 12, 105–118. doi: 10.1016/S1474-4422(12)70238-7
- Saez, J. C., Berthoud, V. M., Branes, M. C., Martinez, A. D., and Beyer, E. C. (2003). Plasma membrane channels formed by connexins: their regulation and functions. *Physiol. Rev.* 83, 1359–1400.
- Saidi Brikci-Nigassa, A., Clement, M. J., Ha-Duong, T., Adjadj, E., Ziani, L., Pastre, D., et al. (2012). Phosphorylation controls the interaction of the connexin43 C-terminal domain with tubulin and microtubules. *Biochemistry* 51, 4331–4342. doi: 10.1021/bi201806j
- Sanchez, H. A., Mese, G., Srinivas, M., White, T. W., and Verselis, V. K. (2010). Differentially altered Ca<sup>2+</sup> regulation and Ca<sup>2+</sup> permeability in Cx26 hemichannels formed by the A40V and G45E mutations that cause keratitis ichthyosis deafness syndrome. *J. Gen. Physiol.* 136, 47–62. doi: 10.1085/jgp.201010433
- Sato, P. Y., Coombs, W., Lin, X., Nekrasova, O., Green, K. J., Isom, L. L., et al. (2011). Interactions between ankyrin-G, Plakophilin-2, and Connexin43 at the cardiac intercalated disc. *Circ. Res.* 109, 193–201. doi: 10.1161/CIRCRESAHA.111.247023
- Scemes, E. (2012). Nature of plasma-membrane functional "hemichannels". *Biochim. Biophys. Acta* 1818, 1880–1883. doi: 10.1016/j.bbamem.2011.06.005
- Seki, A., Coombs, W., Taffet, S. M., and Delmar, M. (2004). Loss of electrical communication, but not plaque formation, after mutations in the cytoplasmic loop of connexin43. *Heart Rhythm* 1, 227–233. doi: 10.1016/j.hrthm.2004.03.066
- Shaikh, S. B., Uy, B., Perera, A., and Nicholson, L. F. (2012). AGEs-RAGE mediated up-regulation of connexin43 in activated human microglial CHME-5 cells. *Neurochem. Int.* 60, 640–651. doi: 10.1016/j.neuint.2012.02.023
- Shao, Q., Liu, Q., Lorentz, R., Gong, X. Q., Bai, D., Shaw, G. S., et al. (2012). Structure and functional studies of N-terminal Cx43 mutants linked to oculodentodigital dysplasia. *Mol. Biol. Cell* 23, 3312–3321. doi: 10.1091/mbc.E12-02-0128
- Sheean, G., and McGuire, J. R. (2009). Spastic hypertonia and movement disorders: pathophysiology, clinical presentation, and quantification. *PM R* 1, 827–833. doi: 10.1016/j.pmrj.2009.08.002
- Shibayama, J., Gutierrez, C., Gonzalez, D., Kieken, E., Seki, A., Carrion, J. R., et al. (2006). Effect of charge substitutions at residue his-142 on voltage gating of connexin43 channels. *Biophys. J.* 91, 4054–4063. doi: 10.1529/biophysj.106.085787
- Shibayama, J., Paznekas, W., Seki, A., Taffet, S., Jabs, E. W., Delmar, M., et al. (2005). Functional characterization of connexin43 mutations found in patients with oculodentodigital dysplasia. *Circ. Res.* 96, e83–e91. doi: 10.1161/01.RES.0000168369.79972.d2
- Shintani-Ishida, K., Uemura, K., and Yoshida, K. (2007). Hemichannels in cardiomyocytes open transiently during ischemia and contribute to reperfusion injury following brief ischemia. *Am. J. Physiol. Heart Circ. Physiol.* 293, H1714–H1720. doi: 10.1152/ajpheart.00022.2007
- Simard, M., Arcuino, G., Takano, T., Liu, Q. S., and Nedergaard, M. (2003). Signaling at the gliovascular interface. *J. Neurosci.* 23, 9254–9262.
- Skerrett, I. M., Aronowitz, J., Shin, J. H., Cymes, G., Kasperek, E., Cao, F. L., et al. (2002). Identification of amino acid residues lining the pore of a gap junction channel. *J. Cell Biol.* 159, 349–360. doi: 10.1083/jcb.200207060
- Sokolova, I. V., Martinez, A. M., and Fletcher, W. H. (2002). The highly conserved Gln49 and Ser50 of mammalian connexin43 are present in chick connexin43 and essential for functional gap junction channels. *Cell Commun. Adhes.* 9, 75–86. doi: 10.1080/15419060214149
- Solan, J. L., and Lampe, P. D. (2007). Key connexin 43 phosphorylation events regulate the gap junction life cycle. *J. Membr. Biol.* 217, 35–41. doi: 10.1007/s00232-007-9035-y
- Spray, D. C., Ye, Z. C., and Ransom, B. R. (2006). Functional connexin "hemichannels": a critical appraisal. *Glia* 54, 758–773. doi: 10.1002/glia.20429
- Stehberg, J., Moraga-Amaro, R., Salazar, C., Becerra, A., Echeverria, C., Orellana, J. A., et al. (2012). Release of gliotransmitters through astroglial connexin 43 hemichannels is necessary for fear memory consolidation in the basolateral amygdala. *FASEB J.* 26, 3649–3657. doi: 10.1096/fj.11-198416
- Steinbauer, C., and Seifert, G. (2012). "Astrocyte dysfunction in epilepsy," in *Jasper's Basic Mechanisms of the Epilepsies*, eds J. L. Noebels, M. Avoli, M. A. Rogawski, R. W. Olsen, and A. V. Delgado-Escueta (Bethesda, MD: Oxford University Press), 606–617. doi: 10.1093/med/9780199746545.003.0047
- Sumi, N., Nishioku, T., Takata, F., Matsumoto, J., Watanabe, T., Shuto, H., et al. (2010). Lipopolysaccharide-activated microglia induce dysfunction of the blood-brain barrier in rat microvascular endothelial cells co-cultured with microglia. *Cell. Mol. Neurobiol.* 30, 247–253. doi: 10.1007/s10571-009-9446-7
- Takano, T., Tian, G. F., Peng, W., Lou, N., Libionka, W., Han, X., et al. (2006). Astrocyte-mediated control of cerebral blood flow. *Nat. Neurosci.* 9, 260–267. doi: 10.1038/nn1623
- Takeuchi, H., Jin, S., Suzuki, H., Doi, Y., Liang, J., Kawanokuchi, J., et al. (2008). Blockade of microglial glutamate release protects against ischemic brain injury. *Exp. Neurol.* 214, 144–146. doi: 10.1016/j.expneurol.2008.08.001
- Takeuchi, H., Mizoguchi, H., Doi, Y., Jin, S., Noda, M., Liang, J., et al. (2011). Blockade of gap junction hemichannel suppresses disease progression in mouse models of amyotrophic lateral sclerosis and Alzheimer's disease. *PLoS ONE* 6:e21108. doi: 10.1371/journal.pone.0021108
- Tang, Q., Dowd, T. L., Verselis, V. K., and Bargiello, T. A. (2009). Conformational changes in a pore-forming region underlie voltage-dependent "loop gating" of an unapposed connexin hemichannel. *J. Gen. Physiol.* 133, 555–570. doi: 10.1085/jgp.200910207
- Theis, M., Jauch, R., Zhuo, L., Speidel, D., Wallraff, A., Doring, B., et al. (2003). Accelerated hippocampal spreading depression and enhanced locomotory activity in mice with astrocyte-directed inactivation of connexin43. *J. Neurosci.* 23, 766–776.
- Theodorin, N., Bechberger, J. F., Naus, C. C., and Sin, W. C. (2012). Role of gap junction protein connexin43 in astrogliosis induced by brain injury. *PLoS ONE* 7:e47311. doi: 10.1371/journal.pone.0047311
- Thevenin, A. F., Kowal, T. J., Fong, J. T., Kells, R. M., Fisher, C. G., and Falk, M. M. (2013). Proteins and mechanisms regulating gap-junction assembly, internalization, and degradation. *Physiology (Bethesda)* 28, 93–116. doi: 10.1152/physiol.00038.2012

- Thibodeau, I. L., Xu, J., Li, Q., Liu, G., Lam, K., Veinot, J. P., et al. (2010). Paradigm of genetic mosaicism and lone atrial fibrillation: physiological characterization of a connexin 43-deletion mutant identified from atrial tissue. *Circulation* 122, 236–244. doi: 10.1161/CIRCULATIONAHA.110.961227
- Tong, D., Li, T. Y., Naus, K. E., Bai, D., and Kidder, G. M. (2007). *In vivo* analysis of undocked connexin43 gap junction hemichannels in ovarian granulosa cells. *J. Cell Sci.* 120, 4016–4024. doi: 10.1242/jcs.011775
- Torres, A., Wang, E., Xu, Q., Fujita, T., Dobrowolski, R., Willecke, K., et al. (2012). Extracellular Ca(2+) acts as a mediator of communication from neurons to glia. *Sci. Signal.* 5, ra8. doi: 10.1126/scisignal.2002160
- Trexler, E. B., Bennett, M. V., Bargiello, T. A., and Verselis, V. K. (1996). Voltage gating and permeation in a gap junction hemichannel. *Proc. Natl. Acad. Sci. U.S.A.* 93, 5836–5841. doi: 10.1073/pnas.93.12.5836
- Unger, T., Bette, S., Zhang, J., Theis, M., and Engle, J. (2012). Connexin-deficiency affects expression levels of glial glutamate transporters within the cerebrum. *Neurosci. Lett.* 506, 12–16. doi: 10.1016/j.neulet.2011.10.032
- Unger, V. M., Kumar, N. M., Gilula, N. B., and Yeager, M. (1997). Projection structure of a gap junction membrane channel at 7 Å resolution. *Nat. Struct. Biol.* 4, 39–43. doi: 10.1038/nsb0197-39
- Unger, V. M., Kumar, N. M., Gilula, N. B., and Yeager, M. (1999). Three-dimensional structure of a recombinant gap junction membrane channel. *Science* 283, 1176–1180. doi: 10.1126/science.283.5405.1176
- Van Norstrand, D. W., Asimaki, A., Rubinos, C., Dolmatova, E., Srinivas, M., Tester, D. J., et al. (2012). Connexin43 mutation causes heterogeneous gap junction loss and sudden infant death. *Circulation* 125, 474–481. doi: 10.1161/CIRCULATIONAHA.111.057224
- Vanslyke, J. K., Naus, C. C., and Musil, L. S. (2009). Conformational maturation and post-ER multisubunit assembly of gap junction proteins. *Mol. Biol. Cell* 20, 2451–2463. doi: 10.1091/mbc.E09-01-0062
- Verselis, V. K., Treilles, M. P., Rubinos, C., Bargiello, T. A., and Srinivas, M. (2009). Loop gating of connexin hemichannels involves movement of pore-lining residues in the first extracellular loop domain. *J. Biol. Chem.* 284, 4484–4493. doi: 10.1074/jbc.M807430200
- Vezzani, A., Auvin, S., Ravizza, T., and Aronica, E. (2012). “Glia-neuronal interactions in ictogenesis and epileptogenesis: role of inflammatory mediators,” in *Jasper’s Basic Mechanisms of the Epilepsies*, eds J. L. Noebels, M. Avoli, M. A. Rogawski, R. W. Olsen, and A. V. Delgado-Escueta (Bethesda, MD: Oxford University Press), 618–634. doi: 10.1093/med/9780199746545.003.0048
- Wallraff, A., Kohling, R., Heinemann, U., Theis, M., Willecke, K., and Steinhauser, C. (2006). The impact of astrocytic gap junctional coupling on potassium buffering in the hippocampus. *J. Neurosci.* 26, 5438–5447. doi: 10.1523/JNEUROSCI.0037-06.2006
- Wang, N., De Bock, M., Antoons, G., Gadicherla, A. K., Bol, M., Decrock, E., et al. (2012a). Connexin mimetic peptides inhibit Cx43 hemichannel opening triggered by voltage and intracellular Ca<sup>2+</sup> elevation. *Basic Res. Cardiol.* 107, 304. doi: 10.1007/s00395-012-0304-2
- Wang, X., Bukoreshtliev, N. V., and Gerdes, H. H. (2012b). Developing neurons form transient nanotubes facilitating electrical coupling and calcium signaling with distant astrocytes. *PLoS ONE* 7:e47429. doi: 10.1371/journal.pone.0047429
- Wang, N., De Vuyst, E., Ponsaerts, R., Boengler, K., Palacios-Prado, N., Wauman, J., et al. (2013a). Selective inhibition of Cx43 hemichannels by Gap19 and its impact on myocardial ischemia/reperfusion injury. *Basic Res. Cardiol.* 108, 309. doi: 10.1007/s00395-012-0309-x
- Wang, X., Ma, A., Zhu, W., Zhu, L., Zhao, Y., Xi, J., et al. (2013b). The role of connexin 43 and hemichannels correlated with the astrocytic death following ischemia/reperfusion insult. *Cell. Mol. Neurobiol.* 33, 401–410. doi: 10.1007/s10571-013-9906-y
- Wasseff, S., Abrams, C. K., and Scherer, S. S. (2010). A dominant connexin43 mutant does not have dominant effects on gap junction coupling in astrocytes. *Neuron Glia Biol.* 6, 213–223. doi: 10.1017/S1740925X11000019
- Wei, C. J., Xu, X., and Lo, C. W. (2004). Connexins and cell signaling in development and disease. *Annu. Rev. Cell Dev. Biol.* 20, 811–838. doi: 10.1146/annurev.cellbio.19.111301.144309
- Weissman, T. A., Riquelme, P. A., Ivic, L., Flint, A. C., and Kriegstein, A. R. (2004). Calcium waves propagate through radial glial cells and modulate proliferation in the developing neocortex. *Neuron* 43, 647–661. doi: 10.1016/j.neuron.2004.08.015
- Wiencken-Barger, A. E., Djukic, B., Casper, K. B., and McCarthy, K. D. (2007). A role for Connexin43 during neurodevelopment. *Glia* 55, 675–686. doi: 10.1002/glia.20484
- Willoughby, J. O., Mackenzie, L., Broberg, M., Thoren, A. E., Medvedev, A., Sims, N. R., et al. (2003). Fluorocitrate-mediated astroglial dysfunction causes seizures. *J. Neurosci. Res.* 74, 160–166. doi: 10.1002/jnr.10743
- Wong, C. W., Christen, T., Roth, I., Chadjichristos, C. E., Derouette, J. P., Foglia, B. F., et al. (2006). Connexin37 protects against atherosclerosis by regulating monocyte adhesion. *Nat. Med.* 12, 950–954. doi: 10.1038/nm1441
- Xu, H. L., Mao, L., Ye, S., Paisansathan, C., Vetri, F., and Pellegrino, D. A. (2008). Astrocytes are a key conduit for upstream signaling of vasodilation during cerebral cortical neuronal activation *in vivo*. *Am. J. Physiol. Heart Circ. Physiol.* 294, H622–H632. doi: 10.1152/ajpheart.00530.2007
- Yahuaca, P., Ek-Vitorin, J. F., Rush, P., Delmar, M., and Taffet, S. M. (2000). Identification of a protein kinase activity that phosphorylates connexin43 in a pH-dependent manner. *Braz. J. Med. Biol. Res.* 33, 399–406. doi: 10.1590/S0100-879X2000000400005
- Ye, Z. C., Wyeth, M. S., Baltan-Tekkok, S., and Ransom, B. R. (2003). Functional hemichannels in astrocytes: a novel mechanism of glutamate release. *J. Neurosci.* 23, 3588–3596.
- Yoon, J. J., Green, C. R., O’Carroll, S. J., and Nicholson, L. F. (2010). Dose-dependent protective effect of connexin43 mimetic peptide against neurodegeneration in an *ex vivo* model of epileptiform lesion. *Epilepsy Res.* 92, 153–162. doi: 10.1016/j.epilepsyres.2010.08.014
- Zhou, X. W., Pfahl, A., Werner, R., Hudder, A., Llanes, A., Luebke, A., et al. (1997). Identification of a pore lining segment in gap junction hemichannels. *Biophys. J.* 72, 1946–1953. doi: 10.1016/S0006-3495(97)78840-4
- Zhou, Y., Yang, W., Lurtz, M. M., Ye, Y., Huang, Y., Lee, H. W., et al. (2007). Identification of the calmodulin binding domain of connexin 43. *J. Biol. Chem.* 282, 35005–35017. doi: 10.1074/jbc.M70728200
- Zlokovic, B. V. (2011). Neurovascular pathways to neurodegeneration in Alzheimer’s disease and other disorders. *Nat. Rev. Neurosci.* 12, 723–738.
- Zonta, M., Sebelin, A., Gobbo, S., Fellin, T., Pozzan, T., and Carmignoto, G. (2003). Glutamate-mediated cytosolic calcium oscillations regulate a pulsatile prostaglandin release from cultured rat astrocytes. *J. Physiol.* 553, 407–414. doi: 10.1113/jphysiol.2003.046706

**Conflict of Interest Statement:** The authors declare that the research was conducted in the absence of any commercial or financial relationships that could be construed as a potential conflict of interest.

**Received:** 13 May 2013; **paper pending published:** 04 June 2013; **accepted:** 02 September 2013; **published online:** 26 September 2013.

**Citation:** De Bock M, Kerrebrouck M, Wang N and Leybaert L (2013) Neurological manifestations of oculodentodigital dysplasia: a Cx43 channelopathy of the central nervous system? *Front. Pharmacol.* 4:120. doi: 10.3389/fphar.2013.00120

This article was submitted to *Pharmacology of Ion Channels and Channelopathies*, a section of the journal *Frontiers in Pharmacology*.

Copyright © 2013 De Bock, Kerrebrouck, Wang and Leybaert. This is an open-access article distributed under the terms of the Creative Commons Attribution License (CC BY). The use, distribution or reproduction in other forums is permitted, provided the original author(s) or licensor are credited and that the original publication in this journal is cited, in accordance with accepted academic practice. No use, distribution or reproduction is permitted which does not comply with these terms.